

C-H Bond Functionalization of Selected Azaheterocycles under Metal-Free and Photochemical Conditions

THESIS

Submitted in partial fulfillment of the requirements for the degree

of

DOCTOR OF PHILOSOPHY

by

Sonam

ID. NO. 2018PHXF0008P

Under the supervision of

Prof. Anil Kumar



BITS Pilani
Pilani | Dubai | Goa | Hyderabad

**DEPARTMENT OF CHEMISTRY
BIRLA INSTITUTE OF TECHNOLOGY AND SCIENCE, PILANI
PILANI CAMPUS, RAJASTHAN (INDIA)**

July 2023

BIRLA INSTITUTE OF TECHNOLOGY AND SCIENCE, PILANI

CERTIFICATE

This is to certify that the thesis titled “**C-H Bond Functionalization of Selected Azaheterocycles under Metal-Free and Photochemical Conditions**” submitted by **Sonam** ID No **2018PHXF0008P** for award of Ph.D. of the Institute embodies original work done by him/her under my supervision.

Signature of the Supervisor:

Name in capital letters: Dr. ANIL KUMAR

Designation: Professor

Date: 28/07/2023

Dedicated to
My Beloved Family

Acknowledgment

At the very beginning, I would like to devote myself to the "God Sai Baba" for giving me the strength, knowledge, and ability to carry out this research study and to complete it without failure. Now it is the time of pleasure to recapture the number of memorable moments, several people, who joined in me in this long journey, whose continuous support, guidance, motivation, help and most importantly blessings at each and every step helped to achieve this milestone of my life.

Next, I am extremely grateful to my research supervisor, Prof. Anil Kumar, for mentoring and teaching me the important aspects throughout my Ph.D. tenure. Without his motivation and expertise in synthetic organic chemistry, the achievement of this research work would have remained a dream. I am indebted to Prof. Anil Kumar for mentoring me, teaching me necessary things, and allowing me to work in the laboratory without any pressure. This achievement has been possible only because of his unconditional support whenever I needed his help, both professionally and personally. A person with an amicable and positive disposition, he has always made himself available to clarify my doubts and confusion despite his busy schedule. I consider it a great opportunity to have done my doctoral program under his guidance and to learn from his research expertise. His inspiring hard work and constant motivation helped me to understand better and remain optimistic throughout the course of my study. I am also grateful for the opportunities provided by him to work with HRMS facility and to mentor undergraduate and newcomer students in his laboratory, which added valuable experience to my Ph.D. life. Thank you, Sir, for all your help and support.

I express my thankfulness to the former and present Vice chancellors, Directors, Deans and Associate Deans of Birla Institute of Technology & Science, Pilani (BITS Pilani) for giving me the opportunity to pursue my doctoral studies by providing necessary facilities. I overwhelmingly acknowledge the office staff of AGSRD, whose secretarial assistance helped me in submitting the various evaluation documents in time. I would also like to acknowledge the former and present Head of the Department, DRC, Chemistry, BITS Pilani, Pilani Campus for their official support and encouragement. My truthful thanks to Dr. Ranjan Sinha Thakur, Librarian,

BITS Pilani and other staffs of library for their support and help while utilizing the library facilities.

I also acknowledge department of chemistry, BITS Pilani for providing me Institute fellowship during the tenure of my Ph.D. Moreover, DST-FIST is also sincerely acknowledged for providing instrumentation facilities in the department. I am very thankful for DST-SERB project for financial support.

I am profoundly thankful for the cooperation and affection extended by all the respected teachers. I am grateful to the members of my Doctoral Advisory Committee, Prof. Ajay K. Sah and Prof. Rajeev Sakhuja for their great cooperation during my Ph.D. At the onset, their valuable suggestion for refining my proposal and seminar had a great impact to begin my research. I acknowledge them for continuous suggestions and corrections for improving my thesis without any time limits. The other respectful faculty members of chemistry department Prof. Mr S. C. Sivasubramanian, Prof. Dalip Kumar, Prof. Indresh Kumar, Prof. Saumi Ray, Prof. R. K. Roy, Prof. Inamur R. Laskar, Prof. Madhushree Sarkar, Prof. Bharti Khungar, Prof. Paritosh Shukla, Prof. Surojit Pande, Prof. Shamik Chakraborty, and Prof. Bibhas R. Sarkar, Dr. Prashant Uday Manohar, Dr. Mrinmoyee Basu, Dr. Partha Sarathi Addy, Dr. Avik Kumar Pati, Dr. Pritam Jana, Dr. Satyajit Patra are respected for their cooperation during my PhD Programme. I am also delightful to thank Dr. Hemant Joshi, Dr. Kiran Bajaj for their inspirational support during my research work. My special thanks to Mrs. Pusplata Ji, Mr. Suresh Ji and Mr. Nandalal Ji for making available for me some general required chemical and allowing me to use few laboratory equipment over the years and also necessary help during the graduate and postgraduate student's class when I was the instructor.

I wish to acknowledge Prof. R. Krishnan from Department of Chemistry, BITS Pilani, Hyderabad Campus for providing us single X-ray crystal analysis.

My special thanks to Prof. Mahiuddin Badiya (IIT Madras), Prof. S. P. Rath (IIT Kanpur) and Dr. Chandī Malakar (NIT Manipur) for their invaluable guidance, support, and encouragement during my internship period. They have been an outstanding role model, providing me with the opportunity to learn and develop a basic research background.

My special thanks to former members of my lab colleague Dr. Kasiviswanadharaju Pericherla, Dr. Pinku, Dr. Poonam for their achievement and inspiration to my professional life at BITS

Pilani. I also like to show my sincere thanks to Dr. Santosh Khandagale, Dr. Manish Kumar, Dr. Vishal, Dr. Vaishali Saini, Dr. Vimal, Dr. Moyna Das, Dr. Chavvi, Dr. Mamta Devi Sharma, Dr. Jagriti for their moral support during my practical work.

I extend my warm thank to dozens of remarkable friends belonging from Chemistry Department, Dr. Amol Pawar, Dr. Jyothi, Dr. Bintu Kumar, Ms. Aishwarya, Ms. Prachi, Dr. Dhritabrata, for their continuous direct or indirect support in my research work. I am also thanking to my departmental colleagues Mr. Santosh Mishra, Mr. Pramod, Mr. Sumit, Dr. Mahesha, Ms. Soumona, Ms. Gurpreet. Ms. Divya, Ms. Pragya, Ms. Payal, Ms. Nidhi, Mr. Ram Prasad Bhatta, Ms. Shivani, Ms. Vishakha, Ms. Anuvasita, Ms. Monika, Ms. Prakriti, Mr. Narsimha, Mr. Prakash, Ms. Heena, Mr. Bharat, Ms. Mamta Katewa, Mr. Narendra, Mr. Yadav, Ms, Sonika, Ms. Shilpa, Ms. Sakshi Jangir, Ms. Sakshi Bajaj, Mr. Ajeet Sheoran, Mr. Ajeet Singh, Ms. Aastha, Ms. Sushma, Ms. Nandani, Mr. Saurajit, Mr. Subhro, Mr. Somnath, Ms. Manisha, Mr. Imtiyaz, Ms. Disha, Ms. Annu, Ms. Sushmita, Ms. Ritu, Ms. Khushika, Mr. Sumit, Mr. Atul, Ms Aarjoo, Ms Nidhi. I also thankful to all my pharmacy department (BITS, Pilani) friends for their help.

The congenial and inspiring atmosphere, coupled with the remarkable achievements made in Lab 3145, have left an indelible mark on my life. I am immensely proud and grateful to express my heartfelt thanks to my labmates, Dr. Om Prakash Patel, Dr. Hitesh Kumar Saini, Dr. Khima Pandey, Dr. Saroj Budania, Dr. Shiv Dhiman, Dr. Vikki Shinde, Ms. Neha Meena, Mr. Dhanajay Nipate, Ms. Bhawani, Mr. Prakash Swami, Mr. Amol Gadekar, and Ms. Diksha Rohilla, for their love and support. I thank each one of you individually for your cooperation, caring, and company, which made my Ph.D. journey more comfortable at BITS Pilani. I also extend my gratitude to graduate students, Mr. Aniket Kulkarni, Mr. Shivanshu, Mr. Raghav, and Ms. Radhika, for their patience and support during our interactions.

I am extremely thankful to Dr. Hemant Joshi for his guidance and motivation throughout my Ph.D., which helped me to apply for a Postdoctoral Research Associate position and work smartly towards my goals. His valuable suggestions and help are truly appreciated.

My thesis would be incomplete without acknowledging the invaluable contributions of my friends, Ms. Divya Saini, Dr. Aashna Nagar, Dr. Divya Susan Koshy, Dr. Khyati Anand, and Ms.

Nidhi, for their continuous and unwavering support during my Ph.D. years. Their presence made my life more vibrant and meaningful, and I am forever grateful.

I owe a special debt of gratitude to Mr. Vikki Shinde for his unwavering moral support during my hard times, which motivated me to reach my destination. His belief in me never faltered, even when I doubted myself. His valuable suggestions and help will remain unforgettable throughout my life.

I am deeply grateful to my parents, Mr. Raj Karan Jaspal and Mrs. Kiran Bala, for their unwavering love, endless patience, and sacrifices they made to educate and prepare me to reach this milestone. Their presence has always been a source of comfort during stressful times. Words and this limited space cannot adequately express my gratitude to my parents. I owe everything I am today to them and my family's support. My heartfelt thanks to my wonderful siblings, Sagar Jaspal and Komal Jaspal, who celebrated my success as their own and provided me with immense pleasure and motivation over the years. They have always been there for me, offering guidance, providing a listening ear, and helping me through difficult times. Their unwavering faith in me helped me overcome obstacles and strive for success. I am truly blessed to have such loving siblings, and I could not have reached this point without them.

I would like to express my sincere gratitude to my teachers from school, college, and post-graduation who supported me directly or indirectly in reaching this level of achievement.

Lastly, I would like to extend my thanks to my well-wishers, including teachers, relatives, and friends, whose faith, encouragement, and constant moral support contributed significantly to the completion of this work. I am deeply grateful to all of them.

Finally, I humbly bow my head to the Almighty, who gave me the strength to work hard and overcome challenging situations.

SONAM

ABSTRACT

Nitrogen containing heterocycles have a wide range of applications in various fields of science such as medicine, pharmaceuticals, and material chemistry. The synthesis and functionalization of these heterocycles through inert C-H bond activation has attracted the attention of synthetic organic chemists. The thesis titled “**C-H Bond Functionalization of Selected Azaheterocycles under Metal-Free and Photochemical Conditions**” aims to develop new synthetic methodologies for the direct functionalization of biologically active nitrogen containing heterocycles. The thesis is divided into five chapters.

The first chapter of the thesis gives a brief introduction of transition-metal-free reactions and iodine(III) reagents. The commercially available I(III) reagent, PIDA was utilized for the [1,2]-*ipso*-migration in Mannich bases derived from imidazo[1,2-*a*]pyridines for the preparation of 3-aminoimidazo[1,2-*a*]pyridine derivatives which were easily transformed to the corresponding 2-aryl-*N*-(pyridin-2-yl)imidazo[1,2-*a*]pyridin-3-amines by treating with NaHCO₃ in methanol. The reaction is believed to proceed through [1,2]-*ipso*-heteroaryl migration *via* formation of a Wheland-type aziridine intermediate followed by nucleophile-assisted ring opening reaction and thereby forming a series of forty-one compounds in moderate to good yields.

The second chapter of the thesis focuses on the development of a new synthetic methodology for regioselective benzylation of imidazoheterocycles using arylglyoxylic acids as a benzoyl source. The reaction was achieved without the need for metal- or photocatalysts, instead utilizing K₂S₂O₈ as the oxidant. The reaction was shown to produce good yields and tolerate a wide range of functional groups, making it a versatile tool for the synthesis of 5-arylimidazo[1,2-*a*]pyridines. Control experiments suggested that the reaction proceeds *via* radical pathway. Importantly, the protocol is amenable for scale-up, and the mild reaction conditions make it a promising approach for the synthesis of a variety of biologically active compounds under metal-free conditions.

The third chapter of the thesis describes a highly selective difluoroalkoxylation of imidazo[1,2-*a*]pyridines under visible-light irradiation. The developed protocol has high functional group tolerance and is compatible with a wide range of alcohols (1° and 2°) without any electronic and steric constraints. This sustainable and environmentally benign reaction provides moderate to

excellent yields of difluoroalkoxylated products. Control experiments suggested that the reaction proceeds *via* radical pathway. The salient features of this protocol include broad substrate scope, sustainable source of energy, and mild reaction conditions. Additionally, the post-functionalization of Zolimidine, a gastroprotective drug, under the standard conditions demonstrates the potential utility of this method in pharmaceutical synthesis.

The fourth chapter of the thesis describes the TEMPO-mediated cross-dehydrogenative coupling of C(sp³-H) bond and C(sp²-H) bond for direct hydroxyfluoroalkylation of indoles and imidazo[1,2-*a*]pyridines by fluorinated alcohols. The developed synthetic protocol is operationally simple and provides a wide range of C3-hydroxyfluoroalkylated indoles and imidazo[1,2-*a*]pyridines in good to excellent yields. The synthetic utility of the protocol was showcased through gram-scale synthesis of the target products. Mechanistic investigation revealed that the reaction involves a radical process.

The fifth chapter of the thesis describes a developed synthetic strategy for the regioselective decoration of quinoxalin-2(1*H*)-ones with alkoxy, alkylthio, alkylamino, and arylseleno groups at the C3 position under metal- and photocatalyst-free conditions. The method offers a broad substrate scope, including bioactive molecules, and provides mild reaction conditions, readily available coupling partners, high yields, scalability, step-economy, and environmentally benign conditions. The protocol's synthetic utility was demonstrated through gram-scale synthesis and C3-alkoxylation of quinoxalin-2(1*H*)-one with natural alcohols, and the synthesis of aldose reductase (ALR2) inhibitor in excellent yields. Control experiments support a radical pathway for the reaction.

Finally, in the **sixth chapter** of the thesis, summary of the thesis work is presented along with the future scope of the research work.

TABLE OF CONTENTS

	Page No	
Certificate	I	
Dedication	II	
Acknowledgements	III	
Abstract	VII	
Table of contents	IX	
List of tables	XIV	
List of figures	XVI	
List of abbreviations	XX	
Chapter 1: PIDA-Mediated Synthesis of 3-Aminoimidazo[1,2- <i>a</i>]pyridine Derivatives		
1.1	Introduction	1
1.1.1	Transition metal-catalyzed reaction	1
1.1.2	Transition-metal-free reactions	3
1.1.3	Chemistry of hypervalent-iodine reagents	4
1.2	Results and discussion	11
1.3	Conclusions	22
1.4	Experimental section	23
1.4.1	General information	23
1.4.2	Experimental procedure for the preparation of acetoxy	23

	products or hemiaminals	
1.4.3	Experimental procedure for the preparation of alkoxy product	29
1.4.4	Experimental procedure for the preparation of 2-phenyl- <i>N</i> -(pyridin-2-yl)imidazo[1,2- <i>a</i>]pyridin-3-amine	36
1.4.5	X-ray crystallographic analysis of compounds 45a, 47aa and 49a	33
1.5	References	39

Chapter 2: C5-Aroylation of Imidazoheterocycles by Oxidative Decarboxylation of Arylglyoxylic Acids

2.1	Introduction	47
2.1.1	Minisci reaction	47
2.2	Results and discussion	53
2.3	Conclusions	62
2.4	Experimental section	62
2.4.1	General materials and methods	62
2.4.2	Experimental procedure for the preparation of benzoylated products	70
2.4.3	Experimental procedure for the synthesis of compound 48	75
2.4.4	X-ray crystallographic data of compound 46aa	76
2.5	References	77

Chapter 3: Visible-Light Driven Regioselective Difluoroalkoxylation of Imidazo[1,2-*a*]pyridines using *N*-Fluorobenzenesulfonimide

3.1	Introduction	81
3.2	Results and discussion	87
3.3	Conclusions	96
3.4	Experimental section	96
3.4.1	General information	96
3.4.2	General procedure for the difluoroalkoxylation of imidazo[1,2- <i>a</i>]pyridines	97
3.4.3	Analytical data of synthesized products	97
3.4.4	X-ray crystallographic analysis of 5ga and 5ai	112
3.5	References	112

Chapter 4: TEMPO-Mediated Cross-Dehydrogenative Coupling of Indoles and Imidazo[1,2-*a*]pyridines with Perfluorinated Alcohols

4.1	Introduction	116
4.2	Results and discussion	123
4.3	Conclusions	135
4.4	Experimental section	136
4.4.1	General information	136
4.4.2	General procedure for the C3-fluoroalkylation of indoles	136

4.4.3	Analytical data of synthesized products	136
4.4.4	General procedure for the C3-fluoroalkylation of imidazopyridines	146
4.4.5	General Procedure for the Synthesis of 27 and 28	153
4.4.6	X-ray crystallographic analysis of 3ba, 3fa, 25aa and 25ba	155
4.5	References	157

Chapter 5: Selectfluor Mediated Regioselective C3-Alkoxylation, Sulfenylation, Amination and Selenylation of Quinoxalin-2(1*H*)-ones

5.1	Introduction	160
5.2	Results and discussion	168
5.3	Conclusions	178
5.4	Experimental section	179
5.4.1	General information	179
5.4.2	General procedure for the synthesis of quinoxalin-2(1 <i>H</i>)-ones	180
5.4.3	General Procedure for the C3-sulfenylation of quinoxalin-2(1 <i>H</i>)-ones)	192
5.4.4	General procedure for the C3-amination of quinoxalin-2(1 <i>H</i>)-ones)	195
5.4.5	General procedure for the C3-selenylation of quinoxalin-2(1 <i>H</i>)-ones)	199

5.4.7	Experimental procedure for the synthesis of 16	200
5.4.8	Experimental procedure for the synthesis of 17	201
5.4.9	Experimental procedure for the synthesis of 18	201
5.4.10	Procedure for radical trapping experiment	202
5.4.11	X-ray crystallographic analysis of compound 5aa, 5ca, 9da and 9ia	202
5.5	References	204

Chapter 6: Conclusions

5.1	General conclusions	208
5.2	Future scope of the research work	212

Appendices

List of publications	A-1
Snapshots of the published articles	A-2
List of conferences attended	A-3
Brief Biography of the candidate	A-4
Brief Biography of the supervisor	A-5

LIST OF TABLES

No	Title	Page No
1.1	Optimization of reaction conditions	14
1.2	Substrate scope for acetoxyated derivatives	15
1.3	Substrate scope for alkoxyated derivatives	18
1.4	Substrate scope for mannich bases derived from arylamines	19
1.5	Crystal data and structure refinement for 45a , 47aa and 49a	38
2.1	Optimization of the reaction condition for 46aa	54
2.2	Substrate scope for benzylation of imidazoheterocycles	59
2.3	Crystal data and structure refinement for 46aa	71
3.1	Optimization of the reaction condition for 5aa	81
3.2	Scope and versatility of imidazo[1,2- <i>a</i>]pyridines	84
3.3	Scope and versatility of alcohols	86
3.4	Crystal data and structure refinement for 5ga and 5ai	103
4.1	Optimization of reaction conditions for 3aa	114
4.2	Hydroxyfluoroalkylation of indoles	117
4.3	Hydroxyfluoroalkylation of imidazo[1,2- <i>a</i>]pyridines	122
4.4	Crystal data and structure refinement for 3ba and 3fa	142
4.5	Crystal data and structure refinement for 25aa and 25ba	143
5.1	Optimization of reaction conditions for 3aa	156

5.2	Alkoxylation of quinoxalin-2(1 <i>H</i>)-ones	158
5.3	Fluoroalkoxylation of quinoxalin-2(1 <i>H</i>)-ones	160
5.4	Thioalkoxylation of quinoxalin-2(1 <i>H</i>)-ones	161
5.5	Amination of quinoxalin-2(1 <i>H</i>)-ones	162
5.6	Selenylation of quinoxalin-2(1 <i>H</i>)-ones	163
5.7	Crystal data and structure refinement for 5aa and 5ca	190
5.8	Crystal data and structure refinement for 9da and 9ia	191

LIST OF FIGURES

Figure No.	Caption	Page No
1.1	Some commercially available bioactive N-heterocyclic compounds	1
1.2	Types of transition-metal catalyzed C-H functionalization	3
1.3	General representation of transition-metal free C-H functionalization	3
1.4	Commonly used organohypervalent iodine compounds	5
1.5	Shape and geometry of trivalent iodanes (RIX ₂)	5
1.6	¹ H NMR spectrum of ((2-phenylimidazo[1,2- <i>a</i>]pyridin-3-yl)(pyridin-2-yl)amino)methyl acetate (45a) recorded in CDCl ₃	11
1.7	¹³ C{ ¹ H} NMR spectrum of ((2-phenylimidazo[1,2- <i>a</i>]pyridin-3-yl)(pyridin-2-yl)amino)methyl acetate (45a) recorded in CDCl ₃	12
1.8	DEPT-135 NMR spectra of ((2-phenylimidazo[1,2- <i>a</i>]pyridin-3-yl)(pyridin-2-yl)amino)methyl acetate (45a) recorded in CDCl ₃	12
1.9	LC-HRMS of ((2-phenylimidazo[1,2- <i>a</i>]pyridin-3-yl)(pyridin-2-yl)amino)methyl acetate 45a	13
1.10	ORTEP diagram of 45a (CCDC No 1957417). The thermal ellipsoids are drawn at 50% probability level	13
1.11	¹ H NMR spectrum of <i>N</i> -(methoxymethyl)-2-phenyl- <i>N</i> -(pyridin-2-yl)imidazo [1,2- <i>a</i>]pyridin-3-amine (47aa) recorded in CDCl ₃	16
1.12	¹³ C{ ¹ H} NMR spectrum of <i>N</i> -(methoxymethyl)-2-phenyl- <i>N</i> -(pyridin-2-yl)imidazo [1,2- <i>a</i>]pyridin-3-amine (47aa) recorded in CDCl ₃	16
1.13	LC-HRMS spectrum of <i>N</i> -(methoxymethyl)-2-phenyl- <i>N</i> -(pyridin-2-yl)imidazo [1,2- <i>a</i>]pyridin-3-amine (47aa)	17
1.14	ORTEP diagram of 47aa (CCDC No 1913162). The thermal ellipsoids are drawn at 50% probability level	17
1.15	ORTEP diagram of 49a (CCDC No 1913162). The thermal ellipsoids are drawn at 50% probability level.	20
2.1	Generalized mechanism of Minisci-type reactions	45

2.2	Array of radical precursors used for Minisci-type reaction	46
2.3	Some commercially accessible drugs containing imidazopyridine skeleton	51
2.4	¹ H NMR spectrum of phenyl(2-phenylimidazo[1,2- <i>a</i>]pyridin-5-yl)methanone 46aa recorded in CDCl ₃	56
2.5	¹³ C{ ¹ H} NMR spectrum of phenyl(2-phenylimidazo[1,2- <i>a</i>]pyridin-5-yl)methanone 46aa recorded in CDCl ₃	56
2.6	NOE spectra of phenyl(2-phenylimidazo[1,2- <i>a</i>]pyridin-5-yl)methanone 46aa recorded in CDCl ₃	57
2.7	HRMS spectrum of phenyl(2-phenylimidazo[1,2- <i>a</i>]pyridin-5-yl)methanone 46aa	58
2.8	ORTEP diagram of 46aa (CCDC No 1978834). The thermal ellipsoids are drawn at 50% probability level.	58
3.1	Organofluorine compounds in pharmaceuticals, agrochemicals and polymer	75
3.2	Examples of fluorinating reagents	76
3.3	¹ H NMR spectrum of 3,3-difluoro-2-methoxy-2-phenyl-2,3-dihydroimidazo[1,2- <i>a</i>]pyridine (5aa) recorded in CDCl ₃	82
3.4	¹³ C{ ¹ H} NMR spectrum of 3,3-difluoro-2-methoxy-2-phenyl-2,3-dihydroimidazo [1,2- <i>a</i>]pyridine (5aa) recorded in CDCl ₃	82
3.5	¹⁹ F NMR spectrum of 3,3-difluoro-2-methoxy-2-phenyl-2,3-dihydroimidazo[1,2- <i>a</i>]pyridine (5aa) recorded in CDCl ₃	83
3.6	HRMS spectrum of phenyl(2-phenylimidazo[1,2- <i>a</i>]pyridin-5-yl)methanone 5aa	83
3.7	ORTEP diagram of 5ga (CCDC 2244256). The thermal ellipsoids are drawn at 50% probability level.	85
3.8	ORTEP diagram of 5ai (CCDC 2244257). The thermal ellipsoids are drawn at 50% probability level.	86
4.1	Bioactive C3-substituted indole and imidazopyridine molecules	107
4.2	¹ H NMR of 2,2,2-trifluoro-1-(2-phenyl-1 <i>H</i> -indol-3-yl)ethan-1-ol (3aa) recorded in CDCl ₃	115

4.3	¹³ C{ ¹ H} NMR of 2,2,2-trifluoro-1-(2-phenyl-1 <i>H</i> -indol-3-yl)ethan-1-ol (3aa) recorded in CDCl ₃	115
4.4	¹⁹ F NMR of 2,2,2-trifluoro-1-(2-phenyl-1 <i>H</i> -indol-3-yl)ethan-1-ol (3aa) recorded in CDCl ₃	116
4.5	HRMS of 2,2,2-trifluoro-1-(2-phenyl-1 <i>H</i> -indol-3-yl)ethan-1-ol (3aa)	116
4.6	ORTEP diagram of 3ba (CCDC No 2033964). The thermal ellipsoids are drawn at 50% probability level	118
4.7	ORTEP diagram of 3fa (CCDC No 2033965). The thermal ellipsoids are drawn at 50% probability level	118
4.8	¹ H NMR spectrum of 2,2,2-trifluoro-1-(2-phenylimidazo[1,2- <i>a</i>]pyridin-3-yl)ethan-1-ol (25aa) recorded in DMSO- <i>d</i> ₆	119
4.9	¹³ C{ ¹ H} NMR spectrum of 2,2,2-trifluoro-1-(2-phenylimidazo[1,2- <i>a</i>]pyridin-3-yl)ethan-1-ol (25aa) recorded in DMSO- <i>d</i> ₆	119
4.10	¹⁹ F NMR spectrum of 2,2,2-trifluoro-1-(2-phenylimidazo[1,2- <i>a</i>]pyridin-3-yl)ethan-1-ol (25aa) recorded in DMSO- <i>d</i> ₆	120
4.11	HRMS of 2,2,2-trifluoro-1-(2-phenylimidazo[1,2- <i>a</i>]pyridin-3-yl)ethan-1-ol (25aa)	120
4.12	ORTEP diagram of 45aa (CCDC No 2033967). The thermal ellipsoids are drawn at 50% probability level	121
4.13	ORTEP diagram of 45ba (CCDC No 2033968). The thermal ellipsoids are drawn at 50% probability level	122
5.1	Biologically active C3-substituted quinoxalin-2(1 <i>H</i>)-ones	147
5.2	C3-Functionalization of quinoxalin-2(1 <i>H</i>)-ones	148
5.3	¹ H NMR spectrum of 3-ethoxyquinoxalin-2(1 <i>H</i>)-one (3aa) recorded in CDCl ₃	157
5.4	¹³ C{ ¹ H} NMR of 3-ethoxyquinoxalin-2(1 <i>H</i>)-one (3aa) recorded in CDCl ₃	157
5.5	ORTEP diagram of 5aa (CCDC No 2178009). The thermal ellipsoids are drawn at 50% probability level	159
5.6	ORTEP diagram of 5ca (CCDC No 2178501). The thermal ellipsoids	160

- are drawn at 50% probability level
- 5.7 ORTEP diagram of **9da** (CCDC No 2206580). The thermal ellipsoids are drawn at 50% probability level 162
- 5.8 ORTEP diagram of **9ia** (CCDC No 2207035). The thermal ellipsoids are drawn at 50% probability level 163

LIST OF ABBREVIATIONS

Abbreviation	Description
AcOH	Acetic acid
acac	Acetylacetone
ADA	1-Adamantancarboxylic acid
Aq	Aqueous
Ar	Aryl
AIDS	Acquired immunodeficiency syndrome
BHT	Butylated hydroxy toluene
<i>t</i> -BuOK	Potassium <i>tert</i> -butoxide
<i>t</i> -BuONO	<i>tert</i> -Butyl nitrite
Cat.	Catalytic
¹³ C	Carbon-13
CH ₃ CN	Acetonitrile
CDCl ₃	Deuterated chloroform
<i>m</i> -CPBA	<i>meta</i> -Chloroperoxybenzoic acid
CDC	Cross-dehydrogenative coupling
CAN	Ceric ammonium nitrate
<i>p</i> -Cymene	1-Methyl-4-(propan-2-yl)benzene
DMAP	4-Dimethylaminopyridine
d	Doublet
DBU	1,8-Diazabicyclo[5.4.0]undec-7-ene
dd	Doublet of doublet
DCE	1,2-Dichloroethane
DCM	Dichloromethane

DMA	<i>N,N</i> -Dimethylacetamide
DME	Dimethoxyethane
DMF	<i>N,N</i> -Dimethylformamide
DMSO- <i>d</i> ₆	Deuterated dimethylsulfoxide
DMSO	Dimethylsulfoxide
DMAc	Dimethylacetamide
DMAP	4-Dimethylaminopyridine
DDQ	2,3-Dichloro-5,6-dicyano-1,4-benzoquinone
dppf	1,1'-Bis(diphenylphosphino)ferrocene
EDC.HCl	1-Ethyl-3-(3-dimethylaminopropyl)carbodiimide
EI	Electron Ionization
ESI	Electron Spray Ionization (MS)
EtOAc	Ethyl acetate
equiv.	Equivalent
ESI-MS	Electrospray ionization mass spectrometry
EtOH	Ethanol
FID	Free induction decay
FT-IR	Fourier transform infrared
g	Gram
h	Hours
HFIP	1,1,1,3,3,3-Hexafluoro-2-propanol
HRMS	High Resolution Mass Spectra
Hz	Hertz

HOMO	Highest occupied molecular orbital
IR	Infra-red
IPA	Isopropanol
IBD	Iodobenzene diacetate
IOC	Intramolecular oxidative coupling
IP	Imidazo[1,2- <i>a</i>]pyridines
<i>J</i>	Coupling constant
KOAc	Potassium acetate
KIE	Kinetic isotope effect
Lit.	Literature
LUMO	Lowest unoccupied molecular orbital
mp	Melting point
<i>m</i>	Multiplet
mg	Milligram
MHz	Mega hertz
min	Minutes
mmol	Millimole
MW	Microwave
nm	Nanometer
N ₂	Nitrogen
DIPEA	N,N-Diisopropylethylamine
Nu	Nucleophile
NMR	Nuclear Magnetic Resonance

NBS	<i>N</i> -Bromosuccinimide
NCS	<i>N</i> -Chlorosuccinimide
NIS	<i>N</i> -Iodosuccinimide
NMP	<i>N</i> -Methyl-2-pyrrolidone
O ₂	Oxygen
OTf	Trifluoromethanesulfonate
OLEDs	Organic light-emitting diode
PEG400	Polyethylene glycol 400
PIDA	Phenyl iodine (III) diacetate
1,10-Phen	1,10-Phenanthroline
PivOH	Pivalic acid
PhCl	Chlorobenzene
ppm	Parts per million
r.t.	Room temperature
s	Singlet
SET	Single electron transfer
<i>S_EAr</i>	Friedel crafts types electrophilic aromatic substitution
TFA	Trifluoroacetic acid
TFE	2,2,2-Trifluoroethanol
TEA	Triethyl amine
t	Triplet
TMDEA	Tetramethylethylenediamine

TBAB	Tetrabutylammonium bromide
TBHP	<i>tert</i> -Butyl hydroperoxide
THF	Tetrahydrofuran
TEMPO	2,2,6,6-Tetramethyl-1-piperidinyloxy, free radical
<i>p</i> -TSA or <i>p</i> -TsOH	<i>p</i> -Toluenesulfonic acid
qTOF	Quadrupole time-of-flight
TLC	Thin layer chromatography
TfOH	Trifluoromethanesulfonic acid
TFAA	Trifluoroacetic anhydride
TMS	Tetramethylsilane
TMSCl	Trimethylsilyl chloride
TD-DFT	Time dependent density functional theory
UV	Ultraviolet-visible

CHAPTER 1

PIDA-Mediated Synthesis of 3-Aminoimidazo[1,2-*a*]pyridine Derivatives

1.1 INTRODUCTION

Heterocyclic chemistry constitutes one of the major and esteemed branches of organic compounds, due to the widespread role of heterocyclic compounds in the natural product synthesis,¹ pharmaceutical industry,² and material chemistry.³ Especially, nitrogen containing heterocycles are part of many important bioactive molecules and exhibits interesting pharmacological properties such as anti-microbial,⁴⁻⁵ anti-spasmodics,⁶ anti-viral,⁷ tubulin inhibitor,⁸ anti-tumor,⁹ anti-infective,¹⁰ anxiolytic agent,¹¹ gastroprotective agent¹² and hypnotics¹³ (**Figure 1.1**). Moreover, their strong DNA intercalating property makes them suitable candidates as anti-neoplastic and mutagenic agents.¹⁴⁻¹⁶ Over the last two decades, considerable efforts have been devoted by researchers for developing simple, efficient and straightforward strategies for the synthesis and functionalization of nitrogen heterocycles.¹⁷⁻¹⁹

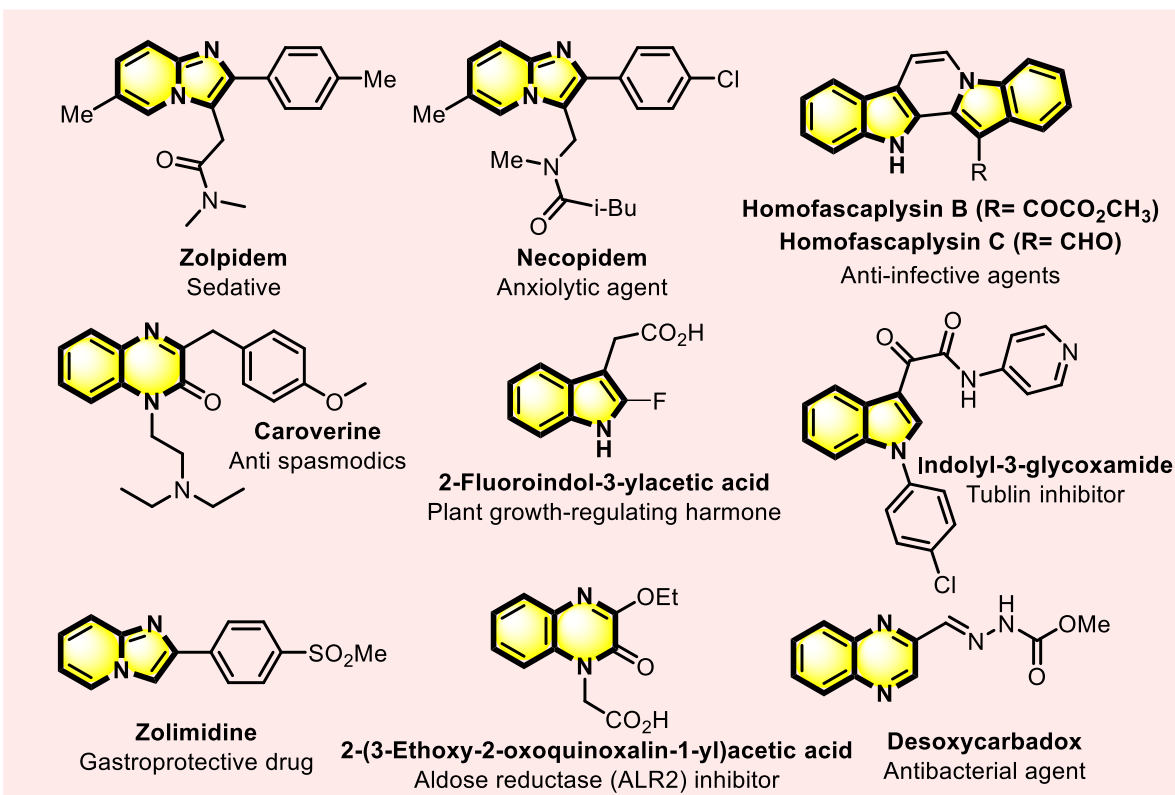


Figure 1.1 Selected commercially available bioactive N-heterocyclic compounds

1.1.1 Transition-metal catalyzed reactions

The development of innovative protocols that either involve the advanced or novel process to construct complex molecules or improve the green aspects, like atom- and step-economy of existing methods, is the perpetual aim of synthetic chemists. In this regard, transition-metal catalyzed C-H activation has emerged as one of the most proficient and continuously growing approaches over the past century and has affected the industries like environmental protection fine chemicals, food processing and energy processing. The direct construction of C-X (X = C or heteroatom) bonds from unactivated C-H bonds truncate the unnecessary requirement of prefunctionalized starting materials and therefore, turn-up into a more economic and straightforward strategy in comparison to traditional cross-coupling reactions (**Figure 1.2**). Delightedly in 2010, the remarkable successes and contributions made *via* transition-metal catalyzed reactions were honored by the Noble Prize in chemistry. A classical synthetic mechanism generally involves the metal or metal salts as catalysts to activate the inert C-H bond *via* oxidative addition which followed by pi-insertion and reductive elimination affords the desired product. Nevertheless, several challenges perceived in catalytic C-H functionalization reactions have restricted their widespread applicability or practicality to some extent. As a first point, most of the transition-metal catalysts are generally very expensive, and usually requires the assistance of auxiliary ligands, which can be even more expensive and sometimes follows laborious synthetic protocols.²⁰⁻²¹ Secondly, air and moisture sensitivity of most of the transition-metal catalysts limits their use only under precise conditions.²² Third issue deals with the varying degrees of toxicity in most of the transition-metal catalysts.²³ Also, contributing to health problems exclusion of even the trace amount of these transition-metal residues from desired products is not only challenging and expensive but also imperative, especially in pharmaceuticals.²⁴⁻²⁵ Next, the requirement of cocatalysts and additives for the promotion in reactivity and selectivity is also a critical and inevitable step in such reactions.²⁶ Last but not the least is low catalyst turnover in transition-metal catalyzed C-H functionalization, which is a big concern for the reactions which involves C-H activation step.²⁷ As a matter of fact, excessive employment of transition-metal catalysts is not consistent with sustainable development.²⁰ Obviously, for direct formation of carbon-heteroatom bond an alternative pathway under transition-metal-free conditions is highly appealing which not only accomplish traditional metal catalyzed route but also

overcome the inadequacies of such transformations. Owing to the rapid development in the research methodologies, synthetic chemists always sought to find out an easy alternate route for direct C-X bond formation. In this regard, researchers are focusing on the gradual shift towards the transition-metal-free chemistry that has been receiving a substantial attention for the past few decades.

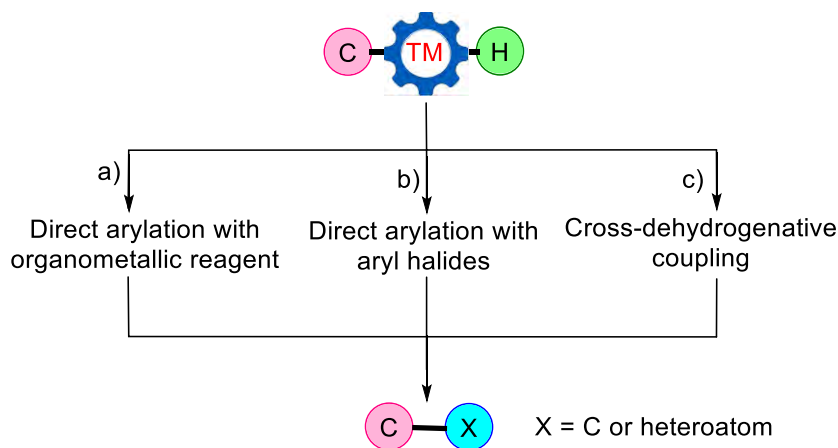


Figure 1.2 Types of transition-metal catalyzed C-H functionalization

1.1.2 Transition-metal-free reactions

Unlike metal-based catalysis, metal-free protocols have been globally adopted due to their greater sustainability,²⁸ cost-effectiveness²⁹ and durability.³⁰ In addition, such methodologies include utilization of less toxic compounds, which makes them more suitable for long-term usage. In the context of green chemistry, the development of new synthetic protocols that deliver high atom-economy, reduce chemical waste generation, and compatible with environment are highly desirable. This can be very well accomplished using transition-metal-free C-H functionalization, as this approach provides a combination of easily handleable reagents along with the eco-friendly reaction medium.³¹ Despite making significant efforts for the advancement of transition-metal-free reactions and paying attention to their promotion, this field still lacks basic knowledge and systematic exploration. The reason being the unavoidable utilization of transition-metal catalyst for the synthesis of substrates and difficulty to root-out the transition-metal residues from the reaction medium. A trace amount of transition-metals remaining in the reaction system will fundamentally influence the exact reaction pathway in some cases, thus making it difficult to classify the corresponding reactions. So far, the term is used to define the reactions

which may produce similar results as those of transition-metal catalyzed reactions, without employing transition-metal catalysts (**Figure 1.3**). Due to the simplicity of transition-metal-free approach and its application in synthesis and functionalization of biologically active molecules, pharmaceuticals, and natural products, this area has been emerged as a hot topic for researchers.

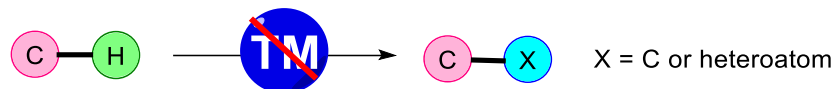


Figure 1.3 General representation of transition-metal-free C-H functionalization

Proven mechanistic pathways for transition-metal-free protocol includes: 1) Radical pathway, during these processes a radical species is added to the radical acceptor substrate to create a σ -complex which undergoes SET followed by loss of proton, or elimination of the leaving group for the formation of product. 2) Hypervalent iodine pathway, similar to radical processes hypervalent iodine reagent follows two types of mechanistic pathway with nucleophiles, *viz.* electrophilic oxidation pathway and radical pathway. In electrophilic oxidation type reactions (i) ligand exchange, (ii) reductive elimination, and (iii) ligand coupling is the typical reactivity pattern whereas, in radical type reactions, single-electron transfer (SET) and homolytic reactions are commonly observed under appropriate conditions. 3) Substitution (electrophilic and nucleophilic) reactions, in such reactions the electrophiles and nucleophiles are respectively added to electron-rich and electron-deficient aromatic rings followed by rapid proton loss. 4) Aryne mechanism, one of the most electrophilic reactive intermediates is aryne intermediate, the reaction of which includes addition of nucleophile followed by attack of aryl anion intermediate to the electrophile. 5) Photoinduced reactions, the reactions in which energy are transferred to organic compounds *via* photochemical methods are photoinduced reactions. Such reactions are initiated by SET (single electron transfer) process in the presence of visible light and followed by the generation of ionic or radical intermediates which contribute to the product formation.

Transition-metal catalysts and/or transition-metal containing oxidants are key ingredients in many organic transformations. It is, however, possible to perform these reactions under metal-free conditions in the presence of some inorganic oxidants that mimic the role of transition-metal catalysts. Such oxidants exhibit distinctive characteristics that allow them to initiate as well as continue the reaction or alter its course resulting in different outcome. Hypervalent-

iodine reagents are one class of such oxidants, which have emerged as an alternative tool to transition-metal catalysts in modern synthetic chemistry.

1.1.3 Chemistry of hypervalent-iodine reagents

Iodine being one of the most heavy and large elements in the periodic table, forms anomalous three-center-four-electron ($3c-4e^-$) bond by the overlapping of 5p orbitals rather than the regular interatomic π -overlapping of lighter group-17 elements. Such $3c-4e^-$ bonds are termed as hypervalent bonds as the compound bearing such bonds can form stable compounds even with higher oxidation states. Notably, the chemical reactivity patterns and the structural characteristics of polyvalent iodine compounds could be very well explained considering the low strength and highly polarized nature of these hypervalent bonds. Some commonly used organohypervalent iodine compounds are depicted in **Figure 1.4**. On the basis of oxidation states, commonly known polyvalent iodine compounds are classified as (i) trivalent iodine derivatives (λ^3 -iodanes) and, (ii) pentavalent iodine derivatives (λ^5 -iodanes). In iodine(III) compounds, the central iodine atom have 10 electrons with bipyramidal geometry in which the axial position is occupied by the more electronegative heteroatomic atom X whereas, the equatorial positions are occupied by the lone pairs of electron and less electronegative atom R. Pseudo trigonal bipyramidal geometry is observed in case of iodonium salts (**6**) where central iodine atom consists of 8 electrons along with the weakly bonded counter anion.

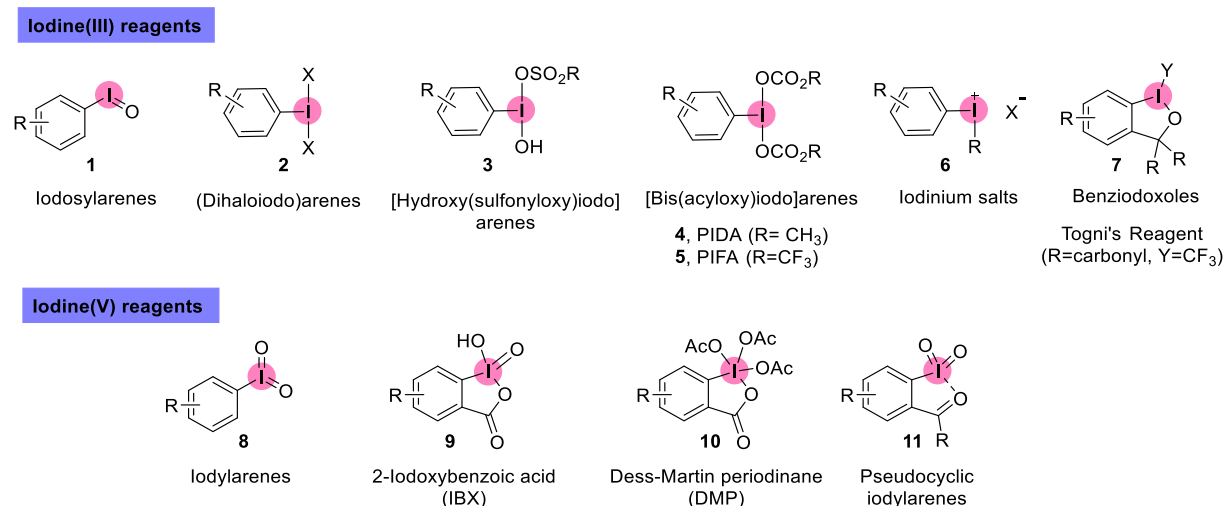
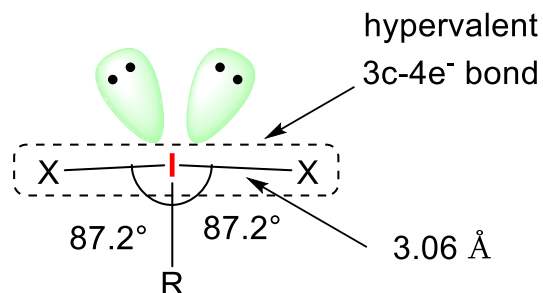


Figure 1.4 Commonly used organohypervalent iodine compounds

The shape of trivalent iodanes (RIX_2) is approximately T-shape where X–I–R bond angle is close to 90° and the linear X–I–X bond is formed by the pure p– π overlapping. On evaluation of the bond lengths in λ^3 -iodanes, the I–X bond is found to be longer than the normal I–X covalent bond length which not only makes the bond weaker and highly polarized but also justifies the high electrophilic character of such scaffolds (**Figure 1.5**).



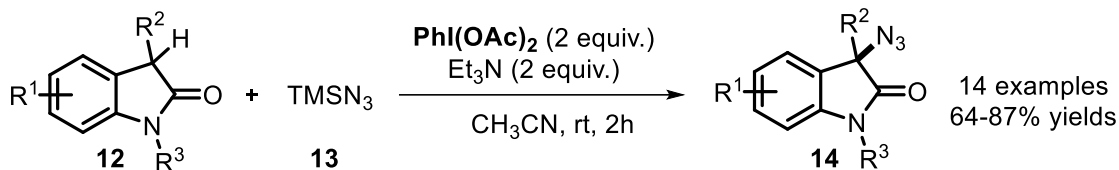
Geometry = pseudotrigonal bipyramidal
 Shape = T shape

Figure 1.5 Shape and geometry of trivalent iodanes (RIX_2)

These properties of hypervalent iodine compounds (especially, λ^3 -iodanes) allows them to find wide application in the field of synthetic chemistry.³² In general, such molecules provide their valuable contribution as electrophilic ligand transfer reagents and selective oxidants in many organic transformations which are classically performed using transition-metal chemistry. Most common synthetic processes performed by these reagents include oxidative C–H functionalization, rearrangements, stereoselective synthesis, SET processes, spirocyclization, heterocyclization, and numerous reactions resulting in the formation of new C–C, C–N and other C–heteroatom or heteroatom–heteroatom bonds.^{33–36} Not only this, there is a great interest in applying hypervalent iodine(III) reagents in the total synthesis of natural products due to their admirable efficiency, single-step conversion, low cost, and low toxicity as compared to heavy metals.³⁷ The escalating interest of researchers in the synthetic applications of such compounds is highlighted by the numerous book chapters and several comprehensive reviews.^{38–41}

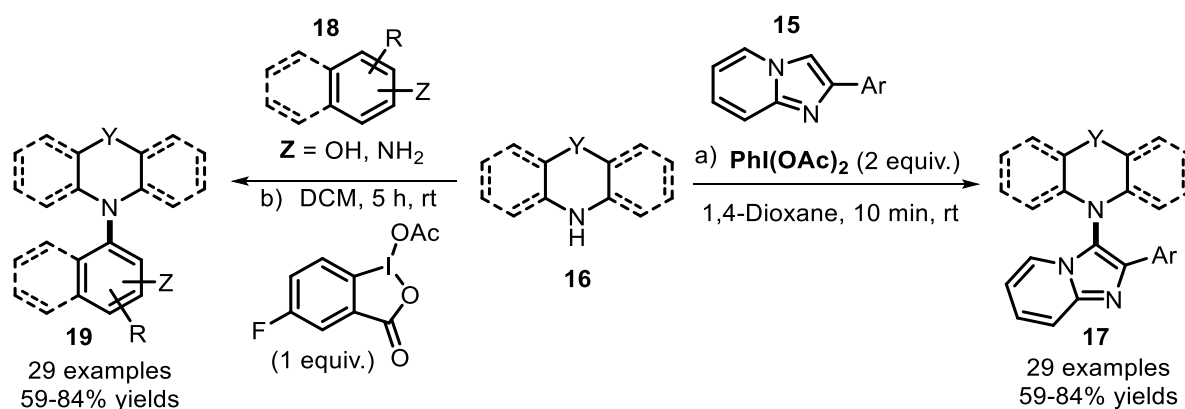
Wei group described a λ^3 -iodane mediated synthetic route for the azidation of 2-oxindoles (**12**). The structurally important 3-azido-2-oxindoles (**14**) were obtained using TMSN_3 (**13**) in the presence of PIDA as an oxidant, triethylamine as a base, and acetonitrile as solvent at room

temperature. The protocol provided a wide range of azide substituted oxindoles in good to excellent yields indicating the broad functional group tolerance along with large scale applicability (**Scheme 1.1**).⁴²



Scheme 1.1 PIDA-mediated azidation of oxindoles

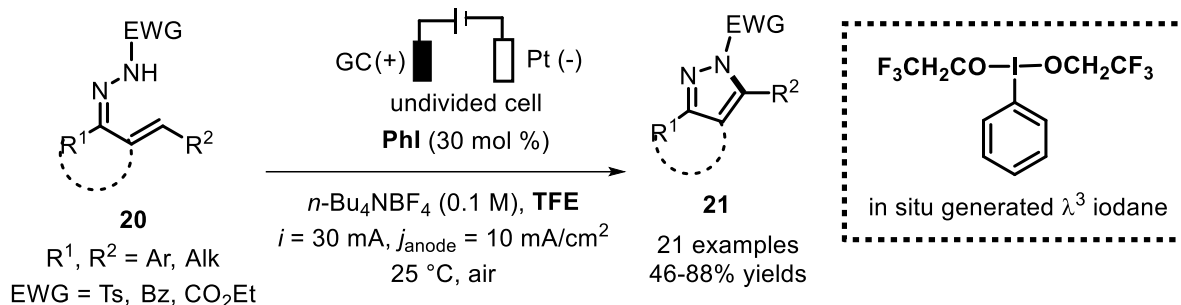
Hajra and his team showcased that imidazopyridines (**15**) could be oxidatively aminated using saturated azaheterocycles (**16**) in the presence of PIDA (**Scheme 1.2a**).⁴³ Various aliphatic nitrogen containing heterocycles such as piperidine, thiomorpholine, and morpholine were effectively tolerated by the reaction condition and thus, furnished a diverse library of aminated compounds (**17**) in moderate to good yields. Based on the preliminary tests, a radical pathway was proposed by the authors. Later, Kita group demonstrated the direct C-N coupling of phenothiazines (**16**) with nucleophiles (**18**) such as phenols and anilines in the presence of substituted benziodoxole as oxidizing agent to afford the selective *N*-arylphenothiazines (**19**) (**Scheme 1.2b**).⁴⁴



Scheme 1.2 λ^3 -iodane mediated intermolecular C-N cross-coupling of saturated azaheterocycle with various nucleophiles

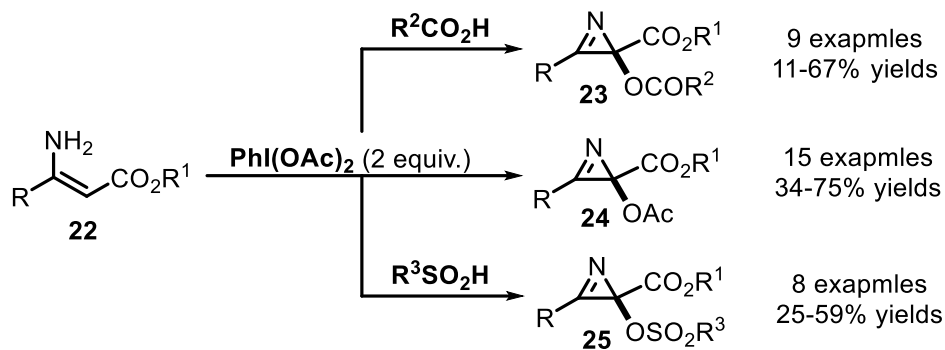
Paveliev *et al.* reported the hypervalent iodine (III) catalyzed intramolecular C-N coupling of α,β -unsaturated hydrazones (**20**) (**Scheme 1.3**).⁴⁵ Electrochemical treatment of substituted hydrazones in situ generated an active λ^3 -iodane *via* anodic oxidation aryl iodide in the presence of TFE, which eventually affords the substituted pyrazoles (**21**) in 46% - 88% yields. The key

role of *in-situ* constructed hypervalent iodine reagent in the newly formed C–N bond, was predicted through NMR and CV experiments.



Scheme 1.3 PIDA-mediated intramolecular C–N coupling of substituted hydrazones

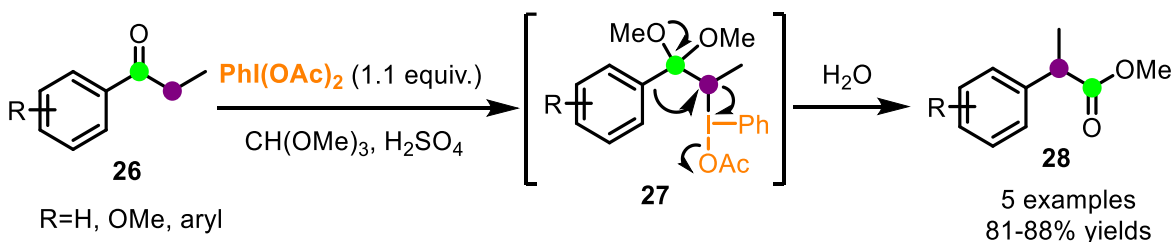
Tang and co-workers have developed a facile route for the functionalization of unsubstituted β -enamino esters (**22**). Substituted acyloxy-2*H*-azirine (**23**) and sulfonyloxy-2*H*-azirine (**25**) derivatives were efficiently synthesized in the presence of PIDA (2 equiv.) with carboxylic acids or sulfonic acids in moderate to good yields (Scheme 1.4).⁴⁶ Moreover, the control experiments predicted the formation of tosyloxy substituted β -enamino ester as an intermediate step, which is further cyclized to afford tosyloxy-2*H*-azirine. Acetyloxy 2*H*-azirine derivatives (**24**) could also be synthesized following the parallel pathway.



Scheme 1.4 PIDA-mediated oxidative acyloxylation, acetoxylation, and sulfonylation of β -enamino esters

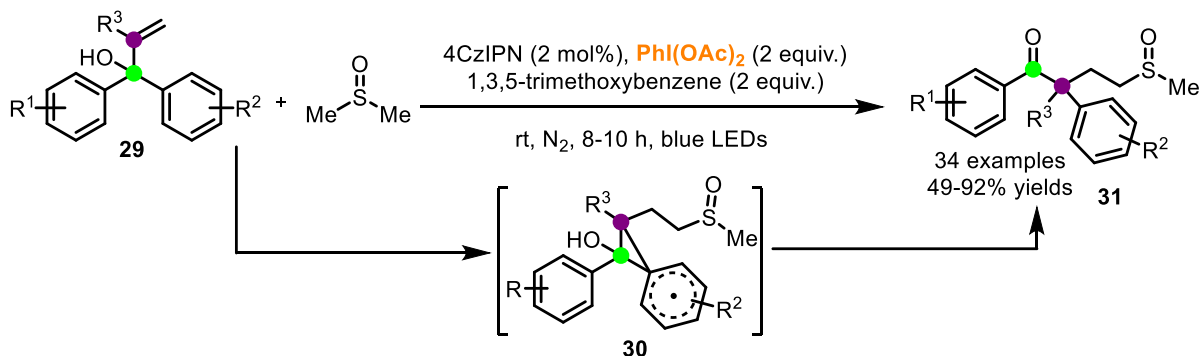
Hypervalent iodine reagents mediated rearrangement reactions are of great interest due to their prominent electrophilic nature that leads to the unique transformations.⁴⁷⁻⁵¹ A careful literature survey indicates that hypervalent iodine reagents can realize [1,2]-migration, [3,3]-sigmatropic/iodonium-Claisen rearrangement, ring contraction, ring expansion, Beckmann rearrangement, and Hofmann rearrangement. Over the past few years, a considerable upsurge is observed in the [1,2]-migratory rearrangement reactions mediated through hypervalent iodine reagents.

Among all, PIDA mediated [1,2]-carbon-to-carbon migration is very well investigated.⁵²⁻⁵⁷ In 1984 the Tamura group, for the first time reported the [1,2]-aryl migration reaction of aryl ethyl ketones (**26**) in the presence of $\text{PhI}(\text{OAc})_2$. The reaction was assumed to give an intermediate (**27**), which underwent [1,2]-aryl migration, followed by hydrolysis, to afford methyl 2-arylpropionate (**28**) as the desired products (**Scheme 1.5**).⁵⁸



Scheme 1.5 PIDA-mediated [1,2]-oxidative rearrangement reaction of propiophenones

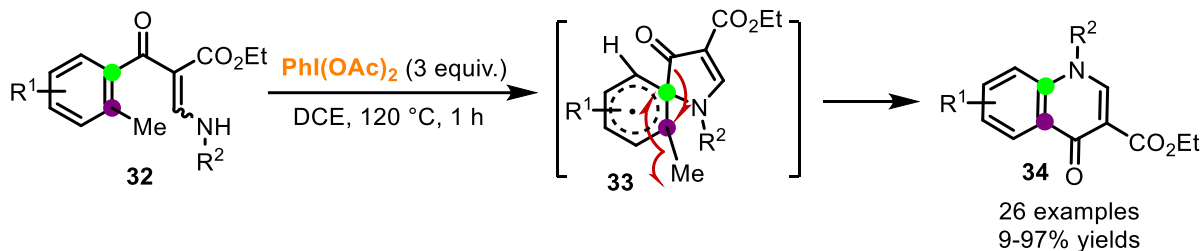
Cai *et al.* reported an efficient protocol for the development of a variety of α -aryl- γ -methylsulfinyl ketones (**31**) via oxidative [1,2]-alkylarylation of unactivated alkenes (**29**) with DMSO. The reaction is postulated to proceed through intermediate (**30**) with the collaborative interactions of $\text{PhI}(\text{OAc})_2$ with visible light irradiation and organic photosensitizer 4CzIPN under transition-metal-free conditions (**Scheme 1.6**).⁵⁹ Good to excellent yields of sulfinyl ketones, high regioselectivity, functional group compatibility and remarkable kinetic isotope effect are the promising features of the designed strategy.



Scheme 1.6 PIDA-mediated [1,2]-alkylarylation of unactivated alkenes and DMSO

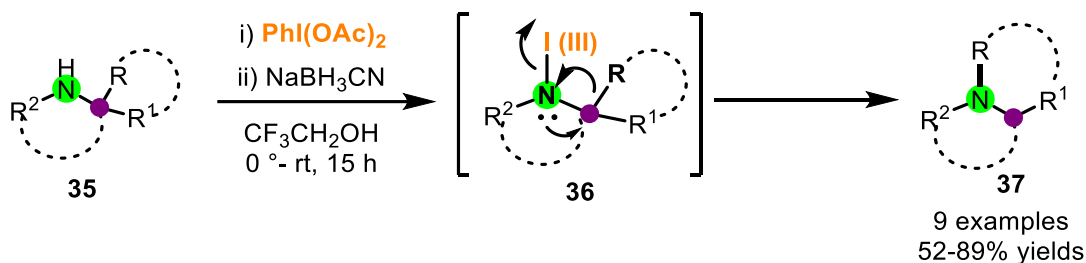
Song and co-workers reported $\text{PhI}(\text{OAc})_2$ -mediated radical cyclization followed by 1,2-carbonyl migration of β -aminoenones (**32**) for the synthesis of quinolones (**34**) via intermediate (**33**) (**Scheme 1.7**).⁶⁰ It appears attractive that the method follows selective cleavage of inert $\text{C}(\text{sp}^3)\text{-C}(\text{sp}^2)$ ortho to carbonyl carbon which overcomes the requirement to pre-functionalize the substrates. Notably, wide functional group tolerance, diverse substrate scope with excellent

selectivity and no metal additive made this strategy more concise to access pharmaceutically important 4-quinolone derivatives.



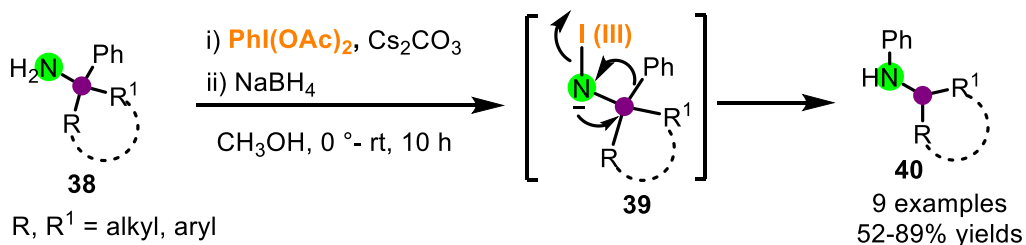
Scheme 1.7 PIDA-mediated [1,2]-oxidative rearrangement reaction of β -aminoenones

In 2018, Muarai group reported the first PIDA mediated [1,2]-carbon-to-nitrogen oxidative rearrangement reaction by using secondary amines (**35**) in the presence of TFE (**Scheme 1.11**).⁶¹ Synthetic application of this approach in affording diverse macrocyclic and polycyclic fused heterocycles (**37**) by utilizing various amines makes it more versatile.



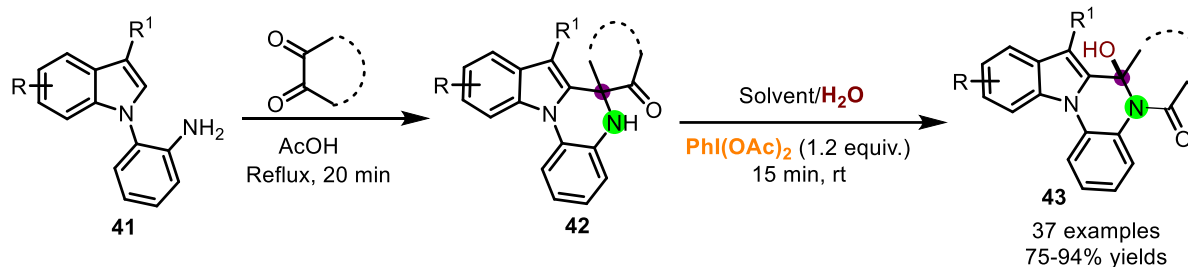
Scheme 1.8 PIDA-mediated [1,2]-oxidative rearrangement reaction of secondary amines

Extending this strategy, the same group in 2019 reported the PIDA mediated oxidative rearrangement reaction of primary amines (**38**). Unlike the reaction of secondary amines, this method utilizes $\text{PhI}(\text{OAc})_2$ and Cs_2CO_3 synergistically for the efficient construction of cyclic, acyclic and large ring compounds (**40**) (**Scheme 1.9**).⁶² Several preliminary experiments suggested a concerted mechanism for the reaction *via* intermediate (**39**), rather than nitrene or radical based mechanism. Chang group in 2021 also reported the *ipso* rearrangement of primary amines under similar conditions but used iodine as a promotor.⁶³



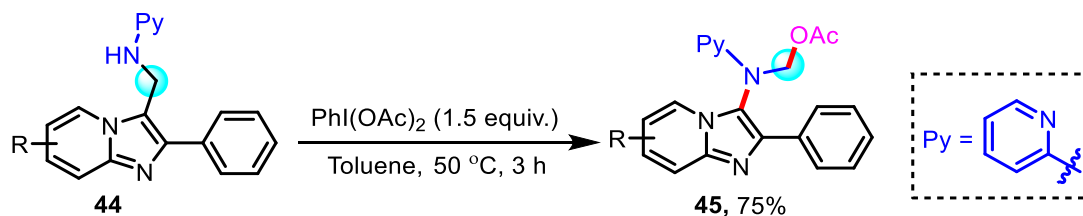
Scheme 1.9 PIDA-mediated [1,2]-oxidative rearrangement reaction of primary amines

Mandal and Pramanik developed an operationally simple and highly diastereoselective strategy involving ring expansion *via* 1,2-bond migration and simultaneous hydroxy insertion in the presence of $\text{PhI}(\text{OAc})_2$. Commenced from the spiro-fused quinoxaline (**42**) (which were synthesized by condensation of (**41**) and 1,2-cyclic diones), hydroxylated polycyclic pyrrolo/indolo[1,2-*a*]quinoxaline-fused lactam derivatives (**43**) were afforded in good-to-excellent yield with significant functional group tolerance in very rapid timeframe (**Scheme 1.10**).⁶⁴ Additionally, having a chiral center at the bridgehead along with one or two axially chiral biaryl or *N*-aryldolyl bridges makes the molecule nonplanar.



Scheme 1.10 PIDA-mediated [1,2]-oxidative rearrangement reaction of spiro-fused quinoxaline

As part of our interest in synthesis and functionalization of azaheterocycles, herein, we report PIDA-mediated [1,2]-*ipso*-migration of heteroaryl rings in Mannich bases (**44**) to give the corresponding *N*-acetoxyethyl/*N*-alkoxyethyl-*N*-aryl-imidazo[1,2-*a*]pyridine-3-amines (**45**) under mild reaction conditions (**Scheme 1.11**).



Scheme 1.11 Synthesis of 3-aminoimidazo[1,2-*a*]pyridine

1.2 RESULTS AND DISCUSSION

Our studies commenced with the reaction of Mannich base *i.e.* *N*-((2-phenylimidazo[1,2-*a*]pyridin-3-yl)methyl)pyridin-2-amine (**44a**) using iodobenzene diacetate as an oxidant. Model reaction of **44a** with PIDA in ethyl acetate at 50 °C produced ((2-phenylimidazo[1,2-*a*]pyridin-3-yl)(pyridin-2-yl)amino)methyl acetate (**45a**) in 75% yield within 3 h (**Table 1.1, entry 1**).

The molecular structure of **45a** was established by the ^1H (Figure 1.6) and ^{13}C NMR (Figure 1.7), DEPT-135 NMR (Figure 1.8), LC-HRMS spectroscopic data (Figure 1.9) and was further confirmed unambiguously by a single crystal X-ray diffraction analysis (Figure 1.10, CCDC No. 1957417).

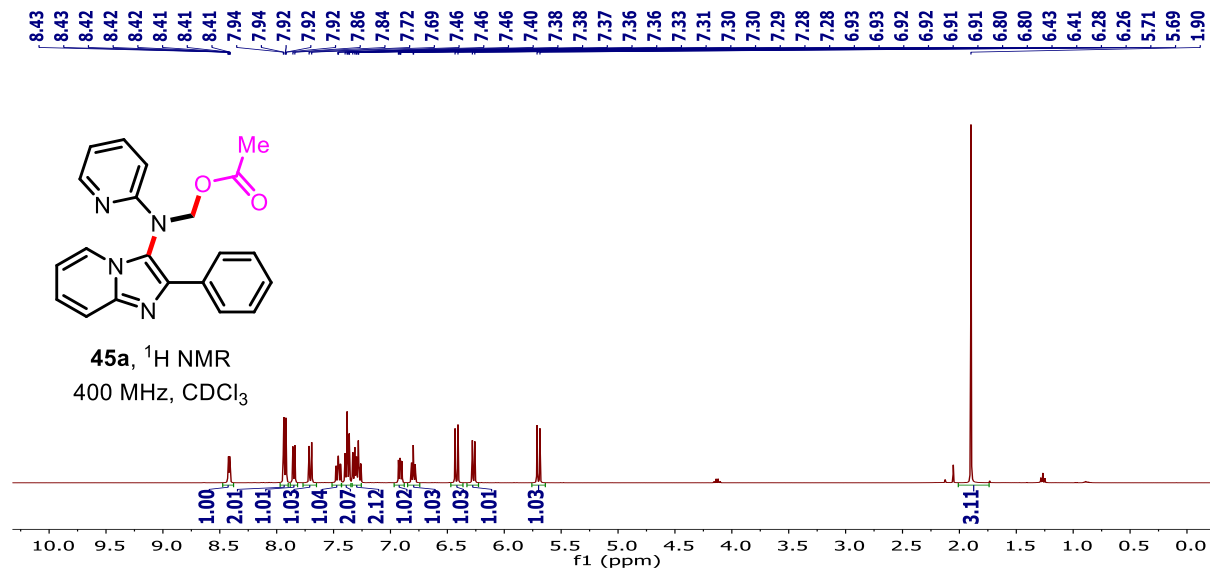


Figure 1.6 ^1H NMR spectrum of ((2-phenylimidazo[1,2-*a*]pyridin-3-yl)(pyridin-2-yl)amino)methyl acetate (**45a**) recorded in CDCl_3

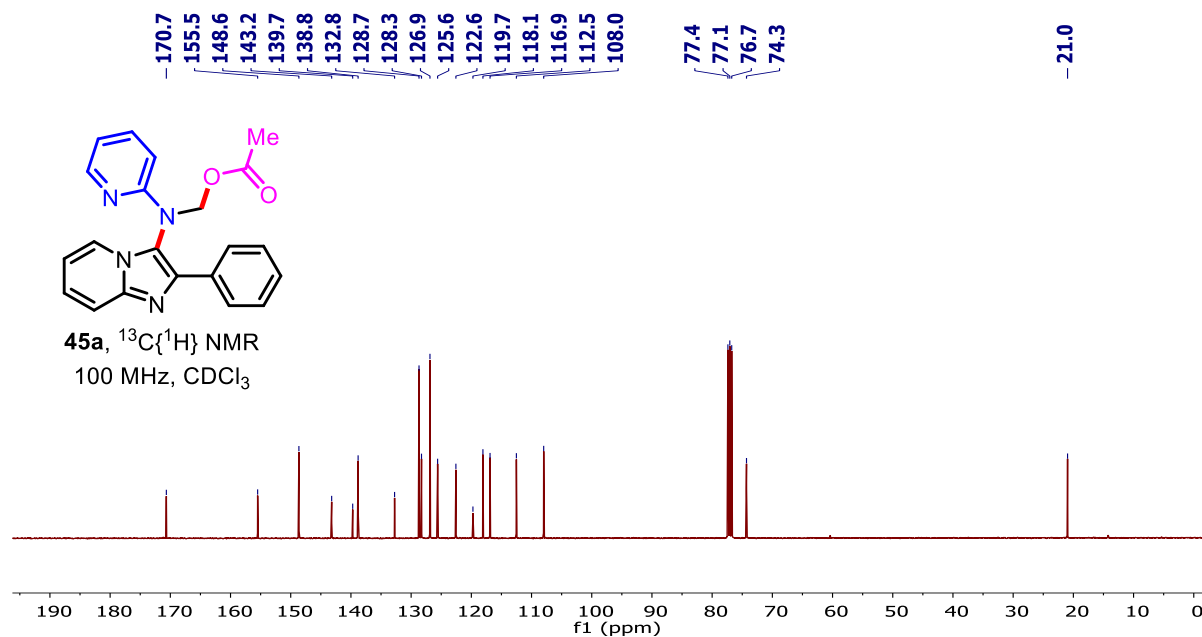


Figure 1.7 $^{13}\text{C}\{^1\text{H}\}$ NMR spectrum of ((2-phenylimidazo[1,2-*a*]pyridin-3-yl)(pyridin-2-yl)amino)methyl acetate (**45a**) recorded in CDCl_3

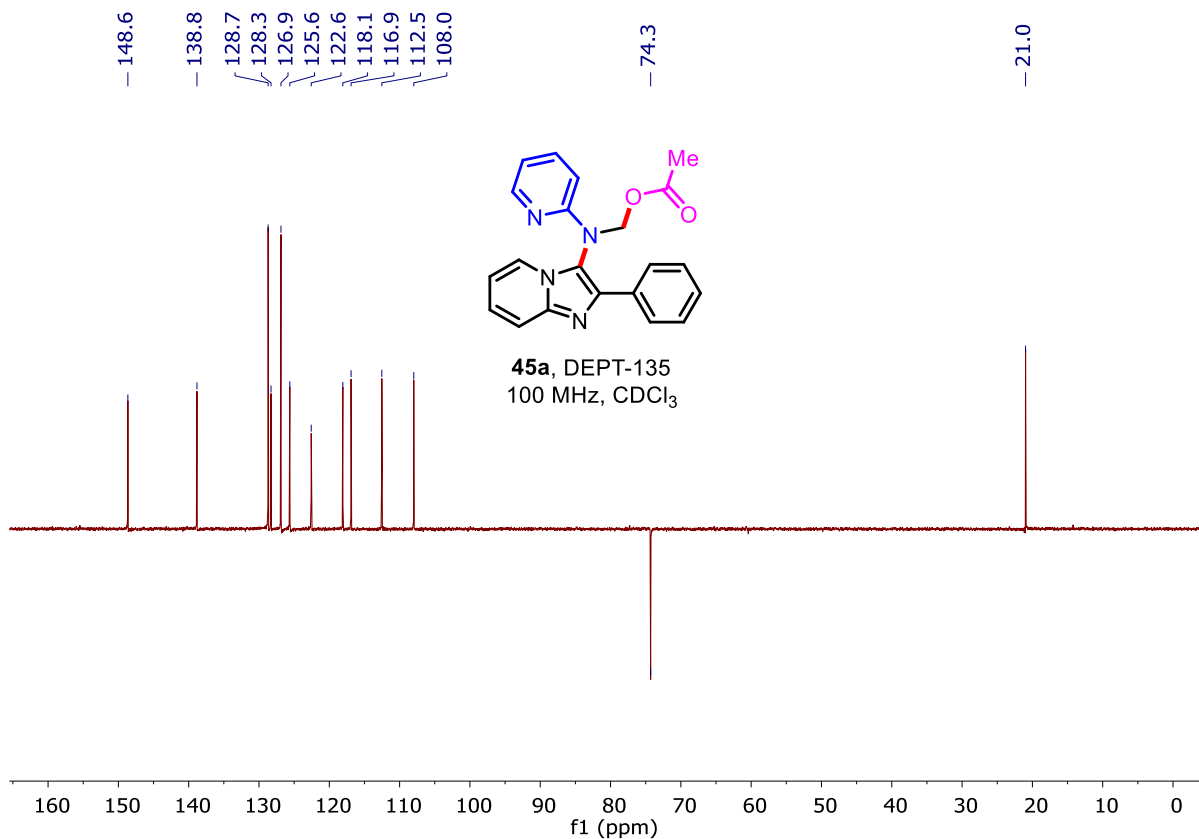


Figure 1.8 DEPT-135 NMR spectra of ((2-phenylimidazo[1,2-*a*]pyridin-3-yl)(pyridin-2-yl)amino)methyl acetate (**45a**) recorded in CDCl₃

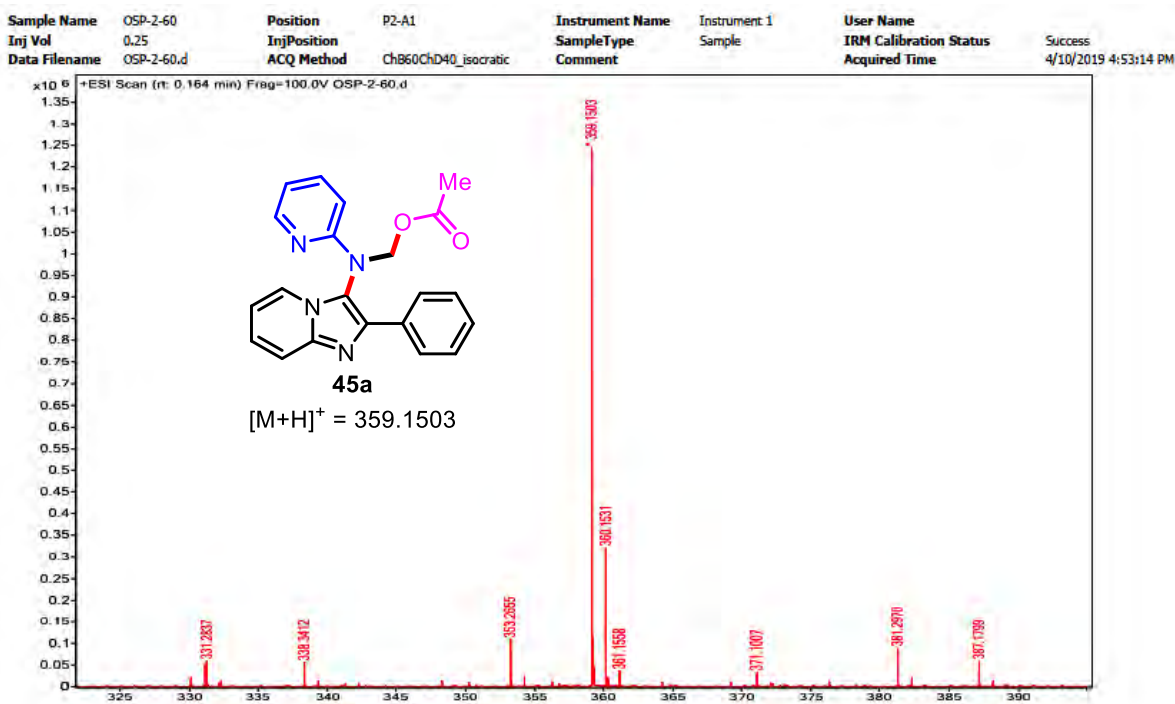


Figure 1.9 LC-HRMS of ((2-phenylimidazo[1,2-*a*]pyridin-3-yl)(pyridin-2-yl)amino)methyl acetate **45a**

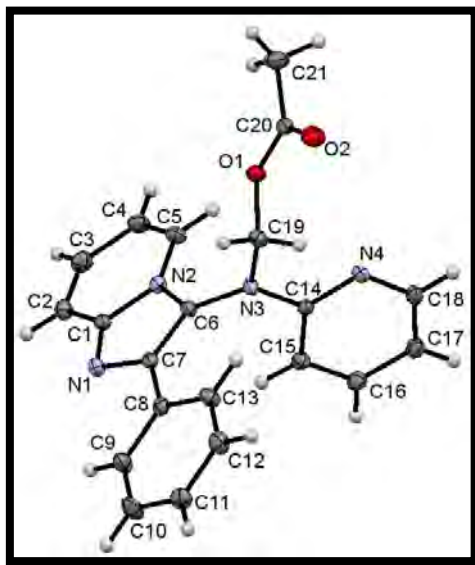
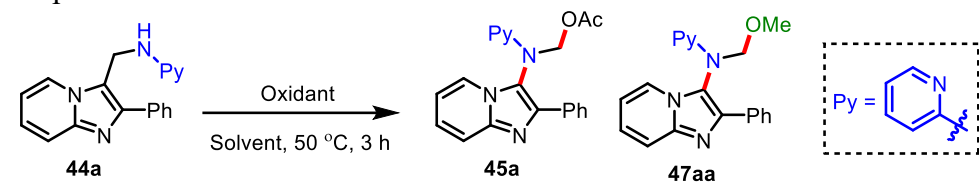


Figure 1.10 ORTEP diagram of **45a** (CCDC No 1957417). The thermal ellipsoids are drawn at 50% probability level

The initial results prompted us to evaluate the effect of different solvents such as 1,2-DCE, toluene, THF, 1,4-dioxane, DMSO, DMF, DMA, H₂O and MeOH on the outcome of reaction (**Table 1.1**, entries 1-11). The screening results concluded that the use of 1,2-DCE and toluene increased the yield of **45a** from 75% to 82% and 90%, respectively (**Table 1.1**, entries 1 vs 2 and 3). Meanwhile, other solvents (THF, 1,4-Dioxane, DMSO, DMF and DMA) resulted in reduced yields of **45a** (**Table 1.1**, entry 1 vs entries 4-8). The use of environmentally benign solvent such as water with or without phase-transfer-catalyst (SLS) did not improve the yield of **45a** (**Table 1.1**, entries 9-10). On the other hand, *N*-(methoxymethyl)-2-phenyl-*N*-(pyridin-2-yl)imidazo[1,2-*a*]pyridin-3-amine (**48aa**) was obtained in 90% yield with trace of **45a** when methanol was used as solvent (**Table 1.1**, entry 11). Decreasing amount of PIDA (1.2 equiv.) showed detrimental effect on the yield of **45a** (**Table 1.1**, entry 12). The use of PIFA (bis(trifluoroacetoxy)iodo)benzene) and organo-catalytic conditions⁶⁶⁻⁶⁷ did not produce the desired product **45a** (**Table 1.1**, entry 13, 14). The reaction did not proceed in presence of Koser's reagent as an oxidant in the reaction and **44a** remained unreacted after 3 h (**Table 1.1**, entry 15).

Table 1.1 Optimization of reaction conditions^a


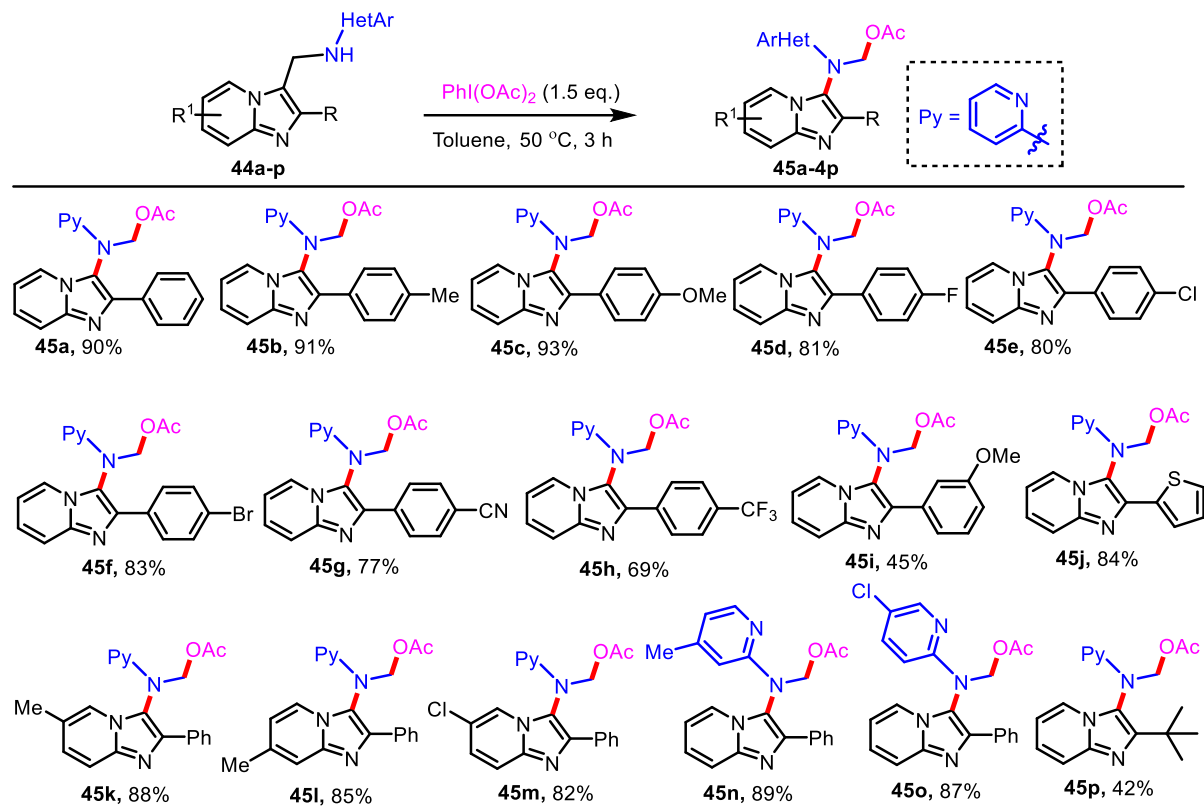
Entry	Oxidant	Solvent	% Yield 45a ^b
1	PhI(OAc) ₂	EtOAc	75
2	PhI(OAc) ₂	1,2-DCE	82
3	PhI(OAc)₂	Toluene	90
4	PhI(OAc) ₂	THF	37
5	PhI(OAc) ₂	1,4-Dioxane	48
6	PhI(OAc) ₂	DMSO	39
7	PhI(OAc) ₂	DMF	70
8	PhI(OAc) ₂	DMA	29
9	PhI(OAc) ₂	H ₂ O	7
10 ^c	PhI(OAc) ₂	H ₂ O	16
11	PhI(OAc) ₂	MeOH	<5 ^d
12 ^e	PhI(OAc) ₂	Toluene	83
13	PhI(OCOCF ₃) ₂	Toluene	0
14 ^f	PhI + <i>m</i> -CPBA	Toluene	Trace
15	HTIB	Toluene	- ^g

^aReaction conditions: **44a** (0.5 mmol), oxidant (1.5 equiv.), solvent (5 mL), 50 °C, 3 h. ^bIsolated yield. ^cSLS (20 mol %) was used. ^dMethoxylated product **47aa** was obtained in 90% yield. ^e1.2 equiv. of PIDA was used. ^fPhI (20 mol %) with *m*-CPBA (3 equiv.) and AcOH (5 equiv.) was used. ^gNo reaction.

With the optimized conditions in hand (**Table 1.1**, entry 3), the scope and generality of the methodology was investigated systematically (**Table 1.2**). At the beginning, Mannich bases of imidazopyridine with various substituents (Me, OMe, F, Cl, Br, CN and CF₃) on C-2 aryl ring reacted smoothly under optimized reaction conditions and produced the corresponding acetoxylated products (**45a-h**) in good to excellent (69-93%) yields. It was observed that Mannich bases with the electron-donating groups on C-2 aryl ring provided better yields than the elec-

tron-withdrawing groups on C2 aryl ring (**Table 1.2**, compare **45a** and **45b-c** vs **45d-h**). Mannich base with thiophene ring at the C2 position also afforded the desired acetoxyated product (**45j**) in 84% yield.

Table 1.2 Substrate scope for acetoxyated derivatives^{a,b}



^aReaction conditions: **44** (0.5 mmol), PIDA (1.5 equiv.), toluene (5 mL), 50 °C, 3 h. ^bIsolated yields.

Next, Mannich bases decorated with substituents (Me and Cl) at different positions on imidazo[1,2-*a*]pyridine nucleus and pyridine ring delivered the corresponding acetoxyated products (**45k-m**) in high (82-88%) yield under the identical reaction conditions. Interestingly, the *tert*-butyl group at C2 position of Mannich base also afforded the desired product (**45p**) in 42% yield.

During the reaction condition optimization studies it was observed that the use of methanol as solvent resulted **47aa** in 90% yield along with a trace amount (<5%) of acetoxy product **45a** (**Table 1.1**, entry 11). It might be due to the relatively high nucleophilicity of methoxide group as compared to the acetate group, which facilitated the ring opening of aziridine intermediate

better than the acetate group resulting the methoxylated product in excellent yield. The structure of **47aa** was established by the ^1H NMR (Figure 1.11), $^{13}\text{C}\{^1\text{H}\}$ NMR (Figure 1.12), and HRMS spectroscopic data (Figure 1.13) and was further confirmed unambiguously by a single crystal X-ray diffraction analysis ((Figure 1.14, CCDC No. 1913162).

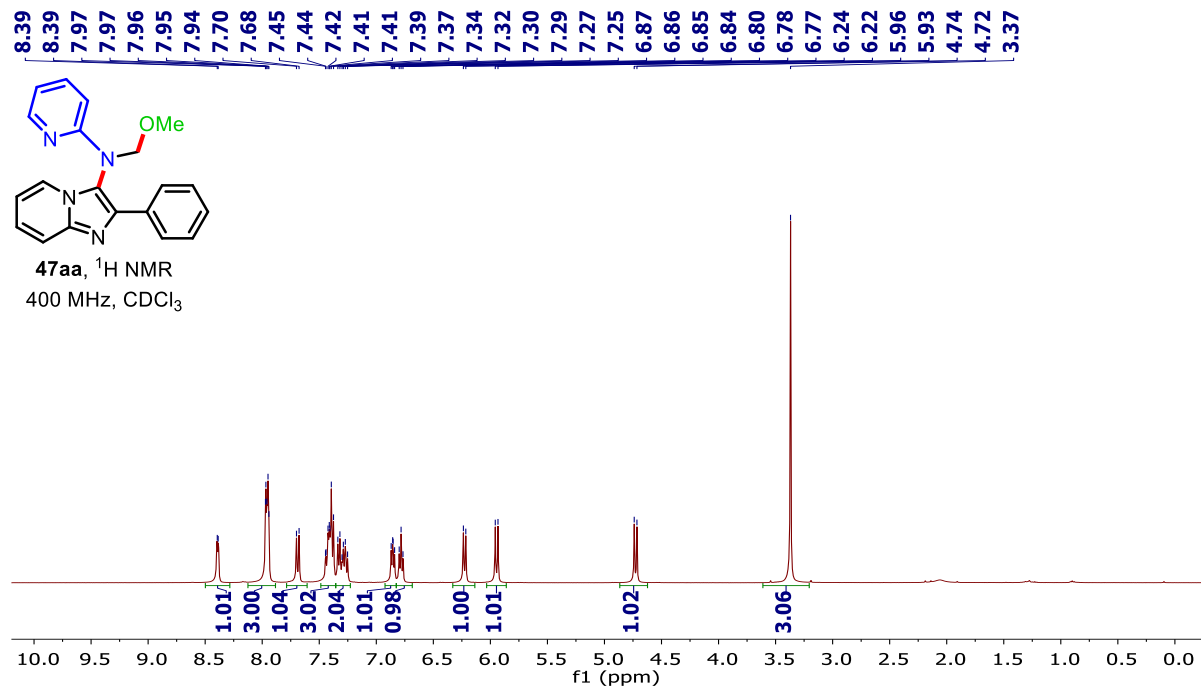


Figure 1.11 ^1H NMR spectrum of *N*-(methoxymethyl)-2-phenyl-*N*-(pyridin-2-yl)imidazo [1,2-*a*]pyridin-3-amine (**47aa**) recorded in CDCl_3

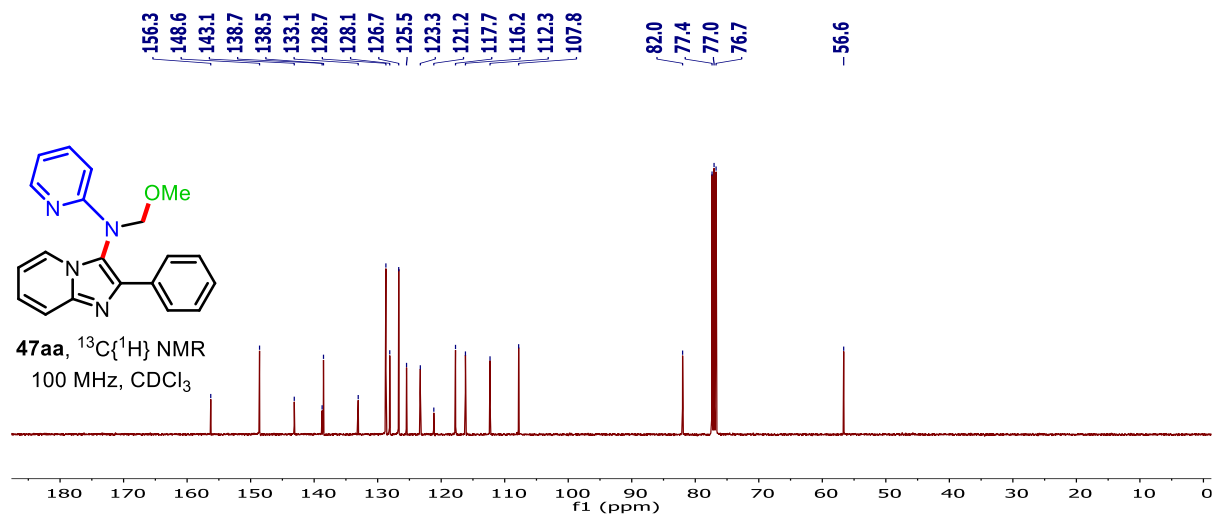


Figure 1.12 $^{13}\text{C}\{^1\text{H}\}$ NMR spectrum of *N*-(methoxymethyl)-2-phenyl-*N*-(pyridin-2-yl)imidazo [1,2-*a*]pyridin-3-amine (**47aa**) recorded in CDCl_3

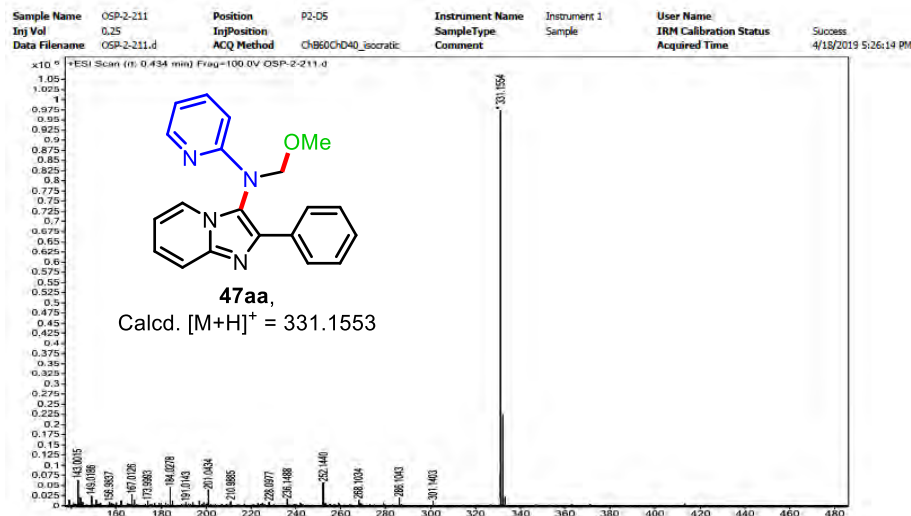


Figure 1.13 LC-HRMS spectrum of *N*-(methoxymethyl)-2-phenyl-*N*-(pyridin-2-yl)imidazo [1,2-*a*]pyridin-3-amine (**47aa**)

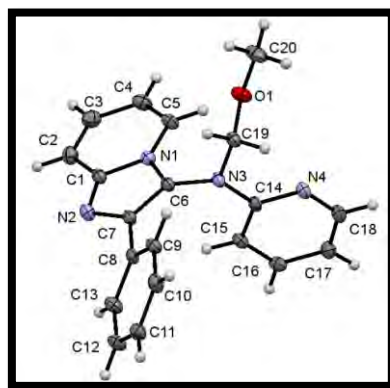


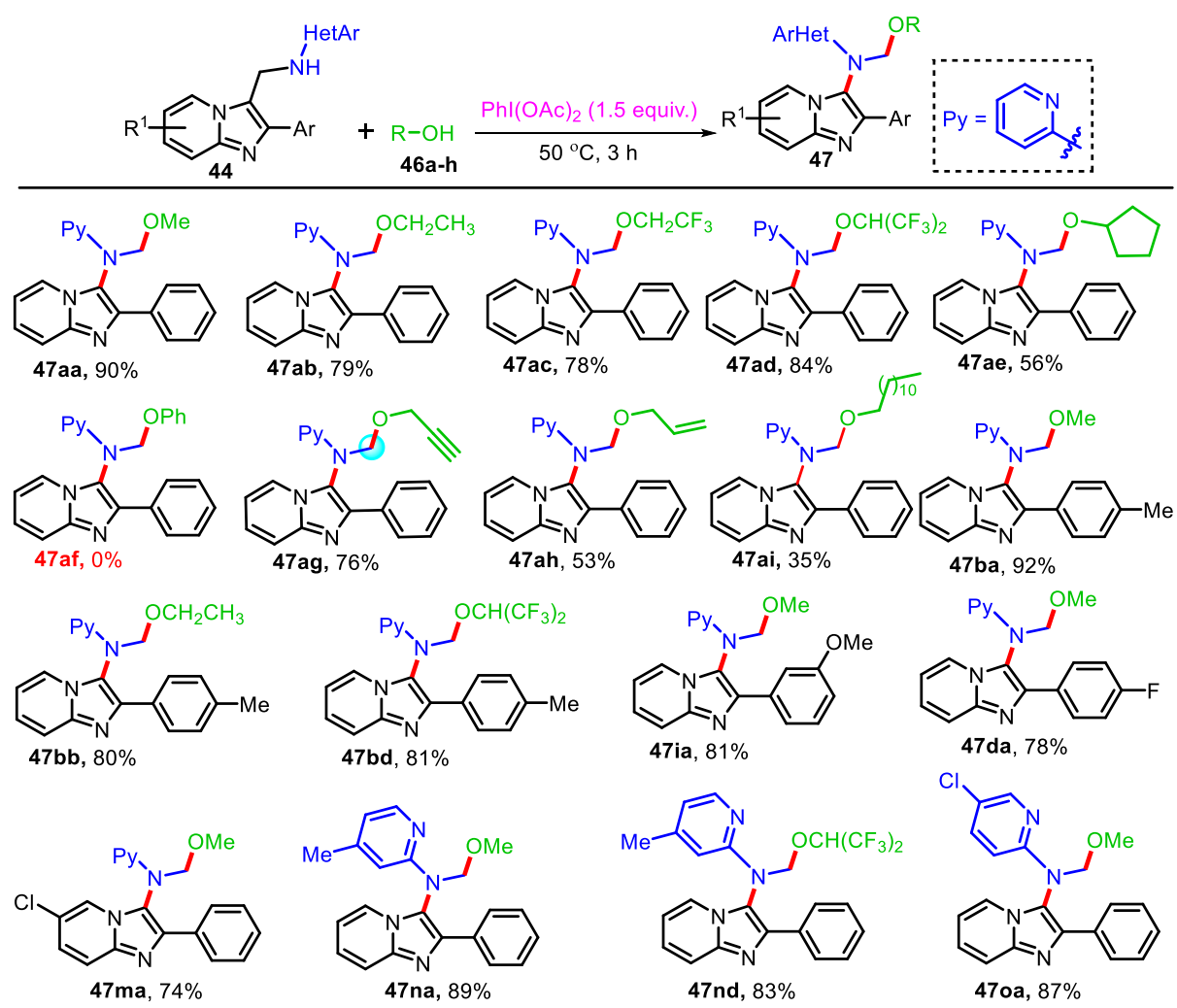
Figure 1.14 ORTEP diagram of **47aa** (CCDC No 1913162). The thermal ellipsoids are drawn at 50% probability level

We then took up a systematic study to evaluate the formation of alkoxyated products by employing different alcohols **46** as solvent with **44a** (Table 1.3). It was found that primary alcohols such as methanol, ethanol, isopropyl alcohol, propargyl alcohol, allyl alcohol, fluorinated alcohol (hexafluoro-2-propanol and 2-trifluoroethanol) as well as secondary alcohol such as cyclopentanol smoothly reacted with **44a** and delivered the desired alkoxyated products **47aa-47ah** in 53-90% yields. A long chain alcohol *i.e.* lauryl alcohol also reacted and gave the desired product **47ai** in low yield (35%), while phenol could not afford the respective product **47af**, most likely due to the weak nucleophilicity of phenol.⁶⁸ Functionalized alcohols such as propargyl alcohol **46g** and allyl alcohol **46h** also reacted well and furnished the respective products

47ag and **47ah** in 76% and 53% yields, respectively. This transformation is interesting from the view-point of medicinal chemistry as it further opens scope of post-modification.

Further, Mannich bases bearing methyl (**44b**), methoxy (**44i**) and fluoro (**44d**) groups on the C2 aryl ring, chloro (**44m**) group on imidazo[1,2-*a*]pyridine nucleus reacted smoothly with different alcohols (MeOH, EtOH and HFIP) in the presence of PIDA to give corresponding alkoxyated products (**47ba-47ma**) in good to excellent (74-92%) yields. Similarly, Mannich bases with methyl (**44n**) and chloro (**44o**) groups on the pyridine ring also participated in the reaction and gave corresponding alkoxyated products **47na-47oa** in excellent yield (83-89%).

Table 1.3 Substrate scope for alkoxyated derivatives^{a,b}

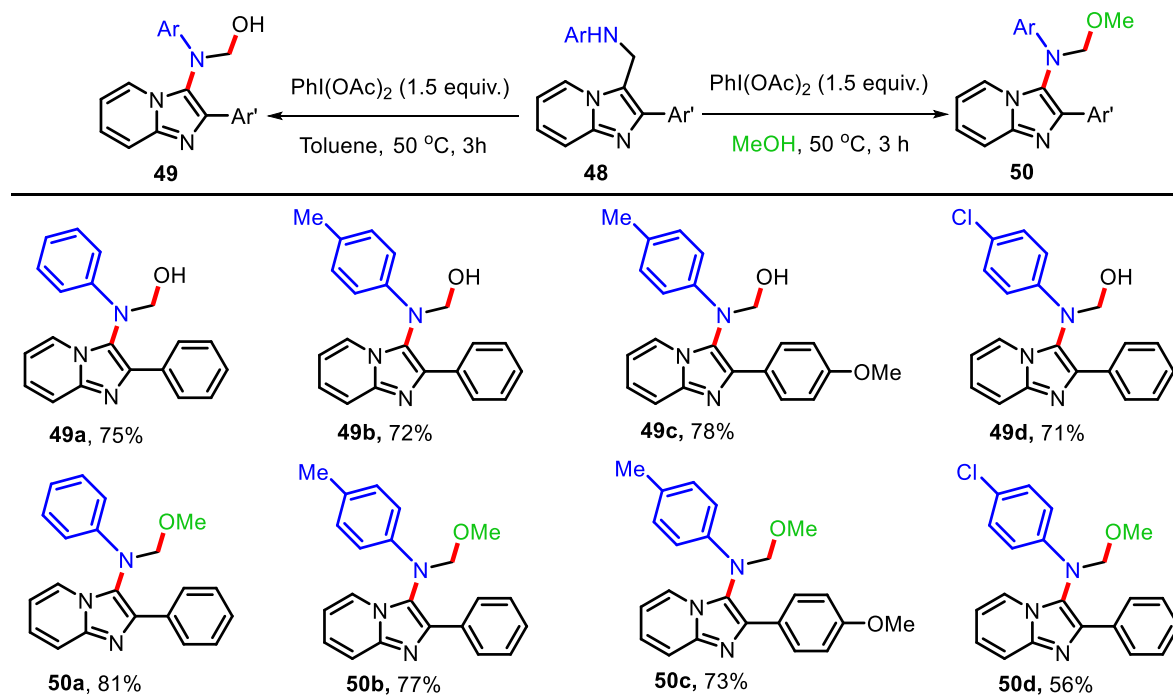


^aReaction conditions: **44** (0.5 mmol), PIDA (1.5 equiv.), ROH (**46**) (5 mL), 50 °C for 3 h.

^bIsolated yields.

Next, scope of the reaction for Mannich bases derived from imidazo[1,2-*a*]pyridines and anilines was studied (Table 1.4). To our satisfaction, rearranged product methoxymethyl amines **50** were obtained in good to excellent yields (73-81%) from the reaction of **48** with PIDA in methanol. On the other hand, (aryl(2-arylimidazo[1,2-*a*]pyridin-3-yl)amino)methanols **49** were obtained when **48** was allowed to react with PIDA in toluene. Results from these reactions indicated that the pyridyl ring has no specific role in the 1,2-*ipso*-migration in Mannich bases. Structure of compounds **49** and **50** was confirmed by NMR (^1H , ^{13}C) and HRMS analysis. Further, structure of **49a** was also elucidated by single crystal X-ray diffraction analysis (CCDC 1986133) (Figure 1.15). It is worth mentioning that the reaction of *N*-((1-tosyl-1*H*-indol-3-yl)methyl)aniline with PIDA in toluene resulted 1-tosyl-1*H*-indole-3-carbaldehyde instead of the desired rearranged product. Formation of 3-formylindole derivative can be explained *via* PIDA mediated oxidation of secondary amine to imine followed by hydrolysis.⁶⁹

Table 1.4 Substrate scope for Mannich bases derived from arylamines^{a,b}



^aReaction conditions: **48** (0.5 mmol), PIDA (1.5 equiv.), MeOH (5 mL), 50 °C for 3 h. ^bIsolated yields.

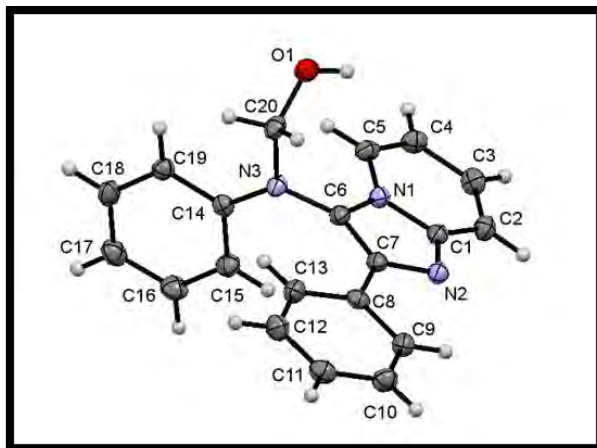
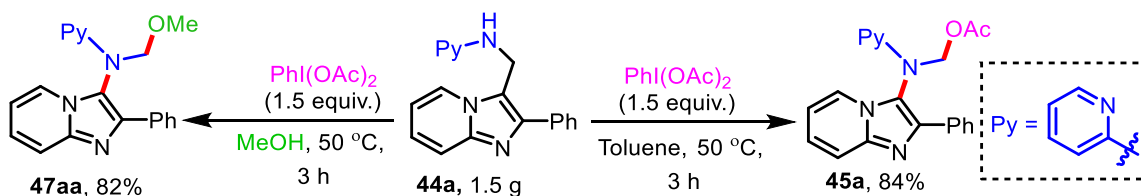


Figure 1.15 ORTEP diagram of **49a** (CCDC No 1913162). The thermal ellipsoids are drawn at 50% probability level

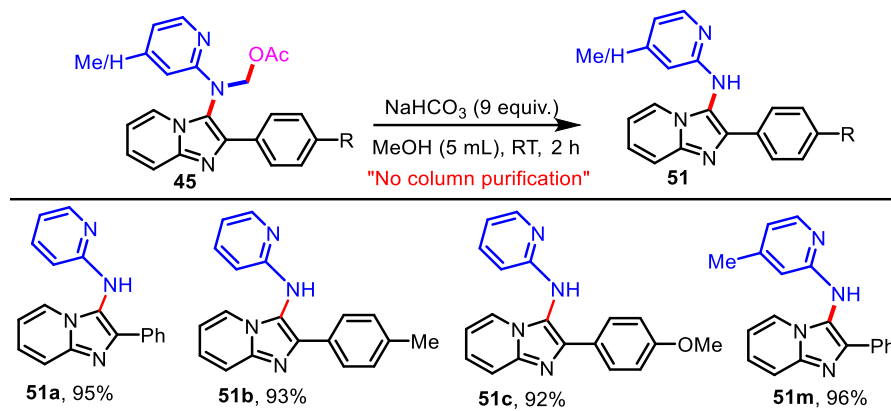
Furthermore, to evaluate the potentiality of the developed methodology for the large-scale synthesis of acetylated and alkoxyated compounds, we performed gram-scale reaction of **44a** (1.5 g) under standard reaction conditions in toluene and MeOH (**Scheme 1.12**). To our expectation, the desired products **45a** and **47aa** were obtained in 84% and 82% yields, respectively.



Scheme 1.12 Gram scale experiment

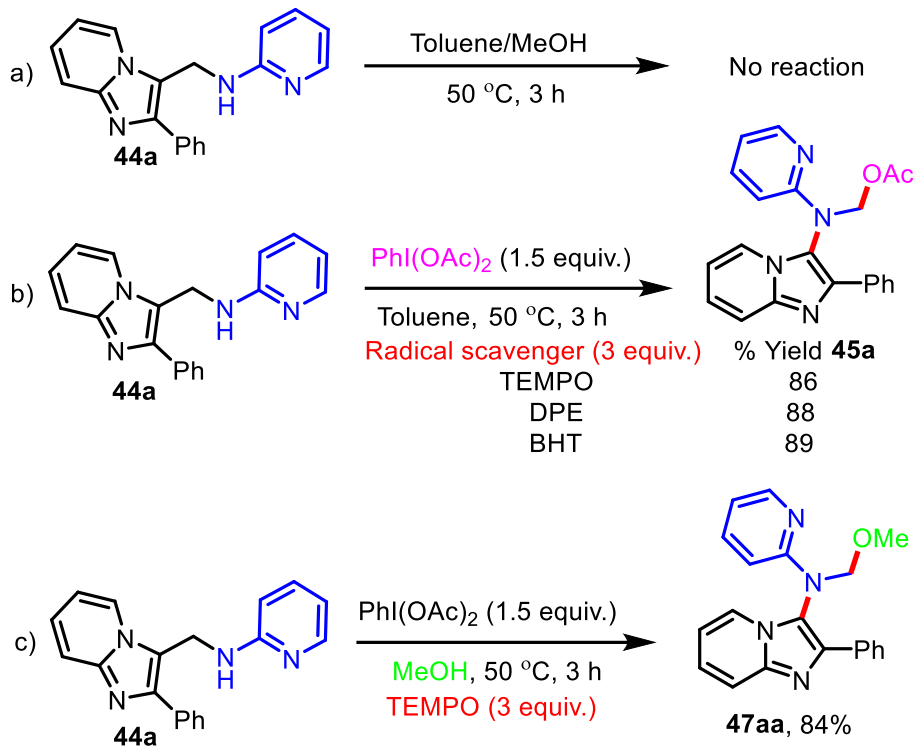
To demonstrate the synthetic utility of the developed protocol, acetylated derivatives **45** were transformed to 3-(pyridin-2-yl)aminoimidazo[1,2-*a*]pyridines (**Scheme 1.13**). On stirring acetylated product **45a** with NaHCO₃ for 2 h in MeOH, 2-phenyl-*N*-(pyridin-2-yl)imidazo[1,2-*a*]pyridin-3-amine (**51a**) was obtained in 95% yield. Similarly, 2-aryl-*N*-(pyridin-2-yl)aminoimidazo[1,2-*a*]pyridines **51b**, **51c** and **51m** were obtained in 93%, 92% and 96% yields from **45b**, **45c** and **45m**, respectively. This is noteworthy to mention that the purity of the products **51** was obtained in >96% through HPLC analysis without using column chromatography. The 3-arylaminoimidazo[1,2-*a*]pyridines are generally prepared by the Groebke-Blackburn-Bienaymé reaction which require isocyanides as one of the substrate.⁷⁰ The developed method

provides a simple and straightforward synthetic strategy for the preparation of bioactive 3-arylaminimidazo[1,2-*a*]pyridines.⁷¹⁻⁷²



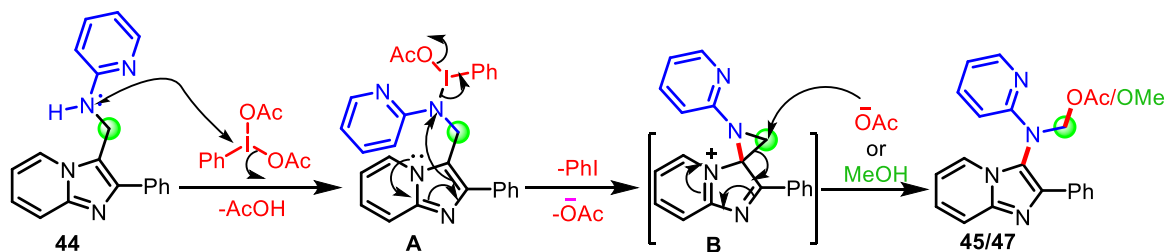
Scheme 1.13 Synthetic utility: removal of methyl acetate

To gain an insight into the mechanism for the oxidative 1,2-migration followed by functionalization, a set of control experiments were performed (**Scheme 1.14**). First, to confirm the role of PIDA, we performed the reaction of **44a** in toluene and methanol in the absence of PIDA. The reaction did not produce the corresponding products **45a** and **47aa**, justifying the essential role of PIDA in the reaction (**Scheme 1.14a**). Second, reaction of **44a** under standard reaction conditions in the presence of different radical scavengers including 2,2,6,6-tetramethylpiperidine-1-oxyl (TEMPO), 1,2-diphenylethylene (DPE) and butylated hydroxytoluene (BHT) resulted **45a** in 86%, 88% and 89% yields, respectively (**Scheme 1.14b**). Similarly, product **47aa** was also formed in 84% yield from the reaction of **44a** with PIDA in methanol in the presence of TEMPO (**Scheme 1.14c**). The results from radical scavengers experiments ruled out the involvement of the radical pathway which is in stark contrast to what is observed by Murai in the PIDA-mediated direct 1,2-C-to-N migration of amines.⁶¹⁻⁶² Based on these results and effect of substituents on C2 aryl ring on the yields of products, we believe that the reaction involves a non-radical, ionic mechanism.



Scheme 1.14 Control experiments

Based on the control experiments and literature reports,⁷³⁻⁷⁴ a plausible mechanistic pathway is depicted in **Scheme 1.15**. It is believed that initially, the reaction of **44** with $\text{PhI}(\text{OCOCH}_3)_2$ gives the iodinated intermediate **A** with the removal of acetic acid. The intermediate **A** is further converted into a Wheland-type aziridine intermediate **B** via nucleophilic *ipso*-attack of imidazo[1,2-*a*]pyridinyl group and subsequent removal of iodobenzene and acetate group. The intermediate **B** is then attacked by acetate/alkoxy nucleophile at strained methylene carbon initial and results in the formation of [1,2]-*ipso*-migrated acetoxyated or alkoxyated product **45/47**.



Scheme 1.15 Proposed reaction mechanism

1.3 CONCLUSIONS

In summary, this chapter delineates a novel protocol for the preparation of 3-amino-imidazo[1,2-*a*]pyridine derivatives in moderate to excellent yields through PIDA-mediated [1,2]-*ipso*-migration in Mannich bases derived from imidazo[1,2-*a*]pyridines, 2-aminopyridines/aryl amines and formaldehyde. The reaction is believed to proceed through [1,2]-*ipso*-heteroaryl migration *via* the formation of a Wheland-type aziridine intermediate followed by nucleophile-assisted ring opening reaction. The protocol is amenable for a scale-up reaction and the acetoxylated products **45** were easily transformed to the corresponding 2-aryl-*N*-(pyridin-2-yl)imidazo[1,2-*a*]pyridin-3-amines **51** by treating with NaHCO₃ in methanol. Given the high pharmaceutical importance of 3-amino-imidazo[1,2-*a*]pyridine derivatives, the newly developed methodology will be useful for the synthesis of highly versatile 3-arylaminoimidazo[1,2-*a*]pyridines under metal-free and mild conditions.

1.4 EXPERIMENTAL SECTION

1.4.1. General Information

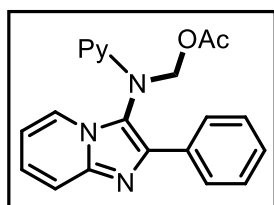
Melting points were determined in open capillary tubes on EZ-Melt automated melting point apparatus and are uncorrected. All the compounds were fully characterized by ¹H, ¹³C{¹H}, and further confirmed by ESI-HRMS analysis. Reactions were monitored by using thin layer chromatography (TLC) on 0.2 mm silica gel F254 plates (Merck). ¹H and ¹³C{¹H} NMR spectra were recorded on Bruker Avance 400 NMR spectrometer at 400 MHz and 100 MHz frequency, respectively, with CDCl₃ as the solvent using TMS as an internal standard. Peak multiplicities of ¹H NMR signals were designated as s (singlet), d (doublet), dd (doublet of doublet), dt (doublet of triplet), td (triplet of doublet), t (triplet), q (quartet), m (multiplet), etc. Chemical shifts (δ) and coupling constants (*J*) are reported in parts per million (ppm) relative to the residual signal of TMS in deuterated solvents and hertz, respectively. ESI-HRMS were recorded using Agilent 6545 Q-TOF LC/MS. IR spectra were recorded using an FT-IR spectrophotometer, and values are reported in cm⁻¹. Column chromatography was performed over silica gel (60-120 mesh) using EtOAc–hexanes as eluent. All the chemicals were obtained from the commercial suppliers and used without further purification. The Mannich bases of imidazo[1,2-*a*]pyridines (**44** and **48**) were prepared either by the reaction of 2-arylimidazo[1,2-*a*]pyridines (5.33 mmol)

and 2-aminopyridines in TBHP⁷⁵ or by reductive amination of 2-arylimidazo[1,2-*a*]pyridine-3-carbaldehyde (5.33 mmol) with arylamines.⁷⁶

1.4.2 Experimental Procedure for the Preparation of Acetoxy Products (45) or Hemiaminals (49)

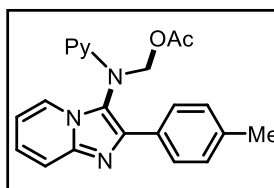
To a solution of **44** or **48** (0.5 mmol; 1 equiv.) in toluene (5 mL) was added $\text{PhI}(\text{OAc})_2$ (1.5 equiv.) at room temperature and the reaction mixture was stirred at 50 °C for 3 h. After completion of the reaction, observed by TLC, the mixture was allowed to attain room temperature. The reaction mixture was poured into water (20 mL) and extracted with ethyl acetate (3 × 15 mL). The combined organic layer was dried over anhydrous Na_2SO_4 and evaporated under vacuum. The resulting crude solid was purified by column chromatography (silica gel 60-120 mesh) using EtOAc-*hexanes* as an eluent to afford **45** or **49**.

*((2-Phenylimidazo[1,2-*a*]pyridin-3-yl)(pyridin-2-yl)amino)methyl acetate (45a)*: White solid;



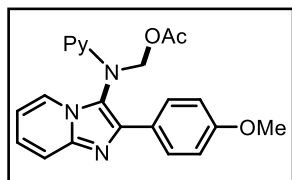
161 mg, 90% yield; Eluent system: EtOAc:hexanes (25:75); mp = 195-196 °C; ¹H NMR (400 MHz, CDCl_3) δ = 8.42-8.40 (m, 1H), 7.94-7.91 (m, 2H), 7.85 (d, J = 6.8 Hz, 1H), 7.70 (d, J = 9.0 Hz, 1H), 7.48-7.43 (m, 1H), 7.40-7.36 (m, 2H), 7.33-7.25 (m, 2H), 6.91 (ddd, J = 7.3, 5.0, 0.9 Hz, 1H), 6.79 (td, J = 6.7, 1.2 Hz, 1H), 6.42 (d, J = 10.3 Hz, 1H), 6.27 (d, J = 8.4 Hz, 1H), 5.69 (d, J = 10.2 Hz, 1H), 1.89 (s, 3H); ¹³C{¹H} NMR (100 MHz, CDCl_3) δ = 170.6, 155.5, 148.6, 143.2, 139.7, 138.8, 132.7, 128.6, 128.2, 126.8, 125.6, 122.5, 119.7, 118.0, 116.8, 112.5, 107.9, 74.2, 20.9; HRMS (ESI) m/z : $[\text{M} + \text{H}]^+$ Calcd for $\text{C}_{21}\text{H}_{19}\text{N}_4\text{O}_2$ 359.1503; found 359.1503.

*(Pyridin-2-yl(2-(*p*-tolyl)imidazo[1,2-*a*]pyridin-3-yl)amino)methyl acetate (45b)*: White solid;



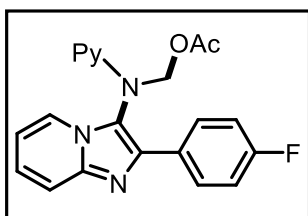
169 mg, 91% yield; Eluent system: EtOAc:hexanes (25:75); mp = 195-196 °C; ¹H NMR (400 MHz, CDCl_3) δ = 8.40-8.38 (m, 1H), 7.83-7.79 (m, 3H), 7.67 (dt, J = 9.0, 1.1 Hz, 1H), 7.45-7.40 (m, 1H), 7.27-7.23 (m, 1H, overlapped with CDCl_3 residual signal), 7.17 (d, J = 8.0 Hz, 2H), 6.90-6.87 (m, 1H), 6.76 (td, J = 6.7, 1.1 Hz, 1H), 6.42 (d, J = 10.2 Hz, 1H), 6.23 (d, J = 8.4 Hz, 1H), 5.64 (d, J = 10.2 Hz, 1H), 2.33 (s, 3H), 1.90 (s, 3H); ¹³C{¹H} NMR (100 MHz, CDCl_3) δ = 170.6, 155.5, 148.6, 143.1, 139.7, 138.7, 138.1, 129.8, 129.4, 126.7, 125.4, 122.5, 119.4, 117.9, 116.8, 112.3, 108.0, 74.4, 21.2, 20.9; HRMS (ESI) m/z : $[\text{M} + \text{H}]^+$ Calcd for $\text{C}_{22}\text{H}_{21}\text{N}_4\text{O}_2^+$ 373.1659; found 373.1651.

((2-(4-Methoxyphenyl)imidazo[1,2-a]pyridin-3-yl)(pyridin-2-yl)amino)methyl acetate (**45c**):



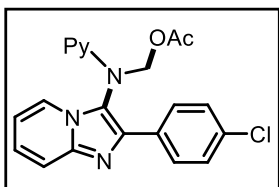
White solid; 180 mg, 93% yield; Eluent system: EtOAc:hexanes (30:70); mp = 167-169 °C; ^1H NMR (400 MHz, CDCl_3) δ = 8.41-8.39 (m, 1H), 7.87-7.83 (m, 2H), 7.82 (dt, J = 6.8, 1.2 Hz, 1H), 7.66 (dt, J = 9.0, 1.1 Hz, 1H), 7.45-7.41 (m, 1H), 7.27-7.22 (m, 1H, overlapped with CDCl_3 residual signal), 6.92-6.87 (m, 3H), 6.76 (td, J = 6.7, 1.1 Hz, 1H), 6.41 (d, J = 10.2 Hz, 1H), 6.24 (d, J = 8.4 Hz, 1H), 5.67 (d, J = 10.2 Hz, 1H), 3.81 (s, 3H), 1.91 (s, 3H); $^{13}\text{C}\{^1\text{H}\}$ NMR (100 MHz, CDCl_3) δ = 170.7, 159.7, 155.5, 148.6, 143.1, 139.6, 138.8, 128.1, 125.4, 125.3, 122.4, 118.8, 117.8, 116.8, 114.1, 112.3, 108.0, 74.3, 55.2, 21.0; HRMS (ESI) m/z : $[\text{M} + \text{H}]^+$ Calcd for $\text{C}_{22}\text{H}_{21}\text{N}_4\text{O}_3^+$ 389.1608; found 389.1598.

((2-(4-Fluorophenyl)imidazo[1,2-a]pyridin-3-yl)(pyridin-2-yl)amino)methyl acetate (**45d**):



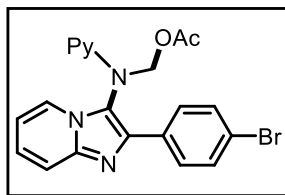
White solid; 152 mg, 81% yield; Eluent system: EtOAc:hexanes (25:75); mp = 177-179 °C; ^1H NMR (400 MHz, CDCl_3) δ = 8.41 (d, J = 4.6 Hz, 1H), 7.92-7.89 (m, 2H), 7.84 (d, J = 6.8 Hz, 1H), 7.69 (d, J = 9.1 Hz, 1H), 7.49-7.44 (m, 1H), 7.31-7.27 (m, 1H), 7.07 (t, J = 8.7 Hz, 2H), 6.92 (dd, J = 6.8, 5.2 Hz, 1H), 6.81 (t, J = 6.6 Hz, 1H), 6.37 (d, J = 10.2 Hz, 1H), 6.26 (d, J = 8.4 Hz, 1H), 5.72 (d, J = 10.2 Hz, 1H), 1.91 (s, 3H); $^{13}\text{C}\{^1\text{H}\}$ NMR (100 MHz, CDCl_3) δ = 170.6, 162.7 (d, $^1J_{\text{C-F}}$ = 246 Hz), 155.4, 148.7, 143.1, 138.9, 138.8, 128.9 (d, $^3J_{\text{C-F}}$ = 3.0 Hz), 128.7 (d, $^3J_{\text{C-F}}$ = 8.0 Hz), 125.7, 122.5, 119.4, 118.0, 117.0, 115.6 (d, $^2J_{\text{C-F}}$ = 22 Hz), 112.6, 107.8, 74.1, 20.9; HRMS (ESI) m/z : $[\text{M} + \text{H}]^+$ Calcd for $\text{C}_{21}\text{H}_{18}\text{FN}_4\text{O}_2^+$ 377.1408; found 377.1420.

((2-(4-Chlorophenyl)imidazo[1,2-a]pyridin-3-yl)(pyridin-2-yl)amino)methyl acetate (**45e**):



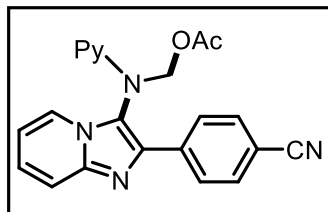
White solid; 166 mg, 80% yield; Eluent system: EtOAc:hexanes (25:75); mp = 164-166 °C; ^1H NMR (400 MHz, CDCl_3) δ = 8.39 (d, J = 3.0 Hz, 1H), 7.86-7.81 (m, 3H), 7.66 (d, J = 9.0 Hz, 1H), 7.46-7.42 (m, 1H), 7.34-7.26 (m, 3H, overlapped with CDCl_3 residual signal), 6.90 (d, J = 7.4, 5.0 Hz, 1H), 6.79 (t, J = 6.8 Hz, 1H), 6.34 (d, J = 10.3 Hz, 1H), 6.23 (d, J = 8.4 Hz, 1H), 5.69 (d, J = 10.3 Hz, 1H), 2.97 (unassigned impurity other than compound), 1.89 (s, 3H); $^{13}\text{C}\{^1\text{H}\}$ NMR (100 MHz, CDCl_3) δ = 170.6, 155.3, 148.7, 143.2, 138.9, 138.6, 134.1, 131.2, 128.8, 128.1, 125.8, 122.5, 119.8, 118.0, 117.0, 112.7, 107.8, 74.1, 20.9; HRMS (ESI) m/z : $[\text{M} + \text{H}]^+$ Calcd for $\text{C}_{21}\text{H}_{18}\text{ClN}_4\text{O}_2^+$ 393.1113; found 393.1115.

((2-(4-Bromophenyl)imidazo[1,2-a]pyridin-3-yl)(pyridin-2-yl)amino)methyl acetate (**45f**):



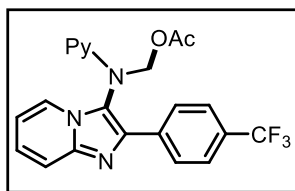
White solid; 181 mg, 83% yield; Eluent system: EtOAc:hexanes (20:80); mp = 174-176 °C; ^1H NMR (400 MHz, CDCl_3) δ = 8.40-8.38 (m, 1H), 7.83-7.78 (m, 3H), 7.67 (d, J = 9.1 Hz, 1H), 7.50-7.42 (m, 3H), 7.30-7.27 (m, 1H), 6.91 (dd, J = 6.9, 5.2 Hz, 1H), 6.79 (td, J = 6.8, 0.8 Hz, 1H), 6.34 (d, J = 10.3 Hz, 1H), 6.23 (d, J = 8.4 Hz, 1H), 5.69 (d, J = 10.3 Hz, 1H), 1.90 (s, 3H); $^{13}\text{C}\{^1\text{H}\}$ NMR (100 MHz, CDCl_3) δ = 170.6, 155.3, 148.7, 143.2, 138.8, 138.6, 131.8, 131.7, 128.4, 125.8, 122.5, 122.4, 119.8, 118.1, 117.0, 112.7, 107.8, 74.1, 20.9; HRMS (ESI) m/z : $[\text{M} + \text{H}]^+$ Calcd for $\text{C}_{21}\text{H}_{18}\text{BrN}_4\text{O}_2^+$ 437.0608; found 437.0593.

((2-(4-Cyanophenyl)imidazo[1,2-a]pyridin-3-yl)(pyridin-2-yl)amino)methyl acetate (**45g**):



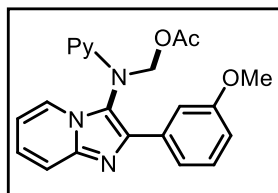
Colorless semi-solid; 147.5 mg, 77% yield; Eluent system: EtOAc:hexanes (25:75); ^1H NMR (400 MHz, CDCl_3) δ = 8.40 (d, J = 4.0 Hz, 1H), 8.04 (d, J = 8.4 Hz, 2H), 7.83 (d, J = 6.8 Hz, 1H), 7.68 (d, J = 9.1 Hz, 1H), 7.64 (d, J = 8.3 Hz, 2H), 7.49-7.45 (m, 1H), 7.34-7.29 (m, 1H), 6.93 (dd, J = 7.3, 5.0 Hz, 1H), 6.83 (t, J = 6.8 Hz, 1H), 6.32 (d, J = 10.4 Hz, 1H), 6.25 (d, J = 8.3 Hz, 1H), 5.72 (d, J = 10.4 Hz, 1H), 1.89 (s, 3H); $^{13}\text{C}\{^1\text{H}\}$ NMR (100 MHz, CDCl_3) δ = 170.5, 155.0, 148.8, 143.4, 139.0, 137.5, 137.3, 132.5, 132.4, 127.2, 126.4, 122.6, 121.0, 118.8, 118.3, 117.3, 113.1, 111.4, 107.8, 74.0, 20.9; HRMS (ESI) m/z : $[\text{M} + \text{H}]^+$ Calcd for $\text{C}_{22}\text{H}_{18}\text{N}_5\text{O}_2^+$ 384.1455, found 384.1443.

(Pyridin-2-yl(2-(4-(trifluoromethyl)phenyl)imidazo[1,2-a]pyridin-3-yl)amino)methyl acetate



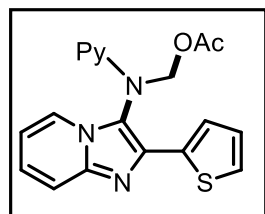
(**45h**): White solid; 147 mg, 69% yield; Eluent system: EtOAc:hexanes (25:75); mp = 144-146 °C; ^1H NMR (400 MHz, CDCl_3) δ = 8.40 (d, J = 5.0 Hz, 1H), 8.03 (d, J = 8.1 Hz, 2H), 7.84 (d, J = 6.9 Hz, 1H), 7.70 (d, J = 9.1 Hz, 1H), 7.62 (d, J = 8.1 Hz, 2H), 7.47 (t, J = 8.0 Hz, 1H), 7.30 (t, J = 7.8 Hz, 1H), 6.92 (t, J = 6.0 Hz, 1H), 6.82 (t, J = 6.8 Hz, 1H), 6.33 (d, J = 10.4 Hz, 1H), 6.26 (d, J = 8.4 Hz, 1H), 5.72 (d, J = 10.3 Hz, 1H), 1.88 (s, 3H); $^{13}\text{C}\{^1\text{H}\}$ NMR (100 MHz, CDCl_3) δ = 170.6, 155.2, 148.8, 143.3, 138.9, 138.2, 136.3, 129.9 (q, $^2J_{\text{C-F}}$ = 32 Hz), 127.0, 126.1, 125.6 (q, $^3J_{\text{C-F}}$ = 3.0 Hz), 124.1 (q, $^1J_{\text{C-F}}$ = 270 Hz), 122.6, 120.6, 118.3, 117.1, 112.9, 107.8, 74.0, 20.9; HRMS (ESI) m/z : $[\text{M} + \text{H}]^+$ Calcd for $\text{C}_{22}\text{H}_{18}\text{F}_3\text{N}_4\text{O}_2^+$ 427.1376; found 427.1359.

((2-(3-Methoxyphenyl)imidazo[1,2-a]pyridin-3-yl)(pyridin-2-yl)amino)methyl acetate (**45i**):



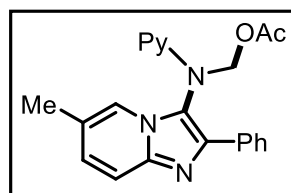
White solid; 87 mg, 45% yield; Eluent system: EtOAc:hexanes (30:70); mp = 97–99 °C; ^1H NMR (400 MHz, CDCl_3) δ 8.42 (d, J = 5.2 Hz, 1H), 7.87 (d, J = 6.8 Hz, 1H), 7.72 (d, J = 9.2 Hz, 1H), 7.52–7.46 (m, 3H), 7.32–7.27 (m, 2H), 6.94–6.87 (m, 2H), 6.82 (t, J = 6.8 Hz, 1H), 6.42 (d, J = 10.0 Hz, 1H), 6.28 (d, J = 8.4 Hz, 1H), 5.72 (d, J = 10.4 Hz, 1H), 3.77 (s, 3H), 1.92 (s, 3H); $^{13}\text{C}\{^1\text{H}\}$ NMR (100 MHz, CDCl_3) δ 170.6, 159.8, 155.6, 148.6, 143.1, 139.6, 138.8, 134.0, 129.7, 125.6, 122.5, 119.9, 119.2, 118.1, 116.9, 114.9, 112.6, 111.6, 108.0, 74.2, 55.2, 20.9; HRMS (ESI) m/z : $[\text{M} + \text{H}]^+$ Calcd for $\text{C}_{22}\text{H}_{21}\text{N}_4\text{O}_3^+$ 389.1608; found 389.1598.

(Pyridin-2-yl(2-(thiophen-2-yl)imidazo[1,2-a]pyridin-3-yl)amino)methyl acetate (**45j**): White



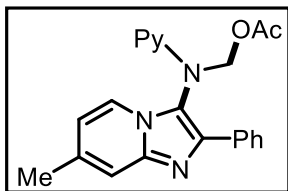
solid; 153 mg, 84% yield; Eluent system: EtOAc:hexanes (30:70); mp = 116–118 °C; ^1H NMR (400 MHz, CDCl_3) δ = 8.40 (d, J = 3.9 Hz, 1H), 7.87 (d, J = 6.7 Hz, 1H), 7.67 (d, J = 9.1 Hz, 1H), 7.46 (d, J = 3.2 Hz, 1H), 7.44–7.40 (m, 1H), 7.31–7.25 (m, 2H), 7.04 (dd, J = 4.8, 3.8 Hz, 1H), 6.89 (dd, J = 6.9, 5.2 Hz, 1H), 6.80 (t, J = 6.6 Hz, 1H), 6.54 (d, J = 10.3 Hz, 1H), 6.20 (d, J = 8.4 Hz, 1H), 5.68 (d, J = 10.3 Hz, 1H), 2.98 (unassigned impurity other than compound), 1.98 (s, 3H); $^{13}\text{C}\{^1\text{H}\}$ NMR (100 MHz, CDCl_3) δ = 170.6, 155.1, 148.5, 143.3, 138.7, 135.9, 135.3, 127.8, 126.0, 125.8, 124.9, 122.5, 118.5, 117.8, 117.0, 112.6, 108.0, 74.2, 21.1; HRMS (ESI) m/z : $[\text{M} + \text{H}]^+$ Calcd for $\text{C}_{19}\text{H}_{17}\text{N}_4\text{O}_2\text{S}^+$ 365.1067; found 365.1058.

((6-Methyl-2-phenylimidazo[1,2-a]pyridin-3-yl)(pyridin-2-yl)amino)methyl acetate (**45k**):



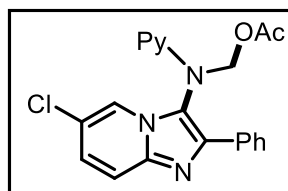
White solid; 164 mg, 88% yield; Eluent system: EtOAc:hexanes (25:75); mp = 169–171 °C; ^1H NMR (400 MHz, CDCl_3) δ = 8.42–8.40 (m, 1H), 7.89–7.86 (m, 2H), 7.60–7.56 (m, 2H), 7.46–7.42 (m, 1H), 7.37–7.33 (m, 2H), 7.30–7.25 (m, 1H, overlapped with CDCl_3 residual signal), 7.11 (dd, J = 9.2, 1.7 Hz, 1H), 6.92–6.89 (m, 1H), 6.33 (d, J = 10.3 Hz, 1H), 6.25 (dt, J = 8.4, 1.0 Hz, 1H), 5.75 (d, J = 10.2 Hz, 1H), 2.98 (unassigned impurity other than compound), 2.27 (s, 3H), 1.86 (s, 3H); $^{13}\text{C}\{^1\text{H}\}$ NMR (100 MHz, CDCl_3) δ = 170.6, 155.6, 148.6, 142.2, 139.5, 138.8, 132.8, 128.8, 128.6, 128.1, 126.7, 122.4, 120.0, 119.3, 117.4, 116.8, 108.0, 74.1, 20.9, 18.3; HRMS (ESI) m/z : $[\text{M} + \text{H}]^+$ Calcd for $\text{C}_{22}\text{H}_{21}\text{N}_4\text{O}_2^+$ 373.1659; found 373.1649.

((7-Methyl-2-phenylimidazo[1,2-a]pyridin-3-yl)(pyridin-2-yl)amino)methyl acetate (**45l**):



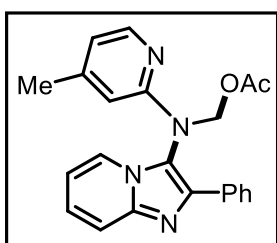
White solid; 158 mg, 85% yield; Eluent system: EtOAc:hexanes (25:75); mp = 163-165 °C; ^1H NMR (400 MHz, CDCl_3) δ = 8.41 (dd, J = 5.0, 1.8 Hz, 1H), 7.90 (d, J = 7.2 Hz, 2H), 7.72 (d, J = 6.9 Hz, 1H), 7.46-7.42 (m, 2H), 7.36 (t, J = 7.2 Hz, 2H), 7.29 (t, J = 7.2 Hz, 1H), 6.90 (dd, J = 7.3, 5.0 Hz, 1H), 6.62 (dd, J = 7.0, 1.6 Hz, 1H), 6.42 (d, J = 10.2 Hz, 1H), 6.26 (d, J = 8.4 Hz, 1H), 5.67 (d, J = 10.2 Hz, 1H), 2.43 (s, 3H), 1.90 (s, 3H); ^{13}C $\{^1\text{H}\}$ NMR (100 MHz, CDCl_3) δ = 170.7, 155.6, 148.5, 143.6, 139.3, 138.7, 136.6, 132.8, 128.6, 128.1, 126.7, 121.8, 119.2, 116.8, 116.4, 115.1, 108.0, 74.3, 21.4, 21.0; HRMS (ESI) m/z : $[\text{M} + \text{H}]^+$ Calcd for $\text{C}_{22}\text{H}_{21}\text{N}_4\text{O}_2^+$ 373.1659; found 373.1645.

((6-Chloro-2-phenylimidazo[1,2-a]pyridin-3-yl)(pyridin-2-yl)amino)methyl acetate (**45m**):



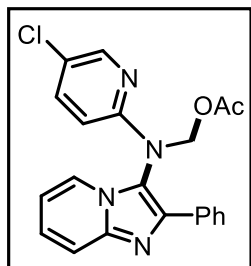
White solid; 161 mg, 82% yield; Eluent system: EtOAc:hexanes (25:75); mp = 170-172 °C; ^1H NMR (400 MHz, CDCl_3) δ = 8.41 (d, J = 4.0 Hz, 1H), 7.89-7.86 (m, 3H), 7.62 (d, J = 9.5 Hz, 1H), 7.48 (t, J = 8.2 Hz, 1H), 7.38-7.29 (m, 3H), 7.23 (dd, J = 9.5, 2.0 Hz, 1H), 6.93 (t, J = 6.1 Hz, 1H), 6.40 (d, J = 10.4 Hz, 1H), 6.27 (d, J = 8.4 Hz, 1H), 5.64 (d, J = 10.3 Hz, 1H), 1.91 (s, 3H); ^{13}C $\{^1\text{H}\}$ NMR (100 MHz, CDCl_3) δ = 170.6, 155.1, 148.7, 141.5, 140.7, 138.9, 132.3, 128.7, 128.5, 127.0, 126.8, 121.0, 120.5, 120.2, 118.4, 117.2, 107.8, 74.1, 20.9; HRMS (ESI) m/z : $[\text{M} + \text{H}]^+$ Calcd for $\text{C}_{21}\text{H}_{18}\text{ClN}_4\text{O}_2^+$ 393.1113; found 393.1110.

((4-Methylpyridin-2-yl)(2-phenylimidazo[1,2-a]pyridin-3-yl)amino)methyl acetate (**45n**):



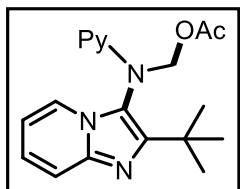
White solid; 165.5 mg, 89% yield; Eluent system: EtOAc:hexanes (25:75); mp = 156-158 °C; ^1H NMR (400 MHz, CDCl_3) δ = 8.25 (d, J = 5.1 Hz, 1H), 7.92-7.90 (m, 2H), 7.82 (dt, J = 6.8, 1.2 Hz, 1H), 7.69 (d, J = 9.0 Hz, 1H), 7.38-7.34 (m, 2H), 7.31-7.24 (m, 2H, overlapped with CDCl_3 residual signal), 6.77 (td, J = 6.8, 0.8 Hz, 1H), 6.72 (d, J = 5.0 Hz, 1H), 6.37 (d, J = 10.2 Hz, 1H), 6.06 (s, 1H), 5.66 (d, J = 10.3 Hz, 1H), 2.10 (s, 3H), 1.86 (s, 3H) ppm; ^{13}C $\{^1\text{H}\}$ NMR (100 MHz, CDCl_3) δ = 170.6, 155.7, 150.2, 148.2, 143.2, 139.6, 132.7, 128.6, 128.2, 126.8, 125.6, 122.6, 119.9, 118.4, 118.0, 112.5, 108.1, 74.4, 21.2, 20.9 ppm; HRMS (ESI) m/z : $[\text{M} + \text{H}]^+$ Calcd for $\text{C}_{22}\text{H}_{21}\text{N}_4\text{O}_2^+$ 373.1659; found 373.1670.

((5-Chloropyridin-2-yl)(2-phenylimidazo[1,2-a]pyridin-3-yl)amino)methyl acetate (45o):



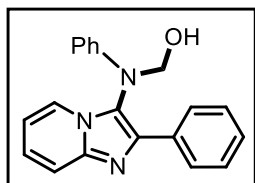
White solid; 170.5 mg, 87% yield; Eluent system: EtOAc:hexanes (25:75); mp = 156-158 °C; ^1H NMR (400 MHz, CDCl_3) δ = 8.32 (d, J = 2.5 Hz, 1H), 7.87 (d, J = 7.8 Hz, 2H), 7.81 (d, J = 6.8 Hz, 1H), 7.69 (d, J = 9.1 Hz, 1H), 7.41-7.27 (m, 5H), 6.80 (t, J = 6.8 Hz, 1H), 6.33 (d, J = 10.3 Hz, 1H), 6.21 (d, J = 8.8 Hz, 1H), 5.63 (d, J = 10.3 Hz, 1H), 1.88 (s, 3H); $^{13}\text{C}\{^1\text{H}\}$ NMR (100 MHz, CDCl_3) δ = 170.5, 153.9, 147.1, 143.2, 139.7, 138.5, 132.5, 128.7, 128.4, 126.8, 125.8, 124.4, 122.4, 119.3, 118.1, 112.7, 108.9, 74.3, 20.9; HRMS (ESI) m/z : $[\text{M} + \text{H}]^+$ Calcd for $\text{C}_{21}\text{H}_{18}\text{ClN}_4\text{O}_2^+$ 393.1113; found 393.1100.

((2-(tert-Butyl)imidazo[1,2-a]pyridin-3-yl)(pyridin-2-yl)amino)methyl acetate (45p): White



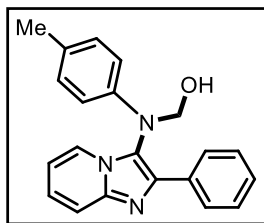
solid; 71 mg, 42% yield; Eluent system: EtOAc:hexanes (40:60); mp = 126–128 °C; ^1H NMR (400 MHz, CDCl_3) δ 8.36 (d, J = 4.0 Hz, 1H), 7.86 (d, J = 6.8 Hz, 1H), 7.64 (d, J = 9.2 Hz, 1H), 7.45–7.40 (m, 1H), 7.22 (t, J = 8.0 Hz, 1H), 6.86 (dd, J = 7.2, 5.0 Hz, 1H), 6.73 (t, J = 6.8 Hz, 1H), 6.63 (d, J = 10.0 Hz, 1H), 6.04 (d, J = 8.4 Hz, 1H), 5.52 (d, J = 10.4 Hz, 1H), 2.06 (s, 3H), 1.41 (s, 9H); $^{13}\text{C}\{^1\text{H}\}$ NMR (100 MHz, CDCl_3) δ 170.7, 155.9, 150.0, 148.3, 142.3, 138.3, 125.0, 122.6, 119.0, 117.6, 116.4, 111.8, 108.1, 76.0, 33.3, 30.0, 21.2; HRMS (ESI) m/z : $[\text{M} + \text{H}]^+$ Calcd for $\text{C}_{19}\text{H}_{23}\text{N}_4\text{O}_2^+$ 339.1816; found 339.1425.

(Phenyl(2-phenylimidazo[1,2-a]pyridin-3-yl)amino)methanol (49a): White solid; 119 mg, 75%



yield; Eluent system: EtOAc:hexanes (35:65); mp = 135-137 °C; ^1H NMR (400 MHz, CDCl_3) δ 7.86 (d, J = 7.4 Hz, 2H), 7.79 (d, J = 6.8 Hz, 1H), 7.45 (d, J = 9.0 Hz, 1H), 7.26 – 7.22 (m, 5H), 7.10 (dd, J = 9.1, 6.6 Hz, 1H), 6.93 (t, J = 7.3 Hz, 1H), 6.85 (d, J = 8.2 Hz, 2H), 6.62 (t, J = 6.7 Hz, 1H), 5.37 (d, J = 11.5 Hz, 1H), 5.13 (d, J = 11.2 Hz, 1H); $^{13}\text{C}\{^1\text{H}\}$ NMR (100 MHz, CDCl_3): δ 145.0, 142.5, 138.4, 132.6, 129.8, 128.6, 128.0, 126.6, 125.4, 123.1, 122.1, 120.6, 117.2, 114.4, 112.3, 76.1; HRMS (ESI) m/z : $[\text{M} + \text{H}]^+$ Calcd for $\text{C}_{20}\text{H}_{18}\text{N}_3\text{O}^+$ 316.1444; found 316.1431.

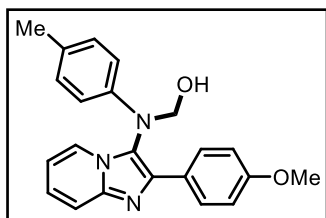
((2-Phenylimidazo[1,2-a]pyridin-3-yl)(p-tolyl)amino)methanol (**49b**): Off-white solid; 119



mg, 72% yield; Eluent system: EtOAc:hexanes (35:65); mp = 140-142 °C; ^1H NMR (400 MHz, CDCl_3) δ 7.92 (d, J = 7.3 Hz, 2H), 7.83 (d, J = 6.8 Hz, 1H), 7.53 (d, J = 9.1 Hz, 1H), 7.34 – 7.25 (m, 3H), 7.16 – 7.13 (m, 1H), 7.07 (d, J = 8.0 Hz, 2H), 6.78 (d, J = 8.1 Hz, 2H), 6.67 – 6.63 (m, 1H), 5.34 (s, 1H), 5.14 (s, 1H), 2.29 (s, 3H); $^{13}\text{C}\{^1\text{H}\}$ NMR (100

MHz, CDCl_3) δ 142.6, 138.6, 132.9, 130.3, 130.0, 128.0, 127.1, 126.6, 125.3, 123.2, 122.4, 117.4, 114.3, 113.5, 112.3, 76.5, 20.4; HRMS (ESI) m/z : $[\text{M} + \text{H}]^+$ Calcd for $\text{C}_{21}\text{H}_{20}\text{N}_3\text{O}^+$ 330.1601; found 330.1599.

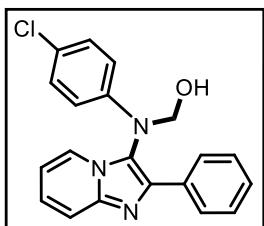
((2-(4-Methoxyphenyl)imidazo[1,2-a]pyridin-3-yl)(p-tolyl)amino)methanol (**49c**): White solid;



140 mg, 78% yield; Eluent system: EtOAc:hexanes (40:60); mp = 118-120 °C; ^1H NMR (400 MHz, CDCl_3) δ 7.88 – 7.86 (m, 2H), 7.82 (dt, J = 6.8, 1.2 Hz, 1H), 7.54 (dt, J = 9.0, 1.1 Hz, 1H), 7.16 (ddd, J = 9.0, 6.7, 1.3 Hz, 1H), 7.09 – 7.04 (m, 2H), 6.89 – 6.84 (m, 2H), 6.80 – 6.75 (m, 2H), 6.67 (td, J = 6.8, 1.1 Hz, 1H), 5.32 (s,

1H), 5.16 (s, 1H), 3.81 (s, 3H), 2.29 (s, 3H); $^{13}\text{C}\{^1\text{H}\}$ NMR (100 MHz, CDCl_3) δ 159.5, 142.6, 142.5, 138.7, 130.3, 129.9, 128.0, 125.5, 125.1, 122.9, 121.5, 117.3, 114.2, 114.1, 112.1, 76.2, 55.2, 20.4; HRMS (ESI) m/z : $[\text{M} + \text{H}]^+$ Calcd for $\text{C}_{22}\text{H}_{22}\text{N}_3\text{O}_2^+$ 360.1707; found 360.1693.

((4-Chlorophenyl)(2-phenylimidazo[1,2-a]pyridin-3-yl)amino)methanol (**49d**): White solid;



124 mg, 71% yield; Eluent system: EtOAc:hexanes (45:55); mp = 173–175 °C; ^1H NMR (400 MHz, CDCl_3) δ 7.84–7.82 (m, 2H), 7.77 (dd, J = 6.6, 1.4 Hz, 1H), 7.50–7.46 (m, 1H), 7.26–7.24 (m, 3H), 7.20–7.12 (m, 3H), 6.77 (d, J = 8.8 Hz, 2H), 6.67 (t, J = 6.8 Hz, 1H), 5.30 (d, J = 11.6 Hz, 1H), 5.12 (d, J = 11.6 Hz, 1H); $^{13}\text{C}\{^1\text{H}\}$ NMR (100 MHz, CDCl_3) δ

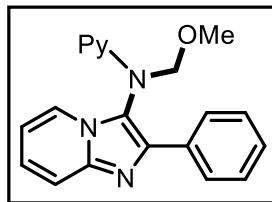
143.7, 142.6, 138.6, 132.4, 129.6, 128.6, 128.2, 126.5, 125.7, 125.5, 122.8, 121.6, 117.4, 115.6, 112.5, 76.2; HRMS (ESI) m/z : $[\text{M} + \text{H}]^+$ Calcd for $\text{C}_{20}\text{H}_{17}\text{ClN}_3\text{O}^+$ 350.1055; found 350.1051.

1.4.3 Experimental Procedure for the Preparation of Alkoxy Product (47 or 50).

To a solution of **44** or **48** (0.5 mmol; 1 equiv.) in alcohol (5 mL) was added $\text{PhI}(\text{OAc})_2$ (1.5 equiv.) at room temperature and the reaction mixture was stirred at 50 °C for 3 h. After completion of the reaction, alcohol was evaporated under vacuum. The resulting crude solid was

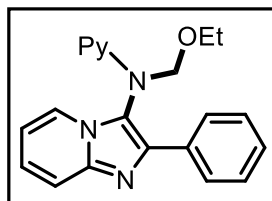
purified by column chromatography (silica gel 60-120 mesh) using EtOAc-*hexanes* as an eluent to afford **47** or **50**.

N-(Methoxymethyl)-2-phenyl-*N*-(pyridin-2-yl)imidazo[1,2-*a*]pyridin-3-amine (**47aa**): White



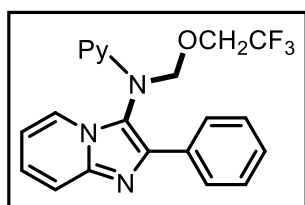
solid; 148.5 mg, 90% yield; Eluent system: EtOAc:hexanes (35:65); mp = 116-117 °C; ^1H NMR (400 MHz, CDCl_3) δ = 8.39 (d, J = 3.2 Hz, 1H), 7.97-7.94 (m, 3H), 7.68 (d, J = 9.1 Hz, 1H), 7.44-7.37 (m, 3H), 7.33-7.25 (m, 2H), 6.85 (dd, J = 6.7, 5.3 Hz, 1H), 6.78 (t, J = 6.6 Hz, 1H), 6.22 (d, J = 8.4 Hz, 1H), 5.94 (d, J = 9.5 Hz, 1H), 4.72 (d, J = 9.5 Hz, 1H), 3.36 (s, 3H); ^{13}C $\{^1\text{H}\}$ NMR (100 MHz, CDCl_3) δ = 156.2, 148.6, 143.1, 138.7, 138.5, 133.0, 128.7, 128.1, 126.6, 125.4, 123.2, 121.1, 117.7, 116.1, 112.3, 107.8, 82.0, 56.6; HRMS (ESI) m/z : $[\text{M} + \text{H}]^+$ Calcd for $\text{C}_{20}\text{H}_{19}\text{N}_4\text{O}^+$ 331.1553; found 331.1554.

N-(Ethoxymethyl)-2-phenyl-*N*-(pyridin-2-yl)imidazo[1,2-*a*]pyridin-3-amine (**47ab**): White



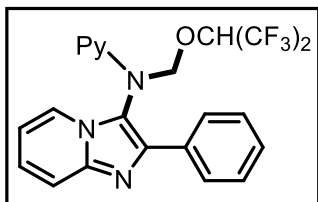
solid; 136 mg, 79% yield; Eluent system: EtOAc:hexanes (32:68); mp = 120-122 °C; ^1H NMR (400 MHz, CDCl_3) δ = 8.36-8.34 (m, 1H), 7.94-7.91 (m, 3H), 7.66 (d, J = 9.1 Hz, 1H), 7.41-7.34 (m, 3H), 7.31-7.22 (m, 2H, overlapped with CDCl_3 residual signal), 6.82 (dd, J = 6.6, 5.1 Hz, 1H), 6.75 (td, J = 6.7, 1.2 Hz, 1H), 6.20 (d, J = 8.6 Hz, 1H), 5.98 (d, J = 10.0 Hz, 1H), 4.78 (d, J = 9.9 Hz, 1H), 3.63-3.55 (m, 1H), 3.55-3.45 (m, 1H), 1.08 (t, J = 7.0 Hz, 3H); ^{13}C $\{^1\text{H}\}$ NMR (100 MHz, CDCl_3) δ = 156.4, 148.5, 143.1, 138.7, 138.5, 133.0, 128.6, 128.0, 126.7, 125.4, 123.3, 121.1, 117.7, 116.0, 112.1, 107.7, 80.0, 64.8, 15.2; HRMS (ESI) m/z : $[\text{M} + \text{H}]^+$ Calcd for $\text{C}_{21}\text{H}_{21}\text{N}_4\text{O}^+$ 345.1710; found 345.1715.

2-Phenyl-*N*-(pyridin-2-yl)-*N*-((2,2,2-trifluoroethoxy)methyl)imidazo[1,2-*a*]pyridin-3-amine



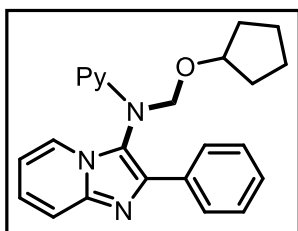
(**47ac**): Colorless viscous oil; 132 mg, 78% yield; Eluent system: EtOAc:hexanes (35:65); ^1H NMR (400 MHz, CDCl_3) δ = 8.29-8.27 (m, 1H), 7.81 (d, J = 7.0 Hz, 3H), 7.59 (d, J = 9.1 Hz, 1H), 7.35-7.26 (m, 3H), 7.23-7.15 (m, 2H), 6.78 (dd, J = 7.0, 5.2 Hz, 1H), 6.69 (t, J = 6.8 Hz, 1H), 6.11 (d, J = 8.4 Hz, 1H), 5.97 (d, J = 10.1 Hz, 1H), 4.94 (d, J = 10.1 Hz, 1H), 4.05 (q, J = 8.8 Hz, 2H); ^{13}C $\{^1\text{H}\}$ NMR (100 MHz, CDCl_3) δ = 155.8, 148.4, 143.2, 139.1, 138.8, 132.8, 128.7, 128.2, 126.7, 125.7, 123.9 (q, $^1J_{\text{C-F}}$ = 278 Hz), 122.9, 120.3, 117.8, 116.7, 112.5, 107.9, 81.7, 67.4 (q, $^2J_{\text{C-F}}$ = 34 Hz); HRMS (ESI) m/z : $[\text{M} + \text{H}]^+$ Calcd for $\text{C}_{21}\text{H}_{18}\text{F}_3\text{N}_4\text{O}^+$ 339.1427; found 339.1425.

N-(((1,1,1,3,3,3-Hexafluoropropan-2-yl)oxy)methyl)-2-phenyl-*N*-(pyridin-2-yl)imidazo[1,2-



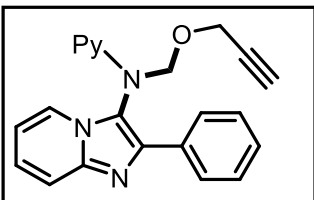
a]pyridin-3-amine (**47ad**): White solid; 196 mg, 84% yield; Eluent system: EtOAc:hexanes (35:65); mp = 151-153 °C; ^1H NMR (400 MHz, CDCl_3) δ = 8.41-8.39 (m, 1H), 7.91-7.88 (m, 3H), 7.70 (d, J = 9.1 Hz, 1H), 7.49-7.45 (m, 1H), 7.42-7.27 (m, 4H), 6.96-6.92 (m, 1H), 6.80 (td, J = 6.8, 1.2 Hz, 1H), 6.23-6.20 (m, 2H), 5.55 (sept, J = 6.1 Hz, 1H), 5.16 (d, J = 10.8 Hz, 1H); ^{13}C { ^1H } NMR (100 MHz, CDCl_3) δ = 155.1, 148.1, 143.3, 139.1, 139.0, 132.6, 128.8, 128.3, 126.6, 125.9, 122.94, 122.93, 121.8 (q, $^1J_{\text{C-F}}$ = 282 Hz), 119.8, 117.8, 117.1, 112.7, 108.1, 83.9, 75.8 (p, $^1J_{\text{C-F}}$ = 32 Hz); HRMS (ESI) m/z : $[\text{M} + \text{H}]^+$ Calcd for $\text{C}_{22}\text{H}_{17}\text{F}_6\text{N}_4\text{O}^+$ 467.1301; found 467.1294.

N-((Cyclopentyloxy)methyl)-2-phenyl-*N*-(pyridin-2-yl)imidazo[1,2-*a*]pyridin-3-amine (**47ae**):



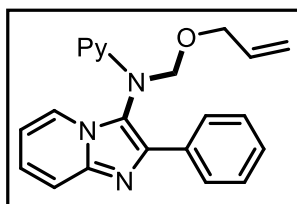
Colorless semi-solid; 107.5 mg, 56% yield; Eluent system: EtOAc:hexanes (30:70); ^1H NMR (400 MHz, CDCl_3) δ = 8.33(dd, J = 5.0, 1.8 Hz, 1H), 7.96-7.93 (m, 3H), 7.65 (dt, J = 9.0, 1.2 Hz, 1H), 7.41-7.34 (m, 3H), 7.30-7.21 (m, 2H, overlapped with CDCl_3 residual signal), 6.80 (dd, J = 7.2, 5.0 Hz, 1H), 6.73 (td, J = 6.8, 0.9 Hz, 1H), 6.20 (d, J = 8.4 Hz, 1H), 5.99 (d, J = 9.8 Hz, 1H), 4.74 (d, J = 9.8 Hz, 1H), 4.07-4.03 (m, 1H), 1.65-1.41 (m, 8H); ^{13}C { ^1H } NMR (100 MHz, CDCl_3) δ = 156.4, 148.5, 143.1, 138.7, 138.4, 133.1, 128.6, 128.0, 126.7, 125.4, 123.6, 121.2, 117.6, 115.9, 111.9, 107.7, 79.7, 78.2, 32.6, 32.3, 23.5, 23.4; HRMS (ESI) m/z : $[\text{M} + \text{H}]^+$ Calcd for $\text{C}_{24}\text{H}_{25}\text{N}_4\text{O}^+$ 385.2023; found 385.2012.

2-Phenyl-*N*-((prop-2-yn-1-yloxy)methyl)-*N*-(pyridin-2-yl)imidazo[1,2-*a*]pyridin-3-amine



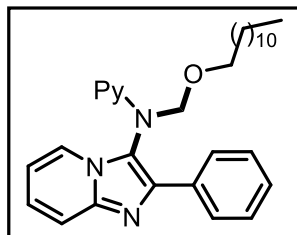
(**47ag**): White solid; 134.5 mg, 76% yield; Eluent system: EtOAc:hexanes (25:75); mp = 105-107 °C; ^1H NMR (400 MHz, CDCl_3) δ = 8.36 (d, J = 4.0 Hz, 1H), 7.96-7.91 (m, 3H), 7.70 (d, J = 8.9 Hz, 1H), 7.44-7.35 (m, 3H), 7.32-7.27 (m, 2H), 6.86-6.83 (m, 1H), 6.78 (t, J = 6.6 Hz, 1H), 6.24 (d, J = 8.4 Hz, 1H), 6.05 (d, J = 10.0 Hz, 1H), 4.89 (d, J = 10.0 Hz, 1H), 4.33-4.23 (m, 2H), 2.30 (t, J = 2.4 Hz, 1H); ^{13}C { ^1H } NMR (100 MHz, CDCl_3) δ = 156.0, 148.5, 142.9, 138.6, 128.7, 128.2, 126.7, 125.93, 125.90, 123.4, 120.8, 117.5, 116.4, 112.5, 107.8, 79.8, 79.3, 74.4, 56.5; HRMS (ESI) m/z : $[\text{M} + \text{H}]^+$ Calcd for $\text{C}_{22}\text{H}_{19}\text{N}_4\text{O}^+$ 355.1553; found 355.1556.

N-((Allyloxy)methyl)-2-phenyl-*N*-(pyridin-2-yl)imidazo[1,2-*a*]pyridin-3-amine (**47ah**): White



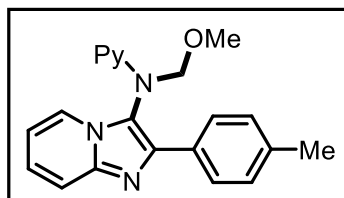
solid; 94 mg, 53% yield; Eluent system: EtOAc:hexanes (25:75); mp = 65-67 °C; ^1H NMR (400 MHz, CDCl_3) δ = 8.38 (s, 1H), 7.95 (d, J = 3.4 Hz, 3H), 7.69 (d, J = 9.1 Hz, 1H), 7.44-7.25 (m, 4H, overlapped with CDCl_3 residual signal), 6.86-6.75 (m, 2H), 6.23 (d, J = 8.5 Hz, 1H), 6.02 (d, J = 9.9 Hz, 1H), 5.85-5.76 (m, 1H), 5.17-5.07 (m, 2H), 4.83 (d, J = 9.9 Hz, 1H), 4.09 (s, 2H); $^{13}\text{C}\{^1\text{H}\}$ NMR (100 MHz, CDCl_3) δ = 156.3, 148.5, 143.1, 138.8, 138.5, 134.3, 133.0, 128.7, 128.0, 126.7, 125.4, 123.3, 121.0, 117.7, 116.8, 116.1, 112.2, 107.8, 79.7, 70.0; HRMS (ESI) m/z : $[\text{M} + \text{H}]^+$ Calcd for $\text{C}_{22}\text{H}_{21}\text{N}_4\text{O}^+$ 357.1710; found 357.1725.

N-((Dodecyloxy)methyl)-2-phenyl-*N*-(pyridin-2-yl)imidazo[1,2-*a*]pyridin-3-amine (**47ai**): Yellow



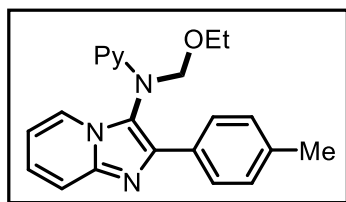
oil; 85 mg, 35% yield; Eluent system: EtOAc:hexanes (20:80); ^1H NMR (400 MHz, CDCl_3) δ = 8.35-8.33 (m, 1H), 7.94-7.91 (m, 3H), 7.66 (dt, J = 9.0, 1.2 Hz, 1H), 7.42-7.34 (m, 3H), 7.31-7.22 (m, 2H, overlapped with CDCl_3 residual signal), 6.83-6.80 (m, 1H), 6.74 (td, J = 6.7, 1.1 Hz, 1H), 6.22 (d, J = 8.6 Hz, 1H), 5.95 (d, J = 9.8 Hz, 1H), 4.77 (d, J = 9.8 Hz, 1H), 3.54-3.48 (m, 1H), 3.42-3.47 (m, 1H), 1.61-1.52 (m, 2H), 1.44 (t, J = 6.5 Hz, 2H), 1.25 (br s, 16H), 0.88-0.85 (m, 3H); $^{13}\text{C}\{^1\text{H}\}$ NMR (100 MHz, CDCl_3) δ = 156.4, 148.5, 143.1, 138.7, 138.4, 133.0, 128.6, 128.0, 126.7, 125.4, 123.4, 121.2, 117.6, 116.0, 112.1, 107.7, 80.3, 69.4, 31.9, 29.7, 29.66, 29.63, 29.61, 29.5, 29.4, 29.38, 29.35, 26.0, 22.6, 14.1; HRMS (ESI) m/z : $[\text{M} + \text{H}]^+$ Calcd for $\text{C}_{31}\text{H}_{41}\text{N}_4\text{O}^+$ 485.3275; found 485.3243.

N-(Methoxymethyl)-*N*-(pyridin-2-yl)-2-(*p*-tolyl)imidazo[1,2-*a*]pyridin-3-amine (**47ba**): White



solid; 158 mg, 92% yield; Eluent system: EtOAc:hexanes (35:65); mp = 126-128 °C; ^1H NMR (400 MHz, CDCl_3) δ = 8.36-8.34 (m, 1H), 7.92 (dt, J = 6.8, 1.2 Hz, 1H), 7.82 (d, J = 8.2 Hz, 2H), 7.66 (d, J = 9.0, 1H), 7.39 (m, 1H), 7.26-7.22 (m, 1H, overlapped with CDCl_3 residual signal), 7.17 (d, J = 8.0 Hz, 2H), 6.83-6.80 (m, 1H), 6.75 (td, J = 6.8, 1.2 Hz, 1H), 6.19 (d, J = 8.4 Hz, 1H), 5.91 (d, J = 9.6 Hz, 1H), 4.69 (d, J = 9.6 Hz, 1H), 3.34 (s, 3H), 2.33 (s, 3H); $^{13}\text{C}\{^1\text{H}\}$ NMR (100 MHz, CDCl_3): δ = 156.2, 148.5, 142.9, 138.6, 138.5, 138.0, 130.0, 129.4, 126.5, 125.5, 123.2, 120.8, 117.5, 116.1, 112.3, 107.8, 81.9, 56.6, 21.3; HRMS (ESI) m/z : $[\text{M} + \text{H}]^+$ Calcd for $\text{C}_{21}\text{H}_{21}\text{N}_4\text{O}^+$ 345.1710 found 345.1711.

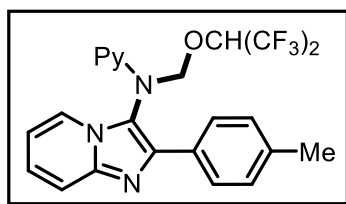
N-(Ethoxymethyl)-*N*-(pyridin-2-yl)-2-(*p*-tolyl)imidazo[1,2-*a*]pyridin-3-amine (**47bb**): White



solid; 143 mg, 80% yield; Eluent system: EtOAc:hexanes (35:65); mp = 150-152 °C; ^1H NMR (400 MHz, CDCl_3) δ = 8.35-8.33 (m, 1H), 7.92 (d, J = 6.8 Hz, 1H), 7.83 (d, J = 8.2 Hz, 2H), 7.68 (d, J = 9.0 Hz, 1H), 7.41-7.36 (m, 1H), 7.27-7.22 (m, 1H,

overlapped with CDCl_3 residual signal), 7.17 (d, J = 7.9 Hz, 2H), 6.82-6.79 (m, 1H), 6.75 (td, J = 6.8, 1.1 Hz, 1H), 6.20 (d, J = 8.6 Hz, 1H), 5.98 (d, J = 9.9 Hz, 1H), 4.76 (d, J = 9.9 Hz, 1H), 3.63-3.55 (m, 1H), 3.53-3.45 (m, 1H), 2.33 (s, 3H), 1.08 (t, J = 7.1 Hz, 3H); $^{13}\text{C}\{^1\text{H}\}$ NMR (100 MHz, CDCl_3) δ = 156.3, 148.5, 142.9, 138.5, 138.4, 138.0, 129.9, 129.4, 126.5, 125.5, 123.3, 120.8, 117.5, 116.0, 112.2, 107.7, 80.0, 64.7, 21.3, 15.2; HRMS (ESI) m/z : $[\text{M} + \text{H}]^+$ Calcd for $\text{C}_{22}\text{H}_{23}\text{N}_4\text{O}^+$ 359.1866; found 359.1878.

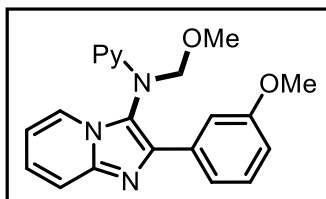
N-(((1,1,1,3,3,3-Hexafluoropropan-2-yl)oxy)methyl)-*N*-(pyridin-2-yl)-2-(*p*-tolyl)imidazo[1,2-



a]pyridin-3-amine (**47bd**): White solid; 194 mg, 81% yield; Eluent system: EtOAc:hexanes (35:65); mp = 154-156 °C; ^1H NMR (400 MHz, CDCl_3) δ = 8.38-8.36 (m, 1H), 7.85 (d, J = 6.8 Hz, 1H), 7.76 (d, J = 8.2 Hz, 2H), 7.66 (d, J = 9.0 Hz, 1H), 7.46-7.41

(m, 1H), 7.28-7.24 (m, 1H, overlapped with CDCl_3 residual signal), 7.18 (d, J = 7.8 Hz, 2H), 6.92-6.89 (m, 1H), 6.77 (td, J = 6.8, 1.2 Hz, 1H), 6.20-6.17 (m, 2H), 5.52 (sept, J = 6.1 Hz, 1H), 5.12 (d, J = 10.7 Hz, 1H), 2.34 (s, 3H); $^{13}\text{C}\{^1\text{H}\}$ NMR (100 MHz, CDCl_3) δ = 155.1, 148.0, 143.3, 139.2, 139.0, 138.3, 129.8, 129.5, 126.5, 125.8, 122.87, 122.86, 121.8 (q, $^1J_{\text{C-F}}$ = 281 Hz), 119.4, 117.7, 117.0, 112.5, 108.2, 83.9, 75.8 (p, $^2J_{\text{C-F}}$ = 32 Hz), 21.3; HRMS (ESI) m/z : $[\text{M} + \text{H}]^+$ Calcd for $\text{C}_{23}\text{H}_{19}\text{F}_6\text{N}_4\text{O}^+$ 481.1458; found 481.1438.

N-(Methoxymethyl)-2-(3-methoxyphenyl)-*N*-(pyridin-2-yl)imidazo[1,2-*a*]pyridin-3-amine

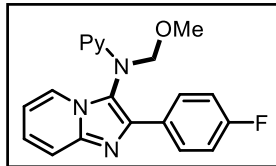


(**47ia**): Off-white solid; 88 mg, 49% yield; EtOAc:hexanes (40:60); mp = 136-138 °C; ^1H NMR (400 MHz, CDCl_3) δ 8.38 (dd, J = 4.8, 2.0 Hz, 1H), 7.97 (d, J = 6.8 Hz, 1H), 7.69 (d, J = 8.8 Hz, 1H), 7.56-7.51 (m, 2H), 7.45-7.41 (m, 1H), 7.31-7.26 (m, 2H, overlapped with the CDCl_3 residual signal), 6.89-6.84 (m, 2H), 6.79 (t, J = 6.8 Hz, 1H), 6.23 (d, J = 8.4 Hz, 1H), 5.94 (d, J = 9.6 Hz, 1H), 4.75 (d, J = 9.6 Hz, 1H), 3.78 (s, 3H), 3.38 (s, 3H);

$^{13}\text{C}\{^1\text{H}\}$ NMR (100 MHz, CDCl_3) δ 159.9, 156.3, 148.6, 143.0, 138.6, 138.5, 134.3, 129.7,

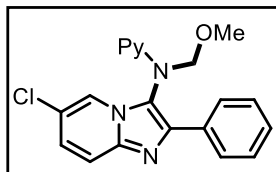
125.5, 123.2, 121.3, 119.1, 117.8, 116.2, 114.7, 112.4, 111.4, 107.8, 82.0, 56.6, 55.2; HRMS (ESI) m/z : $[M + H]^+$ Calcd for $C_{21}H_{21}N_4O_2^+$ 361.1659; found 361.1648.

2-(4-Fluorophenyl)-N-(methoxymethyl)-N-(pyridin-2-yl)imidazo[1,2-a]pyridin-3-amine



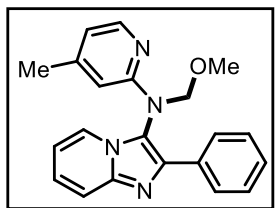
(47da): White solid; 136 mg, 78% yield; Eluent system: EtOAc:hexanes (35:65); mp = 168-170 °C; 1H NMR (400 MHz, $CDCl_3$) δ = 8.34 (d, J = 4.0 Hz, 1H), 7.92-7.88 (m, 3H), 7.64 (d, J = 9.0 Hz, 1H), 7.39 (t, J = 7.2 Hz, 1H), 7.24 (t, J = 8.0 Hz, 1H, overlapped with $CDCl_3$ residual signal), 7.04 (t, J = 8.6 Hz, 2H), 6.82 (t, J = 5.4 Hz, 1H), 6.75 (t, J = 6.7 Hz, 1H), 6.19 (d, J = 8.4 Hz, 1H), 5.84 (d, J = 9.5 Hz, 1H), 4.73 (d, J = 9.5 Hz, 1H), 3.34 (s, 3H); $^{13}C\{^1H\}$ NMR (100 MHz, $CDCl_3$) δ = 162.6 (d, $^1J_{C-F}$, 246 Hz), 156.1, 148.6, 143.1, 138.5, 138.0, 129.2 (d, $^3J_{C-F}$, 3 Hz), 128.5 (d, $^3J_{C-F}$, 8 Hz), 125.6, 123.2, 120.8, 117.6, 116.3, 115.6 (d, $^2J_{C-F}$, 22 Hz), 112.4, 107.7, 81.8, 56.6; HRMS (ESI) m/z : $[M + H]^+$ Calcd for $C_{20}H_{18}FN_4O^+$ 349.1459; found 349.1475.

6-Chloro-N-(methoxymethyl)-2-phenyl-N-(pyridin-2-yl)imidazo[1,2-a]pyridin-3-amine (47la):



White solid; 135 mg, 74% yield; Eluent system: EtOAc:hexanes (35:65); mp = 180-182 °C; 1H NMR (400 MHz, $CDCl_3$) δ = 8.37-8.35 (m, 1H), 7.99 (d, J = 1.4 Hz, 1H), 7.90 (d, J = 7.2 Hz, 2H), 7.60 (d, J = 9.5 Hz, 1H), 7.45-7.41 (m, 1H), 7.38-7.34 (m, 2H), 7.32-7.28 (m, 1H), 7.20 (dd, J = 9.5, 1.9 Hz, 1H), 6.86 (dd, J = 6.8, 5.1, 1H), 6.22 (d, J = 8.7 Hz, 1H), 5.89 (d, J = 9.5 Hz, 1H), 4.67 (d, J = 9.5 Hz, 1H), 3.37 (s, 3H); $^{13}C\{^1H\}$ NMR (100 MHz, $CDCl_3$) δ = 155.9, 148.7, 141.4, 139.7, 138.7, 132.5, 128.8, 128.4, 126.9, 126.6, 121.6, 121.2, 120.8, 118.1, 116.5, 107.6, 81.8, 56.5; HRMS (ESI) m/z : $[M + H]^+$ Calcd for $C_{20}H_{18}ClN_4O^+$ 365.1164; found 365.1173.

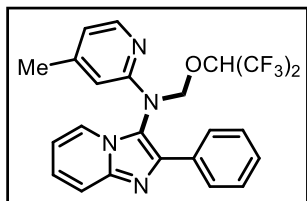
N-(Methoxymethyl)-N-(4-methylpyridin-2-yl)-2-phenylimidazo[1,2-a]pyridin-3-amine (47na):



White solid; 153 mg, 89% yield; Eluent system: EtOAc:hexanes (35:65); mp = 162-164 °C; 1H NMR (400 MHz, $CDCl_3$) δ = 8.20 (d, J = 5.1 Hz, 1H), 7.95-7.90 (m, 3H), 7.69 (dt, J = 9.0, 1.1 Hz, 1H), 7.38-7.34 (m, 2H), 7.31-7.23 (m, 2H, overlapped with $CDCl_3$ residual signal), 6.76 (td, J = 6.8, 1.0 Hz, 1H), 6.66 (d, J = 5.1 Hz, 1H), 6.03 (s, 1H), 5.89 (d, J = 9.6 Hz, 1H), 4.66 (d, J = 9.6 Hz, 1H), 3.31 (s, 3H), 2.09 (s, 3H); $^{13}C\{^1H\}$ NMR (100 MHz, $CDCl_3$) δ = 156.4, 149.8, 148.2, 142.9, 138.3, 132.8, 128.7, 128.1, 126.6, 125.7,

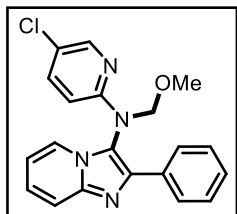
123.3, 121.3, 117.7, 117.5, 112.4, 108.0, 82.1, 56.5, 21.2; HRMS (ESI) m/z : $[M + H]^+$ Calcd for $C_{21}H_{21}N_4O_2^+$ 345.1710; found 345.1736.

N-(((1,1,1,3,3,3-Hexafluoropropan-2-yl)oxy)methyl)-*N*-(4-methylpyridin-2-yl)-2-phenylimidazo[1,2-*a*]pyridin-3-amine (**47nd**): White solid; 199 mg, 83% yield;



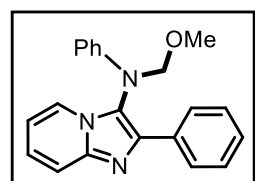
Eluent system: EtOAc:hexanes (30:70); mp = 163-164 °C; 1H NMR (400 MHz, $CDCl_3$) δ = 8.22 (d, J = 5.2 Hz, 1H), 7.90-7.86 (m, 3H), 7.68 (d, J = 9.0 Hz, 1H), 7.40-7.36 (m, 2H), 7.33-7.26 (m, 2H, overlapped with $CDCl_3$ residual signal), 6.78 (t, J = 6.7 Hz, 1H), 6.75 (d, J = 5.1 Hz, 1H), 6.18 (d, J = 10.8 Hz, 1H), 6.01 (s, 1H), 5.57 (sept, J = 6.0 Hz, 1H), 5.10 (d, J = 10.8 Hz, 1H), 2.10 (s, 3H); $^{13}C\{^1H\}$ NMR (100 MHz, $CDCl_3$) δ = 155.3, 150.5, 147.7, 143.3, 139.0, 132.7, 128.8, 128.3, 126.6, 125.9, 123.03, 123.01, 121.9 (q, $^1J_{C-F}$ = 281 Hz), 120.0, 118.6, 117.7, 112.6, 108.3, 84.0, 75.8 (p, $^2J_{C-F}$ = 32 Hz), 21.2; HRMS (ESI) m/z : $[M + H]^+$ Calcd for $C_{23}H_{19}F_6N_4O^+$ 481.1458; found 481.1475.

N-(5-Chloropyridin-2-yl)-*N*-(methoxymethyl)-2-phenylimidazo[1,2-*a*]pyridin-3-amine (**47oa**):



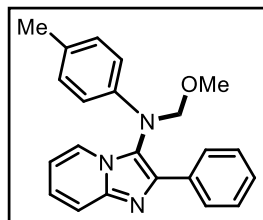
White solid; 158 mg, 87% yield; Eluent system: EtOAc:hexanes (35:65); mp = 150-152 °C; 1H NMR (400 MHz, $CDCl_3$) δ = 8.29 (d, J = 2.6 Hz, 1H), 7.90 (t, J = 6.5 Hz, 3H), 7.66 (d, J = 9.0 Hz, 1H), 7.39-7.24 (m, 5H, overlapped with $CDCl_3$ residual signal), 6.78 (t, J = 6.8 Hz, 1H), 6.16 (d, J = 8.9 Hz, 1H), 5.83 (d, J = 9.6 Hz, 1H), 4.70 (d, J = 9.6 Hz, 1H), 3.34 (s, 3H); $^{13}C\{^1H\}$ NMR (100 MHz, $CDCl_3$) δ = 154.7, 147.0, 143.1, 138.7, 138.3, 132.8, 128.7, 128.2, 126.6, 125.6, 123.6, 123.1, 120.7, 117.8, 112.5, 108.7, 82.1, 56.7; HRMS (ESI) m/z : $[M + H]^+$ Calcd for $C_{20}H_{18}ClN_4O^+$ 365.1164; found 365.1157.

N-(Methoxymethyl)-*N*,2-diphenylimidazo[1,2-*a*]pyridin-3-amine (**50a**): White solid; 133 mg,



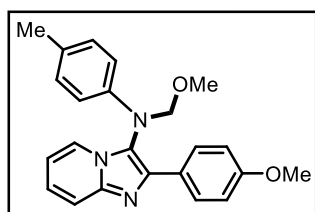
81% yield; Eluent system: EtOAc:hexanes (35:65); mp = 183-185 °C; 1H NMR (400 MHz, $CDCl_3$) δ 8.00 – 7.98 (m, 2H), 7.87 (dt, J = 6.8, 1.2 Hz, 1H), 7.68 (dt, J = 9.1, 1.1 Hz, 1H), 7.41 (m, 2H), 7.36 – 7.30 (m, 2H), 7.32 – 7.20 (m, 2H), 6.98 (m, 1H), 6.88 – 6.84 (m, 2H), 6.75 (td, J = 6.8, 1.1 Hz, 1H), 5.26 (d, J = 10.2 Hz, 1H), 4.75 (d, J = 10.2 Hz, 1H), 3.28 (s, 3H); $^{13}C\{^1H\}$ NMR (100 MHz, $CDCl_3$) δ 145.2, 142.8, 138.7, 133.2, 129.8, 128.7, 128.0, 126.7, 125.3, 123.4, 122.5, 120.9, 117.7, 114.5, 112.2, 85.6, 55.5; HRMS (ESI) m/z : $[M + H]^+$ Calcd for $C_{21}H_{20}N_3O^+$ 330.1601; found 330.1597.

N-(Methoxymethyl)-2-phenyl-*N*-(*p*-tolyl)imidazo[1,2-*a*]pyridin-3-amine (**50b**): White solid;



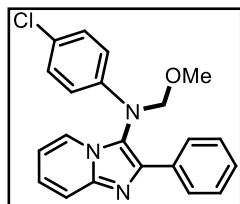
132 mg, 77% yield; Eluent system: EtOAc:hexanes (38:62); mp = 180–182 °C; ¹H NMR (400 MHz, CDCl₃) δ 8.00 (d, *J* = 7.1 Hz, 2H), 7.87 (d, *J* = 6.8 Hz, 1H), 7.67 (d, *J* = 9.0 Hz, 1H), 7.41 (t, *J* = 7.5 Hz, 2H), 7.33 (t, *J* = 7.3 Hz, 1H), 7.29 – 7.19 (m, 1H), 7.09 (d, *J* = 8.1 Hz, 2H), 6.75 (dd, *J* = 15.8, 7.6 Hz, 3H), 5.23 (d, *J* = 10.5 Hz, 1H), 4.73 (d, *J* = 10.3 Hz, 1H), 3.27 (s, 3H), 2.31 (s, 3H); ¹³C{¹H} NMR (100 MHz, CDCl₃) δ 142.9, 142.7, 138.6, 133.3, 130.3, 130.2, 128.7, 128.0, 126.7, 125.2, 123.4, 122.8, 117.6, 114.6, 112.2, 85.8, 55.4, 20.5; HRMS (ESI) *m/z*: [M + H]⁺ Calcd for C₂₂H₂₂N₃O⁺ 344.1757; found 344.1755.

N-(Methoxymethyl)-2-(4-methoxyphenyl)-*N*-(*p*-tolyl)imidazo[1,2-*a*]pyridin-3-amine (**50c**):



Colourless semi-solid; 137 mg, 73% yield; Eluent system: EtOAc:hexanes (40:60); ¹H NMR (400 MHz, CDCl₃) δ 7.93 (d, *J* = 8.4 Hz, 2H), 7.86 (d, *J* = 6.8 Hz, 1H), 7.65 (d, *J* = 9.0 Hz, 1H), 7.24 – 7.20 (m, 1H), 7.08 (d, *J* = 8.1 Hz, 2H), 6.94 (d, *J* = 8.4 Hz, 2H), 6.77 – 6.72 (m, , 3H), 5.21 (d, *J* = 10.3 Hz, 1H), 4.73 (d, *J* = 10.3 Hz, 1H), 3.84 (s, 3H), 3.27 (s, 3H), 2.30 (s, 3H); ¹³C{¹H} NMR (100 MHz, CDCl₃) δ 159.5, 143.0, 142.7, 138.6, 130.2, 130.1, 128.0, 125.9, 125.0, 123.3, 121.9, 117.4, 114.5, 114.2, 112.0, 85.7, 55.5, 55.2, 20.5; HRMS (ESI) *m/z*: [M + H]⁺ Calcd for C₂₃H₂₄N₃O₂⁺ 374.1863; found 374.1857.

N-(4-Chlorophenyl)-*N*-(methoxymethyl)-2-phenylimidazo[1,2-*a*]pyridin-3-amine (**50d**): Off-



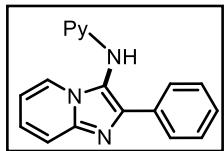
white solid; 101.5 mg, 56% yield; Eluent system: EtOAc:hexanes (35:65); mp = 161–163 °C; ¹H NMR (400 MHz, CDCl₃) δ 7.97–7.94 (m, 2H), 7.86 (d, *J* = 6.4 Hz, 1H), 7.69 (d, *J* = 9.2 Hz, 1H), 7.43–7.39 (m, 2H), 7.35–7.31 (m, 1H), 7.27–7.21 (m, 3H), 6.79–6.72 (m, 3H), 5.21 (d, *J* = 10.0 Hz, 1H), 4.73 (d, *J* = 10.0 Hz, 1H), 3.27 (s, 3H); ¹³C{¹H} NMR (100 MHz, CDCl₃) δ 143.9, 142.8, 138.7, 133.0, 129.6, 128.7, 128.2, 126.6, 125.9, 125.4, 123.1, 122.0, 117.7, 115.8, 112.4, 85.6, 55.5; HRMS (ESI) *m/z*: [M + H]⁺ Calcd for C₂₁H₁₉ClN₃O⁺ 364.1211; found 364.1206.

1.4.4 Experimental Procedure for the Preparation of 2-Phenyl-*N*-(pyridin-2-yl)imidazo[1,2-*a*]pyridin-3-amine (**51**).

To a solution of ((2-phenylimidazo[1,2-*a*]pyridin-3-yl)(pyridin-2-yl)amino)methyl acetate **45a** (0.14 mmol; 1 equiv.) in MeOH (5 mL) was added NaHCO₃ (9 equiv.) at room temperature and the reaction mixture was stirred at 50 °C for 2 h. After completion of the reaction, methanol

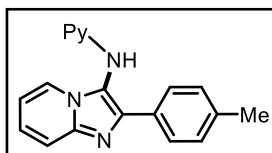
was evaporated under vacuum. The resulting crude solid was washed with diethyl ether to get the pure off-white solid of **51a** in 95% yield. The compound was pure enough based on NMR spectrum analysis.

2-Phenyl-N-(pyridin-2-yl)imidazo[1,2-a]pyridin-3-amine (51a): Off-white solid; 38 mg, 95%



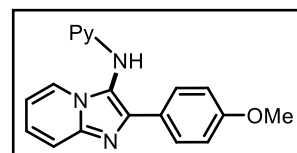
yield; mp = 224-226 °C (lit.,⁷⁷ 225-228 °C); ¹H NMR (400 MHz, CDCl₃) δ = 8.13 (d, *J* = 5.1 Hz, 1H), 8.09-8.06 (m, 2H), 7.89 (d, *J* = 7.0 Hz, 1H), 7.68 (d, *J* = 9.0 Hz, 1H), 7.59 (br s, 1H), 7.41-7.34 (m, 3H), 7.30-7.24 (m, 2H), 6.81 (td, *J* = 6.7, 1.1 Hz, 1H), 6.74 (dd, *J* = 7.1, 5.0 Hz, 1H), 6.12 (d, *J* = 8.4 Hz, 1H); ¹³C{¹H} NMR (100 MHz, CDCl₃) δ = 156.9, 148.5, 142.9, 139.3, 138.7, 133.1, 128.6, 127.9, 126.9, 125.1, 122.5, 117.8, 116.6, 115.6, 112.4, 106.5; HRMS (ESI) *m/z*: [M + H]⁺ Calcd for C₁₈H₁₅N₄⁺ [M + H]⁺ 287.1291; found 287.1299.

N-(Pyridin-2-yl)-2-(p-tolyl)imidazo[1,2-a]pyridin-3-amine (51b): White solid; 39 mg, 93%



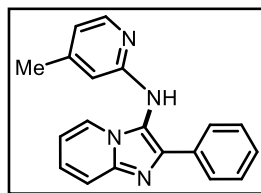
yield; mp = 222-224 °C (lit.,⁷⁷ 223-225 °C); ¹H NMR (400 MHz, CDCl₃) δ = 8.18 (d, *J* = 4.1 Hz, 1H), 7.97 (d, *J* = 7.4 Hz, 2H), 7.89 (d, *J* = 6.8 Hz, 1H), 7.67 (d, *J* = 9.0 Hz, 1H), 7.42-7.37 (m, 1H), 7.28-7.23 (m, 1H, overlapped with CDCl₃ residual signal), 7.18 (d, *J* = 8.2 Hz, 3H), 6.81 (t, *J* = 6.7 Hz, 1H), 6.76 (dd, *J* = 7.2, 5.0 Hz, 1H), 6.12 (d, *J* = 8.4 Hz, 1H), 2.34 (s, 3H); ¹³C{¹H} NMR (100 MHz, CDCl₃) δ = 156.9, 148.6, 142.9, 139.6, 138.6, 137.8, 130.3, 129.3, 126.8, 125.0, 122.5, 117.7, 116.2, 115.6, 112.2, 106.4, 21.2; HRMS (ESI) *m/z*: [M + H]⁺ Calcd for C₁₉H₁₇N₄⁺ 301.1448; found 301.1435.

2-(4-Methoxyphenyl)-N-(pyridin-2-yl)imidazo[1,2-a]pyridin-3-amine (51c): Off-white solid;



41 mg, 92% yield; mp = 203-205 °C (lit.,⁷⁷ 218-221 °C); ¹H NMR (400 MHz, CDCl₃) δ = 8.24 (d, *J* = 5.0 Hz, 1H), 8.01 (d, *J* = 8.5 Hz, 2H), 7.89 (d, *J* = 6.8 Hz, 1H), 7.66 (d, *J* = 9.0 Hz, 1H), 7.42 (t, *J* = 7.7 Hz, 1H), 7.28-7.24 (m, 1H, overlapped with CDCl₃ residual signal), 6.93 (d, *J* = 8.4 Hz, 2H), 6.83-6.78 (m, 2H), 6.69 (s, 1H), 6.14 (d, *J* = 8.3 Hz, 1H), 3.83 (s, 3H); ¹³C{¹H} NMR (100 MHz, CDCl₃) δ = 159.5, 156.8, 148.7, 142.9, 139.6, 138.6, 128.3, 125.8, 125.0, 122.4, 117.6, 115.7, 115.5, 114.0, 112.2, 106.4, 55.2; HRMS (ESI) *m/z*: [M + H]⁺ calcd for C₁₉H₁₇N₄O⁺ 317.1397; found 317.1406.

N-(4-Methylpyridin-2-yl)-2-phenylimidazo[1,2-*a*]pyridin-3-amine (**51m**): Brown solid; 40 mg,



96% yield; mp = 223-225 °C; ^1H NMR (400 MHz, CDCl_3) δ = 8.08-8.04 (m, 3H), 7.88 (dt, J = 6.8, 1.2 Hz, 1H), 7.67 (d, J = 9.0 Hz, 1H), 7.39-7.36 (m, 2H), 7.31-7.23 (m, 2H, overlapped with CDCl_3 residual signal), 6.83-6.79 (m, 2H), 6.60 (d, J = 5.1 Hz, 1H), 5.92 (s, 1H), 2.10 (s, 3H); ^{13}C $\{^1\text{H}\}$ NMR (100 MHz, CDCl_3) δ = 156.9, 150.1, 148.3, 143.0, 139.5, 133.2, 128.6, 127.9, 127.0, 125.2, 122.6, 117.8, 117.3, 116.6, 112.4, 106.6, 21.1; HRMS (ESI) m/z : $[\text{M} + \text{H}]^+$ Calcd for $\text{C}_{19}\text{H}_{17}\text{N}_4^+$ 301.1448; found 301.1460.

1.4.5 X-ray Crystallographic Analysis of Compound **45a**, **47aa** and **49a**

The crystal data collection and data reduction were performed using CrysAlis PRO on a single crystal Rigaku Oxford XtaLab Pro diffractometer. The crystal was kept at 93(2) K during data collection. Using Olex2⁷⁸, the structure was solved with the ShelXT⁷⁹ structure solution program using Intrinsic Phasing and refined with the ShelXL⁸⁰ refinement package using Least Squares minimisation.

The single crystals of the compound **45a** ($\text{C}_{21}\text{H}_{18}\text{N}_4\text{O}_2$) (**Figure 1.10**), **47aa** ($\text{C}_{20}\text{H}_{18}\text{N}_4\text{O}$) (**Figure 1.14**) and **49a** ($\text{C}_{20}\text{H}_{17}\text{N}_3\text{O}$) (**Figure 1.15**) were obtained from slow evaporation of ethyl acetate solutions. The **45a**, **47aa** and **49a** were crystallized in monoclinic, triclinic and monoclinic crystal system with $\text{P}2_1/\text{n}$, $\text{P}-1$ and $\text{P}2_1/\text{c}$ space groups respectively. The crystal structures information of **45a**, **47aa** and **49a** are deposited to Cambridge Crystallographic Data Center and the CCDC numbers for the **45a**, **47aa** and **49a** are 1957417, 1913162 and 1986133, respectively.

Table 1.5 Crystal data and structure refinement for **45a**, **47aa** and **49a**

Identification code	45a	47aa	49a
Empirical formula	$\text{C}_{21}\text{H}_{18}\text{N}_4\text{O}_2$	$\text{C}_{20}\text{H}_{18}\text{N}_4\text{O}$	$\text{C}_{20}\text{H}_{17}\text{N}_3\text{O}$
Formula weight	358.39	330.38	315.36
Temperature/K	93(2)	93(2)	93(2)
Crystal system	monoclinic	triclinic	monoclinic
Space group	$\text{P}2_1/\text{n}$	$\text{P}-1$	$\text{P}2_1/\text{c}$

a/Å	9.0770(3)	8.7653(6)	13.0780(2)
b/Å	17.0044(6)	9.1903(6)	17.8116(2)
c/Å	11.4160(3)	11.0216(7)	13.6505(2)
α /°	90	69.082(6)	90
β /°	93.418(3)	84.898(6)	98.6840(10)
γ /°	90	88.480(5)	90
Volume/Å ³	1758.91(10)	826.04(10)	3143.30(8)
Z	4	2	8
$\rho_{\text{calc}}/\text{cm}^3$	1.353	1.328	1.333
μ/mm^{-1}	0.090	0.085	0.670
F(000)	752.0	348.0	1328.0
Crystal size/mm ³	0.3 × 0.3 × 0.3	0.3 × 0.3 × 0.2	0.2 × 0.08 × 0.05
Radiation	MoK α ($\lambda = 0.71073$)	MoK α ($\lambda = 0.71073$)	CuK α ($\lambda = 1.54184$)
2 Θ range for data collection/°	7.152 to 62.27	6.38 to 62.496	8.22 to 159.586
Index ranges	-12 ≤ h ≤ 11, -24 ≤ k ≤ 24, -15 ≤ l ≤ 16	-12 ≤ h ≤ 11, -13 ≤ k ≤ 13, -15 ≤ l ≤ 15	-16 ≤ h ≤ 10, -22 ≤ k ≤ 22, -16 ≤ l ≤ 17
Reflections collected	19506	14537	22372
Independent reflections	5024 [R _{int} = 0.0103, R _{sigma} = 0.0080]	4603 [R _{int} = 0.0499, R _{sigma} = 0.0461]	6664 [R _{int} = 0.0353, R _{sigma} = 0.0361]
Data/restraints/parameters	5024/0/245	4603/0/227	6664/0/435
Goodness-of-fit on F ²	1.028	1.122	1.054
Final R indexes [I ≥ 2 σ (I)]	R ₁ = 0.0389, wR ₂ = 0.1057	R ₁ = 0.0779, wR ₂ = 0.2427	R ₁ = 0.0484, wR ₂ = 0.1149
Final R indexes [all data]	R ₁ = 0.0409, wR ₂ = 0.1074	R ₁ = 0.0930, wR ₂ = 0.2546	R ₁ = 0.0545, wR ₂ = 0.1184
Largest diff. peak/hole / e Å ⁻³	0.43/-0.38	0.72/-0.48	0.55/-0.29

1.5 REFERENCES

1. Kumar, V.; Kaur, K.; Gupta, G. K.; Sharma, A. K., *European Journal of Medicinal Chemistry* **2013**, *69*, 735-753.
2. Tahlan, S.; Kumar, S.; Narasimhan, B., *BMC Chemistry* **2019**, *13*, 101.
3. Smith, C. A.; Narouz, M. R.; Lummis, P. A.; Singh, I.; Nazemi, A.; Li, C.-H.; Crudden, C. M., *Chemical Reviews* **2019**, *119*, 4986-5056.
4. Ng, V. W. L.; Tan, J. P. K.; Leong, J.; Voo, Z. X.; Hedrick, J. L.; Yang, Y. Y., *Macromolecules* **2014**, *47*, 1285-1291.
5. Sharma, P. K., *Asian Journal of Pharmaceutical and Clinical Research* **2017**, *10*, 47-49.

6. Shah, R.; Vaghani, D.; Merchant, J., *The Journal of Organic Chemistry* **1961**, *26*, 3533-3534.
7. Mermer, A.; Keles, T.; Sirin, Y., *Bioorganic Chemistry* **2021**, *114*, 105076.
8. Liu, X.; Pang, X.-J.; Liu, Y.; Liu, W.-B.; Li, Y.-R.; Yu, G.-X.; Zhang, Y.-B.; Song, J.; Zhang, S.-Y., *Molecules* **2021**, *26*, 4047-4051.
9. Garuti, L.; Roberti, M.; Pizzirani, D., *Mini Reviews in Medicinal Chemistry* **2007**, *7*, 481-489.
10. Silva, D. G.; Junker, A.; de Melo, S. M. G.; Fumagalli, F.; Gillespie, J. R.; Molasky, N.; Buckner, F. S.; Matheussen, A.; Caljon, G.; Maes, L.; Emery, F. S., *ChemMedChem* **2021**, *16*, 966-975.
11. Siddiqui, N.; Andalip; Bawa, S.; Ali, R.; Afzal, O.; Akhtar, M. J.; Azad, B.; Kumar, R., *Journal of Pharmacy and Bioallied Sciences* **2011**, *3*, 146-152.
12. Sepúlveda, B.; Astudillo, L.; Rodríguez, J. A.; Yáñez, T.; Theoduloz, C.; Schmeda-Hirschmann, G., *Pharmacological Research* **2005**, *52*, 429-437.
13. Zhu, J.; Xiao, X.; Qin, H.; Luo, Z.; Chen, Y.; Huang, C.; Jiang, X.; Liu, S.; Zhuang, T.; Zhang, G., *Bioorganic & Medicinal Chemistry Letters* **2023**, *82*, 129165.
14. Jiang, K.; Xing, Y.; Quan, Q.; Sun, Q.; Tian, J.; Liu, C.; Song, X.; Wang, X.; Liu, Y., *Journal of Traditional Chinese Medical Sciences* **2020**, *7*, 393-403.
15. Sahu, C.; Chaurasiya, A.; Chawla, P. A., *Journal of Heterocyclic Chemistry*, **2022**, *1*, 23-29.
16. Wojtaszek, J. L.; Chatterjee, N.; Najeeb, J.; Ramos, A.; Lee, M.; Bian, K.; Xue, J. Y.; Fenton, B. A.; Park, H.; Li, D.; Hemann, M. T.; Hong, J.; Walker, G. C.; Zhou, P., *Cell* **2019**, *178*, 152-159.e111.
17. Kumar, S.; Kumar, A.; Sharma, D.; Das, P., *European Journal of Medicinal Chemistry* **2022**, *22*, e202100171.
18. Yang, W.-C.; Chen, C.-Y.; Li, J.-F.; Wang, Z.-L., *Chinese Journal of Catalysis* **2021**, *42*, 1865-1875.
19. Xiang, Y.; Wang, C.; Ding, Q.; Peng, Y., *Accounts of Chemical Research* **2019**, *361*, 919-944.
20. Anastas, P.; Warner, J. J. N. Y., *Journal of the American Chemical Society* **1998**, *30*, 1822-1824.

21. Zhang, S.; Shi, L.; Ding, Y., *Journal of the American Chemical Society* **2011**, *133*, 20218-20229.
22. Kubota, K.; Takahashi, R.; Ito, H., *Chemical Science* **2019**, *10*, 5837-5842.
23. Maxted, E. B., The Poisoning of Metallic Catalysts. In *Advances in Catalysis*, Frankenburg, W. G.; Komarewsky, V. I.; Rideal, E. K.; Emmett, P. H.; Taylor, H. S., Eds. Academic Press 1951; Vol. 3, pp 129-178.
24. Garrett, C. E.; Prasad, K., *Chemical Reviews* **2004**, *346*, 889-900.
25. Dijkstra, H. P.; van Klink, G. P. M.; van Koten, G., *Accounts of Chemical Research* **2002**, *35*, 798-810.
26. Gansäuer, A.; Bluhm, H., *Chemical Reviews* **2000**, *100*, 2771-2788.
27. Zaitsev, V. G.; Shabashov, D.; Daugulis, O., *Journal of the American Chemical Society* **2005**, *127*, 13154-13155.
28. Shang, S. S.; Gao, S., *Chemical Reviews* **2019**, *11*, 3730-3744.
29. Allen, L. J.; Crabtree, R. H., *Green Chemistry* **2010**, *12*, 1362-1364.
30. Tian, Y.; Xu, D.; Chu, K.; Wei, Z.; Liu, W., *Journal of Materials Science* **2019**, *54*, 9088-9097.
31. Sun, C.-L.; Shi, Z.-J., *Chemical Reviews* **2014**, *114*, 9219-9280.
32. Kitamura, T.; Fujiwara, Y., *Organic Preparations and Procedures International* **1997**, *29*, 409-458.
33. Frei, R.; Courant, T.; Wodrich, M. D.; Waser, J., *Journal of the American Chemical Society* **2015**, *21*, 2662-2668.
34. Zhang, N.; Cheng, R.; Zhang-Negrerie, D.; Du, Y.; Zhao, K., *The Journal of Organic Chemistry* **2014**, *79*, 10581-10587.
35. Kim, H. J.; Kim, J.; Cho, S. H.; Chang, S., *Journal of the American Chemical Society* **2011**, *133*, 16382-16385.
36. Silva, L. F.; Vasconcelos, R. S.; Nogueira, M. A., *Organic Letters* **2008**, *10*, 1017-1020.
37. Silva, J. L. F.; Olofsson, B., *Natural Product Reports* **2011**, *28*, 1722-1754.
38. Yoshimura, A.; Zhdankin, V. V., *Chemical Reviews* **2016**, *116*, 3328-3435.
39. Moriarty, R. M.; Prakash, O., *Accounts of Chemical Research* **1986**, *19*, 244-250.
40. Zhdankin, V. V.; Stang, P. J., *Chemical Reviews* **2002**, *102*, 2523-2584.

41. Wirth, T., Introduction and General Aspects. In *Hypervalent Iodine Chemistry: Modern Developments in Organic Synthesis*, Wirth, T., Ed. Springer Berlin Heidelberg: Berlin, Heidelberg, 2003; pp 1-4.
42. Chen, W.-T.; Gao, L.-H.; Bao, W.-H.; Wei, W.-T., *The Journal of Organic Chemistry* **2018**, *83*, 11074-11079.
43. Mondal, S.; Samanta, S.; Jana, S.; Hajra, A., *The Journal of Organic Chemistry* **2017**, *82*, 4504-4510.
44. Morimoto, K.; Yanase, K.; Toda, K.; Takeuchi, H.; Dohi, T.; Kita, Y., *Organic Letters* **2022**, *24*, 6088-6092.
45. Paveliev, S. A.; Segida, O. O.; Bityukov, O. V.; Tang, H.-T.; Pan, Y.-M.; Nikishin, G. I.; Terent'ev, A. O., **2022**, *364*, 3910-3916.
46. Tang, P.; Wen, L.; Ma, H.-J.; Yang, Y.; Jiang, Y., *Organic & Biomolecular Chemistry* **2022**, *20*, 3061-3066.
47. Charpentier, J.; Früh, N.; Togni, A., *Chemical Reviews* **2015**, *115*, 650-682.
48. Dong, D.-Q.; Hao, S.-H.; Wang, Z.-L.; Chen, C., *Organic & Biomolecular Chemistry* **2014**, *12*, 4278-4289.
49. Samanta, R.; Matcha, K.; Antonchick, A. P., *European Journal of Organic Chemistry* **2013**, *2013*, 5769-5804.
50. Yang, L., Xia G., Jingjun, M., Qian, Y., Feng, A., Cui, J., *Russian Chemical Bulletin* **2020**, *40*, 28-39.
51. Budhwan, R.; Yadav, S.; Murarka, S., *Organic & Biomolecular Chemistry* **2019**, *17*, 6326-6341.
52. Yusubov, M. S.; Zholobova, G. A.; Filimonova, I. L.; Chi, K.-W., *Russian Chemical Bulletin* **2004**, *53*, 1735-1742.
53. Purohit, V. C.; Allwein, S. P.; Bakale, R. P., *Organic Letters* **2013**, *15*, 1650-1653.
54. Qurban, J.; Elsherbini, M.; Wirth, T., *The Journal of Organic Chemistry* **2017**, *82*, 11872-11876.
55. Zhang, D.-Y.; Zhang, Y.; Wu, H.; Gong, L.-Z., *Organic Letters* **2019**, *58*, 7450-7453.
56. Zhang, X.-M.; Tu, Y.-Q.; Zhang, F.-M.; Chen, Z.-H.; Wang, S.-H., *Chemical Society Reviews* **2017**, *46*, 2272-2305.
57. Zhang, B.; Li, X.; Guo, B.; Du, Y., *Chemical Communications* **2020**, *56*, 14119-14136.

58. Tamura, Y.; Shirouchi, Y.; Haruta, J.-i., *Synthesis* **1984**, 1984, 231-232.
59. Lu, M.; Qin, H.; Lin, Z.; Huang, M.; Weng, W.; Cai, S., *Organic Letters* **2018**, 20, 7611-7615.
60. Song, L.-R.; Li, H.; Wang, S.-F.; Lin, J.-P.; Huang, B.; Long, Y.-Q., *Chemical Communications* **2022**, 58, 8340-8343.
61. Murai, K.; Kobayashi, T.; Miyoshi, M.; Fujioka, H., *Organic Letters* **2018**, 20, 2333-2337.
62. Yamakoshi, W.; Arisawa, M.; Murai, K., *Organic Letters* **2019**, 21, 3023-3027.
63. Du, Y.; Hou, J.; Lu, Q.; Hao, W.; Yu, W.; Chang, J., *New Journal of Chemistry* **2021**, 45, 16223-16226.
64. Mandal, S.; Pramanik, A., *The Journal of Organic Chemistry* **2022**, 87, 9282-9295.
65. Xu, X.; Xia, C.; Li, X.; Sun, J.; Hao, L., *RSC Advances* **2020**, 10, 2016-2026.
66. Dohi, T.; Kita, Y., *Chemical Communications* **2009**, 2073-2085.
67. Richardson, R. D.; Wirth, T., *Angewandte Chemie International Edition* **2006**, 45, 4402-4404.
68. He, Y.; Feng, T.; Fan, X., *Organic Letters* **2019**, 21, 3918-3922.
69. Rupanawar, B. D.; Veetil, S. M.; Suryavanshi, G., *European Journal of Organic Chemistry* **2019**, 2019, 6232-6239.
70. Boltjes, A.; Dömling, A., *European Journal of Organic Chemistry* **2019**, 2019, 7007-7049.
71. Elleder, D.; Baiga, T. J.; Russell, R. L.; Naughton, J. A.; Hughes, S. H.; Noel, J. P.; Young, J. A. T., *Virology Journal* **2012**, 9, 305.
72. Nagle, A.; Wu, T.; Kuhen, K.; Gagaring, K.; Borboa, R.; Francek, C.; Chen, Z.; Plouffe, D.; Lin, X.; Caldwell, C.; Ek, J.; Skolnik, S.; Liu, F.; Wang, J.; Chang, J.; Li, C.; Liu, B.; Hollenbeck, T.; Tuntland, T.; Isbell, J.; Chuan, T.; Alper, P. B.; Fischli, C.; Brun, R.; Lakshminarayana, S. B.; Rottmann, M.; Diagana, T. T.; Winzeler, E. A.; Glynne, R.; Tully, D. C.; Chatterjee, A. K., *Journal of Medicinal Chemistry* **2012**, 55, 4244-4273.
73. Liang, D.; He, Y.; Liu, L.; Zhu, Q., *Organic Letters* **2013**, 15, 3476-3479.
74. Manna, S.; Matcha, K.; Antonchick, A. P., *Angewandte Chemie International Edition* **2014**, 53, 8163-8166.

75. Patel, O. P. S.; Nandwana, N. K.; Sah, A. K.; Kumar, A., *Organic & Biomolecular Chemistry* **2018**, *16*, 8620-8628.
76. Li, H.; Li, X.; Yu, Y.; Li, J.; Liu, Y.; Li, H.; Wang, W., *Organic Letters* **2017**, *19*, 2010-2013.
77. Fei, Z.; Zhu, Y.-p.; Liu, M.-c.; Jia, F.-c.; Wu, A.-x., *Tetrahedron Letters* **2013**, *54*, 1222-1226.
78. Dolomanov, O. V.; Bourhis, L. J.; Gildea, R. J.; Howard, J. A.; Puschmann, H., *Journal of Applied Crystallography* **2009**, *42*, 339-341.
79. Sebbar, N.; Ellouz, M.; Essassi, E.; Ouzidan, Y.; Mague, J., *Acta Crystallographica Section E: Crystallographic Communications* **2015**, *71*, o999.
80. Sheldrick, G. M., *Acta Crystallographica Section A: Foundations and Advances* **2015**, *71*, 3-8.

CHAPTER 2

C5-Aroylation of Imidazoheterocycles by Oxidative Decarboxylation of Arylglyoxylic Acids

2.1 INTRODUCTION

Synthetic chemistry has entered a new era of organic transformations with the invention of free radical based C-C bond formation under mild conditions. After a considerable advancement since last half century, free-radical reactions are no longer termed as “notoriously uncontrollable”. The pioneering work from various groups in the diverse fields of free-radical chemistry has grabbed the researcher’s attention and inspired them to venture into this field.¹⁻² As a result, new milestones have been achieved in the arsenal of synthetic methodology *via* free-radical based C-C bond formation reactions. In saturated carbon skeletons, the C-H bond is typically activated through the homolytic abstraction of H-atom by the reactive radical species. However, with the unsaturated systems the process is not that easy and follows an alternative pathway in which the reactive radical species first interact with the conjugated π -system followed by the condition dependent homolytic or heterolytic C-H bond cleavage. In this context, the last decade has witnessed a tremendous emergence of milder, easily operable and environmental benign free-radical reaction conditions especially for C-C bond formation in unsaturated systems. One such easy, efficient and versatile protocol in the expanse of free-radical facilitated reactions is “Minisci reaction”.³

2.1.1 Minisci reaction

A typical Minisci reaction is the one in which an alkyl carboxylic acid generates a free-radical with the help of silver salt and persulphates and is added on the electron deficient heteroarenes. However, Lynch and several other groups in late 1960s already discussed the possibility of adding free-radical to electron deficient heteroarenes.⁴⁻⁵ The commonly used electron deficient heteroarenes are pyridines and quinolines and in both of these regioselective functionalization is a big challenge. In this regard, Lynch disclosed the necessity of acidic reaction condition during phenylation of pyridines in order to majorly achieve the C2-substituted product.⁶ Later on, Minisci *et al.* delineated several methods for the construction of C2- and C4-substituted pyridines and quinolines using alkyl radicals in the presence of iron catalyst and peroxides.⁷⁻⁸ In the consecutive year, an effective method for C-H functionalization of pyridines and quinolines was disclosed by the same group using alkyl radical produced through oxidative decarboxylation of corresponding carboxylic acids.⁹ Since then, an incredible progress was observed in this field, however it is still necessary to maintain the acidic reaction conditions in order to reduce the LUMO energy of the heterocycles for radical addition. The theoretical background

of Minisci type reactions was attractively clarified in a review by Opatz *et al.* in 2014.¹⁰ According to the group, initially the nucleophilic carbon centered radical is added to electron deficient heteroarenes which is already activated in the presence of acid. The resulting intermediate **B** could follow two different plausible pathways for the construction of C–C bond through free-radical mechanism. In one possible pathway, the deprotonation of α -hydrogen affords a neutral radical species **C** which rearomatizes *via* single electron transfer (SET) followed by again deprotonation to showcase the newly formed C–C bond (**Figure 2.1a**). In another prospect, if the reaction proceeds through hydrogen atom transfer (HAT) from the radical cation intermediate **B**, then it could directly afford the rearomatized product in one step (**Figure 2.1b**). Certainly, the majority of Minisci-type reactions follow these basic pathways. However, for any individual reaction, the integration of radical producing mechanism underlying with the Minisci-type addition makes the overall mechanism much more complicated.

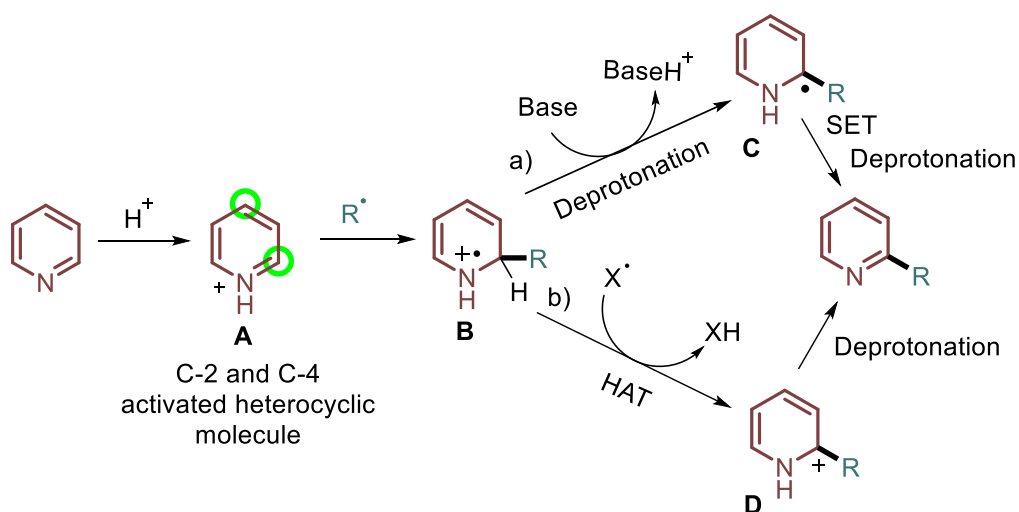


Figure 2.1. Generalized mechanism of Minisci-type reactions

In order to achieve the selective functionalization between uniformly activated positions of pyridine and quinolines, different research groups have studied multiple factors including type of acid used for activation, solvent polarity, solubility of reagents and nature of radical generated. However, due to the similar LUMO coefficient it is often a challenging task which ends up with the formation of mixture of isomers along with low yield. Therefore, regioselectivity and poor yield are the main hurdle faced in Minisci chemistry. The recent analysis of Baran, Blackmond and O'Hara for the regioselectivity of different heterocyclic compounds assures that this aspect remains a challenge and new methods which have ability of controlling this feature are highly

desirable. Moreover, it is worthy to mention that the regio-selectivity issue in some cases can be overcome by making proper substitutions in the ring. Over the years, several research groups worked in this direction and tried to overcome the limitations in Minisci chemistry. Engagement of electrolysis and photocatalysis has also risen as a fascinating approach which is compiled in several independent review articles and book chapters. Multiple radical precursors have been utilized to decorate the basic heterocycles *via* Minisci reaction some of them are mentioned in **Figure 2.2**.

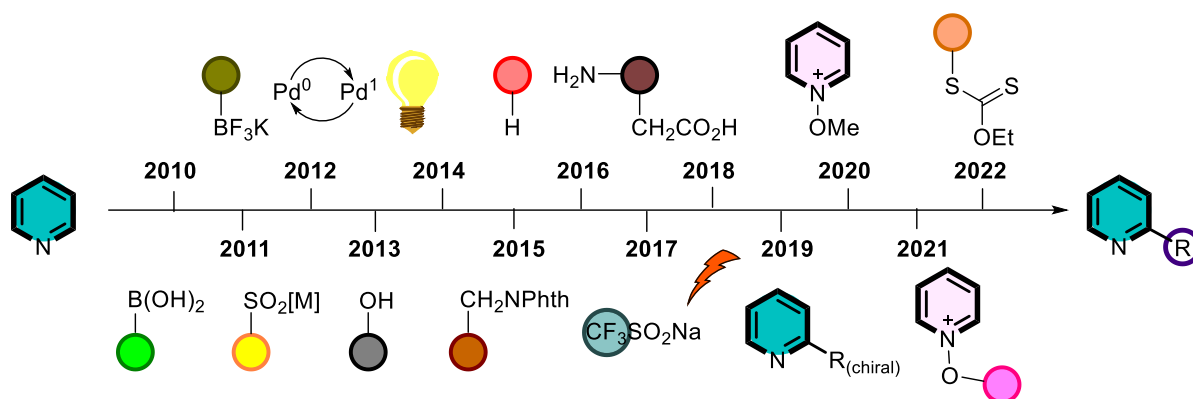
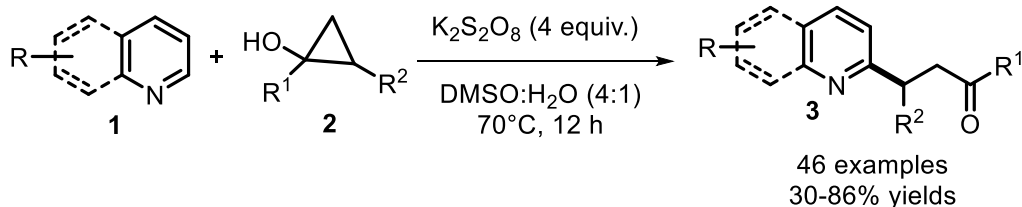


Figure 2.2 Array of radical precursors used for Minisci-type reaction

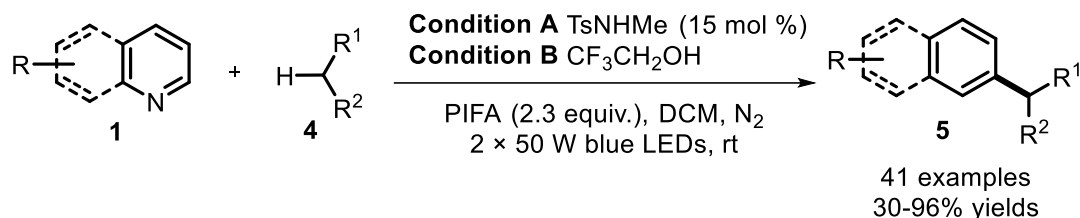
Liu's group in 2020, reported the $K_2S_2O_8$ -mediated ring-opening of cyclopropanols (**2**) for the synthesis of β -heteroarylated ketones (**3**). The metal-free β -carbonyl alkylation devoid any acidic or photocatalytic conditions and tolerates diverse heterocyclic compounds (**1**) such as, pyridines, pyridazine, phenanthroline, benzo[*d*]thiazole, quinolines and isoquinolines affording good to excellent yield of corresponding products (**Scheme 2.1**).¹¹ Eco-friendly conditions which are also amenable for gram scale synthesis, gigantic functional group tolerance and compatibility with diverse heteroarenes are some eye-catching features of their work.



Scheme 2.1 Minisci-type β -carbonyl alkylation of various heteroarenes

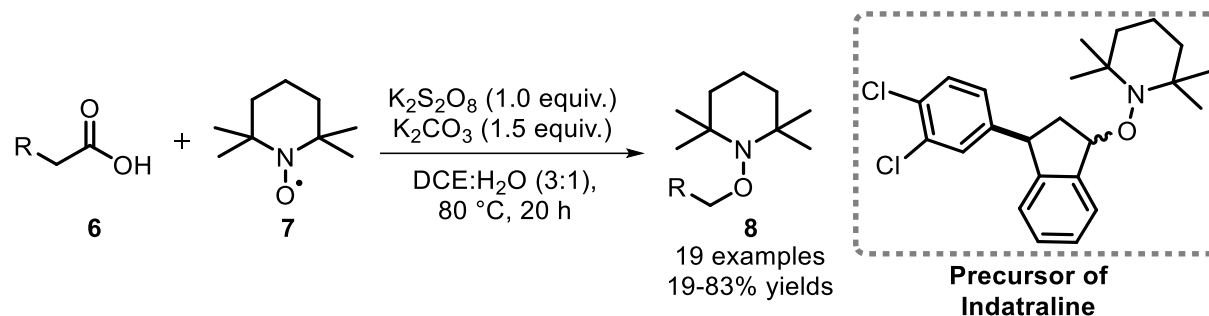
An example of photo-induced Minisci reaction was disclosed by Zhu group which includes the metal-free alkylation of different heteroarenes (**1**) (**Scheme 2.2**).¹² The reaction is believed to

proceed through amidyl/alkoxy radical generation in the presence of visible light, which is responsible for the coupling of cyclic/acyclic alkanes (**4**) with varied heterocycles to subsequently produce site selective alkylated *N*-heteroarenes (**5**). The environmentally benign reaction conditions resulted in moderate to good yield of the alkylated product with discrete functionalized heteroarenes.



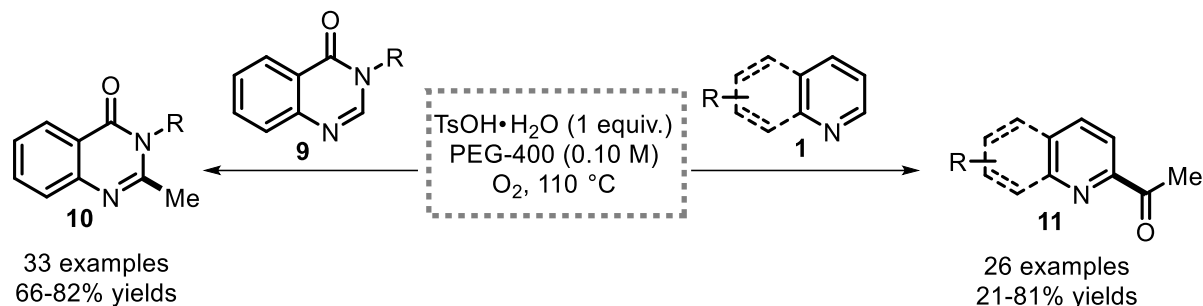
Scheme 2.2 Minisci type alkylation of various heteroarene

Synthesis of alkoxyamines (**8**) from carboxylic acids (**6**) and TEMPO (**7**) was reported for the first time by Goran and Andreas (**Scheme 2.3**).¹³ The developed silver-free Minisci-type oxidative decarboxylation was performed in biphasic solvent system to improve the site-selectivity and avoid the persulfate promoted oxidation of TEMPO. Notably, the developed protocol provided an important step for the synthesis of indatraline, an antidepressant drug.



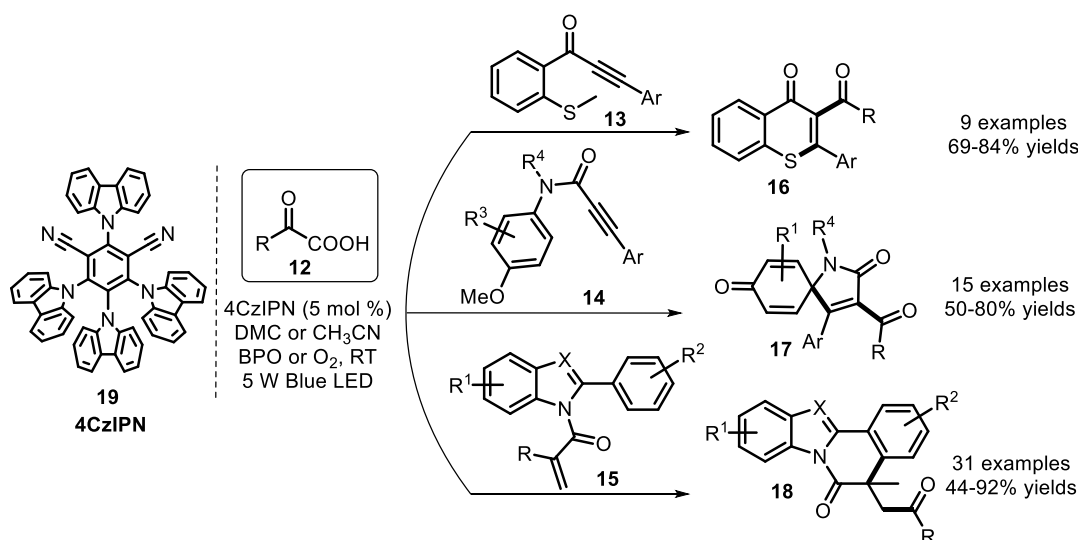
Scheme 2.3 Minisci type aminoxylation of carboxylic acids with TEMPO

A silver-free, substrate dependent method was disclosed by Khudale and Wang for the efficient methylation and acetylation of *N*-heteroarene using PEG 400 as methyl and acetyl surrogate under acidic conditions. C2-methylation (**10**) was obtained when quinazolinones (**9**) were used, however acetylated products (**11**) were observed in case of electron-deficient heteroarenes (**1**) (**Scheme 2.4**).¹⁴ The proposed method has potential for synthesizing methaqualone (a sedative hypnotic drug) and its analogues by one-pot strategy. Extensive substrate scope, good functional group tolerance and sustainable carbon surrogate makes this method more precise for the synthesis of bioactive scaffolds.



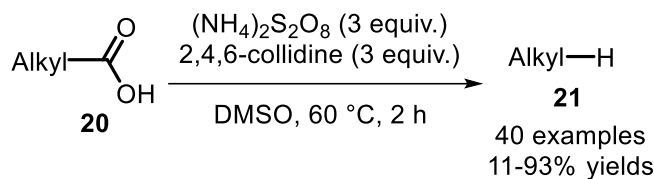
Scheme 2.4 Minisci-type methylation and acetylation of *N*-heteroarenes using PEG-400 as methyl and acetyl surrogate

In 2021, Zhu and colleagues showcased a visible-light induced synthesis of thioflavones (**16**) *via* metal-free Minisci-type decarboxylative arylation of methylthiolated alkynones (**13**) with α -keto acids (**12**) in the presence of 4CzIPN (**19**) as a photocatalyst (**Scheme 2.5**).¹⁵ The described method was equally implemented for *N*-arylpropiolamides (**14**), and *N*-acryloyl-2-phenyl benzoimidazole/indole (**15**) under standard reaction conditions to afford aroylazaspiro [4.5]trienones (**17**) and benzimidazo/indolo[2,1-*a*]isoquinolin-6(5*H*)-ones (**18**), respectively.



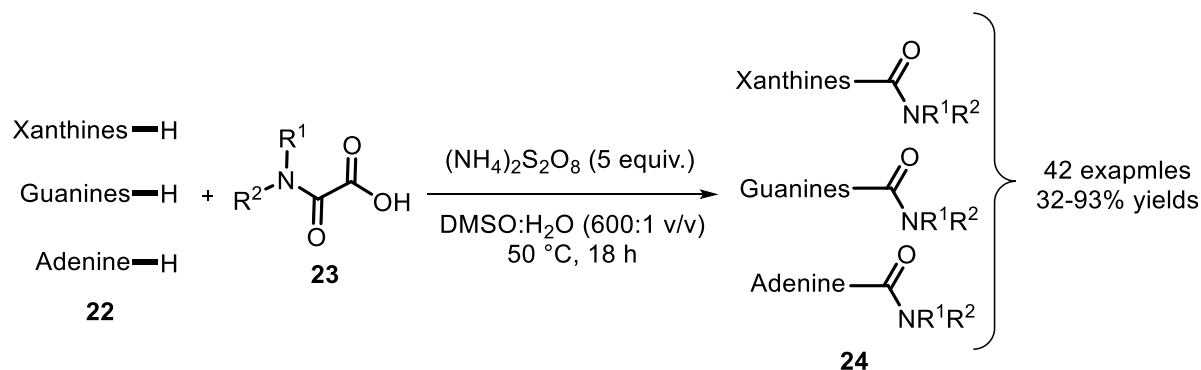
Scheme 2.5 Minisci-type acylation of β -carbolines and indoles

Lee group developed a very straightforward approach for hydrodecarboxylation of carboxylic acids (**20**). A large number of alkyl carboxylic acids such as primary, secondary, tertiary, strained, cyclic, from natural products (ketopinonic acid) and pharmaceuticals (naproxen) were well tolerated under the designed protocol affording decent yield of the hydrodecarboxylated products (**21**) (**Scheme 2.6**).¹⁶ The promising advantage included no use of external hydrogen atom source which is a great limitation in traditional decarboxylation reactions.



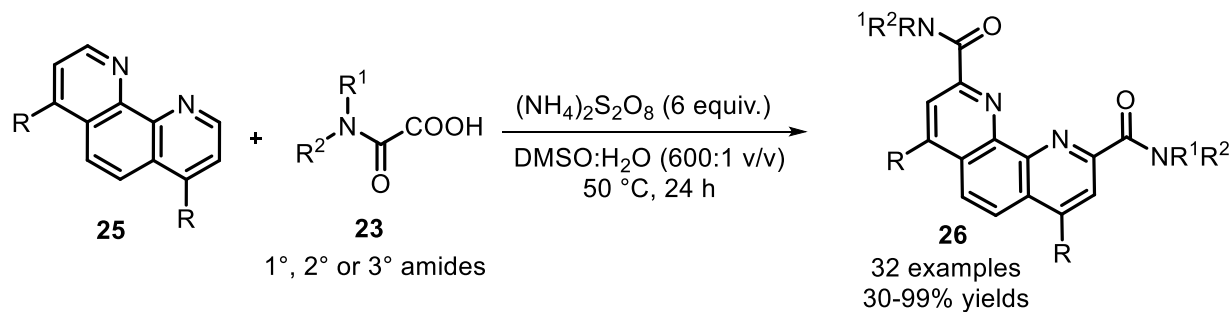
Scheme 2.6 Minisci-type hydrodecarboxylation of aliphatic carboxylic acids

Interestingly, following the aforementioned method for the decarboxylation, the same group reported the C–H carboxyamidation of purine bases (**22**) using oxamic acids (**23**) as amide surrogates. Multiple 1°, 2°, or 3° oxamic acids were compatible and the corresponding amides (**24**) were obtained in excellent yield (**Scheme 2.7**).¹⁷ Late-stage functionalization of purine bases *via* traditional transformations enhanced the utility of this method for the synthesis of bio-relevant molecules.



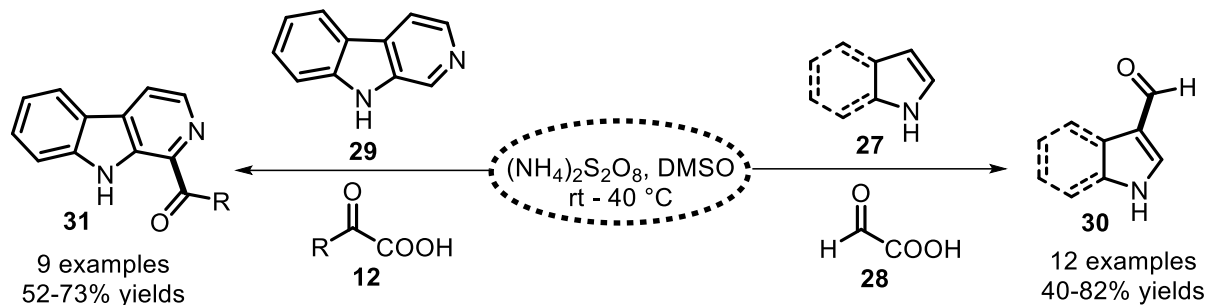
Scheme 2.7 Minisci-type amidation of purine bases

Extending the prior work, a chromatography-free C–H dicarbamoylations (**26**) of phenanthrolines (**25**) has also been reported (**Scheme 2.8**).¹⁸ The developed method provided a 2-step synthesis of 4,7-diisobutoxy-*N*²,*N*⁹-diphenyl-1,10-phenanthroline-2,9-dicarbox amide, which was traditionally produced by following 11 synthetic steps.



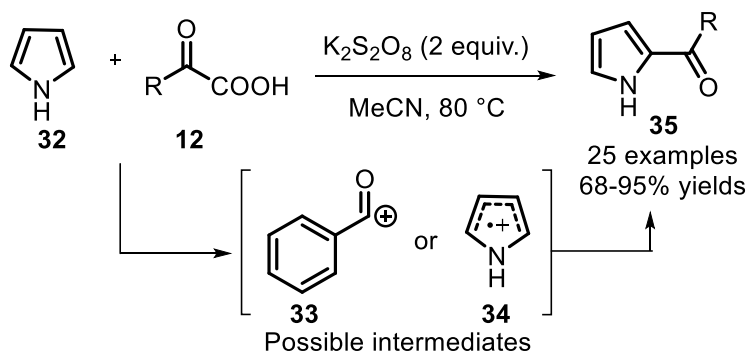
Scheme 2.8 Minisci-type dicarbamoylation of phenanthrolines

Similarly, Dinesh and Nagarajan demonstrated the decarboxylative C-C bond formation of indoles (**27**) and β -carbolines (**28**) with α -oxo (**29**)/ketoacids (**12**) for the effectual construction of 3-carbaldehyde indoles (**30**) and acylated β -carbolines (**31**) in the presence of $(\text{NH}_4)_2\text{S}_2\text{O}_8$. The site selective formylation of indole afforded one-pot synthesis of pityriacitrins, an active indole alkaloid (**Scheme 2.9**).¹⁹



Scheme 2.9 Minisci type acylation/formylation of β -carbolines and indoles

Laha group disclosed a simple, site-selective acylation of electron-rich pyrroles (**32**) with α -ketoacids (**12**) which later come-up as non-classical Minisci-type reaction. The monoacyl substituted pyrroles (**35**) were obtained by following two plausible pathways. Either by umplong reactivity of acyl radical (**33**) followed by electrophilic substitution with **32** or by nucleophilic attack of acyl radical to the electronically-poor pyrrole radical cation (**34**) generated *via* SET from sulfate radical anion (**Scheme 2.10**).²⁰ The developed method avoids imposing acidic and silver catalyzed reaction conditions which were in strong contrast with traditional Minisci-reaction.



Scheme 2.10 Minisci-type amidation of pyrrole

On the other hand, imidazo[1,2-*a*]pyridine is an aromatic, bicyclic heterocycle containing a 5-membered imidazo ring fused with a 6-membered pyridine ring. As a result of fusion of electron-rich and electron-deficient rings, the properties of overall organic molecule become very

diverse since two different charge densities are carried in a single organic molecule. Due to manifold properties, the core imidazopyridine scaffold act as a building block for not only the biologically relevant compounds but also plays significant role in the field of polymer chemistry²¹⁻²² and optoelectronics.²³⁻²⁴⁻²⁵ Many marketed drugs involve imidazopyridine skeleton for example, Zolpidem (or Ambien®) is employed as a sedative and used in the therapy for insomnia.²⁶ Necopidem and Saripidem has binding affinity for central benzodiazepine receptor (CBR) and consumed as anxiolytic agents.²⁷ Olprinone is a cardiotoxic agent and used in the treatment of heart failure.²⁸ Zolimidine, a gastroprotective agent, also exhibits an imidazopyridine in its structure.²⁹ Divaplon acts as partial agonist and anticonvulsant drug³⁰, is from imidazopyridine family as well (**Figure 2.3**). More recently, researchers considered further biological applications for these molecules, such as antitumor, anti-inflammatory, antiviral, antibacterial, and analgesic properties.³¹⁻³⁶

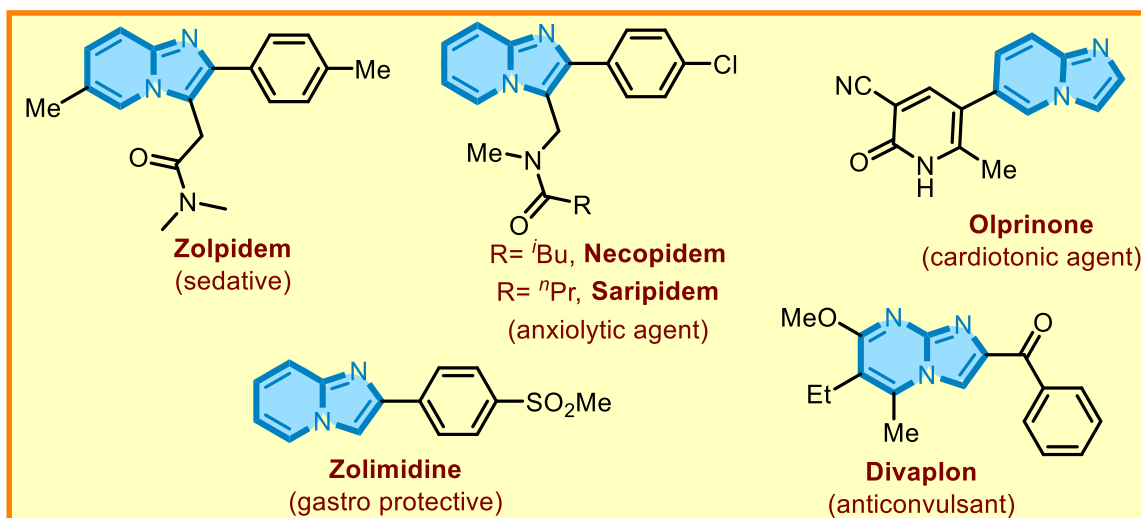
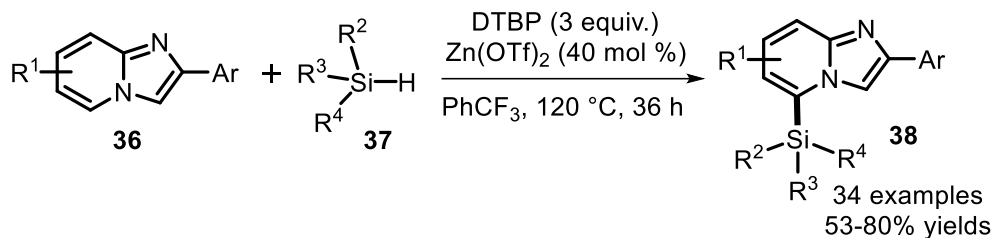


Figure 2.3 Some commercially available drugs containing imidazopyridine skeleton

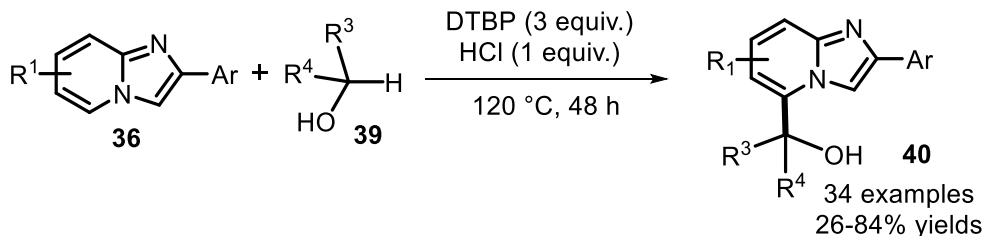
Due to these many applications imidazopyridines have had a long-lasting interest in organic and medicinal chemistry and therefore, it is of great practical significance to construct such a kind of molecular skeleton efficiently and greenly. In this regard numerous amounts of work have been reported of the functionalization of these fused heterocycles, majorly at C3 position³⁷⁻⁴⁰ but the functionalization at C5 position is very less explored. Sun *et al.* reported the regioselective synthesis of C5-silylated imidazo[1,2-*a*]pyridines (**38**) using 2-aryl imidazopyridines

(**36**) and silanes (**37**) in the presence of Lewis acid and peroxide (**Scheme 2.11**).⁴¹ The developed CDC reaction at C5 position was predominantly controlled by coordination of Zn(OTf)₂ with **36**.



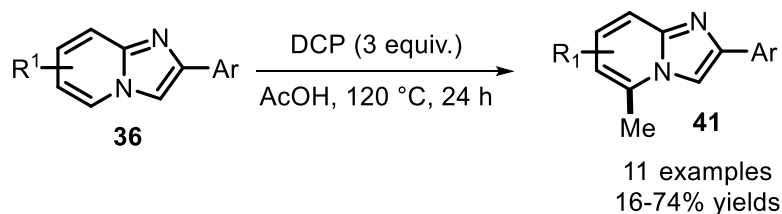
Scheme 2.11 Regioselective C5-silylation of imidazo[1,2-*a*]pyridines

Yan group described the peroxide mediated CDC reaction of imidazo[1,2-*a*]pyridines (**36**) and alcohols (**39**) to afford C5-hydroalkylated product (**40**) (**Scheme 2.12**).⁴² Numerous imidazopyridines substituted at different positions and various primary and secondary alcohols were tolerated under the developed conditions and the corresponding products were obtained in decent yields. Notably, cleavage of C(sp³)-H bond was indicated as the rate-determining step through KIE experiment.



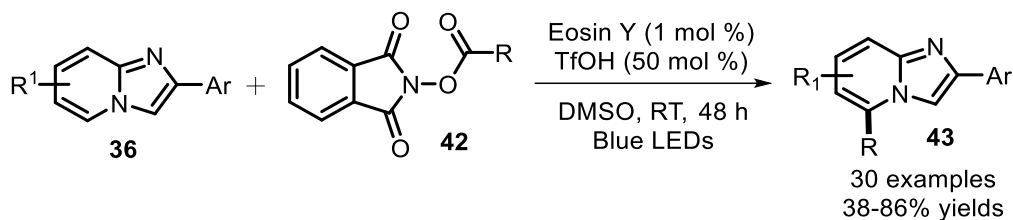
Scheme 2.12 Regioselective C5-hydroalkylation of imidazo[1,2-*a*]pyridines

C5-Methylation of imidazo[1,2-*a*]pyridines (**36**) was investigated by Yan group using peroxides in acetic acid (**Scheme 2.13**).⁴³ Dicumyl peroxide effectively acted as a methyl source as well as the radical initiator in this work and the resulting methylated imidazopyridines (**41**) were obtained in good yields.



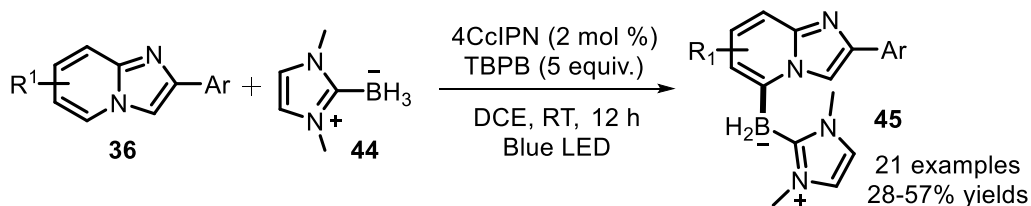
Scheme 2.13 Regioselective C5-methylation of imidazo[1,2-*a*]pyridines

Jin group also disclosed an efficient method for C5-alkylation of imidazo[1,2-*a*]pyridines (**36**) in the presence of visible-light. This method utilized *N*-hydroxyphthalimide (NHPI) esters (**42**) as alkyl source and produced the corresponding C5-alkylated products (**43**) in good yields (**Scheme 2.14**).⁴⁴ Subsequently, a Mn(II)-catalyzed oxidative decarbonylation of aliphatic aldehydes for the regioselective synthesis of C5-alkylated imidazoheterocycles was reported by Sadhanendu and Alaknanda.⁴⁵



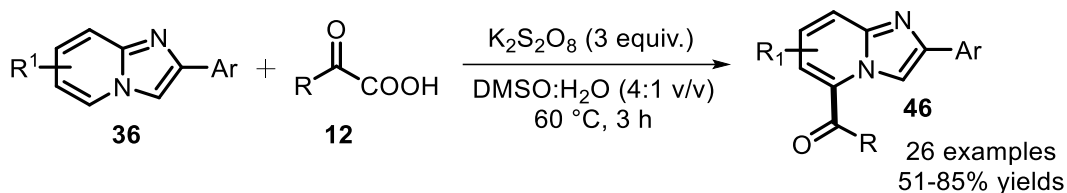
Scheme 2.14 Regioselective C5-alkylation of imidazo[1,2-*a*]pyridines

Among the limited reports on the C5-functionalization of imidazo heterocycles, only one report showcased the Minisci-type reaction which included the visible-light induced C5-borylation of imidazo[1,2-*a*]pyridines (**36**) with NHC-BH₃ (**44**) in the presence of 4CzIPN as a photosensitizer. The method developed by Zheng *et al.* provided a very convenient synthetic strategy for the construction of structurally complex borylated imidazopyridines (**45**) in a regioselective manner. (**Scheme 2.15**).⁴⁶ Environmentally benign reaction conditions, sp² C-B bond formation, huge array of compounds are the fascinating properties of this work.



Scheme 2.15 Minisci-type regioselective C5-borylation of imidazo[1,2-*a*]pyridines

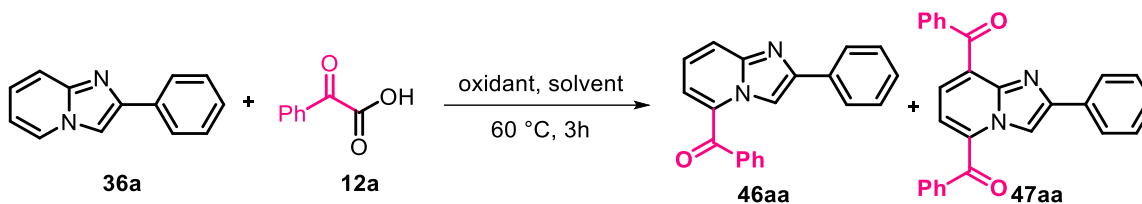
To the best of our knowledge, there is no report for C5-acylation of imidazopyridines. Therefore, in continuation of our interest in functionalization of aza-heterocycles and the importance of biorelevant imidazopyridines (**36**), we have developed a silver-free Minisci-type C5-arylation of imidazo hetroarenes using α -keto acids (**12**) as aroyl source in the presence of K₂S₂O₈ as a radical initiator (**Scheme 2.16**).



Scheme 2.16 Regioselective C5-acylation of imidazo[1,2-*a*]pyridines

2.2 RESULTS AND DISCUSSION

An initial reaction of 2-phenylimidazo[1,2-*a*]pyridine **36a** (0.26 mmol, 1 equiv.) and phenylglyoxylic acid **12a** (0.51 mmol, 2 equiv.) in the presence of $\text{Na}_2\text{S}_2\text{O}_8$ (0.77 mmol, 3.0 equiv.) at 60 °C after 3 h afforded 5-benzoyl-2-phenylimidazo[1,2-*a*]pyridine (**46aa**) and (2-phenylimidazo[1,2-*a*]pyridine-5,8-diyl)bis(phenylmethanone) (**47aa**) in 29% and 10% yields, respectively (**Table 2.1**, entry 1). On changing the oxidant to $\text{K}_2\text{S}_2\text{O}_8$ the yield of **46aa** increased to 49% whereas, the use of $(\text{NH}_4)_2\text{S}_2\text{O}_8$ was found to be less effective for this protocol (**Table 2.1**, entries 2 and 3). Oxidants such as TBHP (*tert*-butyl hydroperoxide) and IBD (iodobenzene diacetate) were also found to be ineffective for this reaction (**Table 2.1**, entries 4 and 5). Screening of different solvents *viz.* DMSO, DMF, DMA, CH_3CN , toluene and H_2O revealed that polar aprotic solvents such as DMSO, DMF and DMA were more suitable media for this reaction (**Table 2.1**, entries 6–10). Interestingly, the yield of **46aa** improved to 56% when a mixture of DMSO and H_2O (3 : 1, v/v) was used as the reaction medium (**Table 2.1**, entry 11). The yield of **46aa** increased to 62% on increasing the amount of **12a** (0.6 mmol, 3 equiv.) but no increment in the yield of **46aa** was observed on further increasing the amount of **12a** (**Table 2.1**, entries 12 and 13). A detrimental effect on the yield of **46aa** was observed when additives such as AgNO_3 , TFA and DIPEA were used in the reaction (**Table 2.1**, entries 14–16). The reaction did not proceed at room temperature and **46aa** was obtained in 12% and 53% yields when the model reaction was performed at 40 °C and 100 °C, respectively (**Table 2.1**, entries 17–19). The yield of **46aa** did not increase on prolonging the reaction time to 24 h (**Table 2.1**, entry 20). Thus, **12a** (3.0 equiv.), $\text{K}_2\text{S}_2\text{O}_8$ (3.0 equiv.), and DMSO/ H_2O (3 mL, 4 : 1 v/v) at 60 °C for 3 h were selected as the optimum reaction conditions for this reaction (**Table 2.1**, entry 12).

Table 2.1 Optimization of reaction conditions for **46aa**^a

Entry	Oxidant	Solvent	% yield ^b	
			46aa	47aa
1	Na ₂ S ₂ O ₈	DMSO	29	10
2	K ₂ S ₂ O ₈	DMSO	49	15
3	(NH ₄) ₂ S ₂ O ₈	DMSO	20	<10
4	TBHP	DMSO	— ^c	—
5	PIDA	DMSO	— ^c	—
6	K ₂ S ₂ O ₈	DMF	47	18
7	K ₂ S ₂ O ₈	DMA	45	15
8	K ₂ S ₂ O ₈	Toluene	— ^c	—
9	K ₂ S ₂ O ₈	CH ₃ CN	— ^c	—
10	K ₂ S ₂ O ₈	H ₂ O	21	<10
11	K ₂ S ₂ O ₈	DMSO/H ₂ O	56	14
12^d	K₂S₂O₈	DMSO/H₂O	62	12
13 ^e	K ₂ S ₂ O ₈	DMSO/H ₂ O	61	17
14 ^{d,f}	K ₂ S ₂ O ₈	DMSO/H ₂ O	26	<10
15 ^{d,g}	K ₂ S ₂ O ₈	DMSO/H ₂ O	29	<10
16 ^{d,h}	K ₂ S ₂ O ₈	DMSO/H ₂ O	29	<10
17 ^{d,i}	K ₂ S ₂ O ₈	DMSO/H ₂ O	— ^c	—
18 ^{d,j}	K ₂ S ₂ O ₈	DMSO/H ₂ O	12	—
19 ^{d,k}	K ₂ S ₂ O ₈	DMSO/H ₂ O	53	17
20 ^{d,l}	K ₂ S ₂ O ₈	DMSO/H ₂ O	60	18

^aReaction conditions: **36a** (0.2 mmol), **12a** (0.5 mmol), K₂S₂O₈ (3.0 equiv.), and solvent (3 mL), 60 °C, 3 h. ^bIsolated yield. ^cNo reaction. ^d**12a** (0.6 mmol) was used. ^e**12a** (0.8 mmol) was used. ^fAgNO₃ (1.5 equiv.) was used as an additive. ^gTFA (1.5 equiv.) was used as an additive. ^hDIPEA (1.5 equiv.) was used as an additive. ⁱReaction at room temperature. ^jReaction at 40 °C. ^kReaction at 100 °C. ^lReaction time: 24 h.

The structure of **46aa** was fully elucidated by ¹H (Figure 2.4) and ¹³C{¹H} NMR (Figure 2.5). In ¹H NMR spectrum the C5 proton of 2-phenylimidazo[1,2-a]pyridine has vanished and the C3 proton

has shifted to the deshielded region at δ 9.24 ppm. In $^{13}\text{C}\{^1\text{H}\}$ NMR spectrum the carbonyl carbon was observed at 190.4 ppm. The remaining protons and carbons of the compound **46aa** were observed at their respective positions in ^1H and $^{13}\text{C}\{^1\text{H}\}$ NMR. The reason of shifting of C3 proton is NOE effect due to the ortho-proton of benzoyl group. Furthermore, the structure of **46aa** was unambiguously confirmed by HRMS analyses (**Figure 2.6**) and a single-crystal X-ray diffraction study (**Figure 2.7**) (CCDC 1978834).

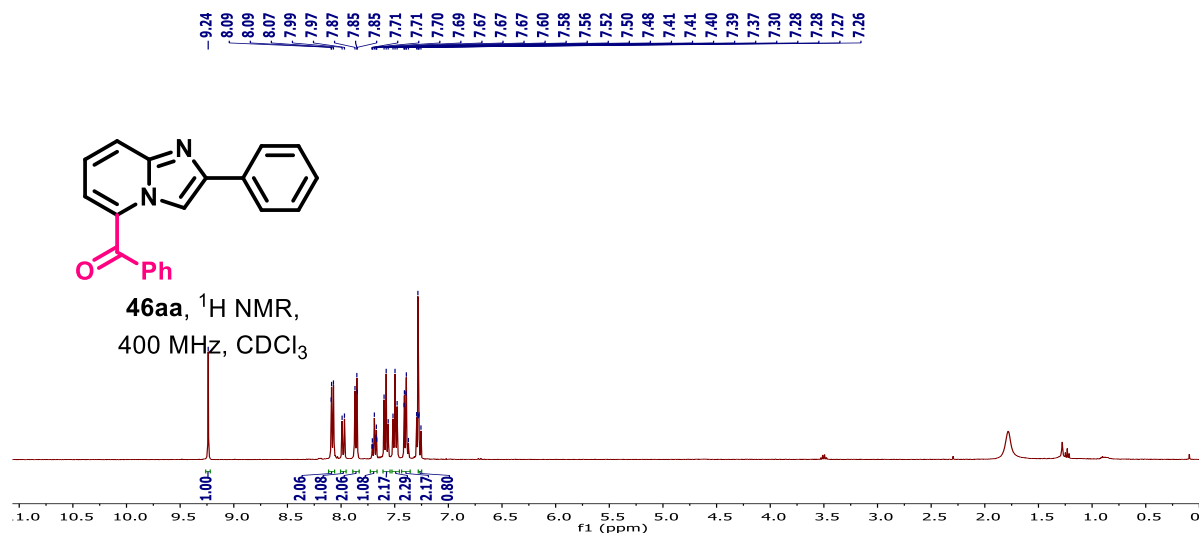


Figure 2.4 ^1H NMR spectrum of phenyl(2-phenylimidazo[1,2-a]pyridin-5-yl)methanone (**46aa**) recorded in CDCl_3

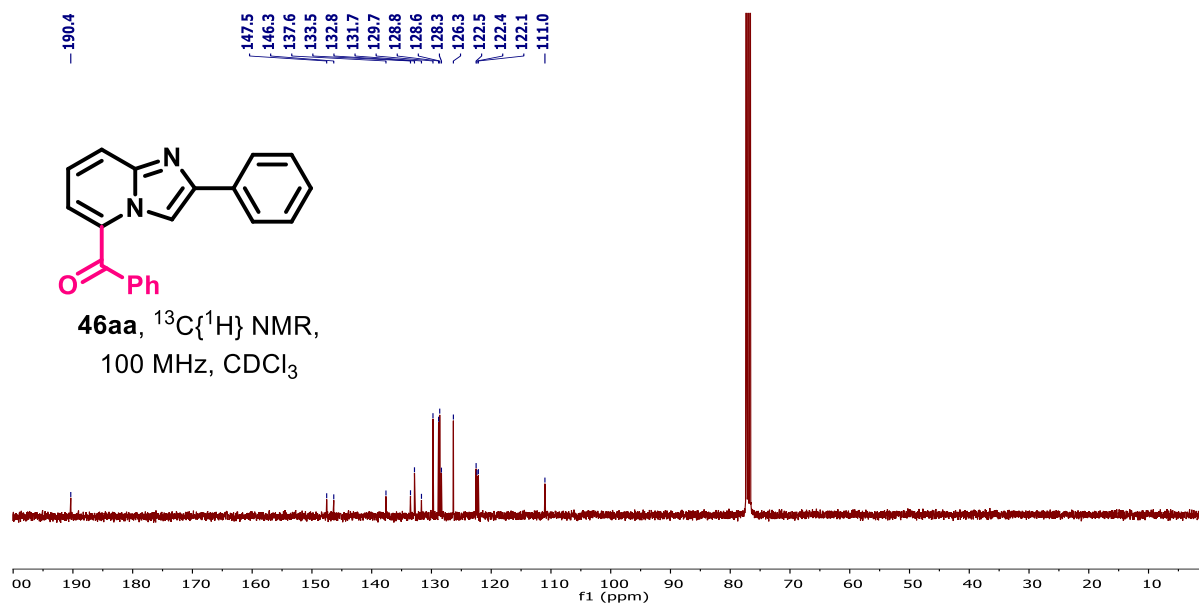


Figure 2.5 $^{13}\text{C}\{^1\text{H}\}$ NMR spectrum of phenyl(2-phenylimidazo[1,2-a]pyridin-5-yl)methanone **46aa** recorded in CDCl_3

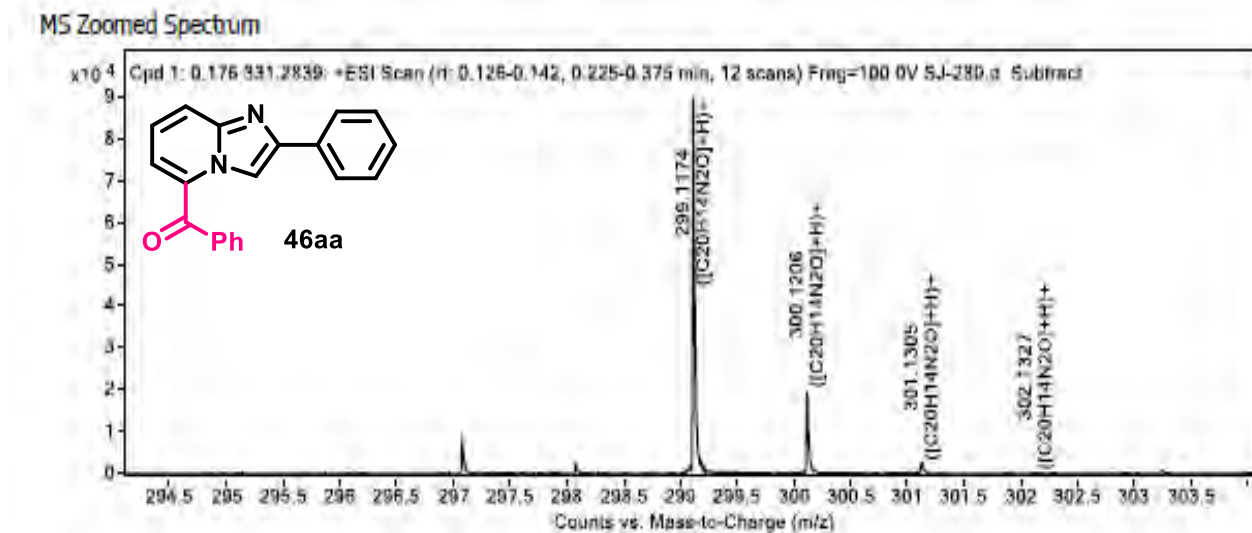


Figure 2.6 HRMS spectrum of phenyl(2-phenylimidazo[1,2-*a*]pyridin-5-yl)methanone **46aa**

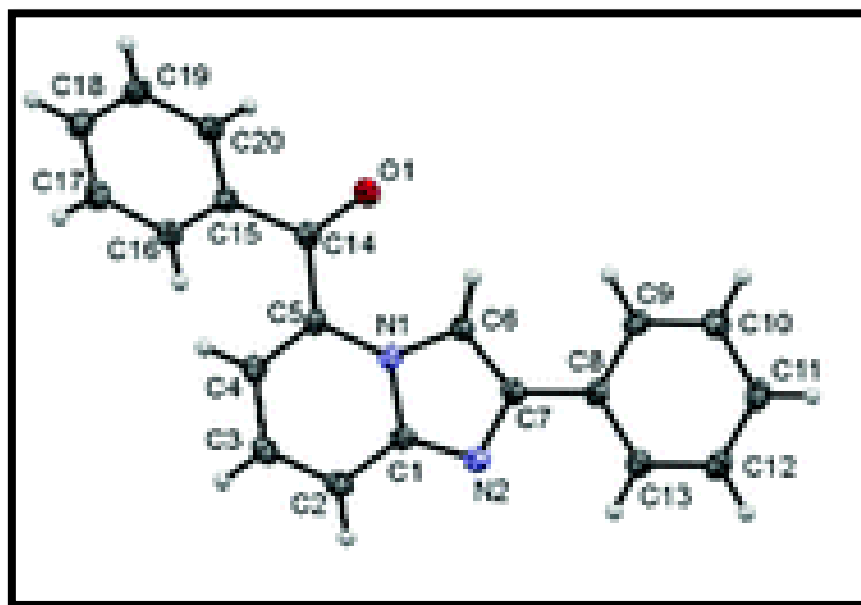
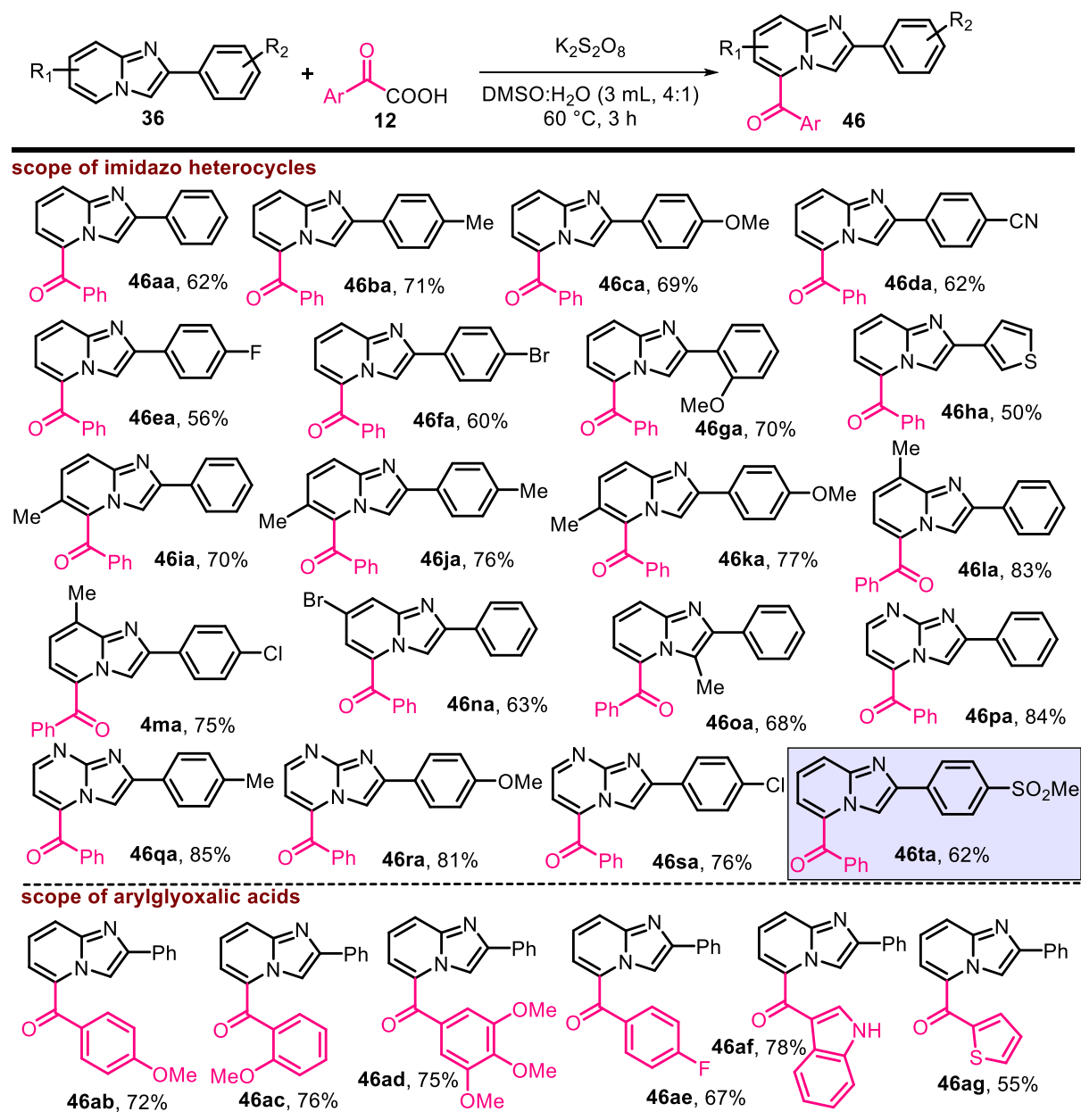


Figure 2.7 ORTEP diagram of **46aa** (CCDC No 1978834). The thermal ellipsoids are drawn at 50% probability level

After confirming the structure of **46aa**, a series of experiments were performed to optimize the reaction conditions for decarboxylative benzoylation of **36a** using **12a** as a benzoyl source (Table 2.1). With the optimized reaction conditions in hand, we investigated the scope of imid-

azo[1,2-*a*]pyridines (**Table 2.2**). A wide range of 2-arylimidazo[1,2-*a*]pyridines with both electron-donating and electron-withdrawing substituents such as Me, OMe, CF₃, CN and halogens at the C2-benzene ring (**36a–g**) on reaction with **12a** afforded the corresponding benzoylated products (**46aa–ga**) with good yields. 2-(Thiophen-2-yl)imidazo[1,2-*a*]pyridine (**36h**) also successfully afforded the desired benzoylated products (**46ha**) in 50% yield. Similarly, the reaction of 2-arylimidazo[1,2-*a*]pyridines substituted with methyl and bromo groups at different positions on the pyridine ring (**36i–n**) afforded the corresponding benzoyl derivatives (**46ia–na**) in good yields (63–83%). It was found that the imidazo[1,2-*a*]pyridines with a methyl substituent on the pyridine ring at C6- and C8-positions provided higher yields as compared to unsubstituted imidazo[1,2-*a*]pyridines. A C3-substituted substrate, 3-methyl-2-phenylimidazo[1,2-*a*]pyridine (**36o**), also reacted under these conditions to give the corresponding C5-benzoyl derivative (**46oa**) in 68% yield. Interestingly, the reaction of imidazo[1,2-*a*]pyrimidines (**36p–s**) with substituents such as methyl, methoxy and chloro groups on the C2-benzene ring with **12a** provided the corresponding C5-benzoyl derivatives **46pa–sa** in high yields (76–85%). The higher yield in the case of imidazo[1,2-*a*]pyrimidines as compared to imidazo[1,2-*a*]pyridines may be due to the extra stability of the radical intermediate by the nitrogen atom of the pyrimidine ring and/or more electron deficient pyrimidine rings. Benzoylation of a commercial drug molecule, Zolimidine, was performed under optimized conditions to give the corresponding C5-benzoylated derivative **46ta** in 62% yield. Finally, the substrate scope of arylglyoxylic acids (**12**) was examined. The reaction of **36a** with a variety of substituted arylglyoxylic acids (**12b–e**) afforded the corresponding benzoylated products (**46ab–ae**) in good yields (67–76%). Heteroaryl glyoxylic acids *viz.* 3-indoleglyoxylic acid (**12f**) and 2-thiophenoglyoxylic acid (**12g**) also reacted successfully under these conditions to afford the corresponding products **46af** and **46ag** in 78% and 55% yields, respectively.

Table 2.2 Substrate scope for benzoylation of imidazoheterocycles^{a,b,c}

^aReaction conditions: **36** (0.5 mmol), **12** (1.5 mmol), $K_2S_2O_8$ (3 equiv.), and DMSO : H_2O (3.0 mL, 4:1 v/v), 60 °C, 3 h. ^bIsolated yields. ^cIn most of the cases, C3-benzoylated derivatives were formed in a small amount (5–10%) which were not isolated.

For additional confirmation 1D NOE experiment with **46pa** was performed which also cleared the regioselectivity at C5 position (**Figure 2.8**). When proton at $\delta = 8.92$ ppm was selectively irradiated, it leads to partial NOE enhancement of the signal at $\delta = 8.14$, 7.92 and 7.62 ppm. It indicates that the benzoyl group is in proximity with the proton at C3 position. Also, irradiation

of signal at $\delta = 8.70$ ppm shows a NOE enhancement of proton at $\delta = 7.23$ ppm only. A clear NOE enhancement of the proton at C3 position ($\delta = 8.92$ ppm) and ortho protons of phenyl ring ($\delta = 7.92$ ppm) was also observed when the signal at $\delta = 8.14$ ppm was selectively irradiated. This confirms the presence of benzoyl group at C5 position of imidazo[1,2-*a*]pyrimidines.

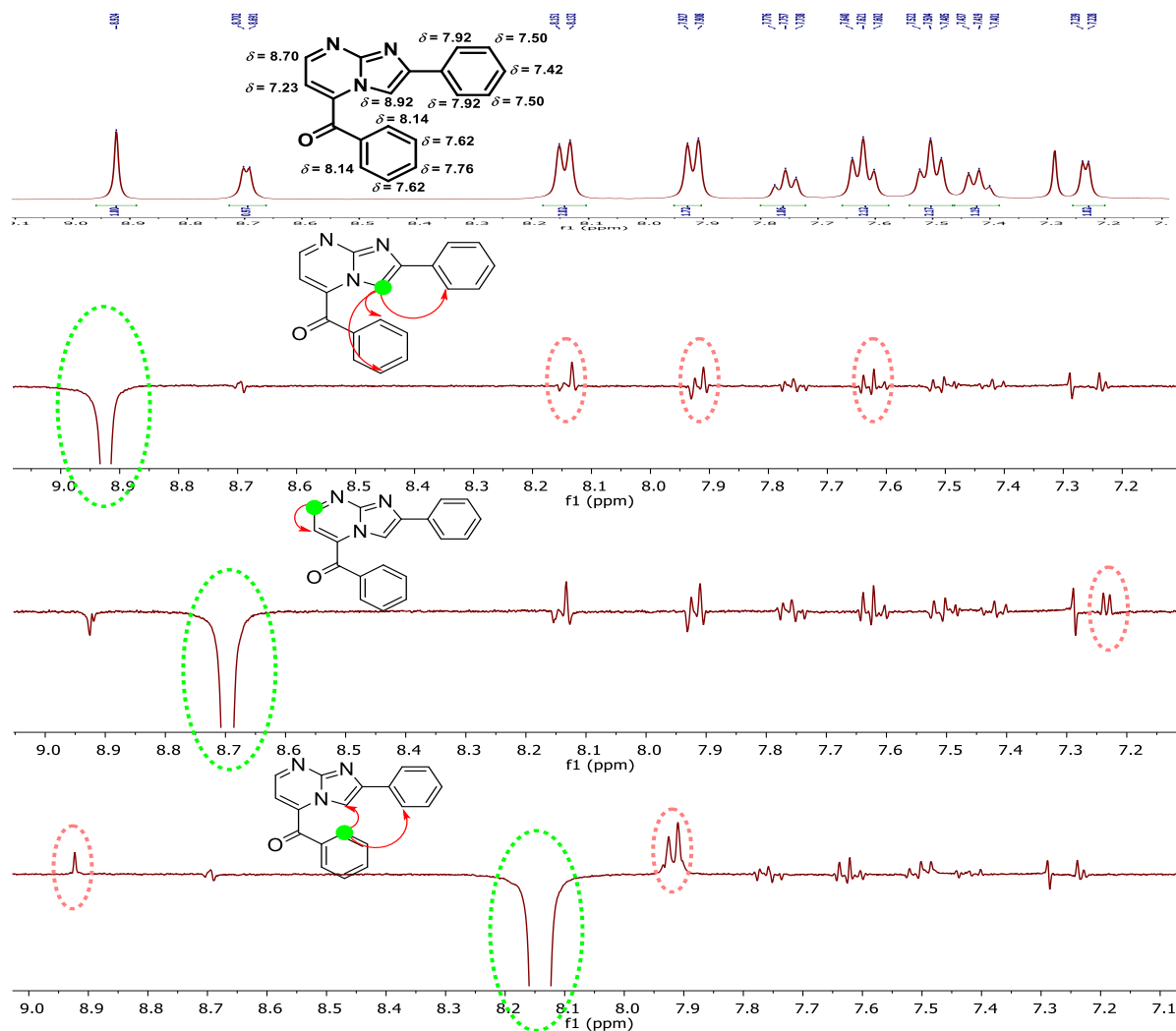
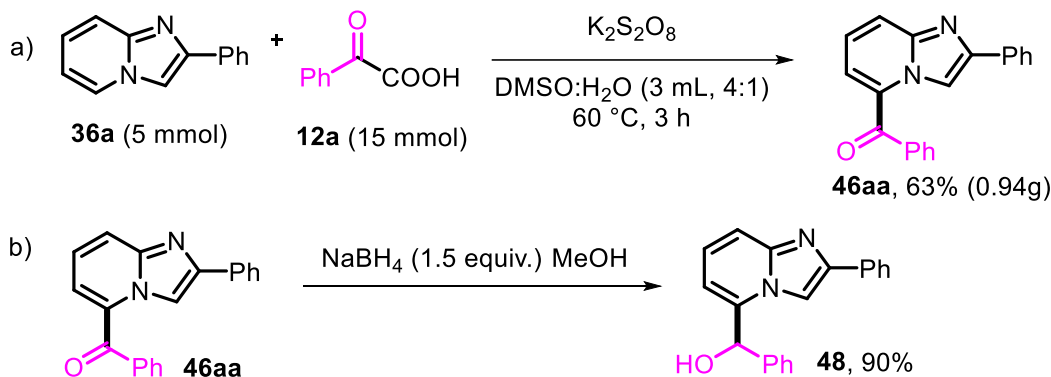


Figure 2.8 NOE spectra of phenyl(2-phenylimidazo[1,2-*a*]pyrimidin-5-yl)methanone **46pa** recorded in CDCl_3

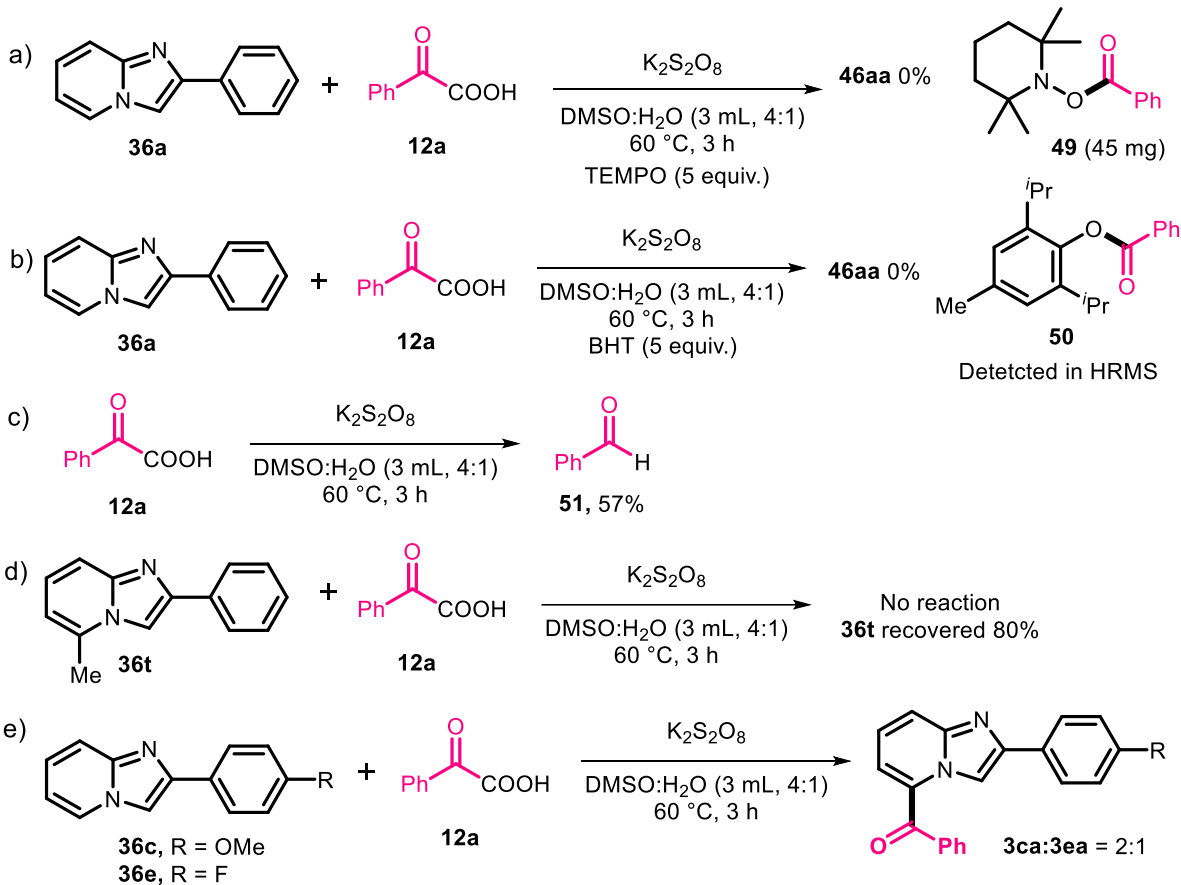
To verify the efficiency of the designed protocol, the gram-scale synthesis of **46aa** was carried out by the reaction of **36a** (5 mmol) with **12a** (15 mmol) under the standard reaction conditions (**Scheme 2.17**). To our expectation, the desired C5-benzoylated product **46aa** was isolated in 63% yield without a significant change in the efficacy of the reaction. Furthermore, synthetic

application of the method was demonstrated by reducing **46aa** to phenyl(2-phenylimidazo[1,2-*a*]pyridin-5-yl)methanol (**48**) in 90% yield using sodium borohydride in methanol (Scheme 2.17).



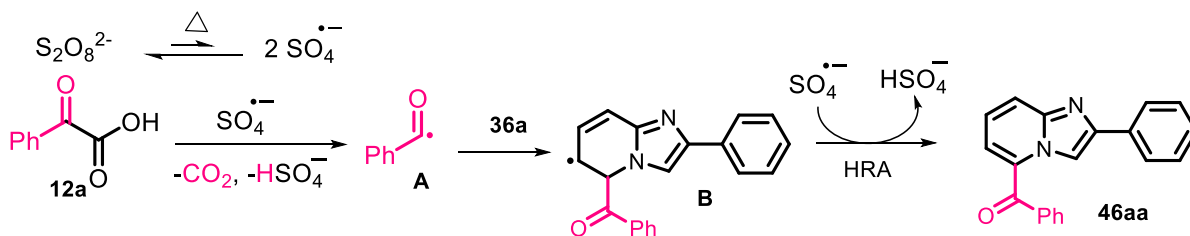
Scheme 2.17 a) Gram scale synthesis of **46aa** and (b) reduction of **46aa** using $NaBH_4$.

To gain insights into the benzoylation reaction mechanism, a few control experiments were performed (Scheme 2.18). The model reaction of **36a** with **12a** failed to produce the desired product **46aa** in the presence of a radical scavenger TEMPO (2,2,6,6-tetramethylpiperidine-1-oxyl), but 2,2,6,6-tetramethylpiperidin-1-yl benzoate (**49**) was isolated (Scheme 2.18a). Similarly, the reaction of **36a** with **12a** in the presence of BHT (butylated hydroxytoluene) under standard reaction conditions also failed to produce the desired product **46aa** (Scheme 2.18b). Formation of 2,6-diisopropyl-4-methylphenyl benzoate (**50**) was detected by HRMS analysis of the reaction mixture. Furthermore, heating **12a** under optimal reaction conditions produced benzaldehyde (**51**) in 57% yield (Scheme 2.18c). The results from these control experiments suggested that the benzoyl radical may be formed through the decarboxylative reaction of phenylglyoxylic acid. The reaction of 5-methyl-2-phenylimidazo[1,2-*a*]pyridine (**36t**) with **12a** under standard reaction conditions failed to produce any product and **36t** was recovered in 80% yield (Scheme 2.18d). Finally, a competitive reaction between 2-arylimidazo[1,2-*a*]pyridines, **36c** and **36e**, produced the corresponding products **46ca** and **46ea** in a 2 : 1 ratio (Scheme 2.18e), indicating that the substrate with electron donating substituents at the C2-benzene ring of the imidazo-[1,2-*a*]pyridines is more favourable for this reaction.



Scheme 2.18 Control experiments

Based on the control experiments and literature reports,^{42-43, 47-48} a plausible mechanistic pathway is depicted in **Scheme 2.19**. First, the thermal decomposition of $K_2S_2O_8$ generated sulfate radicals ($SO_4^{\cdot-}$).⁴⁹ Next, the oxidative decarboxylation of **12a** in the presence of $SO_4^{\cdot-}$ generated benzoyl radicals (**A**), which then reacted regioselectively at the C5-position of **36a** to afford the radical intermediate **B**. Finally, hydrogen radical abstraction (HRA) by $SO_4^{\cdot-}$ or persulfate mediated single-electron transfer (SET) followed by deprotonation produced the desired product **46aa**.



Scheme 2.19 Proposed reaction mechanism

2.3 CONCLUSIONS

In summary, we have developed a metal- and photocatalyst-free $K_2S_2O_8$ -mediated reaction for regioselective benzoylation of imidazoheterocycles using arylglyoxylic acids as a benzoyl source. The reaction produced good yields and tolerated a wide range of functional groups both on imidazoheterocycles as well as on arylglyoxylic acids. Control experiments indicated that the reaction is likely to proceed *via* a radical pathway. The developed protocol is amenable for a scale-up reaction. Given the high pharmaceutical importance of imidazo[1,2-*a*]pyridines, the newly developed method will be useful for the synthesis of a variety of 5-arylimidazo[1,2-*a*]pyridines under metal-free and mild reaction conditions.

2.4 EXPERIMENTAL SECTION

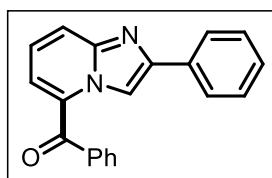
2.4.1 General Information

All the chemicals were obtained from commercial suppliers and used without further purification. Aryl glyoxylic acids were synthesized by the oxidation of the corresponding aryl methyl ketones using selenium dioxide following the reported procedure.⁵⁰ Zolimidine was synthesized by reacting 2-(4-bromophenyl)-imidazo[1,2-*a*]pyridine with sodium methane sulfonate in the presence of CuI/L-proline⁵¹. Reactions were monitored by using thin-layer chromatography (TLC) on 0.2 mm silica gel F254 plates. Column chromatography was performed over silica gel (100–200 mesh) using Hexanes/EtOAc as an Eluent system. Melting points were determined in open capillary tubes on an automated melting point apparatus and are uncorrected. 1H and $^{13}C\{^1H\}$ NMR spectra were recorded on Bruker Avance 400 NMR spectrometer at 400 MHz and 100 MHz frequency, respectively, with $CDCl_3$ as the solvent using TMS as an internal standard or $DMSO-d_6$ as the solvent. Chemical shifts (δ) and coupling constants (J) are reported in parts per million (ppm) and hertz, respectively. The peak multiplicities of 1H NMR signals were designated as s (singlet), d (doublet), dd (doublet of doublet), dt (doublet of triplet), td (triplet of doublet), t (triplet), q (quartet), m (multiplet), *etc.* HRMS (ESI) was performed using Agilent 6545 Q-TOF LC/MS spectrometer.

2.4.2 Experimental Procedure for the Preparation of Benzoylated Products (46)

To a solution of **36** (0.51 mmol, 1.0 equiv.) in DMSO : H₂O (3 mL, 4 : 1 v/v) was added arylglyoxylic acid **12** (1.54 mmol, 3.0 equiv.) and K₂S₂O₈ (1.54 mmol, 3.0 equiv.) at room temperature and the reaction mixture was stirred at 60 °C for 3 h. After completion of the reaction monitored by TLC, the reaction mixture was allowed to attain room temperature. It was poured into water (10 mL) and extracted with ethyl acetate (3 × 5 mL). The combined organic layer was dried over anhydrous Na₂SO₄ and evaporated under vacuum. The resulting crude oil was purified by column chromatography (silica gel 100–200 mesh) using Hexanes/EtOAc as an Eluent system to afford **46**.

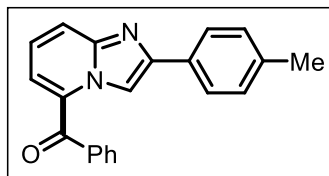
Phenyl(2-phenylimidazo[1,2-a]pyridin-5-yl)methanone (46aa): Yellow solid; 96 mg, 62% yield;



Eluent system: Hexanes/EtOAc (8 : 2 v/v); mp = 163–165 °C; ¹H NMR (400 MHz, CDCl₃) δ = 9.24 (s, 1H), 8.09–8.07 (m, 2H), 7.98 (d, *J* = 8.8 Hz, 1H), 7.87–7.85 (m, 2H), 7.71–7.67 (m, 1H), 7.58 (t, *J* = 7.7 Hz, 2H), 7.50 (t, *J* = 7.7 Hz, 2H), 7.41–7.37 (m, 2H), 7.30–7.26 (m,

1H); ¹³C{¹H} NMR (100 MHz, CDCl₃) δ = 190.4, 147.5, 146.3, 137.6, 133.5, 132.8, 131.7, 129.7, 128.8, 128.6, 128.3, 126.3, 122.5, 122.4, 122.2, 111.0; HRMS (ESI) *m/z*: [M + H]⁺ Calcd for C₂₀H₁₅N₂O⁺ 299.1179; found 299.1174.

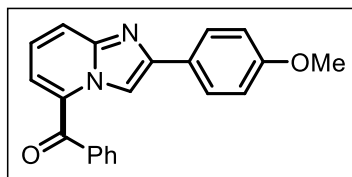
Phenyl(2-(p-tolyl)imidazo[1,2-a]pyridin-5-yl)methanone (46ba): Yellow solid; 105.5 mg, 71%



yield; Eluent system: Hexanes/EtOAc (8 : 2 v/v); mp = 164–166 °C; ¹H NMR (400 MHz, CDCl₃) δ = 9.21 (s, 1H), 7.98–7.95 (m, 3H), 7.86–7.84 (m, 2H), 7.71–7.66 (m, 1H), 7.57 (t, *J* = 7.6 Hz, 2H), 7.39 (dd, *J* = 7.2, 1.2 Hz, 1H), 7.31 (d, *J* = 8.0 Hz, 2H), 7.26

(dd, *J* = 8.8, 7.2 Hz, 1H), 2.43 (s, 3H); ¹³C{¹H} NMR (100 MHz, CDCl₃) δ = 190.4, 147.7, 146.3, 138.2, 137.6, 132.8, 131.6, 130.7, 129.7, 129.5, 128.6, 126.2, 122.4, 122.3, 122.0, 110.7, 21.4; HRMS (ESI) *m/z*: [M + H]⁺ Calcd for C₂₁H₁₇N₂O⁺ 313.1335; found 313.1331.

(2-(4-Methoxyphenyl)imidazo[1,2-a]pyridin-5-yl)(phenyl)methanone (46ca): Yellow solid; 101

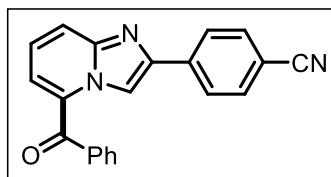


mg, 69% yield; Eluent system: Hexanes/ EtOAc (8 : 2 v/v); mp = 181–183 °C; ¹H NMR (400 MHz, CDCl₃) δ = 9.17 (s, 1H), 8.01 (d, *J* = 8.3 Hz, 2H), 7.95 (d, *J* = 8.9 Hz, 1H), 7.85 (d, *J* = 7.6 Hz, 2H), 7.68 (t, *J* = 7.4 Hz, 1H), 7.57 (t, *J* = 7.7 Hz, 2H), 7.38 (d, *J* =

7.2 Hz, 1H), 7.27–7.23 (m, 1H), 7.03 (d, *J* = 8.3 Hz, 2H), 3.90 (s, 3H); ¹³C{¹H} NMR (100

MHz, CDCl₃) δ = 190.4, 159.9, 147.6, 146.3, 137.7, 132.8, 131.5, 129.7, 128.6, 127.6, 126.2, 122.3, 122.2, 121.9, 114.3, 110.2, 55.4; HRMS (ESI) m/z : [M + H]⁺ Calcd for C₂₁H₁₇N₂O₂⁺ 329.1285, found 329.1279.

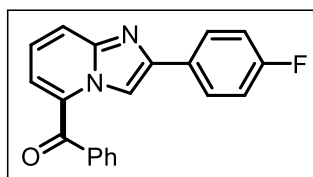
4-(5-Benzoylimidazo[1,2-*a*]pyridin-2-yl)benzonitrile (**46da**): Yellow solid; 91 mg, 62% yield; Eluent system: Hexanes/EtOAc (8:2 v/v); mp = 173–175 °C; ¹H



NMR (400 MHz, CDCl₃) δ = 9.31 (s, 1H), 8.18 (d, J = 8.0 Hz, 2H), 7.97 (d, J = 8.8 Hz, 1H), 7.86 (d, J = 7.6 Hz, 2H), 7.77 (d, J = 7.7 Hz, 2H), 7.70 (t, J = 7.4 Hz, 1H), 7.59 (t, J = 7.6 Hz, 2H), 7.44

(d, J = 7.0 Hz, 1H), 7.35–7.31 (m, 1H); ¹³C{¹H} NMR (100 MHz, CDCl₃) δ = 190.1, 146.1, 144.3, 137.2, 137.1, 133.3, 132.7, 132.0, 129.8, 128.8, 126.8, 124.0, 122.9, 122.4, 118.9, 112.2, 111.8; HRMS (ESI) m/z : Calcd for C₂₁H₁₄N₃O⁺ 324.1131, found 324.1127.

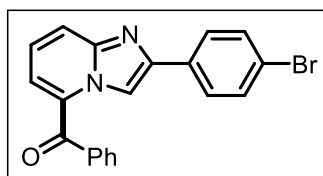
(2-(4-Fluorophenyl)imidazo[1,2-*a*]pyridin-5-yl)(phenyl)methanone (**46ea**): Yellow solid; 83 mg,



56% yield; Eluent system: Hexanes/ EtOAc (8:2 v/v); mp = 171–173 °C; ¹H NMR (400 MHz, CDCl₃) δ = 9.19 (s, 1H), 8.05 (dd, J = 8.8, 5.6 Hz, 2H), 7.96 (d, J = 8.8 Hz, 1H), 7.86 (d, J = 7.2 Hz, 2H), 7.69 (t, J = 7.4 Hz, 1H), 7.58 (t, J = 7.6 Hz, 2H), 7.40 (d, J = 7.2 Hz,

1H), 7.30–7.26 (m, 1H), 7.18 (t, J = 8.6 Hz, 2H); ¹³C{¹H} NMR (100 MHz, CDCl₃) δ = 190.1, 163.2 (d, ¹ J_{C-F} = 248.7 Hz), 145.3, 144.8, 137.1, 133.2, 131.7, 129.8, 128.76, 128.3 (d, ³ J_{C-F} = 8.3 Hz), 123.9, 122.8, 121.6, 116.1, 115.9, 110.6; HRMS (ESI) m/z : [M + H]⁺ Calcd for C₂₀H₁₄FN₂O⁺ 317.1085, found 317.1079.

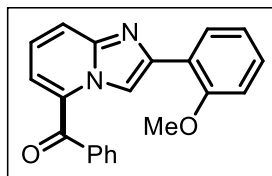
(2-(4-Bromophenyl)imidazo[1,2-*a*]pyridin-5-yl)(phenyl)methanone (**46fa**): Yellow solid; 82.5 mg,



60% yield; Eluent system: Hexanes/ EtOAc (8:2 v/v); mp = 176–178 °C; ¹H NMR (400 MHz, CDCl₃) δ = 9.22 (s, 1H), 7.97–7.93 (m, 3H), 7.85 (dd, J = 8.2, 1.4 Hz, 2H), 7.71–7.67 (m, 1H), 7.63–7.62 (m, 1H), 7.60 (t, J = 2.2 Hz, 2H), 7.58–7.56 (m, 1H), 7.41

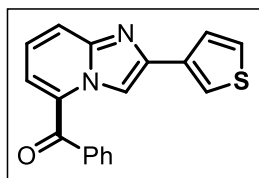
(dd, J = 7.2, 1.2 Hz, 1H), 7.31–7.27 (m, 1H); ¹³C{¹H} NMR (100 MHz, CDCl₃) δ = 190.2, 146.0, 145.7, 137.3, 133.1, 132.0, 131.9, 131.7, 129.8, 128.7, 127.9, 123.1, 122.6, 122.6, 122.2, 111.0; HRMS (ESI) m/z : [M + H]⁺ Calcd for C₂₀H₁₄BrN₂O⁺ 377.0248, found 377.0250.

(2-(2-Methoxyphenyl)imidazo[1,2-a]pyridin-5-yl)(phenyl)-methanone (**46ga**): Yellow solid; 102



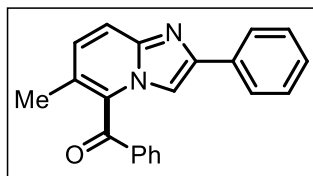
mg, 70% yield; Eluent system: Hexanes/ EtOAc (8 : 2 v/v); mp = 127–129 °C; ^1H NMR (400 MHz, CDCl_3) δ = 9.38 (s, 1H), 8.57 (d, J = 2.8 Hz, 1H), 7.96 (d, J = 8.8 Hz, 1H), 7.87 (d, J = 7.2 Hz, 2H), 7.69 (t, J = 7.6 Hz, 1H), 7.58 (t, J = 7.6 Hz, 2H), 7.46–7.43 (m, 1H), 7.38–7.36 (m, 1H), 7.29–7.25 (m, 2H), 6.92 (d, J = 8.8 Hz, 1H), 4.02 (s, 3H); $^{13}\text{C}\{^1\text{H}\}$ NMR (100 MHz, CDCl_3) δ = 190.0, 156.1, 144.2, 137.2, 133.3, 132.2, 132.0, 131.6, 130.3, 129.9, 128.9, 128.8, 123.9, 122.5, 121.6, 115.0, 113.6, 112.8, 55.9; HRMS (ESI) m/z : $[\text{M} + \text{H}]^+$ Calcd for $\text{C}_{21}\text{H}_{17}\text{N}_2\text{O}_2^+$ 329.1285, found 329.1288.

Phenyl(2-(thiophen-3-yl)imidazo[1,2-a]pyridin-5-yl)methanone (**46ha**): Yellow solid; 75.5 mg,



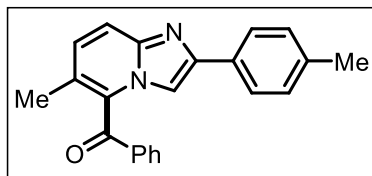
50% yield; Eluent system: Hexanes/EtOAc (8 : 2 v/v); mp = 145–147 °C; ^1H NMR (400 MHz, CDCl_3) δ = 9.12 (s, 1H), 7.95–7.91 (m, 2H), 7.85 (d, J = 7.6 Hz, 2H), 7.69 (t, J = 7.8 Hz, 1H), 7.65 (d, J = 5.2 Hz, 1H), 7.58 (t, J = 7.6 Hz, 2H), 7.45–7.43 (m, 1H), 7.40 (d, J = 7.2 Hz, 1H), 7.26 (d, J = 8.0 Hz, 1H); $^{13}\text{C}\{^1\text{H}\}$ NMR (100 MHz, CDCl_3) δ = 190.4, 146.2, 143.8, 137.6, 135.5, 132.8, 131.6, 129.7, 128.6, 126.2, 126.1, 122.4, 122.3, 122.2, 122.0, 111.0; HRMS (ESI) m/z : $[\text{M} + \text{H}]^+$ Calcd for $\text{C}_{18}\text{H}_{13}\text{N}_2\text{OS}^+$ 305.0743, found 305.0738.

(6-Methyl-2-phenylimidazo[1,2-a]pyridin-5-yl)(phenyl)methanone (**46ia**): Yellow solid; 104.5 mg,



70% yield; Eluent system: Hexanes/EtOAc (8 : 2 v/v); mp = 181–183 °C; ^1H NMR (400 MHz, CDCl_3) δ = 9.09 (s, 1H), 8.05 (d, J = 8, 2H), 7.86 (d, J = 8, 2H), 7.74 (s, 1H), 7.70 (t, J = 7.6 Hz, 1H), 7.59 (t, J = 7.4 Hz, 2H), 7.48 (t, J = 7.4 Hz, 2H), 7.37 (t, J = 7.4 Hz, 1H), 7.20 (s, 1H), 2.46 (s, 3H); $^{13}\text{C}\{^1\text{H}\}$ NMR (100 MHz, CDCl_3) δ = 190.3, 146.9, 146.6, 138.0, 134.1, 133.9, 132.4, 130.0, 129.6, 128.7, 128.5, 128.1, 126.4, 123.2, 121.3, 111.5, 17.8; HRMS (ESI) m/z : $[\text{M} + \text{H}]^+$ Calcd for $\text{C}_{21}\text{H}_{17}\text{N}_2\text{O}^+$ 313.1335, found 313.1337.

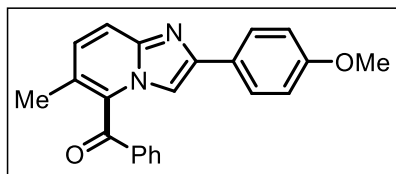
(6-Methyl-2-(*p*-tolyl)imidazo[1,2-a]pyridin-5-yl)(phenyl)-methanone (**46ja**): Yellow solid; 112 mg,



76% yield; Eluent system: Hexanes/ EtOAc (8 : 2 v/v); mp = 173–175 °C; ^1H NMR (400 MHz, CDCl_3) δ = 9.08 (s, 1H), 7.95 (d, J = 8.4 Hz, 2H), 7.86–7.84 (m, 2H), 7.80 (s, 1H), 7.70 (t, J = 7.4 Hz, 1H), 7.58 (t, J = 7.6 Hz, 2H), 7.30 (d, J = 8.8 Hz, 2H), 7.22 (d, J = 2.0 Hz, 1H), 2.46 (s, 3H), 2.42 (s, 3H); $^{13}\text{C}\{^1\text{H}\}$ NMR (100 MHz, CDCl_3) δ = 190.2,

146.3, 146.1, 138.4, 137.4, 133.8, 133.0, 131.0, 130.0, 129.8, 129.6, 128.7, 126.2, 124.7, 120.6, 109.8, 21.4, 21.1; HRMS (ESI) m/z : $[M + H]^+$ Calcd for $C_{22}H_{20}N_2O^+$ 313.1335, found 313.1332.

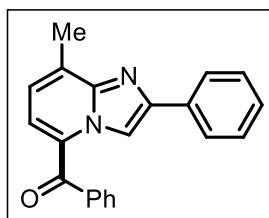
(2-(4-Methoxyphenyl)-6-methylimidazo[1,2-a]pyridin-5-yl)-(phenyl)methanone (**46ka**): Orange



solid; 110 mg, 77% yield; Eluent system: Hexanes/EtOAc (8:2 v/v); mp = 188–190 °C; 1H NMR (400 MHz, $CDCl_3$) δ = 9.01 (s, 1H), 7.98 (d, J = 8.8 Hz, 2H), 7.85 (d, J = 6.8 Hz, 2H), 7.70–7.67 (m, 2H), 7.58 (t, J = 7.6 Hz, 2H), 7.18

(d, J = 1.2 Hz, 1H), 7.01 (d, J = 8.4 Hz, 2H), 3.89 (s, 3H), 2.45 (s, 3H); $^{13}C\{^1H\}$ NMR (100 MHz, $CDCl_3$) δ = 190.4, 159.8, 147.1, 146.7, 137.7, 132.8, 132.7, 130.9, 129.7, 128.6, 127.5, 126.5, 124.4, 120.9, 114.2, 109.4, 55.3, 21.0; HRMS (ESI) m/z : $[M + H]^+$ Calcd for $C_{22}H_{19}N_2O_2^+$ 343.1441, found 343.1440.

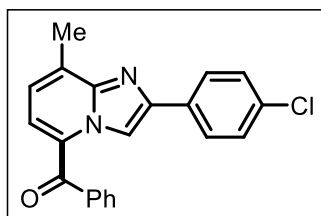
(8-Methyl-2-phenylimidazo[1,2-a]pyridin-5-yl)(phenyl)methanone (**46la**): Yellow solid; 124 mg,



83% yield; Eluent system: Hexanes/EtOAc (8:2 v/v); mp = 156–158 °C; 1H NMR (400 MHz, $CDCl_3$) δ = 9.29 (s, 1H), 8.11–8.09 (m, 2H), 7.84–7.82 (m, 2H), 7.66 (t, J = 7.4 Hz, 1H), 7.56 (t, J = 7.4 Hz, 2H), 7.49 (t, J = 7.6 Hz, 2H), 7.37 (t, J = 7.4 Hz, 1H), 7.33 (d, J = 7.2 Hz, 1H), 7.06 (dd, J = 7.2, 0.8 Hz, 1H), 2.83 (s, 3H); $^{13}C\{^1H\}$ NMR (100

MHz, $CDCl_3$) δ = 190.3, 146.9, 146.6, 138.1, 134.1, 133.9, 132.5, 130.0, 129.6, 128.7, 128.5, 128.1, 126.4, 123.2, 121.3, 111.5, 17.8; HRMS (ESI) m/z : $[M + H]^+$ Calcd for $C_{21}H_{17}N_2O^+$ 313.1335, found 313.1332.

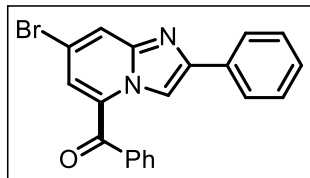
(2-(4-Chlorophenyl)-8-methylimidazo[1,2-a]pyridin-5-yl)(phenyl)-methanone (**46ma**): Yellow solid;



125 mg, 75% yield; Eluent system: Hexanes/EtOAc (8:2 v/v); mp = 169–171 °C; 1H NMR (400 MHz, $CDCl_3$) δ = 9.26 (s, 1H), 8.05–8.02 (m, 2H), 7.83–7.81 (m, 2H), 7.69–7.65 (m, 1H), 7.57 (t, J = 7.6 Hz, 2H), 7.47–7.44 (m, 2H), 7.34 (d, J = 7.6 Hz, 1H), 7.08 (dd, J = 7.2, 0.8 Hz, 1H), 2.81 (s, 3H); $^{13}C\{^1H\}$ NMR (100 MHz,

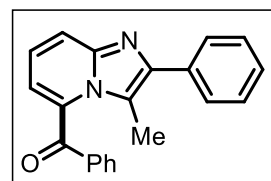
$CDCl_3$) δ = 190.1, 146.2, 145.1, 137.8, 134.1, 133.9, 132.7, 131.7, 130.0, 129.7, 129.0, 128.6, 127.7, 123.4, 122.3, 111.5, 17.9; HRMS (ESI) m/z : $[M + H]^+$ Calcd for $C_{21}H_{16}ClN_2O^+$ 347.0946, found 349.0946.

(7-Bromo-2-phenylimidazo[1,2-a]pyridin-3-yl)(phenyl)methanone (**46na**): Yellow solid; 86.5 mg,



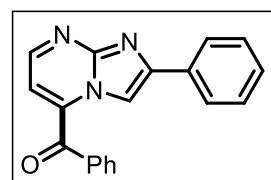
63% yield; Eluent system: Hexanes/EtOAc (8 : 2 v/v); mp = 189–191 °C; ^1H NMR (400 MHz, CDCl_3) δ = 7.95 (dd, J = 8.4, 1.2 Hz, 2H), 7.89 (dd, J = 8.4, 1.2 Hz, 2H), 7.76–7.72 (m, 1H), 7.69 (dd, J = 9.6, 0.4 Hz, 1H), 7.65 (s, 1H), 7.59–7.55 (m, 2H), 7.44–7.39 (m, 3H), 7.36–7.32 (m, 1H); $^{13}\text{C}\{^1\text{H}\}$ NMR (100 MHz, CDCl_3) δ = 189.4, 147.2, 144.4, 135.5, 134.2, 132.8, 132.2, 130.0, 129.5, 128.8, 128.5, 128.4, 126.2, 118.9, 108.0, 105.5; HRMS (ESI) m/z : $[\text{M} + \text{H}]^+$ Calcd for $\text{C}_{20}\text{H}_{14}\text{BrN}_2\text{O}^+$ 377.0284, found 377.0279.

(3-Methyl-2-phenylimidazo[1,2-a]pyridin-5-yl)(phenyl)methanone (**46oa**): Yellow solid; 102 mg,



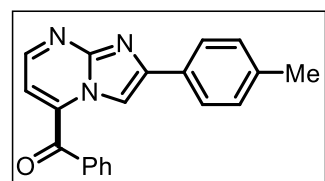
68% yield; Eluent system: Hexanes/EtOAc (8 : 2 v/v); mp = 174–176 °C; ^1H NMR (400 MHz, CDCl_3) δ = 8.04 (d, J = 7.6 Hz, 2H), 7.92 (d, J = 8.8 Hz, 1H), 7.82 (d, J = 7.6 Hz, 2H), 7.72 (t, J = 7.0 Hz, 1H), 7.58 (t, J = 7.6 Hz, 2H), 7.51 (t, J = 7.6 Hz, 2H), 7.40 (t, J = 7.2 Hz, 1H), 7.26 (t, J = 7.8 Hz, 1H), 7.12 (d, J = 6.8 Hz, 1H), 2.33 (s, 3H); $^{13}\text{C}\{^1\text{H}\}$ NMR (100 MHz, CDCl_3) δ = 188.0, 145.3, 145.2, 136.4, 134.3, 134.2, 130.6, 129.9, 129.0, 128.9, 128.5, 127.8, 121.6, 120.7, 119.4, 118.0, 14.4; HRMS (ESI) m/z : $[\text{M} + \text{H}]^+$ Calcd for $\text{C}_{21}\text{H}_{17}\text{N}_2\text{O}^+$ 313.1335, found 313.1329.

Phenyl(2-phenylimidazo[1,2-a]pyrimidin-5-yl)methanone (**46pa**): Yellow solid; 130 mg, 81%



yield; Eluent system: Hexanes/EtOAc (8 : 2 v/v); mp = 190–192 °C; ^1H NMR (400 MHz, CDCl_3) δ = 8.92 (s, 1H), 8.69 (d, J = 4.4 Hz, 1H), 8.14 (d, J = 6.8 Hz, 2H), 7.91 (d, J = 7.2 Hz, 2H), 7.75 (t, J = 7.4 Hz, 1H), 7.62 (t, J = 7.8 Hz, 2H), 7.50 (t, J = 7.4 Hz, 2H), 7.41 (t, J = 7.4 Hz, 1H), 7.22 (d, J = 4.4 Hz, 1H); $^{13}\text{C}\{^1\text{H}\}$ NMR (100 MHz, CDCl_3) δ = 189.8, 150.0, 149.6, 147.5, 136.5, 135.8, 134.1, 132.9, 130.0, 129.0, 128.8, 126.6, 113.1, 108.4; HRMS (ESI) m/z : $[\text{M} + \text{H}]^+$ Calcd for $\text{C}_{19}\text{H}_{14}\text{N}_3\text{O}^+$ 300.1131, found 300.1129.

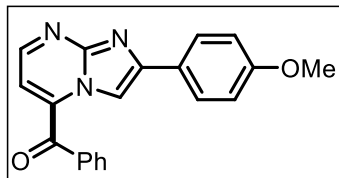
Phenyl(2-(*p*-tolyl)imidazo[1,2-a]pyrimidin-5-yl)methanone (**46qa**): Yellow solid; 127.5 mg, 85%;



Eluent system: Hexanes/EtOAc (8 : 2 v/v); mp = 121–123 °C; ^1H NMR (400 MHz, CDCl_3) δ = 8.89 (s, 1H), 8.67 (d, J = 3.2 Hz, 1H), 8.04 (d, J = 7.6 Hz, 2H), 7.91 (d, J = 8.0 Hz, 2H), 7.77–7.73 (m, 1H), 7.61 (t, J = 7.6 Hz, 2H), 7.32–7.28 (m, 2H), 7.22–7.21 (m, 1H), 2.43 (s, 3H); $^{13}\text{C}\{^1\text{H}\}$ NMR (100 MHz, CDCl_3) δ = 189.8, 150.0, 149.9, 147.2, 139.1, 136.3,

135.9, 134.0, 130.2, 129.9, 129.6, 129.0, 126.5, 112.9, 108.1, 21.4; HRMS (ESI) m/z : $[M + H]^+$
Calcd for $C_{20}H_{16}N_3O^+$ 314.1288, found 314.1281.

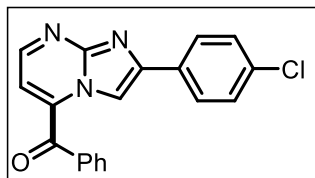
(2-(4-Methoxyphenyl)imidazo[1,2-a]pyrimidin-5-yl)(phenyl)-methanone (**46ra**): Yellow solid; 117.5



mg, 81% yield; Eluent system: Hexanes/ EtOAc (8 : 2 v/v); mp =
159–162 °C; 1H NMR (400 MHz, $CDCl_3$) δ = 8.87 (s, 1H), 8.66
(d, J = 4.4 Hz, 1H), 8.09 (d, J = 8.0 Hz, 2H), 7.91 (d, J = 7.6 Hz,
2H), 7.75 (t, J = 7.6 Hz, 1H), 7.62 (t, J = 7.6 Hz, 2H), 7.21 (d, J =

4.4 Hz, 1H), 7.04 (d, J = 8.4 Hz, 2H), 3.90 (s, 3H); ^{13}C $\{^1H\}$ NMR (100 MHz, $CDCl_3$) δ = 189.9,
160.5, 150.0, 149.8, 147.0, 136.1, 135.9, 134.0, 130.0, 129.0, 128.0, 125.6, 114.3, 113.0, 107.6,
55.4; HRMS (ESI) m/z : $[M + H]^+$ Calcd for $C_{20}H_{16}N_3O_2^+$ 300.1131, found 300.1134.

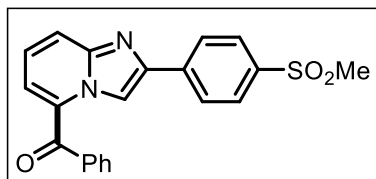
(2-(4-Chlorophenyl)imidazo[1,2-a]pyrimidin-5-yl)(phenyl)-methanone (**46sa**): Yellow solid; 110



mg, 76% yield; Eluent system: Hexanes/EtOAc (8 : 2 v/v); mp =
175–177 °C; 1H NMR (400 MHz, $CDCl_3$) δ = 8.89 (s, 1H), 8.71
(d, J = 4.4 Hz, 1H), 8.08–8.06 (m, 2H), 7.92–7.90 (m, 2H), 7.78–
7.74 (m, 1H), 7.62 (t, J = 7.6 Hz, 2H), 7.48–7.45 (m, 2H), 7.23

(d, J = 4.4 Hz, 1H); ^{13}C $\{^1H\}$ NMR (100 MHz, $CDCl_3$) δ = 189.7, 150.0, 148.4, 147.8, 136.6,
135.8, 134.9, 134.2, 131.5, 130.0, 129.1, 129.0, 127.8, 113.1, 108.5; HRMS (ESI) m/z : $[M +$
 $H]^+$ Calcd for $C_{19}H_{13}ClN_3O^+$ 334.0742, found 334.0737.

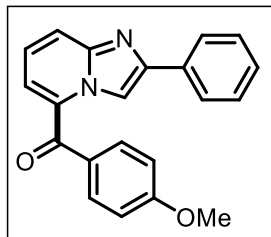
(2-(4-(Methylsulfonyl)phenyl)imidazo[1,2-a]pyridin-5-yl)(phenyl)-methanone (**46ta**): Yellow solid;



70 mg, 51% yield; Eluent system: Hexanes/EtOAc (6 : 4, v/v);
mp = 217–219 °C; 1H NMR (400 MHz, $CDCl_3$) δ = 9.32 (s,
1H), 8.29 (d, J = 8.4 Hz, 2H), 8.08 (t, J = 8.2 Hz, 3H), 7.88
(d, J = 7.2 Hz, 2H), 7.72 (t, J = 7.2 Hz, 1H), 7.60 (t, J = 7.4 Hz,

2H), 7.50 (d, J = 6.8 Hz, 1H), 7.43–7.40 (m, 1H), 3.13 (s, 3H); ^{13}C NMR (100 MHz, $CDCl_3$) δ =
189.9, 140.3, 136.8, 133.5, 132.0, 130.3, 129.9, 129.1, 128.9, 128.6, 128.2, 127.6, 127.2, 123.2,
122.0, 112.3, 44.6; HRMS (ESI) m/z : $[M + H]^+$ Calcd for $C_{21}H_{17}N_2O_3S^+$ 377.0954, found
377.0932.

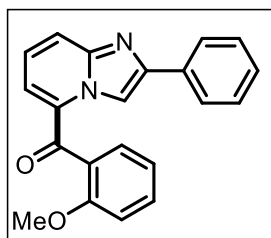
(4-Methoxyphenyl)(2-phenylimidazo[1,2-a]pyridin-5-yl)-methanone (**46ab**): Yellow solid; 121 mg,



72% yield; Eluent system: Hexanes/ EtOAc (8 : 2 v/v); mp = 153–155 °C; ^1H NMR (400 MHz, CDCl_3) δ = 9.02 (s, 1H), 8.05 (d, J = 7.2 Hz, 2H), 7.91 (t, J = 8.4 Hz, 3H), 7.48 (t, J = 7.6 Hz, 2H), 7.38 (t, J = 7.4 Hz, 1H), 7.33 (d, J = 6.8 Hz, 1H), 7.25 (d, J = 7.2 Hz, 1H), 7.05 (d, J = 8.8 Hz, 2H), 3.95 (s, 3H); $^{13}\text{C}\{^1\text{H}\}$ NMR (100 MHz, CDCl_3) δ = 189.0,

163.8, 147.1, 146.3, 133.6, 132.4, 132.2, 129.8, 128.8, 128.2, 126.3, 122.3, 121.8, 120.7, 114.0, 110.6, 55.6; HRMS (ESI) m/z : $[\text{M} + \text{H}]^+$ Calcd for $\text{C}_{21}\text{H}_{17}\text{N}_2\text{O}_2^+$ 329.1285, found 329.1297.

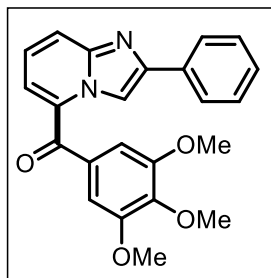
(2-Methoxyphenyl)(2-phenylimidazo[1,2-a]pyridin-5-yl)-methanone (**46ac**): Yellow solid; 128 mg,



76% yield; Eluent system: Hexanes/ EtOAc (8 : 2 v/v); mp = 178–180 °C; ^1H NMR (400 MHz, CDCl_3) δ = 9.52 (s, 1H), 8.13–8.10 (m, 2H), 8.03 (d, J = 8.8 Hz, 1H), 7.56 (td, J = 8.6, 1.6 Hz, 1H), 7.51 (t, J = 7.6 Hz, 2H), 7.45 (dd, J = 7.6, 1.6 Hz, 1H), 7.40 (t, J = 7.4 Hz, 1H), 7.35–7.33 (m, 1H), 7.28–7.24 (m, 1H), 7.15–7.11 (m, 1H), 7.06 (d, J = 8.4

Hz, 1H), 3.78 (s, 3H); $^{13}\text{C}\{^1\text{H}\}$ NMR (100 MHz, CDCl_3) δ = 190.3, 157.3, 147.1, 146.0, 133.0, 132.6, 132.5, 129.5, 128.9, 128.5, 127.8, 126.4, 123.2, 122.9, 122.4, 120.7, 111.6, 111.4, 55.7; HRMS (ESI) m/z : $[\text{M} + \text{H}]^+$ Calcd for $\text{C}_{21}\text{H}_{17}\text{N}_2\text{O}_2^+$ 329.1285, found 329.1278.

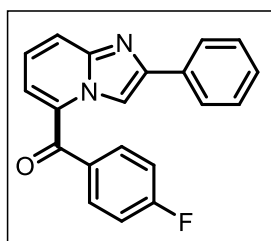
(2-Phenylimidazo[1,2-a]pyridin-5-yl)(3,4,5-trimethoxyphenyl)-methanone (**46ad**): Yellow solid;



150 mg, 75% yield; Eluent system: Hexanes/EtOAc (8 : 2 v/v); mp = 140–142 °C; ^1H NMR (400 MHz, CDCl_3) δ = 9.05 (s, 1H), 8.09 (d, J = 7.2 Hz, 3H), 7.51 (t, J = 7.6 Hz, 2H), 7.47 (d, J = 7.2 Hz, 1H), 7.43–7.39 (m, 1H), 7.36 (d, J = 8.0 Hz, 1H), 7.13 (s, 2H), 4.01 (s, 3H), 3.94 (s, 6H); $^{13}\text{C}\{^1\text{H}\}$ NMR (100 MHz, CDCl_3) δ = 188.9, 153.2, 143.0,

133.0, 131.9, 129.0, 129.0, 128.6, 128.0, 126.5, 123.8, 121.7, 121.4, 110.6, 107.9, 107.6, 61.1, 56.5; HRMS (ESI) m/z : $[\text{M} + \text{H}]^+$ Calcd for $\text{C}_{23}\text{H}_{21}\text{N}_2\text{O}_4^+$ 389.1489, found 389.1486.

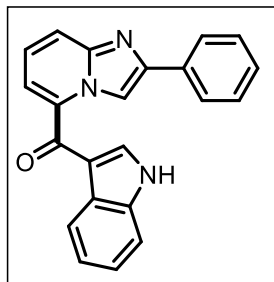
(4-Fluorophenyl)(2-phenylimidazo[1,2-a]pyridin-5-yl)methanone (**46ae**): Yellow solid; 108.5 mg,



67% yield; Eluent system: Hexanes/EtOAc (8 : 2 v/v); mp = 171–173 °C; ^1H NMR (400 MHz, CDCl_3) δ = 9.17 (s, 1H), 8.08–8.06 (dd, J = 8.8, 1.6 Hz, 2H), 7.97 (d, J = 8.8 Hz, 1H), 7.93–7.90 (m, 2H), 7.50 (t, J = 7.7 Hz, 2H), 7.40 (d, J = 7.6 Hz, 1H), 7.36 (dd, J = 7.2, 1.6 Hz, 1H), 7.30–7.24 (m, 3H); $^{13}\text{C}\{^1\text{H}\}$ NMR (100 MHz, CDCl_3) δ = 188.8,

147.5, 146.3, 133.7 (d, $J = 3.3$ Hz), 133.3, 132.4 (d, $J = 9.1$ Hz), 131.5, 128.8, 128.4, 126.3, 122.6, 122.2, 122.0, 116.1, 115.8, 110.9; HRMS (ESI) m/z : $[M + H]^+$ Calcd for $C_{20}H_{14}FN_2O^+$ 317.1085, found 317.1087.

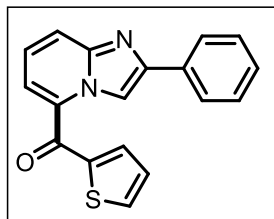
(1*H*-Indol-3-yl)(2-phenylimidazo[1,2-*a*]pyridin-5-yl)methanone (**46af**): Yellow solid; 136 mg, 78%



yield; Eluent system: Hexanes/EtOAc (8 : 2 v/v); mp = 235–237 °C; 1H NMR (400 MHz, $CDCl_3$) δ = 8.80 (d, $J = 4.0$ Hz, 1H), 8.46–8.44 (m, 1H), 8.01–7.99 (m, 2H), 7.84–7.80 (m, 2H), 7.51 (d, $J = 6.8$ Hz, 1H), 7.46–7.41 (m, 2H), 7.37–7.33 (m, 4H), 7.28–7.24 (m, 1H); $^{13}C\{^1H\}$ NMR (100 MHz, $DMSO-d_6$) δ = 183.6, 146.1, 145.5, 137.5, 137.5,

134.6, 134.1, 129.2, 128.4, 126.6, 126.2, 124.6, 124.1, 122.2, 121.9, 120.1, 117.4, 115.4, 113.1, 109.8; HRMS (ESI) m/z : $[M + H]^+$ Calcd for $C_{22}H_{16}N_3O^+$ 338.1288, found 338.1290.

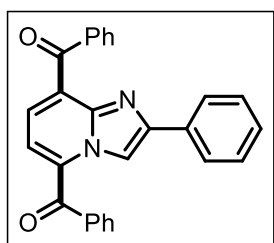
(2-Phenylimidazo[1,2-*a*]pyridin-5-yl)(thiophen-2-yl)methanone (**46ag**): Yellow solid; 86 mg, 55%



yield; Eluent system: Hexanes/EtOAc (8 : 2 v/v); mp = 174–176 °C; 1H NMR (400 MHz, $CDCl_3$) δ = 9.0 (s, 1H), 8.04 (d, $J = 7.2$ Hz, 2H), 7.97 (d, $J = 8.8$ Hz, 1H), 7.84 (d, $J = 4.4$ Hz, 1H), 7.80 (d, $J = 3.6$ Hz, 1H), 7.60 (d, $J = 6.8$ Hz, 1H), 7.48 (t, $J = 7.2$ Hz, 2H), 7.39–7.36 (m, 1H), 7.31 (d, $J = 8.8$ Hz, 1H), 7.26–7.24 (m, 1H); $^{13}C\{^1H\}$ NMR (100 MHz,

$CDCl_3$) δ = 181.4, 147.1, 146.2, 142.7, 135.3, 134.9, 133.4, 131.9, 128.8, 128.3, 128.3, 126.3, 122.4, 122.1, 119.8, 110.5; HRMS (ESI) m/z : $[M + H]^+$ Calcd for $C_{18}H_{13}N_2OS^+$ 305.0743, found 305.0748.

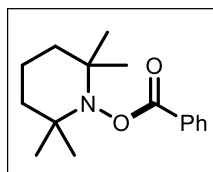
(2-Phenylimidazo[1,2-*a*]pyridine-5,8-diyl)bis(phenylmethanone) (**47aa**): Yellow solid; 31 mg, 15%



yield; Eluent system: Hexanes/EtOAc (8 : 2 v/v); mp = 175–177 °C; 1H NMR (400 MHz, $CDCl_3$) δ = 9.22 (s, 1H), 8.00 (dd, $J = 8.2, 1.4$ Hz, 2H), 7.96 (dd, $J = 8.2, 1.4$ Hz, 2H), 7.91 (dd, $J = 8.2, 1.4$ Hz, 2H), 7.74–7.70 (m, 1H), 7.68–7.64 (m, 1H), 7.62–7.58 (m, 3H), 7.51 (d, $J = 7.6$ Hz, 2H), 7.44 (d, $J = 8.0$ Hz, 2H), 7.41–7.39 (m, 2H); $^{13}C\{^1H\}$ NMR

(100 MHz, $CDCl_3$) δ = 193.1, 190.0, 148.4, 143.8, 137.2, 136.6, 133.8, 133.3, 133.2, 132.7, 132.4, 130.5, 129.9, 128.8, 128.6, 128.5, 128.4, 126.6, 122.4, 120.8, 110.9; HRMS (ESI) m/z : $[M + H]^+$ Calcd for $C_{27}H_{19}N_2O_2^+$ 403.1441, found 403.1439.

2,2,6,6-Tetramethylpiperidin-1-yl benzoate (**49**): Eluent system: Hexanes/EtOAc (8 : 2 v/v); white

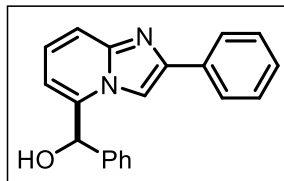


solid; 45 mg; mp = 105–107 °C; ^1H NMR (400 MHz, CDCl_3) δ = 8.14–8.11 (m, 1H), 8.10–8.09 (m, 1H), 7.62–7.58 (m, 1H), 7.51–7.47 (m, 2H), 1.84–1.70 (m, 4H), 1.64–1.60 (m, 2H), 1.30 (s, 6H), 1.15 (s, 6H); ^{13}C $\{^1\text{H}\}$ NMR (100 MHz, CDCl_3) δ = 166.4, 132.8, 129.6, 128.4, 60.4, 39.1, 32.0, 20.9,

17.0; HRMS (ESI) m/z : $[\text{M} + \text{H}]^+$ Calcd for $\text{C}_{16}\text{H}_{24}\text{NO}_2^+$ 262.1802, found 262.1807.

2.4.3 Experimental Procedure for the Synthesis of phenyl(2-phenylimidazo[1,2-*a*]pyridin-5-yl)methanol (**48**)

To a solution of **46aa** (0.17 mmol; 1.0 equiv.) in methanol (10 mL) was added NaBH_4 (0.25 mmol; 1.5 equiv.) portion-wise at room temperature and the reaction mixture was continued for 1 h. After completion of the reaction monitored by TLC, the solvent was evaporated under reduced pressure and the resulting crude solid was washed with diethyl ether and *n*-pentane to get reduced compound phenyl(2-phenylimidazo[1,2-*a*]pyridin-5-yl)methanol (**48**) as white solid;



yield: 45 mg (90%); mp = 96–98 °C; Eluent system: Hexanes/EtOAc (8 : 2 v/v); ^1H NMR (400 MHz, CDCl_3) δ = 7.76–7.74 (m, 3H), 7.34–7.32 (m, 8H), 6.95 (t, J = 8.0 Hz, 1H), 6.59 (d, J = 7.2 Hz, 1H), 5.97 (s, 1H); ^{13}C $\{^1\text{H}\}$ NMR (100 MHz, CDCl_3) δ = 145.9, 144.7, 139.0,

138.8, 133.2, 128.8, 128.6, 128.4, 128.0, 126.8, 126.1, 124.8, 115.7, 111.6, 107.3, 72.6; HRMS (ESI) m/z : $[\text{M} + \text{H}]^+$ Calcd for $\text{C}_{20}\text{H}_{17}\text{N}_2\text{O}^+$ 301.1335, found 301.1337.

2.4.4 X-ray Crystallographic Analysis of Phenyl(2-phenylimidazo[1,2-*a*]pyridin-5-yl)methanone (**46aa**)

The crystals of the compound **46aa** ($\text{C}_{20}\text{H}_{14}\text{N}_2\text{O}$) (**Figure 2.8**) were grown in chloroform solution. **46aa** was crystallized in orthorhombic crystal system with *Pbca* space group. The crystal structure information of **46aa** is deposited to Cambridge Crystallographic Data Center and the CCDC numbers for the **46aa** is 1978834.

The crystal data collection and data reduction were performed using CrysAlis PRO on a single crystal Rigaku Oxford XtaLab Pro diffractometer. The crystal was kept at 93(2) K during data collection. Using Olex2⁵², the structure was solved with the ShelXT⁵³ structure solution program using Intrinsic Phasing and refined with the ShelXL⁵⁴ refinement package using Least Squares minimisation.

Table 2.3: Crystal data and structure refinement for **46aa**

Identification code	46aa
Empirical formula	C ₂₀ H ₁₄ N ₂ O
Formula weight	298.33
Temperature/K	93(2)
Crystal system	orthorhombic
Space group	Pbca
a/Å	8.3127(2)
b/Å	17.1849(3)
c/Å	20.9916(4)
α /°	90
β /°	90
γ /°	90
Volume/Å ³	2998.71(11)
Z	8
$\rho_{\text{calc}}/\text{cm}^3$	1.322
μ/mm^{-1}	0.656
F(000)	1248.0
Crystal size/mm ³	0.1 × 0.1 × 0.1
Radiation	CuK α (λ = 1.54184)
2 Θ range for data collection/°	8.424 to 159.084
Index ranges	-10 ≤ h ≤ 8, -21 ≤ k ≤ 17, -25 ≤ l ≤ 26
Reflections collected	10545
Independent reflections	3204 [R_{int} = 0.0331, R_{sigma} = 0.0312]
Data/restraints/parameters	3204/0/208
Goodness-of-fit on F ²	1.096
Final R indexes [$I \geq 2\sigma(I)$]	R_1 = 0.0442, wR_2 = 0.1217
Final R indexes [all data]	R_1 = 0.0464, wR_2 = 0.1239
Largest diff. peak/hole / e Å ⁻³	0.24/-0.27
CCDC	1978834

2.5 REFERENCES

1. Recupero, F.; Punta, C., *Chemical Reviews* **2007**, *107*, 3800-3842.
2. Yi, H.; Zhang, G.; Wang, H.; Huang, Z.; Wang, J.; Singh, A. K.; Lei, A., *Chemical Reviews* **2017**, *117*, 9016-9085.
3. Duncton, M. A. J., *MedChemComm* **2011**, *2*, 1135-1161.
4. Abramovitch, R. A.; Saha, J. G., *Journal of the Chemical Society* **1964**, 2175-2187.

- Lynch, B. M.; Chang, H. S., *Tetrahedron Letters* **1964**, *5*, 2965-2968.
- Dou, H. J. M.; Lynch, B. M., *Tetrahedron Letters* **1965**, *6*, 897-901.
- Minisci, F.; Galli, R.; Cecere, M.; Malatesta, V.; Caronna, T., *Tetrahedron Letters* **1968**, *9*, 5609-5612.
- Minisci, F.; Galli, R.; Malatesta, V.; Caronna, T., *Tetrahedron* **1970**, *26*, 4083-4091.
- Minisci, F.; Bernardi, R.; Bertini, F.; Galli, R.; Perchinummo, M., *Tetrahedron* **1971**, *27*, 3575-3579.
- Tauber, J.; Imbri, D.; Opatz, T., *Molecules* **2014**, *19*, 16190-16222.
- Liu, Q.; Wang, Q.; Xie, G.; Fang, Z.; Ding, S.; Wang, X., *European Journal of Organic Chemistry* **2020**, *20*, 2600-2604.
- Shao, X.; Wu, X.; Wu, S.; Zhu, C., *Organic Letters* **2020**, *22*, 7450-7454.
- Schulz, G.; Kirschning, A., *Organic & Biomolecular Chemistry* **2021**, *19*, 273-278.
- Kudale, V. S.; Wang, J.-J., *Green Chemistry* **2020**, *22*, 3506-3511.
- Zhu, H.-L.; Zeng, F.-L.; Chen, X.-L.; Sun, K.; Li, H.-C.; Yuan, X.-Y.; Qu, L.-B.; Yu, B., *Organic Letters* **2021**, *23*, 2976-2980.
- McLean, E. B.; Mooney, D. T.; Burns, D. J.; Lee, A.-L., *Organic Letters* **2022**, *24*, 686-691.
- Mooney, D. T.; Moore, P. R.; Lee, A.-L., *Organic Letters* **2022**, *24*, 8008-8013.
- Mooney, D. T.; Donkin, B. D. T.; Demirel, N.; Moore, P. R.; Lee, A.-L., *The Journal of Organic Chemistry* **2021**, *86*, 17282-17293.
- Dinesh, V.; Nagarajan, R., *The Journal of Organic Chemistry* **2022**, *87*, 10359-10365.
- Laha, J. K.; Kaur Hunjan, M.; Hegde, S.; Gupta, A., *Organic Letters* **2020**, *22*, 1442-1447.
- Furukawa, S.; Shono, H.; Mutai, T.; Araki, K., *ACS Applied Materials & Interfaces* **2014**, *6*, 16065-16070.
- Chaudhran, P. A.; Sharma, A., *Critical Reviews in Analytical Chemistry* **2022**, 1-18.
- Cabrele, C.; Reiser, O., *The Journal of Organic Chemistry* **2016**, *81*, 10109-10125.
- Douhal, A.; Amat-Guerri, F.; Acuna, A. U., *The Journal of Physical Chemistry* **1995**, *99*, 76-80.
- Douhal, A.; Amat-Guerri, F.; Acuña, A. U., *Tetrahedron* **1997**, *36*, 1514-1516.

26. Langer, S. Z.; Arbilla, S.; Benavides, J.; Scatton, B., *Adv Biochem Psychopharmacol* **1990**, *46*, 61-72.
27. Boerner, R. J.; Möller, H. J. *Depression and anxiety disorders—epidemiology, theoretical concepts, and treatment options for comorbidity*, Berlin, Heidelberg, 1997; Wolfersdorf, M., Ed. Springer Berlin Heidelberg: Berlin, Heidelberg; pp 210-235.
28. Mizushige, K.; Ueda, T.; Yukiiri, K.; Suzuki, H., *Cardiovascular Drug Reviews* **2002**, *20*, 163-174.
29. Kaminski, J. J.; Doweiko, A. M., *Journal of Medicinal Chemistry* **1997**, *40*, 427-436.
30. Rogawski, M. A., *Epilepsy Res* **2006**, *69*, 273-294.
31. Rival, Y.; Grassy, G.; Michel, G., *Chemical & Pharmaceutical Bulletin* **1992**, *40*, 1170-1176.
32. Fisher, M. H.; Lusi, A., *Journal of Medicinal Chemistry* **1972**, *15*, 982-985.
33. Rival, Y.; Grassy, G.; Taudou, A.; Ecalte, R., *European Journal of Medicinal Chemistry* **1991**, *26*, 13-18.
34. Hamdouchi, C.; de Blas, J.; del Prado, M.; Gruber, J.; Heinz, B. A.; Vance, L., *Journal of Medicinal Chemistry* **1999**, *42*, 50-59.
35. Badawey, E.; Kappe, T., *European Journal of Medicinal Chemistry* **1995**, *30*, 327-332.
36. Hranjec, M.; Kralj, M.; Piantanida, I.; Sedić, M.; Šuman, L.; Pavelić, K.; Karminski-Zamola, G., *Journal of Medicinal Chemistry* **2007**, *50*, 5696-5711.
37. Tran, C.; Hamze, A., *Journal of Medicinal Chemistry* **2022**, *27*, 3461.
38. Ma, C.-H.; Chen, M.; Feng, Z.-W.; Zhang, Y.; Wang, J.; Jiang, Y.-Q.; Yu, B., *New Journal of Chemistry* **2021**, *45*, 9302-9314.
39. Patel, O. P. S.; Nandwana, N. K.; Legoabe, L. J.; Das, B. C.; Kumar, A., *Advanced Synthesis & Catalysis* **2020**, *362*, 4226-4255.
40. Tashrifi, Z.; Mohammadi-Khanaposhtani, M.; Larijani, B.; Mahdavi, M., *European Journal of Organic Chemistry* **2020**, *20*, 269-284.
41. Li, Y.; Shu, K.; Liu, P.; Sun, P., *Organic Letters* **2020**, *22*, 6304-6307.
42. Jin, S.; Xie, B.; Lin, S.; Min, C.; Deng, R.; Yan, Z., *Organic Letters* **2019**, *21*, 3436-3440.
43. Jin, S.; Yao, H.; Lin, S.; You, X.; Yang, Y.; Yan, Z., *Organic & Biomolecular Chemistry* **2020**, *18*, 205-210.
44. Sun, B.; Xu, T.; Zhang, L.; Zhu, R.; Yang, J.; Xu, M.; Jin, C., *Synlett* **2020**, *31*, 363-368.

45. Samanta, S.; Hajra, A., *The Journal of Organic Chemistry* **2019**, *84*, 4363-4371.
46. Zheng, H.; Lu, H.; Su, C.; Yang, R.; Zhao, L.; Liu, X.; Cao, H., *The Journal of Organic Chemistry* **2023**, *41*, 193-198.
47. Ilangovan, A.; Polu, A.; Satish, G., *Organic Chemistry Frontiers* **2015**, *2*, 1616-1620.
48. Semwal, R.; Ravi, C.; Kumar, R.; Meena, R.; Adimurthy, S., *The Journal of Organic Chemistry* **2019**, *84*, 792-805.
49. Liu, Q.; Wang, Q.; Xie, G.; Fang, Z.; Ding, S.; Wang, X., *The Journal of Organic Chemistry* **2020**, *2020*, 2600-2604.
50. Wadhwa, K.; Yang, C.; West, P. R.; Deming, K. C.; Chemburkar, S. R.; Reddy, R. E., *Synthetic Communications* **2008**, *38*, 4434-4444.
51. Zhu, W.; Ma, D., *The Journal of Organic Chemistry* **2005**, *70*, 2696-2700.
52. Dolomanov, O. V.; Bourhis, L. J.; Gildea, R. J.; Howard, J. A.; Puschmann, H., *Journal of Applied Crystallography* **2009**, *42*, 339-341.
53. Sebbar, N.; Ellouz, M.; Essassi, E.; Ouzidan, Y.; Mague, J., *Acta Crystallographica Section E: Crystallographic Communications* **2015**, *71*, o999.
54. Sheldrick, G. M., *Acta Crystallographica Section A: Foundations and Advances* **2015**, *71*, 3-8.

CHAPTER 3

Visible-Light Driven Regioselective Difluoroalkoxylation of Imidazo[1,2-*a*]pyridines using N-Fluorobenzenesulfonimide

4.1 INTRODUCTION

Organofluorine compounds have become increasingly important in modern chemical and pharmaceutical research due to their unique physicochemical properties (**Figure 3.1**).¹⁻³ The incorporation of fluorine into organic compounds greatly enhances their lipophilicity, metabolic stability, membrane permeability, and protein-ligand interactions.⁴⁻⁶ As, fluorine is the most electronegative element, making it highly polarizing, and thus, its introduction into organic molecules can significantly affect their physicochemical properties. Pharmaceuticals are one of the most notable applications of organofluorine compounds. Incorporation of fluorine into an organic compound is vital for drug development because of its tendency to modify the reactivity, selectivity, and specificity of drug molecules towards their target receptors, making them more effective and safer for human use. Apart from the pharmaceutical industry, organofluorine compounds also find extensive use in agrochemicals, materials science, and industrial chemistry. For example, fluoropolymers like Teflon exhibit unique thermal and chemical resistance, making them ideal for various applications, including coatings, insulators, and non-stick surfaces.

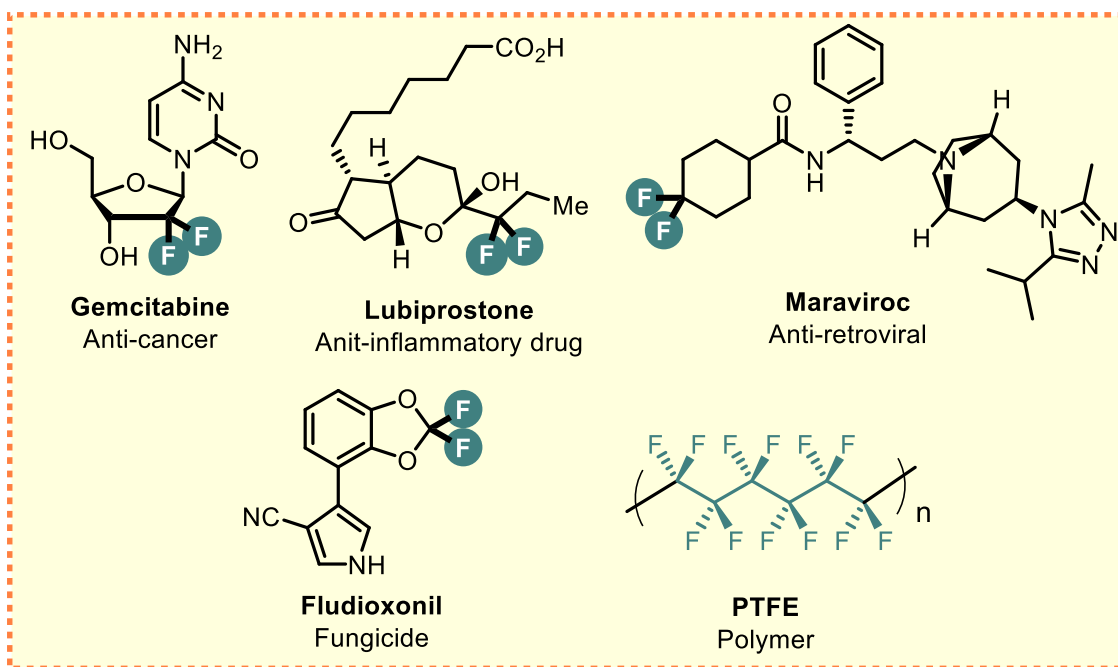
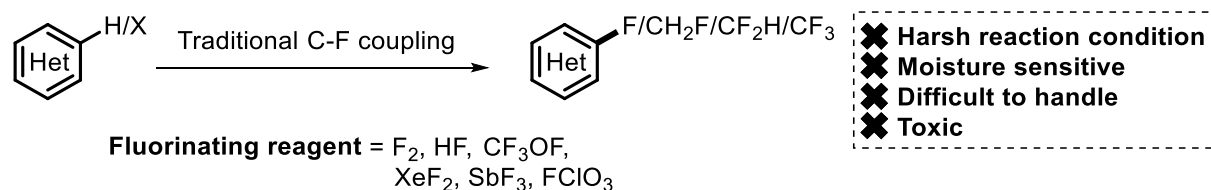


Figure 3.1 Organofluorine compounds in pharmaceuticals, agrochemicals and polymer

Fluorinated solvents and surfactants are also popular in various industrial processes due to their excellent solvent properties and environmental compatibility. Such compounds are also important in modern synthetic organic chemistry as they serve as versatile building blocks for the preparation of complex organic molecules. The unique reactivity and selectivity of fluorine in various reactions, such as nucleophilic substitution and electrocyclic reactions, enable the selective modification of organic molecules in a predictable manner. This makes them indispensable in fields like pharmacology,⁷ agrochemistry,⁸⁻⁹ materials science,¹⁰ and electrochemistry.¹¹ Overall, the importance of organofluorine compounds in various fields cannot be overstated, and their future applications are promising.

Although several methodologies exist for introducing fluorine, geminal difluorination has become a focal point of research due to its unique ability to introduce two fluorine atoms into a molecule.¹²⁻¹⁷ Several research groups have been consistently putting efforts to develop a more convenient, efficient and green protocol for the construction of such motifs. Fluorination is commonly achieved by using F_2 , HF, CF_3OF , XeF_2 , SbF_3 and $FClO_4$ as fluorinating reagents (**Scheme 3.1**).¹⁸⁻²³ Certain limitations like requirement of harsh reaction conditions, which often result in poor selectivity and low yields, toxicity, difficulty in handling, and/or cost hinder their widespread use in organic synthesis. Furthermore, some methods also require the use of hazardous solvents or catalysts, which can be challenging to remove and may lead to environmental concerns. These limitations have spurred the development of new, easy and innovative fluorination methods using fluorinating reagents such as Selectfluor, NFSI, DAST, that are milder, more selective, and more environmentally friendly.



Scheme 3.1 Traditional methods for C-F coupling

Various electrophilic, nucleophilic and radical-based fluorinating agents enables the construction of wide range of fluorinating compounds with diverse properties. Some commonly used fluorinating reagents are depicted in **Figure 3.2**. The importance of fluorinating reagent could

be anticipated through its capability of introducing fluorine atom(s) selectively into organic molecules. This ability makes them essential in the synthesis of various fluorine-containing compounds, modification of functional groups, and late-stage fluorination of complex molecules with high efficiency and selectivity. The importance of fluorinating reagents in synthetic organic chemistry cannot be overstated, as they provide versatile tools for the design and development of new molecules with improved properties and potential applications.

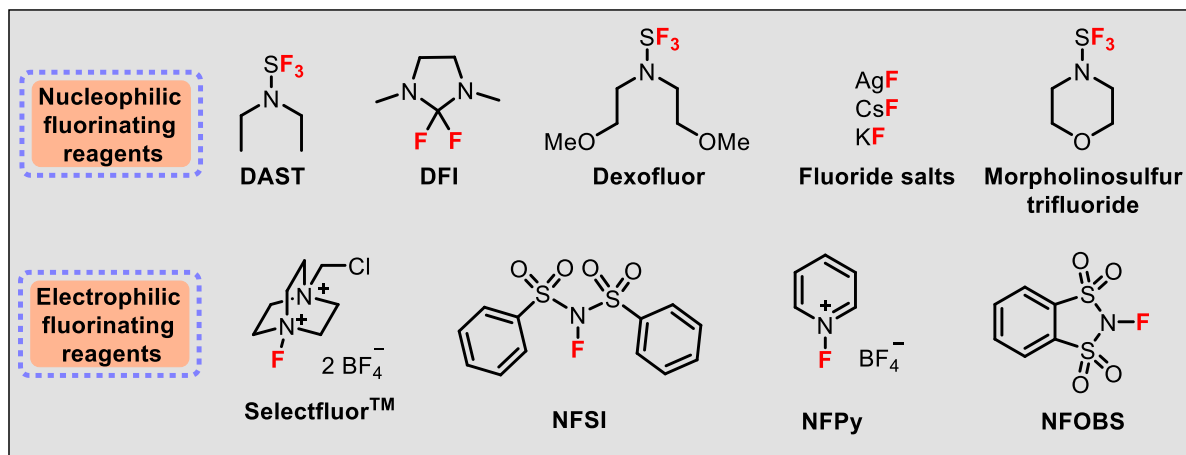
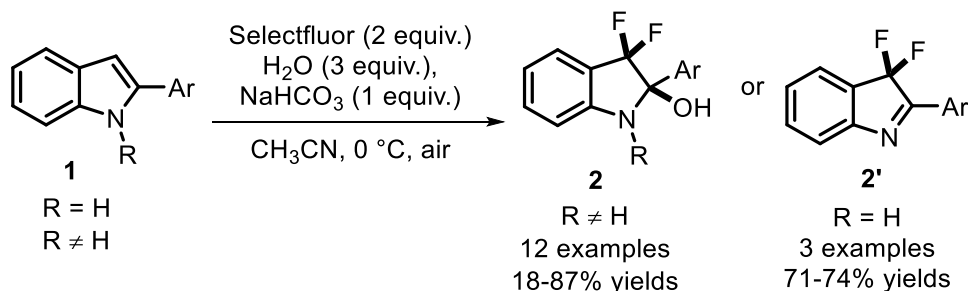


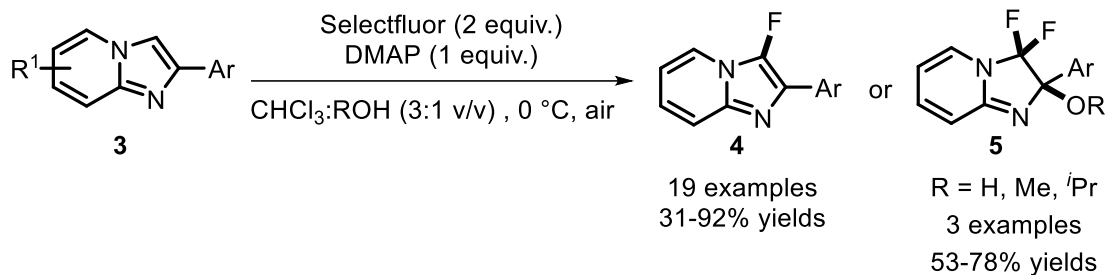
Figure 3.2 Examples of fluorinating reagents

In 2011, Jiao group developed a transition-metal free, highly regioselective difluorination of substituted indoles (**1**) using Selectfluor as the electrophilic fluorinating reagent. 3,3-difluoroindolin-2-ols (**2**) were obtained from *N*-protected indoles while 3,3-difluoro-2-phenyl-3*H*-indole (**2'**) were obtained from free-NH indoles. Control experiments indicated the inevitable role of base and suggested ionic pathway for the reaction (**Scheme 3.2**).²⁴



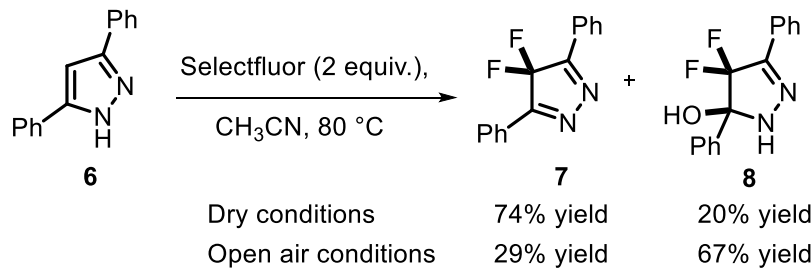
Scheme 3.2 Regioselective difluorohydroxylation of indoles

Liu *et al.* reported a similar method for the regioselective fluorination of imidazo[1,2-*a*]pyridine (**3**) in aqueous conditions by using DMAP as base and Selectfluor as electrophilic fluorinating agent. While focusing on the electrophilic mono-fluorination of imidazo[1,2-*a*]pyridines (**4**), the group also obtained three examples of 3,3-difluoro-2-alkoxy-2-aryl imidazopyridines (**5**) by changing the nucleophile to alcohols. Moreover, the reaction was believed to proceed through electrophilic fluorinated mechanism (**Scheme 3.3**).²⁵



Scheme 3.3 Regioselective fluorination of imidazo[1,2-*a*]pyridines

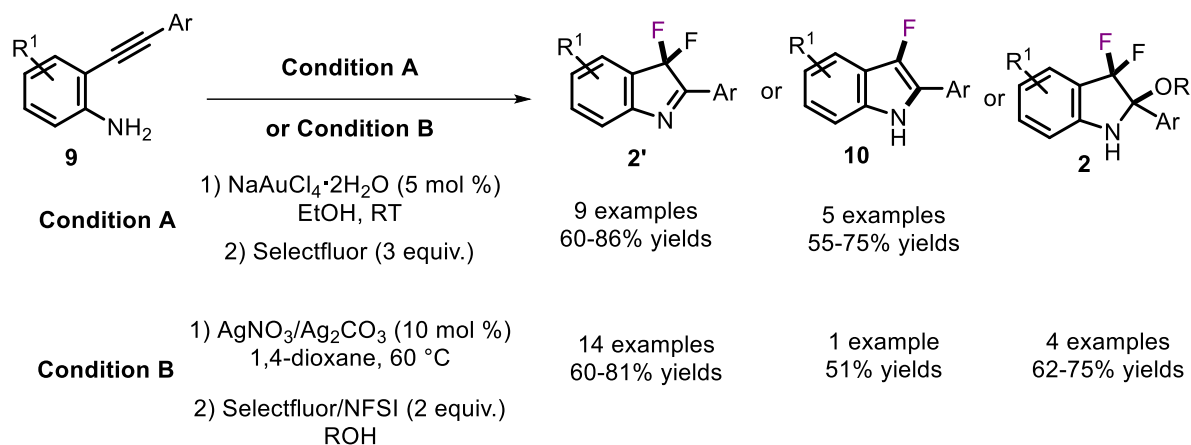
In the same year, Walton *et al.* reported a Selectfluor-mediated difluoroalkylation and difluoro-hydroxylation of 3,5-diphenylpyrazole (**6**) including the detailed charge density study of products (**7**) and (**8**) with respect to parent pyrazole (**Scheme 3.4**). X-ray crystal data and charge density analysis demonstrated the unusually long bond length of the N–N in the substrate molecule. After the difluoro substitution, the electron density between the two nitrogen atoms has also been found to be significantly contracted.²⁶



Scheme 3.4 Regioselective fluorination of imidazo[1,2-*a*]pyridines

Alternatively, 3,3-difluoro-2-substituted-3*H*-indoles (**2'**) were also synthesized *via* one-pot two-step Au-catalyzed cyclization followed by electrophilic fluorination of 2-alkynylanilines (**9**) by Michelet group (**Scheme 3.5a**).²⁷ The procedure was also extended for the synthesis of

2-aryl-3-fluoro-1*H*-indoles (**10**). Notably, this methodology does not require the use of bases, acids, or N-protective groups, making it a simple and efficient process. Similarly Lei *et al.* reported the condition dependent synthesis of 2-aryl-3-fluoro-1*H*-indoles (**10**), 3,3-difluoro-3*H*-indoles (**2'**) and 3,3-difluoro-2-hydroxy-3*H*-indoles (**2**) using Ag-catalyzed one-pot cyclization followed by electrophilic fluorination of **9** (Scheme 3.5a).²⁸



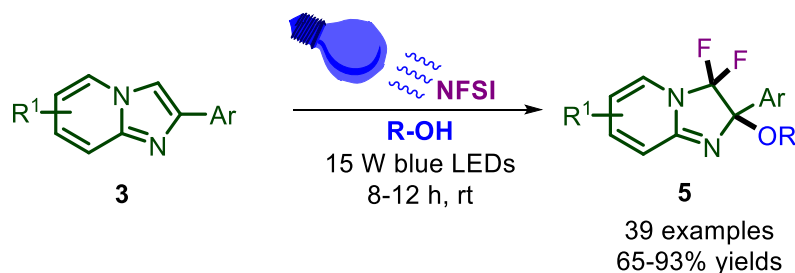
Scheme 3.5 Au/Ag-catalyzed cyclization/fluorination of 2-alkynylianilines

Despite some great advantages, these methods suffer with some challenges such as limited substrate scope, maintenance of low temperature, requirement of metal catalysts, etc. Thus, there is still a need to develop a more effective, economical and green method for the difluorination of heterocycles.

Visible light is considered an ideal reagent for green synthesis due to its non-toxic nature, ability to generate no waste and obtainable from renewable resources.²⁹ Visible light induced reactions have gained significant importance in synthetic organic chemistry in recent years due to their ability to achieve selective transformations and functionalization that are difficult or impossible to achieve using traditional thermal or chemical methods.³⁰ Visible light has the ability to activate specific functional groups, leading to specific bond formation or cleavage, thus offering greater control over reaction kinetics and product selectivity, leading to more efficient and high-yielding reactions.³¹ These advantages have revolutionized the field of synthetic organic chemistry by providing a sustainable, efficient, and selective tool for the preparation of complex organic molecules. Visible-light induced reactions have been used for a diverse range of organic

transformations ranging from oxidative cross-coupling reactions for the formation of C–C or C–heteroatom bonds, rearrangement reactions to various other challenging reactions.³²⁻³⁵ Despite significant progress in the field of synthetic chemistry through visible-light induced transformations, difluorination induced by visible light is still not well explored.

On the other hand, imidazo[1,2-*a*]pyridines are privileged heterocyclic scaffolds that have gained considerable attention in medicinal chemistry,³⁶ synthetic chemistry,³⁷⁻³⁸ and material chemistry.³⁹ Their presence as a building block in various commercially available drugs highlights their importance in pharmaceutical industries.⁴⁰⁻⁴² Additionally, imidazo[1,2-*a*]pyridines exhibit diverse biological activities making them attractive targets for drug discovery.⁴² Owing to the unique structural features, such as the presence of multiple heteroatoms and aromatic rings, imidazo[1,2-*a*]pyridines can interact with various biological targets. As a result of their vast applicability in diverse fields of science, there is a growing interest in developing efficient synthetic methods to functionalize these compounds at specific positions. Among various positions, C3-functionalization of imidazo[1,2-*a*]pyridines has attracted significant attention due to its ability to modulate the biological activity of these compounds.⁴³ Being the most nucleophilic position, the C3-position of imidazo[1,2-*a*]pyridine is susceptible to attack by electrophiles or radicals. A series of methods have been achieved for the C–H bond functionalization specifically at C3-position in the way to construct C–C or C–heteroatom bond however, the difluoroalkoxylation of imidazo[1,2-*a*]pyridine under mild reaction conditions is still challenging. Therefore, in continuation with our interest in the radical-mediated C–H functionalization of heterocyclic compounds, herein we have developed a visible-light induced regioselective difluoroalkoxylation of imidazo[1,2-*a*]pyridines using NFSI as fluorine source (**Scheme 3.6**).



Scheme 3.6 Visible-light induced difluoroalkoxylation of imidazo[1,2-*a*]pyridines

4.2 RESULTS AND DISCUSSION

We initiated our study for optimizing reaction conditions using imidazo[1,2-*a*]pyridine **3a** and methanol **11a** as model substrates. After an extensive survey of the reaction conditions by variation of photocatalyst, additive, fluorine source, solvent, and light source, we achieved 86% yield of 3,3-difluoro-2-methoxy-2-arylimidazo[1,2-*a*]pyridines **5aa** by using NFSI as a fluorinating reagent under the irradiation of 15 W blue LEDs for 8 h (**Table 3.1**, entry 1). The molecular structure of **5aa** was fully characterized by NMR (^1H , **Figure 3.3**, $^{13}\text{C}\{^1\text{H}\}$, **Figure 3.4**, ^{19}F , **Figure 3.5**) and HRMS (**Figure 3.6**). The addition of a catalytic amount of photocatalyst (2 mol %) like (Mes-Acr-Me) $^+$, rose-bengal and rhodamine 6G had no significant effect on the yield (72-75%) of the desired product (**Table 3.1**, entries 2-4). In the presence of TFA as additive, the reaction afforded **5aa** in 23% yield due to the formation of complex reaction mixture, demonstrating the ability to proceed under additive-free conditions (**Table 3.1**, entry 5). When selectfluor was used as a fluorinating reagent, the reaction still produced the desired product **5aa**, but its yield was suppressed to 55% (**Table 3.1**, entry 6). Replacement of blue LEDs with white and green LEDs yielded target product **5aa** in 73% and 17% yield, respectively (**Table 3.1**, entries 7 and 8). Notably, the effect of solvents on the reaction cannot be ignored. It was observed that protic solvent was the most suitable reaction medium providing higher yield, while aprotic solvents such as CH_3CN , DCE, and THF resulted in lower yields (**Table 3.1**, compare entry 1 with entries 9-11). It was also found that the amount of fluorine source was crucial as increasing the amount did not improve the reaction, but decreasing it to 1.5 equivalent resulted in lower yields of **5aa** (**Table 3.1**, entries 12-13). Moreover, prolonging the reaction for 24 h did not have any significant effect, and the target product **5aa** was obtained in 83% yield. Further exploration of the reaction conditions revealed that both NFSI and visible light played vital roles (**Table 3.1**, entries 14-15).

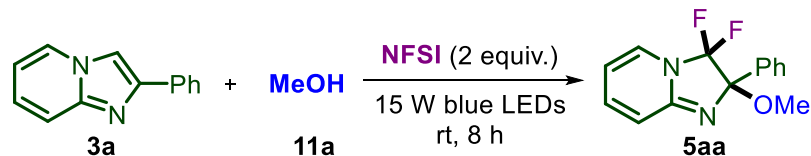


Table 3.1 Optimization of the reaction condition for the synthesis of **5aa**^a

Entry	Deviation in reaction conditions	% Yield of 5aa ^b
1	none	86
2	(Mes-Acr-Me) ⁺ as photocatalyst	72
3	Rose bengal as photocatalyst	75
4	Rhodamine 6G as photocatalyst	73
5	TFA as additive	23
6	Selectfluor as fluorinating reagent	55
7	White light	73
8	Green light	17
9 ^c	CH ₃ CN as solvent	78
10 ^c	DCE as solvent	55
11 ^c	THF as solvent	68
12	NFSI 3.0 equiv.	80
13	NFSI 1.5 equiv.	76
14	Reaction time 24 h	83
15	Without NFSI	nr
16	Without light	nr

^aReaction condition: **3a** (0.26 mmol, 1.0 equiv.), **11a** (1.5 mL), NFSI (0.51 mmol, 2 equiv.), photocatalyst (2 mol %), additive (0.26 mmol, 1.0 equiv), solvent (1.5 mL), under the irradiation of 15 W blue LEDs at RT for 8 h. ^bIsolated yield. ^c**11a** (1.29 mmol, 5 equiv.), nr = No reaction.

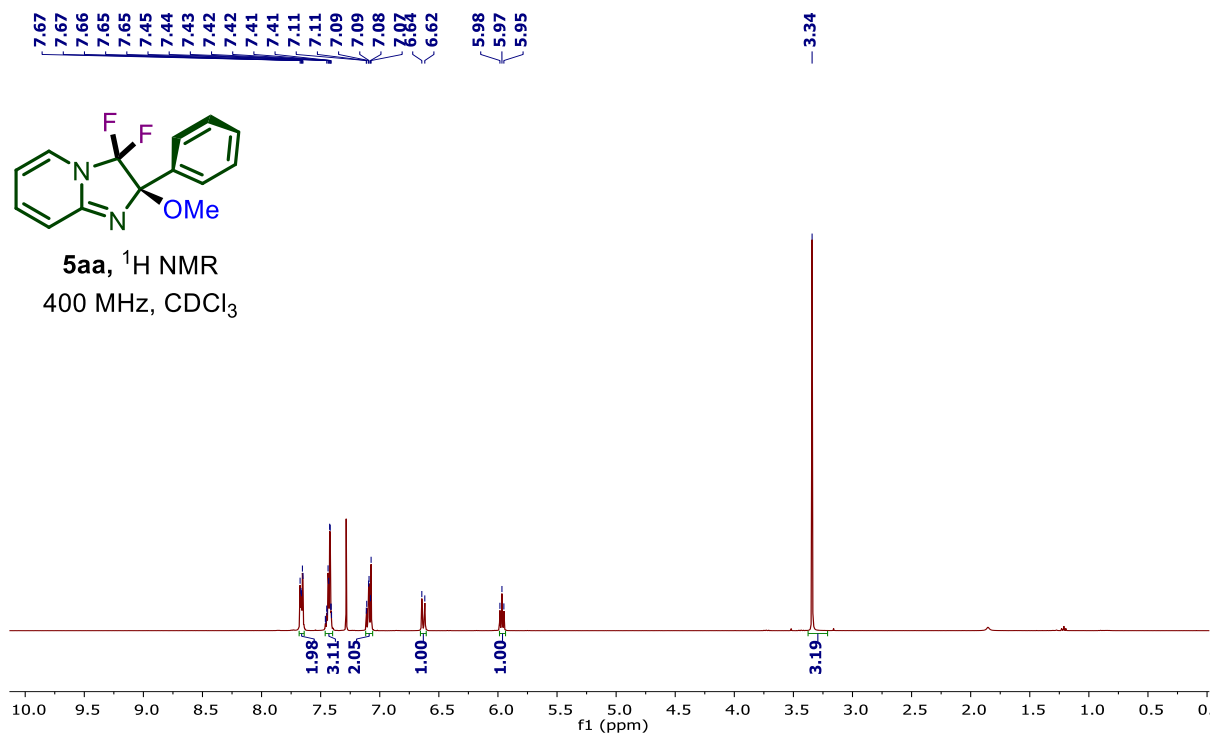


Figure 3.3 ^1H NMR spectrum of 3,3-difluoro-2-methoxy-2-phenyl-2,3-dihydroimidazo[1,2-*a*]pyridine (**5aa**) recorded in CDCl_3

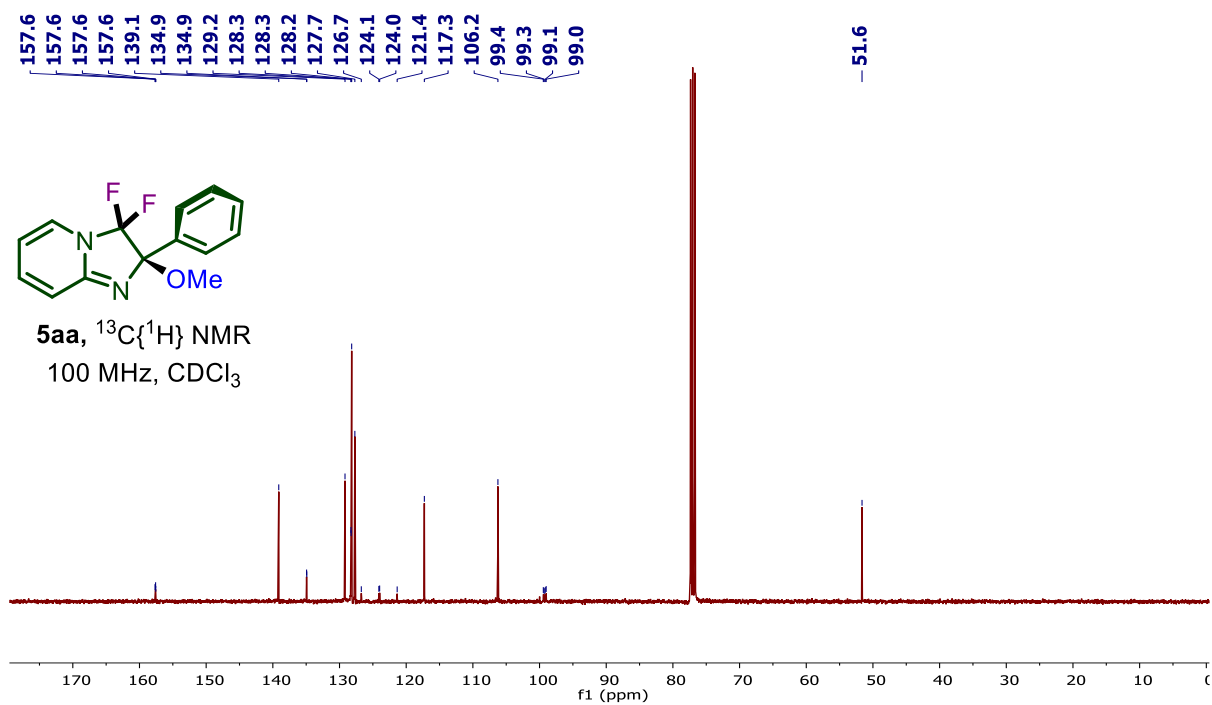


Figure 3.4 $^{13}\text{C}\{^1\text{H}\}$ NMR spectrum of 3,3-difluoro-2-methoxy-2-phenyl-2,3-dihydroimidazo[1,2-*a*]pyridine (**5aa**) recorded in CDCl_3

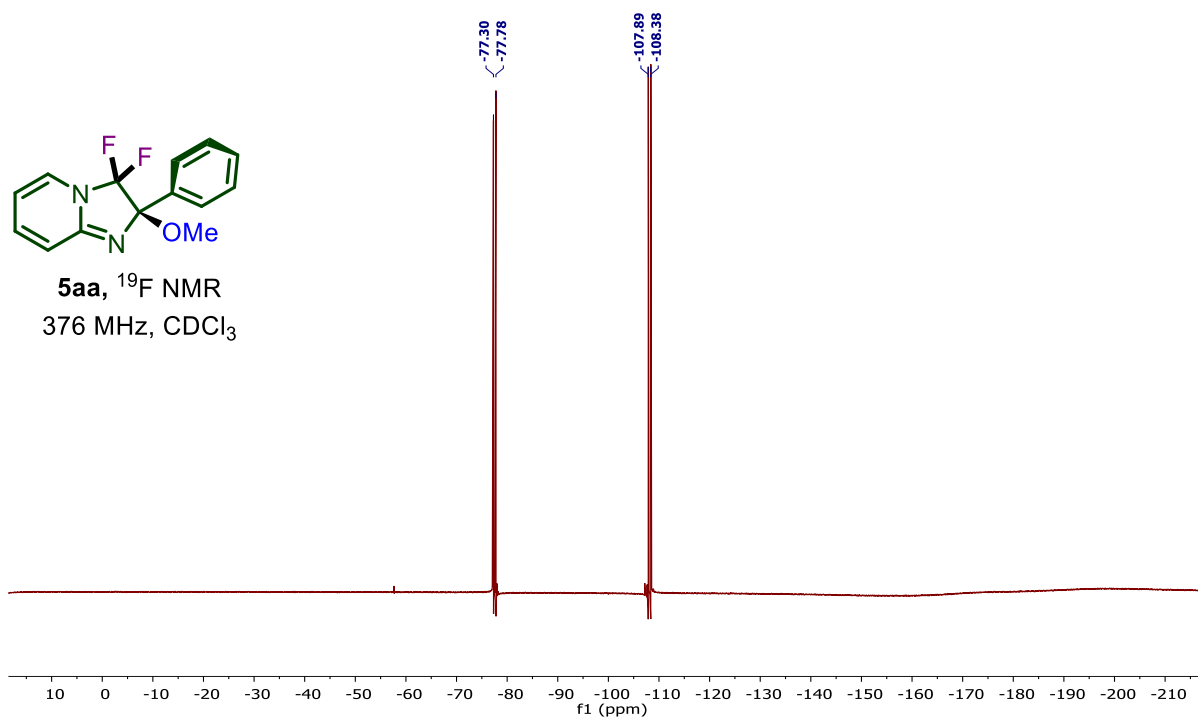
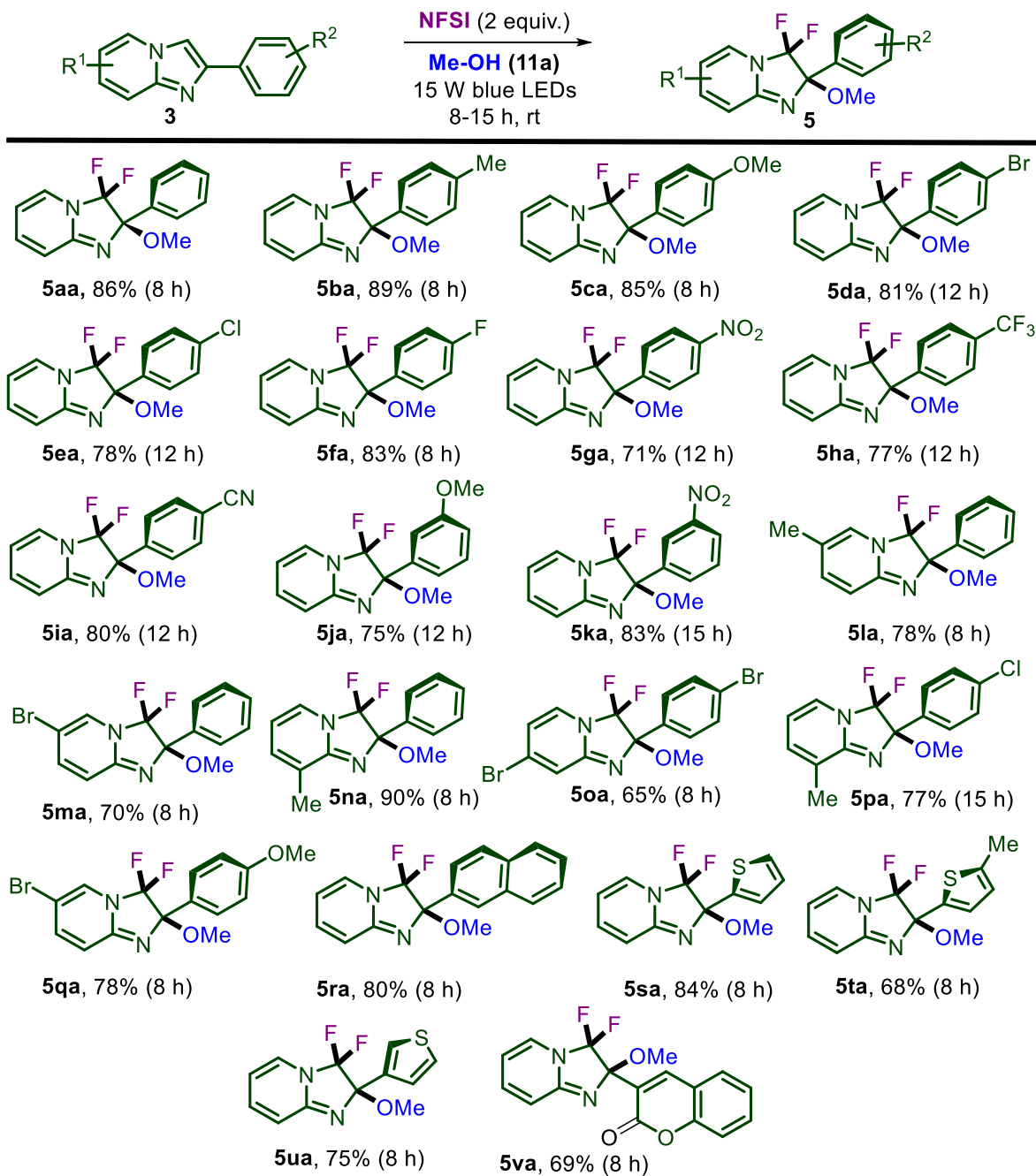


Figure 3.5 ^{19}F NMR spectrum of 3,3-difluoro-2-methoxy-2-phenyl-2,3-dihydroimidazo[1,2-*a*]pyridine (**5aa**) recorded in CDCl_3

After determining the optimized reaction conditions (**Table 3.1**, entry 1), we explored substrate scope for photo-difluoromethoxylation with respect to imidazo[1,2-*a*]pyridines. As shown in **Table 3.2**, various imidazo[1,2-*a*]pyridines with electron-donating as well as electron-withdrawing substituents at the 3- or 4- position of C2-phenyl ring smoothly reacted under the optimized conditions and afforded the corresponding 3,3-difluoro-2-methoxy-2-arylimidazopyridines (**5aa–5ka**) in high yields (71–89%) after the 8–15 h of irradiation. Notably, extended irradiation time was necessary for electronically poor substrates. Sterically encumbered imidazo[1,2-*a*]pyridines with methoxy and nitro groups at the 3-position of the C2-phenyl ring (**5ja–5ka**) showed lower yields. Subsequently, imidazo[1,2-*a*]pyridine derivatives bearing substitution on the pyridyl ring were also investigated. Substrates bearing –Me and –Br substituents at C6-, C7-, and C8- position of the pyridyl ring (**3l–3q**) were well tolerated yielding the corresponding products (**5la–5qa**) 65–90%. To our delight, imidazopyridines bearing 2-naphthyl, 2-thienyl, 2-(2-methyl)thienyl, 3-thienyl, and 3-coumarinyl, readily underwent photo-difluoromethoxylation under the optimized reaction to deliver the corresponding products (**5ra–5va**)

in 68–84% yields. Furthermore, the structure of **5ga** was unambiguously confirmed by single-crystal X-ray diffraction study (CCDC 2244256) (**Figure 3.7**).

Table 3.2 Scope and versatility of imidazo[1,2-*a*]pyridines^{a,b}



^aReaction condition: **3** (0.26 mmol, 1.0 equiv.), **11a** (1.5 mL), NFSI (0.51 mmol, 2 equiv.) under the irradiation of 15 W blue LEDs at rt for 8–15 h. ^bIsolated yield.

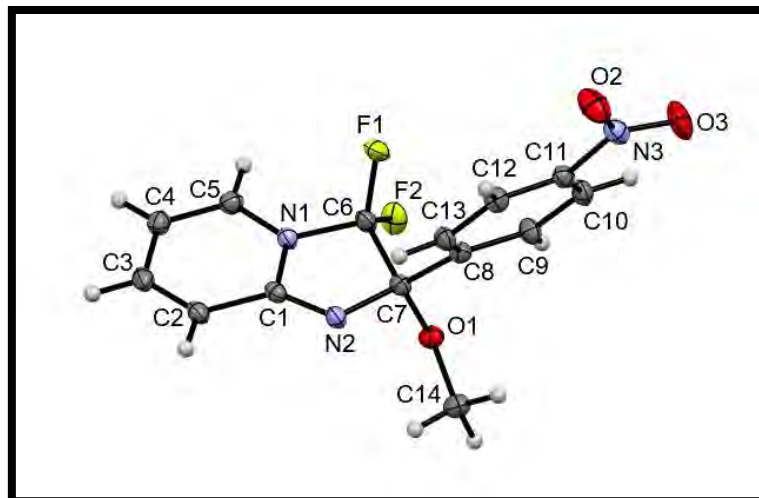
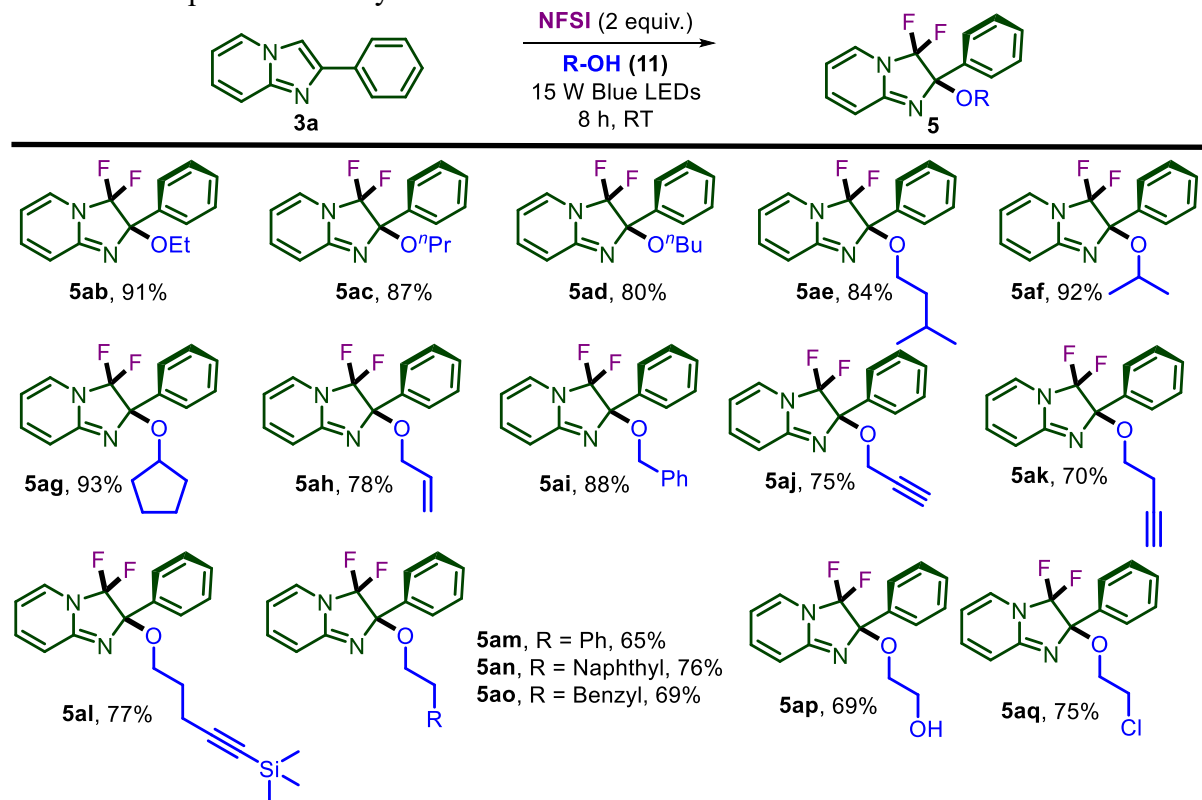


Figure 3.7 ORTEP diagram of **5ga** (CCDC 2244256). The thermal ellipsoids are drawn at 50% probability level

Next, we investigated the scope and versatility of photo-difluoroalkoxylation with respect to a series of alcohols reacting with **3a** under optimal conditions (**Table 3.3**). Primary alcohols such as EtOH (**11b**), *n*-PrOH (**11c**), *n*-BuOH (**11d**) and (CH₃)₂CHCH₂CH₂OH (**11e**) reacted smoothly and afforded the corresponding products **11ab–11ae** in 80–91% yields. Interestingly, secondary alcohols (IPA and cyclopropanol) also reacted smoothly, affording the corresponding products **5af** and **5ag** in 92% and 93% yield, respectively. However, the reaction failed to produce the target product with tertiary alcohol, possibly due to steric hindrance, although the reaction did produce a monofluorinated product (**14**). The reaction also underwent smoothly with allyl alcohol, benzyl alcohol and propargyl alcohol resulting the corresponding products **5ah–5ak** in 70–88% yields. Pleasingly, TMS-substituted pentynol (**11i**), 2-phenylethanol (**11m**), 2-naphthylethanol (**11n**), and 3-phenylpropanol (**11o**) provided corresponding products (**5al–5ao**) in 65–76% yield under standard reaction conditions. It is also noteworthy that out of the two terminal hydroxyl groups in ethylene glycol, only one hydroxyl group reacted with **3a** to yield **5ap** in 69% yield. Finally, 2-chloroethanol, a halogenated alcohol underwent smooth conversion to provide 75% yield of **5aq**. The structure of **5ai** was unambiguously confirmed by single-crystal X-ray diffraction study (CCDC 2244257) (**Figure 3.8**).

Table 3.3 Scope and versatility of alcohols^{a,b}

^aReaction condition: **3a** (0.26 mmol, 1.0 equiv.), **11** (1.5 mL), NFSI (0.51 mmol, 2 equiv.) under the irradiation of 15 W blue LEDs at RT for 8 h. ^bIsolated yield.

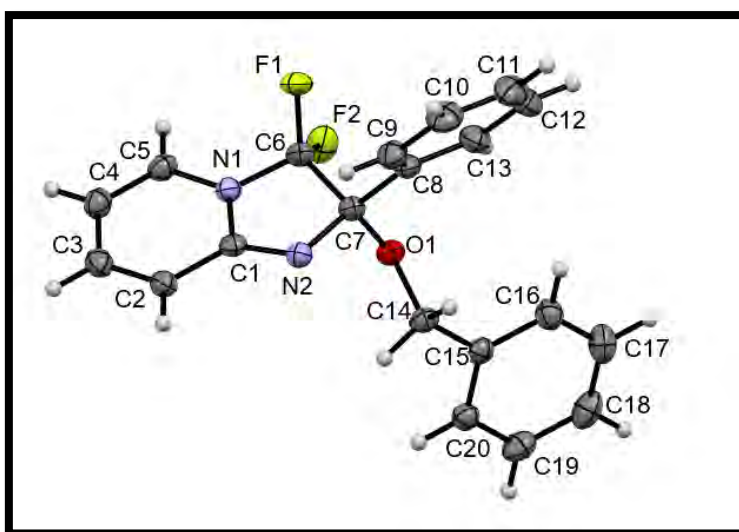
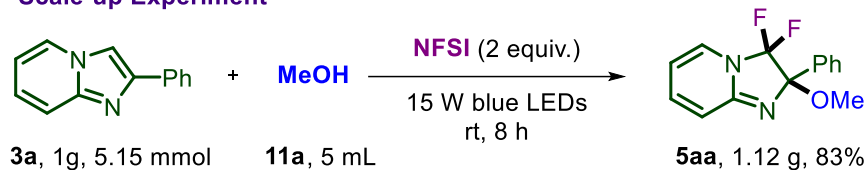


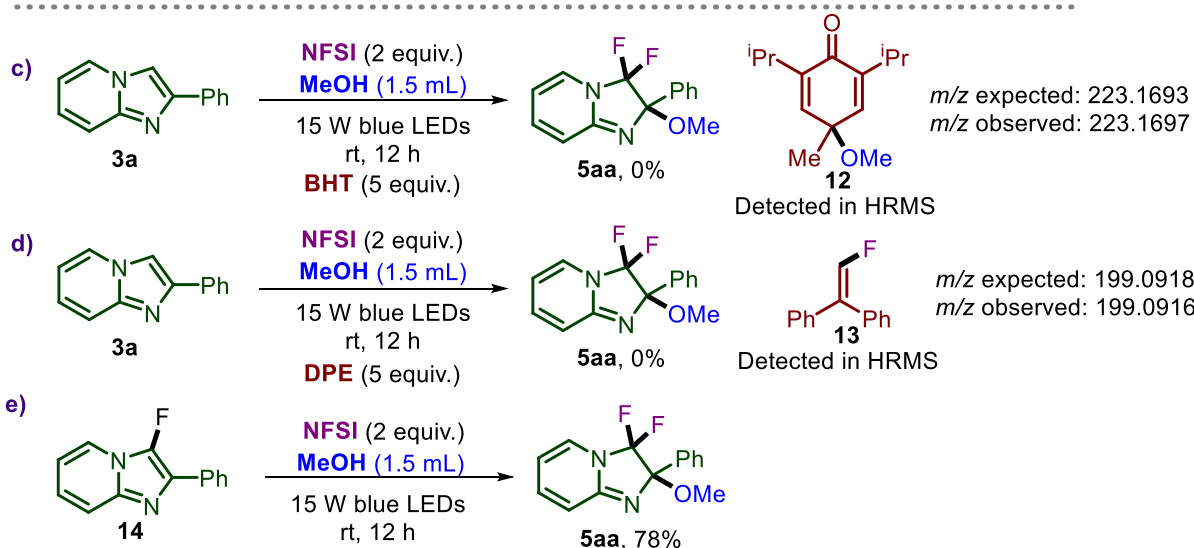
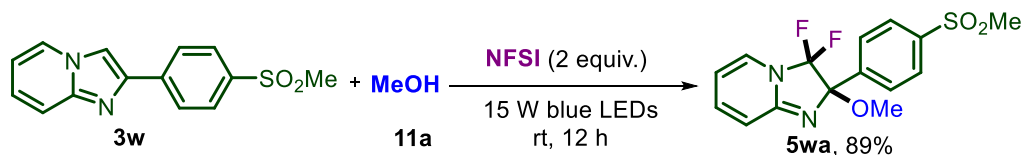
Figure 3.8 ORTEP diagram of **5ai** (CCDC 2244257). The thermal ellipsoids are drawn at 50% probability level

After exploring the substrate scope, the practical applicability of the reaction was demonstrated by a scale-up experiment. The reaction of imidazo[1,2-*a*]pyridine **3a** (1 g, 5.15 mmol) under the optimized conditions afforded **5aa** in 1.12 g (83% yield), without any significant change in the efficacy of the reaction (**Scheme 3.7a**). Furthermore, the synthetic utility of the designed method was demonstrated by the post-functionalization of Zolimidine (**3w**), a gastro-protective drug. Delightfully, the substrate underwent smooth conversion, and the desired 3,3-difluoro-2-methoxy-2-(4-(methylsulfonyl)phenyl)-2,3-dihydroimidazo[1,2-*a*]pyridine (**5wa**) was obtained in 77% yield (**Scheme 3.7b**). To further elucidate the mechanism of this reaction, several preliminary mechanistic investigations were conducted. At first, the effect of radical inhibitors was examined. Addition of butylated hydroxytoluene (BHT) and diphenylethylene to the reaction of **1a** and **11a** under standard reaction conditions led to complete suppression of the formation of product **5aa**. HRMS analysis of the mixture revealed the formation of BHT-OMe (**12**) and DPE-F (**13**) adducts (**Scheme 3.7c, d**). Radical trapping experiments indicated the radical pathway for the reaction, unlike the ionic mechanism reported by Liu *et al.*²⁴ and Lin *et al.*²⁵ Moreover, the formation of the difluoroalkoxylated product **5aa** when starting with a monofluorinated substrate **14** suggested it to be a plausible intermediate during the reaction (**Scheme 3.7e**). To confirm that the reaction was light-induced, an ON/OFF experiment was performed. Under the ON condition, the reaction was irradiated with visible light, while under the OFF condition, the reaction was performed in the dark. The progress of reaction was recorded with ¹H NMR and it was observed that the reaction under the ON condition produced a significant amount of the desired product, while under the OFF condition, there was no detectable product formation. This confirms that the developed difluoroalkoxylation was indeed a photochemical process (**Scheme 3.7f**). The UV/vis absorption spectra of some substrates were recorded at room temperature. The absorption spectra of **3a** and **3a**+NFSI in MeOH indicated the absorption range from UV to visible wavelengths with the absorption edge at about 450–500 nm. The difluoromethoxylation of **3a** was carried out upon the irradiation of blue LED, white LED, and green LED afforded **5aa** in 86%, 73%, and 17% yields, respectively (**Table 3.1**, entry 7 and 8). These yields are correlated with the spectral overlap between the emission of radiation light and the absorbance of **3a**.

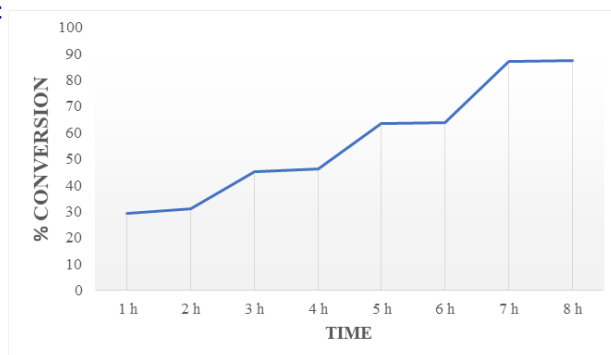
a) Scale-up Experiment



b) Post-functionalization of Zolimidine



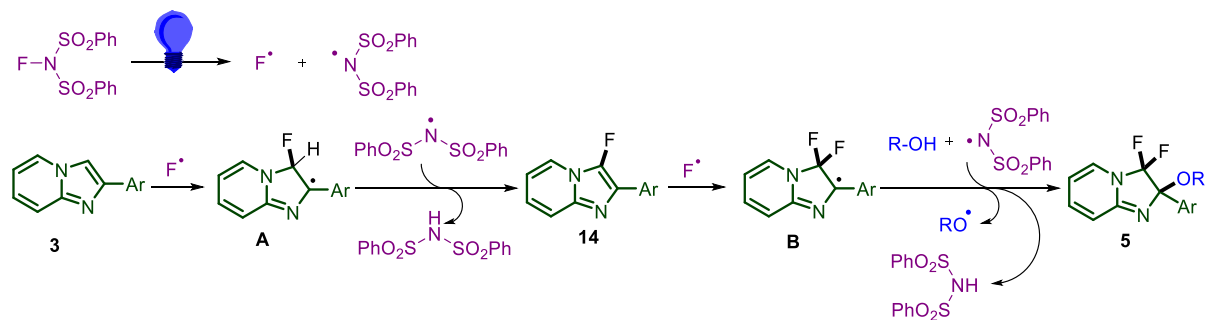
f) ON/OFF experiment



Scheme 3.7. Preliminary mechanistic investigations and synthetic utility

On the basis of the above evidence and previous reports, a plausible mechanism for this visible-light-induced difluoroalkoxylation is proposed (Scheme 3.8). The bond dissociation energy (BDE) of NFSI is 63.5 kcal/mol, which indicates that this transformation initiates with the

cleavage of N–F bond of NFSI under the visible-light irradiation and thus, producing the corresponding radicals. The generated electrophilic fluorine radical reacts regioselectively at the nucleophilic C3-position of imidazo[1,2-*a*]pyridine **3** to produce the highly unstable radical intermediate **A**. Next, hydrogen radical abstraction (HRA) by bisulfonylamidyl radical from C2 position of intermediate **A** formed the monofluorinated intermediate **14**. This compound would undergo a similar process to produce the unstable 3,3-difluorinated radical **B**, which was then attacked by alkoxy radical (generated *via* HRA by bisulfonylamidyl radical) to generate the difluoroalkoxylated product **5**.



Scheme 3.8. Plausible mechanism

4.3 CONCLUSIONS

A highly selective difluoroalkoxylation of imidazo[1,2-*a*]pyridines under the irradiation of visible-light was reported. The reaction was compatible with a large number of imidazo[1,2-*a*]pyridines and alcohols (1° and 2°) without electronic and steric constraints. Broad substrate scope, high functional group tolerance with moderate to excellent yields of difluoroalkoxylated products, environmentally benign reaction conditions and sustainable source of energy are the salient features of the designed protocol. Furthermore, the reaction was believed to follow radical pathway according to the control experiments. Post-functionalization of Zolimidine, a gastro-protective drug under the standard conditions and gram-scale synthesis of **5aa** demonstrates the potential utility of this method.

4.4 EXPERIMENTAL SECTION

4.4.1 General Information

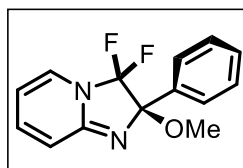
All the chemicals and solvents were purchased from commercial suppliers and used without purification unless otherwise noted. Imidazo[1,2-*a*]pyridines were synthesized by following the

reported procedure. All reactions were monitored by thin layer chromatography (TLC) on pre-coated 0.2 mm silica gel F254 plates (Merck) and visualized under a UV lamp (366 or 254 nm). Desired products were purified by column chromatography (Silica gel 100-200 mesh size) using a gradient of ethyl acetate and hexanes as eluent. Melting points were determined in open capillary tubes on an EZ-Melt automated melting point apparatus and are uncorrected. All the compounds were fully characterized by ^1H , $^{13}\text{C}\{^1\text{H}\}$ and ^{19}F NMR spectra using Bruker Avance 400 spectrometer at 400 MHz, 100 MHz and 376 MHz, respectively. Chemical shifts (δ) are reported in parts per million (ppm) and coupling constants (J) are reported in hertz (Hz) relative to the residual signal of TMS in deuterated solvents. Abbreviations to represent multiplicities are s (singlet), d (doublet), t (triplet), q (quartet), quint (quintet), sext (sextet), sept (septet) dd (double doublet), dt (double triplet), dq (double quartet), td (triplet of doublet), ddd (doublet of doublet of doublet) and m (multiplet). High-resolution mass spectra (HRMS) were recorded by using electrospray ionization (ESI) method on an Agilent Q-TOF 6545 LC-MS spectrometer. Single crystal X-ray analysis was performed on a Rigaku Oxford XtaLAB AFC12 (RINC): Kappa dual home/near diffractometer.

4.4.2 General Procedure for the Difluoroalkoxylation of Imidazo[1,2-*a*]pyridines

An oven dried 10 mL reaction tube was charged with compound **3** (0.26 mmol; 1.0 equiv.), and NFSI (0.51 mmol, 2.0 equiv.) in **11** as solvent at room temperature and the reaction mixture was irradiated under 15 W blue LEDs for 8-15 h. After completion of the reaction as monitored by TLC, reaction mixture was concentrated *in vacuo*. The resulting crude was purified by column chromatography (neutral alumina) using EtOAc/Hexanes as an eluent to afford corresponding products **5**.

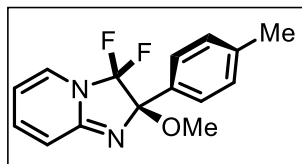
3,3-Difluoro-2-methoxy-2-phenyl-2,3-dihydroimidazo[1,2-*a*]pyridine (5aa): Pale yellow solid



(58 mg, 86% yield); Purification by column chromatography on neutral alumina (eluents: EtOAc/Hexanes = 1.5/8.5); mp = 101-102 °C; ^1H NMR (400 MHz, CDCl_3) δ = 7.67 – 7.65 (m, 2H), 7.46 – 7.41 (m, 3H), 7.11 – 7.07 (m, 2H), 6.64 (d, J = 10.0 Hz, 1H), 5.97 (t, J = 6.6 Hz, 1H), 3.34 (s, 1H); $^{13}\text{C}\{^1\text{H}\}$ NMR (100 MHz, CDCl_3) δ = 157.6 (dd, $^3J_{\text{C-F}}$ = 6.5, 2.4 Hz), 139.1, 134.9 (d, $^3J_{\text{C-F}}$ = 2.9 Hz), 129.2, 128.3 (d, $^4J_{\text{C-F}}$ = 1.8 Hz), 128.2, 127.7, 124.0 (dd, $^1J_{\text{C-F}}$ = 274.7, 262.5 Hz), 117.3, 106.2, 99.2 (dd, $^2J_{\text{C-F}}$ = 29.2, 13.2 Hz), 51.6; ^{19}F NMR (376 MHz, CDCl_3) δ = -77.54

(d, $J = 183.5$ Hz), -108.14 (d, $J = 183.5$ Hz); HRMS (ESI) m/z : $[M + H]^+$ Calcd for $C_{14}H_{12}F_2N_2O^+$ 262.0918; found 262.0921.

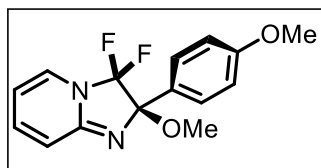
3,3-Difluoro-2-methoxy-2-(*p*-tolyl)-2,3-dihydroimidazo[1,2-*a*]pyridine (5ba): Pale yellow



solid (63 mg, 89% yield); Purification by column chromatography on neutral alumina (eluent: EtOAc/Hexanes = 3.0/7.0); mp = 172-173 °C; 1H NMR (400 MHz, $CDCl_3$) $\delta = 7.57$ (d, $J = 8.8$ Hz, 1H), 7.10 – 7.05 (m, 2H), 6.95 (d, $J = 9.2$ Hz, 1H), 6.61 (d, $J = 10$ Hz, 1H), 5.95

(t, $J = 6.4$ Hz, 1H), 3.84 (s, 3H), 3.32 (s, 3H); $^{13}C\{^1H\}$ NMR (100 MHz, $CDCl_3$) $\delta = 160.2$, 157.4 (dd, $^3J_{C-F} = 6.5, 2.2$ Hz), 139.0, 129.0, 128.3 (d, $^4J_{C-F} = 1.6$ Hz), 126.8 (d, $^3J_{C-F} = 2.8$ Hz), 124.0 (dd, $^1J_{C-F} = 274.8, 262.2$ Hz), 117.3, 113.5, 106.2, 99.1 (dd, $^2J_{C-F} = 29.2, 13.3$ Hz), 55.2, 51.5; ^{19}F NMR (376 MHz, $CDCl_3$) $\delta = -77.48$ (d, $J = 183.1$ Hz), -108.47 (d, $J = 183.1$ Hz); HRMS (ESI) m/z : $[M + H]^+$ Calcd for $C_{15}H_{15}F_2N_2O^+$ 289.1147; found 289.1144.

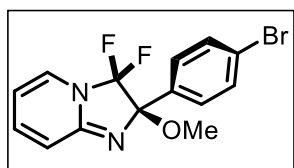
3,3-Difluoro-2-methoxy-2-(4-methoxyphenyl)-2,3-dihydroimidazo[1,2-*a*]pyridine (5ca): Pale



yellow solid (56 mg, 85% yield); Purification by column chromatography on neutral alumina (eluent: EtOAc/Hexanes = 3.0/7.0); mp = 184-186 °C; 1H NMR (400 MHz, $CDCl_3$) $\delta = 7.57$ (d, $J = 8.8$ Hz, 1H), 7.10 – 7.05 (m, 2H), 6.95 (d, $J = 9.2$ Hz, 1H), 6.61 (d, $J =$

10 Hz, 1H), 5.95 (t, $J = 6.4$ Hz, 1H), 3.84 (s, 3H), 3.32 (s, 3H); $^{13}C\{^1H\}$ NMR (100 MHz, $CDCl_3$) $\delta = 160.2$, 157.4 (dd, $^3J_{C-F} = 6.5, 2.2$ Hz), 139.0, 129.0, 128.3 (d, $^4J_{C-F} = 1.6$ Hz), 126.8 (d, $^3J_{C-F} = 2.8$ Hz), 124.0 (dd, $^1J_{C-F} = 274.8, 262.2$ Hz), 117.3, 113.5, 106.2, 99.1 (dd, $^2J_{C-F} = 29.2, 13.3$ Hz), 55.2, 51.5; ^{19}F NMR (376 MHz, $CDCl_3$) $\delta = -77.48$ (d, $J = 183.1$ Hz), -108.47 (d, $J = 183.1$ Hz); HRMS (ESI) m/z : $[M + H]^+$ Calcd for $C_{15}H_{15}F_2N_2O^+$ 289.1147; found 289.1144.

2-(4-Bromophenyl)-3,3-difluoro-2-methoxy-2,3-dihydroimidazo[1,2-*a*]pyridine (5da): Pale

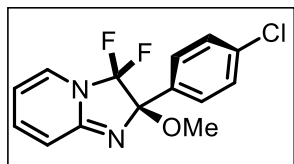


yellow solid (68 mg, 81% yield); Purification by column chromatography on neutral alumina (eluent: EtOAc/Hexanes = 3.0/7.0); mp = 184-186 °C; 1H NMR (400 MHz, $CDCl_3$) $\delta = 7.57 - 7.52$ (m, 4H), 7.14 – 7.09 (m, 2H), 6.63 (d, $J = 9.6$ Hz, 1H), 6.00 (t, $J = 6.8$ Hz, 1H),

3.32 (s, 3H); $^{13}C\{^1H\}$ NMR (100 MHz, $CDCl_3$) $\delta = 157.9$ (dd, $^3J_{C-F} = 6.5, 2.2$ Hz), 139.4, 134.2 (d, $^3J_{C-F} = 2.8$ Hz), 131.4, 129.5, 128.2 (d, $^4J_{C-F} = 1.8$ Hz), 123.8 (dd, $^1J_{C-F} = 275.1, 263.2$ Hz), 123.5, 117.2, 106.5, 98.8 (dd, $^2J_{C-F} = 29.2, 13.6$ Hz), 51.6; ^{19}F NMR (376 MHz, $CDCl_3$) $\delta = -$

77.14 (d, $J = 184.2$ Hz), -108.35 (d, $J = 184.2$ Hz); HRMS (ESI) m/z : $[M + H]^+$ Calcd for $C_{14}H_{12}BrF_2N_2O^+$ 341.0096; found 341.0098.

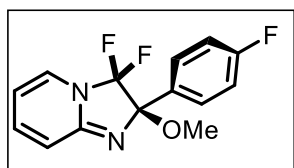
2-(4-Chlorophenyl)-3,3-difluoro-2-methoxy-2,3-dihydroimidazo[1,2-a]pyridine (5ea): Pale



yellow solid (65 mg, 78% yield); Purification by column chromatography on neutral alumina (eluents: EtOAc/Hexanes = 2.0/8.0); mp = 184-186 °C; 1H NMR (400 MHz, $CDCl_3$) $\delta = 7.59$ (d, $J = 8.4$ Hz, 2H), 7.38 (d, $J = 8.4$ Hz, 2H), 7.08 (t, $J = 8.2$ Hz, 2H), 6.60 (d, $J = 9.6$ Hz,

1H), 5.96 (t, $J = 6.8$ Hz, 1H), 3.31 (s, 3H); $^{13}C\{^1H\}$ NMR (100 MHz, $CDCl_3$) $\delta = 157.8$ (dd, $^3J_{C-F} = 6.6, 2.2$ Hz), 139.3, 135.1, 133.7 (d, $^3J_{C-F} = 2.7$ Hz), 129.2, 128.4, 128.2 (d, $^4J_{C-F} = 1.6$ Hz), 124.6 (dd, $^1J_{C-F} = 274.85, 263.05$ Hz), 117.2, 106.4, 98.8 (dd, $^2J_{C-F} = 29.1, 13.5$ Hz), 51.5; ^{19}F NMR (376 MHz, $CDCl_3$) $\delta = -77.21$ (d, $J = 184.2$ Hz), -108.34 (d, $J = 184.2$ Hz); HRMS (ESI) m/z : $[M + H]^+$ Calcd for $C_{14}H_{12}ClF_2N_2O^+$ 297.0601; found 297.0606.

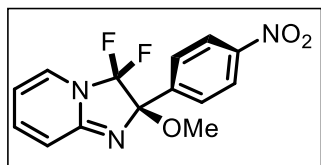
3,3-Difluoro-2-(4-fluorophenyl)-2-methoxy-2,3-dihydroimidazo[1,2-a]pyridine (5fa): Pale



yellow solid (71 mg, 83% yield); Purification by column chromatography on neutral alumina (eluents: EtOAc/Hexanes = 3.0/7.0); mp = 184-186 °C; 1H NMR (400 MHz, $CDCl_3$) $\delta = 7.66 - 7.62$ (m, 2H), 7.13 - 7.08 (m, 4H), 6.62 (d, $J = 9.6$ Hz, 1H), 5.98 (t, $J = 6.8$ Hz, 1H),

3.32 (s, 3H); $^{13}C\{^1H\}$ NMR (100 MHz, $CDCl_3$) $\delta = 163.3$ (d, $^1J_{C-F} = 246.1$ Hz), 157.7 (dd, $^3J_{C-F} = 6.6, 2.1$ Hz), 139.3, 130.9 (t, $^3J_{C-F} = 2.9$ Hz), 129.6 (d, $^3J_{C-F} = 8.4$ Hz), 128.2 (d, $^4J_{C-F} = 1.7$ Hz), 123.93 (dd, $^1J_{C-F} = 274.7, 263.1$ Hz), 117.2, 115.1 (d, $^2J_{C-F} = 21.5$ Hz), 106.4, 98.8 (dd, $^2J_{C-F} = 29.2, 13.6$ Hz), 51.5; ^{19}F NMR (376 MHz, $CDCl_3$) $\delta = -77.09$ (d, $J = 183.4$ Hz), -108.57 (d, $J = 183.4$ Hz), -112.84 ; HRMS (ESI) m/z : $[M + H]^+$ Calcd for $C_{14}H_{12}F_3N_2O^+$ 281.0896; found 281.0900.

3,3-Difluoro-2-methoxy-2-(4-nitrophenyl)-2,3-dihydroimidazo[1,2-a]pyridine (5ga): Pale yellow

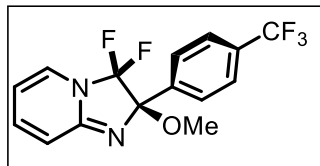


solid (69 mg, 71% yield); Purification by column chromatography on neutral alumina (eluents: EtOAc/Hexanes = 3.0/7.0); mp = 184-186 °C; 1H NMR (400 MHz, $CDCl_3$) $\delta = 8.28 - 8.25$ (m, 2H), 7.86 - 7.83 (m, 2H), 7.18 - 7.09 (m, 2H), 6.65 (d, $J = 9.2$ Hz, 1H),

6.04 (t, $J = 6.8$ Hz, 1H), 3.34 (s, 3H); $^{13}C\{^1H\}$ NMR (100 MHz, $CDCl_3$) $\delta = 158.3$ (dd, $^3J_{C-F} = 6.6, 2.2$ Hz), 148.6, 142.7 (d, $^3J_{C-F} = 2.8$ Hz), 139.8, 128.8, 128.1 (d, $^4J_{C-F} = 1.6$ Hz), 123.3, 123.4 (dd, $^1J_{C-F} = 275.8, 264.0$ Hz), 117.1, 106.9, 98.5 (dd, $^2J_{C-F} = 29.0, 13.9$ Hz), 51.7; ^{19}F

NMR (376 MHz, CDCl₃) δ = -76.81 (d, J = 184.2 Hz), -107.72 (d, J = 184.2 Hz); HRMS (ESI) m/z : [M + H]⁺ Calcd for C₁₄H₁₂F₂N₃O₃⁺ 308.0841; found 308.0839.

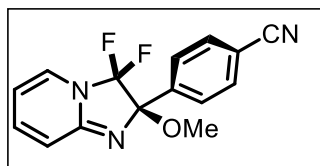
3,3-Difluoro-2-methoxy-2-(4-(trifluoromethyl)phenyl)-2,3-dihydroimidazo[1,2-a]pyridine



(5ha): Pale yellow solid (58 mg, 77% yield); Purification by column chromatography on neutral alumina (eluents: EtOAc/Hexanes = 3.0/7.0); mp = 184-186 °C; ¹H NMR (400 MHz, CDCl₃) δ = 7.79 (d, J = 8.0 Hz, 2H), 7.68 (d, J = 8.0 Hz, 2H), 7.15 – 7.09 (m, 2H),

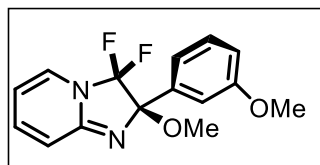
6.66 – 6.63 (m, 1H), 6.01 (t, J = 6.8 Hz, 1H) 3.34 (s, 3H); ¹³C {¹H} NMR (100 MHz, CDCl₃) δ = 158.0 (dd, ³ J_{C-F} = 6.6, 2.3 Hz), 139.5, 139.3 (d, ⁴ J_{C-F} = 1.4 Hz), 131.3 (q, ² J_{C-F} = 32.1 Hz), 128.2, 126.1, 125.15 (q, ³ J_{C-F} = 3.7 Hz), 124.0 (q, ¹ J_{C-F} = 270.7 Hz), 123.9 (dd, ¹ J_{C-F} = 275.3, 263.7 Hz), 117.2, 106.6, 98.8 (dd, ² J_{C-F} = 29.4, 13.8 Hz), 51.7; ¹⁹F NMR (376 MHz, CDCl₃) δ = -62.63, -77.11 (d, J = 183.9 Hz), -108.10 (d, J = 184.2 Hz); HRMS (ESI) m/z : [M + H]⁺ Calcd for C₁₅H₁₂F₅N₂O⁺ 331.0864; found 331.0861.

4-(3,3-Difluoro-2-methoxy-2,3-dihydroimidazo[1,2-a]pyridin-2-yl)benzonitrile (5ia): Pale yellow solid (59 mg, 80% yield); Purification by column chromatography on neutral alumina (eluents: EtOAc/Hexanes = 3.0/7.0); mp = 184-186 °C; ¹H NMR (400 MHz, CDCl₃) δ = 7.78 (d, J = 8.8 Hz,



2H), 7.71 (d, J = 8.4 Hz, 2H), 7.17 – 7.09 (m, 2H), 6.64 (d, J = 9.6 Hz, 1H), 6.03 (t, J = 6.6 Hz, 1H), 3.32 (s, 3H); ¹³C {¹H} NMR (100 MHz, CDCl₃) δ = 158.2 (dd, ³ J_{C-F} = 6.6, 2.3 Hz), 140.8 (d, ³ J_{C-F} = 2.6 Hz), 139.7, 132.0, 128.5 (d, ⁴ J_{C-F} = 0.7 Hz), 128.1 (d, ⁴ J_{C-F} = 1.5 Hz), 123.8 (dd, ¹ J_{C-F} = 275.7, 263.9 Hz), 118.6, 117.1, 113.1, 106.8, 98.6 (dd, ² J_{C-F} = 29.1, 13.6 Hz), 51.7; ¹⁹F NMR (376 MHz, CDCl₃) δ = -76.88 (d, J = 184.2 Hz), -107.76 (d, J = 184.2 Hz); HRMS (ESI) m/z : [M + H]⁺ Calcd for C₁₅H₁₂F₂N₃O⁺ 288.0943; found 288.0944.

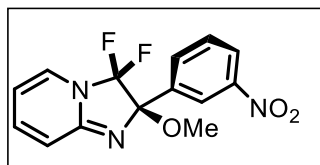
3,3-Difluoro-2-methoxy-2-(3-methoxyphenyl)-2,3-dihydroimidazo[1,2-a]pyridine (5ja): Off-white solid (56 mg, 75% yield); Purification by column chromatography on neutral alumina (eluents: EtOAc/Hexanes = 2.0/8.0); mp = 104-105 °C; ¹H NMR (400 MHz, CDCl₃) δ = 7.35 (t, J = 8.0 Hz,



1H), 7.26 (d, J = 7.6 Hz, 1H), 7.21 (s, 1H), 7.11 – 7.07 (m, 2H), 6.96 (dd, J = 8.2, 1.8 Hz, 1H), 6.63 (d, J = 10.0 Hz, 1H), 5.97 (t, J = 6.6 Hz, 1H), 3.85 (s, 3H), 3.35

(s, 3H); $^{13}\text{C}\{^1\text{H}\}$ NMR (100 MHz, CDCl_3) δ = 159.6, 157.6 (dd, $^3J_{\text{C-F}}$ = 6.6, 2.3 Hz), 139.1, 136.6 (d, $^3J_{\text{C-F}}$ = 2.7 Hz), 129.2, 128.3 (d, $^4J_{\text{C-F}}$ = 1.6 Hz), 124.0 (dd, $^1J_{\text{C-F}}$ = 274.9, 263.1 Hz), 120.1, 117.3, 115.1, 113.0, 106.3, 99.1 (dd, $^2J_{\text{C-F}}$ = 29.1, 13.4 Hz), 55.3, 51.7; ^{19}F NMR (376 MHz, CDCl_3) δ = -77.91 (d, J = 183.5 Hz), -108.30 (d, J = 183.5 Hz); HRMS (ESI) m/z : $[\text{M} + \text{H}]^+$ Calcd for $\text{C}_{15}\text{H}_{15}\text{F}_2\text{N}_2\text{O}_2^+$ 293.1096; found 293.1100.

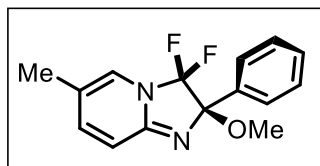
3,3-Difluoro-2-methoxy-2-(3-nitrophenyl)-2,3-dihydroimidazo[1,2-a]pyridine (5ka): Yellow



solid (60 mg, 83% yield); Purification by column chromatography on neutral alumina (eluents: EtOAc/Hexanes = 2.0/8.0); mp = 146-147 °C; ^1H NMR (400 MHz, CDCl_3) δ = 8.54 (t, J = 1.8 Hz, 1H), 8.28 (dd, J = 8.8, 2.0 Hz, 1H), 8.00 (d, J = 8.0 Hz, 1H), 7.61 (t, J =

8.0 Hz, 1H), 7.19 – 7.15 (m, 1H), 7.11 (d, J = 6.8 Hz, 1H), 6.67 (d, J = 9.6 Hz, 1H), 6.05 (t, J = 6.8 Hz, 1H), 3.36 (s, 3H); $^{13}\text{C}\{^1\text{H}\}$ NMR (100 MHz, CDCl_3) δ = 158.3 (dd, $^3J_{\text{C-F}}$ = 6.6, 2.3 Hz), 148.3, 139.8, 138.0 (d, $^3J_{\text{C-F}}$ = 2.8 Hz), 133.8, 129.2 128.1 (d, $^4J_{\text{C-F}}$ = 1.7 Hz), 124.2, 123.8 (dd, $^1J_{\text{C-F}}$ = 277.4, 265.6 Hz), 123.0 (d, $^1J_{\text{C-F}}$ = 0.6 Hz), 117.2, 106.9, 98.5 (dd, $^2J_{\text{C-F}}$ = 29.0, 14.0 Hz), 51.7; ^{19}F NMR (376 MHz, CDCl_3) δ = -76.40 (d, J = 184.3 Hz), -107.72 (d, J = 184.3 Hz); HRMS (ESI) m/z : $[\text{M} + \text{H}]^+$ Calcd for $\text{C}_{14}\text{H}_{12}\text{F}_2\text{N}_3\text{O}_3^+$ $[\text{M} + \text{H}]^+$ 308.0841; found 308.0840.

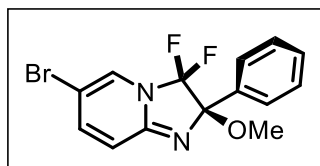
3,3-Difluoro-2-methoxy-6-methyl-2-phenyl-2,3-dihydroimidazo[1,2-a]pyridine (5la): Pale yellow



solid (66 mg, 78% yield); Purification by column chromatography on neutral alumina (eluents: EtOAc/Hexanes = 1.5/8.5); mp = 184-186 °C; ^1H NMR (400 MHz, CDCl_3) δ = 7.67 – 7.64 (m, 2H), 7.45 – 7.40 (m, 3H), 7.01 (d, J = 7.2 Hz, 1H), 6.42 (s, 1H), 5.83 (d,

J = 6.8 Hz, 1H), 3.33 (s, 3H), 2.17 (s, 3H); $^{13}\text{C}\{^1\text{H}\}$ NMR (100 MHz, CDCl_3) δ = 157.9 (dd, $^3J_{\text{C-F}}$ = 6.5, 2.3 Hz), 150.9, 135.2 (d, $^3J_{\text{C-F}}$ = 2.7 Hz), 129.1, 128.1, 127.7, 127.1 (d, $^4J_{\text{C-F}}$ = 1.6 Hz), 123.9 (dd, $^1J_{\text{C-F}}$ = 274.2, 262.8 Hz), 114.5, 109.3, 99.4 (dd, $^2J_{\text{C-F}}$ = 29.1, 13.4 Hz), 51.5, 22.2; ^{19}F NMR (376 MHz, CDCl_3) δ = -77.62 (d, J = 183.1 Hz), -107.94 (d, J = 183.1 Hz); HRMS (ESI) m/z : $[\text{M} + \text{H}]^+$ Calcd for $\text{C}_{15}\text{H}_{15}\text{F}_2\text{N}_2\text{O}^+$ 277.1147; found 277.1143.

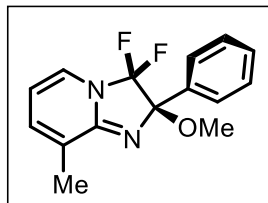
6-Bromo-3,3-difluoro-2-methoxy-2-phenyl-2,3-dihydroimidazo[1,2-a]pyridine (5ma): Pale



yellow solid (63 mg, 70% yield); Purification by column chromatography on neutral alumina (eluents: EtOAc/Hexanes = 1.5/8.5); mp = 184-186 °C; ^1H NMR (400 MHz, CDCl_3) δ = 7.63 – 7.61 (m, 2H), 7.44 – 7.42 (m, 3H), 7.22 (d, J = 1.2 Hz, 1H), 7.11 (dd, J =

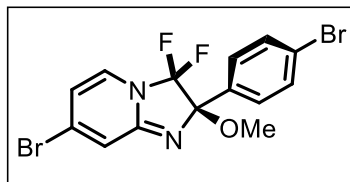
10.0, 2.0 Hz, 1H), 6.58 (d, $J = 10.0$ Hz, 1H), 3.33 (s, 3H); $^{13}\text{C}\{^1\text{H}\}$ NMR (100 MHz, CDCl_3) $\delta = 155.6$ (dd, $^3J_{\text{C-F}} = 6.4, 2.2$ Hz), 142.4, 134.3 (d, $^3J_{\text{C-F}} = 2.8$ Hz), 129.4, 128.3, 128.0 (d, $^4J_{\text{C-F}} = 2.0$ Hz), 127.6, 126.2 (dd, $^1J_{\text{C-F}} = 269.2, 258.6$ Hz), 118.5, 99.6 (dd, $^2J_{\text{C-F}} = 29.2, 13.4$ Hz), 51.8; ^{19}F NMR (376 MHz, CDCl_3) $\delta = -80.73$ (d, $J = 179.3$ Hz), -106.16 (d, $J = 179.3$ Hz); HRMS (ESI) m/z : $[\text{M} + \text{H}]^+$ Calcd for $\text{C}_{14}\text{H}_{12}\text{BrF}_2\text{N}_2\text{O}^+$ 341.0096; found 341.0100

3,3-Difluoro-2-methoxy-8-methyl-2-phenyl-2,3-dihydroimidazo[1,2-a]pyridine (5na): Pale



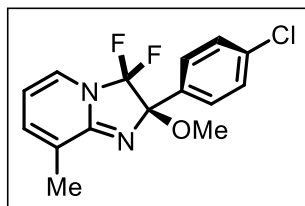
yellow solid (63 mg, 90% yield); Purification by column chromatography on neutral alumina (eluents: EtOAc/Hexanes = 3.0/7.0); mp = 172-173 °C; ^1H NMR (400 MHz, CDCl_3) $\delta = 7.57$ (d, $J = 8.8$ Hz, 1H), 7.10 – 7.05 (m, 2H), 6.95 (d, $J = 9.2$ Hz, 1H), 6.61 (d, $J = 10$ Hz, 1H), 5.95 (t, $J = 6.4$ Hz, 1H), 3.84 (s, 3H), 3.32 (s, 3H); $^{13}\text{C}\{^1\text{H}\}$ NMR (100 MHz, CDCl_3) $\delta = 160.2, 157.4$ (dd, $^3J_{\text{C-F}} = 6.5, 2.2$ Hz), 139.0, 129.0, 128.3 (d, $^4J_{\text{C-F}} = 1.6$ Hz), 126.8 (d, $^3J_{\text{C-F}} = 2.8$ Hz), 124.0 (dd, $^1J_{\text{C-F}} = 274.8, 262.2$ Hz), 117.3, 113.5, 106.2, 99.1 (dd, $^2J_{\text{C-F}} = 29.2, 13.3$ Hz), 55.2, 51.5; ^{19}F NMR (376 MHz, CDCl_3) $\delta = -77.48$ (d, $J = 183.1$ Hz), -108.47 (d, $J = 183.1$ Hz); HRMS (ESI) m/z : $[\text{M} + \text{H}]^+$ Calcd for $\text{C}_{15}\text{H}_{15}\text{F}_2\text{N}_2\text{O}^+$ 289.1147; found 289.1144.

7-Bromo-2-(4-bromophenyl)-3,3-difluoro-2-methoxy-2,3-dihydroimidazo[1,2-a]pyridine



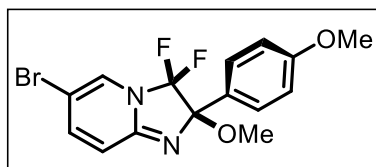
(5oa): Pale yellow solid (54 mg, 65% yield); Purification by column chromatography on neutral alumina (eluents: EtOAc/Hexanes = 1.5/8.5); mp = 184-186 °C; ^1H NMR (400 MHz, CDCl_3) $\delta = 7.56$ (d, $J = 8.8$ Hz, 2H), 7.49 (d, $J = 8.0$ Hz, 2H), 7.23 (m, 1H), 7.11 (dd, $J = 10.0, 2.0$ Hz, 1H), 6.57 (d, $J = 10.0$ Hz, 1H), 3.31 (s, 3H); $^{13}\text{C}\{^1\text{H}\}$ NMR (100 MHz, CDCl_3) $\delta = 155.8$ (dd, $^3J_{\text{C-F}} = 6.5, 2.1$ Hz), 142.6, 133.6 (d, $^3J_{\text{C-F}} = 2.7$ Hz), 131.5, 129.4, 127.9 (d, $^3J_{\text{C-F}} = 2.1$ Hz), 123.6 (dd, $^1J_{\text{C-F}} = 276.6, 264.5$ Hz), 123.7, 118.4, 99.2 (dd, $^2J_{\text{C-F}} = 29.1, 13.6$ Hz), 51.8; ^{19}F NMR (376 MHz, CDCl_3) $\delta = -76.80$ (d, $J = 181.6$ Hz), -107.77 (d, $J = 181.2$ Hz); HRMS (ESI) m/z : $[\text{M} + \text{H}]^+$ Calcd for $\text{C}_{14}\text{H}_{11}\text{Br}_2\text{F}_2\text{N}_2\text{O}^+$ 418.9201; found 418.9197.

2-(4-Chlorophenyl)-3,3-difluoro-2-methoxy-8-methyl-2,3-dihydroimidazo[1,2-a]pyridine

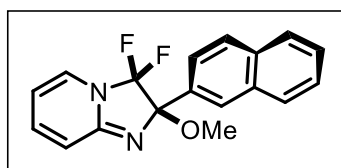


(5pa): Pale yellow solid (60 mg, 77% yield); Purification by column chromatography on neutral alumina (eluent: EtOAc/Hexanes = 1.5/8.5); mp = 184-186 °C; ^1H NMR (400 MHz, CDCl_3) δ = 7.61 (d, J = 8.4 Hz, 2H), 7.39 (d, J = 8.8 Hz, 2H), 7.00 (d, J = 7.2 Hz, 1H), 6.92 (dt, J = 6.8, 1.1 Hz, 1H), 5.95 (t, J = 6.8 Hz, 1H), 3.35 (s, 3H), 2.22 (s, 3H); $^{13}\text{C}\{^1\text{H}\}$ NMR (100 MHz, CDCl_3) δ = 158.6 (dd, $^3J_{\text{C-F}}$ = 6.2, 2.2 Hz), 135.8, 135.0, 134.1 (d, $^3J_{\text{C-F}}$ = 3.0 Hz), 129.2, 128.3, 126.6, 125.4 (d, $^3J_{\text{C-F}}$ = 2.2 Hz), 124.4 (dd, $^1J_{\text{C-F}}$ = 274.7, 263.1 Hz), 106.4, 98.8 (dd, $^2J_{\text{C-F}}$ = 29.1, 13.6 Hz), 51.4, 16.8; ^{19}F NMR (376 MHz, CDCl_3) δ = -76.56 (d, J = 184.2 Hz), -107.27 (d, J = 183.9 Hz); HRMS (ESI) m/z : $[\text{M} + \text{H}]^+$ Calcd for $\text{C}_{15}\text{H}_{14}\text{ClF}_2\text{N}_2\text{O}^+$ 311.0757; found 311.0756.

6-Bromo-3,3-difluoro-2-methoxy-2-(4-methoxyphenyl)-2,3-dihydroimidazo[1,2-a]pyridine



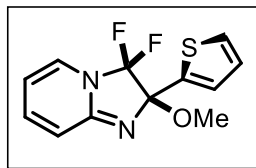
(5qa): Pale yellow solid (55 mg, 78% yield); Purification by column chromatography on neutral alumina (eluent: EtOAc/Hexanes = 1.5/8.5); mp = 184-186 °C; ^1H NMR (400 MHz, CDCl_3) δ = 7.53 (d, J = 8.8 Hz, 2H), 7.22 (d, J = 0.8 Hz, 1H), 7.09 (dd, J = 10.0, 1.6 Hz, 1H), 6.95 (d, J = 8.8 Hz, 2H), 6.57 (d, J = 10.0 Hz, 1H), 3.85 (s, 3H), 3.30 (s, 3H); $^{13}\text{C}\{^1\text{H}\}$ NMR (100 MHz, CDCl_3) δ = 160.4, 155.5 (dd, $^3J_{\text{C-F}}$ = 6.4, 2.0 Hz), 142.4, 129.0, 128.0 (d, $^3J_{\text{C-F}}$ = 2.2 Hz), 126.1 (d, $^3J_{\text{C-F}}$ = 2.9 Hz), 123.8 (dd, $^1J_{\text{C-F}}$ = 276.3, 263.5 Hz), 118.4, 113.6, 99.4 (dd, $^2J_{\text{C-F}}$ = 29.4, 13.4 Hz), 98.5, 55.3, 51.6; ^{19}F NMR (376 MHz, CDCl_3) δ = -77.13 (d, J = 180.8 Hz), -107.85 (d, J = 180.8 Hz); HRMS (ESI) m/z : $[\text{M} + \text{H}]^+$ Calcd for $\text{C}_{15}\text{H}_{14}\text{BrF}_2\text{N}_2\text{O}_2^+$ 371.0201; found 371.0206.

3,3-Difluoro-2-methoxy-2-(naphthalen-2-yl)-2,3-dihydroimidazo[1,2-a]pyridine (**5ra**):

(5ra): Pale yellow solid (61 mg, 80% yield); Purification by column chromatography on neutral alumina (eluent: EtOAc/Hexanes = 1.5/8.5); mp = 184-186 °C; ^1H NMR (400 MHz, CDCl_3) δ = 8.24 (s, 1H), 7.93 – 7.88 (m, 3H), 7.72 (dd, J = 8.8, 1.2 Hz, 1H), 7.55 – 7.50 (m, 2H), 7.14 – 7.12 (m, 1H), 7.10 (d, J = 6.4 Hz, 1H), 6.70 (d, J = 8.0 Hz, 1H), 5.98 (t, J = 6.6 Hz, 1H), 3.37 (s, 3H); $^{13}\text{C}\{^1\text{H}\}$ NMR (100 MHz, CDCl_3) δ = 157.7 (dd, $^3J_{\text{C-F}}$ = 6.6, 2.2 Hz), 139.2, 133.8, 132.9, 132.4 (d, $^3J_{\text{C-F}}$ = 2.9 Hz), 128.5, 128.3 (d, $^3J_{\text{C-F}}$ = 2.2 Hz), 128.0, 127.6, 126.6, 126.2, 124.90, 124.88, 124.1 (dd, $^1J_{\text{C-F}}$ = 275.0, 263.0 Hz), 117.3, 106.3, 99.4 (dd, $^2J_{\text{C-F}}$

= 29.1, 13.5 Hz), 51.7; ^{19}F NMR (376 MHz, CDCl_3) δ = -77.42 (d, J = 184.2 Hz), -107.81 (d, J = 184.2 Hz); HRMS (ESI) m/z : $[\text{M} + \text{H}]^+$ Calcd for $\text{C}_{18}\text{H}_{15}\text{F}_2\text{N}_2\text{O}^+$ 313.1147; found 313.1149.

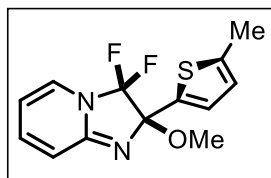
3,3-Difluoro-2-methoxy-2-(thiophen-2-yl)-2,3-dihydroimidazo[1,2-a]pyridine (5sa): Pale yellow



solid (66 mg, 84% yield); Purification by column chromatography on neutral alumina (eluent: EtOAc/Hexanes = 1.5/8.5); mp = 184-186 °C; ^1H NMR (400 MHz, CDCl_3) δ = 7.59 (dd, J = 3.0, 1.0 Hz, 1H), 7.36 (dd, J = 5.0, 3.0 Hz, 1H), 7.19 (d, J = 5.2 Hz, 1H), 7.09 – 7.04 (m, 2H),

6.58 (d, J = 9.2 Hz, 1H), 5.95 (t, J = 6.8 Hz, 1H), 3.34 (s, 3H); $^{13}\text{C}\{^1\text{H}\}$ NMR (100 MHz, CDCl_3) δ = 157.4 (dd, $^3J_{\text{C-F}}$ = 6.1, 2.5 Hz), 139.2, 136.8 (d, $^3J_{\text{C-F}}$ = 3.3 Hz), 128.2 (d, $^4J_{\text{C-F}}$ = 1.6 Hz), 126.7 (d, $^4J_{\text{C-F}}$ = 1.1 Hz), 126.0, 125.8, 123.8 (dd, $^1J_{\text{C-F}}$ = 274.7, 262.8 Hz), 117.1, 106.3, 97.6 (dd, $^2J_{\text{C-F}}$ = 29.0, 14.1 Hz), 51.7; ^{19}F NMR (376 MHz, CDCl_3) δ = -80.14 (d, J = 184.2 Hz), -106.42 (d, J = 184.2 Hz); HRMS (ESI) m/z : $[\text{M} + \text{H}]^+$ Calcd for $\text{C}_{12}\text{H}_{11}\text{F}_2\text{N}_2\text{OS}^+$ 269.0555; found 269.0552.

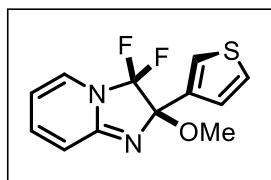
3,3-Difluoro-2-methoxy-2-(5-methylthiophen-2-yl)-2,3-dihydroimidazo[1,2-a]pyridine (5ta):



Pale yellow solid (50 mg, 68% yield); Purification by column chromatography on neutral alumina (eluent: EtOAc/Hexanes = 1.5/8.5); mp = 184-186 °C; ^1H NMR (400 MHz, CDCl_3) δ = 7.12 – 7.09 (m, 2H), 7.07 (d, J = 3.6 Hz, 1H), 6.74 (d, J = 3.4, 1.0 Hz, 1H), 6.60 (d, J = 9.6 Hz,

1H), 5.99 (t, J = 6.6 Hz, 1H), 3.43 (s, 3H), 2.50 (s, 3H); $^{13}\text{C}\{^1\text{H}\}$ NMR (100 MHz, CDCl_3) δ = 157.7 (dd, $^3J_{\text{C-F}}$ = 6.4, 2.6 Hz), 141.6, 139.3, 135.7 (d, $^3J_{\text{C-F}}$ = 3.2 Hz), 128.3 (d, $^4J_{\text{C-F}}$ = 1.7 Hz), 127.8, 125.4, 123.6 (dd, $^1J_{\text{C-F}}$ = 275.4, 262.6 Hz), 117.1, 106.5, 97.7 (dd, $^2J_{\text{C-F}}$ = 28.3, 14.3 Hz), 51.8, 15.4; ^{19}F NMR (376 MHz, CDCl_3) δ = -79.39 (d, J = 180.5 Hz), -107.68 (d, J = 180.5 Hz); HRMS (ESI) m/z : $[\text{M} + \text{H}]^+$ Calcd for $\text{C}_{13}\text{H}_{13}\text{F}_2\text{N}_2\text{OS}^+$ 283.0711; found 283.0715.

3,3-Difluoro-2-methoxy-2-(thiophen-3-yl)-2,3-dihydroimidazo[1,2-a]pyridine (5ua): Pale yellow

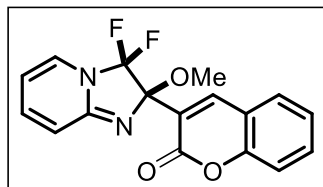


solid (57 mg, 75% yield); Purification by column chromatography on neutral alumina (eluent: EtOAc/Hexanes = 1.5/8.5); mp = 184-186 °C; ^1H NMR (400 MHz, CDCl_3) δ = 7.61 (dd, J = 2.8, 1.2 Hz, 1H), 7.38 (dd, J = 4.8, 3.2 Hz, 1H), 7.21 (d, J = 5.2 Hz, 1H), 7.11 – 7.06 (m, 2H),

6.60 (d, J = 10.0 Hz, 1H), 5.97 (t, J = 6.8 Hz, 1H), 3.35 (s, 3H); $^{13}\text{C}\{^1\text{H}\}$ NMR (100 MHz, CDCl_3) δ = 157.4 (dd, $^3J_{\text{C-F}}$ = 6.6, 2.5 Hz), 139.1, 136.8 (d, $^3J_{\text{C-F}}$ = 3.3 Hz), 128.2 (d, $^4J_{\text{C-F}}$ = 2.2 Hz), 126.7, 126.0, 125.8, 123.8 (dd, $^1J_{\text{C-F}}$ = 275.1, 263.0 Hz), 117.2, 106.2, 97.5 (d, $^2J_{\text{C-F}}$

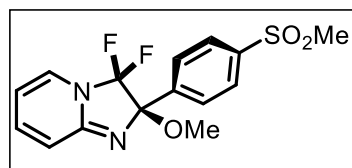
= 29.9, 15.9 Hz), 51.7; ^{19}F NMR (376 MHz, CDCl_3) δ = -80.22 (d, J = 184.2 Hz), -106.40 (d, J = 184.2 Hz); HRMS (ESI) m/z : $[\text{M} + \text{H}]^+$ Calcd for $\text{C}_{12}\text{H}_{11}\text{F}_2\text{N}_2\text{OS}^+$ 269.0555; found 269.0552.

3-(3,3-Difluoro-2-methoxy-2,3-dihydroimidazo[1,2-a]pyridin-2-yl)-2H-chromen-2-one (5va):



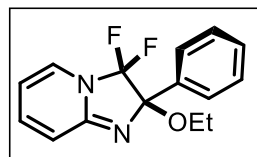
Pale yellow solid (60 mg, 69% yield); Purification by column chromatography on neutral alumina (eluent: EtOAc/Hexanes = 1.5/8.5); mp = 184-186 °C; ^1H NMR (400 MHz, CDCl_3) δ = 8.41 (s, 1H), 7.58 – 7.54 (m, 2H), 7.37 (d, J = 8.4 Hz, 1H), 7.32 – 7.28 (m, 2H), 7.18 – 7.13 (m, 1H), 6.61 (d, J = 9.6 Hz, 1H), 6.03 (t, J = 7.0 Hz, 1H), 3.42 (s, 3H); $^{13}\text{C}\{^1\text{H}\}$ NMR (100 MHz, CDCl_3) δ = 158.7, 157.6 (d, $^3J_{\text{C-F}}$ = 6.2 Hz), 154.3, 143.8, 139.8, 132.3, 128.6, 128.3, 124.4, 123.3 (dd, $^1J_{\text{C-F}}$ = 276.8, 264.6 Hz), 123.2 (d, $^4J_{\text{C-F}}$ = 1.9 Hz), 118.4, 116.8, 116.5, 106.6, 97.4 (dd, $^2J_{\text{C-F}}$ = 29.6, 14.6 Hz), 51.6; ^{19}F NMR (376 MHz, CDCl_3) δ = -77.83 (d, J = 184.2 Hz), -107.71 (d, J = 184.2 Hz); HRMS (ESI) m/z : $[\text{M} + \text{H}]^+$ Calcd for $\text{C}_{17}\text{H}_{13}\text{F}_2\text{N}_2\text{O}_3^+$ 331.0889; found 331.0892.

3,3-difluoro-2-methoxy-2-(4-(methylsulfonyl)phenyl)-2,3-dihydroimidazo[1,2-a]pyridine



(5wa): Pale yellow solid (63 mg, 89% yield); Purification by column chromatography on neutral alumina (eluent: EtOAc/Hexanes = 3.0/7.0); mp = 172-173 °C; ^1H NMR (400 MHz, CDCl_3) δ = 7.57 (d, J = 8.8 Hz, 1H), 7.10 – 7.05 (m, 2H), 6.95 (d, J = 9.2 Hz, 1H), 6.61 (d, J = 10 Hz, 1H), 5.95 (t, J = 6.4 Hz, 1H), 3.84 (s, 3H), 3.32 (s, 3H); $^{13}\text{C}\{^1\text{H}\}$ NMR (100 MHz, CDCl_3) δ = 160.2, 157.4 (dd, $^3J_{\text{C-F}}$ = 6.5, 2.2 Hz), 139.0, 129.0, 128.3 (d, $^4J_{\text{C-F}}$ = 1.6 Hz), 126.8 (d, $^3J_{\text{C-F}}$ = 2.8 Hz), 124.0 (dd, $^1J_{\text{C-F}}$ = 274.8, 262.2 Hz), 117.3, 113.5, 106.2, 99.1 (dd, $^2J_{\text{C-F}}$ = 29.2, 13.3 Hz), 55.2, 51.5; ^{19}F NMR (376 MHz, CDCl_3) δ = -77.48 (d, J = 183.1 Hz), -108.47 (d, J = 183.1 Hz); HRMS (ESI) m/z : $[\text{M} + \text{H}]^+$ Calcd for $\text{C}_{15}\text{H}_{15}\text{F}_2\text{N}_2\text{O}_3\text{S}^+$ 289.1147; found 289.1144.

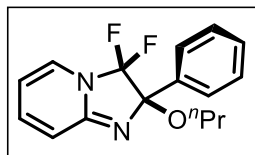
2-Ethoxy-3,3-difluoro-2-phenyl-2,3-dihydroimidazo[1,2-a]pyridine (5ab): Pale yellow solid



(63 mg, 91% yield); Purification by column chromatography on neutral alumina (eluent: EtOAc/Hexanes = 1.5/8.5); mp = 184-186 °C; ^1H NMR (400 MHz, CDCl_3) δ = 7.66 (dd, J = 7.0, 2.2 Hz, 2H), 7.42 (dd, J = 5.2, 1.4 Hz, 2H), 7.35 – 7.33 (m, 1H), 7.11 – 7.07 (m, 1H), 6.64 (d, J = 10.0 Hz, 1H), 5.97 (t, J = 6.6 Hz, 1H), 3.76 – 3.69 (m, 1H), 3.47 – 3.40 (m, 1H), 1.21 (t, J = 7.0 Hz, 3H); $^{13}\text{C}\{^1\text{H}\}$ NMR

(100 MHz, CDCl₃) δ = 157.2 (dd, $^3J_{C-F}$ = 6.1, 2.5 Hz), 139.0, 135.7 (d, $^3J_{C-F}$ = 3.1 Hz), 129.0, 128.1, 128.0, 127.5, 125.9 (dd, $^1J_{C-F}$ = 195.4, 178.4 Hz), 117.2, 106.2, 100.9 (dd, $^2J_{C-F}$ = 29.1, 13.6 Hz Hz), 59.8, 15.6; ^{19}F NMR (376 MHz, CDCl₃) δ = -77.72 (d, J = 180.5 Hz), -107.46 (d, J = 184.2 Hz); HRMS (ESI) m/z : [M + H]⁺ Calcd for C₁₅H₁₅F₂N₂O⁺ 277.1147; found 277.1142.

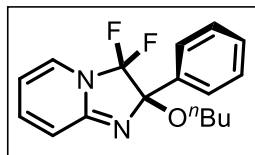
3,3-Difluoro-2-phenyl-2-propoxy-2,3-dihydroimidazo[1,2-a]pyridine (5ac): Pale yellow solid



(59 mg, 87% yield); Purification by column chromatography on neutral alumina (eluents: EtOAc/Hexanes = 1.5/8.5); mp = 184-186 °C; ^1H NMR (400 MHz, CDCl₃) δ = 7.68 – 7.65 (m, 2H), 7.43 – 7.40 (m, 3H), 7.09 – 7.05 (m, 2H), 6.62 (d, J = 10.0 Hz, 1H), 5.95 (t, J = 6.6 Hz, 1H), 3.62

(dt, J = 9.2, 6.8 Hz, 1H), 3.32 (dt, J = 9.2, 7.2 Hz, 1H), 1.61 (sext, J = 7.2 Hz, 2H), 0.90 (t, J = 7.4 Hz, 3H); $^{13}\text{C}\{^1\text{H}\}$ NMR (100 MHz, CDCl₃) δ = 157.3 (dd, $^3J_{C-F}$ = 6.4, 2.5 Hz), 138.9, 135.8 (d, $^3J_{C-F}$ = 2.8 Hz), 129.0, 128.4 (d, $^4J_{C-F}$ = 1.5 Hz), 128.1, 127.6, 124.0 (dd, $^1J_{C-F}$ = 274.8, 264.4 Hz), 117.2, 106.1, 98.9 (dd, $^2J_{C-F}$ = 28.8, 13.5 Hz), 65.6, 23.3, 10.5; ^{19}F NMR (376 MHz, CDCl₃) δ = -77.77 (d, J = 184.2 Hz), -107.44 (d, J = 180.5 Hz); HRMS (ESI) m/z : [M + H]⁺ Calcd for C₁₆H₁₇F₂N₂O⁺ 291.1303; found 291.1301.

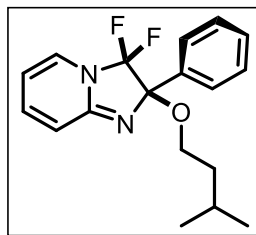
2-Butoxy-3,3-difluoro-2-phenyl-2,3-dihydroimidazo[1,2-a]pyridine (5ad): Pale yellow solid



(57 mg, 80% yield); Purification by column chromatography on neutral alumina (eluents: EtOAc/Hexanes = 1.5/8.5); mp = 184-186 °C; ^1H NMR (400 MHz, CDCl₃) δ = 7.67 – 7.65 (m, 2H), 7.43 – 7.40 (m, 3H), 7.09 – 7.05 (m, 2H), 6.61 (d, J = 10.0 Hz, 1H), 5.94 (t, J = 6.8 Hz, 1H), 3.67

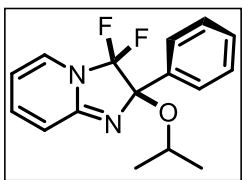
(dt, J = 9.2, 6.4 Hz, 1H), 3.35 (dt, J = 9.2, 6.8 Hz, 1H), 1.65 – 1.51 (quint, J = 7.6 Hz, 2H), 1.40 – 1.30 (m, 2H), 0.88 (t, J = 7.4 Hz, 3H); $^{13}\text{C}\{^1\text{H}\}$ NMR (100 MHz, CDCl₃) δ = 157.3 (dd, $^3J_{C-F}$ = 6.4, 2.3 Hz), 138.9, 135.8 (d, $^3J_{C-F}$ = 2.7 Hz), 129.0, 128.3 (d, $^4J_{C-F}$ = 1.4 Hz), 128.1, 127.6, 124.0 (dd, $^1J_{C-F}$ = 274.7, 262.8 Hz), 117.2, 106.1, 98.9 (dd, $^2J_{C-F}$ = 28.8, 13.5 Hz), 63.8, 32.2, 19.2, 13.9; ^{19}F NMR (376 MHz, CDCl₃) δ = -77.74 (d, J = 184.2 Hz), -107.48 (d, J = 180.5 Hz); HRMS (ESI) m/z : [M + H]⁺ Calcd for C₁₇H₁₉F₂N₂O⁺ 305.1460; found 305.1459.

3,3-Difluoro-2-(isopentyloxy)-2-phenyl-2,3-dihydroimidazo[1,2-a]pyridine (5ae): Pale yellow



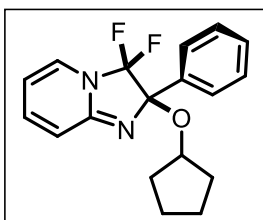
solid (54 mg, 84% yield); Purification by column chromatography on neutral alumina (eluents: EtOAc/Hexanes = 1.5/8.5); mp = 184-186 °C; ^1H NMR (400 MHz, CDCl_3) δ 7.67 – 7.64 (m, 2H), 7.44 – 7.40 (m, 3H), 7.08 – 7.04 (m, 2H), 6.61 (d, J = 10.0 Hz, 1H), 5.94 (t, J = 6.8 Hz, 1H), 3.70 (dt, J = 9.2, 6.8 Hz, 1H), 3.37 (dt, J = 9.2, 6.8 Hz, 1H), 1.69 (sept, J = 6.8 Hz, 1H), 1.49 (q, J = 6.8 Hz, 2H), 0.86 (d, J = 6.8 Hz, 3H), 0.84 (d, J = 6.4 Hz, 3H); $^{13}\text{C}\{^1\text{H}\}$ NMR (100 MHz, CDCl_3) δ = 157.3 (dd, $^3J_{\text{C-F}}$ = 6.5, 2.3 Hz), 138.9, 135.8 (d, $^3J_{\text{C-F}}$ = 2.7 Hz), 129.0, 128.3 (d, $^4J_{\text{C-F}}$ = 1.4 Hz), 128.1, 127.5 (d, $^4J_{\text{C-F}}$ = 0.8 Hz), 124.0 (dd, $^1J_{\text{C-F}}$ = 274.8, 262.8 Hz), 117.2, 106.1, 98.9 (dd, $^2J_{\text{C-F}}$ = 28.9, 13.5 Hz), 62.5, 38.9, 25.0, 22.7, 22.6; ^{19}F NMR (376 MHz, CDCl_3) δ = -77.74 (d, J = 184.2 Hz), -107.50 (d, J = 184.2 Hz); HRMS (ESI) m/z : $[\text{M} + \text{H}]^+$ Calcd for $\text{C}_{18}\text{H}_{21}\text{F}_2\text{N}_2\text{O}^+$ 319.1616; found 319.1611.

3,3-Difluoro-2-isopropoxy-2-phenyl-2,3-dihydroimidazo[1,2-a]pyridine (5af): Pale yellow



solid (58 mg, 92% yield); Purification by column chromatography on neutral alumina (eluents: EtOAc/Hexanes = 1.5/8.5); mp = 101-102 °C; ^1H NMR (400 MHz, CDCl_3) δ = 7.67 – 7.65 (m, 2H), 7.46 – 7.41 (m, 3H), 7.11 – 7.07 (m, 2H), 6.64 (d, J = 10.0 Hz, 1H), 5.97 (t, J = 6.6 Hz, 1H), 3.34 (s, 1H); $^{13}\text{C}\{^1\text{H}\}$ NMR (100 MHz, CDCl_3) δ = 157.6 (dd, $^3J_{\text{C-F}}$ = 6.5, 2.4 Hz), 139.1, 134.9 (d, $^3J_{\text{C-F}}$ = 2.9 Hz), 129.2, 128.3 (d, $^4J_{\text{C-F}}$ = 1.8 Hz), 128.2, 127.7, 124.0 (dd, $^1J_{\text{C-F}}$ = 274.7, 262.5 Hz), 117.3, 106.2, 99.2 (dd, $^2J_{\text{C-F}}$ = 29.2, 13.2 Hz), 51.6; ^{19}F NMR (376 MHz, CDCl_3) δ = -77.54 (d, J = 183.5 Hz), -108.14 (d, J = 183.5 Hz); HRMS (ESI) m/z : $[\text{M} + \text{H}]^+$ Calcd for $\text{C}_{14}\text{H}_{12}\text{F}_2\text{N}_2\text{O}^+$ 262.0918; found 262.0921.

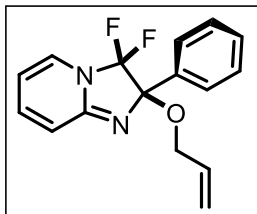
2-(Cyclopentyloxy)-3,3-difluoro-2-phenyl-2,3-dihydroimidazo[1,2-a]pyridine (5ag): Pale yellow



solid (63 mg, 93% yield); Purification by column chromatography on neutral alumina (eluents: EtOAc/Hexanes = 3.0/7.0); mp = 172-173 °C; ^1H NMR (400 MHz, CDCl_3) δ = 7.57 (d, J = 8.8 Hz, 1H), 7.10 – 7.05 (m, 2H), 6.95 (d, J = 9.2 Hz, 1H), 6.61 (d, J = 10 Hz, 1H), 5.95 (t, J = 6.4 Hz, 1H), 3.84 (s, 3H), 3.32 (s, 3H); $^{13}\text{C}\{^1\text{H}\}$ NMR (100 MHz, CDCl_3) δ = 160.2, 157.4 (dd, $^3J_{\text{C-F}}$ = 6.5, 2.2 Hz), 139.0, 129.0, 128.3 (d, $^4J_{\text{C-F}}$ = 1.6 Hz), 126.8 (d, $^3J_{\text{C-F}}$ = 2.8 Hz), 124.0 (dd, $^1J_{\text{C-F}}$ = 274.8, 262.2 Hz), 117.3, 113.5, 106.2, 99.1 (dd, $^2J_{\text{C-F}}$ = 29.2, 13.3 Hz), 55.2, 51.5; ^{19}F NMR (376 MHz, CDCl_3) δ = -77.48 (d, J = 183.1 Hz), -108.47

(d, $J = 183.1$ Hz); HRMS (ESI) m/z : $[M + H]^+$ Calcd for $C_{15}H_{15}F_2N_2O^+$ 289.1147; found 289.1144.

2-(Allyloxy)-3,3-difluoro-2-phenyl-2,3-dihydroimidazo[1,2-a]pyridine (5ah): Pale yellow

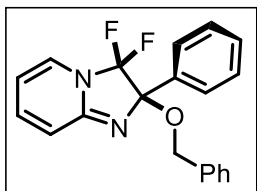


solid (62 mg, 78% yield); Purification by column chromatography on neutral alumina (eluents: EtOAc/Hexanes = 3.0/7.0); mp = 184-186 °C;

1H NMR (400 MHz, $CDCl_3$) $\delta = 7.57$ (d, $J = 8.8$ Hz, 1H), 7.10 – 7.05 (m, 2H), 6.95 (d, $J = 9.2$ Hz, 1H), 6.61 (d, $J = 10$ Hz, 1H), 5.95 (t, $J = 6.4$ Hz, 1H), 3.84 (s, 3H), 3.32 (s, 3H); $^{13}C\{^1H\}$ NMR (100 MHz,

$CDCl_3$) $\delta = 160.2$, 157.4 (dd, $^3J_{C-F} = 6.5$, 2.2 Hz), 139.0, 129.0, 128.3 (d, $^4J_{C-F} = 1.6$ Hz), 126.8 (d, $^3J_{C-F} = 2.8$ Hz), 124.0 (dd, $^1J_{C-F} = 274.8$, 262.2 Hz), 117.3, 113.5, 106.2, 99.1 (dd, $^2J_{C-F} = 29.2$, 13.3 Hz), 55.2, 51.5; ^{19}F NMR (376 MHz, $CDCl_3$) $\delta = -77.48$ (d, $J = 183.1$ Hz), -108.47 (d, $J = 183.1$ Hz); HRMS (ESI) m/z : $[M + H]^+$ Calcd for $C_{15}H_{15}F_2N_2O^+$ 289.1147; found 289.1144.

2-(Benzyloxy)-3,3-difluoro-2-phenyl-2,3-dihydroimidazo[1,2-a]pyridine (5ai): Pale yellow

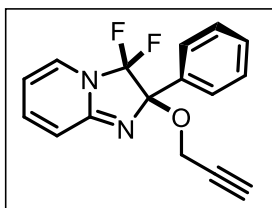


solid (59 mg, 88% yield); Purification by column chromatography on neutral alumina (eluents: EtOAc/Hexanes = 3.0/7.0); mp = 184-186 °C;

1H NMR (400 MHz, $CDCl_3$) $\delta = 7.57 - 7.52$ (m, 4H), 7.14 – 7.09 (m, 2H), 6.63 (d, $J = 9.6$ Hz, 1H), 6.00 (t, $J = 6.8$ Hz, 1H), 3.32 (s, 3H);

$^{13}C\{^1H\}$ NMR (100 MHz, $CDCl_3$) $\delta = 157.9$ (dd, $^3J_{C-F} = 6.5$, 2.2 Hz), 139.4, 134.2 (d, $^3J_{C-F} = 2.8$ Hz), 131.4, 129.5, 128.2 (d, $^4J_{C-F} = 1.8$ Hz), 123.8 (dd, $^1J_{C-F} = 275.1$, 263.2 Hz), 123.5, 117.2, 106.5, 98.8 (dd, $^2J_{C-F} = 29.2$, 13.6 Hz), 51.6; ^{19}F NMR (376 MHz, $CDCl_3$) $\delta = -77.14$ (d, $J = 184.2$ Hz), -108.35 (d, $J = 184.2$ Hz); HRMS (ESI) m/z : $[M + H]^+$ Calcd for $C_{14}H_{12}BrF_2N_2O^+$ 341.0096; found 341.0098.

3,3-Difluoro-2-phenyl-2-(prop-2-yn-1-yloxy)-2,3-dihydroimidazo[1,2-a]pyridine (5aj): Pale



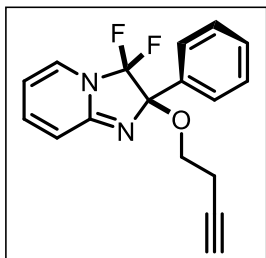
yellow solid (60 mg, 75% yield); Purification by column chromatography on neutral alumina (eluents: EtOAc/Hexanes = 2.0/8.0); mp =

184-186 °C; 1H NMR (400 MHz, $CDCl_3$) $\delta = 7.59$ (d, $J = 8.4$ Hz, 2H), 7.38 (d, $J = 8.4$ Hz, 2H), 7.08 (t, $J = 8.2$ Hz, 2H), 6.60 (d, $J = 9.6$ Hz,

1H), 5.96 (t, $J = 6.8$ Hz, 1H), 3.31 (s, 3H); $^{13}C\{^1H\}$ NMR (100 MHz, $CDCl_3$) $\delta = 157.8$ (dd, $^3J_{C-F} = 6.6$, 2.2 Hz), 139.3, 135.1, 133.7 (d, $^3J_{C-F} = 2.7$ Hz), 129.2, 128.4, 128.2 (d, $^4J_{C-F} = 1.6$ Hz), 124.6 (dd, $^1J_{C-F} = 274.85$, 263.05 Hz), 117.2, 106.4, 98.8 (dd, $^2J_{C-F} = 29.1$, 13.5 Hz), 51.5;

^{19}F NMR (376 MHz, CDCl_3) $\delta = -77.21$ (d, $J = 184.2$ Hz), -108.34 (d, $J = 184.2$ Hz); HRMS (ESI) m/z : $[\text{M} + \text{H}]^+$ Calcd for $\text{C}_{14}\text{H}_{12}\text{ClF}_2\text{N}_2\text{O}^+$ 297.0601; found 297.0606.

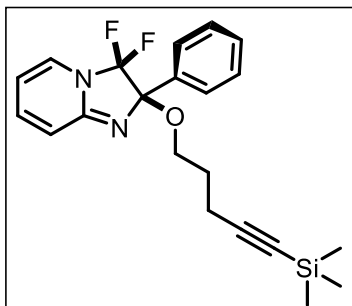
2-(But-3-yn-1-yloxy)-3,3-difluoro-2-phenyl-2,3-dihydroimidazo[1,2-a]pyridine (5ak): Pale



yellow solid (55 mg, 70% yield); Purification by column chromatography on neutral alumina (eluent: EtOAc/Hexanes = 3.0/7.0); mp = 184-186 °C; ^1H NMR (400 MHz, CDCl_3) $\delta = 7.66 - 7.62$ (m, 2H), 7.13 - 7.08 (m, 4H), 6.62 (d, $J = 9.6$ Hz, 1H), 5.98 (t, $J = 6.8$ Hz, 1H), 3.32 (s, 3H); $^{13}\text{C}\{^1\text{H}\}$ NMR (100 MHz, CDCl_3) $\delta = 157.8$ (dd, $^3J_{\text{C-F}} = 6.6$, 2.2 Hz), 139.3, 135.1, 133.7 (d, $^3J_{\text{C-F}} = 2.7$ Hz), 129.2, 128.4, 128.2 (d,

$^4J_{\text{C-F}} = 1.6$ Hz), 124.6 (dd, $^1J_{\text{C-F}} = 274.85$, 263.05 Hz), 117.2, 106.4, 98.8 (dd, $^2J_{\text{C-F}} = 29.1$, 13.5 Hz), 51.5, 21.6; ^{19}F NMR (376 MHz, CDCl_3) $\delta = -77.09$ (d, $J = 183.4$ Hz), -108.57 (d, $J = 183.4$ Hz), -112.84 ; HRMS (ESI) m/z : $[\text{M} + \text{H}]^+$ Calcd for $\text{C}_{14}\text{H}_{12}\text{F}_3\text{N}_2\text{O}^+$ 281.0896; found 281.0900.

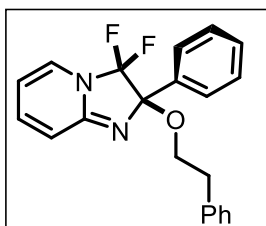
3,3-Difluoro-2-phenyl-2-((5-(trimethylsilyl)pent-4-yn-1-yl)oxy)-2,3-dihydroimidazo[1,2-



a]pyridine (5al): Pale yellow solid (55 mg, 77% yield); Purification by column chromatography on neutral alumina (eluent: EtOAc/Hexanes = 3.0/7.0); mp = 184-186 °C; ^1H NMR (400 MHz, CDCl_3) $\delta = 8.28 - 8.25$ (m, 2H), 7.86 - 7.83 (m, 2H), 7.18 - 7.09 (m, 2H), 6.65 (d, $J = 9.2$ Hz, 1H), 6.04 (t, $J = 6.8$ Hz, 1H), 3.34 (s, 3H); $^{13}\text{C}\{^1\text{H}\}$ NMR (100 MHz, CDCl_3) $\delta = 158.2$ (dd,

$^3J_{\text{C-F}} = 6.6$, 2.3 Hz), 140.8 (d, $^3J_{\text{C-F}} = 2.6$ Hz), 139.7, 132.0, 128.5 (d, $^4J_{\text{C-F}} = 0.7$ Hz), 128.1 (d, $^4J_{\text{C-F}} = 1.5$ Hz), 123.8 (dd, $^1J_{\text{C-F}} = 275.7$, 263.9 Hz), 118.6, 117.1, 113.1, 106.8, 98.6 (dd, $^2J_{\text{C-F}} = 29.1$, 13.6 Hz), 51.7; ^{19}F NMR (376 MHz, CDCl_3) $\delta = -76.88$ (d, $J = 184.2$ Hz), -107.76 (d, $J = 184.2$ Hz); HRMS (ESI) m/z : $[\text{M} + \text{H}]^+$ Calcd for $\text{C}_{21}\text{H}_{25}\text{F}_2\text{N}_2\text{OSi}^+$ 387.1699; found 387.1702.

3,3-Difluoro-2-phenethoxy-2-phenyl-2,3-dihydroimidazo[1,2-a]pyridine (5am): Pale yellow

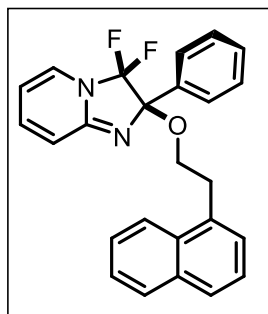


solid (64 mg, 65% yield); Purification by column chromatography on neutral alumina (eluent: EtOAc/Hexanes = 3.0/7.0); mp = 184-186 °C; ^1H NMR (400 MHz, CDCl_3) $\delta = 7.79$ (d, $J = 8.0$ Hz, 2H), 7.68 (d, $J = 8.0$ Hz, 2H), 7.15 - 7.09 (m, 2H), 6.66 - 6.63 (m, 1H), 6.01 (t, $J = 6.8$ Hz, 1H) 3.34 (s, 3H); $^{13}\text{C}\{^1\text{H}\}$ NMR (100 MHz, CDCl_3) $\delta = 158.0$ (dd,

$^3J_{\text{C-F}} = 6.6$, 2.3 Hz), 139.5, 139.3 (d, $^4J_{\text{C-F}} = 1.4$ Hz), 131.3, 128.2, 126.1, 125.15 (q, $^3J_{\text{C-F}} = 3.7$

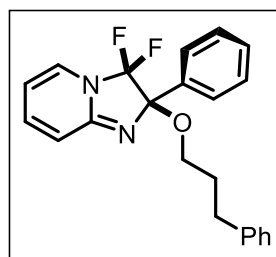
(Hz), 124.0 (dd, $^1J_{C-F} = 275.7, 263.9$ Hz), 117.2, 106.6, 98.8 (dd, $^2J_{C-F} = 29.4, 13.8$ Hz), 51.7, 35.5; ^{19}F NMR (376 MHz, CDCl_3) $\delta = -62.63, -77.11$ (d, $J = 183.9$ Hz), -108.10 (d, $J = 184.2$ Hz); HRMS (ESI) m/z : $[\text{M} + \text{H}]^+$ Calcd for $\text{C}_{15}\text{H}_{12}\text{F}_5\text{N}_2\text{O}^+$ 331.0864; found 331.0861.

3,3-Difluoro-2-(2-(naphthalen-1-yl)ethoxy)-2-phenyl-2,3-dihydroimidazo[1,2-a]pyridine



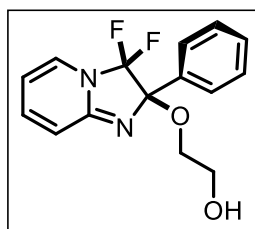
(5an): Pale yellow solid (66 mg, 76% yield); Purification by column chromatography on neutral alumina (eluent: EtOAc/Hexanes = 3.0/7.0); mp = 184-186 °C; ^1H NMR (400 MHz, CDCl_3) $\delta = 7.78$ (d, $J = 8.8$ Hz, 2H), 7.71 (d, $J = 8.4$ Hz, 2H), 7.17 – 7.09 (m, 2H), 6.64 (d, $J = 9.6$ Hz, 1H), 6.03 (t, $J = 6.6$ Hz, 1H), 3.32 (s, 3H); $^{13}\text{C}\{^1\text{H}\}$ NMR (100 MHz, CDCl_3) $\delta = 158.2$ (dd, $^3J_{C-F} = 6.6, 2.3$ Hz), 140.8 (d, $^3J_{C-F} = 2.6$ Hz), 139.7, 132.0, 128.5 (d, $^4J_{C-F} = 0.7$ Hz), 128.1 (d, $^4J_{C-F} = 1.5$ Hz), 123.8 (dd, $^1J_{C-F} = 275.7, 263.9$ Hz), 118.6, 117.1, 113.1, 106.8, 98.6 (dd, $^2J_{C-F} = 29.1, 13.6$ Hz), 51.7; ^{19}F NMR (376 MHz, CDCl_3) $\delta = -76.88$ (d, $J = 184.2$ Hz), -107.76 (d, $J = 184.2$ Hz); HRMS (ESI) m/z : $[\text{M} + \text{H}]^+$ Calcd for $\text{C}_{15}\text{H}_{12}\text{F}_2\text{N}_3\text{O}^+$ 288.0943; found 288.0944.

3,3-Difluoro-2-phenyl-2-(3-phenylpropoxy)-2,3-dihydroimidazo[1,2-a]pyridine (5ao): Off-



white solid (56 mg, 69% yield); Purification by column chromatography on neutral alumina (eluent: EtOAc/Hexanes = 2.0/8.0); mp = 104-105 °C; ^1H NMR (400 MHz, CDCl_3) $\delta = 7.35$ (t, $J = 8.0$ Hz, 1H), 7.26 (d, $J = 7.6$ Hz, 1H), 7.21 (s, 1H), 7.11 – 7.07 (m, 2H), 6.96 (dd, $J = 8.2, 1.8$ Hz, 1H), 6.63 (d, $J = 10.0$ Hz, 1H), 5.97 (t, $J = 6.6$ Hz, 1H), 3.85 (s, 3H), 3.35 (s, 3H); $^{13}\text{C}\{^1\text{H}\}$ NMR (100 MHz, CDCl_3) $\delta = 159.6, 157.6$ (dd, $^3J_{C-F} = 6.6, 2.3$ Hz), 139.1, 136.6 (d, $^3J_{C-F} = 2.7$ Hz), 129.2, 128.3 (d, $^4J_{C-F} = 1.6$ Hz), 124.0 (dd, $^1J_{C-F} = 274.9, 263.1$ Hz), 120.1, 117.3, 115.1, 113.0, 106.3, 99.1 (dd, $^2J_{C-F} = 29.1, 13.4$ Hz), 55.3, 51.7; ^{19}F NMR (376 MHz, CDCl_3) $\delta = -77.91$ (d, $J = 183.5$ Hz), -108.30 (d, $J = 183.5$ Hz); HRMS (ESI) m/z : $[\text{M} + \text{H}]^+$ Calcd for $\text{C}_{15}\text{H}_{15}\text{F}_2\text{N}_2\text{O}_2^+$ 293.1096; found 293.1100.

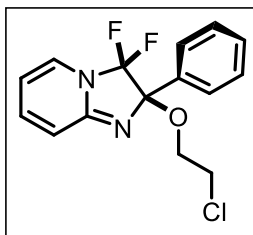
2-((3,3-Difluoro-2-phenyl-2,3-dihydroimidazo[1,2-a]pyridin-2-yl)oxy)ethan-1-ol (5ap): Yel-



low solid (59 mg, 69% yield); Purification by column chromatography on neutral alumina (eluent: EtOAc/Hexanes = 2.0/8.0); mp = 146-147 °C; ^1H NMR (400 MHz, $\text{DMSO}-d_6$) $\delta = 8.54$ (t, $J = 1.8$ Hz, 1H), 8.28 (dd, $J = 8.8, 2.0$ Hz, 1H), 8.00 (d, $J = 8.0$ Hz, 1H), 7.61 (t, $J = 8.0$ Hz, 1H), 7.19 – 7.15 (m, 1H), 7.11 (d, $J = 6.8$ Hz, 1H), 6.67 (d, $J = 9.6$ Hz,

1H), 6.05 (t, $J = 6.8$ Hz, 1H), 3.36 (s, 3H); $^{13}\text{C}\{^1\text{H}\}$ NMR (100 MHz, DMSO- d_6) $\delta = 158.3$ (dd, $^3J_{\text{C-F}} = 6.6, 2.3$ Hz), 148.3, 139.8, 138.0 (d, $^3J_{\text{C-F}} = 2.8$ Hz), 133.8, 129.2, 128.1 (d, $^4J_{\text{C-F}} = 1.7$ Hz), 124.2, 123.8 (dd, $^1J_{\text{C-F}} = 277.4, 265.6$ Hz), 123.0 (d, $^4J_{\text{C-F}} = 0.6$ Hz), 117.2, 106.9, 98.5 (dd, $^4J_{\text{C-F}} = 29.0, 14.0$ Hz), 51.7; ^{19}F NMR (376 MHz, CDCl_3) $\delta = -76.40$ (d, $J = 184.3$ Hz), -107.72 (d, $J = 184.3$ Hz); HRMS (ESI) m/z : $[\text{M} + \text{H}]^+$ Calcd for $\text{C}_{14}\text{H}_{15}\text{F}_2\text{N}_2\text{O}_2^+$ $[\text{M} + \text{H}]^+$ 293.1096; found 293.1091.

2-(2-Chloroethoxy)-3,3-difluoro-2-phenyl-2,3-dihydroimidazo[1,2-a]pyridine (5aq): Pale yellow solid (54 mg, 75% yield); Purification by column chromatography on neutral alumina (eluent: EtOAc/Hexanes = 1.5/8.5); mp = 184-186



low solid (54 mg, 75% yield); Purification by column chromatography on neutral alumina (eluent: EtOAc/Hexanes = 1.5/8.5); mp = 184-186 °C; ^1H NMR (400 MHz, CDCl_3) $\delta = 7.67 - 7.64$ (m, 2H), 7.45 - 7.40 (m, 3H), 7.01 (d, $J = 7.2$ Hz, 1H), 6.42 (s, 1H), 5.83 (d, $J = 6.8$ Hz, 1H), 3.33 (s, 3H), 2.17 (s, 3H); $^{13}\text{C}\{^1\text{H}\}$ NMR (100 MHz, CDCl_3) $\delta = 157.9$ (dd, $J = 6.5, 2.3$ Hz), 150.9, 135.2 (d, $J = 2.7$ Hz), 129.1, 128.1, 127.7, 127.1 (d, $J = 1.6$ Hz), 123.9 (dd, $J = 274.2, 262.8$ Hz), 114.5, 109.3, 99.4 (dd, $J = 29.1, 13.4$ Hz), 51.5, 22.2; ^{19}F NMR (376 MHz, CDCl_3) $\delta = -77.62$ (d, $J = 183.1$ Hz), -107.94 (d, $J = 183.1$ Hz); HRMS (ESI) m/z : $[\text{M} + \text{H}]^+$ Calcd for $\text{C}_{15}\text{H}_{14}\text{ClF}_2\text{N}_2\text{O}^+$ 311.0757; found 311.0753.

4.4.3 X-ray Crystallographic Analysis of Compound 5ga, and 5ai

The single crystals of the compound **5ga** ($\text{C}_{14}\text{H}_{11}\text{F}_2\text{N}_3\text{O}_3$, **Figure 3.7**) and **5ai** ($\text{C}_{20}\text{H}_{16}\text{F}_2\text{N}_2\text{O}$, **Figure 3.8**) was obtained from slow evaporation of chloroform. **5ga** was crystallized in triclinic crystal system with P-1 space group and **5ai** was crystallized in orthorhombic crystal system with Pbcn space group. The crystal structure information of **5ga** and **5ai** is deposited to Cambridge Crystallographic Data Center and the CCDC numbers for the **5ga** is 2244256, and for **5ai** is 2244257.

The crystal data collection and data reduction were performed using CrysAlis PRO on a single crystal Rigaku Oxford XtaLab Pro diffractometer. The crystal was kept at 93(2) K during data collection. Using Olex2⁴⁴, the structure was solved with the ShelXT⁴⁵ structure solution program using Intrinsic Phasing and refined with the ShelXL⁴⁶ refinement package using Least Squares minimization.

Table 3.4: Crystal data and structure refinement for **5ga** and **5ai**

Identification code	5ga	5ai
Empirical formula	C ₁₄ H ₁₁ F ₂ N ₃ O ₃	C ₂₀ H ₁₆ F ₂ N ₂ O
Formula weight	307.26	338.35
Temperature/K	133(2)	133(2)
Crystal system	triclinic	orthorhombic
Space group	P-1	Pbcn
a/Å	7.33770(10)	20.2135(5)
b/Å	7.58970(10)	8.1716(2)
c/Å	12.3784(2)	20.2646(4)
α/°	107.700(2)	90
β/°	99.408(2)	90
γ/°	91.054(2)	90
Volume/Å ³	646.195(18)	3347.24(13)
Z	2	8
ρ _{calc} /g/cm ³	1.579	1.343
μ/mm ⁻¹	1.143	0.826
F(000)	316.0	1408.0
Crystal size/mm ³	0.24 × 0.15 × 0.05	0.15 × 0.08 × 0.05
Radiation	Cu Kα (λ = 1.54184)	Cu Kα (λ = 1.54184)
2θ range for data collection/°	7.618 to 159.482	8.728 to 159.658
Index ranges	-9 ≤ h ≤ 9, -9 ≤ k ≤ 4, -14 ≤ l ≤ 15	-25 ≤ h ≤ 15, -5 ≤ k ≤ 9, -25 ≤ l ≤ 23
Reflections collected	6432	11012
Independent reflections	2712 [R _{int} = 0.0251, R _{sigma} = 0.0274]	3513 [R _{int} = 0.0428, R _{sigma} = 0.0367]
Data/restraints/parameters	2712/0/200	3513/0/226
Goodness-of-fit on F ²	1.054	1.109
Final R indexes [I ≥ 2σ (I)]	R ₁ = 0.0417, wR ₂ = 0.1100	R ₁ = 0.0423, wR ₂ = 0.1230
Final R indexes [all data]	R ₁ = 0.0426, wR ₂ = 0.1110	R ₁ = 0.0463, wR ₂ = 0.1264
Largest diff. peak/hole / e Å ⁻³	0.23/-0.36	0.29/-0.30

4.5 REFERENCES

1. Chambers, R. D., Fluorine in organic chemistry. Chambers, R. D., Ed. Springer Berlin Heidelberg: Berlin, Heidelberg, **2004**; pp 411-476.
2. Postigo, A., Applications of Organofluorine Compounds. *Modern Fluoroorganic Chemistry*, **2004**; pp 203-277.

- Burton, D. J.; Lu, L., Fluorinated Organometallic Compounds. *Organofluorine Chemistry: Techniques and Synthons*, Chambers, R. D., Ed. Springer Berlin Heidelberg: Berlin, Heidelberg, **1997**; pp 45-89.
- Shimizu, M.; Hiyama, T., *Angewandte Chemie International Edition* **2005**, *44*, 214-231.
- Filler, R.; Kobayashi, Y.; Yagupolskii, L. M. In *Organofluorine Compounds in Medicinal Chemistry and Biomedical Applications*, Filler, R., Ed. Elsevier **1993**; pp 126-184.
- Hiyama, T.; Yamamoto, H., Biologically Active Organofluorine Compounds. In *Organofluorine Compounds: Chemistry and Applications*, Yamamoto, H., Ed. Springer Berlin Heidelberg: Berlin, Heidelberg, **2000**; pp 137-182.
- Park, B. K.; Kitteringham, N. R., *Drug metabolism reviews* **1994**, *26*, 605-643.
- Ogawa, Y.; Tokunaga, E.; Kobayashi, O.; Hirai, K.; Shibata, N., *iScience* **2020**, *23*, 101467-101472.
- Theodoridis, G., Fluorine-Containing Agrochemicals: An Overview of Recent Developments. *Advances in Fluorine Science*, Tressaud, A., Ed. Elsevier **2006**; Vol. 2, pp 121-175.
- Cachet, H., Films and Powders of Fluorine-Doped Tin Dioxide. In *Fluorinated Materials for Energy Conversion*, Nakajima, T.; Groult, H., Eds. Elsevier Science: Amsterdam, **2005**; pp 513-534.
- Yamaki, J. I., Thermally Stable Fluoro-Organic Solvents for Lithium Ion Battery. *Fluorinated Materials for Energy Conversion*, Nakajima, T.; Groult, H., Eds. Elsevier Science: Amsterdam, **2005**; pp 267-284.
- Wang, X.; Lei, J.; Liu, Y.; Ye, Y.; Li, J.; Sun, K., *Organic Chemistry Frontiers* **2021**, *8*, 2079-2109.
- Shi, L.; An, D.; Mei, G.-J., *Organic Chemistry Frontiers* **2022**, *9*, 4192-4208.
- Kliš, T., *Catalysts* **2023**, *13*, 94-125.
- Chatterjee, T.; Iqbal, N.; You, Y.; Cho, E. J., *Accounts of Chemical Research* **2016**, *49*, 2284-2294.
- Barata-Vallejo, S.; Cooke, M. V.; Postigo, A., *ACS Catalysis* **2018**, *8*, 7287-7307.
- Song, H.-X.; Han, Q.-Y.; Zhao, C.-L.; Zhang, C.-P., *Green Chemistry* **2018**, *20*, 1662-1731.

18. Sindhe, H.; Chaudhary, B.; Chowdhury, N.; Kamble, A.; Kumar, V.; Lad, A.; Sharma, S., *Organic Chemistry Frontiers* **2022**, *9*, 1742-1775.
19. Rentmeister, A.; Arnold, F. H.; Fasan, R., *Nature Chemical Biology* **2009**, *5*, 26-28.
20. Barton, D. H. R.; Hesse, R. H.; Jackman, G. P.; Pechet, M. M., *Journal of the Chemical Society, Perkin Transactions 1* **1977**, 2604-2608.
21. Yin, B.; Wang, L.; Inagi, S.; Fuchigami, T., *Tetrahedron* **2010**, *66*, 6820-6825.
22. Middleton, W. J.; Bingham, E. M., *The Journal of Organic Chemistry* **1980**, *45*, 2883-2887.
23. Dilman, A. D.; Levin, V. V., *Accounts of Chemical Research* **2018**, *51*, 1272-1280.
24. Lin, R.; Ding, S.; Shi, Z.; Jiao, N., *Organic Letters* **2011**, *13*, 4498-4501.
25. Liu, P.; Gao, Y.; Gu, W.; Shen, Z.; Sun, P., *The Journal of Organic Chemistry* **2015**, *80*, 11559-11565.
26. Walton, L.; Duplain, H. R.; Knapp, A. L.; Eidell, C. K.; Bacsá, J.; Stephens, C. E., *Journal of Fluorine Chemistry* **2015**, *173*, 12-17.
27. Arcadi, A.; Pietropaolo, E.; Alvino, A.; Michelet, V., *Organic Letters* **2013**, *15*, 2766-2769.
28. Yang, L.; Ma, Y.; Song, F.; You, J., *Chemical Communications* **2014**, *50*, 3024-3026.
29. Lang, X.; Chen, X.; Zhao, J., *Chemical Society Reviews* **2014**, *43*, 473-486.
30. Djurišić, A. B.; He, Y.; Ng, A. M. C., *APL Materials* **2020**, *8*, 030903.
31. Marzo, L.; Pagire, S. K.; Reiser, O.; König, B., *Angewandte Chemie International Edition* **2018**, *57*, 10034-10072.
32. Guillemard, L.; Wencel-Delord, J., *Beilstein Journal of Organic Chemistry* **2020**, *16*, 1754-1804.
33. Guo, W.; Wang, Q.; Zhu, J., *Chemical Society Reviews* **2021**, *50*, 7359-7377.
34. Saha, S.; Bagdi, A. K., *Organic & Biomolecular Chemistry* **2022**, *20*, 3249-3262.
35. Revathi, L.; Ravindar, L.; Fang, W.-Y.; Rakesh, K. P.; Qin, H.-L., *Advanced Synthesis & Catalysis* **2018**, *360*, 4652-4698.
36. Khatun, S.; Singh, A.; Bader, G. N.; Sofi, F. A., *Journal of Biomolecular Structure and Dynamics* **2022**, *40*, 14279-14302.
37. Kurteva, V., *ACS Omega* **2021**, *6*, 35173-35185.

38. Bagdi, A. K.; Santra, S.; Monir, K.; Hajra, A., *Chemical Communications* **2015**, *51*, 1555-1575.
39. Purohit, G.; Kharkwal, A.; Rawat, D. S., *ACS Sustainable Chemistry & Engineering* **2020**, *8*, 5544-5557.
40. Nair, D. K.; Mobin, S. M.; Namboothiri, I. N. N., *Organic Letters* **2012**, *14*, 4580-4583.
41. Kim, O.; Jeong, Y.; Lee, H.; Hong, S.-S.; Hong, S., *Journal of Medicinal Chemistry* **2011**, *54*, 2455-2466.
42. Damghani, T.; Moosavi, F.; Khoshneviszadeh, M.; Mortazavi, M.; Pirhadi, S.; Kayani, Z.; Saso, L.; Edraki, N.; Firuzi, O., *Scientific Reports* **2021**, *11*, 3644.
43. Devi, N.; Singh, D.; Rawal, K. R.; Bariwal, J.; Singh, V., *Current Topics in Medicinal Chemistry* **2016**, *16*, 2963-2994.
44. Dolomanov, O. V.; Bourhis, L. J.; Gildea, R. J.; Howard, J. A.; Puschmann, H., *Journal of Applied Crystallography* **2009**, *42*, 339-341.
45. Sebbar, N.; Ellouz, M.; Essassi, E.; Ouzidan, Y.; Mague, J., *Acta Crystallographica Section E: Crystallographic Communications* **2015**, *71*, o999.
46. Sheldrick, G. M., *Acta Crystallographica Section A: Foundations and Advances* **2015**, *71*, 3-8.

CHAPTER 4

TEMPO-Mediated Cross-Dehydrogenative Coupling of Imidazo[1,2-*a*]pyridines and Indoles with Perfluorinated Alcohols

4.6 INTRODUCTION

From more than half past century, an increasing number of heterocyclic compounds continued to penetrate in various research fields especially in medicinal chemistry. It could be very clearly estimated by the unremitting growth of heteroarene ring count of commercial oral drugs since 1960s.¹⁻⁵ According to the recent report by GlaxoSmithKline (GSK) developability assays, the library of successful drug candidates till 21st century has significantly increased the number of heteroaryl rings per molecule from 0.38 to 0.69, which corresponds to approximately 80% growth.⁶⁻⁷ Indoles and imidazopyridines are among such heteroarenes which have been consistently utilized over the years in biologically active scaffolds. C3-functionalized indoles and imidazopyridines not only found their utility in medicinal chemistry, but these privileged skeletons also offer diverse applications in the field of pharmaceuticals, material chemistry, photochemistry, dyes, and agrochemicals as well. In addition, such heterocycles act as valuable building blocks for the construction of multiple complex molecules. Tryptophan, which is a C3-substituted indole amino acid plays a crucial role in protein synthesis. Drugs like indomethacin and plant-based biologically active components like strychnine and LSD are some other essential components of indole. On the other hand, C3-substituted imidazopyridines exhibit a variety of biological activities, including antiviral, antibacterial, and anticancer properties. Several marketed drugs like Zolpidem, Alpidem, Necopidem, Zolimidine, enhance the practical applicability of imidazopyridines. Thus, with their incorporation into medicinal compounds, the indole and imidazopyridine nucleus has become an indispensable and versatile heterocyclic system with a broad range of biological activities, making them crucial pharmacophores in medicine (**Figure 4.1**). Having such a wide application in various fields of science, functionalization of these pharmacophores specifically at C3 position is always a topic of interest for the organic synthetic chemists.

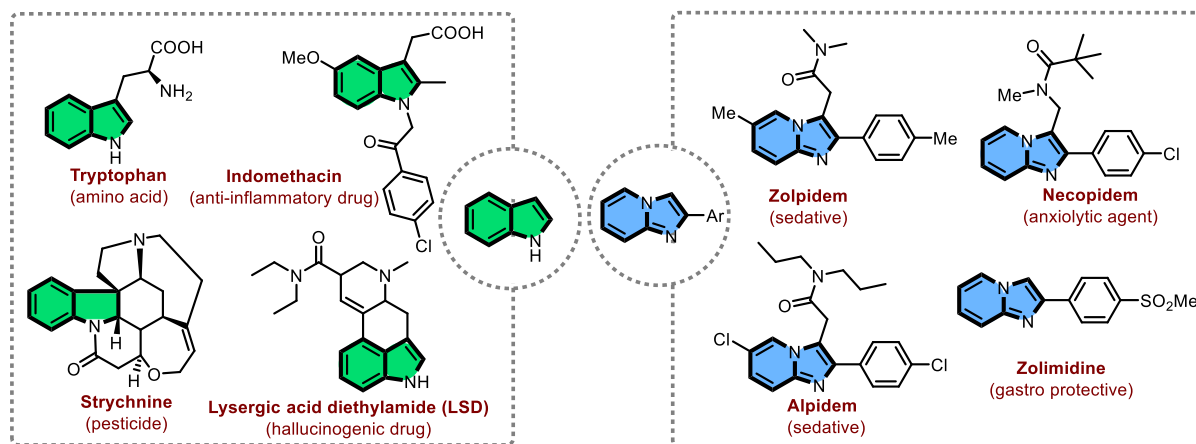
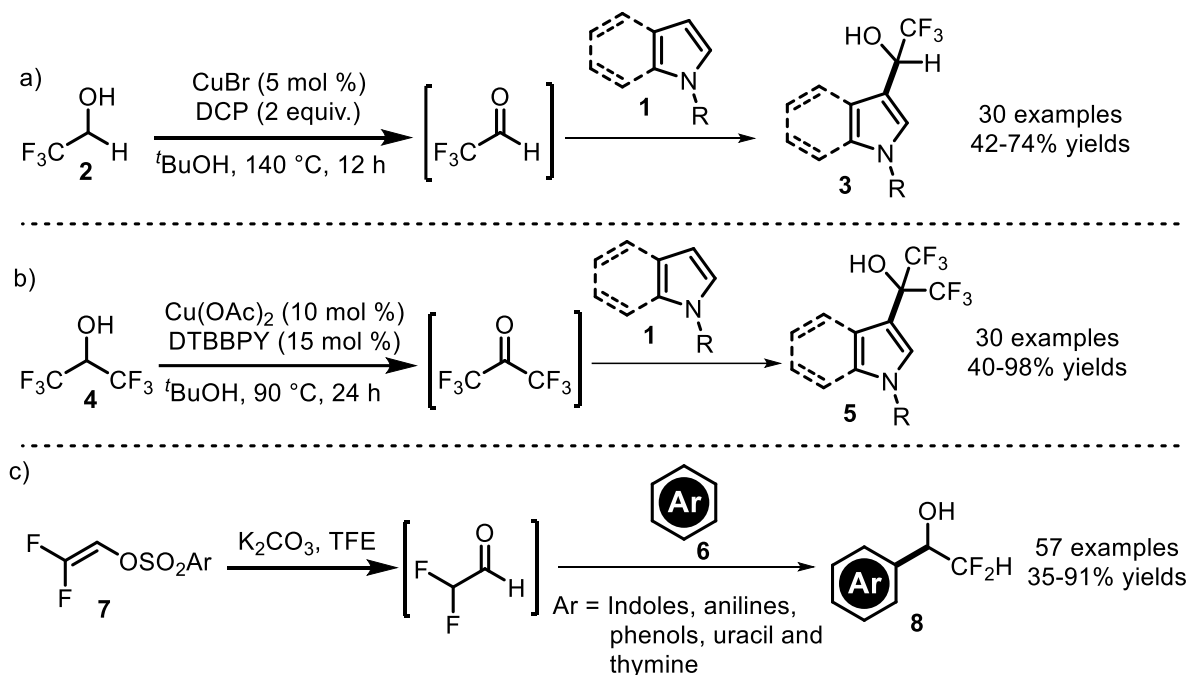


Figure 4.1 Bioactive C3-substituted indole and imidazopyridine molecules

Since, introduction of hydroxyfluoroalkyl groups at the C3-position of indole and imidazopyridine could impart distinctive properties to the molecule, in this regard synthetic chemists are increasingly focusing on the construction of such scaffolds *via* C-H bond activation. One of the key benefits of hydroxyfluoroalkylation is increasing the lipophilicity of a molecule due to the high electronegativity of the fluoroalkyl group. It is useful in drug design, as increased lipophilicity can enhance solubility and subsequently the ability of drug to cross cell membranes and reach its target site.⁸ Moreover, fluorinated alkyl groups can also enhance a molecule's stability, bioavailability, and metabolic profile.⁹⁻¹¹ The hydrogen bonding produced due to fluoro group has potential to increase the stability and efficacy of the molecule by allowing it to interact more effectively with the biological target.¹² Due to their unique electronic properties fluorinated alkyl groups can also enhance the performance of materials used in electronic devices, such as displays and solar cells.¹³ Additionally, they can increase the resistance of agricultural chemicals to environmental degradation, making them more effective in protecting crops.¹⁴⁻¹⁵ In recent years, researchers have developed various methods for achieving hydroxyfluoroalkylation on heterocycles. Friedel-Crafts alkylation with fluorocarboxyls is one of the most common and well-explored approach.

Liu *et al.* and Chen *et al.* independently achieved Cu catalyzed hydroxyfluoroalkylation of electron-rich *N*-heterocycles *via* direct C(sp²)-H/C(sp³)-H coupling with fluorinated alcohols. The former group utilized DCP/CuBr catalytic system for the coupling of pyrroles/indoles (**1**) with 2,2,2-trifluoroethanol (TFE) (**2**) to afford hydroxypolyfluoroalkylated heteroarenes (**3**) in regioselective manner (**Scheme 4.1a**).¹⁶ The latter group employed hexafluoroisopropanol (HFIP)

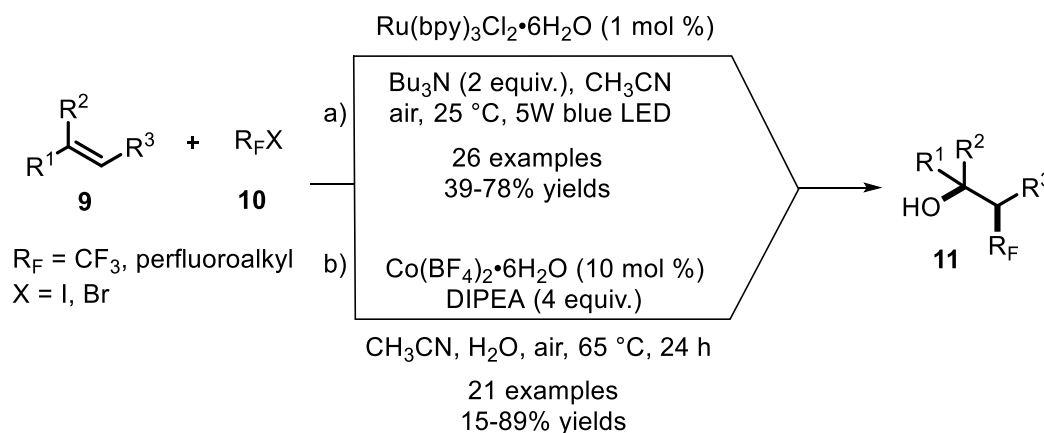
(4) as source of hydroxyfluoroalkylation with pyrroles/indoles (1) in the presence of $\text{Cu}(\text{OAc})_2$ and DTBBPY and obtained the desired product (5) in decent yields (Scheme 4.1b).¹⁷ Subsequently, Cai and co-workers reported an efficient method for the synthesis of α,α -difluoromethyl carbinols (8) utilizing electron-rich arenes (6), such as indoles, phenols, and anilines, in combination with 2,2-difluorovinyl arylsulfonates (7) in trifluoroethanol (Scheme 4.1c).¹⁸ The method is characterized by its simple protocol, readily accessible substrates, wide substrate scope, excellent functional group tolerance, and significant role of α,α -difluoromethyl carbinols as therapeutic agents. The critical role of trifluoroethanol in initiating the reaction was predicted through the control experiments. All these reactions involve a Friedel–Crafts reaction of electron-rich heteroarenes with *in situ* generated fluorocarbonyls. However, limited fluoroalcohols reduces the potency of the reaction.



Scheme 4.1 Hydroxyfluoroalkylation of electron-rich (hetero)arenes *via* Friedel–Crafts reaction

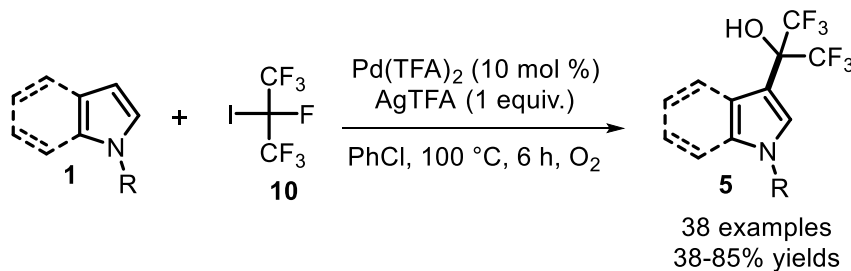
Another approach for hydroxyfluoroalkylation is through fluoroalkyl halides. Jiao group presented the synthesis of β -perfluoroalkylated alcohols (11) with unactivated alkenes (9) and commercially accessible fluoroalkyl iodides (10) in the presence of $\text{Ru}(\text{bpy})_3\text{Cl}_2 \cdot 6\text{H}_2\text{O}$ as photo catalyst under the irradiation of visible light (Scheme 4.2a).¹⁹ The methodology exhibited mild

reaction conditions, a wide substrate scope, and simple operation. According to the control experiments, the generation of fluoroalkyl radicals through the reductive quenching of photocatalytic cycle is the key step to initiate the reaction. Similarly, Sun and coworkers reported the cobalt-catalyzed hydroxyperfluoroalkylation for the synthesis of β -perfluoroalkyl alcohols (**11**) by utilizing fluoroalkyl iodides (**10**) with styrenes as well as other non-activated aliphatic olefins (**9**) (Scheme 4.2b).²⁰



Scheme 4.2 Hydroxyfluoroalkylation of non-activated alkenes with fluoroalkyl halides

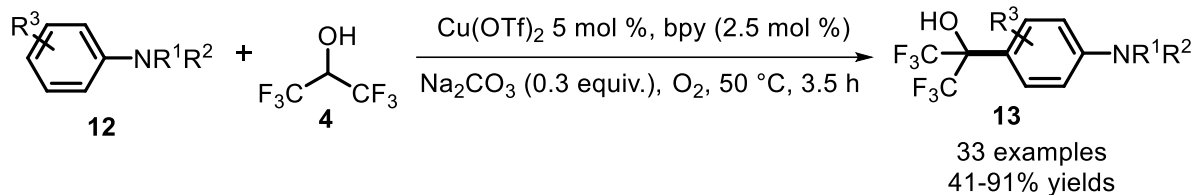
By merging C–I cleavage and C–C bond coupling, Yang and Fang collaboratively developed an efficient method for site-selective C3-hydroxyfluoroalkylation of indole/pyrrole derivatives (**5**) using heptafluoroisopropyl iodides (**10**) and free (NH)-indoles (**1**) as substrates (Scheme 4.3).²¹ The constructed molecules were obtained in average yields and later successfully modified through carbon–oxygen bond, offering excellent derivatizations. Notably, a broad range of organo-fluorine (NH)-heteroarenes derivatives, excellent functional group tolerance and use of molecular oxygen as an oxidant are some salient features of the work.



Scheme 4.3 Pd-catalyzed hydroxyfluoroalkylation of indoles

While the aforementioned methods have proven effective for hydroxyfluoroalkylation of *N*-heteroarenes, they do have their limitations in terms of atom economy, harsh reaction conditions, high costs, and waste generation. Cross-dehydrogenative coupling (CDC) reactions offer an attractive alternative in these terms. CDC reactions can be used to efficiently construct C-C and C-X bonds *via* the direct coupling of two C-H bonds, eliminating the need for external reagents or prefunctionalization steps. This approach has many advantages in organic synthetic chemistry, including improved atom economy, milder reaction conditions, and reduced waste production. In addition, CDC reactions have demonstrated remarkable functional group tolerance, allowing for the selective construction of complex molecules with high regio- and stereo selectivity. As a result, CDC reactions have emerged as a powerful tool for the preparation of structurally diverse fluorinated compounds, including those with hydroxyfluoroalkyl moieties, and have the potential to greatly impact drug discovery and material science.

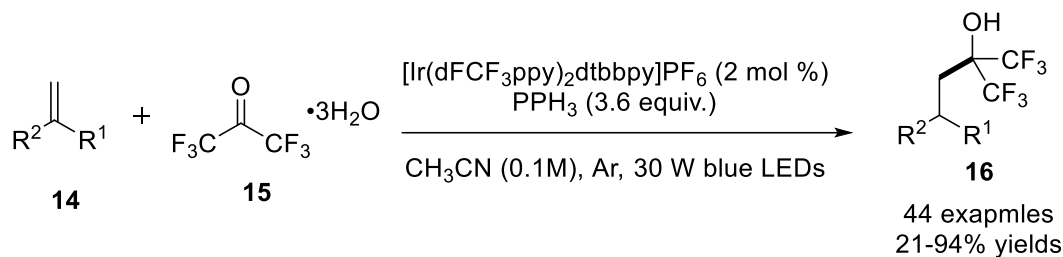
Yao group delineated an efficient copper(II)-catalyzed CDC reaction for the synthesis of fluoroalkylated arylamines (**13**) using substituted anilines (**12**) and hexafluoroisopropanol (**4**) (**Scheme 4.4**).²² Notably, the reaction followed radical pathway and single electron transfer (SET) process was believed to be the key step for initiating the reaction. In addition, tolerance to secondary, tertiary, acyclic, and cyclic anilines substituted at different positions broaden the substrate scope of the developed approach to afford the fluorinated arylamines in excellent yields.



Scheme 4.4 Cu-catalyzed hydroxytrifluoroalkylation of arylamines

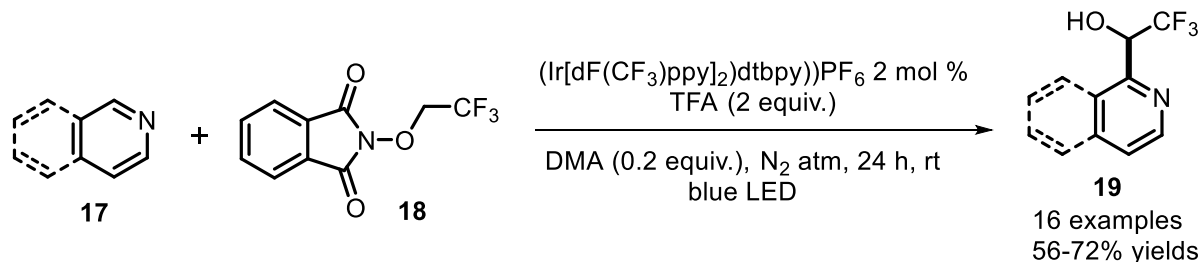
Hydroxypolyfluoroalkylation of electron-deficient alkenes (**14**) using hexafluoroacetone hydrate (**15**) *via* photoredox-catalyzed CDC reaction was reported by Xie *et al.* in 2022. By exploiting the delicate aldehyde/ketone-gem-diol equilibrium, their approach allowed the effective generation of polyfluorocarbonyl radical through phosphine-mediated deoxygenation which performed as the key step to afford bis(trifluoromethyl)carbinols (**16**) in decent yields (**Scheme 4.5**).²³ The reaction is characterized by mild conditions, excellent regioselectivity,

broad functional group tolerance, and readily available substrates, making it a valuable tool for synthesizing underdeveloped polyfluoroalkylated scaffolds.



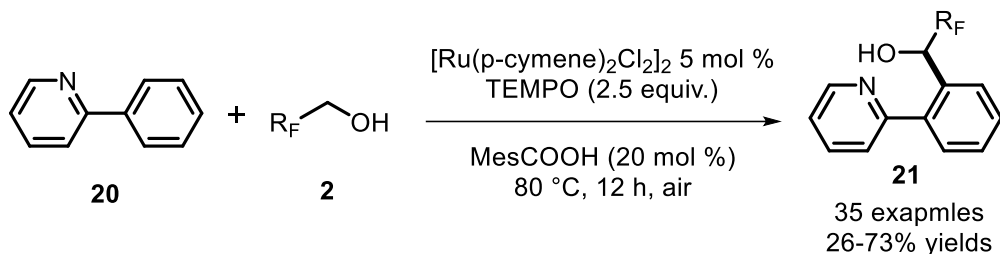
Scheme 4.5 Ir-catalyzed photochemical hydroxytrifluoroalkylation of alkenes

A facile photoredox strategy for the synthesis of hydroxypolyfluoro substituted isoquinolines (**19**) has been developed by Sharma and group. The method utilized incorporation of trifluoroethanol onto isoquinolines (**17**) by using *N*-trifluoroethoxyphthalimide (**18**) as a successful hydroxyfluoroalkyl radical precursor (**Scheme 4.6**).²⁴ Control experiments suggested a radical pathway which is also supported by DFT calculations which disclosed the formation of C-centered trifluoroethanol radical from O-centered trifluoroethoxy radical via 1,2-HAT step. Mild reaction conditions, excellent regioselectivity and good yield are the highlighting features of this work.



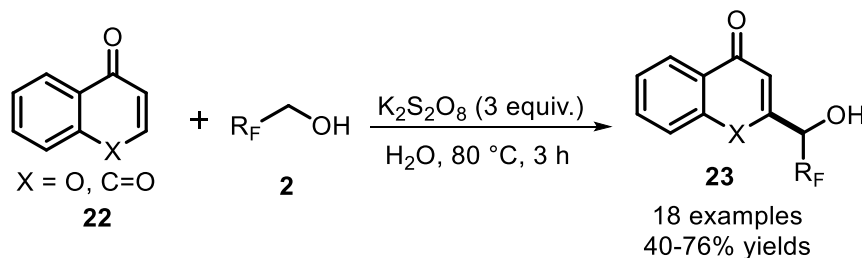
Scheme 4.6 Ir-catalyzed photoredox hydroxytrifluoroalkylation of isoquinolines

Recently, Liu and coworkers disclosed a Ru-catalyzed hydroxyfluoroalkylation of 2-aryl pyridines (**20**) with easily available fluorinated alcohols (**2**) for the synthesis of *ortho*-selective trifluorocarinols (**21**) (**Scheme 4.7**).²⁵ In this reaction TEMPO plays an important role by generating a C-centered radical of TFE which on reaction with **20** affords the corresponding products in moderate to good yields. The key feature of the reaction includes operational simplicity, atom- and step-economy, and excellent selectivity.



Scheme 4.7 Ru-catalyzed hydroxytrifluoroalkylation of 2-arylpyridines

Yu group developed a transition-metal free cross-dehydrogenative coupling for the introduction of polyfluorinated alcohols (**2**) into quinones, coumarins, and chromones (**22**). This one-step hydrogen atom transfer (HAT) method offers a straightforward and efficient approach for the synthesis of hydroxyfluoroalkylated compounds (**23**) (**Scheme 4.8**).²⁶ Control experiments supported a radical mechanism for the reaction, in which the α -OH-polyfluoroalkyl radical was proposed as the key intermediate. Additionally, using water as the solvent and with high atom-economy, this strategy presents a green and valuable option for organic synthesis.

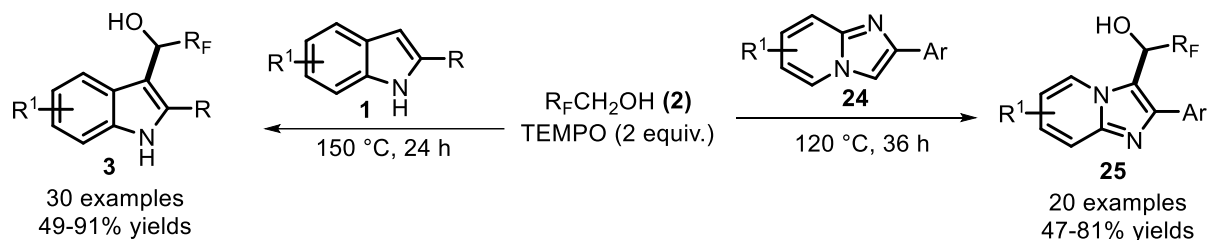


Scheme 4.8 Hydroxytrifluoroalkylation of quinones or chromones

2,2,6,6-Tetramethylpiperidinyl-1-oxyl (TEMPO) is a versatile and widely used stable organic radical in organic synthetic chemistry. It is a small organic molecule with a nitroxyl group that possesses a stable unpaired electron, which imparts its radical character. TEMPO has found extensive applications in many areas of synthetic chemistry due to its unique properties. One of the significant roles of TEMPO is as a radical scavenger in many organic reactions. In the presence of a radical initiator, TEMPO can efficiently trap the radicals generated during the reaction. This role of TEMPO helps to prevent unwanted side reactions and provides a controlled reaction environment.²⁷⁻²⁸ TEMPO-based oxidation reactions have become a popular alternative to metal-catalyzed oxidations, mainly because of their mild conditions, tolerance towards various functional groups, and the generation of non-toxic byproducts.²⁹⁻³⁰ Additionally, TEMPO has been used as a spin probe for studying the kinetics and mechanisms of radical

reactions in various systems.³¹ TEMPO has also found applications in the synthesis of polymers. It has been used as a co-monomer in the radical polymerization of various monomers, such as styrene and acrylates, to introduce controlled amounts of radicals into the polymer chain. This approach has been used to generate new functionalized polymers with unique properties.³²⁻³⁴ Overall valuable properties of TEMPO for organic chemists in designing and synthesizing new molecules and materials has been reported by numerous research groups in the form of reviews.³⁵⁻³⁷

Intrigued by the former studies on the importance of hydroxyfluoroalkylation of different heterocycles and our continuous interest in functionalization of biorelevant indoles (**1**) and imidazopyridines (**24**), we have developed a transition-metal free TEMPO-mediated cross-dehydrogenative coupling of indoles (**1**) and imidazopyridines (**24**) with polyfluorinated alcohols (**2**) for the construction of C3-hydroxyfluoroalkylated indoles (**3**) and imidazoheterocycles (**25**) (**Scheme 4.9**).



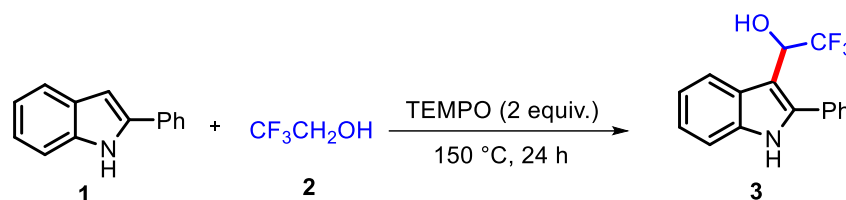
Scheme 4.9 TEMPO-mediated hydroxyfluoroalkylation of indole and 2-aryl imidazopyridine

4.7 RESULTS AND DISCUSSION

We commenced our studies for hydroxyfluoroalkylation with 2-phenylindole (**1a**) and 2,2,2-trifluoroethanol (TFE, **2a**) as the model substrates (**Table 4.1**). Initially, the reaction of **1a** (0.4 mmol) was carried out in TFE (2.0 mL) using (2,2,6,6-tetra-methylpiperidin-1-yl)oxyl (TEMPO, 3 equiv.) as the oxidant at 90 °C. We were delighted to observe formation of 3-(2,2,2-trifluoro-1-hydroxyethyl)indole (**3aa**) in 36% yield within 12 h (**Table 4.1**, entry 1). The molecular structure of **3aa** was fully characterized by NMR (¹H, **Figure 4.2**, ¹³C{¹H}, **Figure 4.3**, ¹⁹F, **Figure 4.4**) and HRMS (**Figure 4.5**). While in the absence of TEMPO, as expected formation of **3aa** was not observed (**Table 4.1**, entry 2). Other oxidants such as K₂S₂O₈, TBHP and DCP were found ineffective (**Table 4.1**, entries 3-5). Increasing the reaction time slightly improved the reaction efficiency and **3aa** was formed in 41% yield (**Table 4.1**, entry 6). Further

prolonging the reaction for 36 h did not improve the yield of **3aa** (Table 4.1, entry 7). Significant improvement in the yield of **3aa** was observed on increasing reaction temperature upto 150 °C (Table 4.1, entries 8-10). Further increase in temperature showed detrimental effect on the yield of **3aa** (Table 4.1, entry 11). On increasing amount of TEMPO to 3 equiv. at 150 °C, **3aa** was formed in 89% NMR yield (85% isolated) (Table 4.1, entry 12). Subsequent increase in the amount of TEMPO to 3.5 equiv. resulted in lower yield of **3aa** (Table 4.1, entry 13). Use of acetic acid as additive decreased the reaction time to 3 h with slightly lower yields (Table 4.1, entry 14)

Table 4.1 Optimization of reaction conditions for the synthesis of **3aa**^a



Entry	Oxidant	Temp (°C)	Time (h)	%Yield (3aa) ^{b,c}
1	TEMPO	90	12	36 (30)
2	-	90	12	0
3	K ₂ S ₂ O ₈	90	12	0
4	TBHP	90	12	0
5	DCP	90	12	0
6	TEMPO	90	24	41 (34)
7	TEMPO	90	36	40 (30)
8	TEMPO	110	24	55 (48)
9	TEMPO	130	24	60 (52)
10	TEMPO	150	24	65 (57)
11	TEMPO	160	24	50 (44)
12 ^d	TEMPO	150	24	89 (85)
13 ^e	TEMPO	150	24	85 (82)
14 ^f	TEMPO	150	3	78 (72)

^aReaction conditions: **1a** (1 equiv., 0.4 mmol), oxidant (2 equiv.), TFE (**2a**, 1.5 mL), sealed tube. ^bYield calculated based on ¹H NMR. ^cValues in parenthesis refers to isolated yield after

column chromatography. ^d3.0 equiv. of TEMPO was used. ^e3.5 equiv. of TEMPO was used.
^fReaction performed in the presence of acetic acid (2 equiv.).

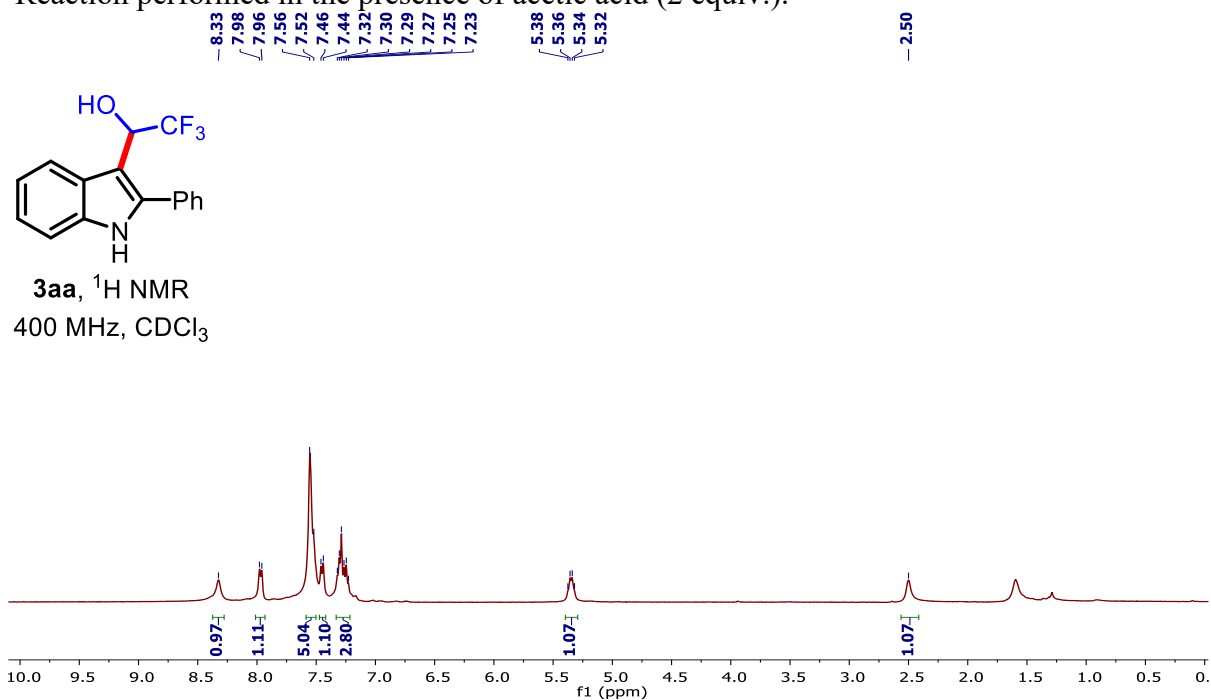


Figure 4.2 ¹H NMR of 2,2,2-trifluoro-1-(2-phenyl-1*H*-indol-3-yl)ethan-1-ol (**3aa**) recorded in CDCl₃

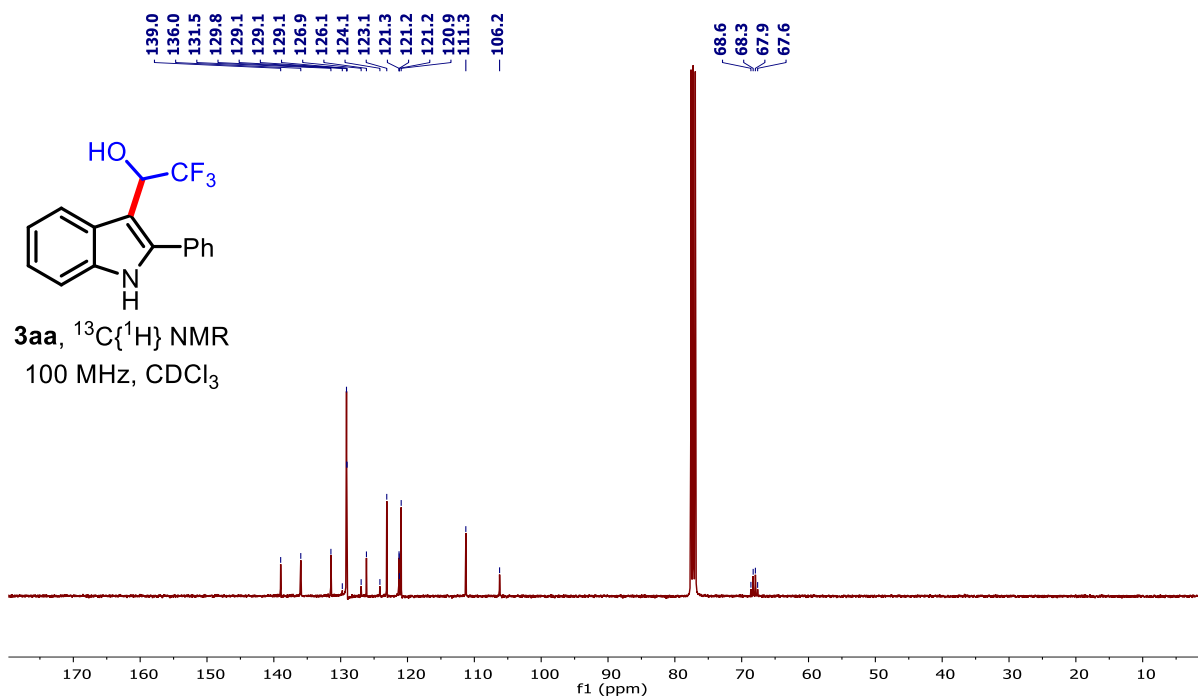


Figure 4.3 ¹³C{¹H} NMR of 2,2,2-trifluoro-1-(2-phenyl-1*H*-indol-3-yl)ethan-1-ol (**3aa**) recorded in CDCl₃

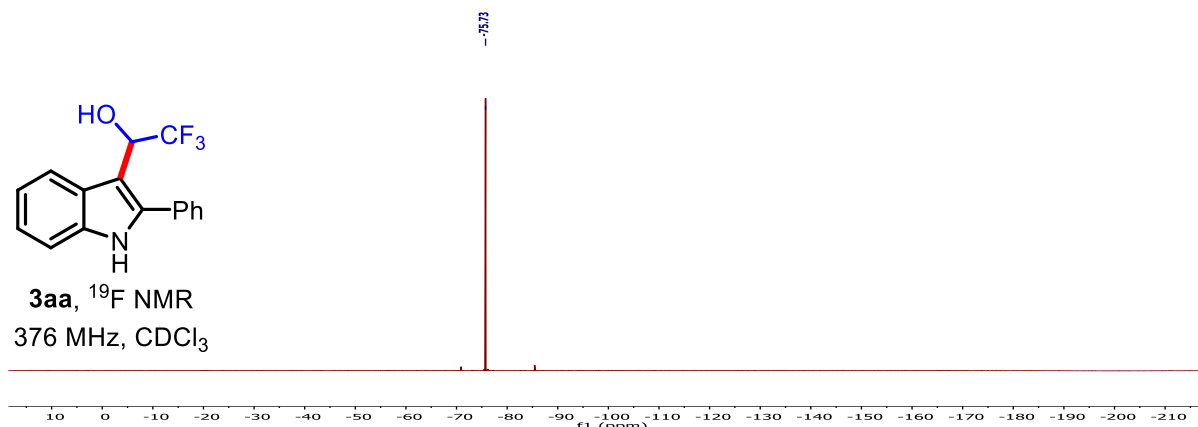


Figure 4.4 ^{19}F NMR of 2,2,2-trifluoro-1-(2-phenyl-1*H*-indol-3-yl)ethan-1-ol (**3aa**) recorded in CDCl_3

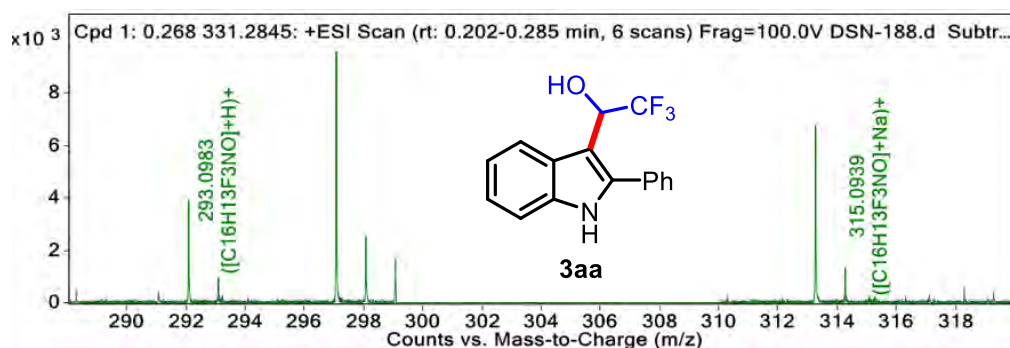


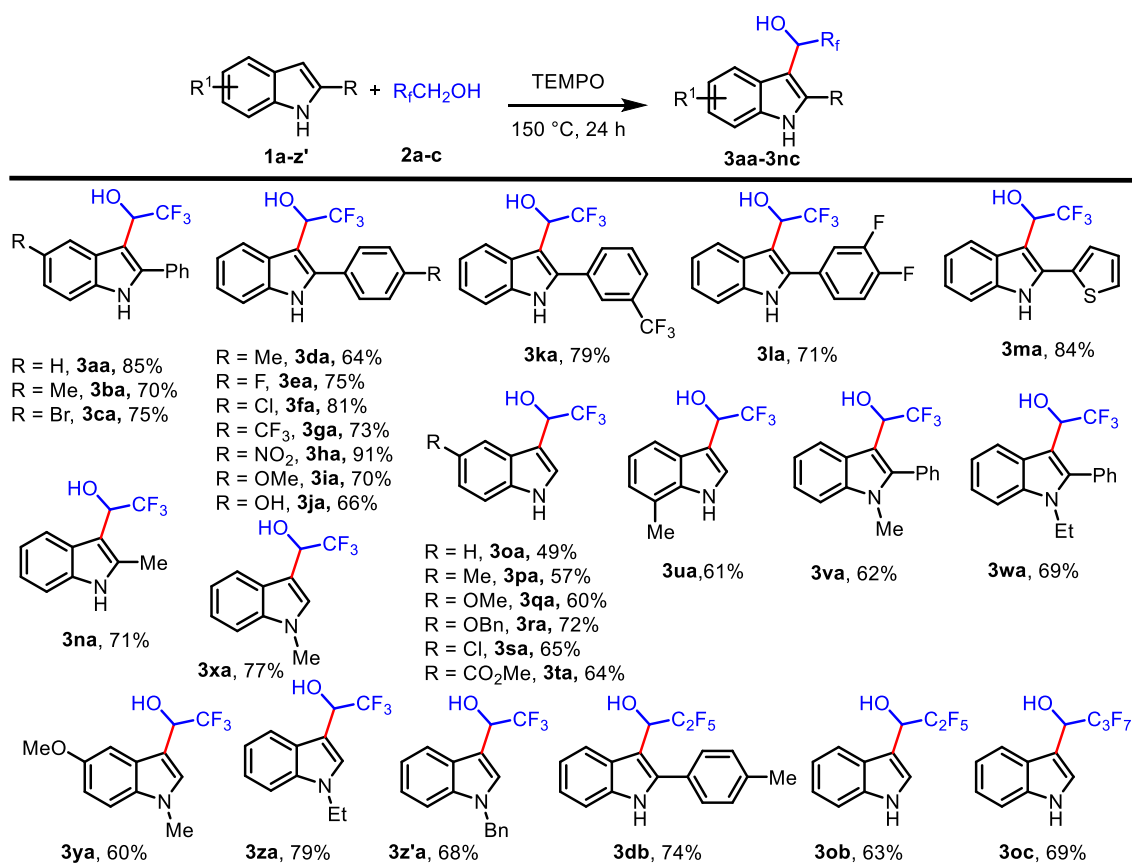
Figure 4.5 HRMS of 2,2,2-trifluoro-1-(2-phenyl-1*H*-indol-3-yl)ethan-1-ol (**3aa**)

With the optimized reaction conditions in hand, we examined the scope and limitations of this strategy against a variety of indoles (**Table 4.2**). Initially, 2-arylindoles (**1a-l**) were reacted with **2a** under standard conditions and corresponding hydroxyfluoroalkylated products **3aa-la** were obtained in good to excellent yields (64-91%). Interestingly, 2-arylindoles with electron-withdrawing groups on C2-aryl ring produced higher yield (compare **3ea-ha** vs **3ga**). 2-(Thiophen-2-yl)-1*H*-indole (**1m**) and 2-methyl-1*H*-indole (**1n**) also gave corresponding products **3ma** and **3na** in 84% and 71% yields, respectively. C2-Unsubstituted indoles (**1o-u**) bearing either electron-donating or -withdrawing groups, such as methyl, methoxy, benzyloxy, chloro and carboxylate at different positions (**1a-u**) reacted smoothly generating the corresponding 3-(2,2,2-trifluoro-1-hydroxyethyl)indoles (**3oa-3ua**) in moderate to good yields (49-72%). Captivatingly, *N*-substituted indoles with methyl, ethyl and benzyl groups (**1v-z'**) also afforded corresponding products **3va-3z'a** in good yields (60-79%). Notably, the tolerance of halogen substituents provided handles for further functionalization. The structures of the products were confirmed by

NMR (^1H , ^{19}F , and $^{13}\text{C}\{^1\text{H}\}$) and HMRS data. The structures of **3ba** (CCDC 2033964, **Figure 4.6**) and **3fa** (CCDC 2033965, **Figure 4.7**) were unambiguously confirmed by single-crystal X-ray analysis.

After evaluating the substrate scope with respect to indoles, we explored the possibility of using different alcohols under optimal conditions. 2,2,3,3,3-Pentafluoropropan-1-ol (**2b**) and 2,2,3,3,4,4,4-heptafluorobutan-1-ol (**2c**) reacted with indole (**1o**) under optimized reaction conditions and afforded the corresponding hydroxyfluoroalkylated products **3ob** and **3oc** in 63% and 69% yield, respectively. Similarly, 2-tolylindole (**1d**) on reaction with **2b** produced hydroxyfluoroalkylated products **3db** in 74% yield. Unfortunately, hydroxyalkylated product could not be isolated from the reaction of **1a** with ethanol, butanol and 2-hexafluoropropanol under these conditions.

Table 4.2. Hydroxyfluoroalkylation of indoles.^{a,b}



^aReaction conditions: **1** (1 equiv., 0.4 mmol), **2** (2.0 mL), TEMPO (3.0 equiv.), 150 °C, 24 h, sealed tube. ^bIsolated yields.

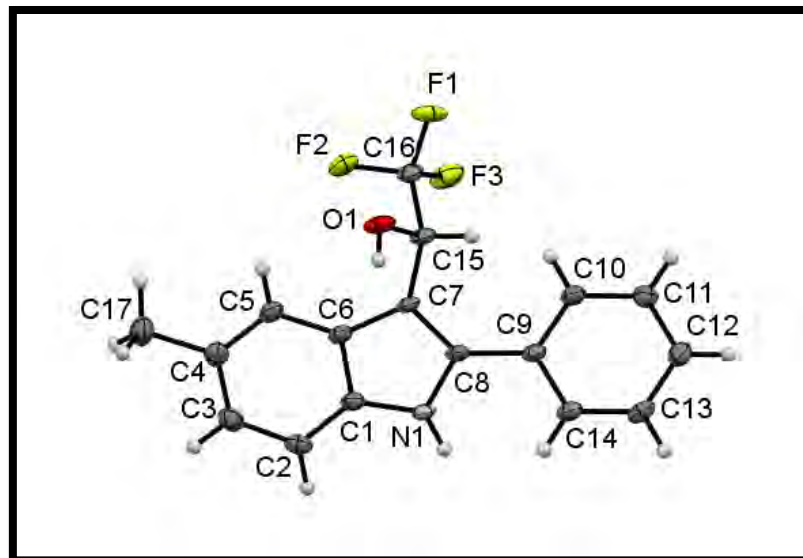


Figure 4.6 ORTEP diagram of **3ba** (CCDC No 2033964). The thermal ellipsoids are drawn at 50% probability level

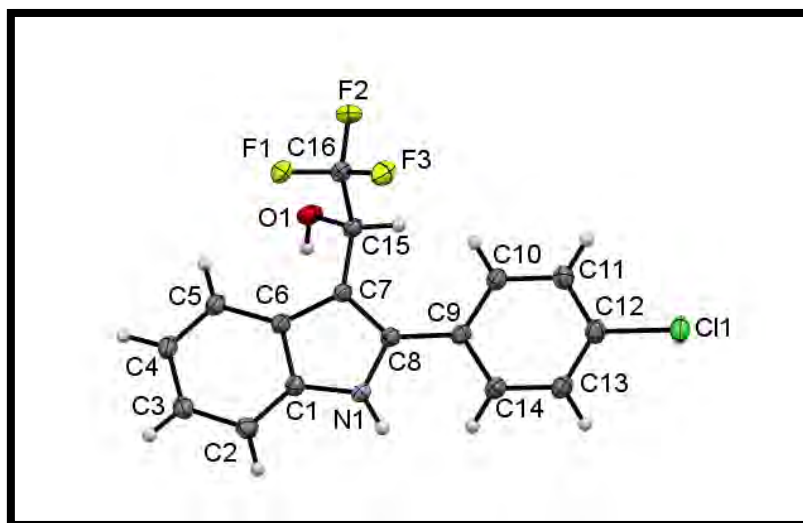


Figure 4.7 ORTEP diagram of **3fa** (CCDC No 2033965). The thermal ellipsoids are drawn at 50% probability level

To further extend the scope of this reaction, imidazo[1,2-*a*]pyridine (**24a**) was allowed to react with **2a**. A small change in the reaction conditions (increase the reaction time to 36 h and lowering reaction temperature to 120 °C) afforded 2,2,2-trifluoro-1-(2-phenylimidazo[1,2-*a*]pyridin-3-yl)ethanol **25aa** in good yield (81%). The product was confirmed by NMR (^1H **Figure 4.8**, $^{13}\text{C}\{^1\text{H}\}$ **Figure 4.9**, and ^{19}F **Figure 4.10**) and HRMS spectra (**Figure 4.11**). The structure

of **25aa** (CCDC 2033967) was unambiguously confirmed by single-crystal X-ray analysis (**Figure 4.12**).

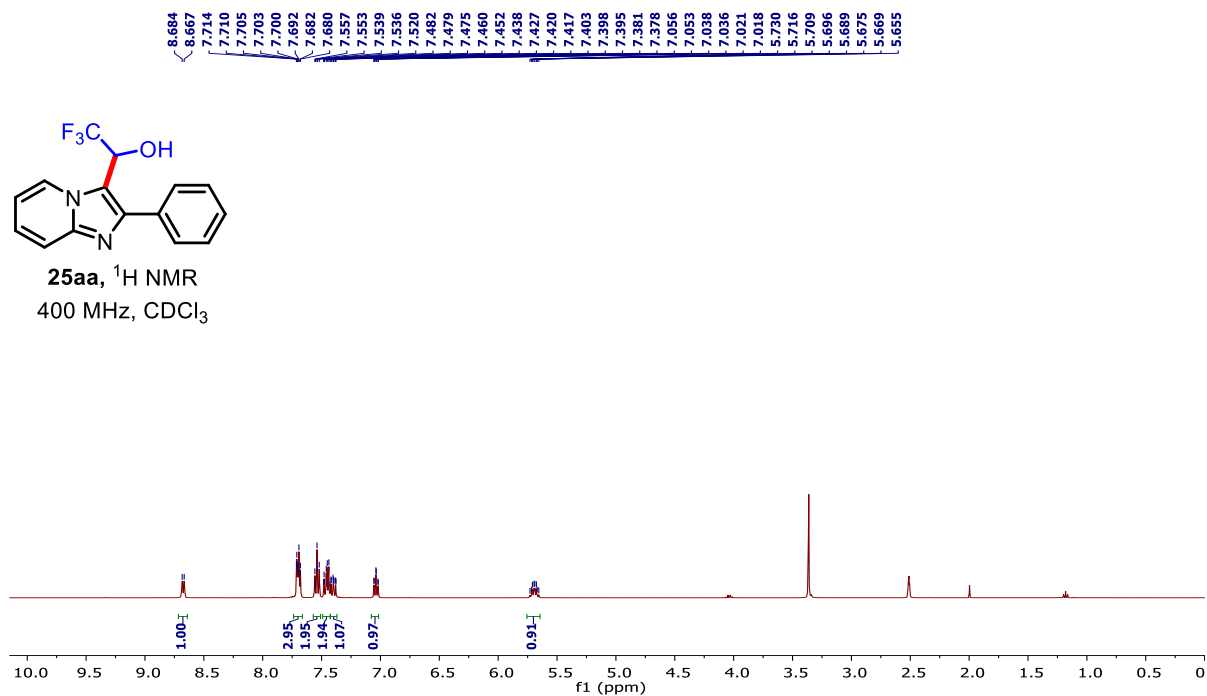


Figure 4.8 ^1H NMR spectrum of 2,2,2-trifluoro-1-(2-phenylimidazo[1,2-*a*]pyridin-3-yl)ethan-1-ol (**25aa**) recorded in $\text{DMSO-}d_6$

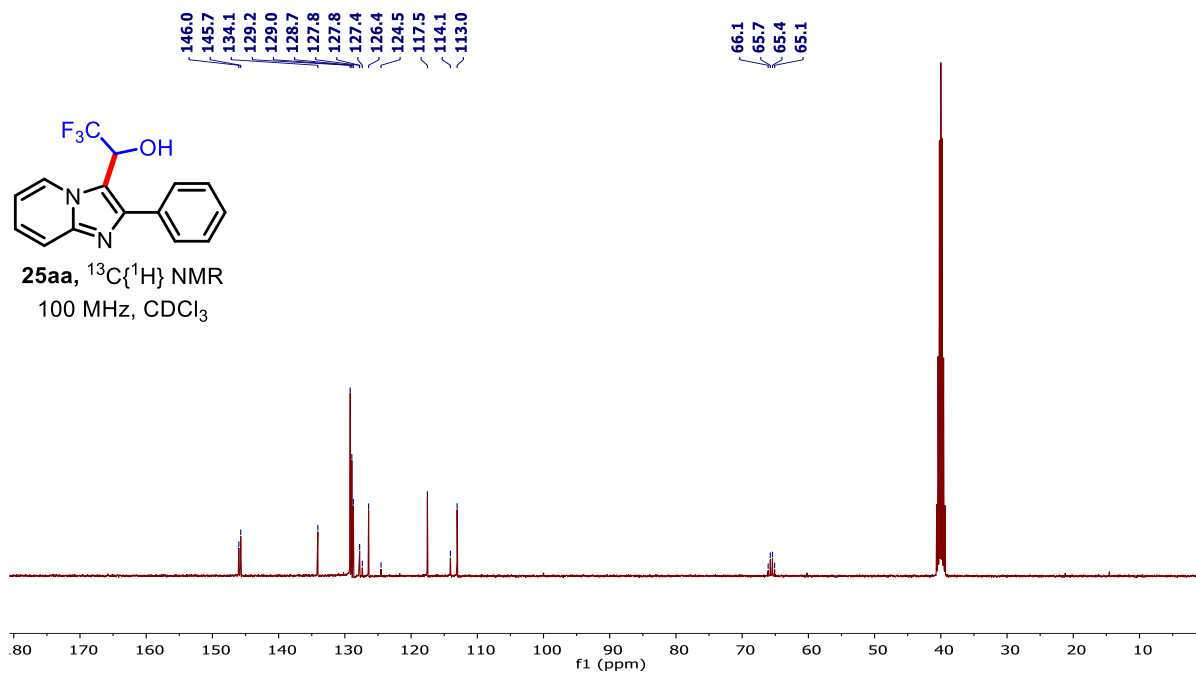


Figure 4.9 $^{13}\text{C}\{^1\text{H}\}$ NMR spectrum of 2,2,2-trifluoro-1-(2-phenylimidazo[1,2-*a*]pyridin-3-yl)ethan-1-ol (**25aa**) recorded in $\text{DMSO-}d_6$

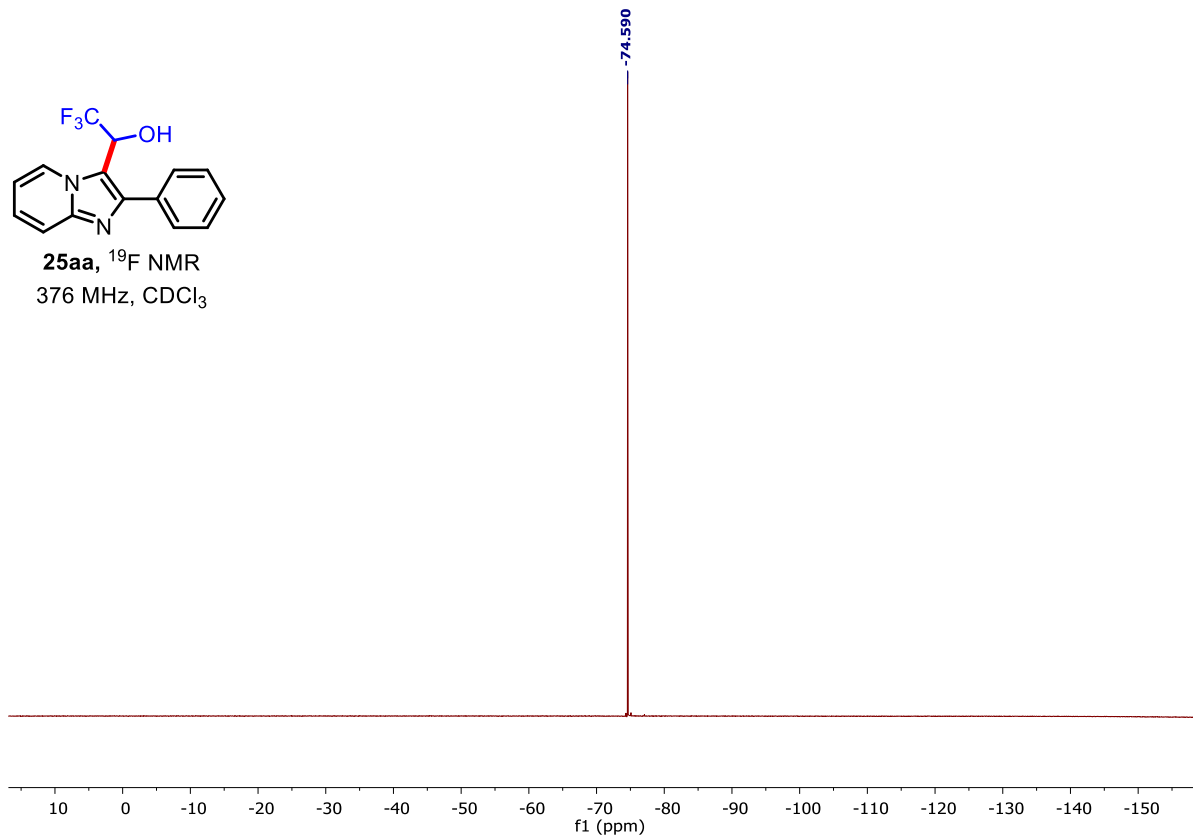


Figure 4.10 ^{19}F NMR spectrum of 2,2,2-trifluoro-1-(2-phenylimidazo[1,2-*a*]pyridin-3-yl)ethan-1-ol (**25aa**) recorded in $\text{DMSO-}d_6$

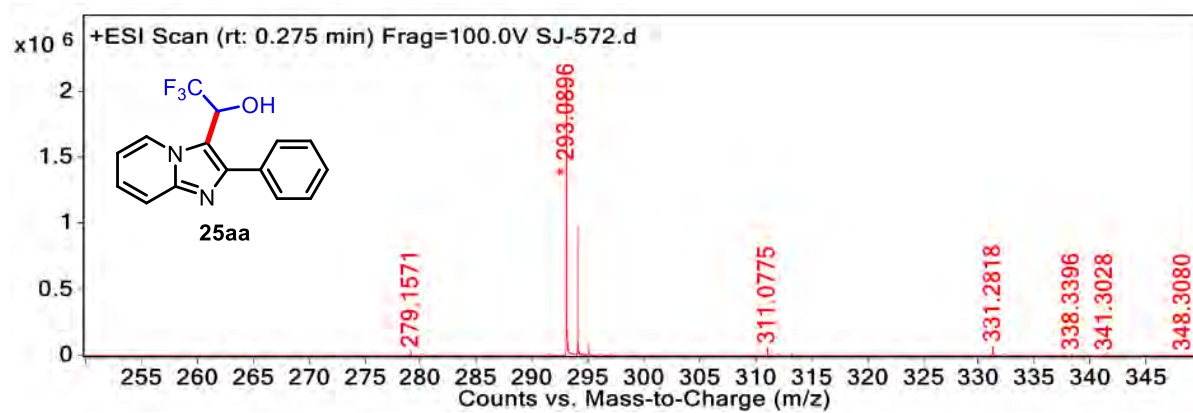


Figure 4.11 HRMS of 2,2,2-trifluoro-1-(2-phenylimidazo[1,2-*a*]pyridin-3-yl)ethan-1-ol (**25aa**)

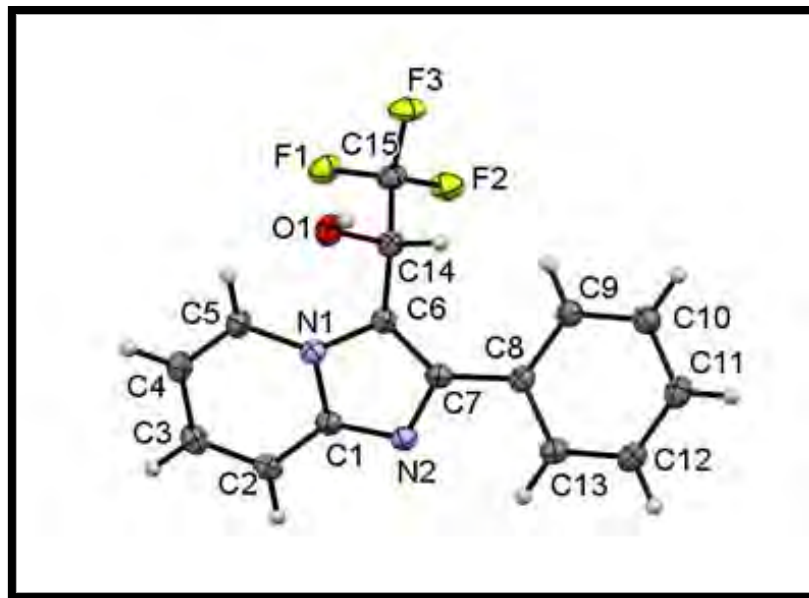
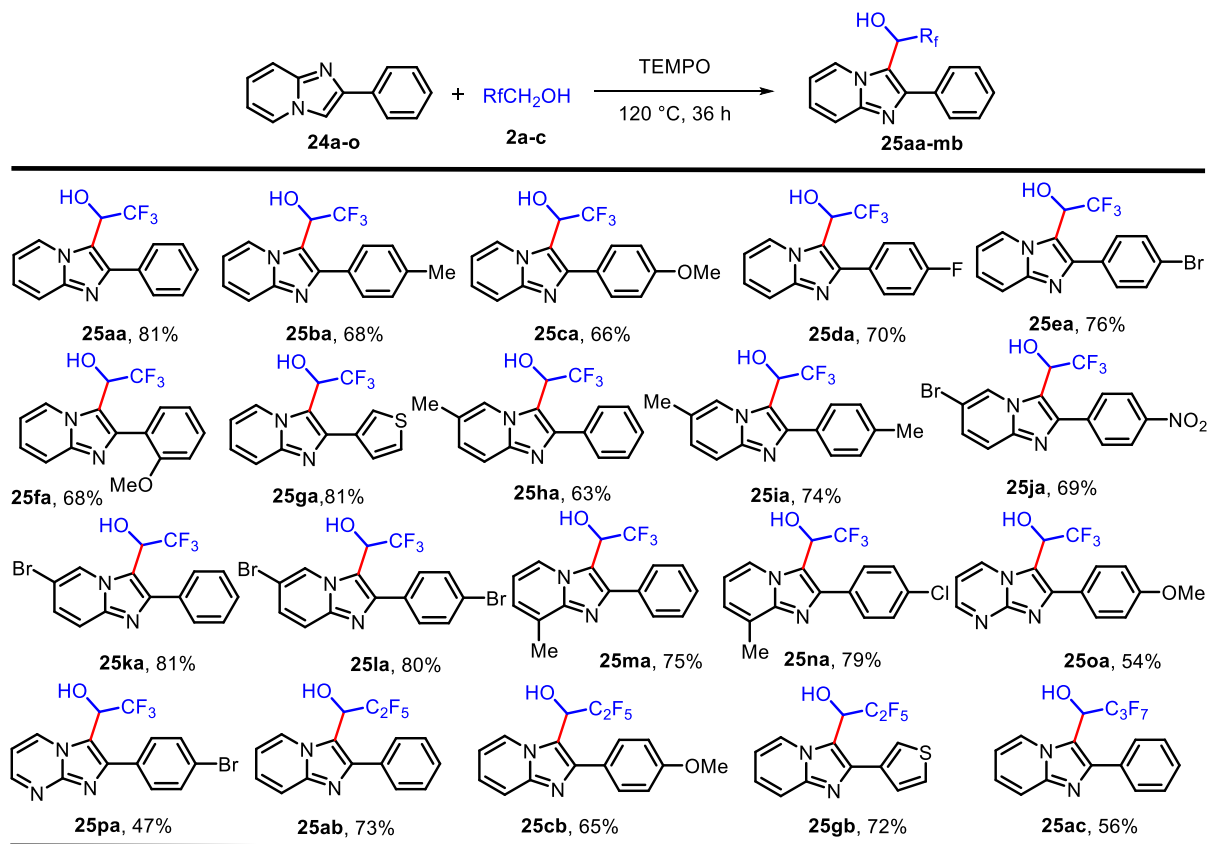


Figure 4.12 ORTEP diagram of **45aa** (CCDC No 2033967). The thermal ellipsoids are drawn at 50% probability level

We then evaluated substrate scope for imidazo[1,2-*a*]pyridines (**Table 4.3**). Reaction of imidazo[1,2-*a*]pyridines having electron-donating as well as electron-withdrawing substituents on the C2-phenyl ring and imidazo[1,2-*a*]pyridine nucleus (**24b-p**) with **2a** afforded the corresponding 2,2,2-trifluoro-1-hydroxyethyl derivatives **25ba-pa** in moderate to good yields (63-81%). 2-(Thiophen-3-yl)imidazo[1,2-*a*]pyridine (**24g**) also successfully afforded the desired product **25ga** in 81% yield. Reaction of imidazo[1,2-*a*]pyrimidines (**24o** and **24p**) with **2a** provided the corresponding 2,2,2-trifluoro-1-hydroxyethyl derivatives **25oa** and **25pa** in 54% and 47%, respectively. Interestingly, reaction of **24a**, **24c** and **24g** with **2b** afforded the corresponding products **25ab**, **25cb** and **25gb** in good yields 73%, 65% and 72% yield respectively. Reaction of **24a** with **2c** also gave the corresponding 2,2,2-trifluoro-1-hydroxyethyl derivative **25ac** in 56% yield. The NMR (^1H , ^{19}F , and $^{13}\text{C}\{^1\text{H}\}$) and HRMS data of **25** were in good agreement with the structures, and the structure **25ba** (CCDC 2033968, **Figure 4.13**) were unambiguously confirmed by single-crystal X-ray analysis.

Table 4.3 Hydroxyfluoroalkylation of imidazo[1,2-*a*]pyridines.^{a,b}

^aReaction conditions: **24** (1 equiv., 0.5 mmol), **2** (2.0 mL), TEMPO (3.0 equiv.), 120 °C, 36 h, sealed tube. ^bIsolated yields.

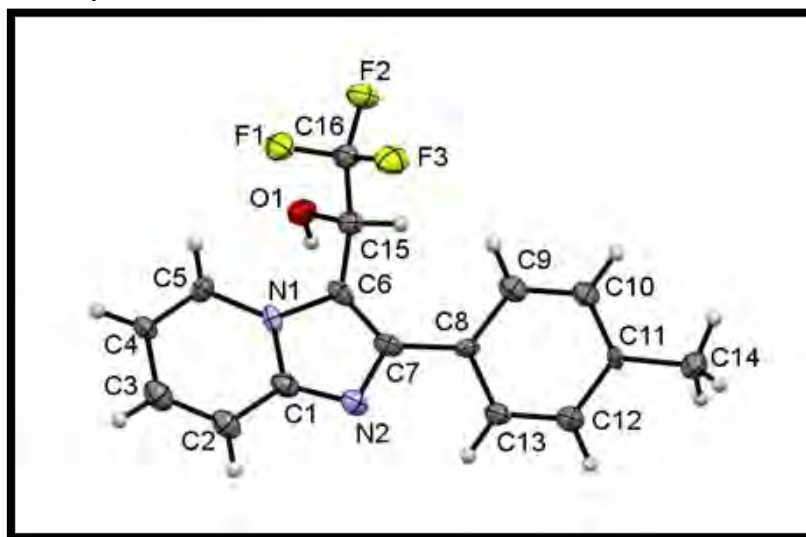
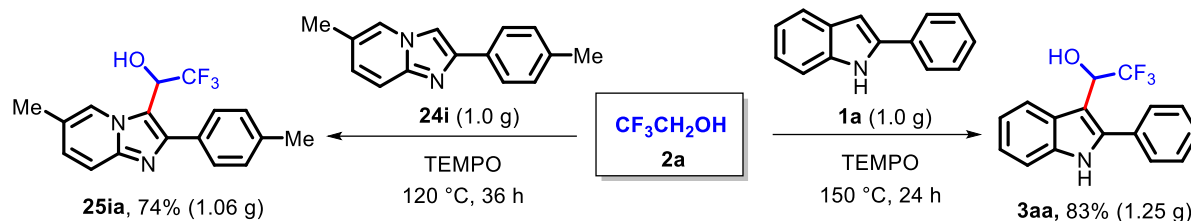


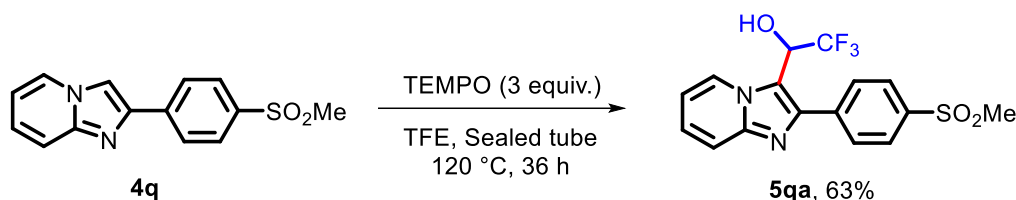
Figure 4.13 ORTEP diagram of **45ba** (CCDC No 2033968). The thermal ellipsoids are drawn at 50% probability level

The robustness of this CDC reaction was demonstrated by generating gram quantities of **3aa** and **25ia**. The gram-scale reaction of **1a** and **24i** with **2a** produced corresponding products **3aa** and **25ia** in 83% (1.25 g) and 74% (1.06 g) yield, respectively (**Scheme 4.10**).



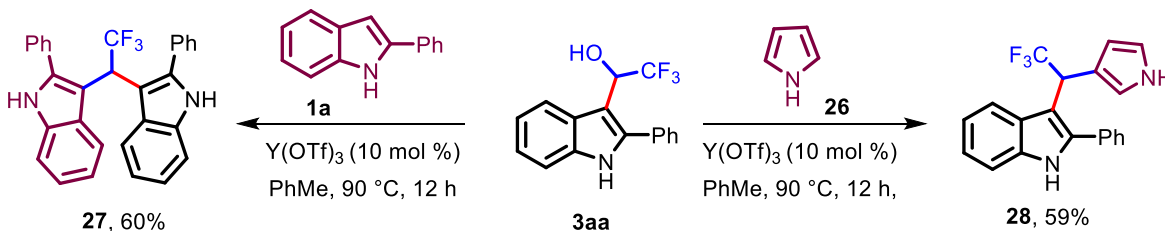
Scheme 4.10 Gram scale synthesis of **3aa** and **25ia**

To demonstrate synthetic utility of the developed protocol, late-stage functionalization of Zolimidine (**24q**), a gastroprotective drug was performed. Delightfully, reaction of **24q** with TFE under standard conditions produced the hydroxyfluoroalkylated product **25qa** in 63% yield (**Scheme 4.11**).



Scheme 4.11 Late-stage functionalization of Zolimidine

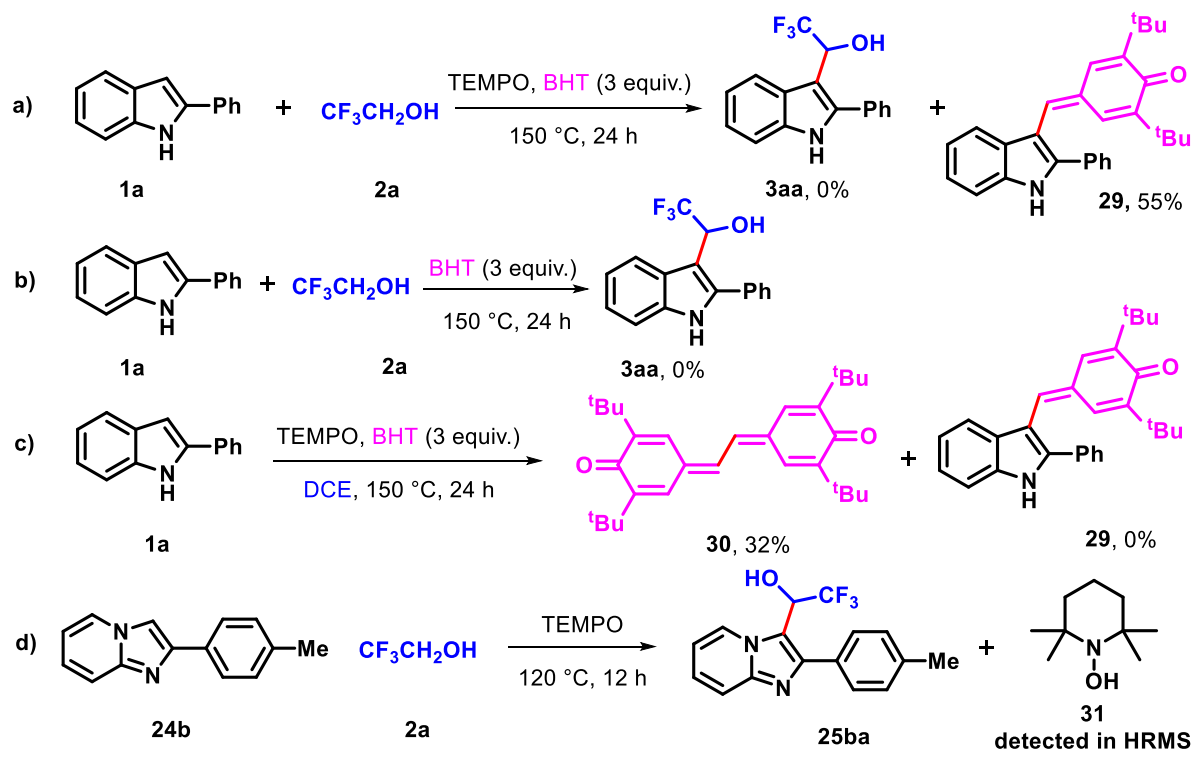
Furthermore, the synthetic application of hydroxyfluoroalkylated products was demonstrated by converting **3aa** to trifluorinated 3-indolyl(heteroaryl)methanols via Yb(OTf)₃ catalyzed Friedel-Crafts reaction (**Scheme 4.12**). Reaction of **3aa** with **1a** and pyrrole (**26**) in the presence of Yb(OTf)₃ (10 mol%) in toluene at 90 °C for 12 h gave 3,3'-(2,2,2-trifluoroethane-1,1-diyl)bis(2-phenyl-1*H*-indole) (**27**) and 2-phenyl-3-(2,2,2-trifluoro-1-(1*H*-pyrrol-3-yl)ethyl)-1*H*-indole (**28**) in 60 and 59% yield, respectively.



Scheme 4.12 Yb(OTf)₃ catalyzed Friedel-Crafts reaction of **3aa**

Some control experiments were performed to gain insights into the reaction mechanism of this CDC reaction (**Scheme 4.13**). First, the effect of radical scavenger was studied by performing

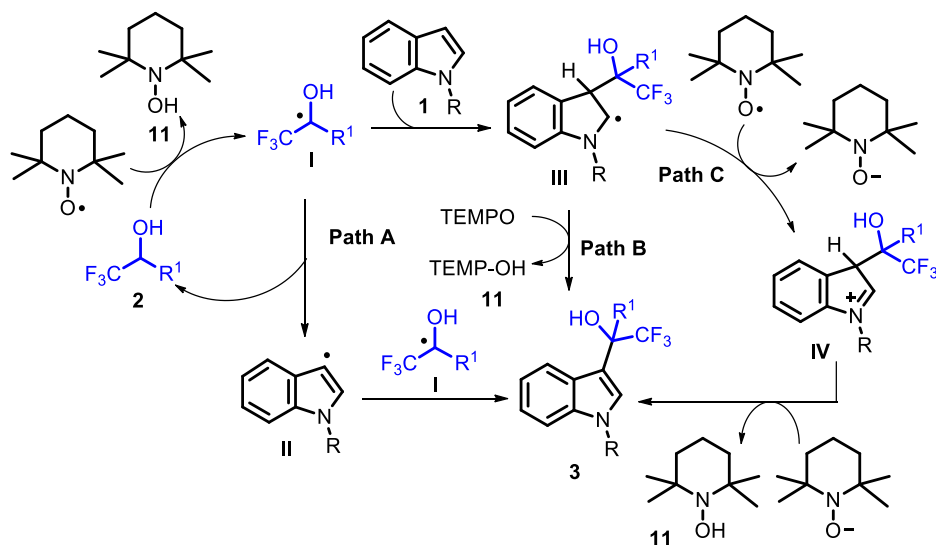
the reaction of **1a** with **2a** in the presence of butylated hydroxytoluene (BHT) (**Scheme 4.13a**). Formation of **3aa** was completely suppressed with concomitant formation of BHT-indole adduct **29** resulting from substitution of a benzylic C–H bond³⁸ indicating that the reaction involves radical pathway which is contrary to the ionic mechanism reported by Jiang group.¹⁷ No product formation was observed from the reaction of **1a** and **2a** in the presence of BHT and absence of TEMPO (**Scheme 4.13b**) indicating crucial role of TEMPO in initiating the reaction. Further, reaction of **1a** in the presence of TEMPO and BHT resulted in the formation of 4,4'-(ethane-1,2-diylidene)bis(2,6-di-tert-butylcyclohexa-2,5-dienone) (**30**) in 32% yield and adduct **29** was not observed under these conditions (**Scheme 4.13c**). A peak at m/z 158.1523 corresponding to TEMP-OH (**31**) was observed along with peaks for **24b** and **25ba** in the HRMS analysis of the reaction mixture of reaction between **24b** and **2a** after 12 h under standard conditions (**Scheme 4.13d**).



Scheme 4.13 Control experiments

Based on the experimental results and literature reports,^{16, 39-40} a plausible mechanism of the developed CDC reaction is proposed in **Scheme 4.14**. First, α -hydrogen atom abstraction by TEMPO generated C-centred radical **I**, which abstracted C3-hydrogen from indole to generate

indole radical (**II**). Recombination of radical **I** and **II** produced product **3**. In another pathway radical **I** on addition to indole (**1**) produced radical intermediate **III**. Next, intermediate **III** either underwent hydrogen atom abstraction by TEMPO to produce product **3** (Path B) or produced iminium ion **IV** by single electron transfer (SET) process (Path C). In path C, elimination of proton from intermediate **IV** produced product **3**. Based on control experiment path A seems to be more probable however, path B and path C can't be ruled out.



Scheme 4.14 Plausible mechanism for TEMPO-mediated hydroxyfluoroalkylation

4.8 CONCLUSIONS

In summary, TEMPO-mediated cross-dehydrogenative coupling of C(sp³-H) bond and C(sp²-H) bond has been developed for direct hydroxyfluoroalkylation of indoles and imidazo[1,2-*a*]pyridines by fluorinated alcohols under metal-free reaction conditions. The developed synthetic protocol is operationally simple and provides a wide range of C3-hydroxyfluoroalkylated indoles and imidazo[1,2-*a*]pyridines in good to excellent yields. Broad substrate scope and high functional group tolerance are the silent features of the developed method. The synthetic utility of the protocol was showcased through gram-scale synthesis of **3aa** and **25ia**. Moreover, 2,2,2-trifluoro-1-(2-phenyl-1*H*-indol-3-yl)ethanol could be elegantly transformed to 3,3'-(2,2,2-trifluoroethane-1,1-diyl)bis(2-phenyl-1*H*-indole) and 2-phenyl-3-(2,2,2-trifluoro-1-(1*H*-pyrrol-3-yl)ethyl)-1*H*-indole. Mechanistic investigation revealed that the reaction involves radical process.

4.9 EXPERIMENTAL SECTION

4.9.1 General Information

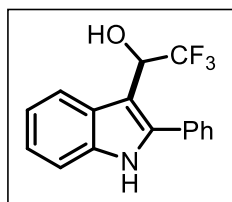
All chemicals and solvents were purchased from commercial suppliers and used without purification, unless otherwise mentioned. 2-Arylindoles⁴¹⁻⁴² and imidazo[1,2-*a*]pyridines⁴³ were synthesized by following the reported procedure. All reactions were monitored by thin layer chromatography (TLC) on pre-coated silica gel 60 F254 aluminium foils and visualised under a UV lamp (366 or 254 nm). Desired products were purified by column chromatography (Silica gel 100-200 mesh size) using a gradient of ethyl acetate and hexane as mobile phase. The ¹H, ¹³C and ¹⁹F NMR spectra were recorded on a 400 MHz spectrometer. Chemical shifts (δ) are reported in parts per million (ppm) and coupling constants (J) are reported in hertz (Hz). High-resolution mass spectra (HRMS) were recorded on a Q-TOF mass spectrometer.

4.9.2 General Procedure for the C3-Fluoroalkylation of Indoles

An oven dried sealed tube charged with compound **1** (0.5 mmol; 1.0 equiv.) in **2** (2 mL) followed by TEMPO (3.0 equiv.) was added at room temperature and the reaction mixture was stirred at 150 °C for 24 h. After completion of the reaction monitored by TLC, then reaction mixture was allowed to attain room temperature. The reaction mixture was poured into water (20 mL) and extracted with ethyl acetate (3 × 15 mL). The combined organic layer was dried over anhydrous Na₂SO₄ and evaporated under vacuum. The resulting crude was purified by column chromatography (silica gel 100-200 mesh) using EtOAc:hexanes as an eluent to afford **3**.

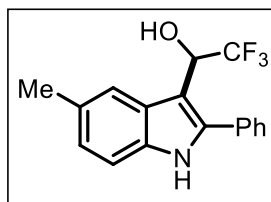
4.9.3 Analytical Data of Synthesized Products

2,2,2-Trifluoro-1-(2-phenyl-1H-indol-3-yl)ethan-1-ol (3aa): White solid; 98.9 mg, 85% yield;



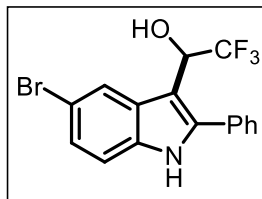
$R_f = 0.7$, Eluent system: EtOAc:hexanes (1.5:8.5); mp = 134-136 °C; ¹H NMR (400 MHz, CDCl₃) δ = 8.32 (s, 1H), 7.97 (d, $J = 8.0$ Hz, 1H), 7.56 – 7.52 (m, 5H), 7.45 (d, $J = 8.0$ Hz, 1H), 7.32 – 7.23 (m, 2H) (with merged CDCl₃ peak), 5.35 (q, $J = 7.3$ Hz, 1H), 2.50 (s, 1H); ¹³C{¹H} (100 MHz, CDCl₃) δ = 138.9, 135.9, 131.4, 129.1, 129.1, 129.0, 126.1, 125.4 (C-F, ¹J_{C-F} = 280.7 Hz), 123.1, 121.2 (C-F, ⁴J_{C-F} = 3.2 Hz), 120.9, 111.1, 106.1, 68.0 (C-F, ²J_{C-F} = 33.3 Hz); ¹⁹F NMR (376 MHz, CDCl₃) δ -75.73 (s, 3F) ppm; HRMS (ESI) m/z : [M + H]⁺ calcd for C₁₆H₁₃F₃NO⁺ 292.0944, found 292.0941.

2,2,2-Trifluoro-1-(5-methyl-2-phenyl-1H-indol-3-yl)ethan-1-ol (3ba): White solid; 112 mg,



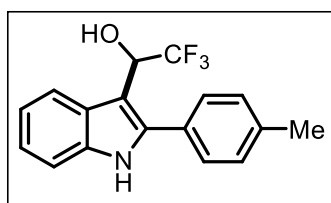
70% yield; $R_f=0.7$, Eluent system: EtOAc:hexanes (1.5:8.5); mp = 146-148 °C; $^1\text{H NMR}$ (400 MHz, CDCl_3) δ = 8.24 (s, 1H), 7.75 (s, 1H), 7.53 – 7.49 (m, 5H), 7.31 (d, J = 8.0 Hz, 1H), 7.13 (d, J = 8.0 Hz, 1H), 5.32 (q, J = 7.3 Hz, 1H), 2.56 (s, 1H), 2.52 (s, 3H); $^{13}\text{C}\{^1\text{H}\}$ (100 MHz, CDCl_3) δ = 139.0, 134.3, 131.6, 130.3, 129.0, 129.0, 128.9, 126.3, 125.5 (C-F, $^1J_{\text{C-F}}$ = 280.9 Hz), 124.7, 120.7 (C-F, $^4J_{\text{C-F}}$ = 2.6 Hz), 110.8, 105.6, 68.1 (C-F, $^2J_{\text{C-F}}$ = 33.3 Hz), 21.6; $^{19}\text{F NMR}$ (376 MHz, CDCl_3) δ = -75.62 (s, 3F) ppm; HRMS (ESI) m/z : $[\text{M} + \text{H}]^+$ calcd for $\text{C}_{17}\text{H}_{15}\text{F}_3\text{NO}^+$ 306.1100, found 306.1087.

1-(5-Bromo-2-phenyl-1H-indol-3-yl)-2,2,2-trifluoroethan-1-ol (3ca): White solid; 148 mg,



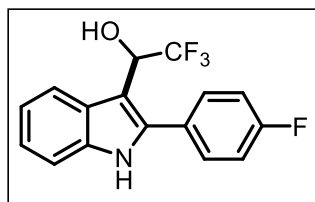
75% yield; $R_f=0.7$, Eluent system: EtOAc:hexanes (1.5:8.5); mp = 158-160 °C; $^1\text{H NMR}$ (400 MHz, CDCl_3) δ = 8.37 (s, 1H), 8.10 (s, 1H), 7.53 (s, 5H), 7.37 (dd, J = 8.8, 1.6 Hz, 1H), 7.29 – 7.27 (m, 1H) (with merged CDCl_3 peak), 5.30 (q, J = 6.4 Hz, 1H), 2.56 (s, 1H); $^{13}\text{C}\{^1\text{H}\}$ (100 MHz, CDCl_3) δ = 139.9, 134.5, 130.9, 129.4, 129.2, 128.9, 127.9, 126.7, 126.0, 123.9 (C-F, $^4J_{\text{C-F}}$ = 2.9 Hz), 114.2, 112.5, 105.8, 67.8 (C-F, $^2J_{\text{C-F}}$ = 33.4 Hz); $^{19}\text{F NMR}$ (376 MHz, CDCl_3) δ -75.87 (s, 3F) ppm; HRMS (ESI) m/z : $[\text{M} + \text{H}]^+$ calcd for $\text{C}_{16}\text{H}_{12}\text{BrF}_3\text{NO}^+$ 370.0049, found 370.0045.

2,2,2-Trifluoro-1-(2-(p-tolyl)-1H-indol-3-yl)ethan-1-ol (3da): White solid; 122 mg, 64% yield;



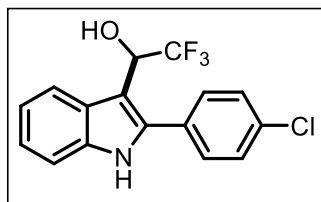
$R_f=0.7$, Eluent system: EtOAc:hexanes (1.5:8.5); mp = 138-140 °C; $^1\text{H NMR}$ (400 MHz, CDCl_3) δ = 8.28 (s, 1H), 7.95 (d, J = 7.2 Hz, 1H), 7.43 (s, 3H), 7.34 (d, J = 6.8 Hz, 2H), 7.31 – 7.27 (m, 1H), 7.25 – 7.23 (m, 1H), 5.34 (q, J = 7.6 Hz, 1H), 2.47 (s, 4H); $^{13}\text{C}\{^1\text{H}\}$ (100 MHz, CDCl_3) δ = 139.2, 139.1, 135.8, 129.8, 128.8, 128.5, 126.1, 125.5 (C-F, $^1J_{\text{C-F}}$ = 281.1 Hz), 122.9, 121.0 (C-F, $^4J_{\text{C-F}}$ = 3.1 Hz), 120.8, 111.0, 105.9, 68.1 (C-F, $^2J_{\text{C-F}}$ = 33.4 Hz), 21.3; $^{19}\text{F NMR}$ (376 MHz, CDCl_3) δ -75.72 (s, 3F) ppm; HRMS (ESI) m/z : $[\text{M} + \text{H}]^+$ calcd for $\text{C}_{17}\text{H}_{15}\text{F}_3\text{NO}^+$ 306.1100, found 306.1094.

2,2,2-Trifluoro-1-(2-(4-fluorophenyl)-1H-indol-3-yl)ethan-1-ol (3ea): White solid; 123.6 mg,



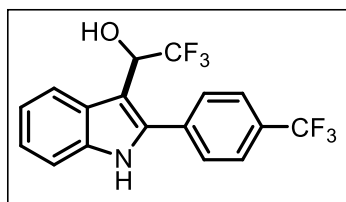
75% yield; $R_f=0.7$, Eluent system: EtOAc:hexanes (1.5:8.5); mp = 142-144 °C; $^1\text{H NMR}$ (400 MHz, CDCl_3) δ 8.31 (s, 1H), 7.95 (d, $J = 8.0$ Hz, 1H), 7.54 – 7.50 (m, 2H), 7.43 (d, $J = 8.0$ Hz, 1H), 7.32 – 7.28 (m, 1H), 7.26 – 7.21 (m, 3H), 5.27 (q, $J = 7.3$ Hz, 1H), 2.58 (s, 1H); $^{13}\text{C}\{^1\text{H}\}$ (100 MHz, CDCl_3) δ 164.4, 162.0, 137.8, 135.9, 130.9, 130.8, 127.5 (C-F, $^4J_{\text{C-F}} = 3.4$ Hz), 126.0, 125.4 (C-F, $^1J_{\text{C-F}} = 280.9$ Hz), 123.2, 121.2 (C-F, $^4J_{\text{C-F}} = 2.7$ Hz), 121.0, 116.3, 116.0, 111.1, 106.3, 68.0 (C-F, $^2J_{\text{C-F}} = 33.2$ Hz); $^{19}\text{F NMR}$ (376 MHz, CDCl_3) δ -75.83 (s, 3F), -111.62 (s, 1F) ppm; HRMS (ESI) m/z : $[\text{M} + \text{H}]^+$ calcd for $\text{C}_{16}\text{H}_{12}\text{F}_4\text{NO}^+$ 310.0850, found 310.0852.

1-(2-(4-Chlorophenyl)-1H-indol-3-yl)-2,2,2-trifluoroethan-1-ol (3fa): White solid; 105.3 mg,



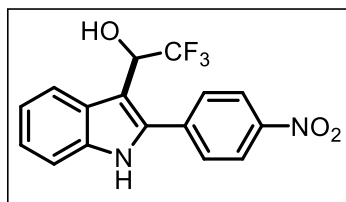
81% yield; $R_f=0.5$, Eluent system: EtOAc:hexanes (2.0:8.0); mp = 132-134 °C; $^1\text{H NMR}$ (400 MHz, CDCl_3) δ = 8.32 (s, 1H), 7.95 (d, $J = 8.0$ Hz, 1H), 7.52 – 7.47 (m, 4H), 7.43 (d, $J = 8.0$ Hz, 1H), 7.32 – 7.29 (m, 1H), 7.26 – 7.22 (m, 1H), 5.28 (q, $J = 7.6$ Hz, 1H), 2.59 (s, 1H); $^{13}\text{C}\{^1\text{H}\}$ (100 MHz, CDCl_3) δ = 137.5, 136.0, 135.3, 130.2, 129.9, 129.3, 126.0, 125.3 (C-F, $^1J_{\text{C-F}} = 280.9$ Hz), 123.4, 121.2 (C-F, $^4J_{\text{C-F}} = 2.6$ Hz), 121.1, 111.2, 106.5, 68.0 (C-F, $^2J_{\text{C-F}} = 33.5$ Hz); $^{19}\text{F NMR}$ (376 MHz, CDCl_3) δ = -75.80 (s, 3F) ppm; HRMS (ESI) m/z : $[\text{M} + \text{H}]^+$ calcd for $\text{C}_{16}\text{H}_{12}\text{ClF}_3\text{NO}^+$ 326.0554, found 326.0550.

2,2,2-Trifluoro-1-(2-(4-(trifluoromethyl)phenyl)-1H-indol-3-yl)ethan-1-ol (3ga): White solid;



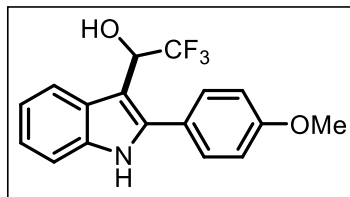
104.8 mg, 73% yield; $R_f = 0.3$, Eluent system: EtOAc:hexanes (1.5:8.5); mp = 136-138 °C; $^1\text{H NMR}$ (400 MHz, CDCl_3) δ = 8.36 (s, 1H), 7.98 (d, $J = 8.0$ Hz, 1H), 7.80 (d, $J = 7.6$ Hz, 2H), 7.68 (d, $J = 7.6$ Hz, 2H), 7.46 (d, $J = 8.0$ Hz, 1H), 7.33 (t, $J = 7.4$ Hz, 1H), 7.28 – 7.24 (m, 1H) (with merged CDCl_3 peak), 5.31 (q, $J = 7.3$ Hz, 1H), 2.55 (s, 1H); $^{13}\text{C}\{^1\text{H}\}$ (100 MHz, CDCl_3) δ = 136.9, 136.1, 135.0, 131.2, 130.9, 129.3, 126.0 (C-F, $^4J_{\text{C-F}} = 3.7$ Hz), 125.3 (C-F, $^1J_{\text{C-F}} = 280.8$ Hz), 123.9 (C-F, $^1J_{\text{C-F}} = 270.7$ Hz), 123.7, 121.5 – 121.4 (C-F, $^4J_{\text{C-F}} = 3.0$ Hz), 121.2, 111.3, 107.2, 67.9 (C-F, $^2J_{\text{C-F}} = 33.5$ Hz); $^{19}\text{F NMR}$ (376 MHz, CDCl_3) δ = -62.73 (s, 3F), -75.83 (s, 3F) ppm; HRMS (ESI) m/z : $[\text{M} + \text{H}]^+$ calcd for $\text{C}_{17}\text{H}_{12}\text{F}_6\text{NO}^+$ 360.0818, found 360.0819.

2,2,2-Trifluoro-1-(2-(4-nitrophenyl)-1H-indol-3-yl)ethan-1-ol (3ha): White solid; 122.3 mg,



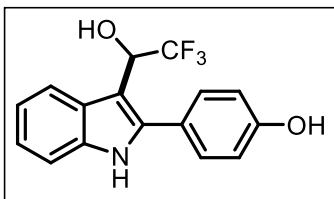
91% yield; $R_f=0.5$, Eluent system: EtOAc:hexanes (2.0:8.0); mp = 144-146 °C; ^1H NMR (400 MHz, CDCl_3) δ = 10.85 (s, 1H), 8.15 – 8.13 (d, J = 8.8 Hz, 2H), 7.78 (d, J = 8.4 Hz, 1H), 7.64 – 7.62 (d, J = 8.8 Hz, 2H), 7.28 (d, J = 8.4 Hz, 1H), 7.06 – 7.02 (m, 1H), 6.97 – 6.93 (m, 1H), 5.96 (d, J = 4.4 Hz, 1H), 5.18 – 5.13 (m, 1H); $^{13}\text{C}\{^1\text{H}\}$ (100 MHz, CDCl_3) δ = 147.0, 138.8, 136.8, 135.4, 129.6, 126.7, 125.7 (C-F, $^1J_{\text{C-F}}$ = 281.3 Hz), 123.7, 123.0, 121.9 (C-F, $^4J_{\text{C-F}}$ = 2.3 Hz), 120.0, 111.5, 108.6, 66.8 (C-F, $^2J_{\text{C-F}}$ = 32.5 Hz); ^{19}F NMR (376 MHz, CDCl_3) δ = -75.52 (d, J = 7.5 Hz, 3F) ppm; HRMS (ESI) m/z : $[\text{M} + \text{H}]^+$ calcd for $\text{C}_{16}\text{H}_{12}\text{F}_3\text{N}_2\text{O}_3^+$ 337.0795, found 337.0779.

2,2,2-Trifluoro-1-(2-(4-methoxyphenyl)-1H-indol-3-yl)ethan-1-ol (3ia): White solid; 89.9 mg,



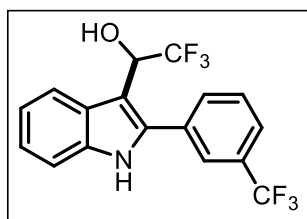
70% yield; $R_f=0.3$, Eluent system: EtOAc:hexanes (1.5:8.5); mp = 132-134 °C; ^1H NMR (400 MHz, CDCl_3) δ = 8.25 (s, 1H), 7.94 (d, J = 7.6 Hz, 1H), 7.47 (d, J = 8.4 Hz, 2H), 7.42 (d, J = 8.0 Hz, 1H), 7.30 – 7.21 (m, 2H) (with merged CDCl_3 peak), 7.05 (d, J = 8.4 Hz, 2H), 5.31 (q, J = 7.3 Hz, 1H), 3.90 (s, 3H), 2.47 (s, 1H); $^{13}\text{C}\{^1\text{H}\}$ (100 MHz, CDCl_3) δ = 160.3, 138.9, 135.8, 130.2, 126.1, 125.5 (C-F, $^1J_{\text{C-F}}$ = 280.8 Hz), 123.7, 122.8, 121.0 – 120.9 (m), 120.8, 114.5, 111.0, 105.7, 68.1 (C-F, $^2J_{\text{C-F}}$ = 33.3 Hz), 55.4; ^{19}F NMR (376 MHz, CDCl_3) δ = -75.74 (s, 3F) ppm; HRMS (ESI) m/z : $[\text{M} + \text{H}]^+$ calcd for $\text{C}_{17}\text{H}_{15}\text{F}_3\text{NO}_2^+$ 322.1049, found 322.1035.

4-(3-(2,2,2-Trifluoro-1-hydroxyethyl)-1H-indol-2-yl)phenol (3ja): White solid; 81.0 mg, 66%



yield; $R_f=0.3$, Eluent system: EtOAc:hexanes (1.5:8.5); mp = 158-160 °C; ^1H NMR (400 MHz, CDCl_3) δ = 10.13 (s, 1H), 7.76 – 7.74 (m, 1H), 7.24 – 7.22 (m, 3H), 7.00 – 6.91 (m, 2H), 6.79 (d, J = 8.0 Hz, 2H), 5.12 (q, J = 7.9 Hz, 1H); $^{13}\text{C}\{^1\text{H}\}$ (100 MHz, CDCl_3) δ = 157.7, 138.9, 136.0, 130.3, 126.6, 126.0 (C-F, $^1J_{\text{C-F}}$ = 280.8 Hz), 123.0, 121.6, 121.3 (C-F, $^4J_{\text{C-F}}$ = 2.3 Hz), 119.6, 115.7, 111.1, 105.6, 67.2 (C-F, $^2J_{\text{C-F}}$ = 32.5 Hz); ^{19}F NMR (376 MHz, CDCl_3) δ = -77.37 (s, 3H) ppm; HRMS (ESI) m/z : $[\text{M} + \text{H}]^+$ calcd for $\text{C}_{16}\text{H}_{13}\text{F}_3\text{NO}_2^+$ 308.0893, found 308.0892.

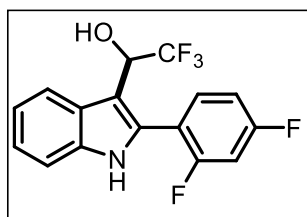
2,2,2-Trifluoro-1-(2-(3-(trifluoromethyl)phenyl)-1H-indol-3-yl)ethan-1-ol (3ka): White solid;



113.4 mg, 79% yield; $R_f = 0.5$, Eluent system: EtOAc:hexanes (2.0:8.0); mp = 130-132 °C; $^1\text{H NMR}$ (400 MHz, CDCl_3) δ 8.36 (s, 1H), 7.98 (d, $J = 8.0$ Hz, 1H), 7.83 (s, 1H), 7.76 (d, $J = 8.4$ Hz, 2H), 7.68 (t, $J = 7.6$ Hz, 1H), 7.46 (d, $J = 8.0$ Hz, 1H), 7.33 (t, $J = 7.2$ Hz, 1H), 7.25 (d, $J = 7.6$ Hz, 1H), 5.29 (q, $J = 7.2$ Hz, 1H), 2.54 (s, 1H);

$^{13}\text{C}\{^1\text{H}\}$ (100 MHz, CDCl_3) δ 136.9, 136.1, 132.3, 131.8, 131.5, 131.2, 129.7, 126.0, 125.7 (C-F, $^4J_{\text{C-F}} = 3.5$ Hz), 125.3 (C-F, $^1J_{\text{C-F}} = 281.1$ Hz), 123.7 (C-F, $^1J_{\text{C-F}} = 270.9$ Hz), 123.6, 121.4 (C-F, $^4J_{\text{C-F}} = 3.0$ Hz), 121.2, 111.3, 107.1, 68.0 (C-F, $^2J_{\text{C-F}} = 33.5$ Hz); $^{19}\text{F NMR}$ (376 MHz, CDCl_3) δ -62.79 (s, 3F), -75.92 (s, 3F); HRMS (ESI) m/z : $[\text{M} + \text{H}]^+$ calcd for $\text{C}_{17}\text{H}_{12}\text{F}_6\text{NO}^+$ 360.0818, found 360.0807.

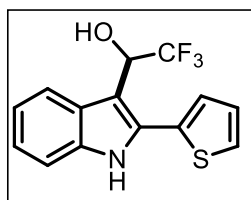
1-(2-(2,4-Difluorophenyl)-1H-indol-3-yl)-2,2,2-trifluoroethan-1-ol (3la): White solid; 92.9



mg, 71% yield; $R_f = 0.5$, Eluent system: EtOAc:hexanes (2.0:8.0); mp = 138-140 °C; $^1\text{H NMR}$ (400 MHz, CDCl_3) δ = 8.42 (s, 1H), 7.97 (d, $J = 8.4$ Hz, 1H), 7.52 – 7.47 (m, 1H), 7.45 (d, $J = 8.0$ Hz, 1H); 7.34 – 7.30 (m, 1H), 7.26 – 7.23 (m, 1H), 7.08 – 7.00 (m, 2H), 5.19 (q, $J = 6.7$ Hz, 1H), 2.62 (s, 1H); $^{13}\text{C}\{^1\text{H}\}$ (100 MHz, CDCl_3) δ =

164.8 (C-F, $^3J_{\text{C-F}} = 12.0$ Hz), 162.3 (C-F, $^3J_{\text{C-F}} = 11.8$ Hz), 161.6 (C-F, $^3J_{\text{C-F}} = 12.1$ Hz), 159.1 (C-F, $^3J_{\text{C-F}} = 12.2$ Hz), 136.0, 132.8 (dd, $J = 9.8, 3.7$ Hz), 131.2, 125.5, 125.2 (C-F, $^1J_{\text{C-F}} = 280.9$ Hz), 123.5, 121.2 (C-F, $^4J_{\text{C-F}} = 2.7$ Hz), 121.0, 112.1 (dd, $J = 21.5, 3.6$ Hz), 111.1, 108.1, 104.9 (C-F, $^2J_{\text{C-F}} = 25.4$ Hz), 68.1 (C-F, $^2J_{\text{C-F}} = 33.7$ Hz); $^{19}\text{F NMR}$ (376 MHz, CDCl_3) δ = -77.07 (s, 3F), -107.04 (d, $J = 8.6$ Hz), -109.8 (d, $J = 8.6$ Hz); HRMS (ESI) m/z : $[\text{M} + \text{H}]^+$ calcd for $\text{C}_{16}\text{H}_{11}\text{F}_5\text{NO}^+$ 328.0755, found 328.0729.

2,2,2-Trifluoro-1-(2-(thiophen-2-yl)-1H-indol-3-yl)ethan-1-ol (3ma): White solid; 99.8 mg,

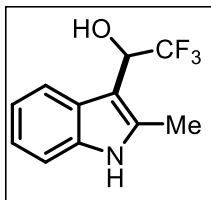


84% yield; $R_f = 0.7$, Eluent system: EtOAc:hexanes (1.5:8.5); mp = 128-130 °C; $^1\text{H NMR}$ (400 MHz, CDCl_3) δ = 8.33 (s, 1H), 7.95 (d, $J = 8.0$ Hz, 1H), 7.50 (dd, $J = 5.0, 1.0$ Hz, 1H), 7.42 (d, $J = 8.0$ Hz, 1H), 7.32 – 7.28 (m, 2H) (with merged CDCl_3 peak), 7.25 – 7.19 (m, 2H), 5.51 (q, J

= 6.9 Hz, 1H), 2.61 (s, 1H); $^{13}\text{C}\{^1\text{H}\}$ (100 MHz, CDCl_3) δ = 136.0, 132.2, 131.7, 128.1, 127.7, 127.3, 126.3, 125.4 (C-F, $^1J_{\text{C-F}} = 280.8$ Hz); 123.5, 121.3 (C-F, $^4J_{\text{C-F}} = 2.4$ Hz), 121.1, 111.1,

107.0, 68.0 (C-F, $^2J_{C-F} = 33.6$ Hz); ^{19}F NMR (376 MHz, CDCl_3) $\delta = -76.12$ (s, 3F) ppm; HRMS (ESI) m/z : $[\text{M} + \text{H}]^+$ calcd for $\text{C}_{14}\text{H}_{11}\text{F}_3\text{NOS}^+$ 298.0508, found 298.0506.

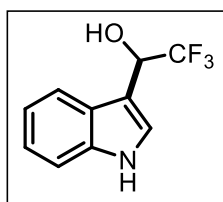
2,2,2-Trifluoro-1-(2-methyl-1H-indol-3-yl)ethan-1-ol (3na): White solid; 65.0 mg, 71% yield;



$R_f = 0.2$, Eluent system: EtOAc:hexanes (3.5:6.5); mp = 118-120 °C; ^1H NMR (400 MHz, $\text{DMSO}-d_6$) $\delta = 11.10$ (s, 1H), 7.68 (d, $J = 8.0$ Hz, 1H), 7.32 (d, $J = 8.0$ Hz, 1H), 7.06 (t, $J = 7.2$ Hz, 1H), 7.00 (t, $J = 7.4$ Hz, 1H), 6.48 (d, $J = 4.4$ Hz, 1H), 5.36 (q, $J = 4.0$ Hz, 1H), 2.44 (s, 3H); $^{13}\text{C}\{^1\text{H}\}$ (100

MHz, $\text{DMSO}-d_6$) $\delta = 140.3, 140.0, 132.3, 131.4$ (C-F, $^1J_{C-F} = 281.4$ Hz), 125.6, 124.6, 124.0, 115.7, 110.3, 71.2 (C-F, $^2J_{C-F} = 31.8$ Hz), 16.9; ^{19}F NMR (376 MHz, $\text{DMSO}-d_6$) $\delta = -71.58$ (s, 3F) ppm; HRMS (ESI) m/z : $[\text{M} + \text{H}]^+$ calcd for $\text{C}_{11}\text{H}_{11}\text{F}_3\text{NO}^+$ 230.0787, found 230.0789.

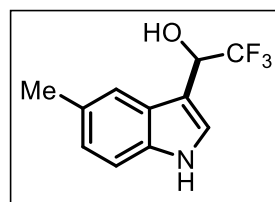
2,2,2-Trifluoro-1-(1H-indol-3-yl)ethan-1-ol (3oa): White solid; 42.1 mg, 49% yield; $R_f = 0.3$,



Eluent system: EtOAc:hexanes (3.0:7.0); mp = 126-128 °C; ^1H NMR (400 MHz, CDCl_3) $\delta = 8.33$ (s, 1H), 7.77 (d, $J = 8.0$ Hz, 1H), 7.43 (d, $J = 8.0$ Hz, 1H), 7.38 (s, 1H), 7.28 (t, $J = 7.6$ Hz, 1H), 7.22 (t, $J = 7.6$ Hz, 1H), 5.39 (q, $J = 6.9$ Hz, 1H), 2.54 (s, 1H); $^{13}\text{C}\{^1\text{H}\}$ (100 MHz, CDCl_3) $\delta = 136.1,$

125.7, 125.0 (C-F, $^1J_{C-F} = 271.0$ Hz), 123.7, 123.0, 120.6, 119.4, 111.5, 109.8, 67.6 (C-F, $^2J_{C-F} = 33.5$ Hz); ^{19}F NMR (376 MHz, CDCl_3) $\delta = -77.86$ (s, 3F) ppm; HRMS (ESI) m/z : $[\text{M} + \text{H}]^+$ calcd for $\text{C}_{10}\text{H}_9\text{F}_3\text{NO}^+$ 216.0631, found 216.0630.

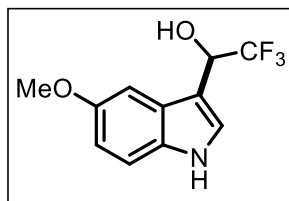
2,2,2-Trifluoro-1-(5-methyl-1H-indol-3-yl)ethan-1-ol (3pa): White solid; 52.2 mg, 57% yield;



$R_f = 0.2$, Eluent system: EtOAc:hexanes (3.5:6.5); mp = 116-118 °C; ^1H NMR (400 MHz, CDCl_3) $\delta = 8.24$ (s, 1H), 7.56 (s, 1H), 7.34 (d, $J = 2.0$ Hz, 1H), 7.31 (s, 1H), 7.11 (dd, $J = 8.0, 1.6$ Hz, 1H), 5.36 (q, $J = 6.9$ Hz, 1H), 2.52 (s, 1H), 2.50 (s, 3H); $^{13}\text{C}\{^1\text{H}\}$ (100 MHz, CDCl_3) $\delta =$

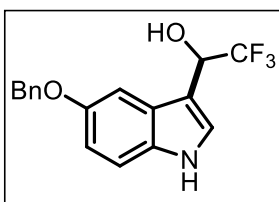
134.4, 130.0, 126.0, 124.9 (C-F, $^1J_{C-F} = 280.2$ Hz), 124.6, 123.8, 118.9, 111.1, 109.3, 67.5 (C-F, $^2J_{C-F} = 33.3$ Hz), 21.5; ^{19}F NMR (376 MHz, CDCl_3) $\delta = -77.78$ (d, $J = 6.8$ Hz, 3F) ppm; HRMS (ESI) m/z : $[\text{M} + \text{H}]^+$ calcd for $\text{C}_{11}\text{H}_{11}\text{F}_3\text{NO}^+$ 230.0787, found 230.0767.

2,2,2-Trifluoro-1-(5-methoxy-1H-indol-3-yl)ethan-1-ol (3qa): White solid; 58.8 mg, 60%



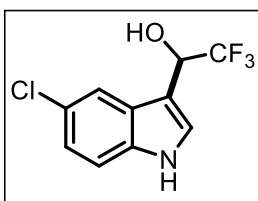
yield; $R_f = 0.3$, Eluent system: EtOAc:hexanes (3.0:7.0); mp = 142–144 °C; $^1\text{H NMR}$ (400 MHz, CDCl_3) $\delta = 9.79$ (s, 1H), 7.18 – 7.16 (m, 2H), 7.07 (s, 1H), 6.73 – 6.70 (m, 1H), 5.55 – 5.50 (m, 1H), 5.19 – 5.14 (m, 1H), 3.73 (s, 3H); $^{13}\text{C}\{^1\text{H}\}$ (100 MHz, CDCl_3) $\delta = 154.0$, 131.4, 126.4, 125.4 (C-F, $^1J_{\text{C-F}} = 280.5$ Hz), 124.8, 112.4, 112.3, 109.6 (C-F, $^4J_{\text{C-F}} = 1.1$ Hz), 101.1, 66.9 (C-F, $^2J_{\text{C-F}} = 32.6$ Hz), 55.8; $^{19}\text{F NMR}$ (376 MHz, CDCl_3) $\delta = -77.66$ (d, $J = 7.1$ Hz, 3F) ppm; HRMS (ESI) m/z : $[\text{M} + \text{H}]^+$ calcd for $\text{C}_{11}\text{H}_{11}\text{F}_3\text{NO}_2^+$ 246.0736, found 246.0735.

1-(5-(Benzyloxy)-1H-indol-3-yl)-2,2,2-trifluoroethan-1-ol (3ra): White solid; 92.4 mg, 72%

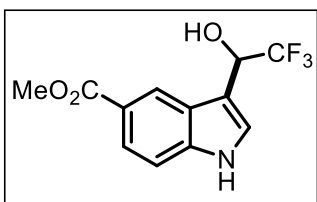


yield; $R_f = 0.2$, Eluent system: EtOAc:hexanes (3.0:7.0); mp = 138–140 °C; $^1\text{H NMR}$ (400 MHz, $\text{DMSO-}d_6$) $\delta = 11.12$ (s, 1H), 7.50 (d, $J = 7.2$ Hz, 2H), 7.44 (d, $J = 2.0$ Hz, 1H), 7.41 (t, $J = 7.4$ Hz, 2H), 7.35 – 7.31 (m, 3H), 6.89 (dd, $J = 8.8, 1.6$ Hz, 1H), 6.50 (d, $J = 5.2$ Hz, 1H), 5.37 (q, $J = 6.7$ Hz, 1H), 5.10 (s, 2H); $^{13}\text{C}\{^1\text{H}\}$ (100 MHz, $\text{DMSO-}d_6$) $\delta = 152.9, 138.2, 131.9, 128.8, 128.1, 128.1, 126.8, 126.3$ (C-F, $^1J_{\text{C-F}} = 281.0$ Hz), 126.0, 112.7, 112.6, 109.9, 103.5, 70.3, 66.3 (C-F, $^2J_{\text{C-F}} = 31.6$ Hz); $^{19}\text{F NMR}$ (376 MHz, $\text{DMSO-}d_6$) $\delta = -76.53$ (d, $J = 7.5$ Hz, 3F) ppm; HRMS (ESI) m/z : $[\text{M} + \text{H}]^+$ calcd for $\text{C}_{17}\text{H}_{15}\text{F}_3\text{NO}_2^+$ 322.1049, found 322.1042.

1-(5-Chloro-1H-indol-3-yl)-2,2,2-trifluoroethan-1-ol (3sa): Semi solid; 64.9 mg, 65% yield; $R_f = 0.3$, Eluent system: EtOAc:hexanes (1.5:8.5); $^1\text{H NMR}$ (400 MHz, CDCl_3) $\delta = 8.45$ (s, 1H), 7.73 (d, $J = 1.6$ Hz, 1H), 7.34 – 7.29 (m, 2H), 7.21 (dd, $J = 8.8, 2.0$ Hz, 1H), 5.30 (q, $J = 6.3$ Hz, 1H); $^{13}\text{C}\{^1\text{H}\}$ (100 MHz, CDCl_3) $\delta = 134.4, 126.8, 126.3, 125.2$ (C-F, $^4J_{\text{C-F}} = 1.8$ Hz), 124.7 (C-F, $^1J_{\text{C-F}} = 280.2$ Hz), 119.0, 119.0, 112.5, 109.4 (C-F, $^4J_{\text{C-F}} = 1.7$ Hz), 67.4 (C-F, $^2J_{\text{C-F}} = 33.5$ Hz); $^{19}\text{F NMR}$ (376 MHz, CDCl_3) $\delta = -77.92$ (s, 3F) ppm; HRMS (ESI) m/z : $[\text{M} + \text{H}]^+$ calcd for $\text{C}_{10}\text{H}_6\text{ClF}_3\text{NO}^+$ 250.0241, found 250.0262.



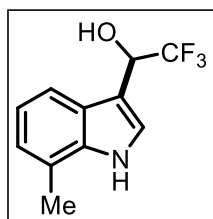
Methyl 3-(2,2,2-trifluoro-1-hydroxyethyl)-1H-indole-5-carboxylate (3ta): White solid; 69.9



mg, 64% yield; $R_f = 0.3$, Eluent system: EtOAc:hexanes (1.5:8.5); mp = 124–126 °C; $^1\text{H NMR}$ (400 MHz, $\text{DMSO-}d_6$) $\delta = 11.61$ (s, 1H), 8.45 (s, 1H), 7.77 (s, 1H), 7.60–7.51 (m, 2H), 6.67 (s, 1H), 5.46 (s, 1H), 3.87 (s, 3H); $^{13}\text{C}\{^1\text{H}\}$ (100 MHz, $\text{DMSO-}d_6$) $\delta = 167.7,$

139.3, 127.4, 126.1 (C-F, $^1J_{\text{C-F}} = 279.9$ Hz), 125.8, 124.7, 123.1, 122.8, 121.1, 112.2, 111.5, 66.4 (C-F, $^2J_{\text{C-F}} = 31.9$ Hz), 52.2; ^{19}F NMR (376 MHz, DMSO- d_6) $\delta = -76.61$ ppm; HRMS (ESI) m/z : $[\text{M} + \text{H}]^+$ calcd for $\text{C}_{12}\text{H}_{11}\text{F}_3\text{NO}_3^+$ 274.0686, found 274.0685.

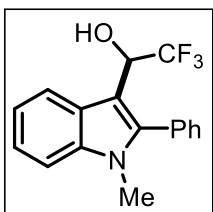
2,2,2-Trifluoro-1-(7-methyl-1H-indol-3-yl)ethan-1-ol (3ua): White solid; 55.9 mg, 61% yield;



$R_f = 0.2$, Eluent system: EtOAc:hexanes (3.5:6.5); mp = 118-120 °C; ^1H NMR (400 MHz, CDCl_3) $\delta = 8.24$ (s, 1H), 7.62 (d, $J = 8.0$ Hz, 1H), 7.36 (d, $J = 1.6$ Hz, 1H), 7.16 (t, $J = 7.4$ Hz, 1H), 7.10 (d, $J = 7.2$ Hz, 1H), 5.37 (q, $J = 6.8$ Hz, 1H), 2.52 (s, 3H), 2.33 (s, 1H); $^{13}\text{C}\{^1\text{H}\}$ (100 MHz, CDCl_3) $\delta = 135.7, 125.3, 124.9$ (C-F, $^1J_{\text{C-F}} = 279.9$ Hz), 123.5, 123.4, 120.8, 120.7,

117.0, 110.3, 67.6 (C-F, $^2J_{\text{C-F}} = 33.6$ Hz), 16.5; ^{19}F NMR (376 MHz, CDCl_3) $\delta = -77.83$ (d, $J = 6.8$ Hz, 3F) ppm; HRMS (ESI) m/z : $[\text{M} + \text{H}]^+$ calcd for $\text{C}_{11}\text{H}_{11}\text{F}_3\text{NO}^+$ 230.0787, found 230.0780.

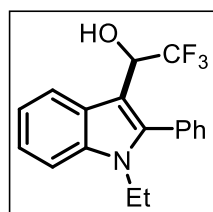
2,2,2-Trifluoro-1-(1-methyl-2-phenyl-1H-indol-3-yl)ethan-1-ol (3va): White solid; 75.6 mg,



62% yield; $R_f = 0.7$, Eluent system: EtOAc:hexanes (1.5:8.5); mp = 84-86 °C; ^1H NMR (400 MHz, CDCl_3) $\delta = 7.95$ (d, $J = 7.6$ Hz, 1H), 7.56 – 7.54 (m, 3H), 7.43 – 7.41 (m, 3H), 7.37 – 7.33 (m, 1H), 7.28 – 7.24 (m, 1H), 5.05 (q, $J = 7.5$ Hz, 1H), 3.61 (s, 3H); $^{13}\text{C}\{^1\text{H}\}$ (100 MHz, CDCl_3) $\delta = 141.5, 137.4, 130.7, 130.3, 129.2, 128.7, 125.0, 125.3$ (C-F, $^1J_{\text{C-F}} = 280.9$ Hz),

122.5, 120.9 (C-F, $^4J_{\text{C-F}} = 3.0$ Hz), 120.6, 109.7, 106.2, 68.4 (C-F, $^2J_{\text{C-F}} = 33.5$ Hz), 30.8; ^{19}F NMR (376 MHz, CDCl_3) $\delta = -76.21$ (s, 3F) ppm; HRMS (ESI) m/z : $[\text{M} + \text{H}]^+$ calcd for $\text{C}_{17}\text{H}_{15}\text{F}_3\text{NO}^+$ 306.1100, found 306.1082.

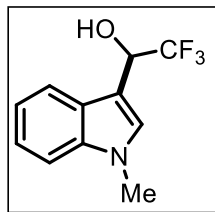
1-(1-Ethyl-2-phenyl-1H-indol-3-yl)-2,2,2-trifluoroethan-1-ol (3wa): White solid; 88.0 mg,



69% yield; $R_f = 0.3$, Eluent system: EtOAc:hexanes (1.5:8.5); mp = 90-92 °C; ^1H NMR (400 MHz, CDCl_3) $\delta = 8.02$ (d, $J = 7.2$ Hz, 1H), 7.60 (s, 3H), 7.52 – 7.50 (m, 3H), 7.40 (t, $J = 7.2$ Hz, 1H), 7.31 (t, $J = 7.0$ Hz, 1H), 5.10 (s, 1H), 4.11 (d, $J = 3.2$ Hz, 2H), 2.23 (s, 1H), 1.34 (t, $J = 6.8$ Hz, 3H); $^{13}\text{C}\{^1\text{H}\}$ (100 MHz, CDCl_3) $\delta = 141.0, 136.1, 130.5, 129.3, 128.7, 125.4,$

125.4 (C-F, $^1J_{\text{C-F}} = 280.9$ Hz), 122.4, 121.1 (C-F, $^4J_{\text{C-F}} = 2.6$ Hz), 120.6, 110.0, 106.4, 68.5 (C-F, $^2J_{\text{C-F}} = 33.7$ Hz), 38.84, 15.37; ^{19}F NMR (376 MHz, CDCl_3) $\delta = -76.13$ (s, 3F) ppm; HRMS (ESI) m/z : $[\text{M} + \text{H}]^+$ calcd for $\text{C}_{18}\text{H}_{17}\text{F}_3\text{NO}^+$ 320.1257, found 320.1260.

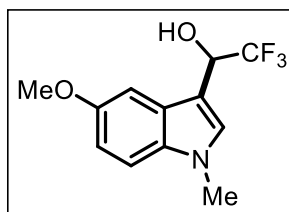
2,2,2-Trifluoro-1-(1-methyl-1H-indol-3-yl)ethan-1-ol (3xa): White solid; 70.5 mg, 77% yield;



$R_f=0.3$, Eluent system: EtOAc:hexanes (1.5:8.5); mp = 68-70 °C; ^1H NMR (400 MHz, DMSO- d_6) δ = 7.76 (s, 1H), 7.48 (s, 2H), 7.23 (s, 1H), 7.13 (s, 1H), 6.60 (s, 1H), 5.43 (s, 1H), 3.81 (s, 3H); $^{13}\text{C}\{^1\text{H}\}$ (100 MHz, DMSO- d_6) δ = 141.8, 134.2, 131.5, 130.9 (C-F, $^1J_{\text{C-F}} = 280.9$ Hz), 126.7, 124.9, 124.4, 115.1, 114.0, 70.9 (C-F, $^2J_{\text{C-F}} = 31.7$ Hz), 37.6; ^{19}F NMR (376 MHz,

DMSO- d_6) δ = -76.61 (s, 3F) ppm; HRMS (ESI) m/z : $[\text{M} + \text{H}]^+$ calcd for $\text{C}_{11}\text{H}_{11}\text{F}_3\text{NO}^+$ 230.0787, found 230.0780.

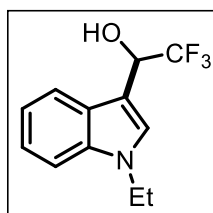
2,2,2-Trifluoro-1-(5-methoxy-1-methyl-1H-indol-3-yl)ethan-1-ol (3ya): White solid; 62.2 mg,



60% yield; $R_f=0.4$, Eluent system: EtOAc:hexanes (2.0:8.0); mp = 106-108 °C; ^1H NMR (400 MHz, DMSO- d_6) δ = 7.39 (s, 1H), 7.34 (d, $J = 8.8$ Hz, 1H), 7.20 (s, 1H), 6.84 (d, $J = 8.8$ Hz, 1H), 6.49 (d, $J = 5.6$ Hz, 1H), 5.39 – 5.32 (m, 1H), 3.77 (s, 3H), 3.76 (s, 3H); $^{13}\text{C}\{^1\text{H}\}$ (100

MHz, DMSO- d_6) δ = 154.0, 132.3, 129.8, 127.2, 126.2 (C-F, $^1J_{\text{C-F}} = 281.0$ Hz), 112.0, 111.1, 108.8, 101.9, 66.0 (C-F, $^2J_{\text{C-F}} = 31.5$ Hz), 55.8, 33.0; ^{19}F NMR (376 MHz, DMSO- d_6) δ = -76.58 (s, 3F) ppm; HRMS (ESI) m/z : $[\text{M} + \text{H}]^+$ calcd for $\text{C}_{12}\text{H}_{13}\text{F}_3\text{NO}_2^+$ 260.0893, found 260.0887.

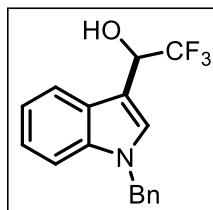
1-(1-Ethyl-1H-indol-3-yl)-2,2,2-trifluoroethan-1-ol (3za): White solid; 76.8 mg, 79% yield; R_f



=0.3, Eluent system: EtOAc:hexanes (1.5:8.5); mp = 76-78 °C; ^1H NMR (400 MHz, CDCl_3) δ = 7.76 (d, $J = 7.6$ Hz, 1H), 7.41 (d, $J = 8.4$ Hz, 1H), 7.33 – 7.29 (m, 2H), 7.24 – 7.20 (m, 1H), 5.38 (q, $J = 6.9$ Hz, 1H), 4.21 (q, $J = 7.3$ Hz, 2H), 2.50 (s, 1H), 1.52 (t, $J = 7.4$ Hz, 3H); $^{13}\text{C}\{^1\text{H}\}$ (100 MHz,

CDCl_3) δ = 136.0, 126.5, 125.0 (C-F, $^2J_{\text{C-F}} = 280.1$ Hz), 122.3, 120.1, 119.5, 109.8, 108.2, 67.5 (C-F, $^2J_{\text{C-F}} = 33.3$ Hz), 41.2, 15.3; ^{19}F NMR (376 MHz, CDCl_3) δ = -77.76 (s, 3F) ppm; HRMS (ESI) m/z : $[\text{M} + \text{H}]^+$ calcd for $\text{C}_{12}\text{H}_{13}\text{F}_3\text{NO}^+$ 244.0944, found 244.0933.

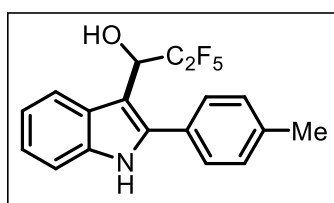
1-(1-Benzyl-1H-indol-3-yl)-2,2,2-trifluoroethan-1-ol (3z'a): White solid; 83.0 mg, 68% yield;



$R_f=0.3$, Eluent system: EtOAc:hexanes (2.0:8.0); mp = 88-90 °C; ^1H NMR (400 MHz, CDCl_3) δ = 7.78 (d, J = 8.0 Hz, 1H), 7.36 – 7.32 (m, 5H), 7.27 (d, J = 7.6 Hz, 1H), 7.24 – 7.20 (m, 1H), 7.16 (d, J = 6.8 Hz, 2H), 5.44 – 5.38 (m, 1H), 5.34 (s, 2H), 2.46 (s, 1H); $^{13}\text{C}\{^1\text{H}\}$ NMR (100 MHz, CDCl_3)

δ = 136.7, 136.6, 128.9, 127.9, 127.6, 127.0, 126.6, 125.0 (C-F, $^1J_{\text{C-F}} = 280.0$ Hz), 122.7, 120.4, 119.6, 110.2, 108.8, 67.6 (C-F, $^2J_{\text{C-F}} = 33.4$ Hz), 50.3; ^{19}F NMR (376 MHz, CDCl_3) δ = -77.79 (s, 3F) ppm; HRMS (ESI) m/z : $[\text{M} + \text{H}]^+$ calcd for $\text{C}_{17}\text{H}_{15}\text{F}_3\text{NO}^+$ 306.1100, found 306.1097.

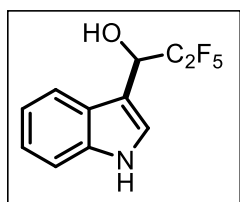
2,2,3,3,3-Pentafluoro-1-(2-(p-tolyl)-1H-indol-3-yl)propan-1-ol (3db): White solid; 105.1 mg,



74% yield; $R_f=0.2$, Eluent system: EtOAc:hexanes (3.5:6.5); mp = 108-110 °C; ^1H NMR (400 MHz, CDCl_3) δ = 8.29 (s, 1H), 7.95 (d, J = 5.2 Hz, 1H), 7.43 (t, J = 7.4 Hz, 3H), 7.35 – 7.33 (m, 2H), 7.29 (d, J = 5.6 Hz, 1H), 7.25 (t, J = 7.4 Hz, 1H), 5.49 – 5.43 (m,

1H), 2.47 (s, 3H), 2.41 (s, 1H); $^{13}\text{C}\{^1\text{H}\}$ (100 MHz, CDCl_3) δ = 139.2, 135.9, 129.8, 128.8, 128.7, 128.4, 126.3, 123.0, 121.1 (dd, $^3J_{\text{C-F}} = 7.3, 1.9$ Hz), 120.9, 111.1, 105.8, 66.9 (C-F, $^2J_{\text{C-F}} = 26.8$), 21.3; ^{19}F NMR (376 MHz, CDCl_3) δ = -81.90 (s, 3F), -117.82 (d, J = 273.5 Hz, 1F), -127.49 (d, J = 273.4 Hz, 1F) ppm; HRMS (ESI) m/z : $[\text{M} + \text{H}]^+$ calcd for $\text{C}_{18}\text{H}_{15}\text{F}_5\text{NO}^+$ 356.1068, found 356.1063.

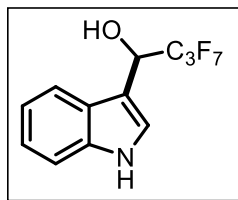
2,2,3,3,3-Pentafluoro-1-(1H-indol-3-yl)propan-1-ol (3ob): White solid; 66.8 mg, 63% yield; R_f



=0.2, Eluent system: EtOAc:hexanes (3.5:6.5); mp = 104-106 °C; ^1H NMR (400 MHz, CDCl_3) δ = 8.28 (s, 1H), 7.79 (d, J = 7.6 Hz, 1H), 7.46 – 7.41 (m, 2H), 7.30 (d, J = 5.6 Hz, 1H), 7.24 (t, J = 7.4 Hz, 1H), 5.52 (dd, J = 17.6, 7.6 Hz, 1H), 2.34 (s, 1H); $^{13}\text{C}\{^1\text{H}\}$ (100 MHz, CDCl_3) δ = 136.0,

125.8, 124.3, 123.0, 120.7, 119.4, 111.6, 109.8, 66.6 (C-F, $^2J_{\text{C-F}} = 29.0$); ^{19}F NMR (376 MHz, CDCl_3) δ = -81.38 (s, 3F), -121.68 (d, J = 272.2 Hz, 1F), -128.47 (d, J = 272.2 Hz, 1F) ppm; HRMS (ESI) m/z : $[\text{M} + \text{H}]^+$ calcd for $\text{C}_{11}\text{H}_9\text{F}_5\text{NO}^+$ 266.0599, found 266.0606.

4,4,4,4,4,4,4-Heptafluoro-1-(1H-indol-3-yl)-418-but-2-yn-1-ol (**3oc**): White solid; 86.9 mg,

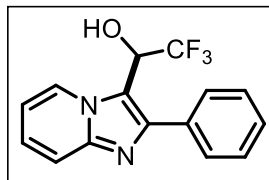


69% yield; $R_f=0.2$, Eluent system: EtOAc:hexanes (3.5:6.5); mp = 96-98 °C; ^1H NMR (400 MHz, CDCl_3) δ = 8.36 (s, 1H), 7.78 (d, J = 7.6 Hz, 1H), 7.46 – 7.42 (m, 2H), 7.32 – 7.22 (m, 2H), 5.61 – 5.55 (m, 1H), 2.39 (s, 1H); $^{13}\text{C}\{^1\text{H}\}$ (100 MHz, CDCl_3) δ = 136.0, 125.8, 124.3, 123.0, 120.7, 119.4, 111.5, 109.8, 66.7 (dd, $^2J_{\text{C-F}}$ = 29.6, 23.1 Hz); ^{19}F NMR (376 MHz, CDCl_3) δ = -80.85 (s, 3F), -118.75 (dp, J = 279.3, 10.7 Hz, 1F), -124.53 – -124.94 (m, 1F), -125.29 – -125.79 (m, 2F) ppm; HRMS (ESI) m/z : $[\text{M} + \text{H}]^+$ calcd for $\text{C}_{12}\text{H}_9\text{F}_7\text{NO}^+$ 316.0567, found 316.0555.

4.9.4 General Procedure for the C3-Fluoroalkylation of Imidazopyridines

An oven dried sealed tube charged with compound **24** (0.5 mmol; 1.0 equiv.) in **2** (2 mL) followed by TEMPO (3.0 equiv.) was added at room temperature and the reaction mixture was stirred at 120 °C for 36 h. After completion of the reaction monitored by TLC, then reaction mixture was allowed to attain room temperature. The reaction mixture was poured into water (20 mL) and extracted with ethyl acetate (3 × 15 mL). The combined organic layer was dried over anhydrous Na_2SO_4 and evaporated under vacuum. The resulting crude was purified by column chromatography (silica gel 100-200 mesh) using EtOAc-hexanes as an eluent to afford **25**.

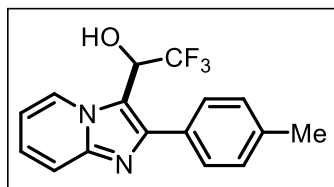
2,2,2-Trifluoro-1-(2-phenylimidazo[1,2-a]pyridin-3-yl)ethan-1-ol (**25aa**): White solid; 118.3



mg, 81% yield; Eluent system: EtOAc:hexanes (3:7); mp = 188-190 °C; ^1H NMR (400 MHz, $\text{DMSO}-d_6$) δ = 8.68 (d, J = 6.8, 1H), 7.71 – 7.68 (m, 3H), 7.56 – 7.52 (m, 2H), 7.48 – 7.43 (m, 2H), 7.42 – 7.38 (m, 1H), 7.04 (td, J = 7.0, 1.1 Hz, 1H), 5.73 – 5.66 (m, 1H); $^{13}\text{C}\{^1\text{H}\}$ NMR (100

MHz, $\text{DMSO}-d_6$) δ = 146.0, 145.7, 134.1, 129.2, 129.0, 128.7, 127.8 (C-F, $^4J_{\text{C-F}}$ = 2.7 Hz), 126.0 (C-F, $^1J_{\text{C-F}}$ = 282.6 Hz), 126.4, 117.5, 114.1, 113.0, 65.6 (C-F, $^2J_{\text{C-F}}$ = 32.4 Hz); ^{19}F NMR (376 MHz, $\text{DMSO}-d_6$) δ = -74.59 (s, 3F); HRMS (ESI) m/z : $[\text{M} + \text{H}]^+$ calcd for $\text{C}_{15}\text{H}_{12}\text{F}_3\text{N}_2\text{O}^+$ 293.0896, found 293.0895.

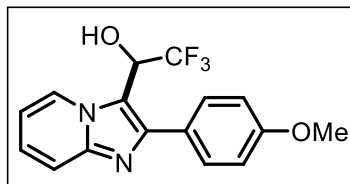
2,2,2-Trifluoro-1-(2-(p-tolyl)imidazo[1,2-a]pyridin-3-yl)ethan-1-ol (**25ba**): White solid; 104.0



mg, 68% yield; Eluent system: EtOAc:hexanes (1.5:8.5); mp = 186-188 °C; ^1H NMR (400 MHz, CDCl_3) δ = 8.55 (t, J = 5.8 Hz, 1H), 7.45 – 7.42 (m, 1H), 7.38 (t, J = 6.8 Hz, 2H), 7.13 – 7.09 (m, 3H), 6.90 – 6.89 (m, 1H), 6.68 (q, J = 6.3 Hz, 1H), 5.47 – 5.42 (m,

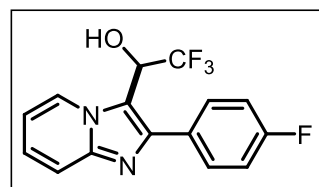
1H), 2.26 (s, 3H); $^{13}\text{C}\{^1\text{H}\}$ NMR (100 MHz, CDCl_3) δ = 146.3, 145.7, 137.9, 130.7, 129.2, 128.6, 127.7 (C-F, $^4J_{\text{C-F}}$ = 3.5 Hz), 127.7, 125.4 (C-F, $^1J_{\text{C-F}}$ = 282.3 Hz), 125.4, 116.9, 114.0, 111.9, 65.8 (C-F, $^2J_{\text{C-F}}$ = 33.2 Hz), 21.2; ^{19}F NMR (376 MHz, CDCl_3) δ = -74.55 (s, 3F); HRMS (ESI) m/z : $[\text{M} + \text{H}]^+$ calcd for $\text{C}_{16}\text{H}_{14}\text{F}_3\text{N}_2\text{O}^+$ 307.1053, found 307.1027.

2,2,2-Trifluoro-1-(2-(4-methoxyphenyl)imidazo[1,2-a]pyridin-3-yl)ethan-1-ol (25ca): White



solid; 106.3 mg, 66% yield; Eluent system: EtOAc:hexanes (2:8); mp = 190-192 °C; ^1H NMR (400 MHz, $\text{DMSO-}d_6$) δ = 8.65 (d, J = 7.2 Hz, 1H), 7.65 (t, J = 9.4 Hz, 3H), 7.42 (d, J = 5.2 Hz, 1H), 7.40 – 7.36 (m, 1H), 7.10 (d, J = 8.8 Hz, 2H), 7.03 – 6.99 (m, 1H),

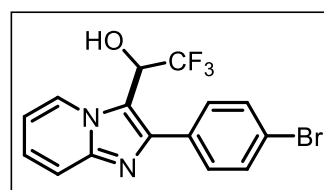
5.70 – 5.63 (m, 1H), 3.83 (s, 3H); $^{13}\text{C}\{^1\text{H}\}$ NMR (100 MHz, $\text{DMSO-}d_6$) δ = 159.8, 145.8, 145.6, 130.2, 127.7 (C-F, $^4J_{\text{C-F}}$ = 3.0 Hz), 126.3, 126.3, 125.9 (C-F, $^1J_{\text{C-F}}$ = 282.3 Hz), 117.3, 114.7, 113.4, 112.9, 65.6 (C-F, $^2J_{\text{C-F}}$ = 32.7 Hz), 55.6; ^{19}F NMR (376 MHz, $\text{DMSO-}d_6$) δ = -73.83 (d, J = 7.9 Hz, 3F); HRMS (ESI) m/z : $[\text{M} + \text{H}]^+$ calcd for $\text{C}_{16}\text{H}_{14}\text{F}_3\text{N}_2\text{O}_2^+$ 323.1002, found 323.0987.



2,2,2-Trifluoro-1-(2-(4-fluorophenyl)imidazo[1,2-a]pyridin-3-yl)ethan-1-ol (25da): White solid; 108.5 mg, 70% yield; Eluent system: EtOAc:hexanes (2:8); mp = 209-211 °C; ^1H NMR (400 MHz, $\text{DMSO-}d_6$) δ = 8.68 (d, J = 6.8 Hz, 1H), 7.76 – 7.72 (m, 2H), 7.68

(d, J = 8.8 Hz, 1H), 7.45 (d, J = 5.6 Hz, 1H), 7.41 – 7.34 (m, 3H), 7.05 – 7.01 (m, 1H), 5.72 – 5.65 (m, 1H); $^{13}\text{C}\{^1\text{H}\}$ NMR (100 MHz, $\text{DMSO-}d_6$) δ = 163.8, 161.4, 145.6, 145.0, 131.0 (C-F, $^3J_{\text{C-F}}$ = 8.3 Hz), 130.5 (C-F, $^4J_{\text{C-F}}$ = 3.0 Hz), 127.8 (C-F, $^4J_{\text{C-F}}$ = 2.5 Hz), 125.9 (C-F, $^1J_{\text{C-F}}$ = 282.5 Hz), 126.5, 117.5, 116.2, 116.0, 114.0, 113.1, 65.5 (C-F, $^2J_{\text{C-F}}$ = 32.6 Hz); ^{19}F NMR (376 MHz, $\text{DMSO-}d_6$) δ = -73.98 (s, 3F), -113.77 (s, 1H); HRMS (ESI) m/z : $[\text{M} + \text{H}]^+$ calcd for $\text{C}_{15}\text{H}_{11}\text{F}_4\text{N}_2\text{O}^+$ 311.0802, found 311.0791.

1-(2-(4-Bromophenyl)imidazo[1,2-a]pyridin-3-yl)-2,2,2-trifluoroethan-1-ol (25ea): White

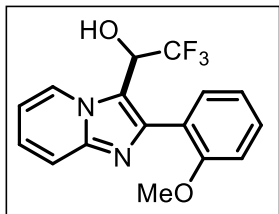


solid; 141.0 mg, 76% yield; Eluent system: EtOAc:hexanes (3:7); mp = 206-208 °C; ^1H NMR (400 MHz, $\text{DMSO-}d_6$) δ = 8.68 (d, J = 7.2 Hz, 1H), 7.75 – 7.72 (m, 2H), 7.70 – 7.65 (m, 3H), 7.45 (d, J = 5.2 Hz, 1H), 7.43 – 7.39 (m, 1H), 7.04 (dt, J = 6.8, 1.2 Hz, 1H),

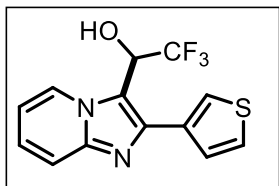
5.75 – 5.68 (m, 1H); $^{13}\text{C}\{^1\text{H}\}$ NMR (100 MHz, $\text{DMSO-}d_6$) δ = 145.7, 144.6, 133.2 (C-F, $^4J_{\text{C-F}}$ = 1.7 Hz), 132.2, 131.0, 127.8 (C-F, $^4J_{\text{C-F}}$ = 2.3 Hz), 125.8 (C-F, $^1J_{\text{C-F}}$ = 283.1 Hz), 126.8, 122.3,

117.4, 114.3, 113.3, 65.4 (C-F, $^2J_{C-F} = 32.3$ Hz); ^{19}F NMR (376 MHz, DMSO- d_6) $\delta = -74.12$ (s, 3F); HRMS (ESI) m/z : $[\text{M} + \text{H}]^+$ calcd for $\text{C}_{15}\text{H}_{11}\text{BrF}_3\text{N}_2\text{O}^+$ 371.0001, found 370.9971.

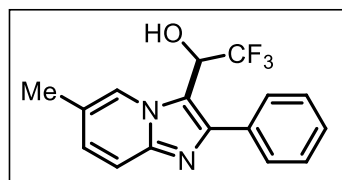
2,2,2-Trifluoro-1-(2-(2-methoxyphenyl)imidazo[1,2-a]pyridin-3-yl)ethan-1-ol (25fa): White solid; 109.5 mg, 68% yield; Eluent system: EtOAc:hexanes (2:8); mp = 206-208 °C; ^1H NMR (400 MHz, CDCl_3) $\delta = 8.64$ (d, $J = 7.2$ Hz, 1H), 7.52 (d, $J = 9.2$ Hz, 1H), 7.34 – 7.30 (m, 1H), 7.28 – 7.26 (m, 1H), 7.23 (ddd, $J = 9.0, 6.8, 1.1$ Hz, 1H), 6.90 – 6.86 (m, 2H), 6.82 (td, $J = 6.8, 1.2$ Hz, 1H), 5.48 (q, $J = 7.8$ Hz, 1H), 3.59 (s, 3H); $^{13}\text{C}\{^1\text{H}\}$ NMR (100 MHz, CDCl_3) $\delta = 156.4, 145.9, 143.2, 132.1, 130.0, 127.1$ (C-F, $^4J_{C-F} = 3.3$ Hz), 125.5, 124.9 (C-F, $^1J_{C-F} = 281.9$ Hz), 122.1, 120.8, 117.0, 115.0, 112.3, 111.1, 66.4 (C-F, $^2J_{C-F} = 33.8$ Hz), 55.4; ^{19}F NMR (376 MHz, CDCl_3) $\delta = -75.28$ (s, 3F); HRMS (ESI) m/z : $[\text{M} + \text{H}]^+$ calcd for $\text{C}_{16}\text{H}_{14}\text{F}_3\text{N}_2\text{O}_2^+$ 323.1002, found 323.0994.



2,2,2-Trifluoro-1-(2-(thiophen-3-yl)imidazo[1,2-a]pyridin-3-yl)ethan-1-ol (25ga): White solid; 120.7 mg, 81% yield; Eluent system: EtOAc:hexanes (1.5:8.5); mp = 220-222 °C; ^1H NMR (400 MHz, DMSO- d_6) $\delta = 8.67$ (d, $J = 6.8$ Hz, 1H), 7.81 (dd, $J = 2.8, 1.2$ Hz, 1H), 7.71 – 7.70 (m, 1H), 7.65 (d, $J = 9.2$ Hz, 1H), 7.55 (dd, $J = 5.2, 1.2$ Hz, 1H), 7.43 (d, $J = 5.6$ Hz, 1H), 7.37 (ddd, $J = 9.0, 6.8, 1.1$ Hz, 1H), 7.01 (td, $J = 6.8, 1.1$ Hz, 1H), 5.86 – 5.79 (m, 1H); $^{13}\text{C}\{^1\text{H}\}$ NMR (100 MHz, DMSO- d_6) $\delta = 145.6, 141.1, 134.4, 128.2, 127.6$ (C-F, $^4J_{C-F} = 2.8$ Hz), 127.5, 127.0, 125.8 (C-F, $^1J_{C-F} = 282.0$ Hz), 124.5, 117.0, 113.6, 113.3, 65.3 (C-F, $^2J_{C-F} = 32.8$ Hz); ^{19}F NMR (376 MHz, DMSO- d_6) $\delta = -69.82$ (s, 3F); HRMS (ESI) m/z : $[\text{M} + \text{H}]^+$ calcd for $\text{C}_{13}\text{H}_{10}\text{F}_3\text{N}_2\text{OS}^+$ 299.0460, found 299.0453.

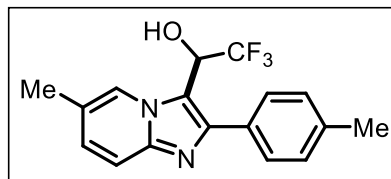


2,2,2-Trifluoro-1-(6-methyl-2-phenylimidazo[1,2-a]pyridin-3-yl)ethan-1-ol (25ha): White solid; 96.4 mg, 63% yield; Eluent system: EtOAc:hexanes (1.5:8.5); mp = 234-236 °C; ^1H NMR (400 MHz, DMSO- d_6) $\delta = 8.45$ (s, 1H), 7.69 – 7.67 (m, 2H), 7.60 (d, $J = 9.2$ Hz, 1H), 7.52 (t, $J = 7.6$ Hz, 2H), 7.46 – 7.42 (m, 1H), 7.41 (d, $J = 5.6$ Hz, 1H), 7.26 (dd, $J = 9.2, 1.6$ Hz, 1H), 5.69 – 5.61 (m, 1H), 2.34 (s, 3H); $^{13}\text{C}\{^1\text{H}\}$ NMR (100 MHz, DMSO- d_6) $\delta = 145.8, 144.8, 134.2, 129.3, 129.1, 128.9, 128.6, 127.4, 125.0$ (C-F, $^1J_{C-F} = 280.0$ Hz), 124.6, 122.1, 117.0, 113.8, 65.6 (C-F, $^2J_{C-F} = 32.5$ Hz), 18.3; ^{19}F NMR (376 MHz, DMSO-



d) $\delta = -73.74$ (s, 3F); HRMS (ESI) m/z : $[M + H]^+$ calcd for $C_{16}H_{14}F_3N_2O^+$ 307.1053, found 307.1026.

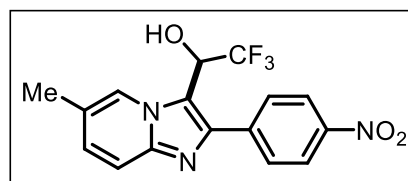
2,2,2-Trifluoro-1-(6-methyl-2-(p-tolyl)imidazo[1,2-a]pyridin-3-yl)ethan-1-ol (25ia): White



solid; 118.4 mg, 74% yield; Eluent system: EtOAc:hexanes (1.5:8.5); mp = 234-236 °C; 1H NMR (400 MHz, DMSO- d_6) $\delta = 8.53$ (d, $J = 7.1$ Hz, 1H), 7.57 (d, $J = 7.8$ Hz, 2H), 7.45 – 7.39 (m, 2H), 7.32 (d, $J = 7.8$ Hz, 2H), 6.86 (dd, $J = 7.1, 1.8$

Hz, 1H), 5.67 – 5.60 (m, 1H), 2.39 (s, 3H), 2.38 (s, 3H); $^{13}C\{^1H\}$ NMR (100 MHz, DMSO- d_6) $\delta = 146.1, 145.8, 138.0, 136.8, 131.4, 129.7, 128.7, 126.9$ (C-F, $^4J_{C-F} = 3.0$ Hz), 126.0 (C-F, $^1J_{C-F} = 282.3$ Hz), 115.6, 115.4, 113.2, 65.6 (C-F, $^2J_{C-F} = 32.3$ Hz), 21.3, 21.2; ^{19}F NMR (376 MHz, DMSO- d_6) $\delta = -69.18$ (s, 3F); HRMS (ESI) m/z : $[M + H]^+$ calcd for $C_{17}H_{16}F_3N_2O^+$ 321.1209, found 321.1212.

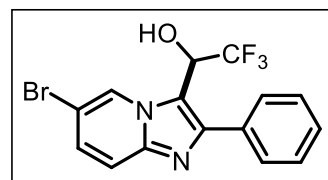
2,2,2-Trifluoro-1-(6-methyl-2-(4-nitrophenyl)imidazo[1,2-a]pyridin-3-yl)ethan-1-ol (25ja):



White solid; 143.5 mg, 69% yield; Eluent system: EtOAc:hexanes (2:8); mp = 254-256 °C; 1H NMR (400 MHz, DMSO- d_6) $\delta = 8.61$ (d, $J = 6.8$ Hz, 1H), 8.36 (d, $J = 8.8$ Hz, 2H), 8.02 (d, $J = 8.8$ Hz, 2H), 7.53 (d, $J = 5.2$ Hz,

1H), 7.49 (s, 1H), 6.92 (dd, $J = 7.2, 1.2$ Hz, 1H), 5.82 (dt, $J = 13.3, 6.7$ Hz, 1H), 2.40 (s, 3H); $^{13}C\{^1H\}$ NMR (100 MHz, DMSO- d_6) $\delta = 147.4, 146.3, 143.1, 140.8, 137.7, 129.9, 127.0$ (C-F, $^4J_{C-F} = 2.1$ Hz), 125.8 (C-F, $^1J_{C-F} = 282.6$ Hz), 124.3, 116.1, 115.9, 115.1, 65.3 (C-F, $^2J_{C-F} = 32.2$ Hz), 21.2; ^{19}F NMR (376 MHz, DMSO- d_6) $\delta = -74.22$ (d, $J = 7.9$ Hz); HRMS (ESI) m/z : $[M + H]^+$ calcd for $C_{16}H_{13}F_3N_3O_3^+$ 352.0904, found 352.0879.

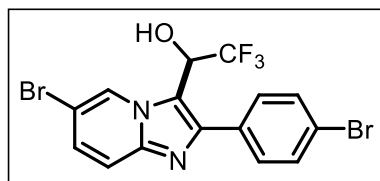
1-(6-Bromo-2-phenylimidazo[1,2-a]pyridin-3-yl)-2,2,2-trifluoroethan-1-ol (25ka): White



solid; 150.2 mg, 81% yield; Eluent system: EtOAc:hexanes (3:7); mp = 228-230 °C; 1H NMR (400 MHz, DMSO- d_6) $\delta = 8.81$ (s, 1H), 7.71 (d, $J = 8.8$ Hz, 3H), 7.56 – 7.52 (m, 3H), 7.48 (d, $J = 7.2$ Hz, 1H), 5.76 (q, $J = 8.0$ Hz, 1H); $^{13}C\{^1H\}$ NMR (100 MHz, DMSO-

d_6) $\delta = 146.6, 144.2, 133.5, 129.3, 129.3, 129.0, 128.9, 127.1$ (C-F, $^4J_{C-F} = 2.7$ Hz), 126.1 (C-F, $^1J_{C-F} = 236.8$ Hz), 118.8, 114.7, 106.9, 65.2 (C-F, $^2J_{C-F} = 35.6$ Hz); ^{19}F NMR (376 MHz, DMSO- d_6) $\delta = -73.74$ (s, 3F); HRMS (ESI) m/z : $[M + H]^+$ calcd for $C_{15}H_{11}BrF_3N_2O^+$ 371.0001 found 370.9980.

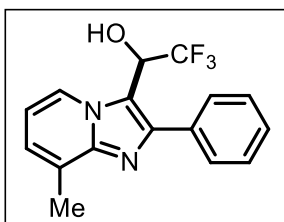
1-(6-Bromo-2-(4-bromophenyl)imidazo[1,2-a]pyridin-3-yl)-2,2,2-trifluoroethan-1-ol (25la):



White solid; 180.0 mg, 80% yield; Eluent system: EtOAc:hexanes (3.5:6.5); mp = 202-204 °C; ^1H NMR (400 MHz, DMSO- d_6) δ = 8.85 (s, 1H), 7.77 – 7.69 (m, 5H), 7.63 (d, J = 5.6 Hz, 1H), 7.58 (dd, J = 9.6, 1.6 Hz, 1H), 5.84 – 5.77 (m, 1H);

$^{13}\text{C}\{^1\text{H}\}$ NMR (100 MHz, DMSO- d_6) δ = 145.3, 144.2, 132.8, 132.2, 131.0, 129.6, 127.1 (C-F, $^4J_{\text{C-F}}$ = 1.7 Hz), 123.0 (C-F, $^1J_{\text{C-F}}$ = 261.8 Hz), 122.5, 118.9, 115.0, 107.2, 65.4 – 65.1 (m); ^{19}F NMR (376 MHz, DMSO- d_6) δ = -74.25 (s, 3F); HRMS (ESI) m/z : $[\text{M} + \text{H}]^+$ calcd for $\text{C}_{15}\text{H}_{10}\text{Br}_2\text{F}_3\text{N}_2\text{O}^+$ 448.9106, found 448.9081.

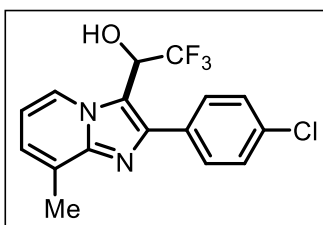
2,2,2-Trifluoro-1-(8-methyl-2-phenylimidazo[1,2-a]pyridin-3-yl)ethan-1-ol (25ma): White



solid; 114.8 mg, 75% yield; Eluent system: EtOAc:hexanes (3:7); mp = 236-238 °C; ^1H NMR (400 MHz, DMSO- d_6) δ = 8.52 (d, J = 6.8 Hz, 1H), 7.70 – 7.68 (m, 2H), 7.53 (t, J = 7.4 Hz, 2H), 7.48 – 7.44 (m, 1H), 7.41 (d, J = 5.6 Hz, 1H), 7.20 (d, J = 6.8 Hz, 1H), 6.93 (t, J = 7.0 Hz, 1H), 5.69 – 5.62 (m, 1H), 2.6 (s, 3H); $^{13}\text{C}\{^1\text{H}\}$ NMR (100 MHz,

DMSO- d_6) δ = 146.1, 145.5, 134.2, 129.1, 129.0, 128.6, 127.0, 125.9 (C-F, $^1J_{\text{C-F}}$ = 282.6 Hz), 125.5 (C-F, $^4J_{\text{C-F}}$ = 3.2 Hz), 124.8, 114.5, 112.9, 65.6 (C-F, $^2J_{\text{C-F}}$ = 32.5 Hz), 17.1; ^{19}F NMR (376 MHz, DMSO- d_6) δ = -73.84 (d, J = 8.1 Hz, 3F); HRMS (ESI) m/z : $[\text{M} + \text{H}]^+$ calcd for $\text{C}_{16}\text{H}_{14}\text{F}_3\text{N}_2\text{O}^+$ 307.1053, found 307.1044.

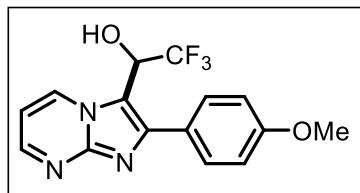
1-(2-(4-Chlorophenyl)-8-methylimidazo[1,2-a]pyridin-3-yl)-2,2,2-trifluoroethan-1-ol (25na):



White solid; 134.0 mg, 79% yield; Eluent system: EtOAc:hexanes (3.5:6.5); mp = 270-272 °C; ^1H NMR (400 MHz, DMSO- d_6) δ = 8.54 (d, J = 6.8 Hz, 1H), 7.75 – 7.73 (m, 2H), 7.61 – 7.58 (m, 2H), 7.44 (d, J = 5.2 Hz, 1H), 7.21 (d, J = 7.2 Hz, 1H), 6.94 (t, J = 7.0 Hz, 1H), 5.68 (dt, J = 8.0, 5.6 Hz, 1H), 2.54 (s, 3H); $^{13}\text{C}\{^1\text{H}\}$ NMR

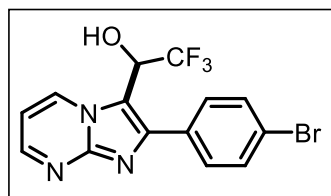
(100 MHz, DMSO- d_6) δ = 146.1, 144.1, 133.4, 133.1, 130.7, 129.2, 127.0, 125.9 (C-F, $^1J_{\text{C-F}}$ = 282.7 Hz), 125.5 (C-F, $^4J_{\text{C-F}}$ = 2.4 Hz), 125.0, 114.8, 113.1, 65.5 (C-F, $^2J_{\text{C-F}}$ = 32.5 Hz), 17.1; ^{19}F NMR (376 MHz, DMSO- d_6) δ = -73.99 (d, J = 8.0 Hz, 3F); HRMS (ESI) m/z : $[\text{M} + \text{H}]^+$ calcd for $\text{C}_{16}\text{H}_{13}\text{ClF}_3\text{N}_2\text{O}^+$ 341.0663, found 341.0641.

2,2,2-Trifluoro-1-(2-(4-methoxyphenyl)imidazo[1,2-a]pyrimidin-3-yl)ethan-1-ol (25oa):



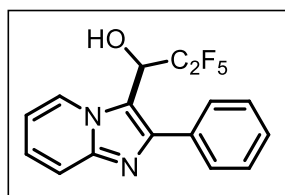
White solid; 87.2 mg, 54% yield; Eluent system: EtOAc:hexanes (2:8); mp = 218-220 °C; ^1H NMR (400 MHz, DMSO- d_6) δ = 9.01 (d, J = 6.8 Hz, 1H), 8.65 (dd, J = 4.0, 2.0 Hz, 1H), 7.68 (d, J = 8.8 Hz, 2H), 7.54 (d, J = 5.2 Hz, 1H), 7.17 (dd, J = 7.0, 4.2 Hz, 1H), 7.12 (d, J = 8.4 Hz, 2H), 5.78 – 5.67 (m, 1H), 3.83 (s, 3H); $^{13}\text{C}\{^1\text{H}\}$ NMR (100 MHz, DMSO- d_6) δ = 160.1, 151.7, 148.5, 146.7, 135.9 (C-F, $^4J_{\text{C-F}}$ = 2.9 Hz), 130.3, 125.9 (C-F, $^1J_{\text{C-F}}$ = 282.5 Hz), 125.7, 124.5, 114.8, 112.1, 109.6, 65.5 (C-F, $^2J_{\text{C-F}}$ = 32.5 Hz), 55.7; ^{19}F NMR (376 MHz, DMSO- d_6) δ = -74.18 (d, J = 7.5 Hz, 3F); HRMS (ESI) m/z : $[\text{M} + \text{H}]^+$ calcd for $\text{C}_{15}\text{H}_{13}\text{F}_3\text{N}_3\text{O}_2^+$ 324.0954, found 324.0941.

1-(2-(4-Bromophenyl)imidazo[1,2-a]pyrimidin-3-yl)-2,2,2-trifluoroethan-1-ol (25pa): White



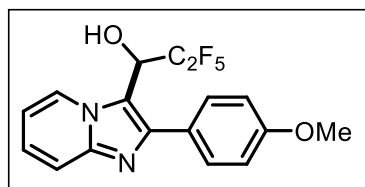
solid; 87.4 mg, 47% yield; Eluent system: EtOAc:hexanes (3:7); mp = 212-214 °C; ^1H NMR (400 MHz, DMSO- d_6) δ = 9.06 (d, J = 6.8 Hz, 1H), 8.69 (dd, J = 4.0, 2.0 Hz, 1H), 7.76 – 7.70 (m, 4H), 7.58 (d, J = 5.2 Hz, 1H), 7.20 (dd, J = 6.8, 4.0 Hz, 1H), 5.82 – 5.75 (m, 1H); $^{13}\text{C}\{^1\text{H}\}$ NMR (100 MHz, DMSO- d_6) δ = 152.3, 148.6, 145.4, 136.1 (C-F, $^4J_{\text{C-F}}$ = 2.6 Hz), 132.7, 132.3, 131.0, 125.8 (C-F, $^1J_{\text{C-F}}$ = 282.1 Hz), 122.7, 113.1, 109.9, 65.3 (C-F, $^2J_{\text{C-F}}$ = 32.5 Hz); ^{19}F NMR (376 MHz, DMSO- d_6) δ = -74.32 (d, J = 7.5 Hz, 3F); HRMS (ESI) m/z : $[\text{M} + \text{H}]^+$ calcd for $\text{C}_{14}\text{H}_{10}\text{BrF}_3\text{N}_3\text{O}^+$ 371.9954, found 371.9942.

2,2,3,3,3-Pentafluoro-1-(2-phenylimidazo[1,2-a]pyridin-3-yl)propan-1-ol (25ab): White solid;



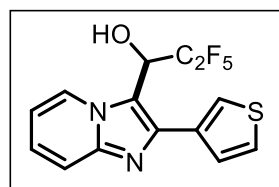
124.8 mg, 73% yield; Eluent system: EtOAc:hexanes (2.5:7.5); mp = 208-210 °C; ^1H NMR (400 MHz, DMSO- d_6) δ = 8.67 (d, J = 5.6 Hz, 1H), 7.72 – 7.64 (m, 4H), 7.54 (t, J = 7.4 Hz, 2H), 7.49 – 7.45 (m, 3H), 7.44 – 7.38 (m, 2H), 7.05 (td, J = 6.9, 1.3 Hz, 1H), 5.77 (dt, J = 24.4, 5.8 Hz, 1H); $^{13}\text{C}\{^1\text{H}\}$ NMR (100 MHz, DMSO- d_6) δ = 146.4, 145.9, 134.1, 129.2, 128.8 (C-F, $^4J_{\text{C-F}}$ = 1.8 Hz), 128.8, 127.8, 127.7, 126.5, 117.6, 113.8, 113.1, 64.7 (dd, $^2J_{\text{C-F}}$ = 28.6, 21.2 Hz); ^{19}F NMR (376 MHz, DMSO- d_6) δ = -81.16 (s, 3F), -116.14 (dd, J = 271.1, 6.1 Hz, 1F), -125.46 (ddd, J = 271.2, 24.0, 2.9 Hz, 1F); HRMS (ESI) m/z : $[\text{M} + \text{H}]^+$ calcd for $\text{C}_{16}\text{H}_{12}\text{F}_5\text{N}_2\text{O}^+$ 343.0864, found 343.0838.

2,2,3,3,3-Pentafluoro-1-(2-(4-methoxyphenyl)imidazo[1,2-a]pyridin-3-yl)propan-1-ol (25cb):



White solid; 120.9 mg, 65% yield; Eluent system: EtOAc:hexanes (2:8); mp = 228-230 °C; ^1H NMR (400 MHz, DMSO- d_6) δ = 8.65 (dd, J = 7.4, 2.6 Hz, 1H), 7.67 (d, J = 8.8 Hz, 1H), 7.60 (d, J = 8.4 Hz, 2H), 7.45 (d, J = 5.2 Hz, 1H), 7.39 (t, J = 7.8 Hz, 1H), 7.10 (d, J = 8.4 Hz, 2H), 7.02 (t, J = 7.0 Hz, 1H), 5.75 (dt, J = 24.8, 5.4 Hz, 1H), 3.83 (s, 3H); $^{13}\text{C}\{^1\text{H}\}$ NMR (100 MHz, DMSO- d_6) δ = 159.8, 146.3, 145.8, 130.1, 130.1, 127.7, 127.6, 126.4, 126.3, 120.7, 117.4, 114.7, 113.2, 112.9, 64.7 (dd, $^2J_{\text{C-F}}$ = 28.8, 21.2 Hz), 55.7; ^{19}F NMR (376 MHz, DMSO- d_6) δ = -81.11 (s, 3F), -115.99 (d, J = 271.1 Hz, 1F), -125.56 (d, J = 271.1 Hz, 1F); HRMS (ESI) m/z : $[\text{M} + \text{H}]^+$ calcd for $\text{C}_{17}\text{H}_{14}\text{F}_5\text{N}_2\text{O}_2^+$ 373.0970, found 373.0945.

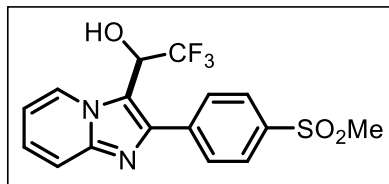
2,2,3,3,3-Pentafluoro-1-(2-(thiophen-3-yl)imidazo[1,2-a]pyridin-3-yl)propan-1-ol (25gb):



White solid; 125.3 mg, 72% yield; Eluent system: EtOAc:hexanes (2:8); mp = 214-216 °C; ^1H NMR (400 MHz, DMSO- d_6) δ = 8.66 (d, J = 6.9, Hz, 1H), 7.77 – 7.71 (m, 3H), 7.66 (d, J = 9.0 Hz, 1H), 7.48 (dd, J = 11.9, 4.6 Hz, 3H), 7.42 – 7.35 (m, 1H), 7.02 (t, J = 6.9 Hz, 1H), 5.89 (dd, J = 24.9, 5.4 Hz, 1H); $^{13}\text{C}\{^1\text{H}\}$ NMR (100 MHz, DMSO- d_6) δ = 145.8, 141.9, 135.9, 128.2, 127.7, 127.6, 127.5, 126.5, 124.2, 124.2, 117.4, 113.3, 113.0, 64.69 (dd, $^2J_{\text{C-F}}$ = 29.4, 21.4 Hz); ^{19}F NMR (376 MHz, DMSO- d_6) δ = -80.87 (s, 3F), -116.19 (d, J = 271.5 Hz, 1F), -126.12 (dd, J = 24.8, 24.4, 1F); HRMS (ESI) m/z : $[\text{M} + \text{H}]^+$ calcd for $\text{C}_{14}\text{H}_{10}\text{F}_5\text{N}_2\text{OS}^+$ 349.0429, found 349.0418.

4,4,4,4,4,4-Heptafluoro-1-(2-phenylimidazo[1,2-a]pyridin-3-yl)-4l8-but-2-yn-1-ol (25ac):

White solid; 109.8 mg, 56% yield; Eluent system: EtOAc:hexanes (2:8); mp = 224-226 °C; ^1H NMR (400 MHz, DMSO- d_6) δ = 8.69 (d, J = 4.3 Hz, 1H), 7.70 (d, J = 9.0 Hz, 1H), 7.68 – 7.63 (m, 3H), 7.53 (t, J = 7.4 Hz, 2H), 7.51 – 7.44 (m, 3H), 7.41 (ddd, J = 8.9, 6.8, 1.0 Hz, 2H), 7.04 (td, J = 6.9, 1.3 Hz, 1H), 5.83 (dt, J = 25.5, 5.2 Hz, 1H); $^{13}\text{C}\{^1\text{H}\}$ NMR (100 MHz, DMSO- d_6) δ = 146.5, 146.0, 134.1, 129.2, 128.8, 127.8, 127.7, 126.6, 117.6, 113.8, 113.1, 64.87 (dd, $^2J_{\text{C-F}}$ = 29.3, 21.2 Hz); ^{19}F NMR (376 MHz, DMSO- d_6) δ = -80.27 (t, J = 8.2 Hz, 3F), -113.46 (d, J = 277.9 Hz, 1F), -122.14 (dtd, J = 277.7, 15.7, 8.0 Hz, 1F), -124.75 (dt, J = 290.4, 7.2 Hz, 1F), -126.89 (ddd, J = 290.4, 10.7, 3.8 Hz, 1F); HRMS (ESI) m/z : $[\text{M} + \text{H}]^+$ calcd for $\text{C}_{17}\text{H}_{12}\text{F}_7\text{N}_2\text{O}^+$ 393.0832, found 393.0793.



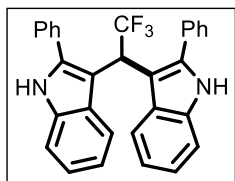
2,2,2-Trifluoro-1-(2-(4-(methylsulfonyl)phenyl)imidazo[1,2-a]pyridin-3-yl)ethan-1-ol (25qa): White solid; 116.6 mg, 63% yield; Eluent system: EtOAc:hexanes (1:1); mp = 236–238 °C; ^1H NMR (400 MHz, DMSO- d_6) δ = 8.73 (d, J = 6.5

Hz, 1H), 8.13 – 7.96 (m, 4H), 7.73 (d, J = 8.9 Hz, 1H), 7.53 (d, J = 5.0 Hz, 1H), 7.48 – 7.37 (m, 1H), 7.07 (t, J = 6.6 Hz, 1H), 5.89 – 5.74 (m, 1H), 3.30 (s, 3H); ^{13}C { ^1H } NMR (100 MHz, DMSO- d_6) δ = 145.9, 144.0, 140.6, 139.0, 129.7, 127.9, 127.2, 127.0, 124.4, 117.7, 115.2, 113.5, 65.4 (C-F, $^2J_{\text{C-F}}$ = 33.0 Hz), 55.3, 44.0; ^{19}F NMR (376 MHz, DMSO- d_6) δ = -74.10 (s, 3F); HRMS (ESI) m/z : $[\text{M} + \text{H}]^+$ calcd for $\text{C}_{16}\text{H}_{14}\text{F}_3\text{N}_2\text{O}_3\text{S}^+$ 371.0672, found 371.0683.

4.9.5 General Procedure for the Synthesis of 27 and 28

To a solution of **3aa** (0.5 mmol; 1.0 equiv.) in toluene (2 mL) was added **1a** or **26** (1.0 equiv.) and $\text{Yb}(\text{OTf})_3$ (10 mol%) at room temperature and the reaction mixture was stirred at 90 °C for 12 h in a sealed tube. After completion of the reaction monitored by TLC, the reaction mixture was allowed to attain room temperature. The reaction mixture was poured into water (20 mL) and extracted with ethyl acetate (3 \times 15 mL). The combined organic layer was dried over anhydrous Na_2SO_4 and evaporated under vacuum. The resulting crude was purified by column chromatography (silica gel 100-200 mesh) using EtOAc-hexanes as an eluent to afford **27** or **28**.

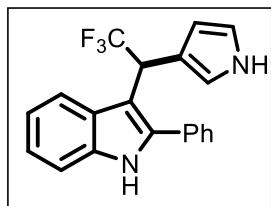
3,3'-(2,2,2-Trifluoroethane-1,1-diyl)bis(2-phenyl-1H-indole) (27): White solid; 139.8 mg, 60%



yield; R_f =0.4, Eluent system: EtOAc:hexanes (3.5:6.5); mp = 246–248 °C; ^1H NMR (400 MHz, DMSO- d_6) δ = 11.43 (s, 2H), 7.76 (d, J = 8.0 Hz, 2H), 7.36 (d, J = 8.4 Hz, 2H), 7.32 (d, J = 7.2 Hz, 2H), 7.27 (t, J = 7.2 Hz, 4H), 7.15 (d, J = 7.6 Hz, 4H), 7.10 (d, J = 7.6 Hz, 2H), 6.98 (t, J = 7.6 Hz, 2H),

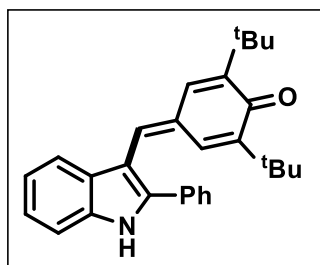
5.55 (q, J = 11.7 Hz, 1H); ^{13}C NMR (100 MHz, DMSO- d_6) δ = 143.0, 141.1, 137.5, 134.1, 133.6, 133.2, 131.6, 126.4, 125.5, 124.5, 116.6, 111.2; ^{19}F NMR (376 MHz, DMSO- d_6) δ = -61.97 (d, J = 12.0 Hz), -74.43 (d, J = 8.3 Hz) ppm; HRMS (ESI) m/z : $[\text{M} + \text{H}]^+$ calcd for $\text{C}_{30}\text{H}_{22}\text{F}_3\text{N}_2^+$ 467.1730, found 467.1712.

2-Phenyl-3-(2,2,2-trifluoro-1-(1H-pyrrol-3-yl)ethyl)-1H-indole (28) : White solid; 100.3 mg,



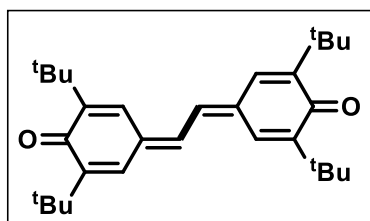
59% yield; $R_f = 0.3$, Eluent system: EtOAc:hexanes (3.5:6.5); mp = 210-212 °C; $^1\text{H NMR}$ (400 MHz, DMSO- d_6) $\delta = 8.32$ (s, 1H), 8.14 (s, 1H), 7.59 (d, $J = 8.0$ Hz, 1H), 7.53 – 7.52 (m, 3H), 7.50 (d, $J = 2.8$ Hz, 1H), 7.46 (d, $J = 8.4$ Hz, 1H), 7.30 – 7.26 (m, 1H) (with merged CDCl₃ peak), 7.16 (t, $J = 7.6$ Hz, 1H), 6.69 (q, $J = 2.4$ Hz, 1H), 6.31 (s, 1H), 6.22 (q, $J = 2.8$ Hz, 1H), 5.19 (q, $J = 9.6$ Hz, 1H); $^{13}\text{C NMR}$ (100 MHz, DMSO- d_6) $\delta = 138.9, 136.0, 131.7, 129.2, 128.9$ (C-F, $^4J_{\text{C-F}} = 2.3$ Hz), 128.0, 126.9, 125.2, 124.3, 122.8, 121.4 (C-F, $^4J_{\text{C-F}} = 3.3$ Hz), 120.7, 117.6, 111.1, 108.8, 108.2 (C-F, $^4J_{\text{C-F}} = 1.8$ Hz), 104.4 (C-F, $^4J_{\text{C-F}} = 2.3$ Hz), 41.4 (C-F, $^2J_{\text{C-F}} = 30.3$ Hz); $^{19}\text{F NMR}$ (376 MHz, DMSO- d_6) $\delta = -66.04$ (s, 3F) ppm; HRMS (ESI) m/z : $[\text{M} + \text{H}]^+$ calcd for C₂₀H₁₆F₃N₂⁺ 341.1260, found 341.1239.

2,6-Di-tert-butyl-4-((2-phenyl-1H-indol-3-yl)methylene)cyclohexa-2,5-dien-1-one (29): Red



solid; 58.3 mg, 55% yield; $R_f = 0.8$, Eluent system: EtOAc:hexanes (1:9); mp = 172-174 °C; $^1\text{H NMR}$ (400 MHz, DMSO- d_6) $\delta = 12.30$ (s, 1H), 7.69 – 7.66 (m, 3H), 7.60 (s, 1H), 7.56 (t, $J = 7.4$ Hz, 2H), 7.53 – 7.48 (m, 2H), 7.46 (d, $J = 2.0$ Hz, 1H), 7.31 (d, $J = 2.0$ Hz, 1H), 7.27 (d, $J = 2.0$ Hz, 1H), 7.21 – 7.17 (m, 1H), 1.30 (s, 9H), 1.12 (s, 9H); $^{13}\text{C}\{^1\text{H}\}$ NMR (100 MHz, DMSO- d_6) $\delta = 185.8, 159.7, 145.9, 145.2, 141.8, 140.0, 137.3, 136.0, 131.8, 130.5, 129.5, 129.3, 128.1, 127.6, 123.7, 121.4, 120.3, 112.7, 110.2, 35.2, 29.8$; HRMS (ESI) m/z : $[\text{M} + \text{H}]^+$ calcd for C₂₉H₃₂NO⁺ 410.2478, found 410.2484.

4,4'-(Ethane-1,2-diylidene)bis(2,6-di-tert-butylcyclohexa-2,5-dien-1-one) (30): Yellow solid;



36.0 mg, 32% yield; $R_f = 0.8$, Eluent system: EtOAc:hexanes (1:9); mp = 142-144 °C; $^1\text{H NMR}$ (400 MHz, CDCl₃) $\delta = 7.55$ (d, $J = 2.4$ Hz, 2H), 7.27 (s, 2H), 7.05 (d, $J = 2.4$ Hz, 2H), 1.40 (s, 18H), 1.36 (s, 18H); $^{13}\text{C}\{^1\text{H}\}$ NMR (100 MHz, CDCl₃) $\delta = 186.4, 150.1, 149.8, 136.1, 134.2, 133.4, 124.5, 35.8, 35.4, 29.7, 29.6$; HRMS (ESI) m/z : $[\text{M} + \text{H}]^+$ calcd for C₃₀H₄₃O₂⁺ 435.3258, found 435.3269.

4.4.6 X-ray Crystallographic Analysis of Compound 3ba, 3fa, 25aa, and 25ba

The crystal data collection and data reduction were performed using CrysAlis PRO on a single crystal Rigaku Oxford XtaLab Pro diffractometer. The crystal was kept at 93(2) K during data

collection. Using Olex2⁵², the structure was solved with the ShelXT⁵³ structure solution program using Intrinsic Phasing and refined with the ShelXL⁵⁴ refinement package using Least Squares minimization.

The single crystals of the compound **3ba** (C₁₇H₁₄F₃NO, **Figure 4.6**) and **3fa** (C₁₆H₁₁ClF₃NO, **Figure 4.7**) was obtained from slow evaporation. **3ba** was crystallized in triclinic crystal system with P-1 space group and **3fa** was crystallized in triclinic crystal system with P-1 space group. The crystal structure information of **3ba** and **3fa** is deposited to Cambridge Crystallographic Data Center and the CCDC numbers for the **3ba** is 2033964 and for **3fa** is 2033965.

Table 4.4: Crystal data and structure refinement for **3ba** and **3fa**

Identification code	3ba	3fa
Empirical formula	C ₁₇ H ₁₄ F ₃ NO	C ₁₆ H ₁₁ ClF ₃ NO
Formula weight	305.29	325.71
Temperature/K	93(2)	93(2)
Crystal system	triclinic	triclinic
Space group	P-1	P-1
a/Å	7.3286(2)	7.4247(3)
b/Å	8.0698(2)	7.7269(2)
c/Å	13.2600(3)	13.8749(2)
α/°	102.542(2)	94.305(2)
β/°	101.298(2)	98.646(2)
γ/°	105.440(2)	112.442(3)
Volume/Å ³	710.53(3)	719.67(4)
Z	2	2
ρ _{calc} /cm ³	1.427	1.503
μ/mm ⁻¹	0.988	2.684
F(000)	316.0	332.0
Crystal size/mm ³	0.15 × 0.12 × 0.1	0.15 × 0.08 × 0.05
Radiation	Cu Kα (λ = 1.54184)	Cu Kα (λ = 1.54184)
2θ range for data collection/°	7.092 to 158.01	12.526 to 159.754
Index ranges	-4 ≤ h ≤ 9, -10 ≤ k ≤ 7, -16 ≤ l ≤ 14	-7 ≤ h ≤ 9, -9 ≤ k ≤ 8, -17 ≤ l ≤ 17
Reflections collected	3824	6808
Independent reflections	2465 [R _{int} = 0.0206, R _{sigma} = 0.0287]	3023 [R _{int} = 0.0297, R _{sigma} = 0.0356]

Data/restraints/parameters	2465/0/201	3023/0/200
Goodness-of-fit on F^2	1.066	1.130
Final R indexes [$I \geq 2\sigma(I)$]	$R_1 = 0.0527$, $wR_2 = 0.1486$	$R_1 = 0.0395$, $wR_2 = 0.1110$
Final R indexes [all data]	$R_1 = 0.0546$, $wR_2 = 0.1523$	$R_1 = 0.0412$, $wR_2 = 0.1122$
Largest diff. peak/hole / $e \text{ \AA}^{-3}$	0.24/-0.43	0.36/-0.43

The single crystals of the compound **25aa** ($C_{15}H_{11}F_3N_2O$, **Figure 4.12**), and **25ba** ($C_{16}H_{13}F_3N_2O$, **Figure 4.13**) was obtained from slow evaporation of $CDCl_3$. **25aa** was crystallized in monoclinic crystal system with $P2_1/c$ space group and **25ba** was crystallized in orthorhombic crystal system with $Pna2_1$ space group. The crystal structure information of **25aa**, and **25ba** is deposited to Cambridge Crystallographic Data Center and the CCDC numbers for the **25aa** is 2033967 and for **25ba** is 2033968.

Table 4.5: Crystal data and structure refinement for **25aa** and **25ba**

Identification code	25aa	25ba
Empirical formula	$C_{15}H_{11}F_3N_2O$	$C_{16}H_{13}F_3N_2O$
Formula weight	292.26	306.28
Temperature/K	93(2)	93(2)
Crystal system	monoclinic	orthorhombic
Space group	$P2_1/c$	$Pna2_1$
$a/\text{\AA}$	11.8860(3)	18.8821(3)
$b/\text{\AA}$	9.2524(2)	7.45630(10)
$c/\text{\AA}$	12.6896(3)	19.7935(4)
$\alpha/^\circ$	90	90
$\beta/^\circ$	111.635(3)	90
$\gamma/^\circ$	90	90
Volume/ \AA^3	1297.21(6)	2786.74(8)
Z	4	8
$\rho_{\text{calc}}/\text{g/cm}^3$	1.496	1.460
μ/mm^{-1}	1.079	1.031
F(000)	600.0	1264.0
Crystal size/ mm^3	$0.1 \times 0.05 \times 0.05$	$0.15 \times 0.05 \times 0.03$
Radiation	$\text{Cu K}\alpha$ ($\lambda = 1.54184$)	$\text{Cu K}\alpha$ ($\lambda = 1.54184$)
2θ range for data collection/ $^\circ$	8.002 to 159.554	8.936 to 159.012

Index ranges	-14 ≤ h ≤ 15, -6 ≤ k ≤ 11, -16 ≤ l ≤ 15	-23 ≤ h ≤ 22, -4 ≤ k ≤ 9, -12 ≤ l ≤ 24
Reflections collected	6786	10447
Independent reflections	2750 [R _{int} = 0.0332, R _{sigma} = 0.0416]	4333 [R _{int} = 0.0339, R _{sigma} = 0.0505]
Data/restraints/parameters	2750/0/191	4333/1/402
Goodness-of-fit on F ²	1.089	1.051
Final R indexes [I ≥ 2σ (I)]	R ₁ = 0.0443, wR ₂ = 0.1278	R ₁ = 0.0979, wR ₂ = 0.2192
Final R indexes [all data]	R ₁ = 0.0478, wR ₂ = 0.1310	R ₁ = 0.1013, wR ₂ = 0.2273
Largest diff. peak/hole / e Å ⁻³	0.25/-0.32	1.67/-0.30

4.10 REFERENCES

1. Bemis, G. W.; Murcko, M. A., *Journal of Medicinal Chemistry* **1996**, *39*, 2887-2893.
2. Gibson, S.; McGuire, R.; Rees, D. C., *Journal of Medicinal Chemistry* **1996**, *39*, 4065-4072.
3. Ertl, P.; Jelfs, S.; Mühlbacher, J.; Schuffenhauer, A.; Selzer, P., *Journal of Medicinal Chemistry* **2006**, *49*, 4568-4573.
4. Broughton, H. B.; Watson, I. A., *Journal of Molecular Graphics and Modelling* **2004**, *23*, 51-58.
5. Lewell, X. Q.; Jones, A. C.; Bruce, C. L.; Harper, G.; Jones, M. M.; McLay, I. M.; Bradshaw, J., *Journal of Medicinal Chemistry* **2003**, *46*, 3257-3274.
6. Ritchie, T. J.; Macdonald, S. J. F.; Young, R. J.; Pickett, S. D., *Drug Discovery Today* **2011**, *16*, 164-171.
7. Ritchie, T. J.; Macdonald, S. J. F., *Drug Discovery Today* **2009**, *14*, 1011-1020.
8. Meanwell, N. A., *Journal of Medicinal Chemistry* **2011**, *54*, 2529-2591.
9. Müller, K.; Faeh, C.; Diederich, F., *Science* **2007**, *317*, 1881-1886.
10. Isanbor, C.; O'Hagan, D., *Journal of Fluorine Chemistry* **2006**, *127*, 303-319.
11. Nenajdenko, V., *Fluorine in Heterocyclic Chemistry Volume 1: 5-Membered Heterocycles and Macrocycles*. Springer2014; Vol. 1; pp 159-232.
12. Yang, W.; Pan, P.; Wang, H.; Cheng, X.; Du, Z., *Polymer International* **2018**, *67*, 1054-1061.
13. Tan, L.; He, Z.; Chen, Y., *RSC Advances* **2015**, *5*, 23213-23223.
14. Jeschke, P., *ChemBioChem* **2004**, *5*, 570-589.

15. Burriss, A.; Edmunds, A. J. F.; Emery, D.; Hall, R. G.; Jacob, O.; Schaezter, J., *Pest Management Science* **2018**, *74*, 1228-1238.
16. Xu, Z.; Hang, Z.; Chai, L.; Liu, Z.-Q., *Organic Letters* **2016**, *18*, 4662-4665.
17. Chen, J.; Li, M.; Zhang, J.; Sun, W.; Jiang, Y., *Organic Letters* **2020**, *22*, 3033-3038.
18. Cai, X.; Xu, J.; Cui, X.; Qu, J.; Sun, W.; Hu, J.; Zhao, S.; Chen, W.-H.; Li, H.; Wu, J.-Q., *Organic Chemistry Frontiers* **2022**, *9*, 6273-6280.
19. Geng, X.; Lin, F.; Wang, X.; Jiao, N., *Journal of Photochemistry and Photobiology A: Chemistry* **2018**, *355*, 194-201.
20. Sun, Q.; Pang, L.; Mao, S.; Fan, W.; Zhou, Y.; Xu, J.; Li, S.; Li, Q., *Synthesis* **2021**, *54*, 1353-1364.
21. Qin, H.; Zhang, Z.; Qiao, K.; Chen, X.; He, W.; Liu, C.; Yang, X.; Yang, Z.; Fang, Z.; Guo, K., *The Journal of Organic Chemistry* **2022**, *87*, 9128-9138.
22. Wu, L.; Song, Y.; Li, Z.; Guo, J.; Yao, X., *Advanced Synthesis & Catalysis* **2021**, *363*, 268-274.
23. Xie, Z.-Z.; Zheng, Y.; Yuan, C.-P.; Guan, J.-P.; Ye, Z.-P.; Xiao, J.-A.; Xiang, H.-Y.; Chen, K.; Chen, X.-Q.; Yang, H., *Angewandte Chemie Int. Ed.* **2022**, *61*, e202211035.
24. Thakur, A.; Gupta, S. S.; Dhiman, A. K.; Sharma, U., *The Journal of Organic Chemistry* **2023**, *88*, 2314-2321.
25. Liu, B.; Chen, X.; Pei, C.; Li, J.; Zou, D.; Wu, Y.; Wu, Y., *The Journal of Organic Chemistry* **2022**, *87*, 14364-14373.
26. Liu, J.; Yu, D.; Yang, Y.; You, H.; Sun, M.; Wang, Y.; Shen, X.; Liu, Z.-Q., *Organic Letters* **2020**, *22*, 4844-4847.
27. Jaspal, S.; Shinde, V. N.; Meena, N.; Nipate, D. S.; Rangan, K.; Kumar, A., *Organic & Biomolecular Chemistry* **2020**, *18*, 9072-9080.
28. Sonam; Shinde, V. N.; Rangan, K.; Kumar, A., *The Journal of Organic Chemistry* **2023**, *88*, 2344-2357.
29. Rafiee, M.; Miles, K. C.; Stahl, S. S., *Journal of the American Chemical Society* **2015**, *137*, 14751-14757.
30. Bruggeman, D. F.; Laporte, A. A. H.; Detz, R. J.; Mathew, S.; Reek, J. N. H., *Angewandte Chemie International Edition* **2022**, *61*, e202200175.

31. Melnyk, A. K.; Sukhoveev, O. V.; Kononets, L. A.; Khilchevsky, O. M.; Shulga, S. M.; Kukhar, V. P.; Vovk, A. I., *Journal of Liposome Research* **2016**, *26*, 80-86.
32. Abbasian, M.; Mahi, R., *Journal of Experimental Nanoscience* **2014**, *9*, 785-798.
33. Janoschka, T.; Morgenstern, S.; Hiller, H.; Friebe, C.; Wolkersdörfer, K.; Häupler, B.; Hager, M. D.; Schubert, U. S., *Polymer Chemistry* **2015**, *6*, 7801-7811.
34. Maji, M. S.; Pfeifer, T.; Studer, A., *Chemistry – A European Journal* **2010**, *16*, 5872-5875.
35. Vogler, T.; Studer, A., *Synthesis* **2008**, *2008*, 1979-1993.
36. Beejapur, H. A.; Zhang, Q.; Hu, K.; Zhu, L.; Wang, J.; Ye, Z., *ACS Catalysis* **2019**, *9*, 2777-2830.
37. Ma, Z.; Mahmudov, K. T.; Aliyeva, V. A.; Gurbanov, A. V.; Pombeiro, A. J. L., *Coordination Chemistry Reviews* **2020**, *423*, 213482.
38. Egami, H.; Ide, T.; Kawato, Y.; Hamashima, Y., *Chemical Communications* **2015**, *51*, 16675-16678.
39. Zhang, B.; Cui, Y.; Jiao, N., *Chemical Communications* **2012**, *48*, 4498-4500.
40. Zhou, W.; Ni, S.; Mei, H.; Han, J.; Pan, Y., *Organic Letters* **2015**, *17*, 2724-2727.
41. Fischer Indole Synthesis. In *Comprehensive Organic Name Reactions and Reagents*; pp 1069-1075.
42. Fischer, E. a. J., F., *Chemische Berichte* **1883**, *16*, 2241.
43. Takizawa, S.-y.; Nishida, J.-i.; Tsuzuki, T.; Tokito, S.; Yamashita, Y., *Inorganic Chemistry* **2007**, *46*, 4308-4319.

CHAPTER 5

**Selectfluor Mediated Regioselective
C3-Alkoxylation, Sulfenylation, Amination
and Selenylation of Quinoxalin-2(1*H*)-ones**

5.1 INTRODUCTION

Quinoxalin-2(1*H*)-one ring system is a highly important heterocyclic framework in organic chemistry due to its wide range of applications in the fields of drug discovery and agrochemicals.¹⁻² In particular, C3-substituted quinoxalin-2(1*H*)-ones have been extensively studied for their diverse biological activities. For instance, several studies have demonstrated that these compounds possess potent anti-tumor activity, making them promising candidates for the development of novel anticancer agents.³ In addition, C3-substituted quinoxalin-2(1*H*)-ones have also been investigated as inhibitors of aldose reductase, an enzyme that has been implicated in various diabetic complications.⁴ Another area where these compounds have shown promise is in the inhibition of serine/threonine kinase STK33, which has been identified as a potential therapeutic target for the treatment of several types of cancer.⁵ C3-substituted quinoxalin-2(1*H*)-ones have also been explored as inhibitors of blood coagulation factor Xa, an important target in the treatment of thromboembolic disorders.⁶ Furthermore, these compounds have been investigated as histamine-4 receptor antagonists, which could have potential applications in the treatment of allergic disorders. Thus, the wide range of biological activities exhibited by C3-substituted quinoxalin-2(1*H*)-ones highlights their potential as valuable lead compounds for the development of novel therapeutics in various fields. Some selected bioactive C3-substituted quinoxalin-2(1*H*)-ones are represented in **Figure 5.1**.

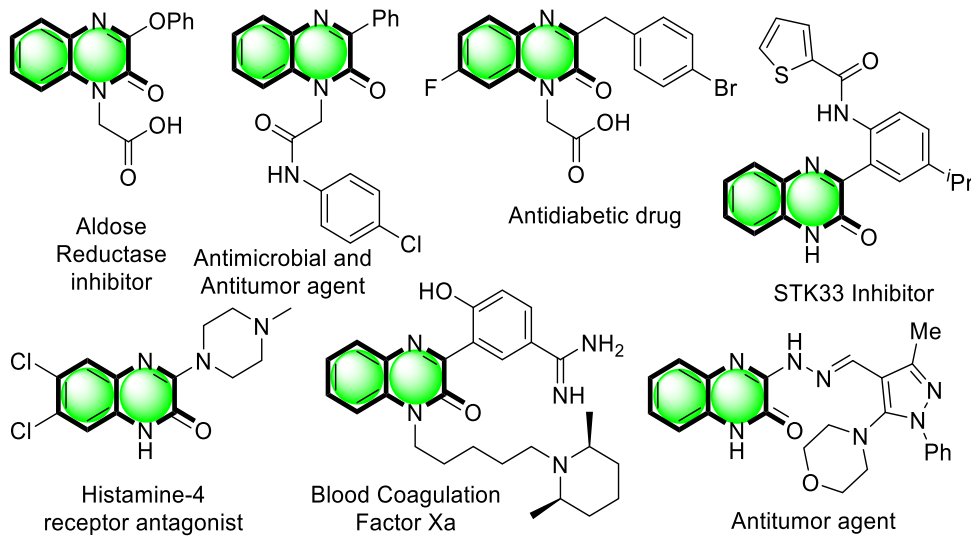


Figure 5.1 Biologically active C3-substituted quinoxalin-2(1*H*)-ones

Specified the importance of the quinoxalin-2(1*H*)-one ring system, significant efforts have been directed toward the development of sustainable and economical methods for its synthesis and

functionalization.⁷⁻⁸ In this context, direct activation/functionalization of C-H bonds at the C3 position has emerged as an important approach for constructing C3-substituted quinoxalin-2(1*H*)-ones. Over the past few years, several research groups have given considerable attention towards the synthesis of C3-substituted quinoxalin-2(1*H*)-ones through direct C-H arylation,⁹⁻¹⁰ alkylation,¹¹⁻¹⁴ acylation,¹⁵⁻¹⁶ alkoxylation,¹⁷ amination,¹⁸⁻¹⁹ amidation,²⁰ sulfenylation,²¹ and phosphorylation²² under transition-metal catalysis or photocatalysis (**Figure 5.2**). The utilization of direct C-H bond functionalization technique not only provide an environmentally friendly option to conventional methods but also enable more flexibility and versatility in the construction and modification of complex molecules.

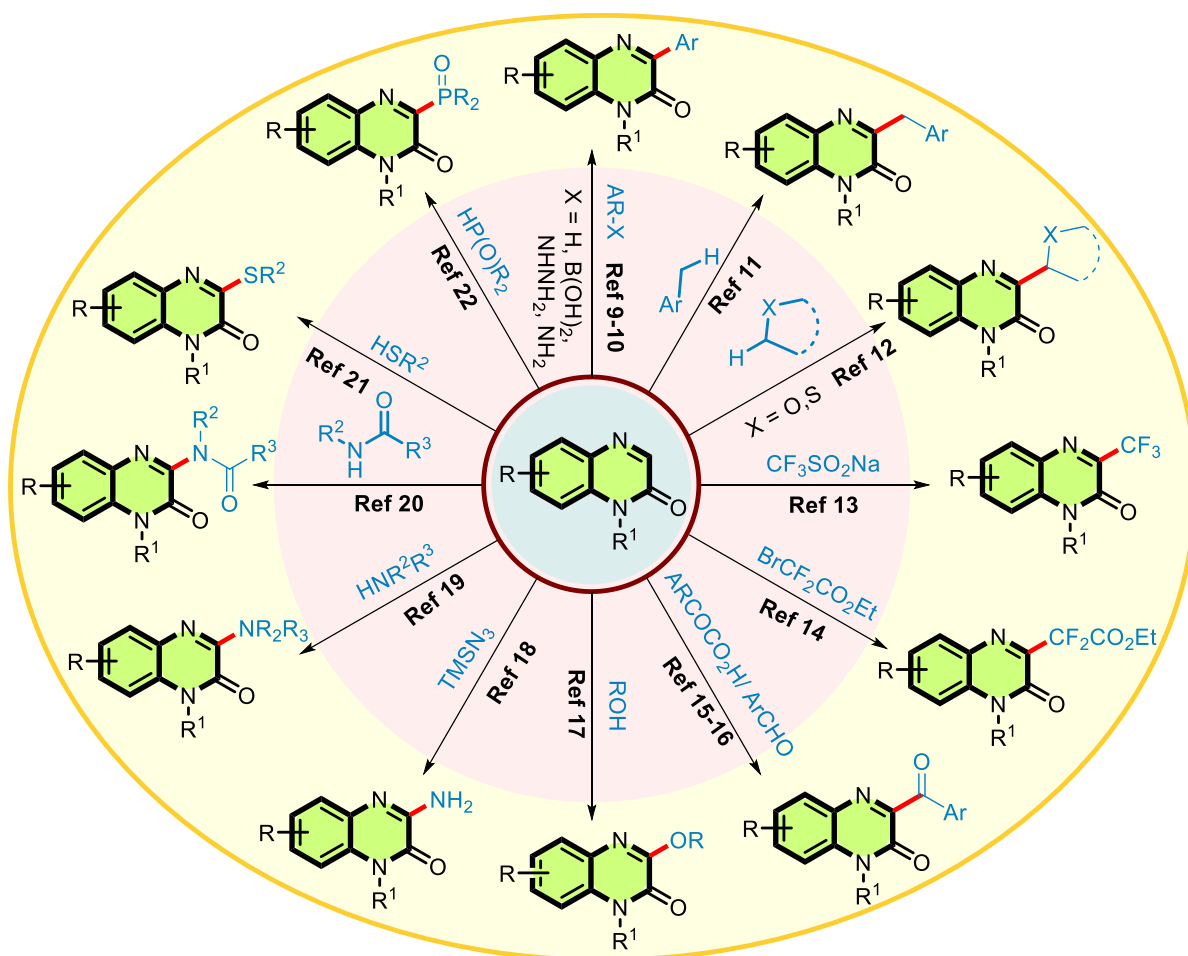
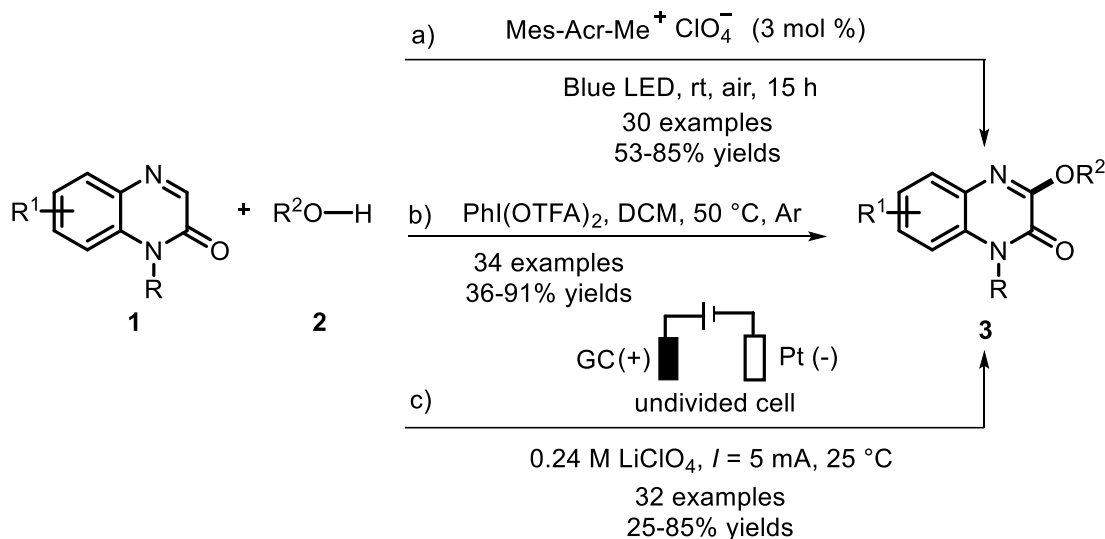


Figure 5.2 C3-Functionalization of quinoxalin-2(1*H*)-ones

Zhao and Xie have independently reported a facile approach for the alkoxylation of quinoxalin-2(1*H*)-ones (**1**) using alcohols (**2**) as the alkoxylation reagent and solvent under visible light irradiation to produce the 3-alkoxy quinoxalin-2(1*H*)-ones (**3**) (**Scheme 5.1a**).²³ The

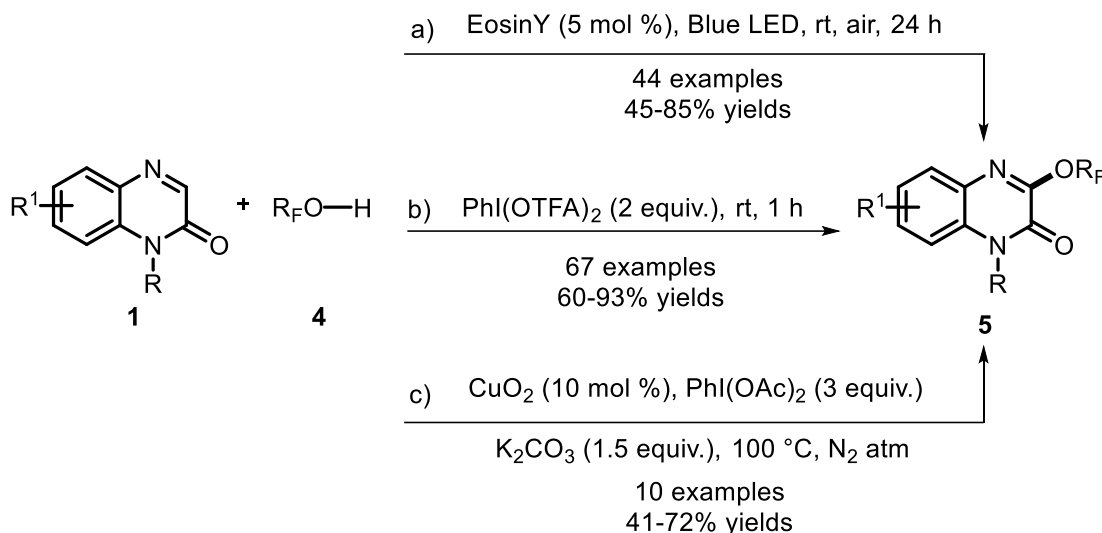
method offers tolerance to commercially available primary and secondary alcohols as reagent and solvent which makes the reaction economically attractive. The protocol exhibits excellent functional group compatibility providing a wide range of products. Similarly, Zhang group reported the synthesis of 3-alkoxylated quinoxalin-2(1*H*)-ones (**3**) *via* transition-metal free cross-dehydrogenative coupling of quinoxalin-2(1*H*)-ones (**1**) and alcohols (**2**) by utilizing $\text{PhI}(\text{OTFA})_2$ as an oxidant as well as radical initiator (**Scheme 5.1b**).¹⁷ Jiang *et al.* further explored the methodology and disclosed the electrochemical construction of the 3-alkoxylated quinoxalin-2(1*H*)-ones (**3**) from quinoxalin-2(1*H*)-ones (**1**) and alcohols (**2**). The metal- and oxidant- free conditions, broad substrate scope and vast functional group tolerance are some of the highlighting features of this method (**Scheme 5.1c**).²⁴



Scheme 5.1 Metal-free C3-alkoxylation of quinoxalin-2(1*H*)-ones

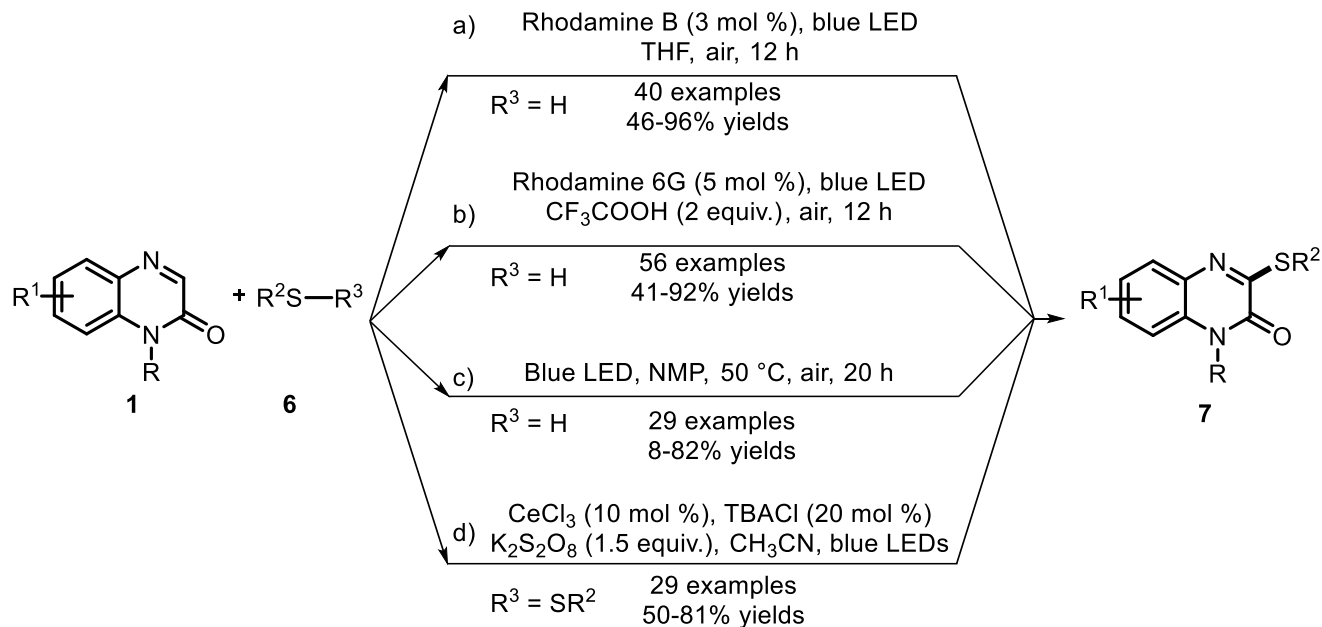
Xia group has developed a resourceful method for fluoroalkoxylation of quinoxalin-2(1*H*)-ones (**1**) at the C3 position under visible light irradiation. This approach employs readily available fluoroalkyl alcohols (**4**) as fluoroalkoxylation reagents, allowing a wide range of substrates to provide moderate to good yields of fluoroalkoxylated products (**5**) (**Scheme 5.2a**).²⁵ This transformation utilizes oxygen as an oxidant, making it more environmentally friendly. Control experiments suggested a radical mechanism for the reaction. Alternatively, Zhang *et al.* reported the synthesis of fluoroalkoxylated products (**5**) through $\text{PhI}(\text{TFA})_2$ mediated SET process. The developed method involved generation of alkoxy radical from (**4**) in the presence of $\text{PhI}(\text{TFA})_2$ which on reaction with (**1**) followed by deprotonation resulted the desired product in excellent

yields (**Scheme 5.2b**).²⁶ Subsequently, Su *et al.* developed a copper-catalyzed cross-dehydrogenative coupling of quinoxalin-2(1*H*)-ones (**1**) and fluoroalkyl alcohol, HFIP (**4**) in the presence of PhI(OAc)₂ as an external oxidizing agent to afford the corresponding fluoroalkylated products (**5**) in average yields (**Scheme 5.2c**).²⁷



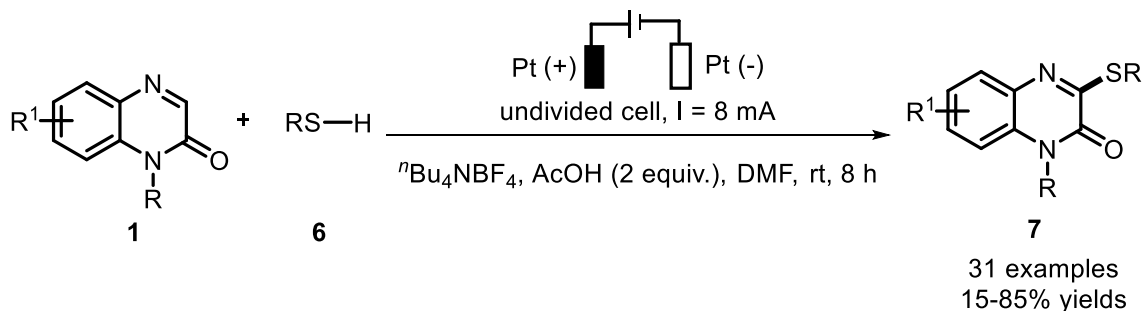
Scheme 5.2 C3-Fluoroalkoxylation of quinoxalin-2(1*H*)-ones

Wei, Li and Pan group have independently disclosed the sulfenylation of quinoxalin-2(1*H*)-ones (**1**) using alkyl/aryl thiols (**6**) under visible-light irradiations. Wei group employed rhodamine B as photocatalyst for constructing 3-sulfenylated quinoxalin-2(1*H*)-ones (**7**) in the presence of 3 W blue LED lamp (**Scheme 5.3a**).²¹ Alternatively, Li group utilized rhodamine 6G as photocatalyst in the presence of TFA as an additive to obtain a variety of 3-sulfenylated quinoxalin-2(1*H*)-ones (**7**) under the irradiation of 3 W blue LEDs (**Scheme 5.3b**). Several mechanistic investigations in both works suggested nucleophilic attack of thiols (**6**) at the nitrogen centered radical generated from quinoxalin-2(1*H*)-ones *via* SET process rather than S-centered radical from thiol. With the further exploration and modification in the existing methods, Pan group disclosed a photocatalyst- and oxidant-free strategy for 3-sulfenylated quinoxalin-2(1*H*)-ones (**7**) by irradiating quinoxalin-2(1*H*)-ones (**1**) and alkyl/aryl thiols (**6**) under a 9 W blue LED lamp (**Scheme 5.3c**).²⁸ Further, Shen *et al.* described a cerium-catalyzed C3-sulfenylation of quinoxalin-2(1*H*)-ones (**1**). The method utilized CeCl₃/K₂S₂O₈ system for the activation of diaryldisulfides (**6**) in presence of 3 W blue LEDs and afforded 3-sulfenylated quinoxalin-2(1*H*)-ones (**7**) in decent yields (**Scheme 5.3d**).²⁹



Scheme 5.3 Visible-light induced C3-sulfonylation of quinoxalin-2(1*H*)-ones

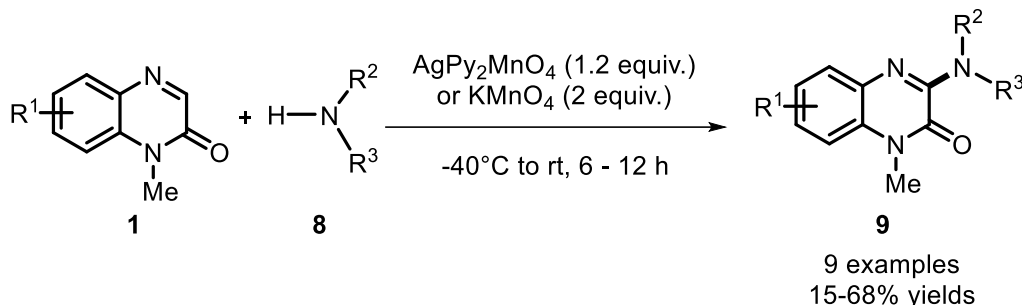
Zhou and co-workers reported the electrochemical synthesis of 3-sulfonylated quinoxalin-2(1*H*)-ones (**7**) by the reaction of quinoxalin-2(1*H*)-ones (**1**) with alkyl/aryl thiols (**6**) using Pt(+) | Pt(-) electrodes containing undivided cell (**Scheme 5.4**).³⁰ In contrast to earlier methods, the formation of S-centered radical was proposed in this method. Control experiments were performed through cyclic voltammetry which also supported the oxidation of **6** due to lower oxidation potential as compared to **1**.



Scheme 5.4 Electrochemical C3-sulfonylation of quinoxalin-2(1*H*)-ones

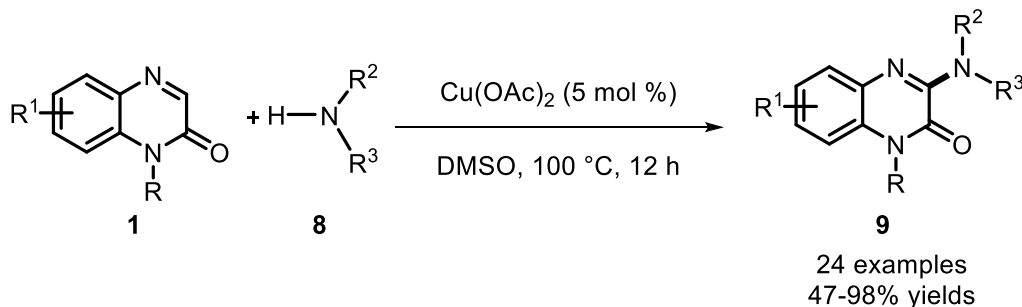
In 2008, Gulevskaya for the first time reported C3-amination of quinoxalin-2(1*H*)-ones. Restricted examples of 3-aminoquinoxalin-2(1*H*)-ones (**9**) have been achieved through nucleophilic aromatic substitution of different 1° or 2° aliphatic amines (**8**) and quinoxalin-2(1*H*)-ones (**1**) in the presence of AgPy₂MnO₄ or KMnO₄ as oxidant (**Scheme 5.5**).³¹ Limited substrate

scope, use of very strong oxidants and specific reaction conditions renders the employment of this method for practical purpose.



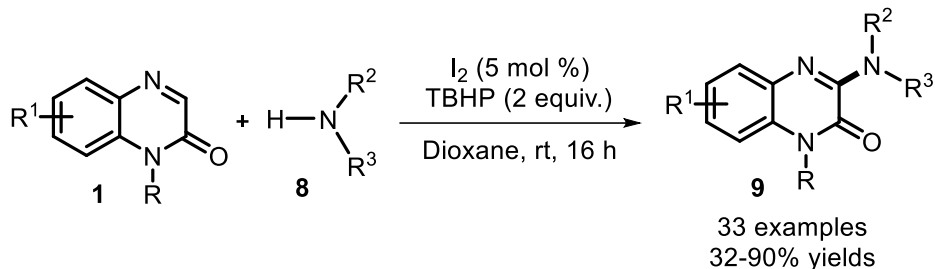
Scheme 5.5 AgPy₂MnO₄/KMnO₄ mediated C3-amination of quinoxalin-2(1*H*)-ones

Li and colleagues have developed a Cu-catalyzed approach for oxidative amination of quinoxalin-2(1*H*)-ones (**1**) enabling the utilization of 1° and 2° aliphatic amines (**8**) in DMSO at 100 °C. The reaction yields numerous 3-aminoquinoxalin-2(1*H*)-ones (**9**) in moderate to good yields, utilizing molecular oxygen as the primary oxidizing agent (**Scheme 5.6**).³² A non-radical mechanism is proposed for this Cu-catalyzed oxidative amination.



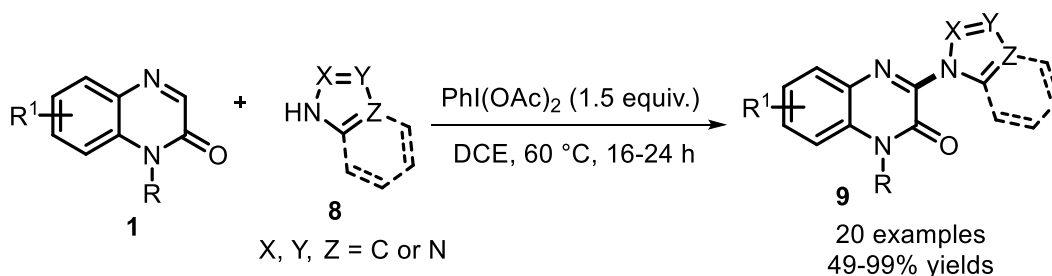
Scheme 5.6 Cu-catalyzed C3-amination of quinoxalin-2(1*H*)-ones

Synthesis of various 3-aminoquinoxalin-2(1*H*)-ones (**9**) has also been reported by Jain group *via* I₂/TBHP catalyzed cross-dehydrogenative coupling of quinoxalin-2(1*H*)-ones (**1**) and aliphatic amines (**8**) (**Scheme 5.6**).³³ One-pot construction of histamine-4 receptor antagonist and two-step synthesis of aldose reductase inhibitor demonstrated the practical utility of the method. Based on control experiments, a non-radical mechanism which involved the *N*-iodination as one of the plausible intermediate is proposed for the reaction.



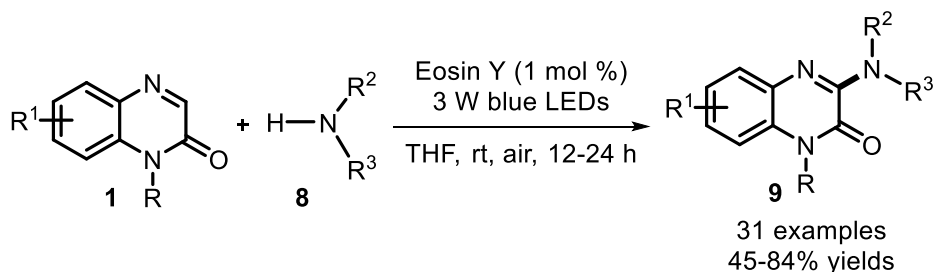
Scheme 5.6 I_2 /TBHP catalyzed C3-amination of quinoxalin-2(1H)-ones

PhI(OAc)₂-mediated oxidative cross-dehydrogenative coupling of quinoxalin-2(1H)-ones (**1**) and azoles (**8**) has been developed by Wiminsong and Yotphan for the effective production of 3-(azol-1-yl)quinoxalin-2-one (**9**) molecules (**Scheme 5.7**).³⁴ Through the control experiments, the reaction was believed to proceed through formation of azole radical intermediate which on reaction with **1** followed by hydrogen radical abstraction resulted the corresponding 3-aminoquinoxalin-2(1H)-ones derivatives.



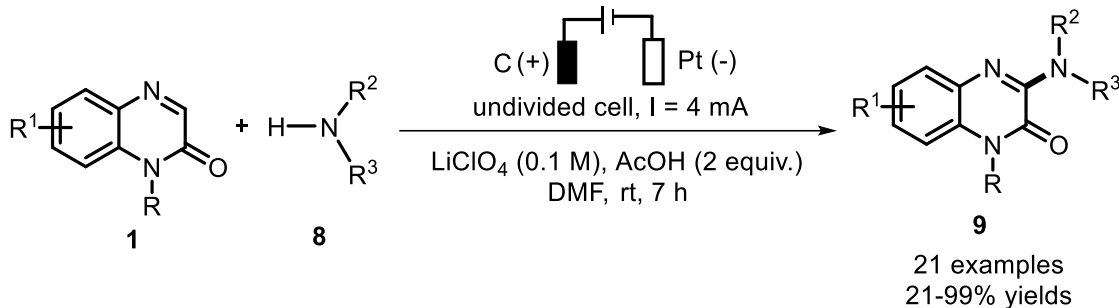
Scheme 5.7 PhI(OAc)₂-mediated C3-amination of quinoxalin-2(1H)-ones

Wei and Zhao group collectively developed a visible-light induced C(sp²)-H/ N-H coupling of quinoxalin-2(1H)-ones (**1**) with 1° and 2° aliphatic amines (**8**) in the presence of Eosin Y as photocatalyst to deliver different 3-aminoquinoxalin-2(1H)-ones (**9**) in good yields (**Scheme 5.8**).³⁵ The effect of photo-irradiation has been proved *via* on/off experiment and the presence of nitrogen radical which is generated after photo-irradiation, has been suggested through ESR experiment.



Scheme 5.8 Visible-light induced C3-amination of quinoxalin-2(1H)-ones

Li *et al.* disclosed an electrochemical cross-dehydrogenative coupling for the synthesis of 3-aminoquinoxalin-2(1*H*)-ones (**9**), by employing quinoxalin-2(1*H*)-ones (**1**) with aliphatic amines and azoles (**8**) in an undivided cell (**Scheme 5.9**).³⁶ Radical scavenging and cyclic voltametric measurements indicated radical mechanism for the developed protocol.



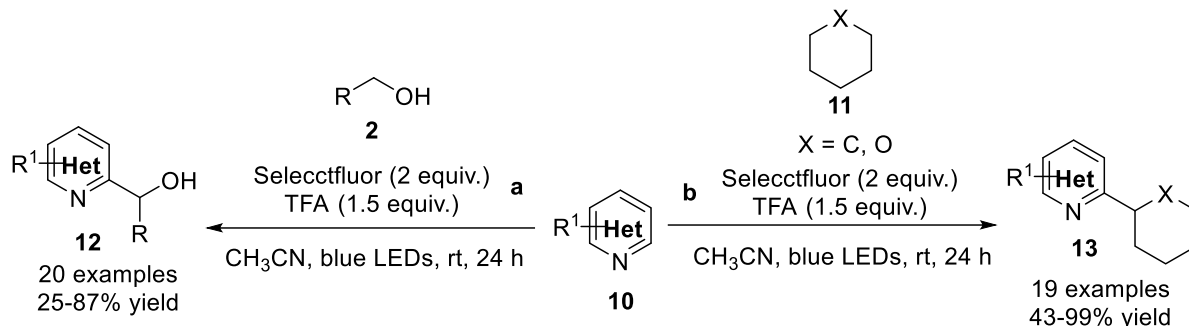
Scheme 5.9 Electrochemical C3-amination of quinoxalin-2(1*H*)-ones

Although the reported methods for the functionalization of quinoxalin-2(1*H*)-ones have proven advantageous in certain aspects, they still face certain limitations like limited substrate scope, the use of toxic solvents, high temperatures, and the use of photocatalysts that obstruct their employment for industrial application. Therefore, it is essential to investigate a more resourceful, versatile, and planet-friendly methods for the synthesis of C3-substituted quinoxalin-2(1*H*)-ones, that is also economically viable.

On the other hand, Selectfluor is a remarkably stable and easy to handle compound which is commonly employed as an effective electrophilic fluorinating reagent and now gaining prominence as a powerful oxidant in numerous organic transformations.³⁷⁻³⁸ Its mild oxidizing properties have enabled the successful synthesis of various functionalized heterocycles.³⁹⁻⁴⁰ In recent years, it has been increasingly recognized as a versatile mediator for metal-free radical-based C-H functionalization reactions, offering a powerful and practical alternative to traditional transition-metal catalyzed reactions.^{22, 41-45}

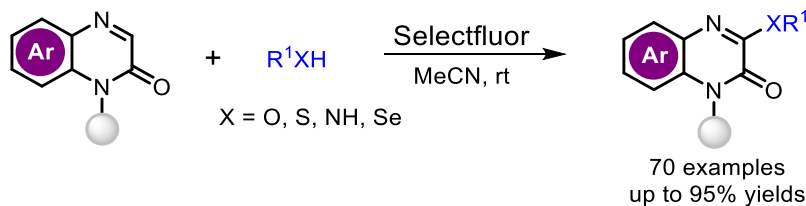
Lei's group recently described an innovative approach using Selectfluor to promote oxidative α C(sp³)-H arylation of alcohols (**2**) with heteroarenes (**10**) under visible light irradiation. The hydroxyalkylated heteroarenes (**12**) were obtained in good yields from primary, secondary, and tertiary alcohols (**Scheme 5.10a**).⁴³ The reaction is believed to initiate through photoinduced N-F bond activation as suggested by the EPR experiment. Later, the same group showcased the alkylation of heteroarenes by employing simple alkanes, ethers, and methylarenes (**11**) with

heteroarenes (**10**), following the same reaction condition under the irradiation of 3 W blue LEDs (Scheme 5.10b).⁴⁶



Scheme 5.10 Selectfluor promoted oxidative α C(sp³)-H arylation of alcohols/alkanes with heteroarenes

In continuation with our interest in the functionalization of aza-heterocycles and radical induced reactions we developed a Selectfluor-promoted oxidative coupling of quinoxalin-2(1*H*)-ones with alcohols, thiols, amines, and selenols leading to the formation of C-O, C-S, C-N, and C-Se bonds in good to excellent (53-95%) yields (Scheme 5.11).



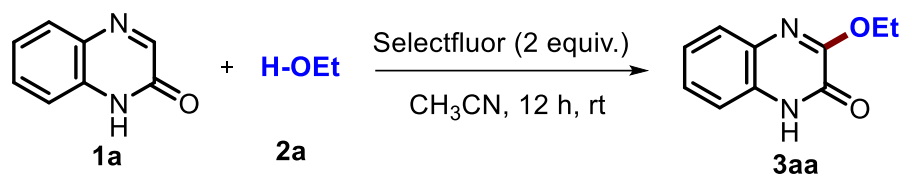
Scheme 5.11 Selectfluor-mediated C3-alkoxylation, sulfenylation, amination, and selenylation of quinoxalin-2(1*H*)-ones

5.2 RESULTS AND DISCUSSION

We commenced our investigation using the model reaction of quinoxalin-2(1*H*)-one **1a** with ethanol **2a** in the presence of Selectfluor in acetonitrile. Interestingly, desired product, 3-ethoxyquinoxalin-2(1*H*)-one **3aa** was obtained in 92% yield after allowing the reaction to continue at room temperature for 12 h. The effect of different parameters like additive, solvent, time, and temperature was investigated on model reaction (Table 5.1). Use of acidic (AcOH, TFA, TsOH, and ADA) or basic additive (Et₃N) led to decrease in the yield of **3aa**. Similarly, no significant increase in the yield of **3aa** was observed by replacing CH₃CN with other solvents (DCM, THF

and DMF), varying equivalence of Selectfluor, reaction temperature or reaction time. The molecular structure of **3aa** was fully characterized by NMR (^1H , **Figure 5.2**, $^{13}\text{C}\{^1\text{H}\}$, **Figure 5.3**) and HRMS (**Figure 5.4**).

Table 5.1 Optimization of reaction conditions for the synthesis **3aa**^a.



Entry	Deviation in reaction conditions	% Yield of 3aa
1	none	92
2	AcOH as additive	72
3	TFA as additive	43
4	TsOH as additive	35
5	ADA as additive	23
6	Et ₃ N as additive	16
7	EtOH as solvent	75
8	DCM as solvent	61
9	THF as solvent	78
10	DMF as solvent	55
11	Selectfluor 3 equiv.	85
12	Selectfluor 1.5 equiv.	63
13	Reaction time 24 h	90
14	Reaction temperature 50 °C	88
15	Reaction temperature 100 °C	78
16	Without Selectfluor	nr

^aReaction conditions: **1a** (0.34 mmol), **2a** (5 equiv.), Selectfluor (2 equiv.), additive (2 equiv.), solvent 2 mL, rt for 12 h. ^bIsolated yield. AcOH = Acetic acid; TFA = Trifluoroacetic acid; TsOH = *p*-Toluenesulfonic acid; ADA = 1-Adamantanecarboxylic acid; DCM = Dichloromethane; THF = Tetrahydrofuran; DMF = *N,N*-dimethylformamide; nr = No reaction.

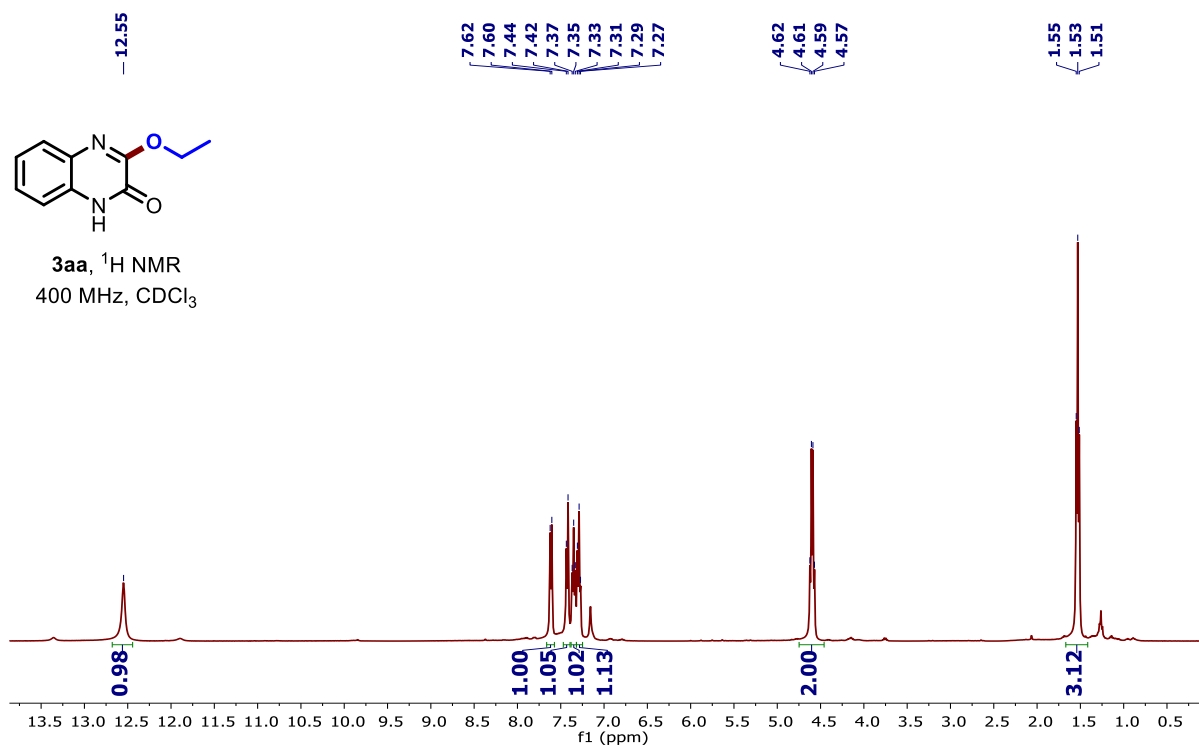


Figure 5.3 ^1H NMR spectrum of 3-ethoxyquinoxalin-2(1*H*)-one (**3aa**) recorded in CDCl_3

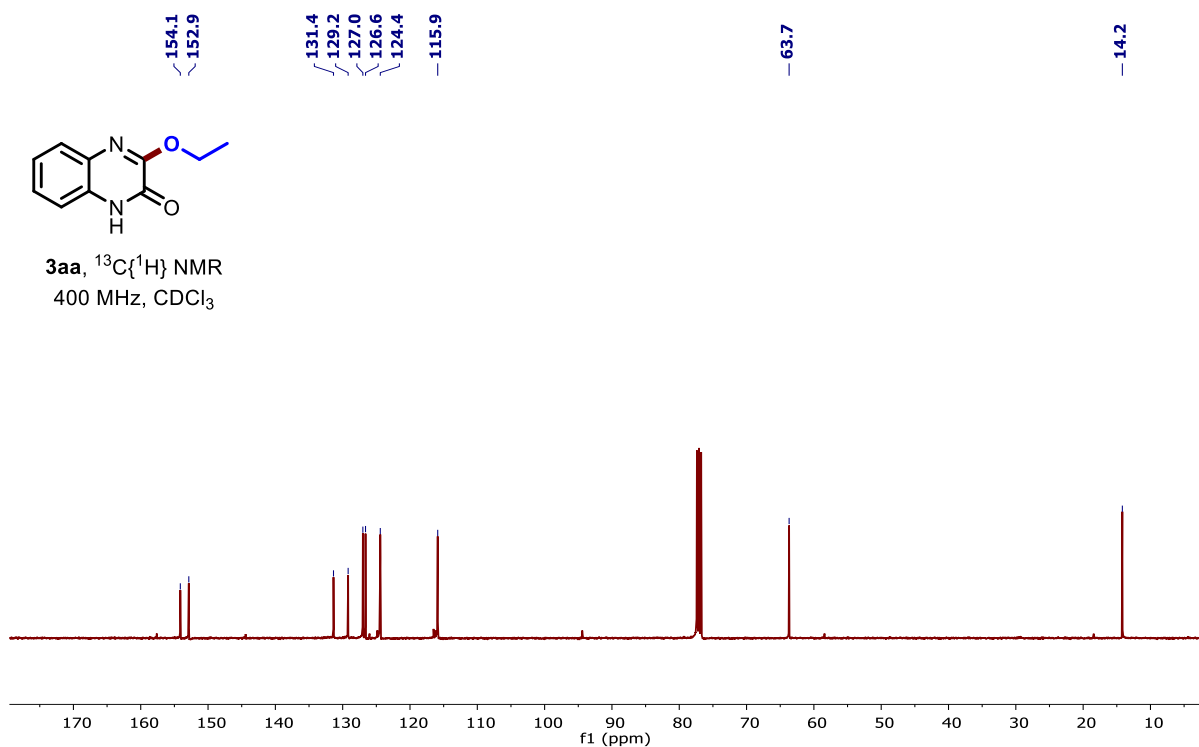
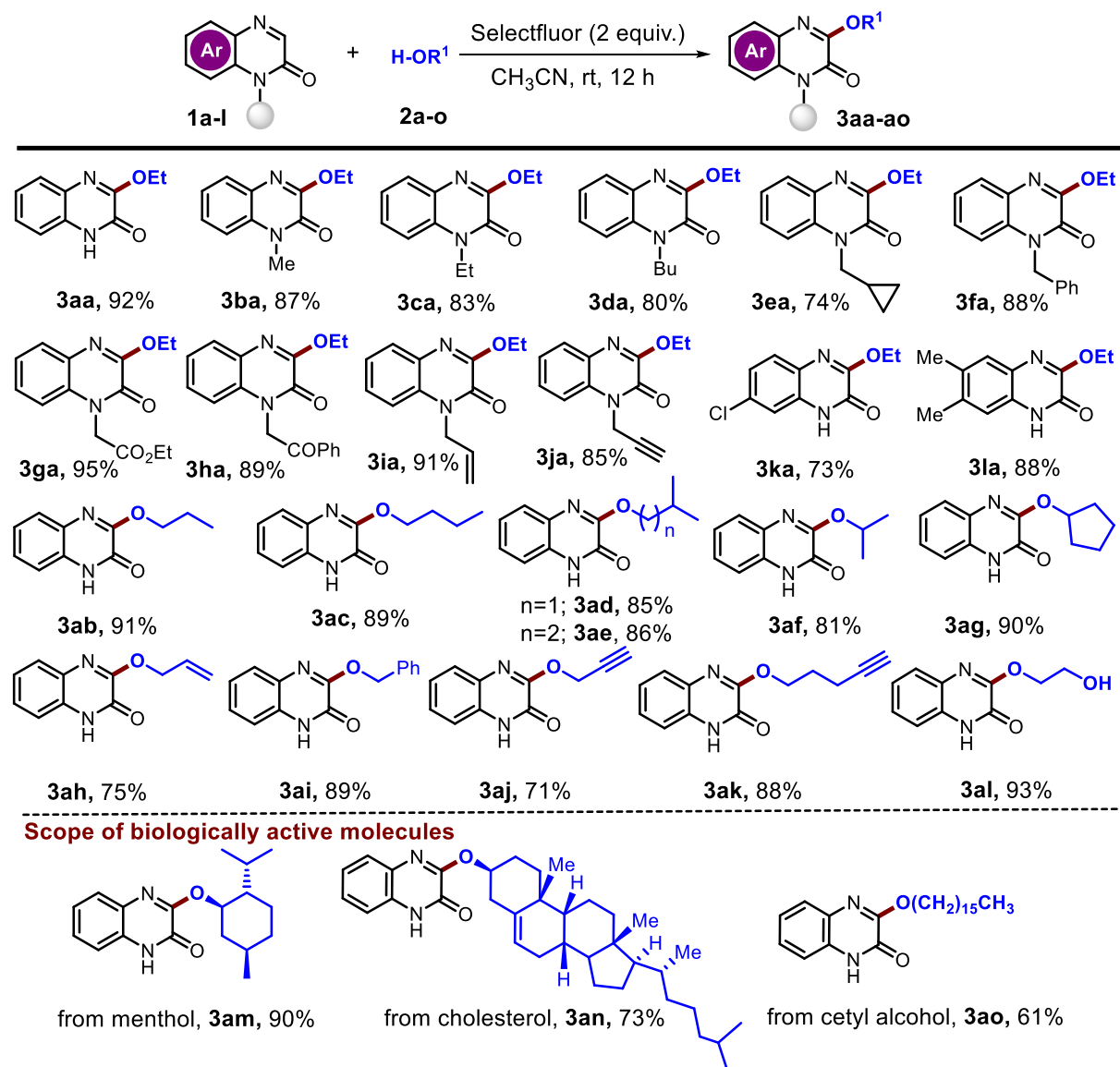


Figure 5.4 $^{13}\text{C}\{^1\text{H}\}$ NMR of 3-ethoxyquinoxalin-2(1*H*)-one (**3aa**) recorded in CDCl_3

With established reaction conditions in hand, we first examined substrate scope of quinoxalin-2(1*H*)-ones **1b-1l** by their reaction with **2a**. As shown in **Table 5.2**, a wide range of quinoxalin-2(1*H*)-ones substituted with various functionalities such as $-\text{CH}_3$, $-\text{C}_2\text{H}_5$, $-\text{n-C}_4\text{H}_9$, cyclopropylmethyl, benzyl, $-\text{CO}_2\text{Et}$, $-\text{CH}_2\text{COPh}$, allyl, propynyl, 4-chloro, and 4,5-dimethyl were well tolerated, and the corresponding alkoxyated products **3ba-3la** were obtained in 73–95% isolated yields.

Table 5.2 Alkoxylation of quinoxalin-2(1*H*)-ones^{a,b}



^aReaction conditions: **1** (0.34 mmol), **2** (5 equiv.), Selectfluor (2 equiv.), CH_3CN (2 mL), rt, 12 h. ^bIsolated yield.

Subsequently, substrate scope of alcohols was examined. A wide range of alcohols **2a-2l** including primary, secondary, allylic, propargylic and benzylic alcohols could smoothly react with **1a**, providing the desired alkoxyated products **3aa-3al** in 71-93% isolated yields. The scope of alcohol was further extended to quinoxalin-2(1*H*)-ones substituted with menthol (**3am**), cholesterol (**3an**) and cetyl alcohol (**3ao**). To our delight the corresponding alkoxyated products were produced in 90%, 73%, and 61% yields, respectively.

The versatility of the current protocol was also demonstrated by fluoroalkoxylation of quinoxalin-2(1*H*)-ones (**Table 5.3**). Reaction of **1a-1m** with trifluoroethanol **4a** in the presence of Selectfluor (2 equiv.) in CH₃CN at room temperature afforded corresponding trifluoroalkoxyated products **5aa-5na** in 53–90% yields. The substrate **1n** was mixture of two isomers and thus we obtained corresponding product **5na** as mixture of two isomers. Reaction of **1a** with 1,1,1,2,2-petrafluoropropanol **4b** also afforded corresponding alkoxyated product **5ab** in 85% yield. Structures of **5aa** (CCDC 2178009) (**Figure 5.5**) and **5ca** (CCDC 2178501) (**Figure 5.6**) were also unambiguously confirmed by single crystal X-ray analysis.

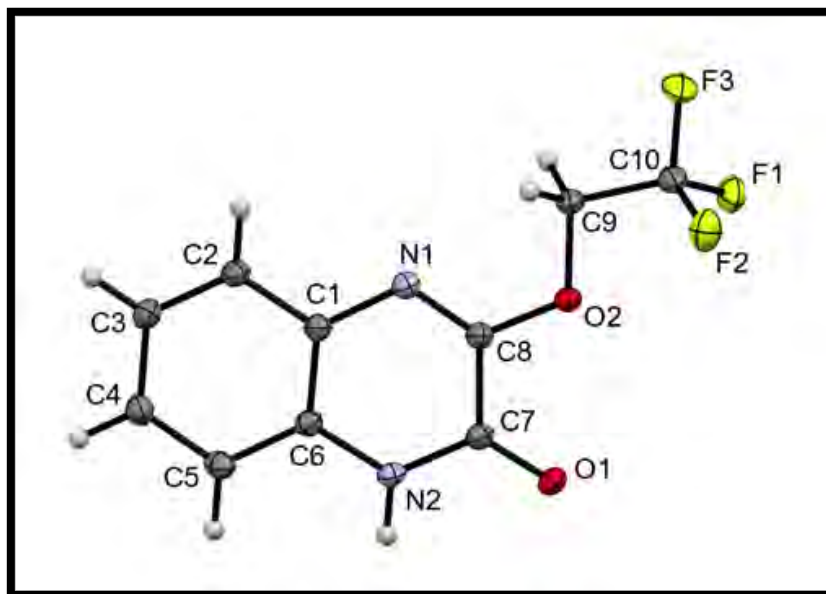


Figure 5.5 ORTEP diagram of **5aa** (CCDC No 2178009). The thermal ellipsoids are drawn at 50% probability level

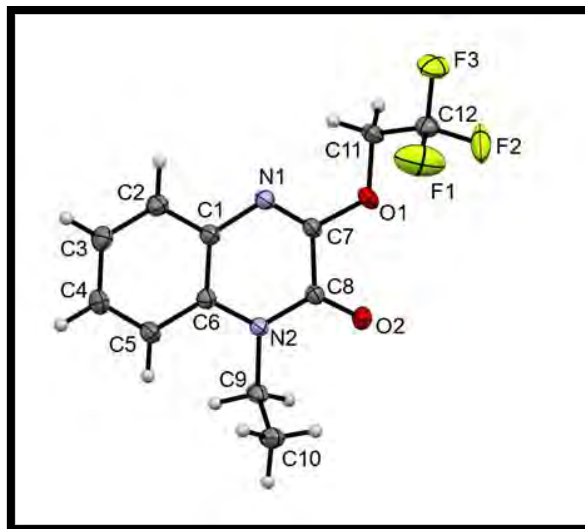
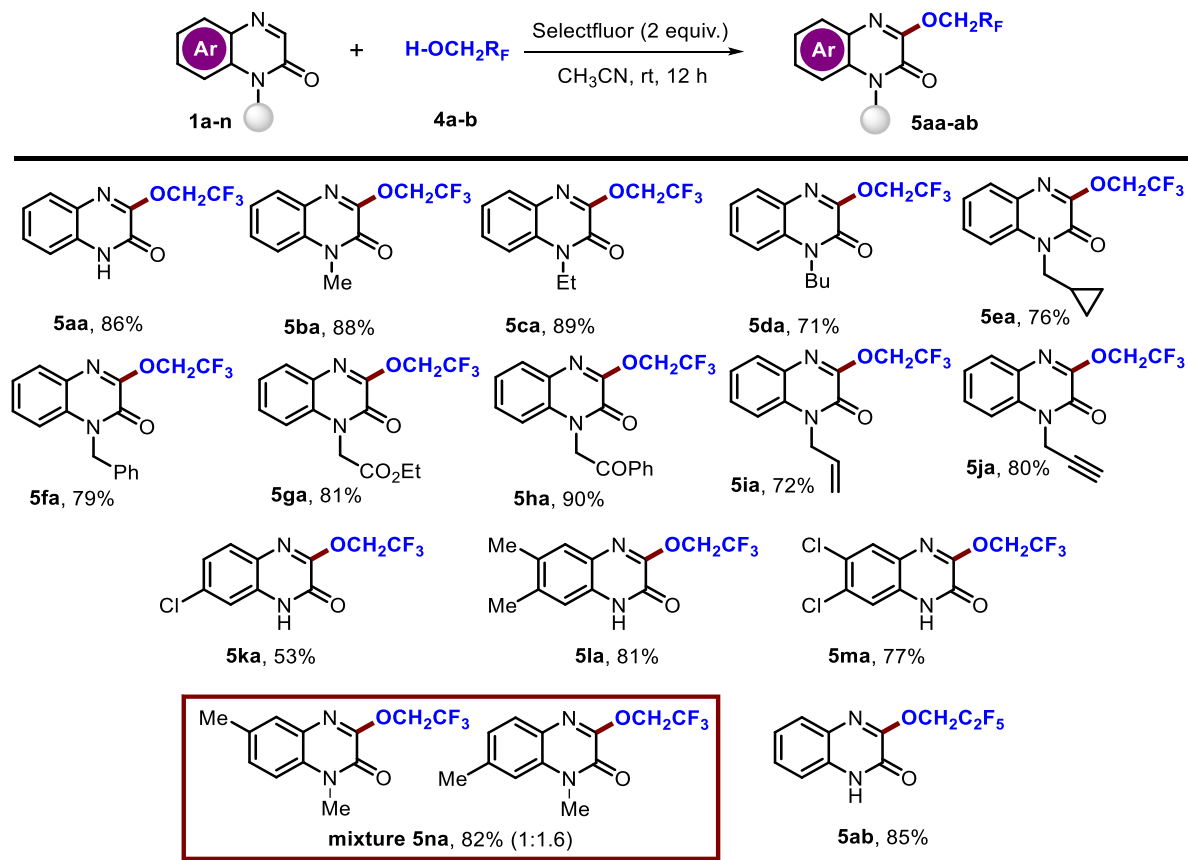


Figure 5.6 ORTEP diagram of **5ca** (CCDC No 2178501). The thermal ellipsoids are drawn at 50% probability level

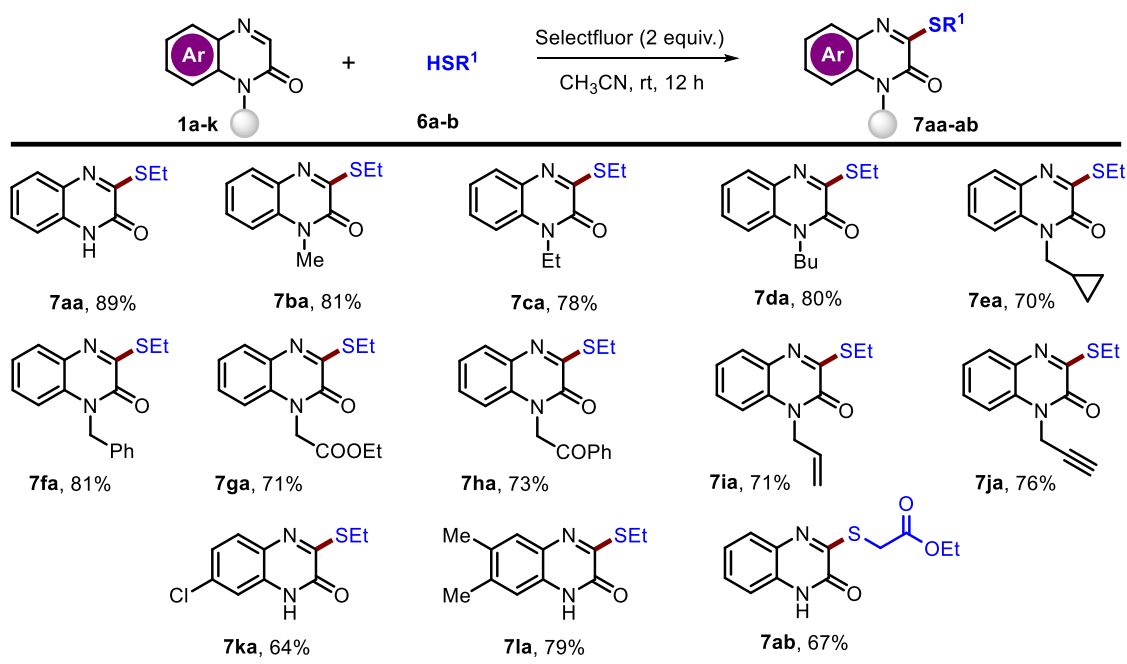
Table 5.3. Fluoroalkoxylation of quinoxalin-2(1*H*)-ones^{a,b}



^aReaction conditions: **1** (0.34 mmol), **4** (5 equiv.), Selectfluor (2 equiv.), CH_3CN (2 mL), rt, 12 h. ^bIsolated yield.

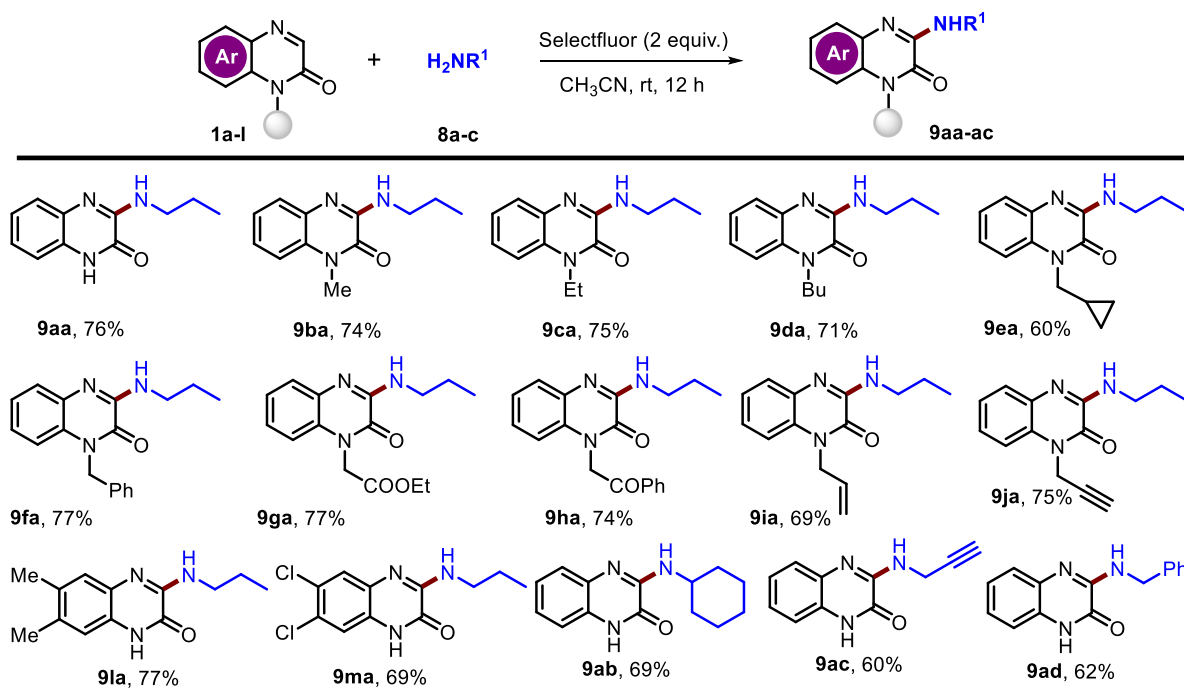
Encouraged by the success of alkoxylation of quinoxalin-2(1*H*)-ones, we proceeded to explore the C3-sulfenylation (**Table 5.4**). To our delight, 3-(ethylthio)quinoxalin-2(1*H*)-one **7aa** was obtained in 89% yield by the reaction of **1a** with ethanethiol **6a** in the presence of Selectfluor (2 equiv.) in CH₃CN at room temperature. Various other quinoxalin-2(1*H*)-ones **1b-1l** also smoothly reacted with **6a** under standard conditions to afford corresponding sulfenylated products **7ba-7la** in 64-81% yields.

Table 5.4. Thioalkoxylation of quinoxalin-2(1*H*)-ones^{a,b}



^aReaction conditions: **1** (0.34 mmol), **6** (5 equiv.), Selectfluor (2 equiv.), CH₃CN (2 mL), rt, 12 h. ^bIsolated yield.

To further illustrate the potential application of this method, we thought to apply our strategy toward amination of quinoxalin-2(1*H*)-ones (**Table 5.5**). We first investigated reaction of **1a** with propyl amine **8a** in the presence of Selectfluor (2 equiv.) in CH₃CN at room temperature. To our satisfaction, the reaction yielded 3-propylaminoquinoxalin-2(1*H*)-one **9aa** in 76% yield. Reaction of other substituted quinoxalin-2(1*H*)-ones **1b-1m** with **8a** also produced corresponding aminated products in good (60-77%) yields. Cyclohexylamine **8b**, propargylamine **8c** and benzylamine **8d** were well tolerated to give target products **9ab**, **9ac** and **9ad** in 69%, 60% and 62% yields, respectively. Structures of **9da** (CCDC 2206580) (**Figure 5.7**) and **9ia** (CCDC 2207035) (**Figure 5.8**) were unambiguously confirmed by single crystal X-ray analysis.

Table 5.5. Amination of quinoxalin-2(1*H*)-ones^{a,b}

^aReaction conditions: **1** (0.34 mmol), **8** (5 equiv.), Selectfluor (2 equiv.), CH₃CN (2 mL), rt, 12 h. ^bIsolated yield.

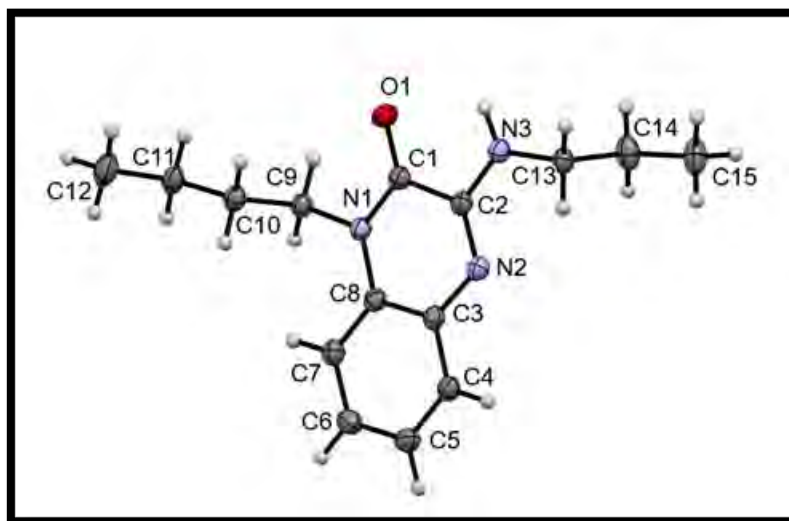


Figure 5.7 ORTEP diagram of **9da** (CCDC No 2206580). The thermal ellipsoids are drawn at 50% probability level

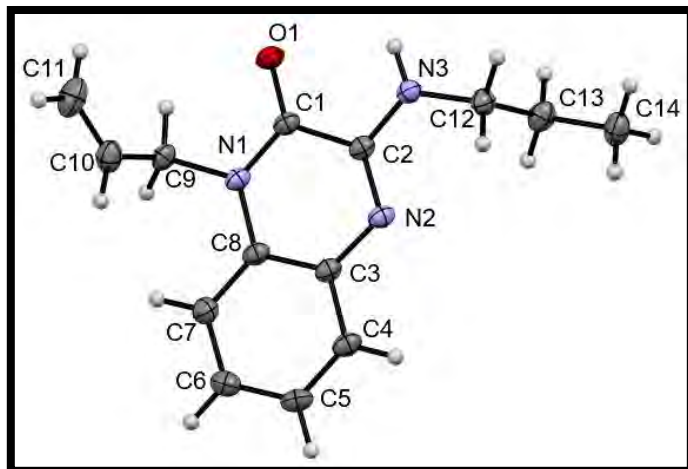
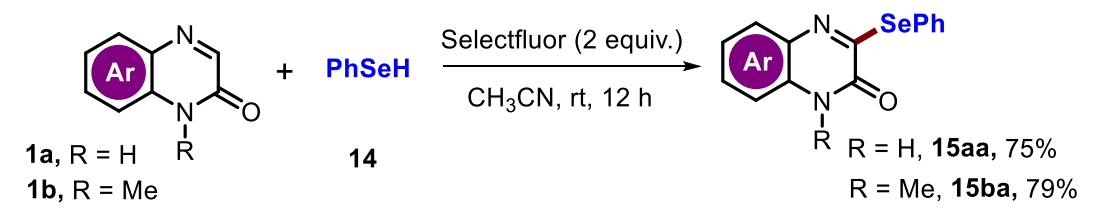


Figure 5.8 ORTEP diagram of **9ia** (CCDC No 2207035). The thermal ellipsoids are drawn at 50% probability level

This method was next utilized for the selenylation of quinoxalin-2(1*H*)-ones (**Table 5.6**). Interestingly, 3-(phenylselanyl)quinoxalin-2(1*H*)-one **15aa** and 1-methyl-3-(phenylselanyl)quinoxalin-2(1*H*)-one **15ba** were isolated in 75% and 79% yield, respectively by the reaction of **1a** and **1b** with benzeneselenol **14** in the presence of Selectfluor (2 equiv.) in CH₃CN at room temperature.

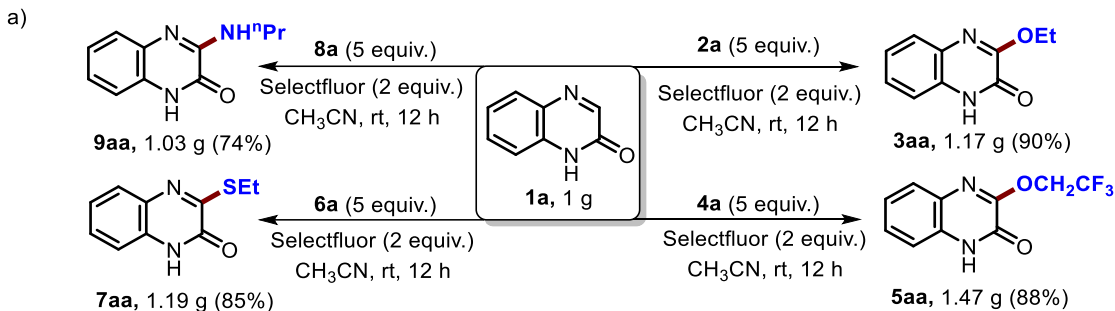
Table 5.6. Selenylation of quinoxalin-2(1*H*)-ones



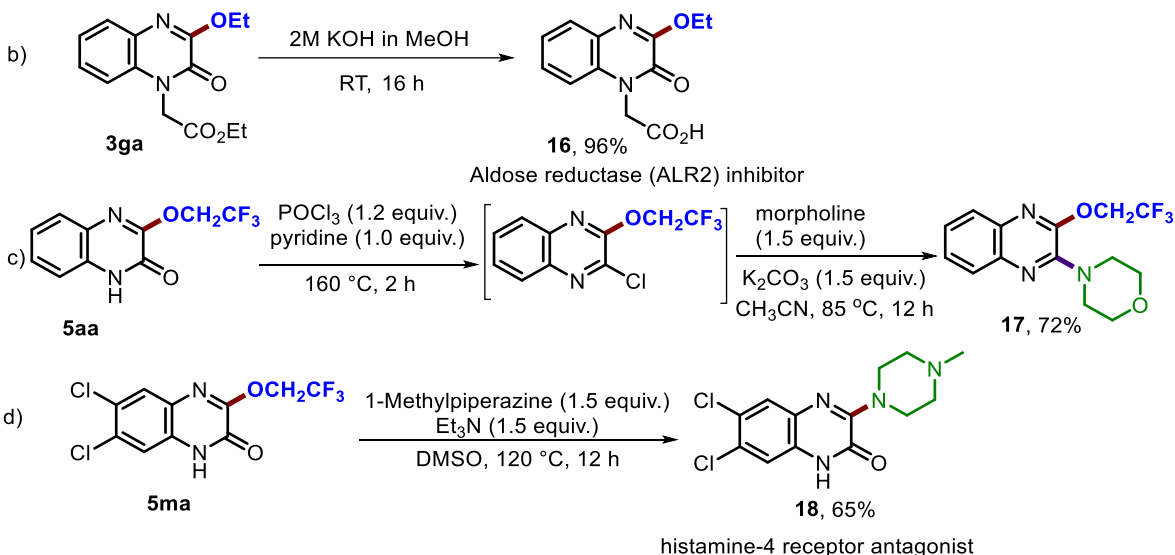
To demonstrate the synthetic utility of our new C–H functionalization method, gram-scale synthesis of representative compounds was performed (**Scheme 5.12**). Notably, the reaction of **1a** (1 g, 6.85 mmol), with **2a**, **4a**, **6a** and **8a** (5 equiv.) under standard reaction conditions afforded desired products **3aa**, **5aa**, **7aa** and **9aa** in 90%, 88%, 85%, and 74% yields, respectively (**Scheme 5.12a**). Further, the synthetic utility of alkoxyated products was demonstrated by conducting subsequent derivatizations. Hydrolysis of **3ga** using KOH in methanol followed by acidification produced an aldose reductase (ALR2) inhibitor **16** in 96% yield (**Scheme 5.12b**). Similarly, reaction of **5aa** with POCl₃ in pyridine followed by reaction with morpholine (**13**)

produced 4-(3-ethoxyquinoxalin-2-yl)morpholine (**17**) in 72% yield (**Scheme 5.12c**). The trifluoroethoxyl group has been used as a good leaving group in S_NAr reactions. We therefore utilized it to prepare histamine-4 receptor antagonist (**18**) by the reaction of **5ma** with 1-methylpiperazine (**Scheme 5.12d**).

Gram scale synthesis of **3aa**, **5aa**, **7aa** and **9aa**

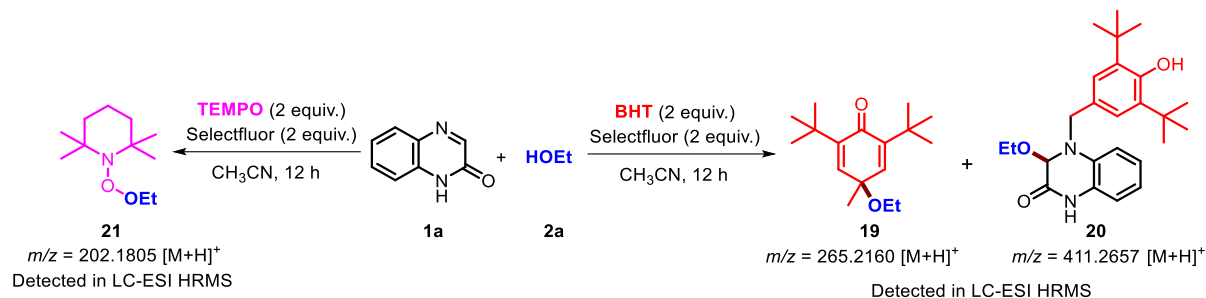


Synthetic manipulation of products **3ga**, **5aa** and **5ma**



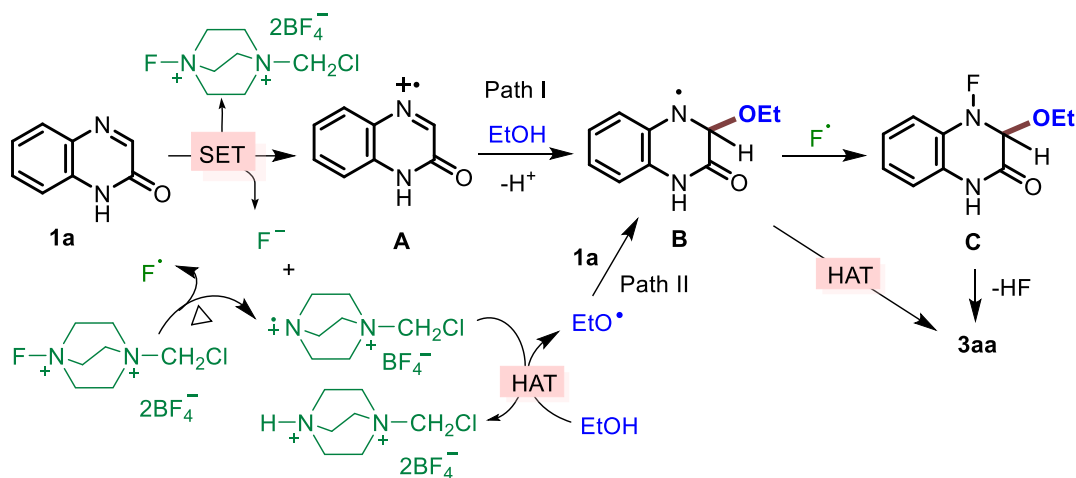
Scheme 5.12 Gram-scale synthesis and synthetic applications

To uncover evidence for the presence of radical intermediate in the reaction mechanism, radical capture experiments were carried out (**Scheme 5.13**). Introducing radical scavenger 2,2,6,6-tetramethylpiperidine N-oxide (TEMPO) or butylated hydroxytoluene (BHT) into model reaction of **1a** with **2a** under standard conditions completely inhibited formation of **3aa**. Further, formation of BHT adducts **19** & **20**, and TEMPO adduct **21** was detected by ESI-HRMS. These results suggest that a radical pathway could be involved in this reaction.



Scheme 5.13 Radical trapping experiments

A plausible mechanism for this transformation is proposed on the basis of previous literature reports^{43, 47} and result of radical trapping experiment (Scheme 5.14). Initially, quinoxalin-2-one derived radical **B** can be generated in two distinct pathways, either through generation of intermediate **A** by single electron transfer (SET) from Selectfluor followed by nucleophilic attack of ethanol to **A** (Path I) or by attack of ethoxy radical generated by hydrogen atom abstraction (HAT) to quinoxalin-2-one (Path II). Finally, product **3aa** is obtained either by HAT from intermediate **B** or elimination of HF from intermediate **C** which is generated by coupling of fluorine radical with intermediate **B**.



Scheme 5.14 Plausible mechanism

5.3 CONCLUSIONS

In summary, we have developed a simple and highly efficient Selectfluor-mediated method for diverse functionalization of quinoxalin-2(1H)-ones under metal- and photocatalyst-free conditions. Various C3-substituted quinoxalin-2(1H)-ones could be prepared in good to excellent yields. The protocol features a broad substrate scope, mild conditions, and excellent functional

group tolerance. The method provides a convenient strategy for alkoxylation, fluoroalkoxylation, sulfenylation, amination, and selenylation at C3-position of quinoxalin-2(1*H*)-ones. Synthetic potential of the method has been demonstrated by gram scale synthesis, C3-alkoxylation of quinoxalin-2(1*H*)-one with natural alcohols and synthesis of aldose reductase (ALR2) inhibitor. These findings are expected to open a new avenue for late-stage functionalization of quinoxalin-2(1*H*)-one based bioactive molecules under mild reaction conditions.

5.4 EXPERIMENTAL SECTION

5.4.1 General Information

All the chemicals and solvents were purchased from commercial suppliers and used without purification, unless otherwise noted. Quinoxalin-2(1*H*)-ones were synthesized by the condensation of *o*-phenylenediamines with ethyl glyoxalate in ethanol/toluene according to a reported procedure.⁴⁸ All reactions were monitored by thin layer chromatography (TLC) on pre-coated 0.2 mm silica gel F254 plates (Merck) and visualised under a UV lamp (366 or 254 nm). Desired products were purified by column chromatography (Silica gel 100-200 mesh size) using a gradient of ethyl acetate and hexanes as mobile phase. Melting points were determined in open capillary tubes on an EZ-Melt automated melting point apparatus and are uncorrected. All the compounds were fully characterized by ¹H, ¹³C and ¹⁹F NMR spectra using Bruker Avance 400 spectrometer at 400 MHz, 100 MHz and 376 MHz, respectively. Chemical shifts (δ) are reported in parts per million (ppm) and coupling constants (*J*) are reported in hertz (Hz) relative to the residual signal of TMS in deuterated solvents. Abbreviations to represent multiplicities are s (singlet), d (doublet), t (triplet), q (quartet), quint (quintet), sext (sextet), sept (septet), dd (double doublet), dt (double triplet), dq (double quartet), td (triplet of doublet), ddd (doublet of doublet) and m (multiplet). High-resolution mass spectra (HRMS) were recorded by using electrospray ionization (ESI) method on an Agilent Q-TOF 6545 LC-MS spectrometer. Single crystal X-ray analysis was performed on a Rigaku Oxford XtaLAB AFC12 (RINC): Kappa dual home/near diffractometer.

5.4.2 General Procedure for the Synthesis of Quinoxalin-2(1*H*)-ones

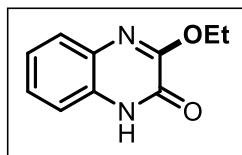
An oven dried 25 mL round bottom flask was charged with *o*-phenylenediamines (10 mmol), ethyl glyoxalate (2.4 g, 12 mmol) and a solution of ethanol and toluene (20 mL, 1: 1 v/v). The reaction mixture was stirred at 85 °C for 12 h. After completion of the reaction monitored by

TLC, reaction mixture was allowed to attain room temperature. The residue was concentrated in vacuum. The obtained solid was washed with H₂O and dried in oven to afford corresponding quinoxalin-2(1*H*)-one. The substrate was used as such without purification for further transformations.

5.4.3 General Procedure for the C3-Alkoxylation/ Fluoroalkoxylation of Quinoxalin-2(1*H*)-ones

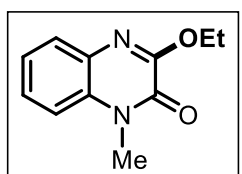
An oven dried 10 mL round bottom flask was charged with quinoxalin-2(1*H*)-ones **1** (0.34 mmol; 1.0 equiv.), **2** or **4** (1.71 mmol; 5.0 equiv.) and Selectflour (2.0 equiv.) in CH₃CN at room temperature and the reaction mixture was stirred for 12 h. After completion of the reaction monitored by TLC, reaction mixture was concentrated in vacuum. The resulting crude was purified by column chromatography (silica gel 100-200 mesh) using EtOAc-hexanes as an eluent to afford corresponding products **3** or **5**.

3-Ethoxyquinoxalin-2(1H)-one (3aa): White solid; 60 mg, 92% yield; purification by column



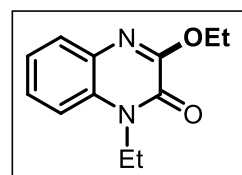
chromatography on silica gel (eluent: EtOAc /Hexane = 1.5/8.5); mp = 184-186 °C; ¹H NMR (400 MHz, CDCl₃) δ 12.55 (s, 1H), 7.61 (d, *J* = 7.6 Hz, 1H), 7.43 (d, *J* = 7.6 Hz, 1H), 7.35 (t, *J* = 7.2 Hz, 1H), 7.29 (t, *J* = 7.2 Hz, 1H), 4.60 (q, *J* = 6.9 Hz, 2H), 1.53 (t, *J* = 7.0 Hz, 3H); ¹³C {¹H} NMR (100 MHz, CDCl₃) δ 154.1, 152.9, 131.4, 129.2, 127.0, 126.6, 124.4, 115.9, 63.7, 14.2; HRMS (ESI) *m/z*: [M + H]⁺ Calcd for C₁₀H₁₁N₂O₂⁺ 191.0815; found 191.0816.

3-Ethoxy-1-methylquinoxalin-2(1H)-one (3ba): White solid; 60 mg, 87% yield; purification by



column chromatography on silica gel (eluent: EtOAc /Hexane = 1.5/7.5); mp = 130-132 °C; ¹H NMR (400 MHz, CDCl₃) δ 7.63 (dd, *J* = 7.8, 1.4 Hz, 1H), 7.43 – 7.39 (m, 1H), 7.33 – 7.25 (m, 2H), 4.56 (q, *J* = 7.1 Hz, 2H), 3.73 (s, 3H), 1.51 (t, *J* = 7.2 Hz, 3H); ¹³C {¹H} NMR (100 MHz, CDCl₃) δ 153.9, 151.2, 131.5, 131.2, 127.5, 126.9, 123.9, 113.6, 63.5, 29.5, 14.2; HRMS (ESI) *m/z*: [M + H]⁺ Calcd for C₁₁H₁₃N₂O₂⁺ 205.0972; found 205.0976.

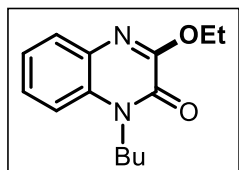
3-Ethoxy-1-ethylquinoxalin-2(1H)-one (3ca): White solid; 61 mg, 83% yield; purification by



column chromatography on silica gel (eluent: EtOAc /Hexane = 2.0/8.0); mp = 112-114 °C; ¹H NMR (400 MHz, CDCl₃) δ 7.66 – 7.64 (m, 1H), 7.44 – 7.40 (m, 1H), 7.32 – 7.28 (m, 2H), 4.56 (q, *J* = 7.1 Hz, 2H), 4.36 (q, *J* = 7.2 Hz, 2H), 1.52 (t, *J* = 7.0 Hz, 3H), 1.40 (t, *J* = 7.0 Hz, 3H);

$^{13}\text{C}\{^1\text{H}\}$ NMR (100 MHz, CDCl_3) δ 153.9, 150.7, 131.6, 130.4, 127.8, 126.9, 123.7, 113.5, 63.4, 37.6, 14.2, 12.4; HRMS (ESI) m/z : $[\text{M} + \text{H}]^+$ Calcd for $\text{C}_{12}\text{H}_{15}\text{N}_2\text{O}_2^+$ 219.1128; found 219.1125.

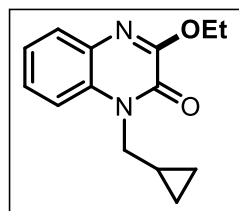
1-Butyl-3-ethoxyquinoxalin-2(1H)-one (3da): White solid; 67 mg, 80% yield; purification by



column chromatography on silica gel (eluent: EtOAc /Hexane = 1.5/3.5); mp = 120-122 °C; ^1H NMR (400 MHz, CDCl_3) δ 7.64 (dd, J = 7.8, 1.4 Hz, 1H), 7.43 – 7.38 (m, 1H), 7.31 – 7.26 (m, 2H), 4.55 (q, J = 7.1 Hz, 2H), 4.31 – 4.27 (m, 2H), 1.80 – 1.72 (m, 2H), 1.52 (t, J = 7.0 Hz, 3H),

1.49 (sext, J = 7.4 Hz, 2H), 1.01 (t, J = 7.2 Hz, 3H); $^{13}\text{C}\{^1\text{H}\}$ NMR (100 MHz, CDCl_3) δ 153.9, 150.9, 131.5, 130.7, 127.8, 126.8, 123.7, 113.6, 63.4, 42.4, 29.3, 20.2, 14.2, 13.8; HRMS (ESI) m/z : $[\text{M} + \text{H}]^+$ Calcd for $\text{C}_{14}\text{H}_{19}\text{N}_2\text{O}_2^+$ 247.1441; found 247.1438.

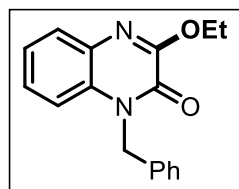
1-(Cyclopropylmethyl)-3-ethoxyquinoxalin-2(1H)-one (3ea): White solid; 61 mg, 74% yield;



purification by column chromatography on silica gel (eluent: EtOAc /Hexane = 3.0/7.0); mp = 100-102 °C; ^1H NMR (400 MHz, CDCl_3) δ 7.63 (d, J = 7.6 Hz, 1H), 7.42 – 7.37 (m, 2H), 7.30 – 7.26 (m, 1H), 4.54 (q, J = 7.2 Hz, 2H), 4.21 (d, J = 6.8 Hz, 2H), 1.51 (t, J = 7.0 Hz, 3H), 1.34 – 1.26 (m, 1H), 0.61 – 0.51 (m, 4H); $^{13}\text{C}\{^1\text{H}\}$ NMR (100 MHz, CDCl_3) δ

154.0, 151.2, 131.5, 130.9, 127.7, 126.8, 123.7, 113.9, 63.5, 46.4, 14.2, 9.6, 4.1; HRMS (ESI) m/z : $[\text{M} + \text{H}]^+$ Calcd for $\text{C}_{14}\text{H}_{17}\text{N}_2\text{O}_2^+$ 245.1285; found 245.1288.

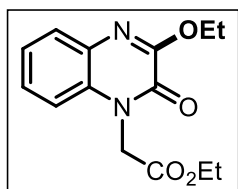
1-Benzyl-3-ethoxyquinoxalin-2(1H)-one (3fa): White solid; 84 mg, 88% yield; mp = 154-156



°C; purification by column chromatography on silica gel (eluent: EtOAc /Hexane = 3.0/7.0); ^1H NMR (400 MHz, CDCl_3) δ 7.66 – 7.64 (m, 1H), 7.35 – 7.26 (m, 7H), 7.23 – 7.21 (m, 1H), 5.54 (s, 2H), 4.60 (q, J = 7.1 Hz, 2H), 1.56 (t, J = 7.0 Hz, 3H); $^{13}\text{C}\{^1\text{H}\}$ NMR (100 MHz, CDCl_3) δ

154.0, 151.4, 135.2, 131.5, 130.8, 128.9, 127.7, 127.6, 127.0, 126.9, 123.9, 114.5, 63.6, 46.2, 14.2; HRMS (ESI) m/z : $[\text{M} + \text{H}]^+$ Calcd for $\text{C}_{17}\text{H}_{17}\text{N}_2\text{O}_2^+$ 281.1285; found 281.1289.

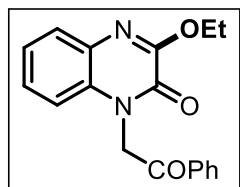
Ethyl 2-(3-ethoxy-2-oxoquinoxalin-1(2H)-yl)acetate (3ga): Purification by column chromatog-



raphy on silica gel (eluent: EtOAc /Hexane = 2.0/8.0); White solid (106 mg, 95% yield); mp = 142-144 °C; ^1H NMR (400 MHz, CDCl_3) δ 7.66 (dd, J = 8.0, 1.2 Hz, 1H), 7.41 – 7.36 (m, 1H), 7.33 – 7.29 (m, 1H), 7.03 (dd, J = 8.2, 1.0 Hz, 1H), 5.07 (s, 2H), 4.58 (q, J = 7.1 Hz, 2H), 4.26 (q, J

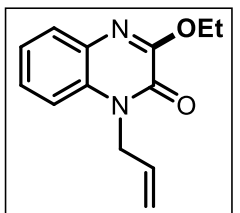
= 7.1 Hz, 2H), 1.53 (t, $J = 7.0$ Hz, 3H), 1.29 (t, $J = 7.2$ Hz, 3H); $^{13}\text{C}\{^1\text{H}\}$ NMR (100 MHz, CDCl_3) δ 167.0, 153.6, 150.9, 131.3, 130.7, 127.8, 127.1, 124.2, 113.0, 63.6, 62.0, 43.8, 14.2, 14.1; HRMS (ESI) m/z : $[\text{M} + \text{H}]^+$ Calcd for $\text{C}_{14}\text{H}_{17}\text{N}_2\text{O}_4^+$ 277.1183; found 277.1180.

3-Ethoxy-1-(2-oxo-2-phenylethyl)quinoxalin-2(1H)-one (3ha): White solid; 93 mg, 89% yield;



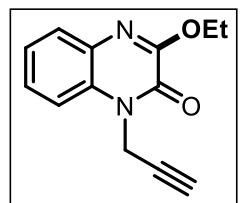
mp = 112-114 °C; Purification by column chromatography on silica gel (eluent: EtOAc /Hexane = 2.5/7.5); ^1H NMR (400 MHz, CDCl_3) δ 8.12 – 8.09 (m, 2H), 7.72 – 7.66 (m, 2H), 7.58 (t, $J = 7.6$ Hz, 2H), 7.31 – 7.28 (m, 2H), 6.92 – 6.89 (m, 1H), 5.78 (s, 2H), 4.61 (q, $J = 7.1$ Hz, 2H), 1.54 (t, $J = 7.0$ Hz, 3H); $^{13}\text{C}\{^1\text{H}\}$ NMR (100 MHz, CDCl_3) δ 191.0, 153.7, 151.1, 134.6, 134.3, 131.4, 130.9, 129.0, 128.2, 127.8, 127.0, 124.0, 113.5, 63.6, 48.7, 14.2; HRMS (ESI) m/z : $[\text{M} + \text{H}]^+$ Calcd for $\text{C}_{18}\text{H}_{17}\text{N}_2\text{O}_3^+$ 309.1234; found 309.1230.

1-Allyl-3-ethoxyquinoxalin-2(1H)-one (3ia): White solid; 71 mg, 91% yield; Purification by



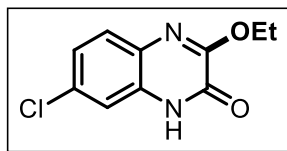
column chromatography on silica gel (eluent: EtOAc /Hexane = 3.0/7.0); mp = 68-70 °C; ^1H NMR (400 MHz, CDCl_3) δ 7.65 (dd, $J = 8.0, 1.6$ Hz, 1H), 7.40 – 7.36 (m, 1H), 7.30 (dd, $J = 7.8, 1.4$ Hz, 1H), 7.28 – 7.24 (m, 1H), 6.00 – 5.90 (m, 1H), 5.28 (dd, $J = 10.4, 0.8$ Hz, 1H), 5.20 (dd, $J = 17.2, 0.8$ Hz, 1H), 4.94 (dt, $J = 5.2, 1.6$ Hz, 2H), 4.57 (q, $J = 7.1$ Hz, 2H), 1.52 (t, $J = 7.0$ Hz, 3H); $^{13}\text{C}\{^1\text{H}\}$ NMR (100 MHz, CDCl_3) δ 153.9, 150.8, 131.4, 130.7, 130.6, 127.62, 127.58, 126.8, 118.1, 114.2, 63.5, 44.8, 14.2; HRMS (ESI) m/z : $[\text{M} + \text{H}]^+$ Calcd for $\text{C}_{13}\text{H}_{15}\text{N}_2\text{O}_2^+$ 231.1128; found 231.1130.

3-Ethoxy-1-(prop-2-yn-1-yl)quinoxalin-2(1H)-one (3ja): White solid; 70 mg, 85% yield; Puri-



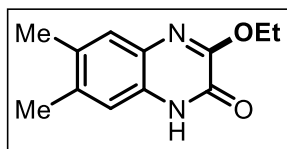
fication by column chromatography on silica gel (eluent: EtOAc /Hexane = 2.0/8.0); mp = 132-134 °C; ^1H NMR (400 MHz, CDCl_3) δ 7.68 – 7.64 (m, 1H), 7.45 (dd, $J = 6.1, 1.4$ Hz, 2H), 7.35 (ddd, $J = 8.3, 6.1, 2.5$ Hz, 1H), 5.10 (d, $J = 2.5$ Hz, 2H), 4.58 (q, $J = 7.1$ Hz, 2H), 2.30 (t, $J = 2.5$ Hz, 1H), 1.52 (t, $J = 7.1$ Hz, 3H); $^{13}\text{C}\{^1\text{H}\}$ NMR (100 MHz, CDCl_3) δ 153.6, 150.4, 131.4, 130.0, 127.7, 127.0, 124.3, 114.1, 76.8, 73.2, 63.7, 31.8, 14.2; HRMS (ESI) m/z : $[\text{M} + \text{H}]^+$ Calcd for $\text{C}_{13}\text{H}_{13}\text{N}_2\text{O}_2^+$ 229.0972; found 229.0976.

7-Chloro-3-ethoxyquinoxalin-2(1H)-one (3ka): White solid; 56 mg, 73% yield; Purification by



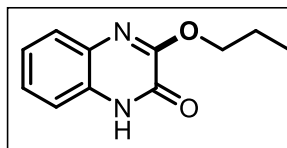
column chromatography on silica gel (eluent: EtOAc /Hexane = 2.0/8.0); mp = 169-171 °C; ^1H NMR (400 MHz, CDCl_3) δ 11.88 (s, 1H), 7.56 (d, J = 8.4 Hz, 1H), 7.41 (d, J = 2.4 Hz, 1H), 7.28 – 7.25 (dd, J = 8.4, 2.0 Hz, 1H), 4.62 (q, J = 7.1 Hz, 2H), 1.56 (t, J = 7.2 Hz, 3H); ^{13}C $\{^1\text{H}\}$ NMR (100 MHz, CDCl_3) δ 154.2, 152.4, 132.6, 130.0, 129.8, 127.8, 124.9, 115.3, 64.0, 14.1; HRMS (ESI) m/z : $[\text{M} + \text{H}]^+$ Calcd for $\text{C}_{10}\text{H}_{10}\text{ClN}_2\text{O}_2^+$ 225.0425; found 225.0427.

3-Ethoxy-6,7-dimethylquinoxalin-2(1H)-one (3la): White solid; 65 mg, 88% yield; Purification



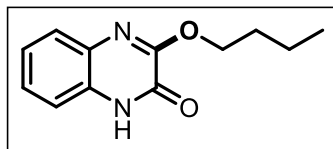
by column chromatography on silica gel (eluent: EtOAc /Hexane = 2.0/8.0); mp = 148-150 °C; ^1H NMR (400 MHz, CDCl_3) δ 11.76 (s, 1H), 7.41 (s, 1H), 7.15 (s, 1H), 4.59 (q, J = 7.1 Hz, 2H), 2.36 (s, 3H), 2.34 (s, 3H), 1.55 (t, J = 7.0 Hz, 3H); ^{13}C $\{^1\text{H}\}$ NMR (100 MHz, CDCl_3) δ 153.7, 152.6, 136.6, 133.4, 129.5, 127.0, 126.9, 116.0, 63.5, 19.6, 19.5, 14.2; HRMS (ESI) m/z : $[\text{M} + \text{H}]^+$ Calcd for $\text{C}_{12}\text{H}_{15}\text{N}_2\text{O}_2^+$ 219.1128; found 219.1131.

3-Propoxyquinoxalin-2(1H)-one (3ab): White solid; 63 mg, 91% yield; mp = 91-93 °C; Purifi-



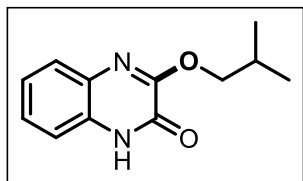
cation by column chromatography on silica gel (eluent: EtOAc /Hexane = 1.5/8.5); ^1H NMR (400 MHz, CDCl_3) δ 11.53 (s, 1H), 7.65 – 7.63 (m, 1H), 7.38 – 7.34 (m, 2H), 7.33 – 7.29 (m, 1H), 4.51 (t, J = 7.0 Hz, 2H), 1.98 (sext, J = 7.3 Hz, 2H), 1.10 (t, J = 7.4 Hz, 3H); ^{13}C $\{^1\text{H}\}$ NMR (100 MHz, CDCl_3) δ 154.4, 152.4, 131.3, 129.2, 127.0, 126.7, 124.4, 115.5, 69.3, 21.8, 10.5; HRMS (ESI) m/z : $[\text{M} + \text{H}]^+$ Calcd for $\text{C}_{11}\text{H}_{13}\text{N}_2\text{O}_2^+$ 205.0972; found 205.0975.

3-Butoxyquinoxalin-2(1H)-one (3ac): White solid; 66 mg, 89% yield; Purification by column



chromatography on silica gel (eluent: EtOAc /Hexane = 2.0/8.0); mp = 80-82 °C; ^1H NMR (400 MHz, CDCl_3) δ 10.90 (s, 1H), 7.65 – 7.63 (m, 1H), 7.40 – 7.35 (m, 1H), 7.33 – 7.29 (m, 2H), 4.54 (t, J = 6.8 Hz, 2H), 1.93 (quint, J = 7.2 Hz, 2H), 1.55 (sext, J = 7.5 Hz, 2H), 1.03 (t, J = 7.4 Hz, 3H); ^{13}C $\{^1\text{H}\}$ NMR (100 MHz, CDCl_3) δ 154.5, 152.0, 131.3, 129.1, 127.0, 126.8, 124.3, 115.2, 67.6, 30.5, 19.2, 13.8; HRMS (ESI) m/z : $[\text{M} + \text{H}]^+$ Calcd for $\text{C}_{12}\text{H}_{15}\text{N}_2\text{O}_2^+$ 219.1128; found 219.1125.

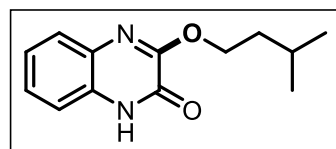
3-Isobutoxyquinoxalin-2(1H)-one (3ad): White solid; 63 mg, 85% yield; Purification by column chromatography on silica gel (eluents: EtOAc /Hexane =



2.0/8.0); mp = 68-70°C; ¹H NMR (400 MHz, CDCl₃) δ 11.82 (s, 1H), 7.64 (d, *J* = 7.6 Hz, 1H), 7.38 – 7.37 (m, 2H), 7.33 – 7.30 (m, 1H), 4.32 (d, *J* = 7.2 Hz, 2H), 2.32 (sept, *J* = 6.7 Hz, 1H), 1.11 (s, 3H),

1.10 (s, 3H); ¹³C{¹H} NMR (100 MHz, CDCl₃) δ 154.5, 152.5, 131.3, 129.2, 127.0, 126.7, 124.3, 115.6, 73.8, 27.6, 19.3; HRMS (ESI) *m/z*: [M + H]⁺ Calcd for C₁₂H₁₅N₂O₂⁺ 219.1128; found 219.1125.

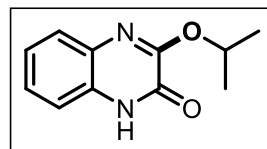
3-(Isopentyloxy)quinoxalin-2(1H)-one (3ae): White solid; 68 mg, 86% yield; Purification by



column chromatography on silica gel (eluents: EtOAc /Hexane = 1.5/8.5); mp = 81-83°C; ¹H NMR (400 MHz, CDCl₃) δ 11.63 (s, 1H), 7.65 (d, *J* = 7.6 Hz, 1H), 7.38 – 7.35 (m, 2H), 7.33 – 7.29 (m,

1H), 4.58 (t, *J* = 6.8 Hz, 2H), 1.92 – 1.82 (m, 3H), 1.04 (s, 3H), 1.02 (s, 3H); ¹³C{¹H} NMR (100 MHz, CDCl₃) δ 154.4, 152.3, 131.3, 129.1, 127.0, 126.7, 124.4, 115.4, 66.4, 37.2, 25.1, 22.6; HRMS (ESI) *m/z*: [M + H]⁺ Calcd for C₁₃H₁₇N₂O₂⁺ 233.1285; found 233.1283.

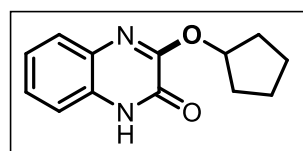
3-Isopropoxyquinoxalin-2(1H)-one (3af): White solid; 56 mg, 81% yield; Purification by column



chromatography on silica gel (eluents: EtOAc /Hexane = 2.5/7.5); mp = 100-102 °C; ¹H NMR (400 MHz, CDCl₃) δ 12.33 (s, 1H), 7.62 (dd, *J* = 7.8, 1.4 Hz, 1H), 7.43 (dd, *J* = 8.0, 1.2 Hz, 1H), 7.36 (td, *J* =

7.6, 1.5 Hz, 1H), 7.30 (td, *J* = 7.6, 1.5 Hz, 1H), 5.55 (sept, *J* = 6.2 Hz, 1H), 1.52 (s, 3H), 1.51 (s, 3H); ¹³C{¹H} NMR (100 MHz, CDCl₃) δ 153.7, 153.0, 131.5, 129.1, 126.8, 126.5, 124.3, 115.9, 70.8, 21.6; HRMS (ESI) *m/z*: [M + H]⁺ Calcd for C₁₁H₁₃N₂O₂⁺ 205.0972; found 205.0969.

3-(Cyclopentyloxy)quinoxalin-2(1H)-one (3ag): White solid; 71 mg, 90% yield; Purification by

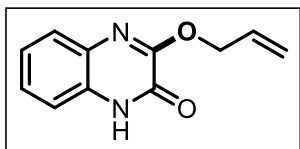


column chromatography on silica gel (eluents: EtOAc /Hexane = 2.0/8.0); mp = 80-82°C; ¹H NMR (400 MHz, CDCl₃) δ 12.03 (s, 1H), 7.63 (d, *J* = 8.0 Hz, 1H), 7.37 – 7.34 (m, 2H), 7.31 – 7.28 (m, 1H),

5.61 – 5.60 (m, 1H), 2.16 – 2.11 (m, 2H), 1.99 – 1.96 (m, 2H), 1.90 – 1.89 (m, 2H), 1.70 – 1.67 (m, 2H); ¹³C{¹H} NMR (100 MHz, CDCl₃) δ 154.2, 152.8, 131.5, 129.1, 126.8, 126.7, 124.3,

115.6, 80.2, 32.6, 24.1; HRMS (ESI) m/z : $[M + H]^+$ Calcd for $C_{13}H_{15}N_2O_2^+$ 231.1128; found 231.1131.

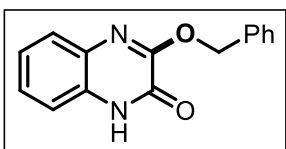
3-(Allyloxy)quinoxalin-2(1H)-one (3ah): White solid; 52 mg, 75% yield; Purification by col-



umn chromatography on silica gel (eluent: EtOAc /Hexane = 1.5/8.5); mp = 144-146 °C; 1H NMR (400 MHz, $CDCl_3$) δ 11.21 (s, 1H), 7.66 – 7.64 (m, 1H), 7.41 – 7.37 (m, 1H), 7.34 – 7.30 (m, 2H),

6.27 – 6.17 (m, 1H), 5.52 (dq, $J = 17.2, 1.3$ Hz, 1H), 5.37 (dd, $J = 10.4, 1.2$ Hz, 1H), 5.07 (dt, $J = 6.0, 1.2$ Hz, 2H); $^{13}C\{^1H\}$ NMR (100 MHz, $CDCl_3$) δ 153.8, 152.3, 132.0, 131.1, 129.3, 127.2, 126.8, 124.4, 119.4, 115.5, 68.3; HRMS (ESI) m/z : $[M + H]^+$ Calcd for $C_{11}H_{11}N_2O_2^+$ 203.0815; found 203.0811.

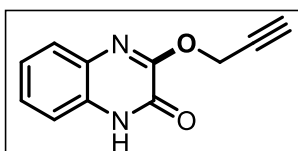
3-(Benzyloxy)quinoxalin-2(1H)-one (3ai): White solid; 77 mg, 89% yield; Purification by col-



umn chromatography on silica gel (eluent: EtOAc /Hexane = 2.0/8.0); mp = 150-152 °C; 1H NMR (400 MHz, $CDCl_3$) δ 12.27 (s, 1H), 7.65 (dd, $J = 7.6, 1.2$ Hz, 1H), 7.58 (d, $J = 7.2$ Hz, 2H), 7.41 –

7.30 (m, 6H), 5.60 (s, 2H); $^{13}C\{^1H\}$ NMR (100 MHz, $CDCl_3$) δ 153.9, 152.6, 135.8, 131.1, 129.4, 128.8, 128.5, 128.3, 127.2, 126.7, 124.4, 115.8, 69.1; HRMS (ESI) m/z : $[M + H]^+$ Calcd for $C_{15}H_{13}N_2O_2^+$ 253.0972; found 253.0970.

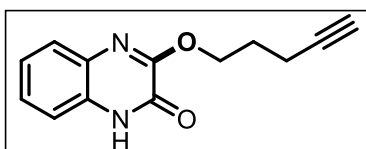
3-(Prop-2-yn-1-yloxy)quinoxalin-2(1H)-one (3aj): White solid; 49 mg, 71% yield; Purification



by column chromatography on silica gel (eluent: EtOAc /Hexane = 2.5/7.5); mp = 112-114 °C; 1H NMR (400 MHz, $CDCl_3$) δ 12.00 (s, 1H), 7.57 (d, $J = 7.6$ Hz, 1H), 7.30 – 7.24 (m, 2H), 7.22 – 7.18 (m, 1H), 5.06 (s, 2H), 2.48 (s, 1H); $^{13}C\{^1H\}$ NMR (100 MHz, $CDCl_3$) δ

153.3, 151.2, 130.4, 130.3, 127.2, 126.7, 123.7, 115.4, 77.9, 75.2, 54.5; HRMS (ESI) m/z : $[M + H]^+$ Calcd for $C_{11}H_9N_2O_2^+$ 201.0659; found 201.0656.

3-(Pent-4-yn-1-yloxy)quinoxalin-2(1H)-one (3ak): White solid; 64 mg, 88% yield; Purification

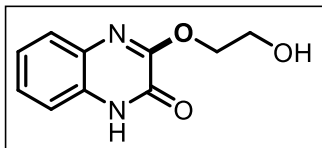


by column chromatography on silica gel (eluent: EtOAc /Hexane = 1.5/8.5); mp = 84-86 °C; 1H NMR (400 MHz, $CDCl_3$) δ 11.80 (s, 1H), 7.65 (d, $J = 7.6$, 1H), 7.42 – 7.37 (m, 2H), 7.34 –

7.30 (m, 1H), 4.65 (t, $J = 6.6$ Hz, 2H), 2.51 (t, $J = 7.0$ Hz, 2H), 2.17 (quin, $J = 6.8$ Hz, 2H); $^{13}C\{^1H\}$ NMR (100 MHz, $CDCl_3$) δ 154.2, 152.4, 131.2, 129.2, 127.1, 126.8, 124.4, 115.6,

106.0, 85.4, 66.3, 27.6, 16.7; HRMS (ESI) m/z : $[M + H]^+$ Calcd for $C_{13}H_{13}N_2O_2^+$ $[M + H]^+$ 229.0972; found 229.0969.

3-(2-Hydroxyethoxy)quinoxalin-2(1H)-one (3al): White solid; 66 mg, 93% yield; Purification

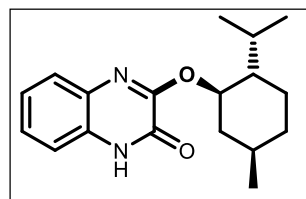


by column chromatography on silica gel (eluent: EtOAc /Hexane = 7.5/2.5); mp = 122-124 °C; 1H NMR (400 MHz, DMSO- d_6) δ 12.37 (s, 1H), 7.51 (d, J = 8.0 Hz, 1H), 7.34 (t, J = 7.4 Hz, 1H),

7.26 – 7.20 (m, 2H), 4.94 (t, J = 5.4 Hz, 1H), 4.38 (t, J = 5.2 Hz, 2H), 3.77 (q, J = 5.2 Hz, 2H);

$^{13}C\{^1H\}$ NMR (100 MHz, DMSO- d_6) δ 155.2, 150.9, 130.75, 130.66, 127.2, 126.5, 123.7, 115.4, 68.9, 63.2; HRMS (ESI) m/z : $[M + H]^+$ Calcd for $C_{10}H_{11}N_2O_3^+$ 207.0764; found 207.0760.

3-(((1R,2R,5R)-2-Isopropyl-5-methylcyclohexyl)oxy)quinoxalin-2(1H)-one (3am): White



solid; 92 mg, 90% yield; Purification by column chromatography on silica gel (eluent: EtOAc /Hexane = 2.0/8.0); mp = 98-100 °C; 1H NMR (400 MHz, $CDCl_3$) δ 12.00 (s, 1H), 7.63 (dd, J = 7.8, 1.0 Hz, 1H), 7.40 (dd, J = 8.0, 1.2 Hz, 1H), 7.38 – 7.32 (dt, J = 7.4, 1.3 Hz,

1H), 7.31 – 7.27 (m, 1H), 5.30 (td, J = 10.8, 4.4 Hz, 1H), 2.30 – 2.27 (m, 1H), 2.14 – 2.07 (m,

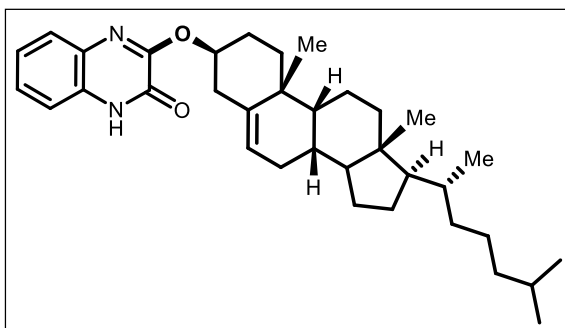
1H), 1.80 – 1.74 (m, 3H), 1.69 – 1.60 (m, 1H), 1.30 – 1.14 (m, 2H), 0.98 (d, J = 6.8 Hz, 3H),

0.94 (d, J = 7.2 Hz, 3H), 0.83 (d, J = 7.2 Hz, 3H); $^{13}C\{^1H\}$ NMR (100 MHz, $CDCl_3$) δ 154.0,

152.8, 131.5, 129.1, 126.64, 126.56, 124.2, 115.7, 47.1, 40.0, 34.4, 31.6, 26.2, 23.6, 22.2, 20.8,

16.5; HRMS (ESI) m/z : $[M + H]^+$ Calcd for $C_{18}H_{25}N_2O_2^+$ 301.1911; found 301.1907.

3-(((3S,8S,9R,10R,13R,17R)-10,13-dimethyl-17-((R)-6-methylheptan-2-yl)-2,3,4,7,8,9,10,11,12,13,14,15,16,17-tetradecahydro-1H-cyclopenta[a]phenanthren-3-yl)oxy)quinoxalin-



2(1H)-one (3an): White solid; 132 mg, 73%

yield; mp = 180-182 °C; Purification by column

chromatography on silica gel (eluent: EtOAc

/Hexane = 1.5/8.5); 1H NMR (400 MHz,

$CDCl_3$) δ 11.74 (s, 1H), 7.63 (d, J = 7.6 Hz, 1H),

7.40 – 7.30 (m, 3H), 5.47 (d, J = 3.6 Hz, 1H),

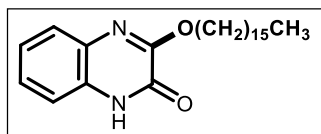
5.22 – 5.14 (m, 1H), 2.64 (d, J = 7.6 Hz, 2H),

2.19 – 1.82 (m, 6H), 1.65 – 1.50 (m, 6H), 1.42 – 1.24 (m, 7H), 1.22 – 1.15 (m, 4H), 1.11 (s,

3H), 1.06 – 1.02 (m, 3H), 0.95 (d, J = 6.8 Hz, 3H), 0.90 (dd, J = 6.6, 1.8 Hz, 6H), 0.72 (s, 3H);

$^{13}\text{C}\{^1\text{H}\}$ NMR (100 MHz, CDCl_3) δ 153.4, 152.8, 140.0, 131.6, 128.7, 127.0, 126.8, 124.6, 122.7, 115.6, 56.8, 56.2, 50.2, 42.4, 39.8, 39.5, 37.8, 37.1, 36.8, 36.2, 35.8, 32.0, 31.9, 28.2, 28.0, 27.4, 24.3, 23.8, 22.8, 22.6, 21.1, 19.4, 18.7, 14.1, 11.9; HRMS (ESI) m/z : $[\text{M} + \text{H}]^+$ Calcd for $\text{C}_{35}\text{H}_{51}\text{N}_2\text{O}_2^+$ 531.3945; found 531.3949.

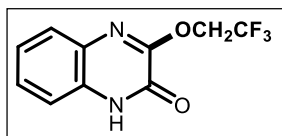
3-(Hexadecyloxy)quinoxalin-2(1H)-one (3ao): White solid; 80 mg, 61% yield; Purification by



column chromatography on silica gel (eluent: EtOAc /Hexane = 1.0/9.0); mp = 92-94 °C; ^1H NMR (400 MHz, CDCl_3) δ 11.97 (s, 1H), 7.64 (d, $J = 7.9$ Hz, 1H), 7.39 – 7.35 (m, 2H), 7.31 (t, $J = 8.0$

Hz, 1H), 4.54 (t, $J = 6.8$ Hz, 2H), 1.94 (quin, $J = 7.1$ Hz, 2H), 1.54 – 1.47 (m, 2H), 1.44 – 1.38 (m, 2H), 1.28 (s, 22H), 0.90 (t, $J = 6.8$ Hz, 3H); $^{13}\text{C}\{^1\text{H}\}$ NMR (100 MHz, CDCl_3) δ 154.5, 152.6, 131.4, 129.1, 126.9, 126.7, 124.4, 115.7, 67.9, 31.9, 29.70, 29.67, 29.63, 29.56, 29.4, 28.5, 25.9, 22.7, 14.1; HRMS (ESI) m/z : $[\text{M} + \text{H}]^+$ Calcd for $\text{C}_{24}\text{H}_{39}\text{N}_2\text{O}_2^+$ 387.3006; found 387.3011.

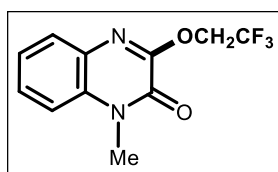
3-(2,2,2-Trifluoroethoxy)quinoxalin-2(1H)-one (5aa): White solid; 72 mg, 86% yield; Purification by



column chromatography on silica gel (eluent: EtOAc /Hexane = 1.5/8.5; mp = 154-156 °C; ^1H NMR (400 MHz, CDCl_3) δ 11.47 (s, 1H), 7.67 (d, $J = 8.0$ Hz, 1H), 7.59 – 7.45 (m, 1H), 7.41 – 7.34 (m,

2H), 4.97 (q, $J = 8.2$ Hz, 2H); $^{13}\text{C}\{^1\text{H}\}$ NMR (100 MHz, CDCl_3) δ 152.4, 151.1, 130.1, 129.8, 128.3, 127.1, 124.7, 124.5 (q, $^1J_{\text{C-F}} = 276.3$ Hz), 115.5, 63.0 (q, $^2J_{\text{C-F}} = 35.3$ Hz); $^{19}\text{F}\{^{13}\text{C}\}$ NMR (376 MHz, CDCl_3) δ -73.00 (t, $J = 8.3$ Hz); HRMS (ESI) m/z : calcd for $\text{C}_{10}\text{H}_8\text{F}_3\text{N}_2\text{O}_2^+$ 245.0532; found 245.0525.

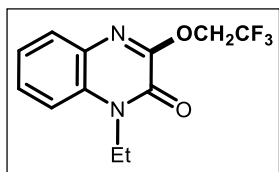
1-Methyl-3-(2,2,2-trifluoroethoxy)quinoxalin-2(1H)-one (5ba): White solid; 77 mg, 88% yield;



Purification by column chromatography on silica gel (eluent: EtOAc /Hexane = 1.5/8.5; mp = 126-128 °C; ^1H NMR (400 MHz, CDCl_3) δ 7.67 (dd, $J = 8.0, 1.6$ Hz, 1H), 7.53 – 7.48 (m, 1H), 7.36 (td, $J = 7.8, 1.2$ Hz, 1H), 7.32 (dd, $J = 8.4, 1.2$ Hz, 1H), 4.93 (q, $J = 8.3$ Hz, 2H),

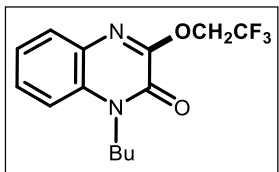
3.77 (s, 3H); $^{13}\text{C}\{^1\text{H}\}$ NMR (100 MHz, CDCl_3) δ 152.0, 150.2, 132.1, 130.0, 128.2, 127.9, 124.2, 123.1 (q, C-F, $^1J_{\text{C-F}} = 273.0$ Hz), 113.8, 62.8 (q, C-F, $^2J_{\text{C-F}} = 36.7$ Hz), 29.6; $^{19}\text{F}\{^{13}\text{C}\}$ NMR (376 MHz, CDCl_3) δ -73.02 (t, $J = 8.3$ Hz); HRMS (ESI) m/z : $[\text{M} + \text{H}]^+$ Calcd for $\text{C}_{11}\text{H}_{10}\text{F}_3\text{N}_2\text{O}_2^+$ 259.0689; found 259.0691.

1-Ethyl-3-(2,2,2-trifluoroethoxy)quinoxalin-2(1H)-one (5ca): White solid; 82 mg, 89% yield;



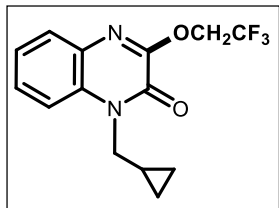
Purification by column chromatography on silica gel (eluent: EtOAc /Hexane = 2.0/8.0); mp = 118-120 °C; ^1H NMR (400 MHz, CDCl_3) δ 7.68 (dd, $J = 8.2, 1.4$ Hz, 1H), 7.51 – 7.47 (m, 1H), 7.36 – 7.32 (m, 2H), 4.92 (q, $J = 8.1$ Hz, 2H), 4.39 (q, $J = 7.2$ Hz, 2H), 1.42 (t, $J = 7.2$ Hz, 3H); $^{13}\text{C}\{^1\text{H}\}$ NMR (100 MHz, CDCl_3) δ 152.0, 149.7, 131.0, 130.3, 128.1, 124.0, 123.1 (q, C-F, $^1J_{\text{C-F}} = 275.6$ Hz), 113.7, 62.7 (q, C-F, $^2J_{\text{C-F}} = 36.7$ Hz), 37.9, 12.4; $^{19}\text{F}\{^{13}\text{C}\}$ NMR (376 MHz, CDCl_3) δ -73.0 (t, $J = 8.3$ Hz); HRMS (ESI) m/z : $[\text{M} + \text{H}]^+$ Calcd for $\text{C}_{12}\text{H}_{12}\text{F}_3\text{N}_2\text{O}_2^+$ 273.0845; found 273.0841.

1-Butyl-3-(2,2,2-trifluoroethoxy)quinoxalin-2(1H)-one (5da): White solid; 72 mg, 71% yield;



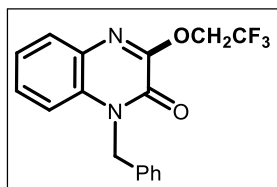
Purification by column chromatography on silica gel (eluent: EtOAc /Hexane = 2.0/8.0); mp = 124-126 °C; ^1H NMR (400 MHz, CDCl_3) δ 7.68 – 7.66 (m, 1H), 7.51 – 7.47 (m, 1H), 7.36 – 7.31 (m, 2H), 4.91 (q, $J = 8.3$ Hz, 2H), 4.33 – 4.29 (m, 2H), 1.82 – 1.74 (m, 2H), 1.56 – 1.47 (m, 2H), 1.03 (t, $J = 7.4$ Hz, 3H); $^{13}\text{C}\{^1\text{H}\}$ NMR (100 MHz, CDCl_3) δ 152.0, 149.9, 131.3, 130.3, 128.1, 128.0, 124.0, 123.2 (q, $^1J_{\text{C-F}} = 268.7$ Hz), 113.8, 62.8 (q, $^2J_{\text{C-F}} = 36.7$ Hz), 42.6, 29.2, 20.2, 13.7; ^{19}F NMR (376 MHz, CDCl_3) δ -73.02 (t, $J = 8.3$ Hz); HRMS (ESI) m/z : $[\text{M} + \text{H}]^+$ Calcd for $\text{C}_{14}\text{H}_{16}\text{F}_3\text{N}_2\text{O}_2^+$ 301.1158; found 301.1160.

1-(Cyclopropylmethyl)-3-(2,2,2-trifluoroethoxy)quinoxalin-2(1H)-one (5ea): White solid; 77



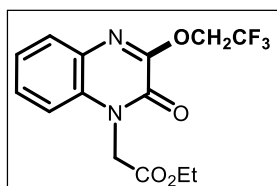
mg, 76% yield; Purification by column chromatography on silica gel (eluent: EtOAc /Hexane = 1.5/8.5); mp = 136-138 °C; ^1H NMR (400 MHz, CDCl_3) δ 7.66 (dd, $J = 8.0, 1.6$ Hz, 1H), 7.43 – 7.40 (m, 1H), 7.33 – 7.27 (m, 2H), 5.97 – 5.87 (m, 1H), 5.17 – 5.10 (m, 2H), 4.56 (q, $J = 7.2$ Hz, 2H), 4.39 – 4.35 (m, 2H), 2.58 – 2.52 (m, 2H); $^{13}\text{C}\{^1\text{H}\}$ NMR (100 MHz, CDCl_3) δ 153.9, 134.0, 127.8, 127.7, 126.9, 125.0, 123.8, 123.2 (q, $^1J_{\text{C-F}} = 268.7$ Hz), 119.8, 117.7, 113.6, 63.5 (q, $^2J_{\text{C-F}} = 36.7$ Hz), 41.8, 31.5, 14.2, 4.1; ^{19}F NMR (376 MHz, CDCl_3) δ -73.02 (t, $J = 8.3$ Hz); HRMS (ESI) m/z : $[\text{M} + \text{H}]^+$ Calcd for $\text{C}_{14}\text{H}_{14}\text{F}_3\text{N}_2\text{O}_2^+$ 299.1002; found 299.1000.

1-Benzyl-3-(2,2,2-trifluoroethoxy)quinoxalin-2(1H)-one (5fa): White solid; 90 mg, 79% yield;



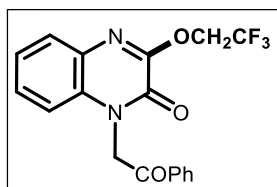
Purification by column chromatography on silica gel (eluents: EtOAc /Hexane = 2.5/7.5); mp = 148-150 °C; ^1H NMR (400 MHz, CDCl_3) δ 7.67 (dd, $J = 7.8, 1.4$ Hz, 1H), 7.40 – 7.34 (m, 2H), 7.33 – 7.27 (m, 6H), 5.56 (s, 2H), 4.95 (q, $J = 8.3$ Hz, 2H); $^{13}\text{C}\{^1\text{H}\}$ NMR (100 MHz, CDCl_3) δ 152.1, 150.4, 134.9, 131.4, 130.2, 129.0, 128.1, 128.0, 127.8, 127.0, 124.2, 123.0 (q, $^1J_{\text{C-F}} = 270.7$ Hz), 114.6, 62.9 (q, $^2J_{\text{C-F}} = 38.0$ Hz), 46.4; ^{19}F NMR (376 MHz, CDCl_3) δ -72.97 (t, $J = 8.5$ Hz); HRMS (ESI) m/z : $[\text{M} + \text{H}]^+$ Calcd for $\text{C}_{17}\text{H}_{14}\text{F}_3\text{N}_2\text{O}_2^+$ 335.1002; found 335.0999.

Ethyl 2-(2-oxo-3-(2,2,2-trifluoroethoxy)quinoxalin-1(2H)-yl)acetate (5ga): White solid; 91 mg,



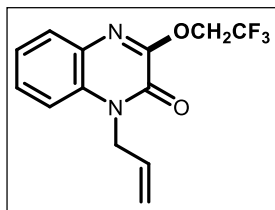
81% yield; Purification by column chromatography on silica gel (eluents: EtOAc /Hexane = 2.0/8.0); mp = 122-124 °C; ^1H NMR (400 MHz, CDCl_3) δ 7.69 (dd, $J = 8.0, 1.2$ Hz, 1H), 7.49 – 7.44 (m, 1H), 7.36 (td, $J = 8.0, 1.2$ Hz, 1H), 7.08 (dd, $J = 8.4, 1.2$ Hz, 1H), 5.08 (s, 2H), 4.93 (q, $J = 8.3$ Hz, 2H), 4.28 (q, $J = 7.1$ Hz, 2H), 1.30 (t, $J = 7.0$ Hz, 3H); $^{13}\text{C}\{^1\text{H}\}$ NMR (100 MHz, CDCl_3) δ 166.8, 151.8, 150.0, 148.3, 131.3, 128.3, 128.2, 125.9 (q, $^1J_{\text{C-F}} = 272.7$ Hz), 124.5, 113.3, 63.7 (q, $^2J_{\text{C-F}} = 38.0$ Hz), 62.2, 43.9, 14.1; ^{19}F NMR (376 MHz, CDCl_3) δ -72.99 (t, $J = 8.2$ Hz); HRMS (ESI) m/z : $[\text{M} + \text{H}]^+$ Calcd for $\text{C}_{14}\text{H}_{14}\text{F}_3\text{N}_2\text{O}_4^+$ 331.0900; found 331.0901.

1-(2-Oxo-2-phenylethyl)-3-(2,2,2-trifluoroethoxy)quinoxalin-2(1H)-one (5ha): White solid;



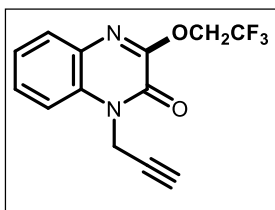
111 mg, 90% yield; Purification by column chromatography on silica gel (eluents: EtOAc /Hexane = 2.5/7.5); mp = 154-156 °C; ^1H NMR (400 MHz, CDCl_3) δ 8.10 (dd, $J = 8.2, 1.4$ Hz, 2H), 7.73 – 7.69 (m, 2H), 7.59 (t, $J = 7.8$ Hz, 2H), 7.39 (td, $J = 7.6, 1.7$ Hz, 1H), 7.33 (td, $J = 8.0, 1.6$ Hz, 1H), 6.95 (dd, $J = 8.4, 1.4$ Hz, 1H), 5.79 (s, 2H), 4.95 (q, $J = 8.3$ Hz, 2H); $^{13}\text{C}\{^1\text{H}\}$ NMR (100 MHz, CDCl_3) δ 190.7, 151.8, 150.1, 134.5, 134.4, 131.5, 130.1, 129.1, 128.19, 128.17, 128.1, 124.3, 123.1 (q, $^1J_{\text{C-F}} = 270.0$ Hz), 113.7, 64.3 (q, $^2J_{\text{C-F}} = 38.0$ Hz), 48.8; ^{19}F NMR (376 MHz, CDCl_3) δ -73.01 (t, $J = 8.5$ Hz); HRMS (ESI) m/z : $[\text{M} + \text{H}]^+$ Calcd for $\text{C}_{18}\text{H}_{14}\text{F}_3\text{N}_2\text{O}_3^+$ 363.0951; found 363.0948.

1-Allyl-3-(2,2,2-trifluoroethoxy)quinoxalin-2(1H)-one (5ia): White solid; 70 mg, 72% yield;



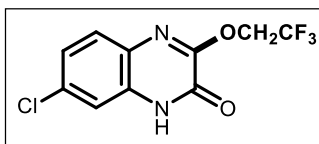
Purification by column chromatography on silica gel (eluents: EtOAc /Hexane = 1.5/8.5); mp = 172-174 °C; ^1H NMR (400 MHz, CDCl_3) δ 7.67 (dd, J = 8.0, 1.6 Hz, 1H), 7.48 – 7.44 (m, 1H), 7.34 (td, J = 7.6, 1.1 Hz, 1H), 7.30 (dd, J = 8.6, 1.0 Hz, 1H), 6.00 – 5.91 (m, 1H), 5.31 (dd, J = 10.4, 0.8 Hz, 1H), 5.23 (dd, J = 17.2, 0.4 Hz, 1H), 4.97 – 4.89 (m, 4H); $^{13}\text{C}\{^1\text{H}\}$ NMR (100 MHz, CDCl_3) δ 152.0, 149.8, 131.3, 130.3, 130.1, 128.0, 124.2, 123.1 (q, C-F, $^1J_{\text{C-F}}$ = 275.9 Hz), 118.5, 114.4, 62.9 (q, $^2J_{\text{C-F}}$ = 38.0 Hz), 45.0; ^{19}F NMR (376 MHz, CDCl_3) δ -73.01 (t, J = 8.5 Hz); HRMS (ESI) m/z : $[\text{M} + \text{H}]^+$ Calcd for $\text{C}_{13}\text{H}_{12}\text{F}_3\text{N}_2\text{O}_2^+$ 285.0845; found 285.0848.

1-(Prop-2-yn-1-yl)-3-(2,2,2-trifluoroethoxy)quinoxalin-2(1H)-one (5ja): White solid; 77 mg,



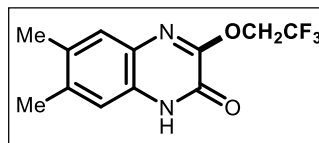
80% yield; Purification by column chromatography on silica gel (eluents: EtOAc /Hexane = 1.5/8.5); mp = 146-148 °C; ^1H NMR (400 MHz, CDCl_3) δ 7.69 (dd, J = 8.0, 1.6 Hz, 1H), 7.56 – 7.52 (m, 1H), 7.49 (dd, J = 8.4, 1.2 Hz, 1H), 7.41 – 7.37 (m, 1H), 5.12 (d, J = 2.4 Hz, 2H), 4.92 (q, J = 8.4 Hz, 2H), 2.33 (t, J = 2.6 Hz, 1H); $^{13}\text{C}\{^1\text{H}\}$ NMR (100 MHz, CDCl_3) δ 151.8, 149.4, 130.6, 130.1, 128.2, 128.0, 124.6, 123.0 (q, $^1J_{\text{C-F}}$ = 269.3 Hz), 114.4, 76.4, 73.5, 62.9 (q, $^2J_{\text{C-F}}$ = 38.0 Hz), 32.0; ^{19}F NMR (376 MHz, CDCl_3) δ -73.00 (t, J = 8.2 Hz); HRMS (ESI) m/z : $[\text{M} + \text{H}]^+$ Calcd for $\text{C}_{13}\text{H}_{10}\text{F}_3\text{N}_2\text{O}_2^+$ 283.0689; found 283.0684.

7-Chloro-3-(2,2,2-trifluoroethoxy)quinoxalin-2(1H)-one (5ka): White solid; 50 mg, 53% yield;



Purification by column chromatography on silica gel (eluents: EtOAc /Hexane = 3.0/7.0); mp = 154-156 °C; ^1H NMR (400 MHz, CDCl_3) δ 11.47 (s, 1H), 7.67 (d, J = 8.0 Hz, 1H), 7.49 – 7.45 (m, 1H), 7.41 – 7.36 (m, 1H), 4.97 (q, J = 8.2 Hz, 2H); $^{13}\text{C}\{^1\text{H}\}$ NMR (100 MHz, CDCl_3) δ 152.5, 151.2, 130.2, 129.9, 128.4, 127.2, 124.8, 124.6 (q, $^1J_{\text{C-F}}$ = 276.3 Hz), 115.6, 63.1 (q, $^2J_{\text{C-F}}$ = 35.3 Hz); $^{19}\text{F}\{^{13}\text{C}\}$ NMR (376 MHz, CDCl_3) δ -73.01 (t, J = 8.3 Hz); HRMS (ESI) m/z : $[\text{M} + \text{H}]^+$ Calcd for $\text{C}_{10}\text{H}_7\text{ClF}_3\text{N}_2\text{O}_2^+$ 279.0143; found 279.0147.

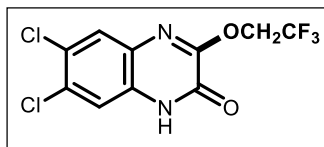
6,7-Dimethyl-3-(2,2,2-trifluoroethoxy)quinoxalin-2(1H)-one (5la): White solid; 75 mg, 81%



yield; Purification by column chromatography on silica gel (eluents: EtOAc /Hexane = 1.0/9.0); mp = 136-138 °C; ^1H NMR (400 MHz, CDCl_3) δ 11.07 (s, 1H), 7.43 (s, 1H), 7.11 (s, 1H), 4.93 (q, J = 8.3 Hz, 2H), 2.38 (s, 3H), 2.36 (s, 3H); $^{13}\text{C}\{^1\text{H}\}$ NMR (100 MHz, CDCl_3) δ 162.3, 156.5,

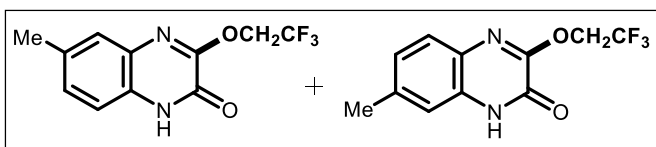
138.0, 133.8, 128.2, 127.2, 125.3 (q, $^1J_{C-F} = 278.8$ Hz), 115.8, 106.6, 62.8 (q, $^2J_{C-F} = 38.7$ Hz), 19.8, 19.5; ^{19}F NMR (376 MHz, CDCl_3) δ -72.99 (t, $J = 8.2$ Hz); HRMS (ESI) m/z : $[\text{M} + \text{H}]^+$ Calcd for $\text{C}_{12}\text{H}_{12}\text{F}_3\text{N}_2\text{O}_2^+$ 273.0845; found 273.0848.

6,7-Dichloro-3-(2,2,2-trifluoroethoxy)quinoxalin-2(1H)-one (5ma): White solid; 81 mg, 77%



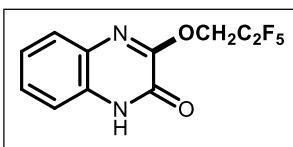
yield; Purification by column chromatography on silica gel (eluent: EtOAc /Hexane = 1.5/8.5); mp = 160-162 °C; ^1H NMR (400 MHz, CDCl_3) δ 12.15 (s, 1H), 7.75 (s, 1H), 7.55 (s, 1H), 4.94 (q, $J = 8.2$ Hz, 2H); $^{13}\text{C}\{^1\text{H}\}$ NMR (100 MHz, CDCl_3) δ 153.0, 151.2, 132.5, 129.4, 128.9, 128.7, 128.0, 122.8 (q, C-F, $^1J_{C-F} = 276.2$ Hz), 116.9, 66.3 (q, C-F, $^2J_{C-F} = 36.9$ Hz); ^{19}F NMR (376 MHz, CDCl_3) δ -72.98 (t, $J = 8.2$ Hz); HRMS (ESI) m/z : $[\text{M} + \text{H}]^+$ Calcd for $\text{C}_{10}\text{H}_6\text{Cl}_2\text{F}_3\text{N}_2\text{O}_2^+$ 312.9753; found 312.975.

6/7-Methyl-3-(2,2,2-trifluoroethoxy)quinoxalin-2(1H)-one (5na): White solid; 75 mg, 82%



yield; Purification by column chromatography on silica gel (eluent: EtOAc /Hexane = 2.0/8.0); mp = 152-154 °C; ^1H NMR (400 MHz, CDCl_3) δ 7.54 (d, $J = 8.0$ Hz, 1H), 7.47 (d, $J = 0.8$ Hz, 1.6H), 7.31 (dd, $J = 8.4, 1.6$ Hz, 1.6H), 7.20 (d, $J = 8.4$ Hz, 1.6H), 7.16 (dd, $J = 8.0, 1.2$ Hz, 1H), 7.10 (s, 1H), 4.94 – 4.87 (m, 5H), 3.74 (s, 3H), 3.74 (s, 5H), 2.52 (s, 3H), 2.46 (s, 5H); $^{13}\text{C}\{^1\text{H}\}$ NMR (100 MHz, CDCl_3) δ 152.1, 151.4, 150.3, 150.1, 138.6, 134.1, 131.9, 129.9, 129.8, 129.2, 127.9, 127.8, 127.5, 125.4, 123.12 (q, $J = 276$ Hz), 123.11 (q, $J = 276$ Hz), 114.0, 113.5, 62.7 (q, $J = 36.9$ Hz), 29.6, 29.5, 21.9, 20.7; ^{19}F NMR (376 MHz, CDCl_3) δ -72.99 – -73.06 (multiplet); HRMS (ESI) m/z : $[\text{M} + \text{H}]^+$ Calcd for $\text{C}_{11}\text{H}_{10}\text{F}_3\text{N}_2\text{O}_2^+$ 259.0689; found 259.0685.

3-(2,2,3,3,3-Pentafluoropropoxy)quinoxalin-2(1H)-one (5ab): White solid; 85 mg, 85% yield;

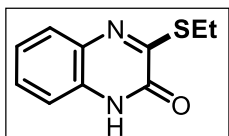


Purification by column chromatography on silica gel (eluent: EtOAc /Hexane = 1.0/9.0); mp = 130-132 °C; ^1H NMR (400 MHz, CDCl_3) δ 11.77 (s, 1H), 7.68 – 7.66 (m, 1H), 7.50 – 7.45 (m, 1H), 7.43 (d, $J = 6.8$ Hz, 1H), 7.39 – 7.34 (m, 1H), 5.04 (t, $J = 13.0$ Hz, 2H); $^{13}\text{C}\{^1\text{H}\}$ NMR (100 MHz, CDCl_3) δ 152.4, 151.3, 130.0, 129.8, 128.4, 127.0, 125.5 (q, $^1J_{C-F} = 270.7$ Hz), 124.8, 115.7, 61.8 (t, $^2J_{C-F} = 27.2$ Hz); ^{19}F NMR (376 MHz, CDCl_3) δ -83.7, -123.0 (t, $J = 13.3$ Hz); HRMS (ESI) m/z : $[\text{M} + \text{H}]^+$ Calcd for $\text{C}_{11}\text{H}_8\text{F}_5\text{N}_2\text{O}_2^+$ 295.0500; found 295.0494.

5.4.4 General Procedure for the C3-Sulfenylation of Quinoxalin-2(1H)-ones

An oven dried 10 mL round bottom flask was charged with quinoxalin-2(1H)-ones **1** (0.34 mmol; 1.0 equiv.), **6** (1.71 mmol; 5.0 equiv.) and Selectflour (2.0 equiv.) in CH₃CN at room temperature and the reaction mixture was stirred for 12 h. After completion of the reaction monitored by TLC, reaction mixture was concentrated in vacuum. The resulting crude was purified by column chromatography (silica gel 100-200 mesh) using EtOAc-hexanes as an eluent to afford corresponding products **7**.

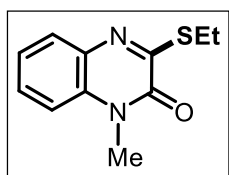
3-(Ethylthio)quinoxalin-2(1H)-one (7aa): White solid; 63 mg, 89% yield; Purification by col-



umn chromatography on silica gel (eluents: EtOAc /Hexane = 1.0/9.0); mp = 112-114 °C; ¹H NMR (400 MHz, CDCl₃) δ 11.80 (s, 1H), 7.80 – 7.77 (m, 1H), 7.47 – 7.42 (m, 1H), 7.40 – 7.32 (m, 2H), 3.27 (q, *J* = 7.5 Hz,

2H), 1.47 (t, *J* = 7.2 Hz, 3H); ¹³C{¹H} NMR (100 MHz, CDCl₃) δ 159.8, 154.8, 133.5, 129.0, 128.3, 127.4, 124.4, 116.1, 23.8, 13.8; HRMS (ESI) *m/z*: [M + H]⁺ Calcd for C₁₀H₁₁N₂OS⁺ 207.0587; found 207.0590.

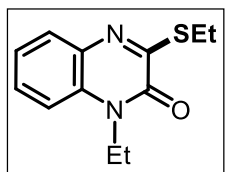
3-(Ethylthio)-1-methylquinoxalin-2(1H)-one (7ba): White solid; 60 mg, 81% yield; Purification



by column chromatography on silica gel (eluents: EtOAc /Hexane = 1.5/8.5); mp = 102-104 °C; ¹H NMR (400 MHz, CDCl₃) δ 7.78 (dd, *J* = 8.0, 1.6 Hz, 1H), 7.49 – 7.45 (m, 1H), 7.35 (dd, *J* = 7.6, 1.2 Hz, 1H), 7.32 – 7.30 (m, 1H), 3.73 (s, 3H), 3.20 (q, *J* = 7.3 Hz, 2H), 1.43 (t, *J* = 7.4 Hz,

3H); ¹³C{¹H} NMR (100 MHz, CDCl₃) δ 160.0, 153.4, 133.5, 131.4, 128.3, 128.1, 123.8, 113.7, 29.3, 23.9, 13.8; HRMS (ESI) *m/z*: [M + H]⁺ Calcd for C₁₁H₁₃N₂OS⁺ 221.0743; found 221.0746.

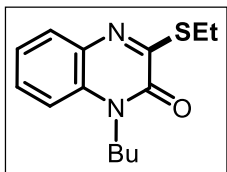
1-Ethyl-3-(ethylthio)quinoxalin-2(1H)-one (7ca): White solid; 63 mg, 78% yield; Purification



by column chromatography on silica gel (eluents: EtOAc /Hexane = 1.5/8.5); mp = 91-93 °C; ¹H NMR (400 MHz, CDCl₃) δ 7.81 – 7.78 (m, 1H), 7.49 – 7.45 (m, 1H), 7.35 – 7.31 (m, 2H), 4.35 (q, *J* = 7.2 Hz, 2H), 3.21 (q, *J* = 7.3 Hz, 2H), 1.44 (t, *J* = 7.0 Hz, 3H), 1.39 (d, *J* = 7.2 Hz, 3H);

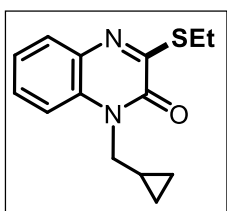
¹³C{¹H} NMR (100 MHz, CDCl₃) δ 160.0, 152.9, 133.9, 130.2, 128.6, 128.1, 123.6, 113.6, 37.5, 23.9, 13.8, 12.4; HRMS (ESI) *m/z*: [M + H]⁺ Calcd for C₁₂H₁₅N₂OS⁺ 235.0900; found 235.0899.

1-Butyl-3-(ethylthio)quinoxalin-2(1H)-one (7da): White solid; 71 mg, 80% yield; Purification



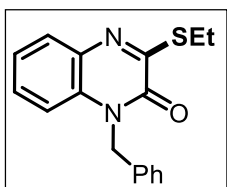
by column chromatography on silica gel (eluents: EtOAc /Hexane = 1.0/9.0); mp = 86-88 °C; ^1H NMR (400 MHz, CDCl_3) δ 7.80 (dd, J = 8.6, 1.4 Hz, 1H), 7.49 – 7.45 (m, 1H), 7.35 – 7.31 (m, 2H), 4.30 – 4.26 (m, 2H), 3.21 (q, J = 7.3 Hz, 2H), 1.82 – 1.74 (m, 2H), 1.55 – 1.48 (m, 2H), 1.44 (t, J = 7.4 Hz, 3H), 1.02 (t, J = 7.2 Hz, 3H); $^{13}\text{C}\{^1\text{H}\}$ NMR (100 MHz, CDCl_3) δ 160.1, 153.1, 133.9, 130.5, 128.6, 128.0, 123.6, 113.8, 42.3, 29.7, 29.3, 23.9, 20.3, 13.8; HRMS (ESI) m/z : $[\text{M} + \text{H}]^+$ Calcd for $\text{C}_{14}\text{H}_{19}\text{N}_2\text{OS}^+$ 263.1213; found 263.1212.

1-(Cyclopropylmethyl)-3-(ethylthio)quinoxalin-2(1H)-one (7ea): White solid; 62 mg, 70%



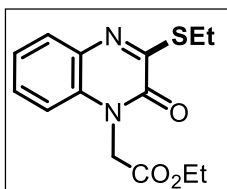
yield; Purification by column chromatography on silica gel (eluents: EtOAc /Hexane = 1.0/9.0); mp = 77-79 °C; ^1H NMR (400 MHz, CDCl_3) δ 7.81 – 7.79 (m, 1H), 7.50 – 7.46 (m, 1H), 7.36 – 7.32 (m, 2H), 5.96 – 5.86 (m, 1H), 5.18 – 5.11 (m, 2H), 4.37 – 4.22 (m, 2H), 3.21 (q, J = 7.5 Hz, 2H), 2.55 (q, J = 7.5 Hz, 2H), 1.44 (t, J = 7.4 Hz, 3H); $^{13}\text{C}\{^1\text{H}\}$ NMR (100 MHz, CDCl_3) δ 160.0, 153.1, 133.8, 128.6, 128.1, 123.7, 117.7, 113.7, 46.4, 41.8, 31.4, 23.9, 13.8, 4.1; HRMS (ESI) m/z : $[\text{M} + \text{H}]^+$ Calcd for $\text{C}_{14}\text{H}_{17}\text{N}_2\text{OS}^+$ 261.1056; found 261.1058.

1-Benzyl-3-(ethylthio)quinoxalin-2(1H)-one (7fa): White solid; 81 mg, 81% yield; Purification



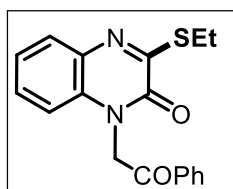
by column chromatography on silica gel (eluents: EtOAc /Hexane = 1.5/8.5); mp = 120-122 °C; ^1H NMR (400 MHz, CDCl_3) δ 7.80 (dd, J = 7.8, 1.4 Hz, 1H), 7.36 – 7.26 (m, 8H), 5.53 (s, 2H), 3.25 (q, J = 7.5 Hz, 2H), 1.47 (t, J = 7.4 Hz, 3H); $^{13}\text{C}\{^1\text{H}\}$ NMR (100 MHz, CDCl_3) δ 160.1, 153.6, 135.1, 133.8, 130.7, 128.9, 128.4, 128.1, 127.7, 127.0, 123.8, 114.6, 46.1, 24.1, 13.8; HRMS (ESI) m/z : $[\text{M} + \text{H}]^+$ Calcd for $\text{C}_{17}\text{H}_{17}\text{N}_2\text{OS}^+$ 297.1056; found 297.1055.

Ethyl 2-(3-(ethylthio)-2-oxoquinoxalin-1(2H)-yl)acetate (7ga): White solid; 70 mg, 71% yield;



Purification by column chromatography on silica gel (eluents: EtOAc /Hexane = 1.5/8.5); mp = 118-120 °C; ^1H NMR (400 MHz, CDCl_3) δ 7.59 (dd, J = 8.0, 1.2 Hz, 1H), 7.33 – 7.29 (m, 1H), 7.26 – 7.22 (m, 1H), 6.96 (dd, J = 8.2, 1.0 Hz, 1H), 5.00 (s, 2H), 4.51 (q, J = 7.1 Hz, 2H), 4.18 (q, J = 7.1 Hz, 2H), 1.45 (t, J = 7.0 Hz, 3H), 1.21 (t, J = 7.2 Hz, 3H); $^{13}\text{C}\{^1\text{H}\}$ NMR (100 MHz, CDCl_3) δ 168.4, 156.0, 139.8, 139.3, 139.0, 130.3, 129.0, 127.3, 127.0, 62.7, 61.4, 14.2; HRMS (ESI) m/z : $[\text{M} + \text{H}]^+$ Calcd for $\text{C}_{14}\text{H}_{17}\text{N}_2\text{O}_3\text{S}^+$ 293.0954; found 293.0950.

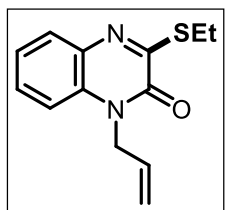
3-(Ethylthio)-1-(2-oxo-2-phenylethyl)quinoxalin-2(1H)-one (7ha): White solid; 80 mg, 73%



yield; Purification by column chromatography on silica gel (eluents: EtOAc /Hexane = 1.0/9.0); mp = 102-104 °C; ^1H NMR (400 MHz, CDCl_3) δ 8.11 – 8.09 (m, 2H), 7.82 (dd, $J = 7.4, 1.6$ Hz, 1H), 7.70 (t, $J = 7.4$ Hz, 1H), 7.58 (t, $J = 7.6$ Hz, 2H), 7.39 – 7.31 (m, 2H), 6.95 (dd, $J = 8.0, 1.2$

Hz, 1H), 5.76 (s, 2H), 3.25 (q, $J = 7.3$ Hz, 2H), 1.46 (t, $J = 7.4$ Hz, 3H); $^{13}\text{C}\{^1\text{H}\}$ NMR (100 MHz, CDCl_3) δ 190.9, 159.6, 153.2, 134.6, 134.3, 133.7, 130.8, 129.1, 128.6, 128.2, 123.9, 113.6, 48.5, 24.0, 13.8; HRMS (ESI) m/z : $[\text{M} + \text{H}]^+$ Calcd for $\text{C}_{18}\text{H}_{17}\text{N}_2\text{O}_2\text{S}^+$ 325.1005; found 325.1008.

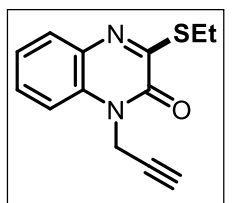
1-Allyl-3-(ethylthio)quinoxalin-2(1H)-one (7ia): White solid; 59 mg, 71% yield; Purification



by column chromatography on silica gel (eluents: EtOAc /Hexane = 2.0/8.0); mp = 88-90 °C; ^1H NMR (400 MHz, CDCl_3) δ 7.80 (dd, $J = 8.0, 1.2$ Hz, 1H), 7.46 – 7.42 (m, 1H), 7.36 – 7.29 (m, 2H), 6.00 – 5.91 (m, 1H), 5.32 – 5.27 (dd, $J = 10.4, 0.4$ Hz, 1H), 5.26 – 5.18 (dd, $J = 17.2, 0.4$ Hz,

1H), 4.94 (dt, $J = 5.2, 1.6$ Hz, 2H), 3.22 (q, $J = 7.5$ Hz, 2H), 1.45 (t, $J = 7.4$ Hz, 3H); $^{13}\text{C}\{^1\text{H}\}$ NMR (100 MHz, CDCl_3) δ 160.0, 153.0, 133.7, 130.6, 130.5, 128.4, 128.0, 123.8, 118.3, 114.3, 44.7, 24.0, 13.8; HRMS (ESI) m/z : $[\text{M} + \text{H}]^+$ Calcd for $\text{C}_{13}\text{H}_{15}\text{N}_2\text{OS}^+$ 247.0900; found 247.0898.

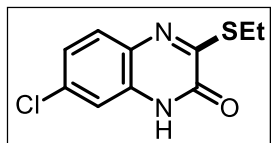
3-(Ethylthio)-1-(prop-2-yn-1-yl)quinoxalin-2(1H)-one (7ja): White solid; 63 mg, 76% yield;



Purification by column chromatography on silica gel (eluents: EtOAc /Hexane = 1.5/8.5); mp = 114-116 °C; ^1H NMR (400 MHz, CDCl_3) δ 7.81 (dd, $J = 8.0, 1.2$ Hz, 1H), 7.54 – 7.47 (m, 2H), 7.40 – 7.36 (m, 1H), 5.09 (d, $J = 2.4$ Hz, 2H), 3.22 (q, $J = 7.3$ Hz, 2H), 2.31 (t, $J = 2.4$ Hz, 1H), 1.44 (t, $J =$

7.4 Hz, 3H); $^{13}\text{C}\{^1\text{H}\}$ NMR (100 MHz, CDCl_3) δ 159.8, 152.5, 133.7, 129.8, 128.4, 128.2, 124.2, 114.3, 76.6, 73.4, 31.7, 24.0, 13.7; HRMS (ESI) m/z : $[\text{M} + \text{H}]^+$ Calcd for $\text{C}_{13}\text{H}_{13}\text{N}_2\text{OS}^+$ 245.0743; found 245.0748.

7-Chloro-3-(ethylthio)quinoxalin-2(1H)-one (7ka): White solid; 51 mg, 64% yield; Purification

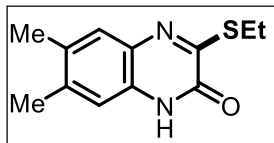


by column chromatography on silica gel (eluents: EtOAc /Hexane = 2.0/8.0); mp = 102-104 °C; ^1H NMR (400 MHz, CDCl_3) δ 12.21 (s, 1H), 7.55 (t, $J = 8.0$ Hz, 1H), 7.29 – 7.24 (m, 1H), 7.12 (t, $J = 7.0$ Hz, 1H),

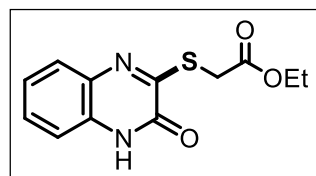
3.13 (q, $J = 7.2$ Hz, 2H), 1.35 (t, $J = 7.0$ Hz, 3H); $^{13}\text{C}\{^1\text{H}\}$ NMR (100 MHz, CDCl_3) δ 160.7,

153.9, 133.3, 131.7, 130.7, 128.2, 123.9, 115.4, 23.7, 13.7; HRMS (ESI) m/z : $[M + H]^+$ Calcd for $C_{10}H_{10}ClN_2OS^+$ 241.0197; found 241.0200.

3-(Ethylthio)-6,7-dimethylquinoxalin-2(1H)-one (71a): White solid; 63 mg, 79% yield; Purification by column chromatography on silica gel (eluent: EtOAc /Hexane = 2.0/8.0); mp = 123-125 °C; 1H NMR (400 MHz, $CDCl_3$) δ 11.54 (s, 1H), 7.55 (s, 1H), 7.13 (s, 1H), 3.24 (q, $J = 7.5$ Hz, 2H), 2.39 (s, 4H), 2.37 (s, 3H), 1.46 (t, $J = 7.4$ Hz, 3H); $^{13}C\{^1H\}$ NMR (100 MHz, $CDCl_3$) δ 158.3, 154.7, 138.1, 133.3, 132.0, 127.5, 127.0, 116.2, 23.8, 19.9, 19.5, 13.8; HRMS (ESI) m/z : $[M + H]^+$ Calcd for $C_{12}H_{15}N_2OS^+$ 235.0900; found 235.0898.



Ethyl 2-((3-oxo-3,4-dihydroquinoxalin-2-yl)thio)acetate (7ab): White solid; 61 mg, 67% yield; Purification by column chromatography on silica gel (eluent: EtOAc /Hexane = 3.0/7.0); mp = 128-130 °C; 1H NMR (400 MHz, $CDCl_3$) δ 12.09 (s, 1H), 7.73 (dd, $J = 8.0, 1.2$ Hz, 1H), 7.49 – 7.45 (m, 1H), 7.42 – 7.40 (m, 1H), 7.36 – 7.32 (m, 1H), 4.28 (q, $J = 7.1$ Hz, 2H), 4.03 (s, 2H), 1.33 (t, $J = 7.2$ Hz, 3H); $^{13}C\{^1H\}$ NMR (100 MHz, $CDCl_3$) δ 168.9, 158.2, 154.6, 133.2, 129.3, 128.9, 127.5, 124.6, 116.2, 61.8, 32.3, 14.3; HRMS (ESI) m/z : $[M + H]^+$ Calcd for $C_{12}H_{13}N_2O_3S^+$ 265.0641; found 265.0638.

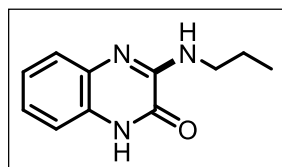


5.4.5 General Procedure for the C3-Amination of Quinoxalin-2(1H)-ones

An oven dried 10 mL round bottom flask was charged with quinoxalin-2(1H)-ones **1** (0.34 mmol; 1.0 equiv.), **8** (1.71 mmol; 5.0 equiv.) and Selectflour (2.0 equiv.) in CH_3CN at room temperature and the reaction mixture was stirred for 12 h. After completion of the reaction monitored by TLC, reaction mixture was concentrated in vacuum. The resulting crude was purified by column chromatography (silica gel 100-200 mesh) using EtOAc-hexanes as an eluent to afford corresponding products **9**.

5.4.5 General Procedure for the C3-Amination of Quinoxalin-2(1H)-ones

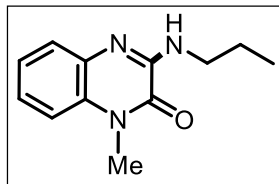
3-(Propylamino)quinoxalin-2(1H)-one (9aa): White solid; 53 mg, 76% yield; Purification by column chromatography on silica gel (eluent: EtOAc /Hexane = 2.5/7.5); mp = 148-150 °C; 1H NMR (400 MHz, $CDCl_3$) δ 11.56 (s, 1H), 7.57 (d, $J = 8.0$ Hz, 1H), 7.28 – 7.24 (m, 1H), 7.22 – 7.20 (m, 2H), 6.35 (t, $J = 5.4$ Hz, 1H), 3.57 (q, $J = 6.8$ Hz, 2H), 1.78 (sext, $J = 7.3$ Hz, 2H), 1.07 (t, $J = 7.4$ Hz, 3H); $^{13}C\{^1H\}$ NMR (100 MHz, $CDCl_3$) δ 152.9, 149.5, 134.2,



152.9, 149.5, 134.2,

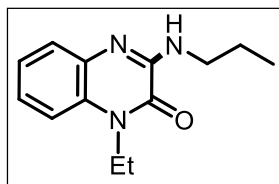
126.9, 125.4, 124.5, 123.9, 115.3, 42.7, 22.4, 11.6; HRMS (ESI) m/z : $[M + H]^+$ Calcd for $C_{11}H_{14}N_3O^+$ 204.1131; found 204.1130.

1-Methyl-3-(propylamino)quinoxalin-2(1H)-one (9ba): White solid; 56 mg, 74% yield; Purification by column chromatography on silica gel (eluent: EtOAc /Hexane = 2.5/7.5); mp = 134-136 °C; 1H NMR (400 MHz, $CDCl_3$) δ 7.57 – 7.55 (m, 1H), 7.28 – 7.19 (m, 3H), 6.42 (s, 1H), 3.71 (s, 3H), 3.52 (q, $J = 6.7$ Hz, 2H), 1.73 (sext, $J = 7.4$ Hz, 2H), 1.04 (t, $J = 7.4$ Hz, 3H);



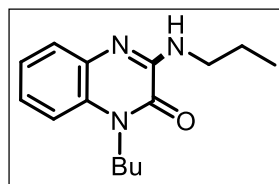
$^{13}C\{^1H\}$ NMR (100 MHz, $CDCl_3$) δ 151.9, 149.0, 134.3, 129.3, 126.0, 124.1, 123.7, 113.5, 42.6, 29.3, 22.4, 11.6; HRMS (ESI) m/z : $[M + H]^+$ Calcd for $C_{12}H_{16}N_3O^+$ 218.1288; found 218.1290.

1-Ethyl-3-(propylamino)quinoxalin-2(1H)-one (9ca): White solid; 60 mg, 75% yield; Purification by column chromatography on silica gel (eluent: EtOAc /Hexane = 2.0/8.0); mp = 152-154 °C; 1H NMR (400 MHz, $CDCl_3$) δ 7.59 – 7.57 (m, 1H), 7.27 – 7.24 (m, 3H), 6.40 (s, 1H), 4.35 (q, $J = 7.2$ Hz, 2H), 3.53 (q, $J = 6.7$ Hz, 2H), 1.74 (sext, $J = 7.3$ Hz, 2H), 1.40 (t, $J = 7.2$ Hz, 3H), 1.05 (t, $J = 7.4$ Hz, 3H); $^{13}C\{^1H\}$ NMR (100 MHz, $CDCl_3$) δ 151.4, 149.0, 134.6,



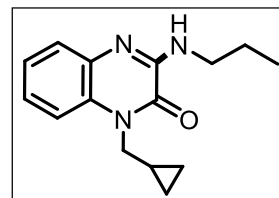
128.1, 126.4, 123.9, 123.7, 113.4, 42.6, 37.4, 22.5, 12.5, 11.6; HRMS (ESI) m/z : $[M + H]^+$ Calcd for $C_{13}H_{18}N_3O^+$ 232.1444; found 232.1440.

1-Butyl-3-(propylamino)quinoxalin-2(1H)-one (9da): White solid; 63 mg, 71% yield; Purification by column chromatography on silica gel (eluent: EtOAc /Hexane = 2.5/7.5); mp = 126-128 °C; 1H NMR (400 MHz, $CDCl_3$) δ 7.57 (d, $J = 6.0$ Hz, 1H), 7.25 – 7.23 (m, 3H), 6.41 (t, $J = 5.6$ Hz, 1H), 4.28 (t, $J = 7.8$ Hz, 2H), 3.53 (q, $J = 6.7$ Hz, 2H), 1.81 – 1.71 (m, 4H), 1.50 (sext, $J = 7.5$ Hz, 2H), 1.05 (t, $J = 7.2$ Hz, 3H), 1.02 (t, $J = 7.2$ Hz, 3H); $^{13}C\{^1H\}$ NMR (100 MHz, $CDCl_3$) δ 151.6, 149.0, 134.6, 128.3, 126.3, 123.9, 123.7, 113.6, 42.6, 42.3, 29.3, 22.4, 20.3,



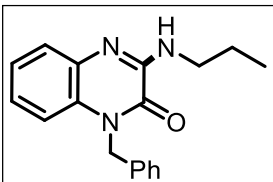
13.8, 11.6; HRMS (ESI) m/z : $[M + H]^+$ Calcd for $C_{15}H_{22}N_3O^+$ 260.1757; found 260.1755.

1-(Cyclopropylmethyl)-3-(propylamino)quinoxalin-2(1H)-one (9ea): White solid; 52 mg, 60% yield; Purification by column chromatography on silica gel (eluent: EtOAc /Hexane = 2.0/8.0); mp = 112-114 °C; 1H NMR (400 MHz, $CDCl_3$) δ 7.59 – 7.76 (m, 1H), 7.27 – 7.22 (m, 4H), 6.39 (s, 1H), 5.97 – 5.86 (m, 1H), 5.19 – 5.11 (m, 2H), 4.37 – 4.22 (m, 2H), 3.55 – 3.50



(m, 2H), 2.55 (q, $J = 7.5$ Hz, 2H), 1.74 (sext, $J = 7.3$ Hz, 2H), 1.05 (t, $J = 7.4$ Hz, 3H); $^{13}\text{C}\{^1\text{H}\}$ NMR (100 MHz, CDCl_3) δ 153.9, 150.9, 134.0, 127.8, 126.9, 123.8, 117.7, 113.6, 63.5, 46.4, 41.8, 31.5, 14.2, 9.6, 4.1; HRMS (ESI) m/z : $[\text{M} + \text{H}]^+$ Calcd for $\text{C}_{15}\text{H}_{20}\text{N}_3\text{O}^+$ 258.1601; found 258.1598.

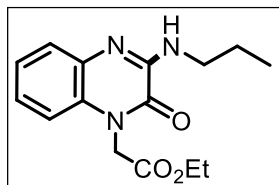
1-Benzyl-3-(propylamino)quinoxalin-2(1H)-one (9fa): White solid; 77 mg, 77% yield; Purification by column chromatography on silica gel (eluent: EtOAc /Hexane = 2.0/8.0); mp = 141-143 °C; ^1H NMR (400 MHz, CDCl_3) δ 7.59



(dd, $J = 7.8, 1.4$ Hz, 1H), 7.36 – 7.32 (m, 2H), 7.29 – 7.25 (m, 3H), 7.25 – 7.21 (m, 1H), 7.17 – 7.09 (m, 2H), 6.51 (t, $J = 5.8$ Hz, 1H), 5.53

(s, 2H), 3.57 (q, $J = 6.7$ Hz, 2H), 1.77 (sext, $J = 7.4$ Hz, 2H), 1.07 (t, $J = 7.4$ Hz, 3H); $^{13}\text{C}\{^1\text{H}\}$ NMR (100 MHz, CDCl_3) δ 152.2, 149.0, 135.4, 134.6, 128.9, 128.6, 127.6, 126.7, 126.2, 124.1, 123.8, 114.4, 46.2, 42.7, 22.5, 11.6; HRMS (ESI) m/z : $[\text{M} + \text{H}]^+$ Calcd for $\text{C}_{18}\text{H}_{20}\text{N}_3\text{O}^+$ 294.1601; found 294.1595.

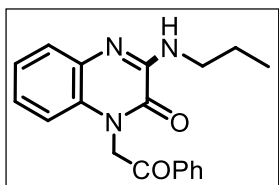
Ethyl 2-(2-oxo-3-(propylamino)quinoxalin-1(2H)-yl)acetate (9ga): White solid; 69 mg, 77%



yield; Purification by column chromatography on silica gel (eluent: EtOAc /Hexane = 2.5/7.5); mp = 143-145 °C; ^1H NMR (400 MHz, CDCl_3) δ 7.58 (dd, $J = 7.8, 1.8$ Hz, 1H), 7.26 (dd, $J = 7.8, 1.4$ Hz, 1H), 7.21 (td, $J = 7.8, 1.5$ Hz, 1H), 6.98 (dd, $J = 8.0, 1.2$ Hz, 1H), 6.36 (s,

1H), 5.05 (s, 2H), 4.27 (q, $J = 7.1$ Hz, 2H), 3.55 – 3.51 (m, 2H), 1.75 (sext, $J = 7.3$ Hz, 2H), 1.29 (t, $J = 7.2$ Hz, 3H), 1.05 (t, $J = 7.4$ Hz, 3H); $^{13}\text{C}\{^1\text{H}\}$ NMR (100 MHz, CDCl_3) δ 167.2, 151.9, 148.6, 134.3, 128.5, 126.4, 124.4, 123.9, 112.9, 62.0, 43.9, 42.7, 22.4, 14.1, 11.6; HRMS (ESI) m/z : $[\text{M} + \text{H}]^+$ Calcd for $\text{C}_{15}\text{H}_{20}\text{N}_3\text{O}_3^+$ 290.1499; found 290.1496.

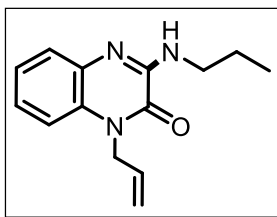
1-(2-Oxo-2-phenylethyl)-3-(propylamino)quinoxalin-2(1H)-one (9ha): White solid; 81 mg,



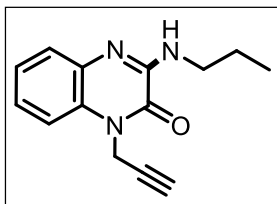
74% yield; Purification by column chromatography on silica gel (eluent: EtOAc /Hexane = 2.5/7.5); mp = 156-156 °C; ^1H NMR (400 MHz, CDCl_3) δ 8.12 (dd, $J = 8.4, 1.2$ Hz, 2H), 7.73 – 7.69 (m, 1H), 7.62 – 7.57 (m, 3H), 7.27 – 7.23 (m, 1H), 7.16 – 7.11 (m, 1H), 6.85

(dd, $J = 8.2, 1.0$ Hz, 1H), 6.37 (t, $J = 4.6$ Hz, 1H), 5.76 (s, 2H), 3.59 – 3.54 (m, 2H), 1.76 (sext, $J = 7.4$ Hz, 2H), 1.06 (t, $J = 7.4$ Hz, 3H); $^{13}\text{C}\{^1\text{H}\}$ NMR (100 MHz, CDCl_3) δ 191.1, 152.0, 148.7, 134.6, 134.4, 134.3, 129.1, 128.7, 128.6, 126.4, 124.3, 123.8, 113.3, 48.7, 42.7, 22.4, 11.6; HRMS (ESI) m/z : $[\text{M} + \text{H}]^+$ Calcd for $\text{C}_{19}\text{H}_{20}\text{N}_3\text{O}_2^+$ 322.1550, found 322.1546.

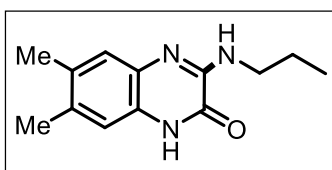
1-Allyl-3-(propylamino)quinoxalin-2(1H)-one (9ia): White solid; 57 mg, 69% yield; Purification by column chromatography on silica gel (eluents: EtOAc /Hexane = 2.5/7.5); mp = 136-138 °C; ^1H NMR (400 MHz, CDCl_3) δ 7.59 – 7.57 (m, 1H), 7.28 – 7.22 (m, 1H), 7.21 – 7.18 (m, 2H), 6.41 (s, 1H), 6.01 – 5.92 (m, 1H), 5.28 (d, J = 11.2 Hz, 1H), 5.20 (d, J = 17.6 Hz, 1H), 4.93 (d, J = 5.2 Hz, 2H), 3.54 (q, J = 6.7 Hz, 2H), 1.74 (sext, J = 7.3 Hz, 2H), 1.05 (t, J = 7.4 Hz, 3H); ^{13}C $\{^1\text{H}\}$ NMR (100 MHz, CDCl_3) δ 151.6, 148.9, 134.4, 130.8, 128.4, 126.2, 124.1, 123.7, 117.8, 114.1, 44.7, 42.6, 22.4, 11.6; HRMS (ESI) m/z : $[\text{M} + \text{H}]^+$ Calcd for $\text{C}_{14}\text{H}_{18}\text{N}_3\text{O}^+$ 244.1444; found 244.1447.



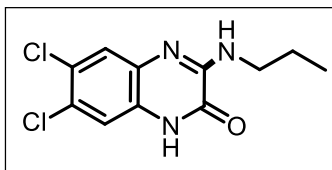
1-(Prop-2-yn-1-yl)-3-(propylamino)quinoxalin-2(1H)-one (9ja): White solid; 61 mg, 75% yield; Purification by column chromatography on silica gel (eluents: EtOAc /Hexane = 2.5/7.5); mp = 118-120 °C; ^1H NMR (400 MHz, CDCl_3) δ 7.60 – 7.57 (m, 1H), 7.39 – 7.37 (m, 1H), 7.30 – 7.27 (m, 2H), 6.39 (s, 1H), 5.08 (d, J = 2.4 Hz, 2H), 3.56 – 3.51 (m, 2H), 2.31 (t, J = 2.6 Hz, 1H), 1.74 (sext, J = 7.5 Hz, 2H), 1.05 (t, J = 7.4 Hz, 3H); ^{13}C $\{^1\text{H}\}$ NMR (100 MHz, CDCl_3) δ 151.3, 148.7, 134.5, 127.8, 126.3, 124.5, 123.9, 114.0, 76.9, 73.1, 42.7, 31.8, 22.4, 11.6; HRMS (ESI) m/z : $[\text{M} + \text{H}]^+$ Calcd for $\text{C}_{14}\text{H}_{16}\text{N}_3\text{O}^+$ 242.1288; found 242.1290.



6,7-Dimethyl-3-(propylamino)quinoxalin-2(1H)-one (9la): White solid; 60 mg, 77% yield; Purification by column chromatography on silica gel (eluents: EtOAc /Hexane = 2.0/8.0); mp = 146-148 °C; ^1H NMR (400 MHz, CDCl_3) δ 9.85 (s, 1H), 7.60 (s, 1H), 6.96 (s, 1H), 2.95 – 2.91 (m, 2H), 2.39 (s, 3H), 2.36 (s, 3H), 1.84 (sext, J = 7.1 Hz, 2H), 1.08 (t, J = 7.4 Hz, 3H); ^{13}C $\{^1\text{H}\}$ NMR (100 MHz, CDCl_3) δ 151.4, 138.1, 133.9, 128.3, 127.7, 127.1, 115.9, 106.8, 62.6, 20.5, 19.8, 19.5, 11.4; HRMS (ESI) m/z : $[\text{M} + \text{H}]^+$ Calcd for $\text{C}_{13}\text{H}_{18}\text{N}_3\text{O}^+$ 232.1444; found 232.1440.

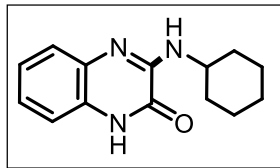


6,7-Dichloro-3-(propylamino)quinoxalin-2(1H)-one (9ma): White solid; 63 mg, 69% yield; Purification by column chromatography on silica gel (eluents: EtOAc /Hexane = 2.5/7.5); mp = 158-160 °C; ^1H NMR (400 MHz, CDCl_3) δ 11.51 (s, 1H), 7.64 (s, 1H), 6.44 (s, 1H), 3.53 (q, J = 6.8 Hz, 3H), 1.80 – 1.76 (m, 2H), 1.07 (t, J = 7.4 Hz, 3H); ^{13}C $\{^1\text{H}\}$



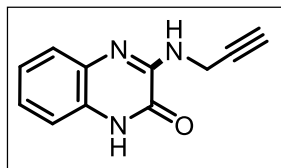
NMR (100 MHz, CDCl₃) δ 152.7, 149.6, 133.8, 127.9, 126.9, 126.5, 126.1, 116.2, 42.7, 22.3, 11.6; HRMS (ESI) m/z : [M + H]⁺ Calcd for C₁₃H₁₈N₃O⁺ 272.0352; found 272.0356.

3-(cyclohexylamino)quinoxalin-2(1H)-one (9ab): White solid; 41 mg, 69% yield; Purification



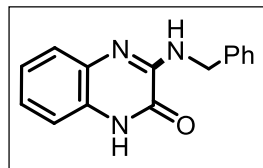
by column chromatography on silica gel (eluent: EtOAc /Hexane = 3.0/7.0); mp = 132-134 °C; ¹H NMR (400 MHz, CDCl₃) δ 10.21 (s, 1H), 7.60 (dd, J = 7.6, 2.0 Hz, 1H), 7.26 – 7.22 (m, 2H), 7.14 (dd, J = 7.8, 1.8 Hz, 1H), 6.42 (s, 1H), 4.40 (dd, J = 5.4, 2.6 Hz, 2H), 2.32 (t, J = 2.4 Hz, 1H); ¹³C {¹H} NMR (100 MHz, CDCl₃) δ 151.9, 148.6, 133.5, 127.4, 125.9, 124.7, 124.6, 115.0, 79.6, 71.7, 30.6; HRMS (ESI) m/z : [M + H]⁺ Calcd for C₁₁H₁₀N₃O⁺ 200.0818; found 200.0819.

3-(Prop-2-yn-1-ylamino)quinoxalin-2(1H)-one (9ac): White solid; 41 mg, 60% yield; Purification



by column chromatography on silica gel (eluent: EtOAc /Hexane = 3.0/7.0); mp = 132-134 °C; ¹H NMR (400 MHz, CDCl₃) δ 10.21 (s, 1H), 7.60 (dd, J = 7.6, 2.0 Hz, 1H), 7.26 – 7.22 (m, 2H), 7.14 (dd, J = 7.8, 1.8 Hz, 1H), 6.42 (s, 1H), 4.40 (dd, J = 5.4, 2.6 Hz, 2H), 2.32 (t, J = 2.4 Hz, 1H); ¹³C {¹H} NMR (100 MHz, CDCl₃) δ 151.9, 148.6, 133.5, 127.4, 125.9, 124.7, 124.6, 115.0, 79.6, 71.7, 30.6; HRMS (ESI) m/z : [M + H]⁺ Calcd for C₁₁H₁₀N₃O⁺ 200.0818; found 200.0819.

3-(Benzylamino)quinoxalin-2(1H)-one (9ad): White solid; 53 mg, 62% yield; Purification by



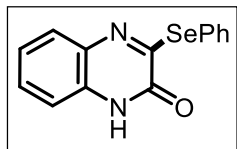
column chromatography on silica gel (eluent: EtOAc /Hexane = 2.5/7.5); mp = 128-130°C; ¹H NMR (400 MHz, CDCl₃) δ 11.30 (s, 1H), 7.61 – 7.59 (m, 1H), 7.46 (d, J = 7.2 Hz, 2H), 7.40 (t, J = 7.2 Hz, 2H), 7.36 – 7.32 (m, 1H), 7.30 – 7.25 (m, 1H), 7.24 – 7.18 (m, 2H), 6.61 (t, J = 5.6 Hz, 1H), 4.80 (d, J = 5.6 Hz, 2H); ¹³C {¹H} NMR (100 MHz, CDCl₃) δ 152.7, 149.2, 138.2, 134.0, 128.7, 128.1, 127.6, 127.1, 125.6, 124.6, 124.2, 115.3, 45.0; HRMS (ESI) m/z : [M + H]⁺ Calcd for C₁₅H₁₄N₃O⁺ 252.1131; found 252.1135.

5.4.6 General Procedure for the C3-Selenylation of Quinoxalin-2(1H)-ones

An oven dried 10 mL round bottom flask was charged with quinoxalin-2(1H)-ones **1** (0.34 mmol; 1.0 equiv.), **14** (1.71 mmol; 5.0 equiv.) and Selectflour (2.0 equiv.) in CH₃CN at room temperature and the reaction mixture was stirred for 12 h. After completion of the reaction

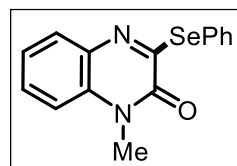
monitored by TLC, reaction mixture was concentrated in vacuum. The resulting crude was purified by column chromatography (silica gel 100-200 mesh) using EtOAc-hexanes as an eluent to afford corresponding products **15**.

3-(Phenylselanyl)quinoxalin-2(1H)-one (15aa): Off-white solid; 52 mg, 75% yield; Purifica-



tion by column chromatography on silica gel (eluent: EtOAc /Hexane = 2/3); mp = 170-172°C; ^1H NMR (400 MHz, CDCl_3) δ 12.13 (s, 1H), 8.27 (s, 1H), 7.71 (d, J = 8.8 Hz, 1H), 7.64 – 7.63 (m, 2H), 7.43 – 7.38 (m, 3H), 7.33 (s, 1H), 7.27 – 7.23 (dd, J = 8.4, 1.2 Hz, 1H); $^{13}\text{C}\{^1\text{H}\}$ NMR (100 MHz, CDCl_3) δ 156.6, 149.7, 138.0, 135.2, 131.9, 131.3, 129.8, 128.8, 128.4, 126.8, 117.1; HRMS (ESI) m/z : $[\text{M} + \text{H}]^+$ Calcd for $\text{C}_{14}\text{H}_{11}\text{NOSe}^+$ 303.0031; found 303.0045.

1-Methyl-3-(phenylselanyl)quinoxalin-2(1H)-one (15ba): White solid; 53 mg, 79% yield; puri-

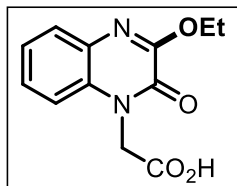


fication by column chromatography on silica gel (eluent: EtOAc /Hexane = 1/4); mp = 158-160°C; ^1H NMR (400 MHz, CDCl_3) δ 8.26 (s, 1H), 7.71 (d, J = 8.8 Hz, 1H), 7.65 – 7.63 (m, 2H), 7.44 – 7.39 (m, 3H), 7.30 – 7.28 (m, 2H), 3.56 (s, 3H); $^{13}\text{C}\{^1\text{H}\}$ NMR (100 MHz, CDCl_3) δ 154.9, 149.5, 137.8, 135.1, 133.7, 132.1, 130.7, 129.9, 128.9, 128.6, 126.0, 115.2, 28.6; HRMS (ESI) m/z : $[\text{M} + \text{H}]^+$ Calcd for $\text{C}_{15}\text{H}_{13}\text{N}_2\text{OSe}^+$ 317.0188; found 317.0185.

5.4.7 Experimental Procedure for the Synthesis of 16

An oven dried 10 mL round bottom flask was charged with compound **3ga** (0.09 mmol; 1.0 equiv.) and 2M KOH in MeOH at room temperature. The reaction mixture was stirred for 16 h at ambient temperature. After completion of the reaction monitored by TLC, the reaction mixture was filtered and the residue was washed with diethyl ether. The white powder was dried under high vacuum to obtain **16**.

2-(3-Ethoxy-2-oxoquinoxalin-1(2H)-yl)acetic acid (16): White solid; 21 mg, 96% yield; mp =



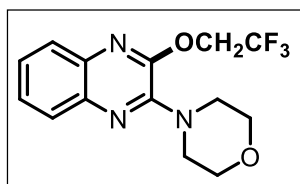
172-174 °C; ^1H NMR (400 MHz, $\text{DMSO}-d_6$) δ 7.60 – 7.58 (m, 1H), 7.44 – 7.37 (m, 2H), 7.31 (t, J = 6.8 Hz, 1H), 4.96 (s, 1H), 4.49 – 4.38 (q, J = 6.8 Hz, 2H), 1.39 (t, J = 7.0 Hz, 3H); $^{13}\text{C}\{^1\text{H}\}$ NMR (100 MHz, $\text{DMSO}-d_6$) δ 169.2, 153.8, 150.5, 131.4, 130.8, 127.6, 124.2, 114.9, 63.4, 44.5,

14.5; HRMS (ESI) m/z : $[\text{M} + \text{H}]^+$ Calcd for $\text{C}_{12}\text{H}_{13}\text{N}_2\text{O}_4^+$ 249.0870; found 249.0875.

5.4.8 Experimental Procedure for the Synthesis of 17

A mixture of **5aa** (0.16 mmol, 1 equiv.), POCl₃ (1.2 equiv.) and pyridine (1.0 equiv.) in a 10 mL pressure tube was stirred at 160 °C (in an oil bath) for 2 hours. After the completion of reaction as monitored by TLC, the reaction mixture was allowed to attain the room temperature and then quenched with saturated NaHCO₃ solution. The mixture was extracted with EtOAc and the collected organic layer was washed with brine, dried with Na₂SO₄. The solvent was removed under reduced pressure, the resulting crude was used dried and taken in a 10 mL pressure tube. Morpholine (1.5 equiv.), K₂CO₃ (1.5 equiv.) and CH₃CN (1.5 mL) was added to the tube and reaction mixture was stirred at 85 °C (in an oil bath) for 12 hours. After completion of the reaction as monitored by TLC, the reaction mixture was diluted with H₂O (3 mL) and extracted with EtOAc (2 × 3 mL). The collected organic layer was washed with brine, dried with Na₂SO₄. The solvent was removed under reduced pressure, and the resulting crude was purified by column chromatography (silica gel 100-200 mesh) using EtOAc-hexanes as an eluent to afford **17**.

4-(3-(2,2,2-trifluoroethoxy)quinoxalin-2-yl)morpholine (**17**): White solid; 26 mg, 72% yield;



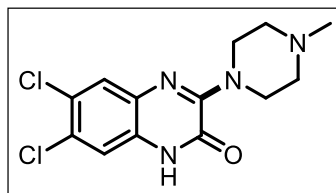
mp = 131-133 °C; ¹H NMR (400 MHz, CDCl₃) δ 7.77 (d, *J* = 7.6 Hz, 1H), 7.72 (d, *J* = 7.6 Hz, 1H), 7.52 (t, *J* = 7.0 Hz, 1H), 7.46 (t, *J* = 7.2 Hz, 1H), 4.95 (q, *J* = 8.4 Hz, 2H), 3.91 – 3.89 (m, 4H), 3.75 – 3.73 (m, 4H); ¹³C{¹H} NMR (100 MHz, CDCl₃) δ 148.2, 146.2, 138.9,

135.6, 127.4, 126.4, 126.21, 126.19, 123.5 (q, *J* = 275.4 Hz) 66.8, 62.5 (q, *J* = 36.0 Hz), 48.3; HRMS (ESI) *m/z*: [M + H]⁺ Calcd for C₁₄H₁₅F₃N₃O₂⁺ 314.1111; found 314.1106.

5.4.9 Experimental Procedure for the Synthesis of 18

An oven dried 10 mL pressure tube was charged with compound **5ma** (0.08 mmol; 1.0 equiv.), 1-methylpiperazine (0.012 mmol, 1.5 equiv.), Et₃N (1.5 equiv.), DMSO at room temperature. The reaction mixture was stirred for 12 h at 120 °C (in an oil bath). After completion of the reaction as monitored by TLC, the reaction mixture was diluted with H₂O (3 mL) and extracted with EtOAc (2 × 3 mL). The collected organic layer was washed with brine, dried with Na₂SO₄. The solvent was removed under reduced pressure, and the resulting crude was purified by column chromatography (silica gel 100-200 mesh) using EtOAc-hexanes as an eluent to afford **18**.

6,7-Dichloro-3-(4-methylpiperazin-1-yl)quinoxalin-2(1H)-one (**18**): Off-white solid; 26 mg,



65% yield; mp = 131-133 °C; ^1H NMR (400 MHz, DMSO- d_6) δ 7.38 (d, J = 2.5 Hz, 1H), 7.17 (s, 3H), 3.92 – 3.77 (m, 4H), 2.43 – 2.40 (m, 4H), 2.20 (s, 3H); ^{13}C { ^1H } NMR (100 MHz, DMSO- d_6) δ 152.8, 151.7, 132.8, 130.4, 125.5, 125.0, 123.4, 115.2, 55.0, 46.5,

46.2; HRMS (ESI) m/z : $[\text{M} + \text{H}]^+$ Calcd for $\text{C}_{13}\text{H}_{15}\text{Cl}_2\text{N}_4\text{O}^+$ 313.0617; found 313.0611.

5.4.10 Procedure for Radical Trapping Experiment. An oven dried 10 mL round bottom flask was charged with compound **1** (0.17 mmol; 1.0 equiv.), **2** (0.85 mmol; 5.0 equiv.), BHT (2 equiv.) and Selectflour (2.0 equiv.) in CH_3CN (1 mL) at room temperature and the reaction mixture was stirred for 12 h. An aliquot of the reaction mixture was analysed using HRMS spectrometry. Peaks at m/z 265.2160 and 411.2567 corresponding to $[\text{M} + \text{H}]^+$ ions of **19** and **20**, respectively were observed in the HRMS spectrum of the reaction mixture. Similarly, TEMPO (2 equiv.) was used instead of BHT and reaction mixture was analysed by HRMS. A peak at m/z = 202.1805 corresponding to **21** with molecular formula $\text{C}_{11}\text{H}_{24}\text{NO}_2^+$ was observed.

5.4.11 X-ray Crystallographic Analysis of Compound **5aa**, **5ca**, **9da** and **9ia**

The crystal data collection and data reduction were performed using CrysAlis PRO on a single crystal Rigaku Oxford XtaLab Pro diffractometer. The crystal was kept at 93(2) K during data collection. Using Olex2⁴⁹, the structure was solved with the ShelXT⁵⁰ structure solution program using Intrinsic Phasing and refined with the ShelXL⁵¹ refinement package using Least Squares minimisation.

The single crystals of the compound **5aa** ($\text{C}_{10}\text{H}_7\text{F}_3\text{N}_2\text{O}_2$) (**Figure 5.4**) and **5ca** ($\text{C}_{12}\text{H}_{11}\text{F}_3\text{N}_2\text{O}_2$) (**Figure 5.5**) were obtained from chloroform solution. **5aa** was crystallized in monoclinic crystal system with $\text{P}2_1/\text{c}$ space group and **5ca** was crystallized in triclinic crystal system with $\text{P}-1$ space group.. The crystal structure information of **5aa** and **5ca** is deposited to Cambridge Crystallographic Data Center and the CCDC numbers for **5aa** is 2178009 and for **5ca** is 2178501.

Table 5.7: Crystal data and structure refinement for **5aa** and **5ca**

Identification code	5aa	5ca
Empirical formula	$\text{C}_{10}\text{H}_7\text{F}_3\text{N}_2\text{O}_2$	$\text{C}_{12}\text{H}_{11}\text{F}_3\text{N}_2\text{O}_2$
Formula weight	244.18	272.23
Temperature/K	93(2)	123(2)

Crystal system	monoclinic	triclinic
Space group	P2 ₁ /c	P-1
a/Å	7.40700(10)	9.3781(2)
b/Å	14.9774(3)	10.2596(2)
c/Å	8.9193(2)	12.8663(3)
α/°	90	90.405(2)
β/°	101.306(2)	94.661(2)
γ/°	90	107.158(2)
Volume/Å ³	970.28(3)	1178.31(5)
Z	4	4
ρ _{calc} /cm ³	1.672	1.535
μ/mm ⁻¹	1.382	1.200
F(000)	496.0	560.0
Crystal size/mm ³	0.4 × 0.1 × 0.04	0.2 × 0.14 × 0.08
Radiation	Cu Kα (λ = 1.54184)	Cu Kα (λ = 1.54184)
2θ range for data collection/°	11.716 to 158.258	9.026 to 159.406
Index ranges	-9 ≤ h ≤ 9, -14 ≤ k ≤ 19, -11 ≤ l ≤ 9	-11 ≤ h ≤ 7, -13 ≤ k ≤ 12, -15 ≤ l ≤ 16
Reflections collected	5167	12828
Independent reflections	2032 [R _{int} = 0.0192, R _{sigma} = 0.0234]	4939 [R _{int} = 0.0322, R _{sigma} = 0.0370]
Data/restraints/parameters	2032/0/154	4939/0/345
Goodness-of-fit on F ²	1.083	1.078
Final R indexes [I ≥ 2σ (I)]	R ₁ = 0.0329, wR ₂ = 0.0885	R ₁ = 0.0374, wR ₂ = 0.0988
Final R indexes [all data]	R ₁ = 0.0346, wR ₂ = 0.0898	R ₁ = 0.0405, wR ₂ = 0.1014
Largest diff. peak/hole / e Å ⁻³	0.29/-0.28	0.33/-0.30

The single crystals of the compound **9da** (C₁₅H₂₁N₃O) (**Figure 5.6**) and **9ia** (C₁₄H₁₇N₃O) were obtained from chloroform solution. **9da** was crystallized in triclinic crystal system with P-1 space group and **9ia** was crystallized in monoclinic crystal system with P2₁/n space group. The crystal structure information of **9da** and **9ia** are deposited to Cambridge Crystallographic Data Center and the CCDC numbers for **9da** is 2206580 and for **9ia** is 2207035.

Table 5.8: Crystal data and structure refinement for **9da** and **9ia**

Identification code	9da	9ia
Empirical formula	C ₁₅ H ₂₁ N ₃ O	C ₁₄ H ₁₇ N ₃ O
Formula weight	259.35	243.30
Temperature/K	123	123(2)

Crystal system	triclinic	monoclinic
Space group	P-1	P2 ₁ /n
a/Å	8.7991(2)	11.9983(3)
b/Å	8.9233(3)	4.78150(10)
c/Å	10.0097(3)	22.0370(5)
α/°	110.064(3)	90
β/°	98.948(2)	96.867(2)
γ/°	99.827(2)	90
Volume/Å ³	707.67(4)	1255.19(5)
Z	2	4
ρ _{calc} /g/cm ³	1.217	1.288
μ/mm ⁻¹	0.618	0.667
F(000)	280.0	520.0
Crystal size/mm ³	0.17 × 0.08 × 0.03	0.15 × 0.06 × 0.04
Radiation	Cu Kα (λ = 1.54184)	Cu Kα (λ = 1.54184)
2θ range for data collection/°	9.67 to 159.242	8.016 to 158.832
Index ranges	-11 ≤ h ≤ 11, -10 ≤ k ≤ 11, -10 ≤ l ≤ 12	-14 ≤ h ≤ 13, -5 ≤ k ≤ 3, -25 ≤ l ≤ 28
Reflections collected	6909	5885
Independent reflections	2949 [R _{int} = 0.0295, R _{sigma} = 0.0390]	2596 [R _{int} = 0.0322, R _{sigma} = 0.0427]
Data/restraints/parameters	2949/0/174	2596/0/164
Goodness-of-fit on F ²	1.095	1.082
Final R indexes [I ≥ 2σ (I)]	R ₁ = 0.0409, wR ₂ = 0.1122	R ₁ = 0.0402, wR ₂ = 0.1091
Final R indexes [all data]	R ₁ = 0.0454, wR ₂ = 0.1174	R ₁ = 0.0465, wR ₂ = 0.1128
Largest diff. peak/hole / e Å ⁻³	0.19/-0.26	0.16/-0.23

5.5 REFERENCES

1. Carta, A.; Piras, S.; Loriga, G.; Paglietti, G., *Mini-Reviews in Medicinal Chemistry* **2006**, *6*, 1179-1200.
2. Qin, X.; Hao, X.; Han, H.; Zhu, S.; Yang, Y.; Wu, B.; Hussain, S.; Parveen, S.; Jing, C.; Ma, B.; Zhu, C., *Journal of Medicinal Chemistry* **2015**, *58*, 1254-1267.
3. Galal, S. A.; Khairat, S. H. M.; Ragab, F. A. F.; Abdelsamie, A. S.; Ali, M. M.; Soliman, S. M.; Mortier, J.; Wolber, G.; El Diwani, H. I., *European Journal of Medicinal Chemistry* **2014**, *86*, 122-132.

- Shi, L.; Hu, W.; Wu, J.; Zhou, H.; Zhou, H.; Li, X., *Mini-Reviews in Medicinal Chemistry* **2018**, *18*, 392-413.
- Weïwer, M.; Spoonamore, J.; Wei, J.; Guichard, B.; Ross, N. T.; Masson, K.; Silkworth, W.; Dandapani, S.; Palmer, M.; Scherer, C. A.; Stern, A. M.; Schreiber, S. L.; Munoz, B., *ACS Medicinal Chemistry Letters* **2012**, *3*, 1034-1038.
- Willardsen, J. A.; Dudley, D. A.; Cody, W. L.; Chi, L.; McClanahan, T. B.; Mertz, T. E.; Potoczak, R. E.; Narasimhan, L. S.; Holland, D. R.; Rapundalo, S. T.; Edmunds, J. J., *Journal of Medicinal Chemistry* **2004**, *47*, 4089-4099.
- Ghosh, P.; Das, S., *Synthetic Communications* **2020**, *50*, 2266-2312.
- Shi, L.; Zhou, H.; Wu, J.; Li, X., *Mini-Reviews in Organic Chemistry* **2015**, *12*, 96-112.
- Carrër, A.; Brion, J.-D.; Messaoudi, S.; Alami, M., *Organic Letters* **2013**, *15*, 5606-5609.
- Mou, C.-X.; Yuan, J.-W.; Hu, Q.; Han, B.-J.; Yang, L.-R.; Xiao, Y.-M.; Fan, L.-L.; Zhang, S.-R.; Qu, L.-B., *New Journal of Chemistry* **2023**, *47*, 3783-3792.
- Yan, Q.; Cui, W.; Li, J.; Xu, G.; Song, X.; Lv, J.; Yang, D., *Organic Chemistry Frontiers* **2022**, *9*, 2653-2658.
- Yuan, J.; Fu, J.; Yin, J.; Dong, Z.; Xiao, Y.; Mao, P.; Qu, L., *Organic Chemistry Frontiers* **2018**, *5*, 2820-2828.
- Wang, L.; Zhang, Y.; Li, F.; Hao, X.; Zhang, H.-Y.; Zhao, J., *Advanced Synthesis & Catalysis* **2018**, *360*, 3969-3977.
- Wang, L.; Liu, H.; Li, F.; Zhao, J.; Zhang, H.-Y.; Zhang, Y., *Advanced Synthesis & Catalysis* **2019**, *361*, 2354-2359.
- Ni, H.; Shi, X.; Li, Y.; Zhang, X.; Zhao, J.; Zhao, F., *Organic & Biomolecular Chemistry* **2020**, *18*, 6558-6563.
- Yuan, J.-W.; Fu, J.-H.; Liu, S.-N.; Xiao, Y.-M.; Mao, P.; Qu, L.-B., *Organic & Biomolecular Chemistry* **2018**, *16*, 3203-3212.
- Yang, Q.; Han, X.; Zhao, J.; Zhang, H.-Y.; Zhang, Y., *The Journal of Organic Chemistry* **2019**, *84*, 11417-11424.
- Yang, Q.; Yang, Z.; Tan, Y.; Zhao, J.; Sun, Q.; Zhang, H.-Y.; Zhang, Y., *Advanced Synthesis & Catalysis* **2019**, *361*, 1662-1667.
- Sumunnee, L.; Pimpasri, C.; Noikham, M.; Yotphan, S., *Organic & Biomolecular Chemistry* **2018**, *16*, 2697-2704.

20. Xie, L.-Y.; Peng, S.; Fan, T.-G.; Liu, Y.-F.; Sun, M.; Jiang, L.-L.; Wang, X.-X.; Cao, Z.; He, W.-M., *Science China Chemistry* **2019**, *62*, 460-464.
21. Xie, L.-Y.; Chen, Y.-L.; Qin, L.; Wen, Y.; Xie, J.-W.; Tan, J.-X.; Huang, Y.; Cao, Z.; He, W.-M., *Organic Chemistry Frontiers* **2019**, *6*, 3950-3955.
22. Mai, W.-P.; Yuan, J.-W.; Zhu, J.-L.; Li, Q.-Q.; Yang, L.-R.; Xiao, Y.-M.; Mao, P.; Qu, L.-B., *ChemistrySelect* **2019**, *4*, 11066-11070.
23. Zhao, L.; Wang, L.; Gao, Y.; Wang, Z.; Li, P., *Advanced Synthesis Catalysis* **2019**, *361*, 5363-5370.
24. Jiang, X.; Yang, L.; Ye, Z.; Du, X.; Fang, L.; Zhu, Y.; Chen, K.; Li, J.; Yu, C., *European Journal of Organic Chemistry* **2020**, 1687-1694.
25. Xu, X.; Xia, C.; Li, X.; Sun, J.; Hao, L., *RSC Advances* **2020**, *10*, 2016-2026.
26. Xu, J.; Yang, H.; Cai, H.; Bao, H.; Li, W.; Zhang, P., *Organic Letters* **2019**, *21*, 4698-4702.
27. Su, H.-Y.; Zhu, X.-L.; Huang, Y.; Xu, X.-H.; Qing, F.-L., *Chemical Communications* **2020**, *56*, 12805-12808.
28. Teng, Q.-H.; Yao, Y.; Wei, W.-X.; Tang, H.-T.; Li, J.-R.; Pan, Y.-M., *Green Chemistry* **2019**, *21*, 6241-6245.
29. Zhang, L.; He, J.; Zhang, P.; Zhu, D.; Zheng, K.; Shen, C., *Green Synthesis and Catalysis* **2022**.
30. Zhou, J.; Li, Z.; Sun, Z.; Ren, Q.; Zhang, Q.; Li, H.; Li, J., *The Journal of Organic Chemistry* **2020**, *85*, 4365-4372.
31. Gulevskaya, A. V.; Burov, O. N.; Pozharskii, A. F.; Kletskii, M. E.; Korbukova, I. N., *Tetrahedron* **2008**, *64*, 696-707.
32. Li, Y.; Gao, M.; Wang, L.; Cui, X., *Organic & Biomolecular Chemistry* **2016**, *14*, 8428-8432.
33. Gupta, A.; Deshmukh, M. S.; Jain, N., *The Journal of Organic Chemistry* **2017**, *82*, 4784-4792.
34. Wimonsong, W.; Yotphan, S., *Tetrahedron* **2021**, *81*, 131919.
35. Wei, W.; Wang, L.; Bao, P.; Shao, Y.; Yue, H.; Yang, D.; Yang, X.; Zhao, X.; Wang, H., *Organic Letters* **2018**, *20*, 7125-7130.

36. Li, K. J.; Xu, K.; Liu, Y. G.; Zeng, C. C.; Sun, B. G., *Advanced Synthesis & Catalysis* **2019**, *361*, 1033-1041.
37. Aguilar Troyano, F. J.; Merkens, K.; Gómez-Suárez, A., *Asian Journal of Organic Chemistry* **2020**, *9*, 992-1007.
38. Stavber, S., *Molecules* **2011**, *16*, 6432-6464.
39. Galloway, J. D.; Mai, D. N.; Baxter, R. D., *Organic Letters* **2017**, *19*, 5772-5775.
40. Hu, J.; Zhou, G.; Tian, Y.; Zhao, X., *Organic & Biomolecular Chemistry* **2019**, *17*, 6342-6345.
41. Yuan, J.-W.; Chen, Q.; Wu, W.-T.; Zhao, J.-J.; Yang, L.-R.; Xiao, Y.-M.; Mao, P.; Qu, L.-B., *New Journal of Chemistry* **2022**, *46*, 9451-9460.
42. Kalari, S.; Karale, U. B.; Rode, H. B., *The Journal of Organic Chemistry* **2022**, *87*, 2435-2445.
43. Niu, L.; Liu, J.; Liang, X.-A.; Wang, S.; Lei, A., *Nature Communications* **2019**, *10*, 467.
44. Kulthe, A. D.; Nadiveedhi, M. R.; Mainkar, P. S.; Akondi, S. M., *ARKIVOC* **2021**, *2021*, 115-124.
45. Belladonna, A. L.; Cervo, R.; Alves, D.; Barcellos, T.; Cargnelutti, R.; Schumacher, R. F., *Tetrahedron Letters* **2020**, *61*, 152035.
46. Liang, X.-A.; Niu, L.; Wang, S.; Liu, J.; Lei, A., *Organic Letters* **2019**, *21*, 2441-2444.
47. Xie, L.-Y.; Qu, J.; Peng, S.; Liu, K.-J.; Wang, Z.; Ding, M.-H.; Wang, Y.; Cao, Z.; He, W.-M., *Green Chemistry* **2018**, *20*, 760-764.
48. Zhu, H.; Mishra, R.; Yuan, L.; Abdul Salam, S. F.; Liu, J.; Gray, G.; Sterling, A. D.; Wunderlich, M.; Landero-Figueroa, J.; Garrett, J. T.; Merino, E. J., *ChemMedChem* **2019**, *14*, 1933-1939.
49. Dolomanov, O. V.; Bourhis, L. J.; Gildea, R. J.; Howard, J. A.; Puschmann, H., *Journal of Applied Crystallography* **2009**, *42*, 339-341.
50. Sebbar, N.; Ellouz, M.; Essassi, E.; Ouzidan, Y.; Mague, J., *Acta Crystallographica Section E: Crystallographic Communications* **2015**, *71*, o999.
51. Sheldrick, G. M., *Acta Crystallographica Section A: Foundations and Advances* **2015**, *71*, 3-8.

CHAPTER 6

Conclusions and Future Scope

6.1 General conclusions

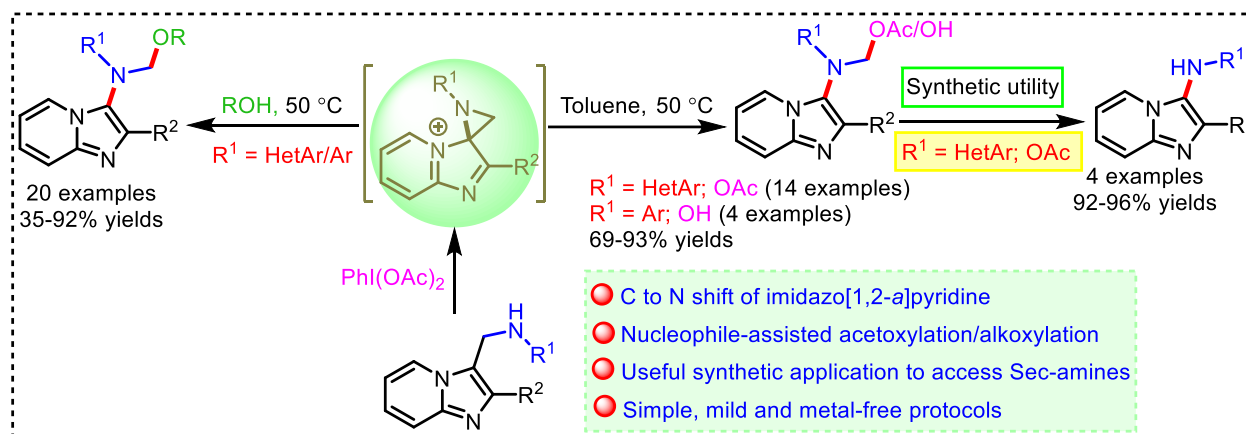
Across the world, synthetic chemist always plays pivotal role in design and synthesis of biologically potent fused heterocyclic molecules due to its wide applications in agrochemical, pharmaceuticals and their ubiquity in various natural products. However, to achieve these complex bioactive organic molecules with not only minimization of synthetic steps and with high atom economy but also easily from available precursors are the major concern. In this regards, synthesis of the complex heterocyclic frameworks in a single step is always on high priority. Besides, transition-metal-free C-H activation has attracted great attention over traditional transition-metal catalyzed methods for the construction of complex heterocyclic moieties without pre-functionalization of starting materials.

In the recent years, C-H functionalization through transition-metal-free protocol has received great attention for the C-C and C-X (X = heteroatom.) bond formation. These methodologies provide high molecular complexity, excellent regioselectivity and exhibit high functional group tolerance. In the thesis entitled “**C-H Bond Functionalization of Selected Aza-Heterocycles under Metal-free and Photochemical Conditions**” describes the functionalization of various nitrogen heterocycles through ionic/radical processes.

Chapter 1 of the thesis describes the advantages of metal-free reactions over transition-metal catalyzed reactions for the functionalization of aza-heterocycles. The plenty of literature reports describes the scope of transition-metal-free reactions for synthetic chemists in decorating the *N*-heterocyclic skeletons with diverse functionalities.

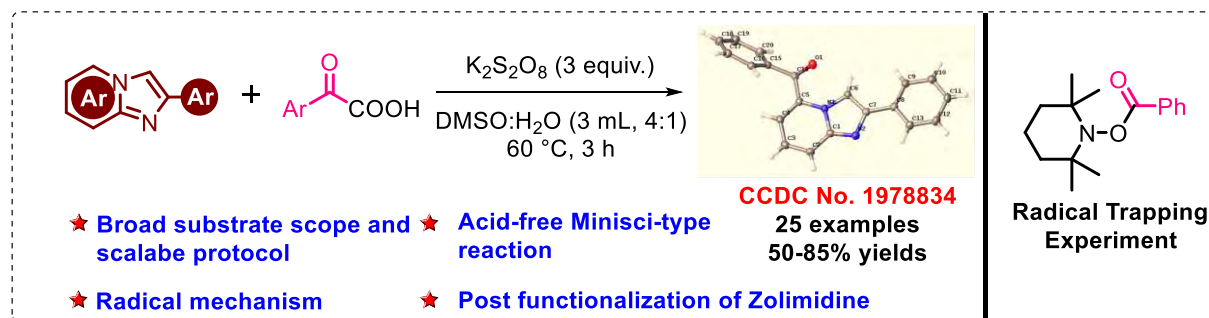
Further, the synthesis of *N*-acetoxymethyl, *N*-alkoxymethyl and *N*-hydroxymethyl *N*-aryl-imidazopyridine-3-amines has been described in the presence of PIDA as an oxidant (**Scheme 6.1**). The reaction is believed to pursue *via* formation of aziridine intermediate followed by nucleophile assisted ring opening in imidazopyridine derived mannich bases. The described method was found to be tolerated by different substituted imidazopyridine and alcohols despite of their electronic nature providing excellent yields (upto 96%) of the corresponding products. All the synthesized compounds were characterized by NMR and mass spectroscopy and selected examples were unambiguously characterized by single-crystal XRD studies. The constructed molecules were easily transformed to *N*-pyridyl imidazopyridine 3-amines with high purity even

without performing column chromatography. Control experiments indicated non-radical pathway for the reaction.



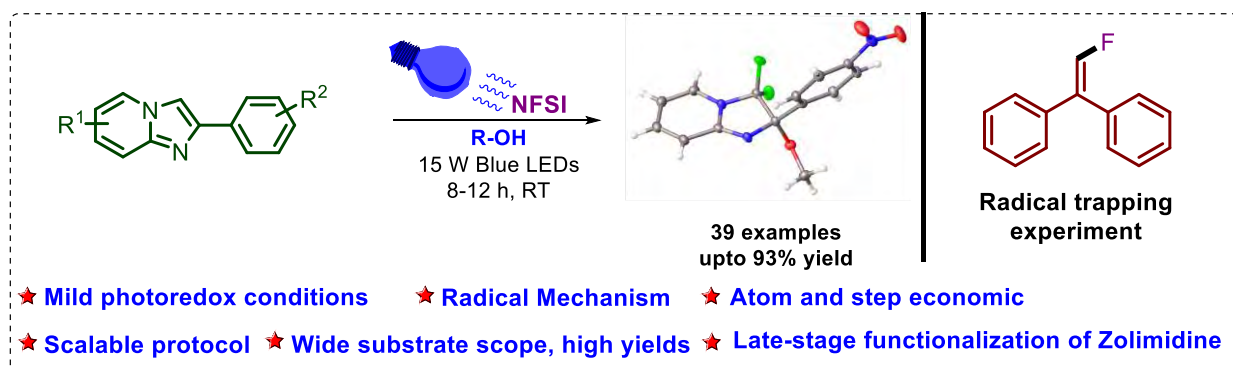
Scheme 6.1 PIDA-mediated synthesis of 3-aminoimidazo[1,2-*a*]pyridine

Chapter 2 deals with the Minisci-reaction type C5-arylation of imidazopyridines using potassium persulfate as an oxidant. In this chapter we have demonstrated the development of a new synthetic methodology for regioselective benzylation of imidazoheterocycles using arylglyoxylic acids as a aryl source (**Scheme 6.2**). The reaction was accomplished without the need for metal- or photocatalysts. A total of 25 examples of 5-aryl imidazo[1,2-*a*]pyridines were synthesized using this method, along with late-stage modification of the gastroprotective drug molecule, Zolimidine. The reaction was shown to produce good yields and tolerate a wide range of functional groups on both imidazoheterocycles and arylglyoxylic acids. Control experiments suggested that the reaction proceeds *via* a radical pathway. Importantly, the protocol is amenable for scale-up, and the mild reaction conditions make it a promising approach for the synthesis of a variety of biologically active compounds under metal-free conditions.



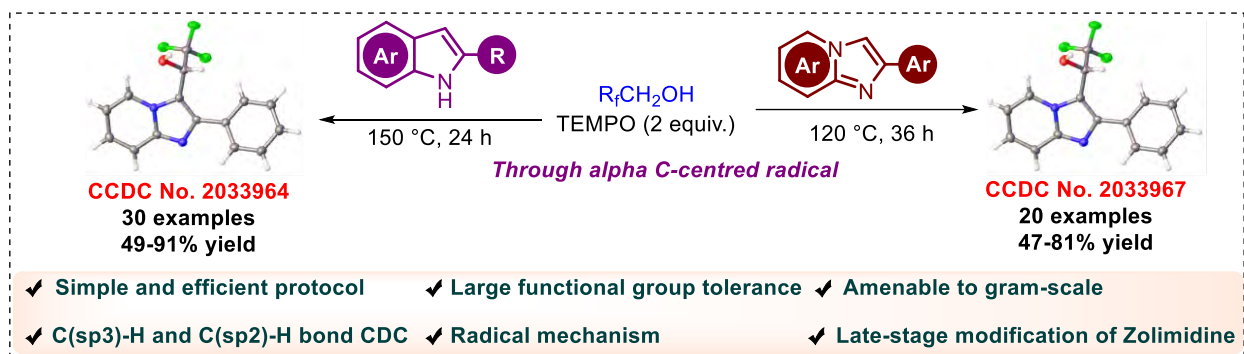
Scheme 6.2 Regioselective C5-arylation of imidazo[1,2-*a*]pyridines

Chapter 3 describes significance of visible-light induced reactions along with the importance of organofluorine compounds. In this chapter a highly selective difluoroalkoxylation of imidazo[1,2-*a*]pyridines under visible-light irradiation was developed (**Scheme 6.3**). The reaction featured high functional group tolerance with moderate to excellent yields of difluoroalkoxylated products, as well as a broad substrate scope and environmentally benign reaction conditions. Interestingly, several bioactive alcohols and imidazopyridines, including Zolimidine, a gastroprotective drug were well compatible with the developed method. The protocol was found to follow a radical pathway based on control experiments.



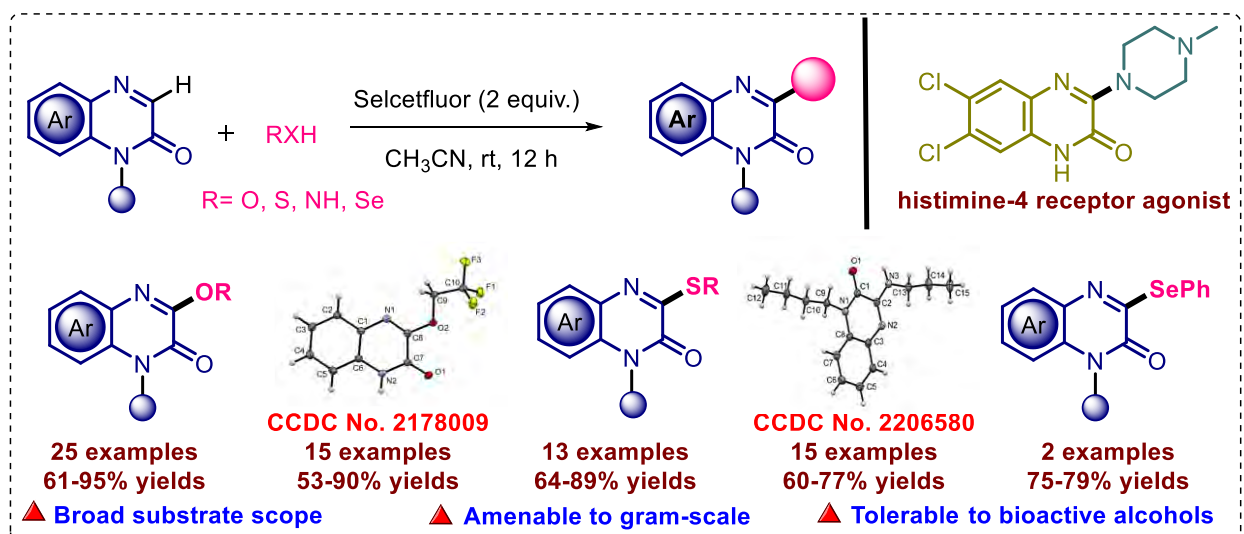
Scheme 6.3 Visible-light induced difluoroalkoxylation of imidazo[1,2-*a*]pyridines

In **chapter 4**, a TEMPO-mediated cross-dehydrogenative coupling of C(sp³)-H bond and C(sp²)-H bond was developed for direct hydroxyfluoroalkylation of indoles and imidazo[1,2-*a*]pyridines by fluorinated alcohols under metal-free conditions (**Scheme 6.4**). The synthetic protocol was shown to be operationally simple, providing a wide range of C3-hydroxyfluoroalkylated indoles and imidazo[1,2-*a*]pyridines in good to excellent yields with high functional group tolerance. The developed method was showcased through gram-scale synthesis of **3aa** and **25ia**, and two elegant transformations of 2,2,2-trifluoro-1-(2-phenyl-1H-indol-3-yl)ethanol were demonstrated. Mechanistic investigation revealed that the reaction involves a radical process.



Scheme 6.4 TEMPO-mediated hydroxyfluoroalkylation of indole and 2-aryl imidazopyridine

Chapter 5 elaborates an interesting synthetic strategy for affording a wide range of quinoxalin-2(1*H*)-ones decorated with alkoxy, alkylthio, alkylamino, and arylseleno groups at C3 positions under metal- and photocatalyst-free conditions. The method was shown to have broad substrate scope, including bioactive molecules. The mild reaction conditions, readily available coupling partners, high yields, scalability, step-economy, and metal- and photocatalyst-free conditions make it a promising approach for the synthesis of biologically active compounds. The synthetic utility of the developed protocol was demonstrated by gram-scale synthesis, C3-alkoxylation of quinoxalin-2(1*H*)-one with natural alcohols, and synthesis of aldose reductase (ALR2) inhibitor in excellent yields. Through control experiments, the mechanism of the reaction was proposed to involve radical pathway.



Scheme 6.5 Selectfluor-mediated C3-alkoxylation, sulfenylation, amination, and selenylation of quinoxalin-2(1*H*)-ones

6.2 Future scope of the research work

Nitrogen containing fused heterocyclic compounds have significant role in organic synthesis due to their wide range of applications in natural products, pharmaceuticals, medicinal chemistry, and material science. The major concern for the access of these potent heterocyclic compounds is the requirement of pre-functionalized starting materials, ultimate multistep synthesis causes low atom and step economy. Thus, transition-metal-free C-H functionalization engrossed more attention in chemical transformations to afford the *N*-fused heterocycles in one step synthesis from readily available substrate.

Although the thesis is primarily focused on the C-H reactions, still, there is broad scope for the synthesis of fused aza-heterocycles and their C-H activation. In particular, biologically important 2-arylimidazo[1,2-*a*]pyridines, 2-arylindoles and quinoxalin-2(1*H*)-ones were exclusively explored and used for further C-H functionalization. Some of the target molecules are demonstrated below which can be prepared by minor modification of the reaction condition developed for the C-H bond functionalization and cross-coupling/annulation reactions (**Figure 6.1**). Furthermore, it would be very interesting to explore synthesis of the target molecules using photo-induced process which is cheaper and environment friendly.

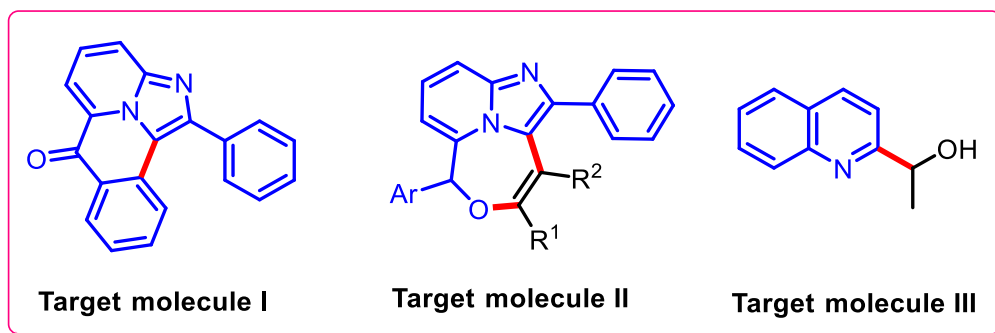
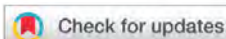


Figure 6.1 Proposed target molecules for future study

1. Om P. S. Patel, Shiv Dhiman, Shahid Khan, Vikki N. Shinde, **Sonam**, Manu R. Srivathsa, Prabhat N. Jha, Anil Kumar, A straightforward TBHP-mediated synthesis of 2-amidobenzoic acids from 2-arylidols and their antimicrobial activity. *Org. Biomol. Chem.*, **2019**, *17*, 5962-5970.
2. **Sonam**, Om P. S. Patel, Vikki N. Shinde, Nitesh K. Nandwana, Krishnan Rangan, Anil Kumar, Phenylodine(III) diacetate-mediated 1,2-*ipso*-migration in mannich bases of imidazo[1,2-*a*]pyridines: Preparation of *N*-acetoxymethyl/alkoxymethyl-*N*-arylimidazo[1,2-*a*]pyridine-3-amines. *J. Org. Chem.* **2020**, *85*, 7309-7321.
3. **Sonam**, Vikki N. Shinde, Neha Meena, Dhanajay S. Nipate, Krishnan Rangan, Anil Kumar, Metal-free benzoylation of imidazoheterocycles by oxidative decarboxylation of arylglyoxylic acids. *Org. Biomol. Chem.*, **2020**, *18*, 9072-9080.
4. Vikki N. Shinde, Tapta Kumar Roy, **Sonam**, Dhanajay S. Nipate, Neha Meena, Krishnan Rangan, Anil Kumar, Rhodium(III)-catalyzed annulation of 2-arylimidazo[1,2-*a*]pyridines with maleimides: synthesis of 1*H*-benzo[*e*]pyrido[1',2':1,2]imidazo[4,5-*g*]isoindole-1,3(2*H*)-diones and their photophysical studies. *Adv. Synth. Catal.*, **2020**, *362*, 5751-5764.
5. **Sonam**, Dhananjay S. Nipate, Vikki N. Shinde, Krishnan Rangan, Anil Kumar, TEMPO-mediated cross-dehydrogenative coupling of indoles and imidazo[1,2-*a*]pyridines with fluorinated alcohols. *Org. Lett.* **2021**, *23*, 1373-1377.
6. **Sonam**, Dhananjay S. Nipate, Vikki N. Shinde, Krishnan Rangan, Anil Kumar, TEMPO-Mediated synthesis of indolyl/Imidazo[1,2-*a*]pyridinyl-substituted *para*-Quinone methides from butylated hydroxytoluene. *J. Org. Chem.* **2021**, *86*, 17090–17100.
7. **Sonam**, Vikki N. Shinde, Anil Kumar “KPF₆-Mediated esterification and amidation of carboxylic acids. *J. Org. Chem.* **2022**, *87*, 2651–2661.
8. Vikki N. Shinde, Bhawani, **Sonam**, Krishnan Rangan, Dalip Kumar, Anil Kumar, Mechanochemical ruthenium-catalyzed *ortho*-alkenylation of *N*-heteroaryl arenes with alkynes under ball-milling conditions. *J. Org. Chem.* **2022**, *87*, 5994–6005.
9. **Sonam**, Nitesh K. Nandwana, Vikki N. Shinde, Krishnan Rangan, Anil Kumar, Ruthenium(II)-catalyzed annulation of 2-arylimidazoles with arylglyoxals: synthesis of 5-hydroxyimidazo[2,1-*a*]isoquinolin-6(5*H*)-ones and their photophysical studies. *Eur. J. Org. Chem.* **2022**, e202201065

10. **Sonam**, Vikki N. Shinde, Krishnan Rangan, Anil Kumar, Selectfluor-mediated regioselective C3-alkoxylation, sulfenylation and amination of quinoxalin-2(1*H*)-ones. *J. Org. Chem.* **2023**, *88*, 2344–2357.
11. Neha Meena, Bhawani, **Sonam**, Krishnan Rangan, Anil Kumar, A ball-milling-enabled Zn(OTf)₂-catalyzed Friedel-Crafts hydroxylation of imidazo[1,2-*a*]pyridines and indoles. *J. Org. Chem.* **2023**, *88*, 3022–3034.
12. Vikki N. Shinde, Bhawani, **Sonam**, Krishnan Rangan, Anil Kumar, Manganese-catalyzed site-selective C-H activation at *ortho*-position of 2-arylimidazo[1,2-*a*]pyridines with maleimides. DOI: 10.1055/a-2066-1131.
13. Vikki N. Shinde, Neha Meena, **Sonam**, Krishnan Rangan, Anil Kumar, Catalyst switchable regioselective oxidative annulation of 2-arylimidazo[1,2-*a*]pyridines with cinnamaldehydes. Manuscript submitted to *J. Org. Chem.*
14. **Sonam**, Amol B. Gadekar, Vikki N. Shinde, Krishnan Rangan, Anil Kumar, “Visible-light driven regioselective difluoroalkoxylation of imidazo[1,2-*a*]pyridines using N-fluorobenzenesulfonimide.” (Manuscript under preparation).
15. Vikki N. Shinde, Bhawani, **Sonam**, Krishnan Rangan, Anil Kumar, C3-Alkenylation of indole/Imidazo[1,2-*a*]pyridine with propargyl alcohol. (Manuscript under preparation).



Cite this: *Org. Biomol. Chem.*, 2019, 17, 5962

A straightforward TBHP-mediated synthesis of 2-amidobenzoic acids from 2-arylindoles and their antimicrobial activity†

Om P. S. Patel,^{‡a} Shiv Dhiman,^{‡a} Shahid Khan,^b Vikki N. Shinde,^a Sonam Jaspal,^a Manu R. Srivathsa,^a Prabhat N. Jha^b and Anil Kumar^{†*}

A simple and highly efficient strategy has been developed for the synthesis of 2-amidobenzoic acids through the *tert*-butyl hydroperoxide (TBHP)-mediated oxygenation and sequential ring opening of 2-arylindoles in a one-pot fashion under metal-free aerobic conditions. The developed synthetic protocol is operationally simple, tolerates a wide range of functional groups, and is amenable to the gram-scale. Radical trapping experiments revealed that the reaction involves a radical pathway. The syn-


Phenyliodine(III) Diacetate-Mediated 1,2-*ipso*-Migration in Mannich Bases of Imidazo[1,2-*a*]pyridines: Preparation of *N*-Acetoxymethyl/Alkoxyethyl-*N*-arylimidazo[1,2-*a*]pyridine-3-amines


Om P. S. Patel,[§] Sonam Jaspal,[§] Vikki N. Shinde, Nitesh K. Nandwana, Krishnan Rangan, and Anil Kumar^{*}


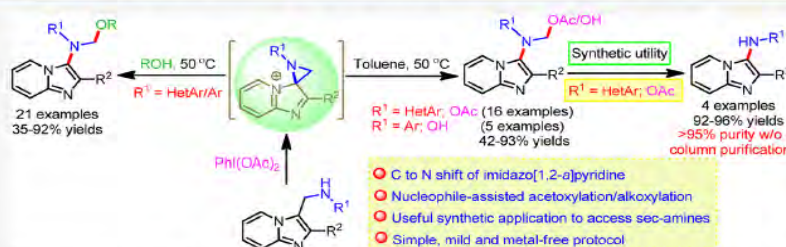
Cite This: *J. Org. Chem.* 2020, 85, 7309–7321

Read Online

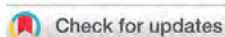
ACCESS |


 Metrics & More


 Article Recommendations


 Supporting Information


ABSTRACT: Phenyliodine(III) diacetate-mediated 1,2-*ipso*-migration of an imidazo[1,2-*a*]pyridine ring via the formation of an aziridine intermediate in Mannich bases derived from imidazo[1,2-*a*]pyridines, 2-pyridylamines or arylamines, and formaldehyde is reported. The imidazo[1,2-*a*]pyridines bearing different substituents showed excellent migratory aptitude and resulted in corresponding *N*-acetoxymethyl-, *N*-alkoxyethyl-, and *N*-hydroxyethyl-*N*-arylimidazo[1,2-*a*]pyridine-3-amine derivatives in moderate to excellent (42 examples; 35–93%) yields. Radical trapping experiments confirmed the involvement of a non-radical intermediate. The developed protocol is amenable for a scale-up reaction, and synthetic utility of *N*-acetoxymethyl products was demonstrated by transforming them to corresponding *N*-(pyridin-2-yl)imidazo[1,2-*a*]pyridin-3-amines.



Cite this: *Org. Biomol. Chem.*, 2020, **18**, 9072

Metal-free benzoylation of imidazoheterocycles by oxidative decarboxylation of arylglyoxylic acids†

Sonam Jaspal,^a Vikki N. Shinde,^a Neha Meena,^a Dhananjay S. Nipate,^a Krishnan Rangan^b and Anil Kumar^b  ^{*,a}

A simple and straightforward approach has been realized for the direct benzoylation of imidazoheterocycles by oxidative decarboxylation of arylglyoxylic acids in the presence of $K_2S_2O_8$ as an oxidant. Various functional groups were tolerated on both imidazoheterocycles and arylglyoxylic acids and a wide range of C5-benzoyl-imidazoheterocycles were obtained in good to high yields (50–84%). Radical trapping experiments confirmed the involvement of the radical pathway. The developed protocol is amenable for a

Received 6th September 2020,
Accepted 15th October 2020
DOI: 10.1039/d0ob01842b



pubs.acs.org/OrgLett

Letter


TEMPO-Mediated Cross-Dehydrogenative Coupling of Indoles and Imidazo[1,2-*a*]pyridines with Fluorinated Alcohols


Dhananjay S. Nipate,[§] Sonam Jaspal,[§] Vikki N. Shinde, Krishnan Rangan, and Anil Kumar^{*§}


Cite This: *Org. Lett.* 2021, **23**, 1373–1377

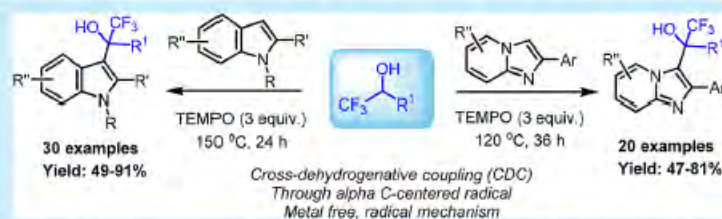
 Read Online

ACCESS |

 Metrics & More

 Article Recommendations

 Supporting Information



ABSTRACT: A simple and highly efficient metal-free method has been developed for hydroxyfluoroalkylation of indoles and imidazo[1,2-*a*]pyridines via TEMPO-mediated C(sp³)-H and C(sp²)-H bond cross-dehydrogenative coupling of fluorinated alcohols and indoles. The protocol showed broad substrate scope, afforded good yields of hydroxyfluoroalkylated products, and was amenable for scale-up. Mechanistic investigation indicated involvement of the radical pathway.

TEMPO-Mediated Synthesis of Indolyl/Imidazo[1,2-*a*]pyridinyl-Substituted *para*-Quinone Methides from Butylated HydroxytolueneDhananjay S. Nipate,[§] Sonam,[§] Vikki N. Shinde, Krishnan Rangan, and Anil Kumar*Cite This: *J. Org. Chem.* 2021, 86, 17090–17100

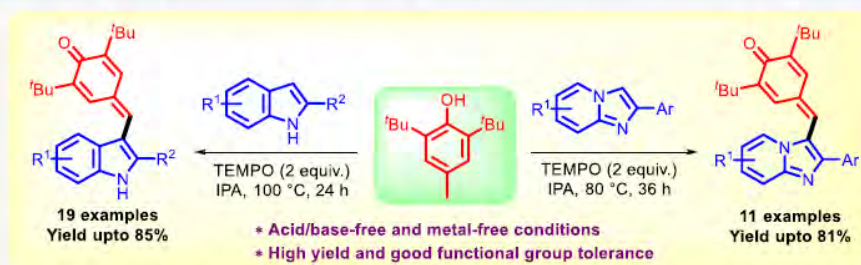
Read Online

ACCESS |

Metrics & More

Article Recommendations

Supporting Information



ABSTRACT: A series of indolyl or imidazo[1,2-*a*]pyridinyl-substituted *para*-quinone methides (*p*-QMs) is prepared by a metal-free, TEMPO-mediated cross-dehydrogenative coupling of butylated hydroxytoluene (BHT) with indoles or imidazo[1,2-*a*]pyridines in good to high yields. Broad substrate scope with respect to indoles and imidazo[1,2-*a*]pyridines, good functional group tolerance, and acid/base-free conditions are advantageous features of the developed protocol. The method was amenable for scale-up on the gram scale. Based on control experiments, a reaction mechanism is proposed to describe this transformation.

KPF₆-Mediated Esterification and Amidation of Carboxylic Acids

Sonam, Vikki N. Shinde, and Anil Kumar*

Cite This: <https://doi.org/10.1021/acs.joc.1c02611>

Read Online

ACCESS |

Metrics & More

Article Recommendations

Supporting Information

ABSTRACT: A novel KPF₆-promoted green method has been developed for the synthesis of esters and amides. A wide range of carboxylic acids and alcohols or amines worked well under the developed reaction conditions, thus providing good to excellent (61–98%) yields of the corresponding esters and amides. The method worked well with bioactive substrates such as cholesterol, levulinic acid, and linoleic acid. Wide substrate scope, operational simplicity, scalability, and sustainability make this protocol a practical and economically attractive approach for the preparation of ester and amides.



Selectfluor-Mediated Regioselective C-3 Alkoxylation, Amination, Sulfenylation, and Selenylation of Quinoxalin-2(1H)-ones

Sonam, Vikki N. Shinde, Krishnan Rangan, and Anil Kumar*

Cite This: <https://doi.org/10.1021/acs.joc.2c02756>

Read Online

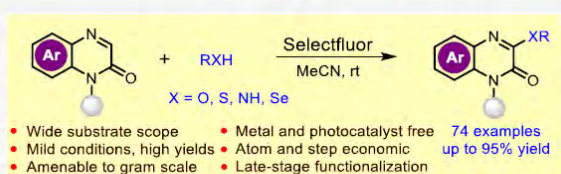
ACCESS |

Metrics & More

Article Recommendations

Supporting Information

ABSTRACT: A Selectfluor-promoted oxidative coupling of quinoxalin-2(1H)-ones with alcohols, amines, thiols, and selenols leading to the formation of C–O, C–N, C–S, and C–Se bonds has been developed. The protocol provided good to excellent (53–95%) yields of a wide range of quinoxalin-2(1H)-ones decorated with alkoxy, alkylamino, alkylthio, and arylselenyl groups at the C3-position under metal- and photocatalyst-free conditions. The reaction is believed to proceed through a radical pathway. A broad substrate scope including bioactive molecules, mild reaction conditions, readily available coupling partners, high yields, scalability, step-economy, and metal- and photocatalyst-free conditions are the highlighting features of the method. The synthetic utility of the developed protocol was demonstrated by gram-scale synthesis, C3-alkoxylation of quinoxaline-2(1H)-one with natural alcohols, and synthesis of aldose reductase (ALR2) inhibitor and histamine-4 receptor antagonist in good yields.



European Journal of Organic Chemistry

10.1002/ejoc.202201065

WILEY-VCH

RESEARCH ARTICLE

Ruthenium(II)-Catalyzed Annulation of 2-Arylimidazoles with Arylglyoxals: Synthesis of 5-Hydroxyimidazo[2,1-a]isoquinolin-6(5H)-ones and Their Photophysical Studies

Sonam,^{§[a]} Nitesh K. Nandwana,^{§[a,†]} Vikki N. Shinde,^[a,‡] Krishnan Rangan,^[b] and Anil Kumar*^[a]

[a] Sonam, N. K. Nandwana, V. N. Shinde and Prof. A. Kumar
Department of Chemistry
Birla Institute of Technology and Science Pilani, Pilani Campus, Rajasthan, 333031, India
E-mail: anilkumar@pilani.bits-pilani.ac.in

[b] Prof. K. Rangan
Department of Chemistry, Birla Institute of Technology and Science Pilani, Hyderabad Campus, Telangana, 500078, India

§Authors contributed equally.

†#Current address

‡The Wistar Institute, Philadelphia, PA 19104, USA

#Department of Chemistry, Texas A&M University, P.O. Box 30012, College Station, Texas 77842-3012, United States

*Corresponding author, E-mail: anilkumar@pilani.bits-pilani.ac.in

Supporting information for this article is given via a link at the end of the document.

Abstract: Synthesis of novel 5-hydroxyimidazo[2,1-a]isoquinolin-6(5H)-ones have been achieved by Ru(II)-catalyzed reaction of 2-arylimidazoles with arylglyoxals. The method provided moderate to good yields of 5-hydroxyimidazo[2,1-a]isoquinolin-6(5H)-ones and is amenable for gram-scale synthesis. The reaction involves imidazole-directed Ru(II)-catalyzed *ortho*-dicarbonylation followed by nucleophilic cyclization of the NH-group with the carbonyl group. Photophysical properties of the newly synthesized 5-hydroxyimidazo[2,1-a]isoquinolin-6(5H)-ones were investigated.

Transition metal-catalyzed C–H bond functionalization has inarguably emerged as one of the most important tool for the construction of carbon-carbon (C–C) and carbon-heteroatom (C–X) bonds in modern organic synthesis in the past two decades.^[3] Compared to conventional cross-coupling reactions, this strategy precludes the pre-functionalization steps, thus making this reaction as an atom- and step-economic, and sustainable alternative. 2-Aryl(benz)imidazoles have been functionalized using this approach by taking advantage of the inherent directing ability of imidazole ring.^[4] Transition metal-

FULL PAPER

Rhodium(III)-Catalyzed Annulation of 2-Arylimidazo[1,2-*a*]pyridines with Maleimides: Synthesis of 1*H*-Benzo[*e*]pyrido[1',2':1,2]imidazo[4,5-*g*]isoindole-1,3(2*H*)-diones and their Photophysical Studies

Vikki N. Shinde,^[a] Tapta Kanchan Roy,^[b] Sonam Jaspal,^[a] Dhananjay S. Nipate,^[a] Neha Meena,^[a] Krishnan Rangan,^[c] Dalip Kumar^[a] and Anil Kumar^{*[a]}

- [a] Department of Chemistry
Birla Institute of Technology and Science Pilani, Pilani Campus
Pilani, Rajasthan, 333031 (India)
E-mail: anilkadian@gmail.com and anilkumar@pilani.bits-pilani.ac.in
- [b] Department of Chemistry and Chemical Sciences
Central University of Jammu
Rahya Suchani, J&K, 181143 (India)
- [c] Department of Chemistry
Birla Institute of Technology and Science Pilani, Hyderabad Campus
Hyderabad, Telangana, 500078 (India)

Supporting information for this article is available on the WWW under <https://doi.org/10.1002/adsc.202000960>

JOC | The Journal of Organic Chemistry

pubs.acs.org/joc

Article

Ball-Milling-Enabled Zn(OTf)₂-Catalyzed Friedel–Crafts Hydroxyalkylation of Imidazo[1,2-*a*]pyridines and Indoles

Neha Meena,[§] Bhawani,[§] Sonam,[§] Krishnan Rangan, and Anil Kumar^{*§}

Cite This: <https://doi.org/10.1021/acs.joc.2c02719>

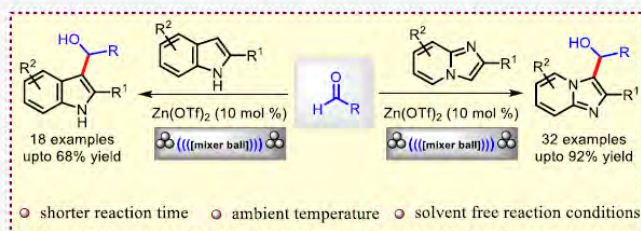
Read Online

ACCESS |

Metrics & More

Article Recommendations

Supporting Information



ABSTRACT: A facile and efficient synthetic method for the construction of C3-hydroxyalkylated imidazo[1,2-*a*]pyridines and indoles by a Zn(OTf)₂-catalyzed Friedel–Crafts hydroxyalkylation of imidazo[1,2-*a*]pyridines and indoles with carbonyl compounds under mechanochemical conditions is reported. Good product selectivity, shorter reaction time, ambient reaction temperature, tolerance of a wide range of functional groups, broad substrate scope, moderate to good yield of products, and scalability are the salient features of the developed methodology.

Mechanochemical Ruthenium-Catalyzed *Ortho*-Alkenylation of *N*-Heteroaryl Arenes with Alkynes under Ball-Milling Conditions

Bhawani,[§] Vikki N. Shinde,[§] Sonam,[§] Krishnan Rangan, and Anil Kumar^{*§}

Cite This: <https://doi.org/10.1021/acs.joc.2c00257>

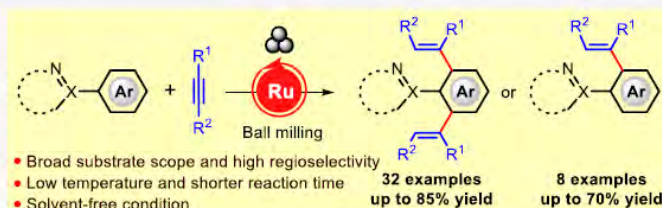
Read Online

ACCESS |

Metrics & More

Article Recommendations

Supporting Information



ABSTRACT: The mechanochemical, solvent-free Ru(II)-catalyzed alkenylation of *N*-heteroaryl arenes with alkynes has been successfully described. A wide spectrum of arenes bearing *N*-heteroaryl moieties such as imidazo[1,2-*a*]pyridine, imidazo[1,2-*a*]pyrimidine, benzo[*d*]imidazo[2,1-*b*]thiazole, imidazo[2,1-*b*]thiazole, 2*H*-indazole, 1*H*-indazole, 1*H*-pyrazole, and 1,2,4-oxadiazol-5(4*H*)-one as a directing group reacted with various substituted alkynes under ball milling in the presence of [Ru(*p*-cymene)Cl₂]₂, affording dialkenylated products in moderate to good yields. The reaction of 2,3-dihydrophthalazine-1,4-dione with 1-phenyl-1-propyne afforded a monoalkenylated product. Similarly, reaction of 2-phenylimidazo[1,2-*a*]pyridine with aliphatic terminal alkynes produced a monoalkenylated derivative as the major product along with minor amount of dialkenylated product. The developed method exhibited excellent functional group compatibility, broad substrate scope, shorter reaction times, and no external heating. Moreover, the method can be readily scaled-up as demonstrated by gram-scale synthesis of 2-(2,6-bis((*E*)-1-phenylprop-1-en-2-yl)phenyl)imidazo[1,2-*a*]pyridine.

Synthesis

Manganese-Catalyzed *ortho*-Hydroalkylation of Aryl Substituted *N*-Heteroaromatic Compounds with Maleimides

Vikki N Shinde, Bhawani Bhawani, Dhananjay S Nipate, Sonam Sonam, Neha Meena, Dalip Kumar, Krishan Rangan, Anil Kumar.

Affiliations below.

DOI: 10.1055/a-2066-1131

Please cite this article as: Shinde V N, Bhawani B, Nipate D S et al. Manganese-Catalyzed *ortho*-Hydroalkylation of Aryl Substituted *N*-Heteroaromatic Compounds with Maleimides. *Synthesis* 2023. doi: 10.1055/a-2066-1131

Conflict of Interest: The authors declare that they have no conflict of interest.

This study was supported by Science and Engineering Research Board (<http://dx.doi.org/10.13039/501100001843>), CRG/2020/002220, Department of Science and Technology, Ministry of Science and Technology (<http://dx.doi.org/10.13039/501100001409>), SR/FST/CSI-270/2015

Abstract:

1. **Sonam**, Vikki N. Shinde, Shiv Dhiman, Anil Kumar, Synthesis of Coumarin and Quinolinones Fused Aza-heterocycles via Ullmann Type C-N Coupling Reaction and Cross-dehydrogenative Coupling, 25th ISCB International conference, 12th – 14th January, 2019, Hotel Golden Tulip, Lucknow, India
2. **Sonam**, Vikki N. Shinde, Anil Kumar, *N*-Heteroarylation and Solvent-Switched Acetoxylation and Alkoxylation in Mannich Bases of Imidazopyridines *via* PIDA-Mediated 1,2-*Ips*o-Migration, at 26th ISCB International conference, Nirma University of Gujrat, 22st – 24th January, 2020. (**BEST POSTER AWARD**)
3. **Sonam**, Vikki N. Shinde, Anil Kumar Metal-Free Selectfluor-Mediated C3 Alkoxylation, Sulfenylation and Amination of Quinoxalin-2(1*H*)-ones 29th CRSI National symposium in chemistry, 7th – 9th Jul, 2022, IISER Mohali, India.

Brief Biography of the Candidate

[A-4]

Sonam, born in January 1993 in Gurgaon, Haryana, India, holds a Bachelor's degree in Chemistry (Hons.) from Rajdhani College, Delhi University (2011-2014), and a Master's degree in Chemistry from Dr. B. R. Ambedkar National Institute of Technology, Jalandhar, Punjab, India (2015-2017). During her Master's, she completed one-month internships at IIT Kanpur under the guidance of Prof. S. P. Rath and a two-month internship at IIT Madras under the supervision of Prof. Md. Mahiuddin Baidya.

In March 2018, Sonam joined as a Project Fellow in the DST-SERB sponsored project, working under the guidance of Prof. Anil Kumar at the Department of Chemistry, BITS Pilani, Pilani Campus, Rajasthan. Later, in August 2018, she enrolled for the Ph.D. program at BITS Pilani under Prof. Anil Kumar's mentorship. Her research revolves around the C-H bond functionalization of selected azaheterocycles, employing metal-free and photochemical conditions.

Throughout her academic journey, Sonam has made significant contributions to the field of synthetic organic chemistry, publishing twelve research articles in peer-reviewed international journals, with seven of them being as the first author. She has also actively participated in three international/national conferences, presenting her work as poster presentations and even receiving the Best Poster Award in one of the conferences.

Sonam's passion lies in exploring the application of transition-metal-free C-H functionalization reactions with novel heterocyclic compounds, and she continues to strive for excellence in her research endeavors.

Brief Biography of the Supervisor

[A-5]

Dr. Anil Kumar is a distinguished professor of chemistry at Birla Institute of Technology and Science (BITS), Pilani. He completed his PhD from the department of chemistry, University of Delhi, under the esteemed guidance of professor SMS Chauhan in 2004. During his doctoral research, Dr. Kumar focused on developing heterogeneous catalysts for organic synthesis, with a strong emphasis on green chemistry principles.

Following his doctoral studies, Dr. Kumar pursued his postdoctoral research at the department of biomedical and pharmaceutical sciences, University of Rhode Island, Kingston, USA, under the mentorship of Prof. Keykavous Parang. His postdoctoral work involved the synthesis of novel Src kinase inhibitory agents and solid-phase synthesis.

In 2006, Dr. Kumar joined the department of chemistry at BITS Pilani as an assistant professor, and through his dedication and exceptional contributions, he was promoted to associate professor in February 2013 and later to the prestigious position of Professor in August 2018. Throughout his career, he has displayed outstanding leadership, serving as the Associate Dean for Work Integrated Learning Programmes (WILP) from May 2014 to August 2018, and as the Head of the Department of Chemistry, BITS Pilani, Pilani Campus, from September 2014 to August 2016.

Dr. Kumar is highly regarded for his remarkable achievements and has earned several accolades, including the CRSI Bronze Medal (2020) from CRSI Bangalore, Prof. S. Venkateswaran Faculty Excellence Award (2017) from BITS Alumni Association, Dr. Arvind Kumar Memorial Award (2014) from Indian Council of Chemists, ISCB Young Scientist Award in Chemical Sciences (2013) from ISCB Lucknow, and Harrison McCain Foundation Award (2012) from Acadia University, Canada. He is currently serving as a council member of CRSI Bangalore for the period 2023-2026.

With over 23 years of extensive research experience and more than 17 years of teaching experience, Dr. Kumar's expertise lies in developing novel reaction methodologies using transition metal catalyzed C-C, N, S, O coupling reactions, green chemistry, ionic liquids, and medicinal chemistry. He has an impressive publication record, with over 181 research papers published in reputed international journals covering the areas of synthetic organic chemistry, green chemistry, and medicinal chemistry. Additionally, he has contributed significantly to the field through four book chapters and has delivered more than 45 invited lectures at national and international symposiums/conferences.

Dr. Kumar is an accomplished mentor, having supervised thirteen PhD students and co-supervised two others. Currently, he is supervising six PhD students. His exceptional leadership is evident in his successful completion of six research projects as Principal Investigator (PI), sponsored by esteemed organizations

Brief Biography of the Supervisor

[A-5]

such as SERB, DST, CSIR, and UGC, and one project as Co-PI sponsored by DST. At present, he is leading a major CSIR New Delhi project.

A respected member of various professional organizations, Dr. Kumar is a life member of Chemical Research Society of India, Bangalore; Indian Society of Chemists and Biologists, Lucknow; and Indian Council of Chemists, Agra. He serves as a valuable member of the editorial advisory board for The Open Catalysis Journal and actively contributes as a reviewer for numerous esteemed journals.

Dr. Anil Kumar's relentless pursuit of excellence in research and his dedication to imparting knowledge to the next generation of scientists have made him a prominent figure in the field of chemistry, earning him admiration and respect from peers and students alike. His passion for exploring novel chemical transformations and fostering sustainable practices in chemistry continues to inspire and shape the future of the discipline.